ADULT NEUROGENESIS: BEYOND RATS AND MICE

EDITED BY: Luca Bonfanti and Irmgard Amrein
PUBLISHED IN: Frontiers in Neuroscience

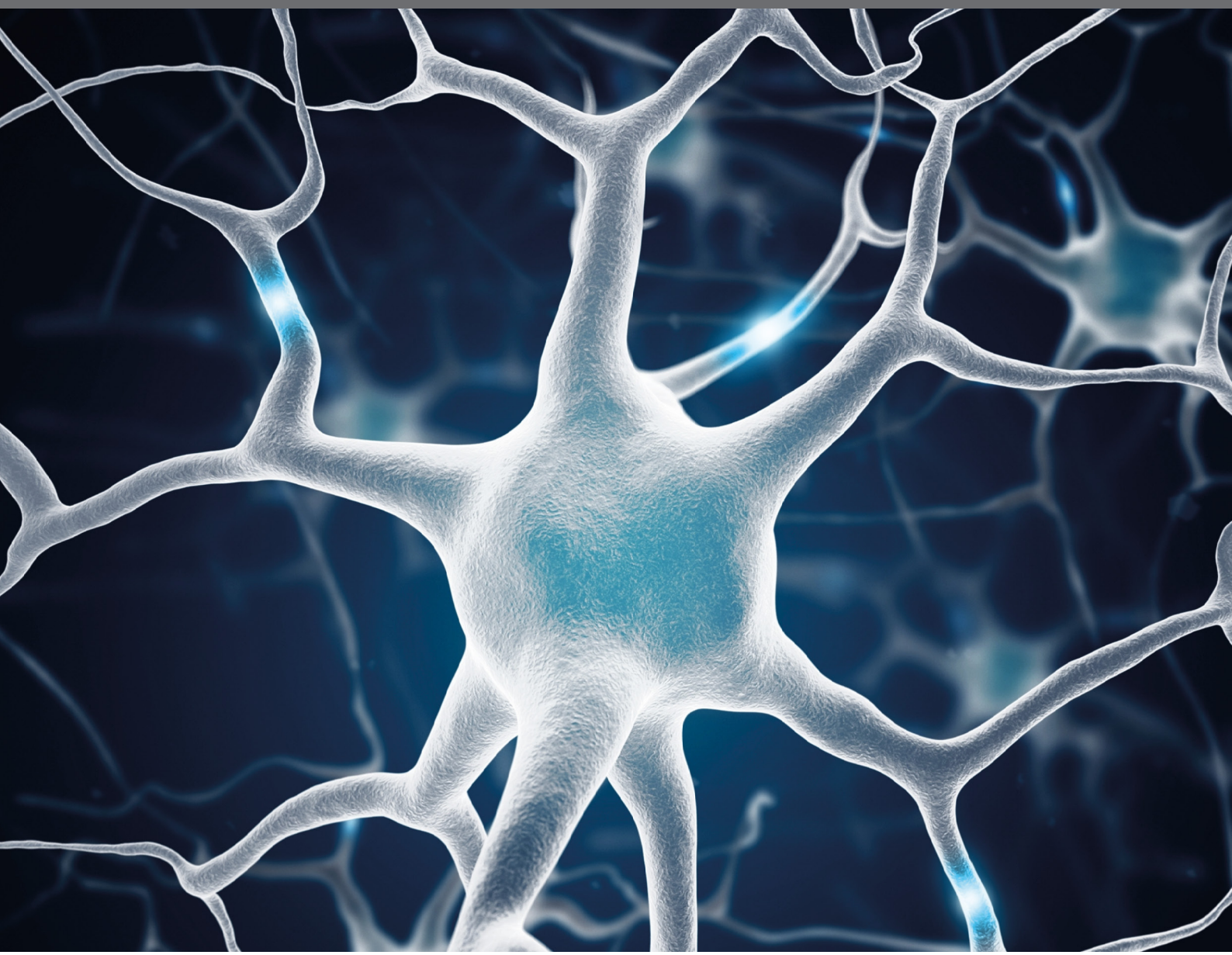

frontiers Research Topics

frontiers

ISSN 1664-8714
ISBN 978-2-88945-761-8
DOI 10.3389/978-2-88945-761-8

About Frontiers

Frontiers is more than just an open-access publisher of scholarly articles: it is a pioneering approach to the world of academia, radically improving the way scholarly research is managed. The grand vision of Frontiers is a world where all people have an equal opportunity to seek, share and generate knowledge. Frontiers provides immediate and permanent online open access to all its publications, but this alone is not enough to realize our grand goals.

Frontiers Journal Series

The Frontiers Journal Series is a multi-tier and interdisciplinary set of open-access, online journals, promising a paradigm shift from the current review, selection and dissemination processes in academic publishing. All Frontiers journals are driven by researchers for researchers; therefore, they constitute a service to the scholarly community. At the same time, the Frontiers Journal Series operates on a revolutionary invention, the tiered publishing system, initially addressing specific communities of scholars, and gradually climbing up to broader public understanding, thus serving the interests of the lay society, too.

Dedication to Quality

Each Frontiers article is a landmark of the highest quality, thanks to genuinely collaborative interactions between authors and review editors, who include some of the world's best academicians. Research must be certified by peers before entering a stream of knowledge that may eventually reach the public - and shape society; therefore, Frontiers only applies the most rigorous and unbiased reviews.
Frontiers revolutionizes research publishing by freely delivering the most outstanding research, evaluated with no bias from both the academic and social point of view. By applying the most advanced information technologies, Frontiers is catapulting scholarly publishing into a new generation.

What are Frontiers Research Topics?

Frontiers Research Topics are very popular trademarks of the Frontiers Journals Series: they are collections of at least ten articles, all centered on a particular subject. With their unique mix of varied contributions from Original Research to Review Articles, Frontiers Research Topics unify the most influential researchers, the latest key findings and historical advances in a hot research area! Find out more on how to host your own Frontiers Research Topic or contribute to one as an author by contacting the Frontiers Editorial Office: researchtopics@frontiersin.org

ADULT NEUROGENESIS: BEYOND RATS AND MICE

Topic Editors:
Luca Bonfanti, University of Turin, Italy
Irmgard Amrein, ETH Zurich, Switzerland

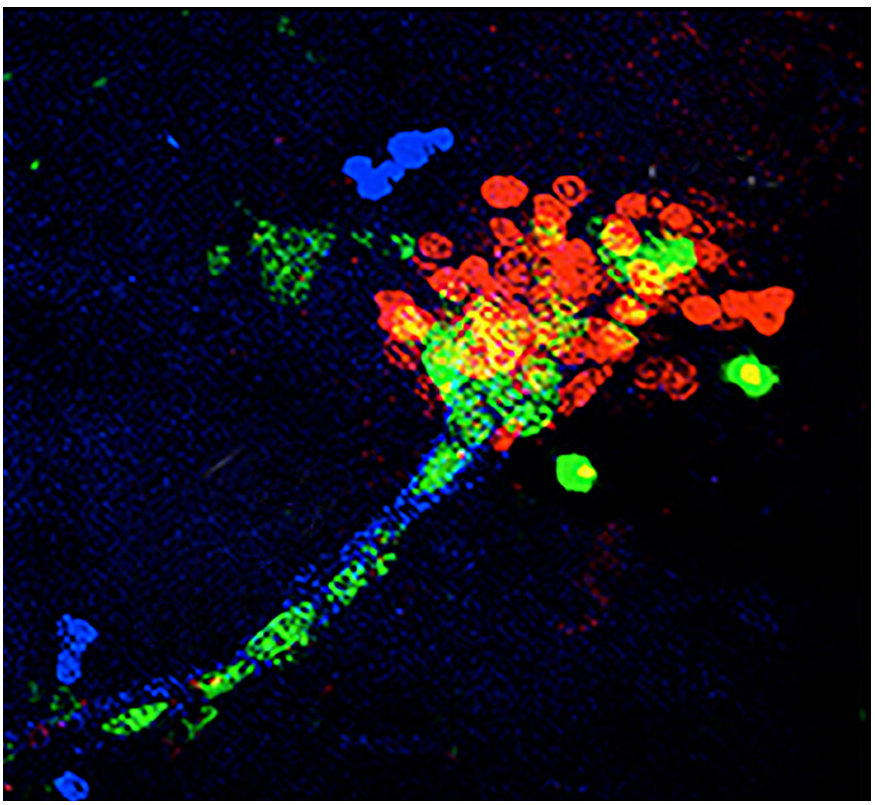

Neural precursor cells in the Lateral Proliferation Zone (LPZ) of the crayfish brain - *Procambarus clarkii* (from Beltz and Benton 2017, *Front Neurosci*).

Beltz BS and Benton JL (2017) From Blood to Brain: Adult-Born Neurons in the Crayfish Brain Are the Progeny of Cells Generated by the Immune System. *Front. Neurosci*. 11:662. doi: 10.3389/fnins.2017.00662

Cover image: dreamerb/Shutterstock.com

Researchers working on adult neurogenesis have focused largely on inbred laboratory rodents. While this provides a strong advantage of restricting genetic variation in the group, it also narrows our perspective on adult neurogenesis as a biological phenomenon. Many unsolved issues and open questions cannot be resolved without the contribution of comparative studies spanning through widely different species: how did adult neurogenesis evolve, what is the link between adult neurogenesis and brain complexity, how do adult neurogenesis and animal behavior influence

each other, how does adult neurogenesis contribute to brain plasticity, cognition and, possibly, repair, and how do experimental conditions affect adult neurogenesis. The main message from the comparative approach to adult neurogenesis is that the relative exclusive focus on laboratory rodents can result in a bias on how we think about this biological process.

Citation: Bonfanti, L., Amrein, I., eds. (2019). Adult Neurogenesis: Beyond Rats and Mice. Lausanne: Frontiers Media. doi: 10.3389/978-2-88945-761-8

Table of Contents

frontiers in Neuroscience

EDITORIAL
published: 04 December 2018
doi: 10.3389/fnins.2018.00904

Editorial: Adult Neurogenesis: Beyond Rats and Mice

Luca Bonfanti[1,2]* *and Irmgard Amrein*[3,4]*

[1] Neuroscience Institute Cavalieri Ottolenghi, Orbassano, Italy, [2] Department of Veterinary Sciences, University of Turin, Torino, Italy, [3] Division of Functional Neuroanatomy, Institute of Anatomy, University of Zurich, Zurich, Switzerland, [4] Department of Health Sciences and Technology, ETH Zurich, Zurich, Switzerland

Keywords: comparative studies, evolution, brain plasticity, adult neurogenesis, brain repair, translation

Editorial on the Research Topic

Adult Neurogenesis: Beyond Rats and Mice

Most biological tissues routinely replace old cells with new ones. Unlike other tissues, the nervous system–being the most complex biological device found in nature–uniquely maintains most of its neurons throughout life and replaces relatively few. It preserves hotspots where it generates new neurons from resident stem cells during adulthood in a process known as adult neurogenesis, which varies among different species in its features, dynamics, and regulation. In spite of its widespread prevalence in the animal kingdom, the preponderance of studies conducted on a few laboratory rodent species such as rats and mice limits our understanding of the evolution, regulation, and function of adult neurogenesis. The anatomy, complexity and functions of the brain vary greatly in the animal kingdom: striking differences exist from simple bilaterians to humans, and, to a lesser extent, also among mammals. Therefore, both comparative and focused studies on different species will shed more light on the origin, development, and purpose of adult neurogenesis.

Adult neurogenesis was discovered and described by Joseph Altman and Das in rats (Altman and Das, 1965) and has been investigated in many species such as the zebrafish, frog, songbird, mole, mole-rat, vole, bat, fox, dog, dolphin, elephant, shrew, rabbit, monkey, and human. With the development of genetic manipulation techniques, researchers have focused largely on inbred laboratory rodents. While this provides a strong advantage of restricting genetic variation in the group, it also narrows our perspective on adult neurogenesis as a biological phenomenon (Bolker, 2017). Moreover, the rapid development of genetic tools has made *Mus musculus* the species of choice in studying adult neurogenesis. Yet, many unsolved issues and open questions cannot be resolved without the contribution of comparative studies spanning through widely different species. Such issues involve: how did adult neurogenesis evolve, whether our survival depend on adult neurogenesis, what is the link between adult neurogenesis and brain complexity, how do adult neurogenesis and animal behavior influence each other, how does adult neurogenesis contribute to brain plasticity, cognition and, possibly, repair, and how do experimental conditions affect adult neurogenesis.

Studying unconventional species will give us insights into the evolution and function of the brain, strengthening our understanding of the cellular basis of cognition and behavior, thus helping adult neurogenesis to find its place in the puzzle. With this Research Topic we, along with contributors from different areas, tried to answer the open questions and to encourage engaging discussions on the comparative and evolutionary aspects of adult neurogenesis. The diversity in adult neurogenesis indeed spans the *de-novo* formation of the entire adult brain in planaria (Brown and Pearson), neurogenesis in diverse brain areas in fish (Olivera-Pasilio et al.), reptiles (LaDage et al.; Lutterschmidt et al.), and birds (Barkan et al.; Kosubek-Langer et al.) to animals with restricted neurogenic niches such as invertebrates (Beltz and Benton; Simões and Rhiner) and mammals (Taylor et al.; Lévy et al.; Oosthuizen; Wiget et al.). The striking differences do not only concern

OPEN ACCESS

Edited by:
Magdalena Götz,
German Research Center for Environmental Health (HZ), Germany

Reviewed by:
Armen Saghatelyan,
Laval University, Canada
Kazunobu Sawamoto,
Nagoya City University, Japan

***Correspondence:**
Luca Bonfanti
luca.bonfanti@unito.it
Irmgard Amrein
irmgard.amrein@hest.ethz.ch

Specialty section:
This article was submitted to Neurogenesis, a section of the journal Frontiers in Neuroscience

Received: *19 September 2018*
Accepted: *19 November 2018*
Published: *04 December 2018*

Citation:
Bonfanti L and Amrein I (2018) Editorial: Adult Neurogenesis: Beyond Rats and Mice. Front. Neurosci. 12:904. doi: 10.3389/fnins.2018.00904

the sites of occurrence and relative amounts (Brown and Pearson; Lévy et al.; Olivera-Pasilio et al.; Wiget et al.) but also in mechanistic aspects of stem cell biology. Intriguing examples are given by the adult-born neurons generated from the immune system and then traveling to the neurogenic niche via the circulatory system in the crayfish brain (Beltz and Benton; Simões and Rhiner), or the heterogeneity of neoblasts, putative stem cells, in flatworms enabling the regeneration of the entire brain (Brown and Pearson). Yet, the main message from the comparative approach to adult neurogenesis is that the relative exclusive focus on laboratory rodents can result in a bias on how we think about this biological process. For instance, promising neuroprotective treatments developed in rodent models can fail in preclinical trials, and animal models with gyrencephalic brains might be necessary to study the behavior of neuroblasts in large white matter tracts (Taylor et al.). The bias is well-illustrated by the article of Faykoo-Martinez et al.: "species-specific adaptations in brain and behavior are paramount to survival and reproduction in diverse ecological niches and it is naive to think adult neurogenesis escaped these evolutionary pressures. A neuroethological approach to the study of adult neurogenesis is essential for a comprehensive understanding of the phenomenon." Indeed, interactions of adult neurogenesis with neuroethological traits such as migration and mating behavior in snakes (Lutterschmidt et al.), territoriality in lizards (LaDage et al.), sociality and social interactions in mole-rats, birds, and sheep (Barkan et al.; Lévy et al.; Oosthuizen), or migratory lifestyle in birds (Barkan et al.) are presented here. The complexity of interactions is, to date, more an obstruction than a help in terms of publishability, but as Faykoo-Martinez et al. put it "most of us are guilty of making strong assertions about our data in order to have impact yet this ultimately creates bias in how work is performed, interpreted, and applied." Such concerns are confirmed by the finding of remarkable reduction of adult neurogenesis in some large-brained, long-living mammals, including humans and dolphins (Sanai et al., 2011; Sorrells et al., 2018), as reviewed and discussed in the article by Parolisi et al. More and more comparative data strongly support the view that adult neurogenesis is maintained in evolution only depending on strict relationships with its functional need(s). E.g., olfactory systems, mostly linked to paleocortical-hippocampal structures, were important in early mammalian evolution working as a reference system for spatial navigation for the location of food sources and mates, then replaced/integrated by the expansion of the isocortex as a "multimodal interface" for behavioral navigation based on vision and audition (Aboitiz and Montiel, 2015; see article by Parolisi et al.). The complex evolutionary aspects of adult neurogenesis role(s) and age-related reduction in mammals are addressed in the contribution by Hans-Peter Lipp. The main message of this opinion article is that no simple explanations can be called upon on such topic, a heavily actual conclusion even 30 years after neural stem cell discovery.

Animal models other than laboratory mice are by no means "out-of-reach" for advanced techniques, and the following examples could encourage and facilitate creative thinking in terms of research questions and how to approach them. Lindsey et al. present a thorough step-by-step protocol for visualizing cell proliferation in the *whole* zebrafish brain in 3 dimension. LaDage et al. used hormonal implants in lizards to study the interaction of testosterone and neurogenesis on territorial behavior. In fish and birds, Neurobiotin or lentivirus can be used to trace and characterize newly born neurons (Kosubek-Langer et al.; Olivera-Pasilio et al.), and Brown and Pearson summarize the single-cell genomic data collected in planaria. Ideally, studies in laboratory rodents and non-conventional animal models can support and foster each other. For example, increased neurogenesis in laboratory mice confers stress resilience mediated by the temporal hippocampus (Anacker et al., 2018). Strikingly, wild rodents, naturally exposed to high stress levels, show more neurogenesis in the temporal hippocampus than the commonly used laboratory mouse C57BL/6 (Wiget et al.). Similarly, Reyes-Aguirre and Lamas identified the mechanism why the mouse retina cannot regenerate after damage, much in contrast to what has been reported in fish (Raymond et al., 2006). Finally, by using meta-analyses and a model to compare the neurodevelopmental sequences of different mammals, Charvet and Finlay try to put in a common time frame the envelopes of hippocampal neurogenesis, in order to interpret them in species with highly different lifespan.

In conclusion, with this Research Topic we strongly assert that adult neurogenesis research cannot rely exclusively on laboratory rodents, as each animal model can only cover certain aspects of the various flavors in which neuronal stem cells and their progeny in the postnatal brain can behave. The papers presented here emphasize the value of "… taking a step back and actually placing our results in a much larger, non-biomedical context, …[helping]… to reduce dogmatic thinking and create a framework for discovery" (Faykoo-Martinez et al.). After all, the failure of many clinical trials based on pre-clinical studies carried out on mice (Lindvall and Kokaia, 2010; Donegà et al., 2013), do confirm the need for investments in comparative medicine (specifically on brain structural plasticity, see La Rosa and Bonfanti, 2018). A comparative view can indeed foster a more careful interpretation of the final impact of the biological process of neurogenesis in brain functioning and animal behavior.

AUTHOR CONTRIBUTIONS

All authors listed have made a substantial, direct and intellectual contribution to the work, and approved it for publication.

ACKNOWLEDGMENTS

The Topic Editors would like to acknowledge the contribution of Nambirajan Govindarajan to the success of this Research Topic. Thanks to him, this important topic was brought to life, allowing the scientific community to contribute to an open debate on adult neurogenesis.

REFERENCES

Aboitiz, F., and Montiel, J. F (2015). Olfaction, navigation, and the origin of isocortex. *Front. Neurosci.* 9:402. doi: 10.3389/fnins.2015.00402

Altman, J., and Das, G. D (1965). Post-natal origin of microneurones in the rat brain. *Nature* 207, 953–956. doi: 10.1038/207953a0

Anacker, C., Luna, V. M., Stevens, G. S., Millette, A., Shores, R., Jimenez, J. C., et al. (2018). Hippocampal neurogenesis confers stress resilience by inhibiting the ventral dentate gyrus. *Nature* 559, 98–102. doi: 10.1038/s41586-018-0262-4

Bolker, J. A (2017). Animal models in translational research: rosetta stone or stumbling block? *Bioessays* 39, 1–8. doi: 10.1002/bies.201700089

Donegà, M., Giusto, E., Cossetti, C., and Pluchino, S (2013). "Systemic neural stem cell-based therapeutic interventions for inflammatory CNS disorders," in Neural Stem Cells: New Perspectives, ed. L. Bonfanti (Rijeka: INTECH), 287–347.

La Rosa, C., and Bonfanti, L (2018). Brain plasticity in mammals: An example for the role of comparative medicine in the Neurosciences. *Front. Vet. Sci.* 5:274. doi: 10.3389/fvets.2018.00274

Lindvall, O., and Kokaia, Z (2010). Stem cells in human neurodegenerative disorders-time for clinical translation? *J. Clin. Invest.* 120, 29–40. doi: 10.1172/JCI40543

Raymond, P. A., Barthel, L. K., Bernardos, R. L., and Perkowski, J (2006). Molecular characterization of retinal stem cells and their niches in adult zebrafish. *BMC Dev. Biol.* 6:36. doi: 10.1186/1471-213X-6-36

Sanai, N., Nguyen, T., Ihrie, R. A., Mirzadeh, Z., Tsai, H.-H., Wong, M., et al. (2011). Corridors of migrating neurons in the human brain and their decline during infancy. *Nature* 478, 382–386. doi: 10.1038/nature10487

Sorrells, S. F, Paredes, M. F., Cebrian-Silla, A., Sandoval, K., Qi, D., Kelley, K. W., et al. (2018). Human hippocampal neurogenesis drops sharply in children to undetectable levels in adults. *Nature* 555, 377–381. doi: 10.1038/nature 25975

Conflict of Interest Statement: The authors declare that the research was conducted in the absence of any commercial or financial relationships that could be construed as a potential conflict of interest.

frontiers in Neuroscience

PERSPECTIVE
published: 23 May 2017
doi: 10.3389/fnins.2017.00289

A Brain Unfixed: Unlimited Neurogenesis and Regeneration of the Adult Planarian Nervous System

David D. R. Brown[1,2] *and Bret J. Pearson*[1,2,3]*

[1] Program in Developmental and Stem Cell Biology, The Hospital for Sick Children, Toronto, ON, Canada, [2] Department of Molecular Genetics, University of Toronto, Toronto, ON, Canada, [3] Ontario Institute for Cancer Research, Toronto, ON, Canada

Powerful genetic tools in classical laboratory models have been fundamental to our understanding of how stem cells give rise to complex neural tissues during embryonic development. In contrast, adult neurogenesis in our model systems, if present, is typically constrained to one or a few zones of the adult brain to produce a limited subset of neurons leading to the dogma that the brain is primarily fixed post-development. The freshwater planarian (flatworm) is an invertebrate model system that challenges this dogma. The planarian possesses a brain containing several thousand neurons with very high rates of cell turnover (homeostasis), which can also be fully regenerated *de novo* from injury in just 7 days. Both homeostasis and regeneration depend on the activity of a large population of adult stem cells, called neoblasts, throughout the planarian body. Thus, much effort has been put forth to understand how the flatworm can continually give rise to the diversity of cell types found in the adult brain. Here we focus on work using single-cell genomics and functional analyses to unravel the cellular hierarchies from stem cell to neuron. In addition, we will review what is known about how planarians utilize developmental signaling to maintain proper tissue patterning, homeostasis, and cell-type diversity in their brains. Together, planarians are a powerful emerging model system to study the dynamics of adult neurogenesis and regeneration.

Keywords: regeneration, planarian, adult neurogenesis, brain plasticity, stem cell heterogeneity

OPEN ACCESS

Edited by:
Luca Bonfanti,
University of Turin, Italy

Reviewed by:
Alice Powers,
Stony Brook University, United States
Annalisa Buffo,
University of Turin, Italy

***Correspondence:**
Bret J. Pearson
bret.pearson@sickkids.ca

Specialty section:
This article was submitted to Neurogenesis, a section of the journal Frontiers in Neuroscience

Received: *31 March 2017*
Accepted: *08 May 2017*
Published: *23 May 2017*

Citation:
Brown DDR and Pearson BJ (2017) A Brain Unfixed: Unlimited Neurogenesis and Regeneration of the Adult Planarian Nervous System. Front. Neurosci. 11:289. doi: 10.3389/fnins.2017.00289

INTRODUCTION

The adult brain has long been thought to be a fixed structure due to its immense complexity as is illustrated succinctly in the following quote from prominent nineteenth century neuroscientist and Nobel laureate Santiago Ramón y Cajal:

> *"Once the development was ended, the founts of growth and regeneration of the axons and dendrites dried up irrevocably. In the adult centers, the nerve paths are something fixed, ended, and immutable. Everything may die, nothing may be regenerated. It is for the science of the future to change, if possible, this harsh decree."*

Although, genetic laboratory model organisms have taught us volumes about neural development, they do not strongly challenge the view of Ramón y Cajal as adult organisms. For example, the roundworm *C. elegans* has no known adult neurogenesis. Adult *Drosophila* have little

to no cell division in the adult brain, although this is (amazingly) still controversial (Ito and Hotta, 1992; von Trotha et al., 2009; Fernández-Hernández et al., 2013). Finally, mouse and human have limited neurogenesis in the sub-ventricular zone (SVZ) of the cortex and in the dentate gyrus (DG) (Altman and Das, 1965, 1967; Doetsch et al., 1999), resulting in a neuronal turnover of ∼1–2% per year in humans (Spalding et al., 2013). Correlative to the paucity of adult neurogenesis, these model systems also have extremely limited neural-regenerative capacity (Cebrià, 2007).

As new experimental model systems can be functionally interrogated with CRISPR/Cas9 technology, as well as molecular and genomic techniques, the dogma of Ramón y Cajal is now being challenged. In fact, high levels of adult neurogenesis and neural regeneration have been found in cnidarians, invertebrates, and vertebrates alike, suggesting that the ancestral state was that of significant neural plasticity (Holstein et al., 2003; Reddien and Sánchez Alvarado, 2004; Tanaka and Reddien, 2011; Kizil et al., 2012; Ross et al., 2017). Highly-regenerative organisms that can replace much of their nervous system offer a unique opportunity to study the cellular and molecular underpinnings of adult neurogenesis in an unrestricted context. For example, zebrafish are vertebrates that demonstrate adult neurogenesis along the entire rostral-caudal axis of the brain (Grandel et al., 2006) and have some ability to regenerate damaged regions of their central nervous system (CNS; brain and spinal cord; Kroehne et al., 2011). Although, humans have limited capacity to generate adult neurons, it has been demonstrated that transplanted neurons are capable of integrating into the brain (Falkner et al., 2016). Despite this finding, proper and full functional integration of neurons into the adult brain has been problematic and requires refinement before therapies can be effective (Brundin et al., 2010). It is currently thought that if we can understand the biology of adult neurogenesis and neural regeneration in other model systems, we will be able to drive a patient's own cells to become hyper-regeneration-competent and differentiate into neurons that can integrate into existing neural circuitry (Kim et al., 2013). Thus, inducing adult neurogenesis and cell integration in humans may hold the potential to regenerate and heal a brain after disease or injury.

Perhaps the most powerful CNS-regenerator in the laboratory is the invertebrate freshwater planarian, *Schmidtea mediterranea*, which is a flatworm of the phylum Platyhelminthes and is capable of limitless regeneration (Tan et al., 2012). The asexual laboratory strain is an extremely long-lived, constitutive adult animal with a brain possessing on the order of 1,000–10,000 cells, which can completely regenerate its whole brain and functionally reintegrate the new tissue in ∼7 days without scaring (Cebrià, 2007). In addition, the planarian brain can be rescaled in size and proportion as the animal grows or shrinks, which can be a ∼10-fold change in length and ∼100-fold change in area (Newmark and Sánchez Alvarado, 2002; Hill and Petersen, 2015). Finally, the planarian brain undergoes constant neuronal turnover of ∼25% per week (**Figure 1**; Zhu et al., 2015; Currie et al., 2016). Altogether, the planarian brain may represent the most dynamic adult CNS found in animals.

Planarians owe their regenerative ability and neuronal turnover (homeostasis) to a large population of somatic stem cells, called "neoblasts," which populate the mesenchyme of the worm and account for ∼20% of all cells in the animal (Baguñà et al., 1989; Sánchez Alvarado and Kang, 2005; Baguñà, 2012; Zhu and Pearson, 2016; **Figure 1**). As far as has been examined, every tissue in the adult animal undergoes some level of turnover without injury, and every tissue can be regenerated. However, it should be noted that the regulators of cellular lifespan and whether dying cells secrete signals, are completely unknown. Thus, the field has recently focused on the tissue-specific nature of the stem cells and whether or not heterogeneity exists (Reddien, 2013). To this end, several key questions are raised when considering a long-lived flatworm's potential for continuous adult neurogenesis: (1) How does the planarian dedicate a sub-fraction of its large stem cell population to neural homeostasis in order to generate the diversity of neuronal subtypes found in the adult flatworm? and (2) How does the planarian dynamically modulate neurogenesis to entirely regenerate or maintain scale and proportion of the adult brain?

Here we will highlight candidate-based functional and single-cell sequencing studies that have focused on characterizing the heterogeneity that exists within the planarian stem cell pool to drive the continual generation of a plethora of neuronal subtypes. Additionally, we will review what is known about how planarians utilize conserved developmental signaling pathways to define neurogenic zones that dynamically couple neoblasts, capable of continuous and unlimited adult neurogenesis, with mature and fully patterned neurons of the adult brain.

FROM NEOBLAST TO NEURON: STEM CELL HETEROGENEITY UNDERPINS ADULT NEUROGENESIS

Although, planarians possess a massive population of neoblasts, it remains unclear how flatworms dedicate a fraction of these neoblasts to adult neurogenesis. The vast majority of these cells express *piwi-1*, a member of the PIWI/Argonaute family of proteins (Reddien et al., 2005; van Wolfswinkel, 2014), and are constantly dividing (Newmark and Sánchez Alvarado, 2000). Recent studies have begun to tease apart the heterogeneity that exists within this once seemingly homogenous population of adult stem cells. Wagner and colleagues demonstrated, through single-cell transplants into lethally irradiated hosts, that there exists a sub-population of pluripotent neoblasts (cNeoblasts) capable of generating every tissue in the adult worm (Wagner et al., 2011). The discovery of the cNeoblast suggested that a cellular hierarchy existed within the neoblasts and that stem cell heterogeneity was likely underlying the diverse array of cellular lineages present in the flatworm. Further exploration of neoblast heterogeneity led to the classification of the (zeta)ζNeoblasts, which appear to be restricted to generate epidermal lineages. Additional analysis demonstrated the presence of non-ζNeoblasts, known as (sigma)σNeoblasts, which may contain the cNeoblast population due to the ability of the σNeoblasts to regenerate the ζNeoblast population (van Wolfswinkel et al., 2014). Lastly, (gamma)γNeoblasts were

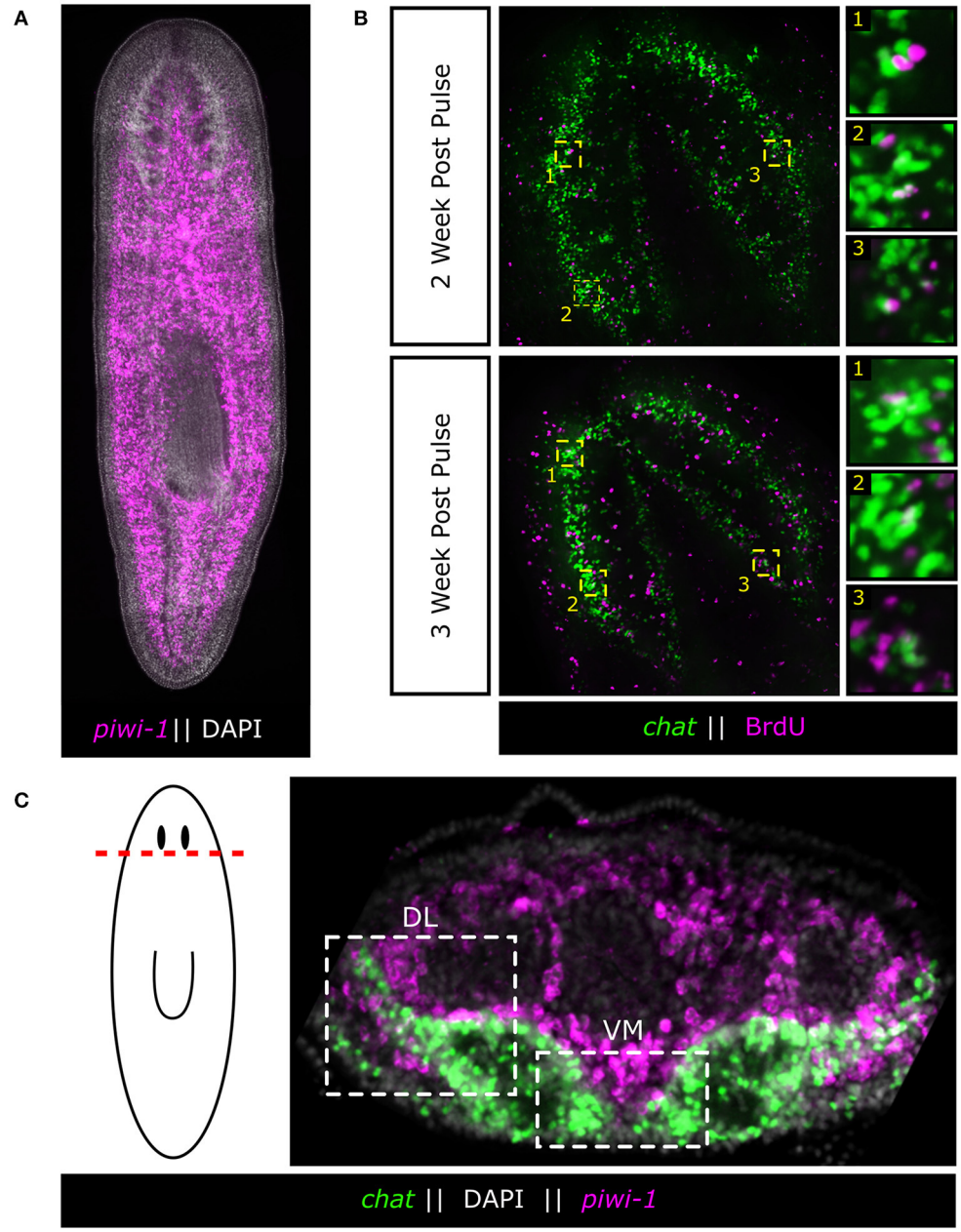

FIGURE 1 | Adult neurons are born continuously in the adult flatworm from a large population of adult stem cells. (A) Fluorescent *in situ* hybridization (FISH) of planarian adult stem cells (neoblasts) as marked by *piwi-1*. Neoblasts span the entire length of the body except for the region anterior to the eyes. **(B)** BrdU pulse chase experiments demonstrating the continuous nature of adult neurogenesis in the planarian. Worms were fed BrdU food (25 mg/mL) 2 days in a row and chased for 2 and 3 weeks. BrdU was detected and combined with FISH of the brain marker *chat* to mark acetylcholine neurons. Panels are representative single slice confocal planes. **(C)** Adult stem cells surround the Ventral-Medial (VM) and Dorsal-Lateral (DL) zones of the brain, two putative neurogenic zones. These stem cells are the likely source of new neurons during adult neurogenesis.

identified as a molecularly-distinct subpopulation of neoblasts, which express gut markers (van Wolfswinkel et al., 2014).

Despite the heterogeneity that has been observed in the neoblast population, the presence of a *bona fide* neural stem cell has not yet been demonstrated. A study employing a single-cell genomics approach investigating neoblast heterogeneity in the head of the animal identified the (nu)νNeoblasts, a class of neoblast that exhibits neural gene expression (Molinaro and Pearson, 2016). Through the use of an *in silico* lineage tracing technique, known as waterfall (Shin et al., 2015), gene markers enriched in the νNeoblasts were identified and detected in a subpopulation of dividing stem cells adjacent to the brain

(Molinaro and Pearson, 2016). Although, functional studies remain to be done to cement the νNeoblast as a true neural stem cell, the presence of a dividing neoblast population with neural character that can be found directly adjacent to the brain, a putative neurogenic zone, is suggestive that a *bona fide* neural stem cell does exist in the planarian. It will be interesting to see whether there are multiple populations of neuronal stem cells, or if the νNeoblast is responsible for generating the diversity of neural subtypes found in the planarian brain. Regardless, νNeoblasts may represent a mechanism by which planarians dedicate a sub-fraction of their neoblasts toward adult neurogenesis.

NEUROGENIC ZONES: HOW IS ADULT NEUROGENESIS DYNAMICALLY MODULATED?

Upon amputation the planarian is able to rapidly re-establish its head and generate a fully functional brain without any pieces of the original tissue. To remake its brain the planarian must (1) form a blastema, (2) define a neurogenic zone and generate the brain primordium, (3) properly pattern newly generated brain tissue, (4) form the proper neural connections, and (5) functionally integrate the new tissue into existing neural tissue (Agata and Umesono, 2008). Exactly what causes the brain primordium to form is currently unknown, but several conserved developmental signaling pathways act to create a signaling landscape in the head that is permissive for neurogenesis. Briefly, the planarian must first re-establish its anterior-posterior (AP) axis which is accomplished via canonical WNT (Gurley et al., 2008) and Hedgehog (Hh) (Rink et al., 2009) signaling. After the anterior pole is established, anterior WNT inhibition (Petersen and Reddien, 2011), FGF signaling (Cebrià et al., 2002) and BMP signaling (Molina et al., 2007) create an environment that is permissive for the formation of the brain primordium in the ventral anterior of the head (**Figure 1**). This permissive signaling landscape must be maintained in the intact flatworm because disruption of any of these signaling pathways can lead to diminished neurogenesis, such as in *apc*(RNAi), or ectopic neurogenesis, as is observed in β–*catenin*(RNAi), *ndk*(RNAi), and *bmp*(RNAi) (Cebrià et al., 2002; Molina et al., 2007; Gurley et al., 2008). It is unclear exactly how ectopic neurogenesis is triggered, but it is clear that when the planarian neoblasts are not properly controlled, neural tissue can form in improper locations. The link between the signaling landscape and brain neurogenesis suggests either (1) that the neoblast population is poised for neurogenesis in all regions of the animal but must be prevented from acquiring a neural fate, or (2) that a subset of neoblasts can be biased toward neural fates through positional signaling. Further defining neurogenic zones and characterizing how they form *de novo* will be vital to our understanding of how the flatworm integrates its unlimited capacity for adult neurogenesis with the ability to dynamically scale, pattern and regenerate a complex neural tissue from a pool of adult stem cells.

The adult planarian brain is a highly plastic and dynamic structure. Not only is the entire brain turned over with new neurons arising from the neoblast compartment continuously, but the brain is constantly being scaled and patterned during periods of growth and degrowth (Baguñà, 2012). This raises the question of how planarians are able to dynamically coordinate the number of new neurons that are born vs. those that must be turned over and removed. Several WNT molecules are involved in scaling the brain relative to body size. *wnt5* has been shown to pattern the mediolateral axis through repression of medial fates and acts to restrict lateral brain growth while *wnt11-6* acts to restrict brain length along the AP axis (Gurley et al., 2010; Hill and Petersen, 2015). *wnt11-6*, which is expressed in posterior brain neurons, forms a spatial feedback loop through the induction of its inhibitor, *notum*, in anterior brain commissural neurons allowing the animal to dynamically regulate the length of its brain along the AP axis (Hill and Petersen, 2015). The feedback loop formed between *wnt11-6* and *notum* affects brain size through a neoblast-dependent mechanism and not through cell death (Hill and Petersen, 2015). *wnt11-6(RNAi)* animals possess a posteriorly-expanded brain and a concomitant increase in the number of brain progenitor cells during tissue remodeling while *notum(RNAi)* animals exhibit the opposite effect (Hill and Petersen, 2015), indicating that this spatial feedback loop somehow influences the generation of new neurons from the neoblast population to control brain length.

If neurons are expressing signaling molecules to dynamically shape the brain through communication with stem cells, then stem cells must express the signal-transduction machinery in order to respond. A recent study on Hedgehog (Hh) signaling demonstrated its role in directing adult neurogenesis through signaling from neurons to the stem cell compartment (Currie et al., 2016). The authors found that the Hh ligand was primarily expressed by cholinergic neurons in the ventral-medial (VM) region of the brain. Interestingly, decreased Hh signaling results in animals that exhibit fewer neural progenitor cells and fewer newly born VM acetylcholine neurons, whereas increased Hh signaling increases the number of several types of neural progenitors (Currie et al., 2016). Currie and colleagues then further employed single-cell RNA-sequencing data (Molinaro and Pearson, 2016) specifically from head stem cells to demonstrate that many of these stem cells expressed both WNT and Hh signal transduction machinery suggesting they could be receptive to signaling cues from the brain (Currie et al., 2016). Both WNT and Hh signaling appear capable of influencing neoblasts close to the brain. It is currently unclear which neoblasts are being influenced, but with Hh expression being confined to the VM nervous system it would stand to reason that neoblasts which receive this message are in the pocket of cells between the brain lobes and nerve cords (**Figure 2**). It remains unknown whether stem cells that contribute to the brain do so in a regionally biased manner, or if any neoblast flanking the brain is free to contribute new neurons when signaled to do so. Hedgehog signaling affects VM neuronal fates, but what signaling directs dorsal-lateral (DL) fates is unclear. There is a large range of neuronal subtypes (*cintillo*+, *gpas*+, *chat*+, *gad*+, and many others; Oviedo et al., 2003; Nishimura et al., 2008, 2010; Iglesias et al., 2011) located in the DL regions of the brain and determining what signals direct DL neoblasts (**Figure 1C**) to

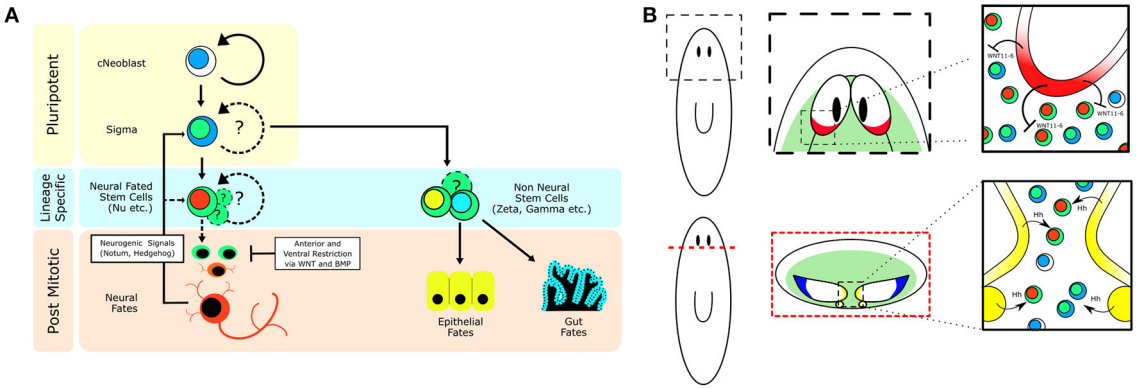

FIGURE 2 | Stem cell heterogeneity and conserved developmental signaling define planarian neurogenic zones. (A) Cartoon showing how a population of pluripotent adult stem cells (cNeoblasts) are capable of generating stem cell heterogeneity and a multitude of differentiated cell types in the adult flatworm. Emphasis on how environmental signaling restricts cellular fate. **(B)** Depiction of planarian neurogenic zones near the brain, which involve signaling between mature brain neurons and nearby stem cells to coordinate adult neurogenesis and brain patterning. (Top—Top down view of the planarian brain, anterior is up; Bottom—Cross section of the planarian brain, dorsal is up.) Green zones illustrate where adult stem cells can be found. The red brain region is a source of WNT11-6, which restricts brain length through signaling to the stem cells. The yellow region denotes the ventral-medial brain and nerve cords which express Hh and signal to nearby stem cells to promote adult neurogenesis. The blue region defines a unique dorsal-lateral zone of the brain that possesses several cell types, of which the progenitors are currently unknown. Black ovals denote the planarian anterior photoreceptors (eyes).

integrate into this region and acquire these fates will be important in understanding the full link between mature brain neurons and nearby stem cells. From the single-stem cell RNAseq data, the complex "code" of over 10 WNT receptors (Gurley et al., 2008), the frizzled genes, are very heterogeneously expressed, suggesting more heterogeneous responses to WNT signals than with the Hh pathway (Currie et al., 2016). In the future, it will be interesting to tease apart how local WNT signals direct stem cells toward specific cell fates, perhaps through the action of various TCF/LEF transcription factors.

CONCLUSIONS

The planarian is unique in its ability to maintain and regenerate its full adult brain continuously and is a powerful model with which to study adult neurogenesis in an *in vivo* context. In order to maintain continuous and unlimited adult neurogenesis the planarian employs a robust and self-organizing landscape of developmental signaling pathways to link mature neuronal tissue with nearby populations of adult stem cells, ensuring the controlled generation and integration of new neurons that can scale in real time. Coupled with the planarian's ability to instruct the generation of a brain primordium *de novo* after complete tissue loss, the flatworm is able to both regenerate and maintain its entire brain without limits. Underlying this dynamic link between mature neurons and stem cells, the neoblasts are capable of generating every neuronal subtype found in the adult flatworm. Additional studies into the full heterogeneity of the adult stem cells and the lineages between stem cell and neuron are still needed to fully understand how planarians are able to direct and control unlimited adult neurogenesis without negative consequences to the organism. Although, much remains to be discovered, the planarian turns the idea of a fixed brain on its head and raises the larger question of whether this total brain plasticity is possible in other organisms such as humans.

AUTHOR CONTRIBUTIONS

BP and DB wrote and edited the manuscript.

FUNDING

DB was funded by Natural Sciences and Engineering Research Council award # RGPIN-2016-06354. BP was funded by Ontario Institute for Cancer Research award #IA-026.

ACKNOWLEDGMENTS

We would like to thank Shu Jun Zhu and Dr. Ko Currie for providing images and quantifications of BrdU pulse-chases.

REFERENCES

Agata, K., and Umesono, Y. (2008). Brain regeneration from pluripotent stem cells in planarian. *Philos. Trans. R. Soc. Lond. B Biol. Sci.* 363, 2071–2078. doi: 10.1098/rstb.2008.2260

Altman, J., and Das, G. D. (1965). Autoradiographic and histological evidence of postnatal hippocampal neurogenesis in rats. *J. Comp. Neurol.* 124, 319–335. doi: 10.1002/cne.901240303

Altman, J., and Das, G. D. (1967). Postnatal neurogenesis in the guinea-pig. *Nature* 214, 1098–1101. doi: 10.1038/2141098a0

Baguñà, J. (2012). The planarian neoblast: the rambling history of its origin and some current black boxes. *Int. J. Dev. Biol.* 56, 19–37. doi: 10.1387/ijdb.113463jb

Baguñà, J., Saló, E., and Romero, R. (1989). Effects of activators and antagonists of the neuropeptides substance P and substance K on cell proliferation in planarians. *Int. J. Dev. Biol.* 33, 261–266.

Brundin, P., Barker, R. A., and Parmar, M. (2010). Neural grafting in Parkinson's disease Problems and possibilities. *Prog. Brain Res.* 184, 265–294. doi: 10.1016/S0079-6123(10)84014-2

Cebrià, F. (2007). Regenerating the central nervous system: how easy for planarians! *Dev. Genes Evol.* 217, 733–748. doi: 10.1007/s00427-007-0188-6

Cebrià, F., Kobayashi, C., Umesono, Y., Nakazawa, M., Mineta, K., Ikeo, K., et al. (2002). FGFR-related gene nou-darake restricts brain tissues to the head region of planarians. *Nature* 419, 620–624. doi: 10.1038/nature01042

Currie, K. W., Molinaro, A. M., and Pearson, B. J. (2016). Neuronal sources of hedgehog modulate neurogenesis in the adult planarian brain. *Elife* 5:e19735. doi: 10.7554/eLife.19735

Doetsch, F., Caillé, I., Lim, D. A., García-Verdugo, J. M., and Alvarez-Buylla, A. (1999). Subventricular zone astrocytes are neural stem cells in the adult mammalian brain. *Cell* 97, 703–716. doi: 10.1016/S0092-8674(00)80783-7

Falkner, S., Grade, S., Dimou, L., Conzelmann, K. K., Bonhoeffer, T., Götz, M., et al. (2016). Transplanted embryonic neurons integrate into adult neocortical circuits. *Nature* 539, 248–253. doi: 10.1038/nature20113

Fernández-Hernández, I., Rhiner, C., and Moreno, E. (2013). Adult neurogenesis in Drosophila. *Cell Rep.* 3, 1857–1865. doi: 10.1016/j.celrep.2013.05.034

Grandel, H., Kaslin, J., Ganz, J., Wenzel, I., and Brand, M. (2006). Neural stem cells and neurogenesis in the adult zebrafish brain: origin, proliferation dynamics, migration and cell fate. *Dev. Biol.* 295, 263–277. doi: 10.1016/j.ydbio.2006.03.040

Gurley, K. A., Elliott, S. A., Simakov, O., Schmidt, H. A., Holstein, T. W., and Sánchez Alvarado, A. (2010). Expression of secreted Wnt pathway components reveals unexpected complexity of the planarian amputation response. *Dev. Biol.* 347, 24–39. doi: 10.1016/j.ydbio.2010.08.007

Gurley, K. A., Rink, J. C., and Sánchez Alvarado, A. (2008). Beta-catenin defines head versus tail identity during planarian regeneration and homeostasis. *Science* 319, 323–327. doi: 10.1126/science.1150029

Hill, E. M., and Petersen, C. P. (2015). Wnt/Notum spatial feedback inhibition controls neoblast differentiation to regulate reversible growth of the planarian brain. *Development* 142, 4217–4229. doi: 10.1242/dev.123612

Holstein, T. W., Hobmayer, E., and Technau, U. (2003). Cnidarians: an evolutionarily conserved model system for regeneration? *Dev. Dyn.* 226, 257–267. doi: 10.1002/dvdy.10227

Iglesias, M., Almuedo-Castillo, M., Aboobaker, A. A., and Saló, E. (2011). Early planarian brain regeneration is independent of blastema polarity mediated by the Wnt/β-catenin pathway. *Dev. Biol.* 358, 68–78. doi: 10.1016/j.ydbio.2011.07.013

Ito, K., and Hotta, Y. (1992). Proliferation pattern of postembryonic neuroblasts in the brain of *Drosophila melanogaster*. *Dev. Biol.* 149, 134–148. doi: 10.1016/0012-1606(92)90270-Q

Kim, S. U., Lee, H. J., and Kim, Y. B. (2013). Neural stem cell-based treatment for neurodegenerative diseases. *Neuropathology* 33, 491–504. doi: 10.1111/neup.12020

Kizil, C., Kaslin, J., Kroehne, V., and Brand, M. (2012). Adult neurogenesis and brain regeneration in zebrafish. *Dev. Neurobiol.* 72, 429–461. doi: 10.1002/dneu.20918

Kroehne, V., Freudenreich, D., Hans, S., Kaslin, J., and Brand, M. (2011). Regeneration of the adult zebrafish brain from neurogenic radial glia-type progenitors. *Development* 138, 4831–4841. doi: 10.1242/dev.072587

Molina, M. D., Saló, E., and Cebrià, F. (2007). The BMP pathway is essential for re-specification and maintenance of the dorsoventral axis in regenerating and intact planarians. *Dev. Biol.* 311, 79–94. doi: 10.1016/j.ydbio.2007.08.019

Molinaro, A. M., and Pearson, B. J. (2016). *In silico* lineage tracing through single cell transcriptomics identifies a neural stem cell population in planarians. *Genome Biol.* 17, 87. doi: 10.1186/s13059-016-0937-9

Newmark, P. A., and Sánchez Alvarado, A. (2000). Bromodeoxyuridine specifically labels the regenerative stem cells of planarians. *Dev. Biol.* 220, 142–153. doi: 10.1006/dbio.2000.9645

Newmark, P. A., and Sánchez Alvarado, A. (2002). Not your father's planarian: a classic model enters the era of functional genomics. *Nat. Rev. Genet.* 3, 210–219. doi: 10.1038/nrg759

Nishimura, K., Kitamura, Y., Taniguchi, T., and Agata, K. (2010). Analysis of motor function modulated by cholinergic neurons in planarian Dugesia japonica. *Neuroscience* 168, 18–30. doi: 10.1016/j.neuroscience.2010.03.038

Nishimura, K., Kitamura, Y., Umesono, Y., Takeuchi, K., Takata, K., Taniguchi, T., et al. (2008). Identification of glutamic acid decarboxylase gene and distribution of GABAergic nervous system in the planarian Dugesia japonica. *Neuroscience* 153, 1103–1114. doi: 10.1016/j.neuroscience.2008.03.026

Oviedo, N. J. J., Newmark, P. A., and Sánchez Alvarado, A. (2003). Allometric scaling and proportion regulation in the freshwater planarian *Schmidtea mediterranea*. *Dev. Dyn.* 226, 326–333. doi: 10.1002/dvdy.10228

Petersen, C. P., and Reddien, P. W. (2011). Polarized notum activation at wounds inhibits Wnt function to promote planarian head regeneration. *Science* 332, 852–855. doi: 10.1126/science.1202143

Reddien, P. W. (2013). Specialized progenitors and regeneration. *Development* 140, 951–957. doi: 10.1242/dev.080499

Reddien, P. W., Oviedo, N. J. J., Jennings, J. R., Jenkin, J. C., and Sánchez Alvarado, A. (2005). SMEDWI-2 is a PIWI-like protein that regulates planarian stem cells. *Science* 310, 1327–1330. doi: 10.1126/science.1116110

Reddien, P. W., and Sánchez Alvarado, A. (2004). Fundamentals of planarian regeneration. *Annu. Rev. Cell Dev. Biol.* 20, 725–757. doi: 10.1146/annurev.cellbio.20.010403.095114

Rink, J. C., Gurley, K. A., Elliott, S. A., and Sánchez Alvarado, A. (2009). Planarian Hh signaling regulates regeneration polarity and links Hh pathway evolution to cilia. *Science* 326, 1406–1410. doi: 10.1126/science.1178712

Ross, K. G., Currie, K. W., Pearson, B. J., and Zayas, R. M. (2017). Nervous system development and regeneration in freshwater planarians. *Wiley Interdiscip. Rev. Dev. Biol.* 6. doi: 10.1002/wdev.266

Sánchez Alvarado, A., and Kang, H. (2005). Multicellularity, stem cells, and the neoblasts of the planarian *Schmidtea mediterranea*. *Exp. Cell Res.* 306, 299–308. doi: 10.1016/j.yexcr.2005.03.020

Shin, J., Berg, D. A., Zhu, Y., Shin, J. Y., Song, J., Bonaguidi, M. A., et al. (2015). Single-cell RNA-seq with waterfall reveals molecular cascades underlying adult neurogenesis. *Cell Stem Cell* 17, 360–372. doi: 10.1016/j.stem.2015.07.013

Spalding, K. L., Bergmann, O., Alkass, K., Bernard, S., Salehpour, M., Huttner, H. B., et al. (2013). Dynamics of hippocampal neurogenesis in adult humans. *Cell* 153, 1219–1227. doi: 10.1016/j.cell.2013.05.002

Tan, T. C., Rahman, R., Jaber-Hijazi, F., Felix, D. A., Chen, C., Louis, E. J., et al. (2012). Telomere maintenance and telomerase activity are differentially regulated in asexual and sexual worms. *Proc. Natl. Acad. Sci. U.S.A.* 109, 4209–4214. doi: 10.1073/pnas.1118885109

Tanaka, E. M., and Reddien, P. W. (2011). The cellular basis for animal regeneration. *Dev. Cell* 21, 172–185. doi: 10.1016/j.devcel.2011.06.016

von Trotha, J. W., Egger, B., and Brand, A. H. (2009). Cell proliferation in the Drosophila adult brain revealed by clonal analysis and bromodeoxyuridine labelling. *Neural Dev.* 4:9. doi: 10.1186/1749-8104-4-9

van Wolfswinkel, J. C. (2014). Piwi and potency: PIWI proteins in animal stem cells and regeneration. *Integr. Comp. Biol.* 54, 700–713. doi: 10.1093/icb/icu084

van Wolfswinkel, J. C., Wagner, D. E., and Reddien, P. W. (2014). Single-cell analysis reveals functionally distinct classes within the planarian stem cell compartment. *Cell Stem Cell* 15, 326–339. doi: 10.1016/j.stem.2014.06.007

Wagner, D. E., Wang, I. E., and Reddien, P. W. (2011). Clonogenic neoblasts are pluripotent adult stem cells that underlie planarian regeneration. *Science* 332, 811–816. doi: 10.1126/science.1203983

Zhu, S. J., Hallows, S. E., Currie, K. W., Xu, C., and Pearson, B. J. (2015). A mex3 homolog is required for differentiation during planarian stem cell lineage development. *Elife* 4. doi: 10.7554/eLife.07025

Zhu, S. J., and Pearson, B. J. (2016). (Neo)blast from the past: new insights into planarian stem cell lineages. *Curr. Opin. Genet. Dev.* 40, 74–80. doi: 10.1016/j.gde.2016.06.007

Conflict of Interest Statement: The authors declare that the research was conducted in the absence of any commercial or financial relationships that could be construed as a potential conflict of interest.

The reviewer AB and handling Editor declared their shared affiliation, and the handling Editor states that the process nevertheless met the standards of a fair and objective review.

frontiers in Neuroscience

MINI REVIEW
published: 08 June 2017
doi: 10.3389/fnins.2017.00327

A Cold-Blooded View on Adult Neurogenesis

*Anabel R. Simões and Christa Rhiner**

Champalimaud Centre for the Unknown, Lisbon, Portugal

During brain development, highly complex and interconnected neural circuits are established. This intricate wiring needs to be robust to faithfully perform adult brain function throughout life, but at the same time offer room for plasticity to integrate new information. In the mammalian brain, adult-born neurons are produced in restricted niches harboring neural stem cells. In the fruit fly *Drosophila*, low-level adult neurogenesis arising from a dispersed population of neural progenitors has recently been detected in the optic lobes. Strikingly, these normally quiescent neural stem cells proliferate upon brain injury and produce new neurons for brain regeneration. Here, we review adult neurogenesis in crustaceans and insects and highlight that neurogenesis in the visual system is prominent in arthropods, but its role and underlying mechanisms are unclear. Moreover, we discuss how the study of damage-responsive progenitor cells in *Drosophila* may help to understand robust regenerative neurogenesis and open new avenues to enhance brain repair after injury or stroke in humans.

Keywords: adult neurogenesis in arthropods, *Drosophila*, adult neural stem cells, regenerative neurogenesis, activation of quiescent stem cells

OPEN ACCESS

Edited by:
Luca Bonfanti,
University of Turin, Italy

Reviewed by:
Jan Kaslin,
Australian Regenerative Medicine Institute, Australia
Jorge Valero,
Achucarro Basque Center for Neuroscience (Ikerbasque), Spain

****Correspondence:***
Christa Rhiner
christa.rhiner@research.fchampalimaud.org

Specialty section:
This article was submitted to Neurogenesis, a section of the journal Frontiers in Neuroscience

Received: *29 March 2017*
Accepted: *23 May 2017*
Published: *08 June 2017*

Citation:
Simões AR and Rhiner C (2017) A Cold-Blooded View on Adult Neurogenesis. Front. Neurosci. 11:327. doi: 10.3389/fnins.2017.00327

The generation and integration of new neurons into the adult brain based on quiescent adult neural stem cells is a conserved trait in mammals (Kempermann, 2012). In the rodent brain, where most research has concentrated on so far, two canonical regions of adult neurogenesis exist (Zhao C. et al., 2008). First, the subventricular zone of the lateral ventricle, which produces neuroblasts that will migrate into the olfactory bulb to form new olfactory interneurons and second, the hippocampus, where adult-born neurons are thought to contribute to learning and memory (Bond et al., 2015; Gonçalves et al., 2017).

This review will focus on adult neurogenesis in crustaceans and insects, which have recently gained more protagonism in the field and show the potential to offer new mechanistic insight into aspects of stem cell activation, regeneration, and evolutionary conserved functions of newborn neurons in the mature brain.

ADULT NEUROGENESIS IN CRUSTACEANS

Arthropods represent the most species-rich phylum, comprising myriapods (e.g., centipedes), the extinct trilobites, the chelicerates (e.g., spiders), crustaceans, and insects, whereas the latter two subphyla are more closely related. Adult neurogenesis is well-documented in numerous species of crustaceans. In decapod crustaceans, such as lobster and crayfish, the formation and integration of adult-born neurons has been especially well-studied (Harzsch and Dawirs, 1996; Schmidt, 1997, 2001, 2007; Harzsch et al., 1999a; Sullivan and Beltz, 2005). These aquatic invertebrates are long-lived and show indeterminate growth during adulthood. Since they keep growing as adults, their brain needs to integrate an ever-increasing amount of sensory input from new sensilla on the body and from ommatidia of the eye. Strikingly, new neurons are only incorporated in few brain areas,

mainly the medulla of the optic lobe (Schmidt, 1997; Sullivan and Beltz, 2005) and two clusters associated with the olfactory and accessory lobes (Schmidt and Harzsch, 1999; Beltz and Sandeman, 2003; **Figure 1A**). In contrast, additional afferents from chemo- and mechanosensory neurons are integrated via enhanced arborizations and connectivity of preexisting neurons (Schmidt, 2007).

ADULT NEUROGENESIS SUSTAINED BY IMMIGRANTS

What is the source of new neurons in the crustacean brain? By now, the entire cellular path leading to adult neurogenesis in freshwater crayfish has been discovered (Benton et al., 2011, 2014): Similar to mammals, the brain of crayfish contains a neurogenic niche formed by glial cells, which harbors neural progenitor cells. However, these first-generation precursors are not self-renewing (Benton et al., 2011); they divide symmetrically and both daughter cells, termed second-generation precursors, migrate along fibrous streams to proliferation zones near the olfactory lobe, where they divide at least once more before their progeny differentiates into olfactory interneurons or projection neurons (Sullivan and Beltz, 2005; Kim et al., 2014; **Figure 1A**).

Since the precursors in the niche do not self-renew, there must be a way to replenish the niche to sustain life-long neurogenesis. Recently, Barbara Beltz and group showed that circulating hemocytes (blood cells), which can access the neurogenic niche via the cerebral artery (Chaves da Silva et al., 2013), are a source of first-generation neural precursors (Benton et al., 2014). When they injected labeled hemocytes from a donor crayfish into a recipient animal, these immune cells efficiently homed to the neurogenic niche—an attraction mediated partly by serotonin signaling (Benton et al., 2011)—and gave rise to second generation precursors and ultimately differentiated neurons (Benton et al., 2014). This shows that in crayfish, cells outside the brain are responsible of regulating adult neurogenesis. In contrast, neurogenesis during development is based—very much like in insects—on asymmetric divisions of classic neuroblasts (Harzsch et al., 1999b).

What is the function of neurogenesis in these particular regions? Obviously, neurogenesis is not just a compensatory reaction to accommodate more sensory input in growing crustaceans, as discussed above. In the olfactory system, the integration of new neurons may lead to increased combinatorial coding and therefore the ability to distinguish new odors. This could have a survival advantage for long-lived crustaceans, which often migrate over long distances and change habitat (Schmidt, 2007). In rodents, olfactory bulb neurogenesis seems to be important for efficient odor discrimination learning (Alonso et al., 2012), but also a function in mate choice is likely (Mak et al., 2007). Olfactory neurogenesis may therefore represent

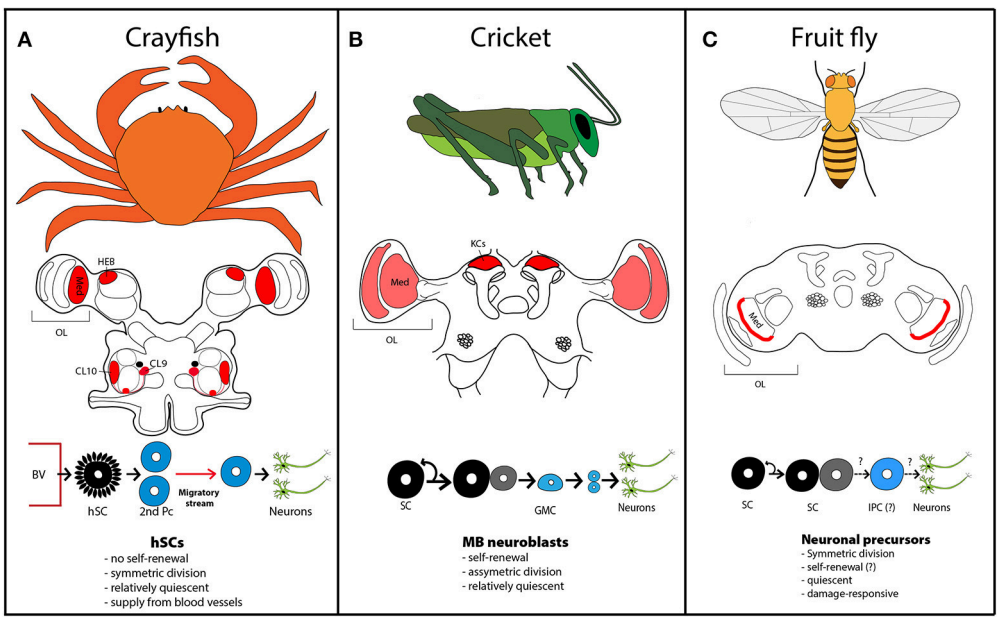

FIGURE 1 | Neurogenic zones in crustacean and insect species. **(A)** Adult neurogenesis in crayfish occurs in the medulla (med) of the optic lobe (OL), the hemiellipsoid body (HEB) and in cluster (CL) 9 and 10 adjacent to the olfactory lobe. The red circle below the clusters designates the niche. Circulating hemocytes in the blood enter the niche in the brain via underlying blood vessels (BVs). The progeny of these hemocyte-derived stem cells (hSCs), called secondary precursors (2nd Pcs) migrate along streams to the proliferation clusters, where they divide and differentiate into olfactory interneurons. **(B)** In crickets, adult-proliferating cells are found in the optic lobes and the cortex of the adult mushroom bodies. New neurons arise from mushroom body (MB) neuroblasts, which divide asymmetrically to self-renew and produce a ganglion mother cell (GMC), which in turn divides to form two neurons. KC, Kenyon cells. **(C)** Low-level adult neurogenesis occurs in the outer medulla of fruit fly. Adult-born neurons derive from symmetric divisions of neural precursors and likely intermediate proliferating cells (IPCs). Neurogenic zones are shaded in red. Light red indicates proliferating zones, where no published images are available.

a conserved trait to allow olfactory fine-tuning in long-lived animals, given that the maturation of adult-born neurons takes several weeks to months.

Overall, neurogenesis in the olfactory pathway of crayfish shows many parallels to adult neurogenesis in the olfactory bulb of rodents, starting from the slow-dividing progenitors (≥48 h) (Benton et al., 2011) to the migratory stream of neuroblasts and their differentiation into olfactory interneurons (**Figure 1A**). On the other hand, neural precursors in crustaceans do not seem to form glial lineages compared to mammalian adult neural stem cells and they are continuously refreshed from hemocytes since they lack self-renewing stem cell properties (Benton et al., 2014).

THE OPTIC LOBE AS NEUROGENIC ZONE

In the small crab and crayfish, adult neurogenesis occurs in the optic lobe, but has not been investigated in detail. Proliferating cells have been observed in several zones of the adult optic lobe, but evidence that they differentiate into neurons has only been obtained for the medulla externa (Sullivan and Beltz, 2005; **Figure 1A**). If new neurons were required to maintain the highly columnar organization of the visual pathway, one would also expect to find adult-born neurons in the lamina. However, it might be very challenging to understand the functions of new neurons in visual circuits of crustaceans because they have very complex eyes. There are species like the mantis shrimp, which show up to 16 different photoreceptors and trinocular vision (Thoen et al., 2014).

Finally, the addition of local interneurons has also been observed in the hemiellipsoid body of the shore crab (Schmidt, 1997). The hemiellipsoid body is located close to the optic lobes and may be homologous to the mushroom bodies of insects, which are higher brain centers required for memory formation. This raises the question if neurogenesis in crustaceans could also be important for orientation or learning. Given that adult neurogenesis in crayfish can be suppressed by reducing peripheral hemocytes, without manipulating the nervous system, it will be interesting to see how altered neurogenesis impacts on behavior.

REGENERATION IN THE CRUSTACEAN BRAIN

In crayfish, the overall level of neurogenesis is regulated by the number of circulating peripheral hemocytes (Benton et al., 2014). This strong link between the immune system and a stem cell niche is remarkable and could represent an efficient mechanism to directly convert immune cell activation into stem cell proliferation and regeneration in case of inflammation and tissue damage.

Regeneration in decapod crustaceans has been described since the 18th century for the appendages and for the compound eye (Steele, 1907; Cooper, 1998). Several species of crustaceans have the ability to regenerate the ommatidia of the eye after partial removal of the cornea, like the hermit crab and several shrimp and crayfish species. Hermit crabs can even regenerate a perfect eye after removal of the cornea and half of the optic ganglion (Steele, 1907). These experiments, together with the observed adult neurogenesis in optic lobes, suggest that neural precursors also migrate to and proliferate in the optic ganglia (Steele, 1907). Now that the cellular basis of adult neurogenesis is known in crayfish, it would be interesting to study its role and regulation in eye and optic ganglion regeneration.

ADULT NEUROGENESIS IN INSECTS

In insects, adult neurogenesis is known to occur in two different regions: the mushroom bodies (MBs) and the optic lobes (Cayre et al., 1996; **Figure 1B**). Strikingly, almost all studies have concentrated on MBs, leaving optic lobe neurogenesis virtually unexplored. Therefore, we will first consider findings in MBs, before shifting the discussion to the visual system.

The MBs represent higher brain centers for multimodal sensory integration in the protocerebrum of insects (Farris and Sinakevitch, 2003). They consist of hundreds to hundreds of thousands densely packed interneurons, called Kenyon cells (KCs), and a neuropil formed by their projections and synaptic contacts. The MBs receive input from the olfactory and gustatory system, in hymenoptera also from the visual pathway (Farris and Sinakevitch, 2003).

Newly generated neurons in adult MBs derive from persisting MB neuroblast proliferation after development is concluded. Such ongoing production of new KCs occurs in house crickets and other coleopterans (Cayre et al., 1994), gryllidae (Cayre et al., 1996; **Figure 1B**), cockroaches (Gu et al., 1999), moths (Dufour and Gadenne, 2006), praying mantis, and milkweed bugs (Cayre et al., 2007). On the other hand, no active neuroblasts have been detected in MBs of honey bees (Fahrbach et al., 1995), ants (Gronenberg et al., 1996) and migratory locusts (Cayre et al., 1996). In *Drosophila*, neurogenesis in adult MB is scarce and was interpreted as last divisions of progeny, generated by neuroblast activity in the pupal stage (Ito and Hotta, 1992).

Integration of adult-born neurons into MBs is best understood in house crickets (*Acheta domesticus*), where life-long production of new interneurons is sustained by a cluster of approximately 100 neuroblasts located at the apex of a cortex formed by KCs (Cayre et al., 2007; **Figure 1B**). Asymmetric division of these neuroblasts leads to self-renewal and the production of a ganglion mother cell, which in turn divides symmetrically to generate two neurons. Newly formed KCs deposit in layers, whereby the most recent KCs are found close to the stem cells and older KCs, which are pushed away by new waves of KCs, settle in more peripheral layers (Cayre et al., 1996).

NEW KENYON CELLS AND OLFACTORY LEARNING?

Adult neurogenesis in crickets is substantial, accounting for an estimated 20% of total KCs in an aged cricket (Malaterre et al., 2002). KCs themselves are heterogeneous differing in size, projection and arborization patterns. In crickets, the adult-born KCs project all to the alpha and beta lobes of the MBs. In

Drosophila, the alpha and beta lobes have been shown to be required for long-term memory formation (Pascual and Préat, 2001).

To understand the contribution of adult-born KCs in crickets, head-restricted gamma irradiation has been used to target adult dividing neuroblasts and study behavioral consequences. These experiments revealed that irradiated crickets showed slower learning in an olfactory association task and impaired long-term memory, whereas learning based on visual cues was mostly unaffected (Scotto-Lomassese et al., 2003). This suggests that new KCs could be important to link olfactory information processed in the antennal lobe to reward or danger signals (food, mates) in the environment. Such odor-reward integration leading to memory formation has been described in *Drosophila*, where olfactory learning leads to reinforcement in dopaminergic neurons innervating the MBs, which in turn drives synaptic plasticity between KCs and MB output neurons (Owald and Waddell, 2015). Hence reactivation of such remodeled MB circuits efficiently re-evokes odor-associated experience and guides appropriate approach or avoidance behavior.

In crickets, sensory stimulation alone is sufficient to increase neurogenesis (Cayre et al., 2005), but how selective memory is formed and retained is unclear, since all newly generated and pre-existing KCs survive. This is different in mammals where the bulk of adult-born neurons undergoes apoptosis (Biebl et al., 2000) and only few new neurons are selected to integrate into hippocampal circuits, which are structurally similar to MBs. It is therefore conceivable that new KCs may first serve to increase the acquisition rate in olfactory learning and then participate in olfactory-associative memories due to reinforcement occurring in specific subsets of KCs, but more functional experiments would be required to support this hypothesis.

In moths, adult-proliferating cells have been detected in MBs and optic lobes (Dufour and Gadenne, 2006). The brain of 3 days-old adults contained new KCs, but proliferation ceased shortly thereafter, when animals reached sexual maturity, which is similar in *Drosophila*. Moths are short-lived and males need to be able to locate females over large distances. This plasticity in the MBs could therefore be related to pheromone-associated learning to detect mates, but experimental evidence is lacking. Moreover, moths are able to associate olfactory cues such as pheromones or flower scents with a sugar reward and form long-term memory (Hartlieb et al., 1999), but learning has not been assessed in conditions of suppressed adult neurogenesis.

Possibly, the actual life span of an insect could be indicative if new neurons are generated in the mature brain. In short-lived insects, the production of new neurons in the adult brain may be too cost-intensive and time-consuming to yield an impact compared to species, which live up to 2 years (e.g. cockroaches). The analysis of more long-lived arthropod species such as spiders or termites, could shed some light on this question.

In the future, the red flour beetle may hold a great potential to uncover the function of neurogenesis in adult MBs since it combines the possibility to monitor adult neuroblast proliferation (lasting up to 2 months of adulthood) with the availability of genetic gain- and loss-of-function tools (Zhao X. et al., 2008).

INSECTS: NEUROGENESIS IN SIGHT?

Visual information in insects and crustaceans is processed in the optic lobe (OL) (**Figure 1**). In insects, the OLs are divided into the neuropils of the lamina, outer, and inner medulla and either lobular plate or a sublobula neuropil. In malacostracan crustaceans, there are four neuropils: the lamina, the medulla, the lobula, and lobular plate (Farris and Sinakevitch, 2003).

Several early histological studies mention the persistence of neuroblasts in adult OLs (Graichen, 1936; Panov, 1960). Proliferating cells verified by BrdU-labeling, have also been observed in OLs of adult moths (Dufour and Gadenne, 2006) and crickets (Cayre et al., 1996), but not further analyzed. In crickets, dividing cells were described to locate close to the medulla of the OLs (Scotto-Lomassese et al., 2003).

More recently, low-level adult neurogenesis has also been detected in the medulla cortex of *Drosophila* (**Figure 1C**), where a scattered population of neural precursors gives rise to new neurons (Fernández-Hernández et al., 2013; Moreno et al., 2015). These neural precursors do not express known neuroblast markers, except for cytoplasmic staining for Deadpan (Bier et al., 1992), a homolog of the vertebrate Hes (hairy and enhancer of split-1) bHLH transcription factors, which is expressed in the nucleus of dividing neuroblasts during development (Bello et al., 2008; Boone and Doe, 2008; Maurange et al., 2008). Lineage-tracing revealed that initial neural precursors and progeny divide mainly symmetrically to generate new neurons (**Figure 1C**). New-born neurons in the medulla cortex mature within 2 weeks, extending projections to lobula or lobular plate (Fernández-Hernández et al., 2013). In *Drosophila*, color-sensitive photoreceptors send their axons to the medulla, whereas light-dark sensitive receptors project to the lamina. The lobula is implicated in color and polarized light vision and spectral preference, the lobular plate is dedicated to motion detection (Behnia and Desplan, 2015).

Still, the proliferation of approximately 30–40 neural precursors per OL is very low given that they contribute to an estimated number of 4–6 divisions per OL per week, meaning that they are mainly quiescent. Based on the location and low activity of the neural progenitors, their function may be related to adjustments in color vision or slow homeostatic turnover.

Apart from neurogenesis, the optic neuropils have long been known to show volumetric plasticity (Heisenberg et al., 1995). If flies are reared in enriched environments (social interactions, light), the neuropils and especially the lamina become larger compared to animals deprived of light and housed alone. This effect is observable even in mature flies.

Workers of a species of nectar-feeding ants, naturally undergo a strong switch in behavior associated with visual input: They spend the first weeks of adulthood dedicated to tasks inside the nest before they set out to forage for food. This requires completely new abilities such as long-distance navigation and memory of food location. It would therefore be interesting to know if this transition is not only accompanied by growth of the optic neuropils and changes in photoreceptor expression (Yilmaz et al., 2016), but also by adult neurogenesis, especially given the context of long-distance navigation.

To conclude, given the scarce evidence on adult neurogenesis in the visual system, we can only speculate about its function. Notwithstanding the lack of data, the medulla seems to emerge as a potentially conserved site of adult neurogenesis in crustaceans and insects (**Figure 1**). To gain further insight into the role of adult neurogenesis in arthropods, it will be vital to conduct more functional experiments. The fact that *Drosophila* shows low-level adult neurogenesis and robust damage-induced formation of new neurons opens the door to address these processes with functional genetic experiments.

THE POWER OF DAMAGE-RESPONSIVE STEM CELLS

Although the physiologic function of adult neurogenesis in *Drosophila* remains elusive, the adult neural progenitors in the OLs are readily activated in case of acute tissue damage. Stab lesion of the optic lobe to the level of the medulla (**Figure 2**), triggers proliferation of adult neural precursors, which involves nuclear translocation of Deadpan and upregulation of *Drosophila* Myc, the homolog of the human *c-myc* protooncogene (Fernández-Hernández et al., 2013). Such activated progenitors either directly or indirectly give rise to new neurons. The latter is more likely to be the case, since the damage-responsive precursors switch back to the resting state >48 h post-injury, but cells in proximity keep dividing (Fernández-Hernández et al., 2013; Fernández-Hernández and Rhiner, 2015). Stab wounding results in local regenerative neurogenesis around the lesioned site, which implies that neural progenitor cells distributed throughout the OL get either locally activated by injury-induced signals or may actively migrate to the site of damage. Remarkably, the newborn neurons mature and persist up to 11 days after injury (Moreno et al., 2015), which points to an efficient endogenous repair system. These findings underline that quiescent adult neural progenitors can serve as a backup population to regenerate brain tissue in case of injury.

In turn, the adult zebrafish brain contains numerous neurogenic regions, which harbor neural progenitors (radial glial cells) that constantly produce neurons in the mature brain (Kizil et al., 2012). Upon stab lesion of the telencephalon, inflammatory signals stimulate radial glial cells to increase proliferation and the damaged brain area is efficiently restored (Kyritsis et al., 2012). Teleost fish show therefore a trend that continuous brain growth during adult life is paralleled by pronounced adult neurogenesis, similar to crustaceans.

A promising therapeutic strategy aims to support local neurogenesis in human patients suffering from trauma or stroke, circumventing the complications of grafting exogenous stem cells for repair. Endogenous adult neural stem cells have been shown to be similarly responsive to injury signals in rodents and humans (Zhang and Chopp, 2009): After stroke, neural stem cells in the SVZ enhance proliferation, reactivate developmental pathways and generate neuroblasts, able to migrate to lesioned brain areas (Zhang and Chopp,

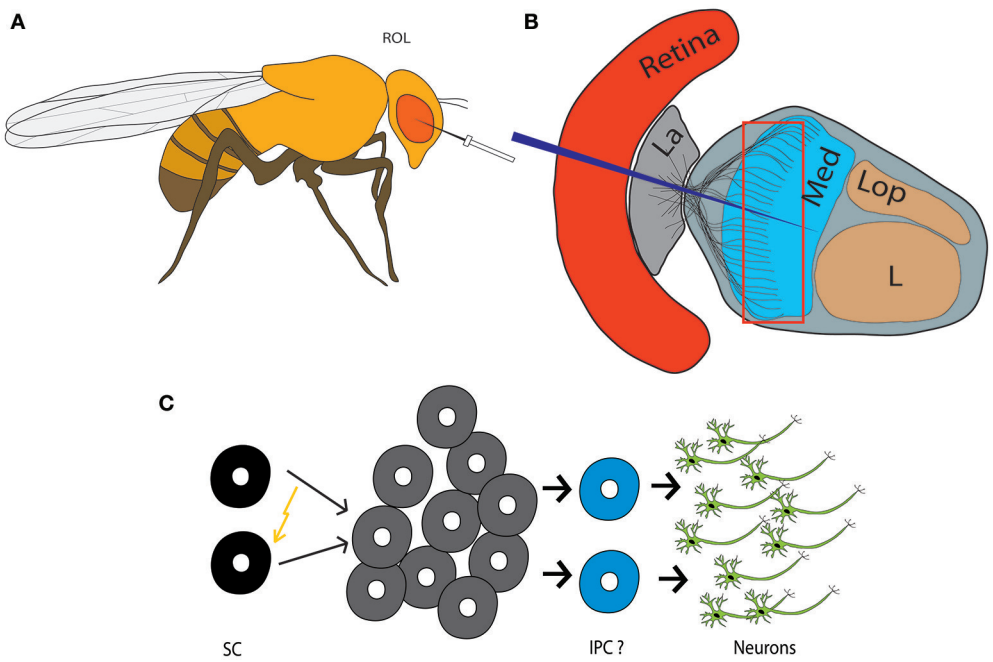

FIGURE 2 | Injury-induced neurogenesis in the adult fly brain. **(A)** Traumatic brain injury paradigm in *Drosophila*: Stab lesions are performed with a thin metal filament to injure the right optic lobe (ROL). **(B)** Scheme depicting the retina and neuropils of the optic lobe. The eye is lesioned to the level of the medulla. La, Lamina; Med, Medulla; L, Lobula; Lop, Lobular plate. **(C)** Injury leads to activation and proliferation of quiescent adult neural progenitor cells, which give rise to new neurons, likely involving generation of a type of intermediate proliferating cell (IPC). SC, Stem cells.

2009). In addition, a large fraction of neuroblasts are produced locally at the ischemic lesion from activated astrocytes, which adopt a neurogenic program (Magnusson et al., 2014). Major challenges are however the survival and successful integration of the newly formed neurons and the tendency of the neural stem cells to form glial instead of neural cells.

The above-described model of brain regeneration in the genetic model organism *Drosophila* allows to screen for conserved genes, which are important for the efficient activation of quiescent neural progenitors and their differentiation into neural lineages *in vivo*. Moreover, the newly-generated cells can be followed up to study how they integrate into circuits. Initially, optic lobe lesions should allow to evaluate the effect of regenerative neurogenesis on recovery of visual skills. Learnt principles may then be tested in other contexts, such as ventral nerve cord regeneration in flies (Kato et al., 2011), which are relevant for human CNS injuries.

So far, crustaceans and insects have played a very small role in the field of adult neurogenesis, which has been dominated by mammalian research. Recent studies have uncovered fascinating aspects of stem cell regulation and regeneration in arthropods, which may open new therapeutic approaches to stimulate neurogenesis after brain injury.

AUTHOR CONTRIBUTIONS

ARS and CR wrote the manuscript. CR elaborated the concept and ARS drew the Figures.

FUNDING

This work has been funded by the Champalimaud Foundation (CR) and a Portuguese Foundation for Science and Technology (FCT) PhD fellowship (grant number SFRH/BD/121028/2016) to ARS.

REFERENCES

Alonso, M., Lepousez, G., Sebastien, W., Bardy, C., Gabellec, M. M., Torquet, N., et al. (2012). Activation of adult-born neurons facilitates learning and memory. *Nat. Neurosci.* 15, 897–904. doi: 10.1038/nn.3108

Behnia, R., and Desplan, C. (2015). Visual circuits in flies: beginning to see the whole picture. *Curr. Opin. Neurobiol.* 34, 125–132. doi: 10.1016/j.conb.2015.03.010

Bello, B. C., Izergina, N., Caussinus, E., and Reichert, H. (2008). Amplification of neural stem cell proliferation by intermediate progenitor cells in Drosophila brain development. *Neural Dev.* 3:5. doi: 10.1186/1749-8104-3-5

Beltz, B. S., and Sandeman, D. C. (2003). Regulation of life-long neurogenesis in the decapod crustacean brain. *Arthropod Struct. Dev.* 32, 39–60. doi: 10.1016/S1467-8039(03)00038-0

Benton, J. L., Kery, R., Li, J., Noonin, C., Söderhäll, I., and Beltz, B. S. (2014). Cells from the immune system generate adult-born neurons in crayfish. *Dev. Cell* 30, 322–333. doi: 10.1016/j.devcel.2014.06.016

Benton, J. L., Zhang, Y., Kirkhart, C. R., Sandeman, D. C., and Beltz, B. S. (2011). Primary neuronal precursors in adult crayfish brain: replenishment from a non-neuronal source. *BMC Neurosci.* 12:53. doi: 10.1186/1471-2202-12-53

Biebl, M., Cooper, C. M., Winkler, J., and Kuhn, H. G. (2000). Analysis of neurogenesis and programmed cell death reveals a self-renewing capacity in the adult rat brain. *Neurosci. Lett.* 291, 17–20. doi: 10.1016/S0304-3940(00)01368-9

Bier, E., Vaessin, H., Younger-Shepherd, S., Jan, L. Y., and Jan, Y. N. (1992). Deadpan, an essential pan-neural gene in Drosophila, encodes a helix-loop-helix protein similar to the hairy gene product. *Genes Dev.* 6, 2137–2151. doi: 10.1101/gad.6.11.2137

Bond, A. M., Ming, G. L., and Song, H. (2015). Adult mammalian neural stem cells and neurogenesis: five decades later. *Cell Stem Cell* 17, 385–395. doi: 10.1016/j.stem.2015.09.003

Boone, J. Q., and Doe, C. Q. (2008). Identification of Drosophila type II neuroblast lineages containing transit amplifying ganglion mother cells. *Dev. Neurobiol.* 68, 1185–1195. doi: 10.1002/dneu.20648

Cayre, M., Malaterre, J., Scotto-Lomassese, S., Aouane, A., Strambi, C., Strambi, A., et al. (2005). Hormonal and sensory inputs regulate distinct neuroblast cell cycle properties in adult cricket brain. *J. Neurosci. Res.* 82, 659–664. doi: 10.1002/jnr.20672

Cayre, M., Scotto-Lomassese, S., Malaterre, J., Strambi, C., and Strambi, A. (2007). Understanding the regulation and function of adult neurogenesis: contribution from an insect model, the house cricket. *Chem. Senses* 32, 385–395. doi: 10.1093/chemse/bjm010

Cayre, M., Strambi, C., Charpin, P., Augier, R., Meyer, M. R., Edwards, J. S., et al. (1996). Neurogenesis in adult insect mushroom bodies. *J. Comp. Neurol.* 371, 300–310. doi: 10.1002/(SICI)1096-9861(19960722)371:2<300::AID-CNE9>3.0.CO;2-6

Cayre, M., Strambi, C., and Strambi, A. (1994). Neurogenesis in an adult insect brain and its hormonal control. *Nature* 368, 57–59. doi: 10.1038/368057a0

Chaves da Silva, P. G., Benton, J. L., Sandeman, D. C., and Beltz, B. S. (2013). Adult neurogenesis in the crayfish brain: the hematopoietic anterior proliferation center has direct access to the brain and stem cell niche. *Stem Cells Dev.* 22, 1027–1041. doi: 10.1089/scd.2012.0583

Cooper, R. L. (1998). Development of sensory processes during limb regeneration in adult crayfish. *J. Exp. Biol.* 201, 1745–1752.

Dufour, M. C., and Gadenne, C. (2006). Adult neurogenesis in a moth brain. *J. Comp. Neurol.* 495, 635–643. doi: 10.1002/cne.20909

Fahrbach, S. E., Strande, J. L., and Robinson, G. E. (1995). Neurogenesis is absent in the brains of adult honey bees and does not explain behavioral neuroplasticity. *Neurosci. Lett.* 197, 145–148. doi: 10.1016/0304-3940(95)11913-H

Farris, S. M., and Sinakevitch, I. (2003). Development and evolution of the insect mushroom bodies: towards the understanding of conserved developmental mechanisms in a higher brain center. *Arthropod Struct. Dev.* 32, 79–101. doi: 10.1016/S1467-8039(03)00009-4

Fernández-Hernández, I., and Rhiner, C. (2015). New neurons for injured brains? The emergence of new genetic model organisms to study brain regeneration. *Neurosci. Biobehav. Rev.* 56, 62–67. doi: 10.1016/j.neubiorev.2015.06.021

Fernández-Hernández, I., Rhiner, C., and Moreno, E. (2013). Adult neurogenesis in Drosophila. *Cell Rep.* 3, 1857–1865. doi: 10.1016/j.celrep.2013.05.034

Gonçalves, J. T., Schafer, S. T., and Gage, F. H. (2017). Adult neurogenesis in the hippocampus: from stem cells to behavior. *Cell* 167, 897–914. doi: 10.1016/j.cell.2016.10.021

Graichen, E. (1936). Das Zentralnerven-system von Nepa cinerea mit Einschluss des sym-pathischen Nervensystems. *Zool. Jahrb. Abt. Anal. U. Ontlog.* 61, 195–238.

Gronenberg, W., Heeren, S., and Hölldobler, B. (1996). Age-dependent and task-related morphological changes in the brain and the mushroom bodies of the ant Camponotus floridanus. *J. Exp. Biol.* 199, 2011–2019.

Gu, S. H., Tsia, W. H., Chiang, A. S., and Chow, Y. S. (1999). Mitogenic effects of 20-hydroxyecdysone on neurogenesis in adult mushroom bodies of the cockroach, Diploptera punctata. *J. Neurobiol.* 39, 264–274. doi: 10.1002/(SICI)1097-4695(199905)39:2<264::AID-NEU10>3.0.CO;2-7

Hartlieb, E., Anderson, P., and Hansson, B. S. (1999). Appetitive learning of odours with different behavioural meaning in moths. *Physiol. Behav.* 67, 671–677. doi: 10.1016/S0031-9384(99)00124-9

Harzsch, S., Benton, J., Dawirs, R. R., and Beltz, B. (1999b). A new look at embryonic development of the visual system in decapod crustaceans: neuropil formation, neurogenesis, and apoptotic cell death. *J. Neurobiol.* 39, 294–306.

Harzsch, S., and Dawirs, R. (1996). Neurogenesis in the developing crab brain: postembryonic generation of neurons persists beyond metamorphosis. *J. Neurobiol.* 29, 384–398. doi: 10.1002/(SICI)1097-4695(199603)29:3<384::AID-NEU9>3.0.CO;2-5

Harzsch, S., Miller, J. H., Benton, J. L., and Beltz, B. S. (1999a). From embryo to adult: persistent neurogenesis and apoptotic cell death shape the lobster deutocerebrum. *J. Neurosci.* 19, 3472–3485.

Heisenberg, M., Heusipp, M., and Wanke, C. (1995). Structural plasticity in the Drosophila brain. *J. Neurosci.* 15, 1951–1960.

Ito, K., and Hotta, Y. (1992). Proliferation pattern of postembryonic neuroblasts in the brain of *Drosophila melanogaster*. *Dev. Biol.* 149, 134–148. doi: 10.1016/0012-1606(92)90270-Q

Kato, K., Forero, M. G., Fenton, J. C., and Hidalgo, A. (2011). The glial regenerative response to central nervous system injury is enabled by pros-notch and pros-NFκB feedback. *PLoS Biol.* 9:e1001133. doi: 10.1371/journal.pbio.1001133

Kempermann, G. (2012). New neurons for 'survival of the fittest'. *Nat. Rev. Neurosci.* 13, 727–736. doi: 10.1038/nrn3319

Kim, Y. F., Sandeman, D. C., Benton, J. L., and Beltz, B. S. (2014). Birth, survival and differentiation of neurons in an adult crustacean brain. *Dev. Neurobiol.* 74, 602–615. doi: 10.1002/dneu.22156

Kizil, C., Kaslin, J., Kroehne, V., and Brand, M. (2012). Adult neurogenesis and brain regeneration in zebrafish. *Dev. Neurobiol.* 72, 429–461. doi: 10.1002/dneu.20918

Kyritsis, N., Kizil, C., Zocher, S., Kroehne, V., Kaslin, J., Freudenreich, D., et al. (2012). Acute inflammation initiates the regenerative response in the adult zebrafish brain. *Science* 338, 1353–1356. doi: 10.1126/science.1228773

Magnusson, J. P., Göritz, C., Tatarishvili, J., Dias, D. O., Smith, E. M., Lindvall, O., et al. (2014). A latent neurogenic program in astrocytes regulated by Notch signaling in the mouse. *Science* 346, 237–241. doi: 10.1126/science.346.6206.237

Mak, G. K., Enwere, E. K., Gregg, C., Pakarainen, T., Poutanen, M., Huhtaniemi, I., et al. (2007). Male pheromone-stimulated neurogenesis in the adult female brain: possible role in mating behavior. *Nat. Neurosci.* 10, 1003–1011. doi: 10.1038/nn1928

Malaterre, J., Strambi, C., Chiang, A. S., Aouane, A., Strambi, A., and Cayre, M. (2002). Development of cricket mushroom bodies. *J. Comp. Neurol.* 452, 215–227. doi: 10.1002/cne.10319

Maurange, C., Cheng, L., and Gould, A. P. (2008). Temporal transcription factors and their targets schedule the end of neural proliferation in Drosophila. *Cell* 133, 891–902. doi: 10.1016/j.cell.2008.03.034

Moreno, E., Fernandez-Marrero, Y., Meyer, P., and Rhiner, C. (2015). Brain regeneration in *Drosophila* involves comparison of neuronal fitness. *Curr. Biol.* 25, 955–963. doi: 10.1016/j.cub.2015.02.014

Owald, D., and Waddell, S. (2015). Olfactory learning skews mushroom body output pathways to steer behavioral choice in Drosophila. *Curr. Opin. Neurobiol.* 35, 178–184. doi: 10.1016/j.conb.2015.10.002

Panov, A. A. (1960). The structure of the brain in insects in successive stages of postembryonic development. III Optic lobes. *Rev. Entomol.* 39, 55–68.

Pascual, A., and Préat, T. (2001). Localization of long-term memory within the Drosophila mushroom body. *Science* 294, 1115–1117. doi: 10.1126/science.1064200

Schmidt, M. (1997). Continuous neurogenesis in the olfactory brain of adult shore crabs, *Carcinus maenas*. *Brain Res.* 762, 131–143. doi: 10.1016/S0006-8993(97)00376-4

Schmidt, M. (2001). Neuronal differentiation and long-term survival of newly generated cells in the olfactory midbrain of the adult spiny lobster, *Panulirus argus*. *J. Neurobiol.* 48, 181–203. doi: 10.1002/neu.1050

Schmidt, M. (2007). The olfactory pathway of decapod crustaceans—an invertebrate model for life-long neurogenesis. *Chem. Senses* 32, 365–384. doi: 10.1093/chemse/bjm008

Schmidt, M., and Harzsch, S. (1999). Comparative analysis of neurogenesis in the central olfactory pathway of adult decapod crustaceans by *in vivo* BrdU labeling. *Biol. Bull.* 196, 127–136. doi: 10.2307/1542558

Scotto-Lomassese, S., Strambi, C., Strambi, A., Aouane, A., Augier, R., Rougon, G., et al. (2003). Suppression of adult neurogenesis impairs olfactory learning and memory in an adult insect. *J. Neurosci.* 23, 9289–9296.

Steele, M. I. (1907). Regeneration in compound eyes of Crustacea. *J. Exp. Zool.* 5, 163–243. doi: 10.1002/jez.1400050203

Sullivan, J. M., and Beltz, B. S. (2005). Newborn cells in the adult crayfish brain differentiate into distinct neuronal types. *J. Neurobiol.* 65, 157–170. doi: 10.1002/neu.20195

Thoen, H. H., How, M. J., Chiou, T.-H., and Marshall, J. (2014). A different form of color vision in mantis shrimp. *Science* 343, 411–413. doi: 10.1126/science.1245824

Yilmaz, A., Lindenberg, A., Albert, S., Grübel, K., Spaethe, J., Rössler, W., et al. (2016). Age-related and light-induced plasticity in opsin gene expression and in primary and secondary visual centers of the nectar-feeding ant Camponotus rufipes. *Dev. Neurobiol.* 76, 1041–1057. doi: 10.1002/dneu.22374

Zhang, Z. G., and Chopp, M. (2009). Neurorestorative therapies for stroke: underlying mechanisms and translation to the clinic. *Lancet Neurol.* 8, 491–500. doi: 10.1016/S1474-4422(09)70061-4

Zhao, C., Deng, W., and Gage, F. H. (2008). Mechanisms and functional implications of adult neurogenesis. *Cell* 132, 645–660. doi: 10.1016/j.cell.2008.01.033

Zhao, X., Coptis, V., and Farris, S. M. (2008). Metamorphosis and adult development of the mushroom bodies of the red flour beetle, *Tribolium castaneum*. *Dev. Neurobiol.* 68, 1487–1502. doi: 10.1002/dneu.20669

Conflict of Interest Statement: The authors declare that the research was conducted in the absence of any commercial or financial relationships that could be construed as a potential conflict of interest.

frontiers in Neuroscience

METHODS
published: 17 January 2018
doi: 10.3389/fnins.2017.00750

A Whole Brain Staining, Embedding, and Clearing Pipeline for Adult Zebrafish to Visualize Cell Proliferation and Morphology in 3-Dimensions

Benjamin W. Lindsey[1†], *Alon M. Douek*[1], *Felix Loosli*[2] *and Jan Kaslin*[1*]

[1] *Australian Regenerative Medicine Institute, Monash University, Clayton, VIC, Australia,* [2] *Institute of Toxicology and Genetics, Karlsruhe Institute of Technology, Karlsruhe, Germany*

OPEN ACCESS

Edited by:
Paolo Peretto,
Università degli Studi di Torino, Italy

Reviewed by:
Giorgio Roberto Merlo,
Università degli Studi di Torino, Italy
Ali Erturk,
Ludwig-Maximilians-Universität München, Germany

****Correspondence:***
Jan Kaslin
jan.kaslin@monash.edu

†Present Address:
Benjamin W. Lindsey,
University of Ottawa, Brain and Mind Research Institute, Department of Biology, Ottawa, ON, Canada

Specialty section:
This article was submitted to Neurogenesis, a section of the journal Frontiers in Neuroscience

Received: *29 September 2017*
Accepted: *22 December 2017*
Published: *17 January 2018*

Citation:
Lindsey BW, Douek AM, Loosli F and Kaslin J (2018) A Whole Brain Staining, Embedding, and Clearing Pipeline for Adult Zebrafish to Visualize Cell Proliferation and Morphology in 3-Dimensions. Front. Neurosci. 11:750. doi: 10.3389/fnins.2017.00750

The field of macro-imaging has grown considerably with the appearance of innovative clearing methods and confocal microscopes with lasers capable of penetrating increasing tissue depths. The ability to visualize and model the growth of whole organs as they develop from birth, or with manipulation, disease or injury, provides new ways of thinking about development, tissue-wide signaling, and cell-to-cell interactions. The zebrafish (*Danio rerio*) has ascended from a predominantly developmental model to a leading adult model of tissue regeneration. The unmatched neurogenic and regenerative capacity of the mature central nervous system, in particular, has received much attention, however tools to interrogate the adult brain are sparse. At present there exists no straightforward methods of visualizing changes in the whole adult brain in 3-dimensions (3-D) to examine systemic patterns of cell proliferation or cell populations of interest under physiological, injury, or diseased conditions. The method presented here is the first of its kind to offer an efficient step-by-step pipeline from intraperitoneal injections of the proliferative marker, 5-ethynyl-2′-deoxyuridine (EdU), to whole brain labeling, to a final embedded and cleared brain sample suitable for 3-D imaging using optical projection tomography (OPT). Moreover, this method allows potential for imaging GFP-reporter lines and cell-specific antibodies in the presence or absence of EdU. The small size of the adult zebrafish brain, the highly consistent degree of EdU labeling, and the use of basic clearing agents, benzyl benzoate, and benzyl alcohol, makes this method highly tractable for most laboratories interested in understanding the vertebrate central nervous system in health and disease. Post-processing of OPT-imaged adult zebrafish brains injected with EdU illustrate that proliferative patterns in EdU can readily be observed and analyzed using IMARIS and/or FIJI/IMAGEJ software. This protocol will be a valuable tool to unlock new ways of understanding systemic patterns in cell proliferation in the healthy and injured brain, brain-wide cellular interactions, stem cell niche development, and changes in brain morphology.

Keywords: macro-imaging, tissue clearing, medaka, optical projection tomography, neurogenesis, stem cell senescence, regeneration, development

INTRODUCTION

How cells in the developing or adult brain are organized and behave following injury or disease remains a fascinating, yet still poorly understood, question. For many years, the ability to visualize the structural composition or global patterns across the neuro-axis of the adult vertebrate brain was limited by the lack of imaging tools available to examine cell phenotypes in larger tissue structures *in situ* in 3-dimensions (3-D). As a result, most interpretations have been derived from 2-dimensional (2-D) analyses of sectioned tissue. Recently however, the field of macro-imaging has become popularized by a growing interest of researchers to understand whole organ development, structure, and the associated morphological and cellular abnormalities that arise with disease (Short et al., 2010; Epp et al., 2015; Lloyd-Lewis et al., 2016; Short and Smyth, 2016). This has been paralleled by innovations in modern clearing techniques and specialized imaging methods designed to visualize thick tissues or whole organs in 3-D space, giving way to a new era of fluorescent, whole organ imaging (Susaki et al., 2014; Azaripour et al., 2016; Susaki and Ueda, 2016; Aswendt et al., 2017; Whitehead et al., 2017).

The value of macro-imaging has been demonstrated across a range of tissues, including embryos (Sharpe et al., 2002; Sharpe, 2003), heart (Kolesová et al., 2016; Aguilar-Sanchez et al., 2017), kidney (Short et al., 2010; Combes et al., 2014; Short and Smyth, 2016, 2017), lymph node (Song et al., 2015), mammary glands (Lloyd-Lewis et al., 2016), and brain (Gleave et al., 2013; Ode and Ueda, 2015), leading to new insight into the cellular behavior of organs under diverse conditions. This progress has been facilitated by the power of multiphoton imaging, newer confocal microscopes with lasers having increasingly better z-axis penetration, the development of light-sheet microscopes, and tomographic techniques such as Optical Projection Tomography (Sharpe et al., 2002; Keller et al., 2010; Parra et al., 2012; Kromm et al., 2016; McGowan and Bidwell, 2016; Susaki and Ueda, 2016; Whitehead et al., 2017). Nevertheless, whole organ imaging of thick tissue of ∼1 mm or greater introduce a number of challenges that must be overcome compared to antibody labeling and confocal imaging of sectioned tissue at the micron scale.

In most cases the biggest obstacle for macro-imaging is the successful sample preparation of thick tissue or organs. A significant challenge continues to be the balance between homogeneous fluorescent labeling through the tissue block and rendering the tissue clear for imaging. Unfortunately, this can only be accomplished by trial and error, with individual tissue types having their own unique set of physical properties. Commonly protein labeling using antibodies or transgenic reporter lines, such as Green Fluorescent Protein (GFP), show excellent fluorescent signal prior to clearing steps. However, reagents used for transitioning tissue to a cleared state often reduce fluorescence levels or quench fluorescence altogether. To circumvent this problem, a variety of different tissue clearing methods have been developed, making use of CLARITY-based methods (i.e., PARS, PACT; Chung and Deisseroth, 2013; Yang et al., 2014; reviewed in Vigouroux et al., 2017), aqueous methods (i.e., CUBIC, Scale; Susaki et al., 2015), and non-aqueous methods such as 3DISCO (Belle et al., 2014, 2017; reviewed in Vigouroux et al., 2017), iDISCO (Renier et al., 2014), uDISCO (Pan et al., 2016), and BABB (Ahnfelt-Rønne et al., 2007). While the success of these methods appear to vary by tissue, some indeed show promise for preserving fluorescence for downstream imaging.

Many of the above clearing methods have been established specifically for studies of neural-circuitry or cell-specific analysis in the mammalian brain (Parra et al., 2012; Chung and Deisseroth, 2013; Susaki et al., 2014; Epp et al., 2015; reviewed in Azaripour et al., 2016; Vigouroux et al., 2017). However, the large size of the adult brain of rodent models, can limit imaging options or restrict imaging of the brain to only a specific subregion during a single scan. Unlike the rodent brain, the smaller brain of teleost fishes such as zebrafish and medaka, show exceptional promise as experimental models to visualize spatial changes along the 3-D neuro-axis in adulthood under physiological or compromised states. Having the opportunity to investigate cell dynamics within a 3-D context offers the chance to address novel questions concerning cell-specific behavior, systemic signaling, stem cell niche development, and morphological variation.

The zebrafish, in particular, has become a rising star in the field of adult neurogenesis, plasticity, and regeneration (Kaslin et al., 2008; Kizil et al., 2012; Lindsey and Tropepe, 2014; Lindsey et al., 2014; Than-Trong and Bally-Cuif, 2015; Alunni and Bally-Cuif, 2016; Ghosh and Hui, 2016). Constitutively cycling adult neural stem cells are found across an extensive number of neurogenic compartments along the anterior-posterior (A-P) neuro-axis (Adolf et al., 2006; Grandel et al., 2006; Chapouton et al., 2007), with these cells capable of producing newly regenerated neurons following brain injury (Kroehne et al., 2011; Baumgart et al., 2012; Kishimoto et al., 2012; Kyritsis et al., 2012; Kaslin et al., 2017). With its well mapped neurogenic niches, heterogeneous mixture of adult stem cell populations (Ganz et al., 2010; Lindsey et al., 2012), array of cell-specific transgenic lines, molecular toolbox, and highly conserved genome compared with its vertebrate counterparts, the zebrafish provides an exquisite experimental system to uncover clues governing stem cell dynamics under homeostasis and regeneration. However, there has yet to be developed a straightforward method to label and visualize adult stem cell populations in a 3-D context. While highly transparent zebrafish mutants lacking skin pigmentation, such as *casper* and *crystal*, have been made available in recent years, these lines only benefit imaging of larvae or early juvenile stages (White et al., 2008; Antinucci and Hindges, 2016), but do not mitigate opacity and light scattering in the adult brain. As a result, developing new clearing and imaging methods permitting 3-D visualization of changes in cell proliferation tailored for the adult zebrafish brain are needed. Therefore, the rationale for establishing the protocol described herein was to develop an efficient and feasible method to visualize and analyze actively cycling adult stem cells in their respective niches, in order to understand how they respond at a global scale to brain injury or when shifted from a homeostatic state.

Our protocol describes an 8-step method for sample preparation in advance of Optical Projection Tomography (OPT) imaging. The protocol takes advantage of the small molecular

size of 5-ethynyl-2′-deoxyuridine (EdU) to reliably label cells in the *S*-phase of the cell cycle and uses individual reagents to avoid the high cost of the commercial "Click-it EdU kit" for staining (Salic and Mitchison, 2008). Clearing of the entire adult zebrafish brain without loss of EdU fluorescent signal is completed using a combination of benzyl benzoate and benzyl alcohol (BABB, also known as "Murray's reagent"), inexpensive, non-aqueous reagents that have been successfully demonstrated to render tissue transparent (Miller et al., 2005; Zucker, 2006; Short et al., 2010; Gleave et al., 2012, 2013). Unlike many lengthy labeling and clearing protocols for thick tissue, our pipeline allows for the proliferative pattern of samples to be readily visualized and analyzed in less than 10 days using software such as IMARIS or FIJI/IMAGEJ. Moreover, following EdU staining, we highlight that the option of whole brain fluorescent labeling of proteins or transgenic reporter lines can be performed, broadening the applications of this protocol. Finally, we present three analysis methods that can be applied to reconstructed OPT-scanned brain samples that can be completed using FIJI/IMAGEJ. OPT allows fluorescent or non-fluorescent imaging of paraformaldehyde fixed specimens with thicknesses of up to ∼15 mm at near cellular resolution (3.21 um/pixel; Sharpe et al., 2002). Three or more fluorescent channels can be sequentially scanned from ultraviolet to infrared (i.e., 350, 488, 555, 647), in addition to brightfield, that can be reconstructed to obtain a 3-D or 2-D view of brains for manipulation. OPT has the added advantage over many newer microscopy techniques in obtaining isotropic datasets that are designed for 3-D volumetric analysis and morphometrics. Taken together, this protocol is the first of its kind to offer a streamlined method of whole brain imaging in the adult zebrafish brain, with the potential to be applied to other small teleost models (i.e., medaka and killifish) or for imaging using modern light-sheet microscopy.

MATERIALS AND METHODS

All animal experiments were assessed and approved by the Monash University Animal Ethics Committee and were conducted under applicable Australian laws governing the care and use of animals for scientific research. Zebrafish (*Danio rerio*) were maintained in line with standard protocols at the Monash University FishCore.

Medaka (*Oryzias latipes*) stocks were maintained at the Institute of Toxicology and Genetics (ITG) of the Karlsruhe Institute of Technology (KIT). Animal husbandry and experimental procedures were performed in accordance with local and European Union animal welfare standards (Tierschutzgesetz 111, Abs. 1, Nr. 1, AZ35-9185.64/BH). The facility is under the supervision of the local representative of the animal welfare agency.

A summary of the workflow for parts 1–8 is shown in **Figure 1A** along with representative images of specific steps in the protocol. To facilitate laboratories in adopting this protocol, we have additionally designed a video demonstrating these key steps and procedures (**Supplementary Video 1**).

PART 1: Labeling Proliferating Cells Using EdU

1.1 Prepare a 10 mM stock of 5-ethynyl-2′-deoxyuridine (EdU) by combining 50 mg of EdU powder (ThermoFisher; A10044) and 20 mL of 1X-Phosphase Buffered Saline (1X-PBS, pH 7.4). Use low heat and vortex as required to dissolve powder in solution.

1.2 Prepare 40 μL aliquots in 0.5 mL PCR tubes (Axygen; 70001981) for injection. This volume of EdU is ideal for intraperitoneal injections of animals between 6-months and 1-year. **Note**: If using newly thawed aliquots of EdU, be sure that the EdU powder has not separated out of solution. If so, use low heat and vortex to reconstitute. Always store EdU solution at −20°C away from light until use. Thawed EdU aliquots should be used within 1–2 days.

1.3 Prepare a solution of 0.04% Tricaine (Sigma; E10521): fish water (i.e., aquarium water) to anesthetize fish prior to injection and setup a separate tank of clean fish water to transfer fish post-EdU injection. Be sure to label tanks clearly.

1.4 Setup a Petri dish for intraperitoneal injections under a dissecting microscope with a large working distance or at the bench. **Note:** To facilitate injections, use a Petri dish with plasticine/modeling clay molded to form a trough lined by the blunt ends of two razor blades (**Figure 1B**). This V-shaped holder allows adult zebrafish to be quickly and easily placed ventral side up following anaesthetization for EdU injection, without the need to use dissecting tools to orient and hold the fish.

1.5 Draw up a single 40 μL aliquot of EdU solution using a 30 gauge × ½ inch needle (Terumo) into a 1 mL syringe and ensure no air bubbles are present.

1.6 Place the fish into anesthetic and monitor until breathing has slowed and swimming ceased. This should occur within less than 1-min. **Note:** Depending on the size and age of adult zebrafish, the water may have to be further titrated with Tricaine for optimal concentration.

1.7 Use a plastic spoon to transfer the fish into the Petri dish ventral side up once the fish is anesthetized.

1.8 Inject zebrafish near the ventral-midline intraperitoneally at an ∼45° angle (**Figure 1B**). **Note:** It is critical that when piercing the skin, the needle only descends below the skin and not into the underlying organs as this will cause injury to internal organs and possible death.

1.9 With the needle in position, slowly inject the EdU solution and remove needle. **Note:** When properly injected there should be no blood observed at the injection site. Commonly a slight increase in the volume of the peritoneal cavity is observed.

1.10 Transfer the fish to fresh facility water and monitor that breathing and swimming is restored to normal. This should occur within a few minutes.

1.11 Provide a 2-h chase period (or longer if desired), before the next EdU injection.

1.12 Repeat steps 1.5–1.11 to provide animals with a second 2-h chase period of EdU. This method will provide robust

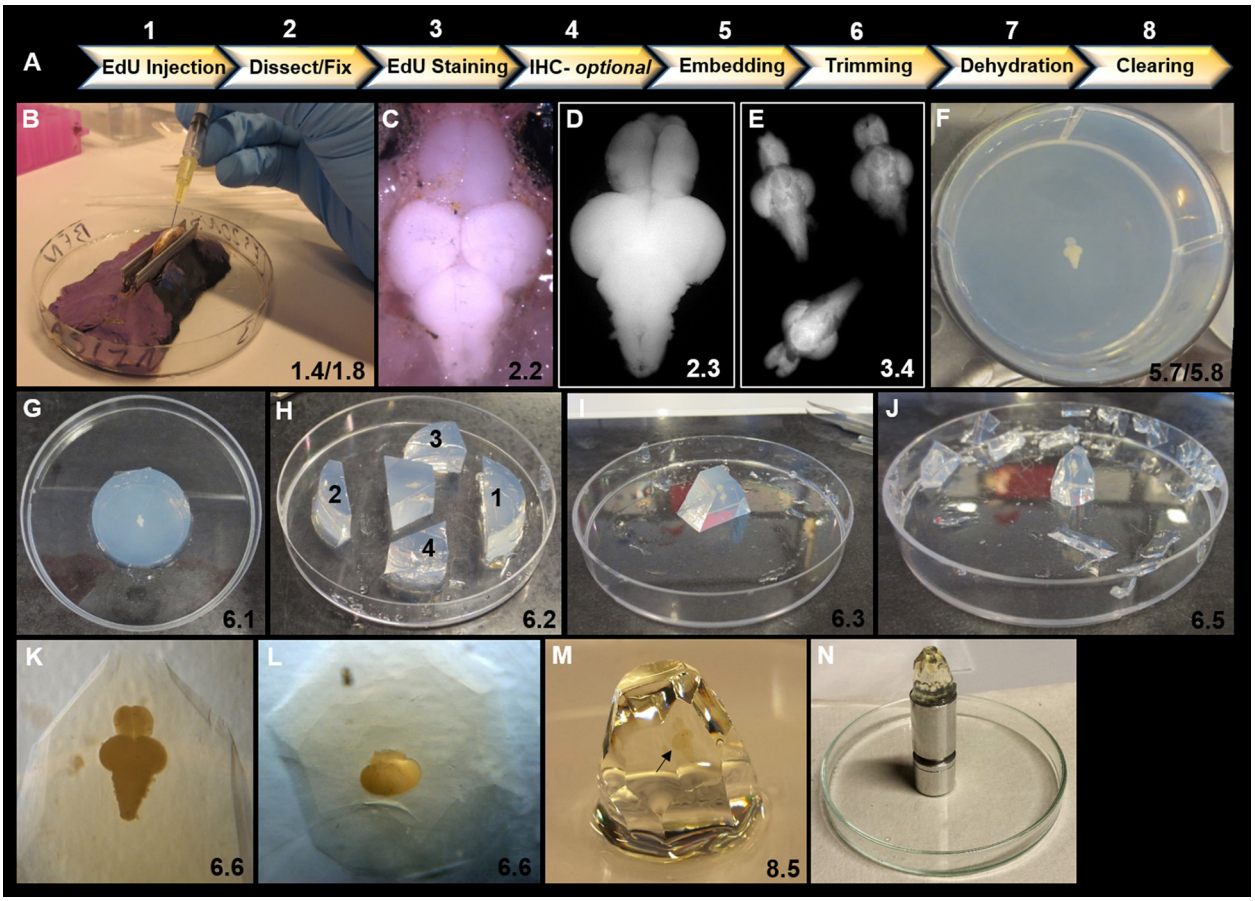

FIGURE 1 | Overview of key steps in sample preparation for optical projection tomography (OPT). **(A)** Summary of 8 step workflow for sample preparation for OPT scanning. **(B)** Intraperitoneal injection of 40 μL of EdU into ventral abdomen of adult zebrafish using a 1 mL syringe and 30 gauge × ½ inch needle. Note the use of V-shaped holder to orient and stabilize the anesthetized specimen during injection. **(C)** Dorsal view of adult zebrafish brain *in situ* prior to excision and fixation. **(D)** Excised adult zebrafish brain fixed in 2% paraformaldyhyde. **(E)** Representative image of three adult brains in EdU staining solution in a 12-well plate. **(F)** Adult brain embedded dorsally and centered in well and in z-plane in low melting agarose in a 6-well plate. **(G)** Low melting agarose cylinder removed from 6-well plate in preparation for trimming. **(H)** Initial trimming using a razor blade to form a trapezoid by 4 sequential cuts: (1) perpendicular to olfactory bulbs, (2) perpendicular to and ~1 cm from spinal cord, and (3 and 4) two lateral diagonal cuts joining 1 and 2 together. **(I)** Trapezoid oriented upright with brain positioned along the long-axis vertically. Olfactory bulbs are localized at the top of the block. **(J)** Trimmed block ready for dehydration and clearing. Notice block is tapered from top to bottom to reduce agarose around brain sample for scanning and to provide a larger base to adhere to mount. **(K–L)** Position of brain within trimmed block viewed under brightfield observed along the long-axis **(K)** and from the dorsal aspect of the block **(L)**. **(M)** Adult zebrafish brain (black arrow) observed *en block* following methanol dehydration and BABB clearing. Note the transparent nature of the brain. **(N)** Sample adhered to an OPT mount in preparation for scanning. In all panels, the corresponding detailed protocol steps are denoted in the bottom right-hand corner.

labeling of all EdU-positive cells in the *S*-phase over the 4-h period prior to sacrifice.

PART 2: Brain Dissection and Fixation

2.1 In a small beaker, sacrifice zebrafish using an overdose of 0.4% Tricaine and ice-cold fish water (aquarium water).

2.2 Carefully dissect out the entire brain, from the olfactory bulbs to the anterior aspect of the spinal cord (**Figure 1C**). Take care to remove any blood, pigment or tissue adhered to the brain, as this will interfere with OPT scanning.

2.3 Transfer clean brains into an ice-cold solution of 2% paraformaldehyde (PFA; Sigma; 158127) diluted in Phosphate Buffer (pH 7.4; **Figure 1D**). **Caution:** PFA is carcinogenic therefore ensure to take proper handling precautions, make solution in a fume hood, and perform dissections in a well-ventilated room. PFA waste should be discarded according to institutional protocols. **Note:** Use glass vials or non-sticky plastic vials to prevent tissue from sticking. Multiple brains can be placed in a single vial for a treatment condition. Continue subsequent steps in glass vials until commencing EdU staining.

2.4 Place samples on a tissue rocker in the dark at 4°C, and rock gently overnight (8–12 h).

PART 3: Rinsing and EdU Staining

3.1 Transfer samples into cooled, syringe-filtered 1X-PBS containing 0.3% Triton X-100 (Tx, Sigma; T9284) and rinse 4 × 30-min in the dark on a tissue rocker at 4°C.

3.2 Transfer brains into a solution of cooled, syringe-filtered 1% Tx/5% dimethyl sulfoxide (DMSO; Millipore; 317275) in 1X-PBS for 24-h in the dark at 4°C on a tissue rocker.
3.3 Rinse brains with cooled, syringe-filtered 1X-PBS-Tx 0.3% 4 × 30-min and leave overnight (8–12 h) on rocker in the dark at 4°C.
3.4 Prepare EdU staining solution at a volume of 3 mL/well using a 12-well plate (Corning, Inc.; 353043). The Alexa Fluor Azide (ThermoFisher) chosen to label EdU-positive cells should be either 555 (red) or 647 (far red), to reserve the 488 (green) channel for autofluorescence scans of brain volume. **Note:** No more than 5–6 brains should be placed in a single well for optimal staining (**Figure 1E**).

Table 1 provides the recipe for making 3 mL of staining solution (enough for a single well of a 12-well plate) from individual reagents (see supplier information in **Table 2**) without the need to purchase the more costly "Click-iT EdU Colorimetric IHC Detection Kit" (ThermoFisher; C10644).

3.5 Decant buffer with brain samples into a Petri dish. Using a plastic transfer pipette, carefully transfer each brain from buffer into the designated well of the 12-well plate (ThermoFisher; 150200). **Note:** Often it is necessary to cut the end of the pipette so that brains are drawn up without damage.
3.6 Using a transfer pipette, remove excess buffer from wells.
3.7 Gently add the EdU staining solution down the sides of the well and stain for 4 consecutive days with gentle agitation in the dark at 4°C.
3.8 Upon completion of staining, rinse tissue continuously with cold 1X-PBS until brains no longer show traces of Azide dye. This normally takes ½-full day of rinsing (4–8 washes).
3.9 Verify staining under a fluorescent dissecting microscope before proceeding to agarose embedding. Staining should be distinct with minimal background.

PART 4: Immunohistochemistry (*Optional*)

In some instances, it may be advantageous to examine changes in cell proliferation (EdU) in association with other proteins or GFP-reporter lines. Outlined below is an exemplary protocol combining EdU labeling in the Tg(mpeg1:gfp) transgenic line that labels resident or infiltrating macrophages (Ellett et al., 2011). However, preliminary experiments should always be done to optimize any immunohistochemistry whole brain labeling for specific transgenic lines or antibodies, as difficulties in tissue penetration or quenching of fluorescence during the dehydration and/or clearing process can occur. From preliminary testing (data not shown), membrane bound reporter lines or small antibodies appear to be good candidates for whole brain labeling.

Whole-Brain Labeling of Green-Fluorescent Protein (GFP) in the Tg(mpeg1:gfp) Line

4.1 Following EdU labeling and rinsing, transfer tissue to new, clean wells of the 12-well plate to commence immunohistochemistry. All steps should be done at 4°C in the dark on a tissue agitator/rocker.
4.2 Block samples in a cooled, syringe-filtered, solution of 1X-PBS with 0.3% Tx, 2% normal goat serum (Sigma; G9023), and 1% bovine serum albumin (Sigma; A7906) for 8-h.
4.3 Incubate brains in the primary antibody, rabbit-anti-GFP (ThermoFisher; A11122) diluted 1:500 with blocking solution (above) for 7-days.
4.4 Rinse samples in 1X-PBS-Tx 0.3% for 4 × 1-h.
4.5 Incubate brains in the secondary antibody, goat-anti-rabbit Alexa 555 (ThermoFisher; A21429) diluted 1:750 with 1X-PBS-Tx 0.3% for 7-days.
4.6 Rinse samples in 1X-PBS-Tx 0.3% for 4 × 1-h.
4.7 Verify staining under a fluorescent dissecting microscope before proceeding to agarose embedding. Staining should be distinct with minimal background throughout the brain tissue (dorsal or cross-sectional view) if successful.

PART 5: Tissue Embedding

5.1 Prior to embedding, wash samples with double distilled Milli-Q water, 3 × 30-min to remove any excess salt from 1X-PBS rinses.
5.2 Combine low melting agarose (Sigma; A9414) with water to yield a 1% solution (Combes et al., 2014). Typically, 0.25 g/25 ml is sufficient for a single well of a 6-well plate (Corning, Inc.; 353046). Heat solution gradually in a flask using a microwave until dissolved. **Caution:** Solution will be extremely hot once dissolved, therefore use proper handling equipment.
5.3 Cool agarose solution under tap water until flask can be comfortably touched to wrist.
5.4 Once cooled, pour solution into a 50 mL Luer lock syringe with a 0.45 μm syringe filter membrane attached and filter solution into wells. Fill each well just below the brim.

TABLE 1 | Recipe for 3 mL of EdU staining solution.

Reagent	Volume
1X- PBS (pH 7.4)	2,241 μL
0.5 M L-Ascorbic acid (dissolved in Milli-Q water)	600 μL
2M Tris buffer (pH 8.5)	150 μL
100 mM Alexa Fluor Azide (dissolved in DMSO)	6 μL
1M Copper Sulfate ($CuSO_4$)	3 μL
Total volume	3 mL

TABLE 2 | Reagent specifications to make EdU staining solution.

Reagent	Supplier	Item #
L-Ascorbic acid	Sigma	A5960
Trizma base	Sigma	T6791
Copper (II) Sulfate	Sigma	C1297
Alexa Fluor 555 Azide	ThermoFisher	A20012
Alexa Fluor 647 Azide	ThermoFisher	A10277
Alexa Fluor 488 Azide	ThermoFisher	A10266

5.5 Monitor the temperature of agarose in wells with a thermometer. Temperature must reach ∼30°C or below before brains are transferred. **Note:** Use a bed of ice to speed up cooling process. Be sure that the temperature does not drop much below 30°C or brain samples cannot be properly oriented as agarose will start solidifying.

5.6 Insert each brain into a single well using a cut plastic transfer pipette or cut pipette tip of a 1,000 μL micropipette. Brains should be placed down one side of the well with as little buffer as possible.

5.7 Use long fire-polished glass Pasteur pipettes (or other) to manipulate each brain sample and orient dorsal side up. **Note:** The goal is to situate samples in the middle of the well (i.e., between top and bottom and in the center; **Figure 1F**). For best imaging tissue should be embedded along the long-axis. For adult zebrafish brains this means that the A-P neuro-axis is oriented vertically when the block is standing up and when mounted for scanning. This method provides less variability in the depth of tissue through which light must pass as the sample is being imaged around 360°.

5.8 Allow agarose to set for a minimum of 1-h at 4°C in the dark (**Figure 1F**). **Note:** The protocol can be paused here.

PART 6: Trimming

6.1 Use the back of a scalpel blade to cut around the agarose cylinder and place it onto a clean glass or plastic surface for trimming (**Figure 1G**).

6.2 With the agarose cylinder in the same orientation as in the 6-well plate (i.e., brain dorsal side up), use a razor blade to make 4 initial cuts to form a trapezoid (**Figure 1H,** labels 1–4).

1. The short side of the trapezoid should be made 1 cm from the anterior aspect of the olfactory bulbs, by making a straight cut perpendicular to the bulbs.
2. The long side of the trapezoid should be made at least 1.5 cm from the posterior aspect of the spinal cord, cutting perpendicular to brain axis.

3&4. Make a single diagonal cut on the lateral sides of the brain to join cuts 1 and 2.

6.3 Use a scalpel blade to gently orient the block so that the olfactory bulbs are up (i.e., brain should be oriented vertically along the long-axis; **Figure 1I**).

6.4 Next use a clean scalpel blade to trim the block. Start by trimming vertically down each of the four corners.

6.5 Continue around the block until there is ∼5 mm of agarose around the brain and the block tapers to a base of ∼1 cm (size of mount face to which block is glued; **Figure 1J**). The goal is to have an equal amount of agarose around the entire brain for consistent penetration of light during imaging. Ensure the height of the block base (i.e., distance from tip of spinal cord and bottom of block) is no <1 cm when finished, as less than this could lead to the glue interfering with OPT imaging.

6.6 Using a brightfield microscope, verify the orientation of the brain within the trimmed agarose block along the long-axis (**Figure 1K**) and in the vertical plane (**Figure 1L**). **Note:** The protocol can be paused here with samples stored at 4°C in the dark.

PART 7: Dehydration

7.1 Transfer trimmed blocks into labeled 50 mL Falcon tubes. Place no more than 4 samples/tube. **Caution:** Perform all methanol dehydration steps in a fume hood taking proper safety measures. Methanol waste should be discarded according to institutional protocols.

7.2 For a single block, fill tube with 25 mL of 100% HPLC grade methanol to dehydrate tissue. If preparing multiple blocks fill to 50 mL. The same Falcon tubes can be used for all subsequent dehydration and clearing steps. **Note:** Label tubes well with a non-removal marker (i.e., china marker), since labels can be easily lost by methanol or BABB exposure.

7.3 Place tubes in the dark at room temperature on a tissue rocker for 4-h. **Note:** To prevent any solution leaking onto the tissue rocker, place the tubes into a secondary plastic container.

7.4 Repeat step 7.2–7.3 with 3 additional methanol changes. If left overnight, this is still considered a single methanol rinse. **Note:** To check if dehydration was successful, take a couple of milliliters of methanol from tissue rinse and mix with BABB in a glass petri dish. If color turns cloudy once mixed tissue is not fully dehydrated and water is left in sample. Consider a further methanol rinse to remove remaining water.

PART 8: Clearing

8.1 Prepare a 2:1 solution of fresh benzyl benzoate: benzyl alcohol (BABB; Sigma: B6630, 402834). **Caution**: BABB is considered hazardous and thus proper safety measures must be taken. Work in the fume hood when making solution and for all subsequent solution changes. BABB solution should be stored out of direct light, and waste discarded according to institutional protocols.

8.2 Using the same tubes as for methanol dehydration, place samples in the first BABB rinse. If previously used BABB is available, use this for the first BABB rinse. Otherwise, use new BABB. **Note:** Previously used BABB can only be used for the first rinse. Thereafter, fresh BABB must be used for proper clearing.

8.3 Place tubes in the dark at room temperature on a tissue rocker for 4-h. **Note:** To prevent any solution leaking onto the tissue rocker, maintain tubes in the secondary plastic container.

8.4 Repeat steps 8.2–8.3 with 3 additional BABB changes. If left overnight, this is still considered a single BABB rinse.

8.5 Upon completion of BABB rinses, verify that the expected staining pattern is observed under a fluorescent dissecting microscope before proceeding to OPT scanning. **Note:** Properly cleared brain samples should appear nearly transparent *en block* under bright light compared to before dehydration and clearing steps (**Figure 1M**).

8.6 Samples should be imaged using OPT within 1–2 days of completion of the above protocol to prevent any fading of fluorescent signal and minimize exposure time during scans.

Comments on Optical Projection Tomography (OPT) Scanning and Post-processing Data Reconstructions for Downstream Visualization and Analysis

The detailed methods of use of the Bioptonics 3001 OPT scanner (Bioptonics, Edinburgh, UK) and Nrecon reconstruction software (Bruker microCT) is beyond the scope of the presented protocol. Nonetheless, below are listed some general guidelines and considerations for scanning cleared adult zebrafish brain tissue, with example parameters of an OPT scan shown in **Table 3**.

OPT Scanning:

1. Provide 20–30 min for blocks to adhere to the OPT mount if using an adhesive (**Figure 1N**). Superglues such as Lock tite and Tarzan grip work well and can be purchased from local suppliers. Note that the types of OPT mounts can vary, and the use of glues and how the block is initially trimmed may require modification.
2. Ensure the BABB in the OPT chamber in which samples are submerged is always clean, as are the sides of the glass chamber.
3. Time should be taken to always properly calibrate the OPT scanner before the first experimental sample is imaged.
4. It is advisable to standardize the magnification at which all samples are scanned.
5. Ensure each channel (i.e., 350, 488, 555, 647) is in focus and that exposure is adjusted so that no "bright spots" are seen on your sample—this will affect post-processing reconstructions. For instance, use a general rule of keeping the exposure for each channel at ∼75% of the maximum, but this must be assessed on a case by case basis. Similar to conventional confocal microscopy, the staining intensity of EdU (or other markers) will vary slightly from sample to sample. However, if downstream analysis is to compare intensity levels under different conditions, appropriate preliminary experiments should be performed to determine consistent parameters for scanning.
6. For scanning, image at least every 0.45° around the 360° axis of the sample. Modifications of this can readily be done, but will influence the length of time to scan a single sample.
7. Averaging can also be applied to each individual channel. When exposure is typically lower than 500 ms, averaging may be advantageous.
8. Upon completion of each scan, use a Data Viewer to review that all frames in the data series were imaged properly before removing sample from the OPT scanner.
9. Samples can be stored in BABB in the dark at room temperature or 4°C for a couple months with EdU fluorescence remaining fairly stable.

Post-processing Data Reconstructions:

1. Reconstruction is done by using the raw OPT files produced from OPT scans.
2. Prior to commencing reconstruction, transfer all raw OPT files onto the PC that houses the reconstruction software. The raw OPT files/channel will have a file size of ∼1.5 GB. Following reconstruction, each dataset/channel will increase to >6 GB so be certain to have sufficient hard drive space on the PC.
3. While processing the raw OPT files to yield a final reconstructed dataset for each individual channel, ensure that the final reconstruction is crisp and in focus. Final datasets should be in focus when viewed either in 3-dimensions (3-D) or in cross-sectional view. If blurry/fussy, adjust parameters for reconstruction and re-run, or omit from downstream analysis if it remains out of focus.
4. Reconstructed datasets can be loaded into software such as Drishti, IMARIS, or FIJI/IMAGEJ for visualization and quantification. Depending on the settings used during OPT scanning, differences in staining intensity, total volume, or surface area of a marker can be reliably quantified between treatment groups. From experience, for 3-D visualization of single or multiple OPT channels, IMARIS is optimal. However, both IMARIS and FIJI/IMAGEJ provide different quantification methods (2-D or 3-D).

Telencephalic Stab Lesion Assay

Adult fish were anesthetized in 0.04% Tricaine (Sigma) in fish water prior to stab lesion. Stab lesions were performed as described in Kroehne et al. (2011). In brief, a 30 gauge cannula was inserted through a single nostril along the rostrocaudal brain-axis, into the olfactory bulb and finally the caudal aspect of the telencephalic hemisphere. Thereafter, fish were returned to their experimental tank and monitored for normal swimming behavior.

Quantification of Whole Brain EdU Stained Tissue

All quantification methods described below were developed and performed using FIJI/IMAGEJ software to investigate systemic,

TABLE 3 | Example parameters for OPT scanning of EdU and GFP in the Tg(mpeg1:gfp) transgenic line of a 6-month adult zebrafish brain.

Visualization	Staining procedure	OPT laser	Exposure (ms)	Averaging	Rotation	Scan time
EdU	Alexa Fluor 647 Azide	647	∼200	2	0.45°	∼1-h
GFP	1° Rabbit-anti-GFP (1:500)	555	∼150	2	0.45°	∼1-h
	2° Goat-anti-rabbit-Alexa555 (1:750)					
Brain volume	none	488	∼800	None	0.45°	∼40-min

brain-wide changes in EdU labeling following adult telencephalic stab lesion. Original OPT scans were taken at a screen resolution of 1,024 pixels. Analysis methods relied on 16-bit grayscale pixel intensity of EdU in the region of interest (ROI). Pixel intensity ranged from 0 to 65,536 (0 = black; 65,536 = white). Preliminary experiments were performed to standardized the exposure for channels during OPT scans between uninjured and injured brains for downstream analysis. Virtual cross-sections were a depth of 1-pixel each following post-processing and 3-D reconstruction of brains, resulting in 1,024 slices through the A-P brain axis.

Histogram Analysis

To examine changes in cell proliferation across the A-P neuro-axis of the adult zebrafish brain under homeostasis and following lesion, we developed an analysis method allowing us to plot the histogram of EdU intensity (**Figure 4A**). 3-D reconstructed, EdU-stained brains were virtually sectioned through the horizontal plane, and a final maximum projection obtained. A threshold mask, was next overlapped on all non-black pixels only and the brain segmented along its A-P axis into individual 20 μm segments. Since all animals were age-matched, a near equal number of segments was derived from each brain for comparison. From each segment, the mean pixel intensity was calculated as a representation of the mean EdU intensity within the segment. The mean EdU intensity per like-segment was then calculated across biological samples and plotted as a histogram for control and lesioned conditions or as the percent change from control levels.

Structure Analysis

To quantify systemic changes in the amount of EdU-positive staining in structures of the lesioned brain compared to control, we developed an analysis method targeted to large tissue depths (**Figure 5A**). ROI's in structures across the brain axis, both proximal and distal to the site of lesion were analyzed, however, only a subset of the data is displayed. For each ROI, the pixel depth in the z-axis was determined, and then converted to 16-color pixel bins. The 16-color pixel bins divided the 65,536 intensity range of pixels into bins of 4,096 each, designated by progressively warmer colors. We then calculated the total number of pixels within each bin and converted pixels into voxels. Pixel size ranged between ∼4.5 and 5 μm, with associated voxel size ∼91–125 μm^3 across brain samples. The underlying hypothesis was that more non-black pixels should be observed in cases where more EdU labeling was present. This approach provided us with 15 non-black bins for downstream analysis of changes in EdU volume within a defined brain structure. For individual biological samples, the pixel count was summed across the 15 bins and converted to volume (μm^3). The mean volume was then calculated across biological samples in the same ROI, upon which statistical analysis was performed.

Slice Analysis

To reliably quantify changes in EdU-positive labeling in distinct adult stem cell niches throughout the brain post-injury, we devised a slice analysis method that sampled EdU volume every 5th section along the z-axis of the neurogenic compartment (**Figure 6A**). This method was developed to avoid EdU labeling of immune cells (i.e., neutrophils, macrophages) that are activated post-lesion and recruited near the site of injury. Following selection of the ROI's for analysis and determination of its z-depth in pixels, in every 5th section the stem cell niche was demarcated by hashed lines, converted to 16-color pixel bins as previous, and the total number of pixels/bin extracted. We next summed all pixels across slices in subsets of non-black bins (e.g., 4,096–12,288) of each biological sample. These values were then converted to voxels to represent EdU volume and the final mean calculated across biological replicates for statistical comparisons.

Larval EdU Labeling and Imaging

Larvae (Tubingen) were housed according to standard protocols. Larvae were transferred into a 50 ng/uL EdU solution with 1% dimethyl sulfoxide (DMSO) in 1x Ringer's media and incubated for 12-h at 28.5°C. At 3-, 5-, and 7-dpf (days post fertilization) animals were sacrificed by an overdose of 0.04% Tricaine, then immediately fixed overnight in ice-cold 4% PFA in 0.1 M phosphate buffer (pH 7.4). Following 1X-PBS rinses, the dorsocranial skin overlaying the brain was removed from larvae for subsequent EdU labeling. Samples were incubated in EdU staining solution as described above for 30-min in the dark at room temperature with gentle rocking. Thereafter, larvae were rinsed then incubated for 30-min in a 1:5,000 solution of 4,6-Diamidino-2-phenylindole (DAPI) for counterstaining. Brains were next excised, washed, and placed through an ascending glycerol series (30%➔50%➔70%), before finally being whole-mounted for confocal imaging in 70% glycerol. Samples were imaged using a Leica TCS SP8 inverted confocal laser scanning microscope equipped with a Leica HyD hybrid detector. Acquisition was performed in 1 μm z-steps using a 20X oil-immersion objective at 1,024 resolution. Acquired z-stacks were visualized in 3-D using IMARIS software.

Statistical Analysis and Data Representation

Statistical analyses and data representation were completed using GraphPad Prism 7. One-way ANOVA was used to compare differences in EdU-positive labeling between the control group and 1-, 3-, and 7-day post lesion (dpl). Where a significant difference was reported, Tukey's *post-hoc* test was applied with significance accepted at $p < 0.05$. All data are represented graphically as either EdU intensity (histogram analysis) or EdU volume (μm^3; structure and slice analysis). All data shown represent mean + standard error of the mean (S.E.M.).

RESULTS

EdU Labeling Is Successfully Visualized Throughout the 3-Dimensional Axis of the Adult Brain

The protocol outlined here successfully demonstrates the ability to label proliferating cells in the whole adult zebrafish brain

with only a short 4-h pulse of the *S*-phase marker, 5-ethynyl-2′-deoxyuridine (EdU; **Figures 2A–C**). OPT scans of EdU injected adult fish show consistency of labeling across constitutively proliferating stem cell populations residing in adult neurogenic niches along the neuro-axis (**Figures 2B,C**; **Supplementary Video 2**). Combining this sample preparation with isotropic imaging by OPT permits near cellular resolution of actively cycling cells that can be visualized in 3-dimensions or by section for analysis (**Figure 2D**). The intense labeling of EdU primarily observed along the midline of the brain where adult stem cell niches reside, closely mimics the proliferative pattern previously shown by standard immunohistochemistry performed on cryosections (Lindsey and Kaslin, 2017). For instance, the specificity of EdU labeling in the dorsal forebrain adjacent the ventricle in virtual cross-sections from our OPT pipeline are consistent with immunolabeling using the common proliferative marker, Proliferating Cell Nuclear Antigen (PCNA) in this same domain (compare **Figure 2E** inset with **Figure 2G**). However, suboptimal EdU labeling and OPT scanning can result in sections that are over-exposed, such as shown in **Figure 2F** (white arrows) in the forebrain ventral midline, and give rise to poor reconstruction post-OPT imaging. Output such as this considerably impairs analysis of EdU using either intensity or volumetric analyses, and therefore such samples should be re-examined or omitted. Since OPT scanning is performed using 1,024 pixels, following reconstruction brains stacks have a depth of 1-pixel each. When considering downstream analyses, it is important to visualize datasets in cross-section to confirm the expected staining pattern, assess for over-exposure and that reconstructions were completed properly. This can be verified immediately using dataset reconstruction software (i.e., NRecon) or using programs such as IMARIS. Additionally, by taking advantage of the autofluorescence of brain tissue, OPT scanning in a channel not reserved for a specific marker (here the 488 laser), allows users to obtain the volume of the brain (or shell) that can be visualized independently for morphometric analysis (**Figure 2H**) or overlaid with the EdU-specific channel using IMARIS software (**Figures 2I–K**). These samples can be visualized in the plane of choice from either the 3-D reconstructed (**Figure 2I**) or rendered (**Figures 2J,K; Supplementary Video 3**) dataset. Merging scans taken of the brain shell with EdU scans is valuable to define the neuro-anatomical localization of EdU patterns under healthy or diseases states.

Immunohistochemistry Can Be Performed on EdU-Labeled Brains but Optimization Is Critical

The ability to observe cell-specific reporter lines or proteins of interest throughout the adult brain alongside proliferative patterns is beneficial to explore interactions between different cell types or changes in the proliferative status of a given population. While a secondary focus of our study and an optional step in the current protocol, presented here are some examples of successful immunostaining accomplished at different stages of the EdU sample preparation pipeline. It is strongly encouraged that optimization of each individual transgenic line or protein is completed prior to implementation with this protocol. Immunohistochemistry (IHC) labeling is performed post-EdU staining. Brains require 1-week incubation in primary and secondary antibodies for reasonable fluorescent labeling through the entire depth of the adult brain. We demonstrate that co-labeling of EdU with the commonly used glial marker, glutamine synthetase (GS), can be accomplished using our OPT pipeline (**Figure 3A**) and that this antibody displays the same labeling pattern observed in cryosections (**Figures 3B,C**). In cases where GFP reporter lines are utilized it is important that antibody labeling (**Figure 3D**) parallels the endogenous pattern of GFP reporter expression (**Figure 3E**) during sample preparation for OPT scanning, and resembles GFP reporter expression in sectioned tissue (**Figure 3F**). It is advisable to verify IHC staining patterns prior to sample embedding, dehydration, and clearing, by cutting through the thickest section of the brain after the 2-week incubation, and in a region where the pattern of staining is well-known. It is not uncommon for some primary antibodies to work well and others poorly in whole brain IHC (**Figure 3G**). Most critical however, is that the fluorescent signal is maintained following the dehydration and clearing steps to allow successful OPT imaging of fluorescent channels. Poor antibody labeling during whole brain staining may be a consequence of many factors, but often can be visually detected by limited penetration into the parenchyma of tissue (**Figure 3G**), unsuccessful labeling of an antibody (**Figure 3H**), or quenching from the dehydration and clearing process (**Figure 3I**). Nonetheless, when IHC labeling protocols are optimized for transgenic lines in combination with EdU labeling, it is possible to readily observe systemic changes in distinct cell populations of interest. For example, performing whole brain EdU labeling in the Tg(mpeg1:gfp) transgenic line specific to tissue macrophages under homeostasis and post-telencephalic injury, one can detect a global increase in the intensity of both EdU and immune cell staining at 1-dpl throughout the lesioned hemisphere (yellow asterisk) that returns near baseline by 7-dpl (**Figures 3J–L**; dpl, days post lesion).

Reconstructed OPT Datasets Can Easily Be Analyzed Using FIJI/IMAGEJ Software

Numerous methods of quantification can be used to analyze OPT datasets. Here, we present three analysis methods we developed and performed using FIJI/IMAGEJ from reconstructed OPT datasets to interrogate changes in EdU intensity or volume across the neuro-axis and within distinct structures or proliferation zones of the brain. By using non-black pixel intensity as a direct proxy of EdU intensity along the A-P axis of the adult brain (**Figure 4A**), our *Histogram Analysis* results demonstrate the ability to create a baseline/reference profile of cell proliferation and to monitor how this profile is perturbed following forebrain telencephalic lesion (**Figures 4B–G**). For example, during constitutive cell proliferation peaks in EdU intensity are closely associated with adult proliferative zones along the ventricular system (**Figure 4B**). One of the most conspicuous peaks in EdU intensity is observed in the midline forebrain (Fb) niche (proliferation zones 2 & 3 in Grandel et al., 2006),

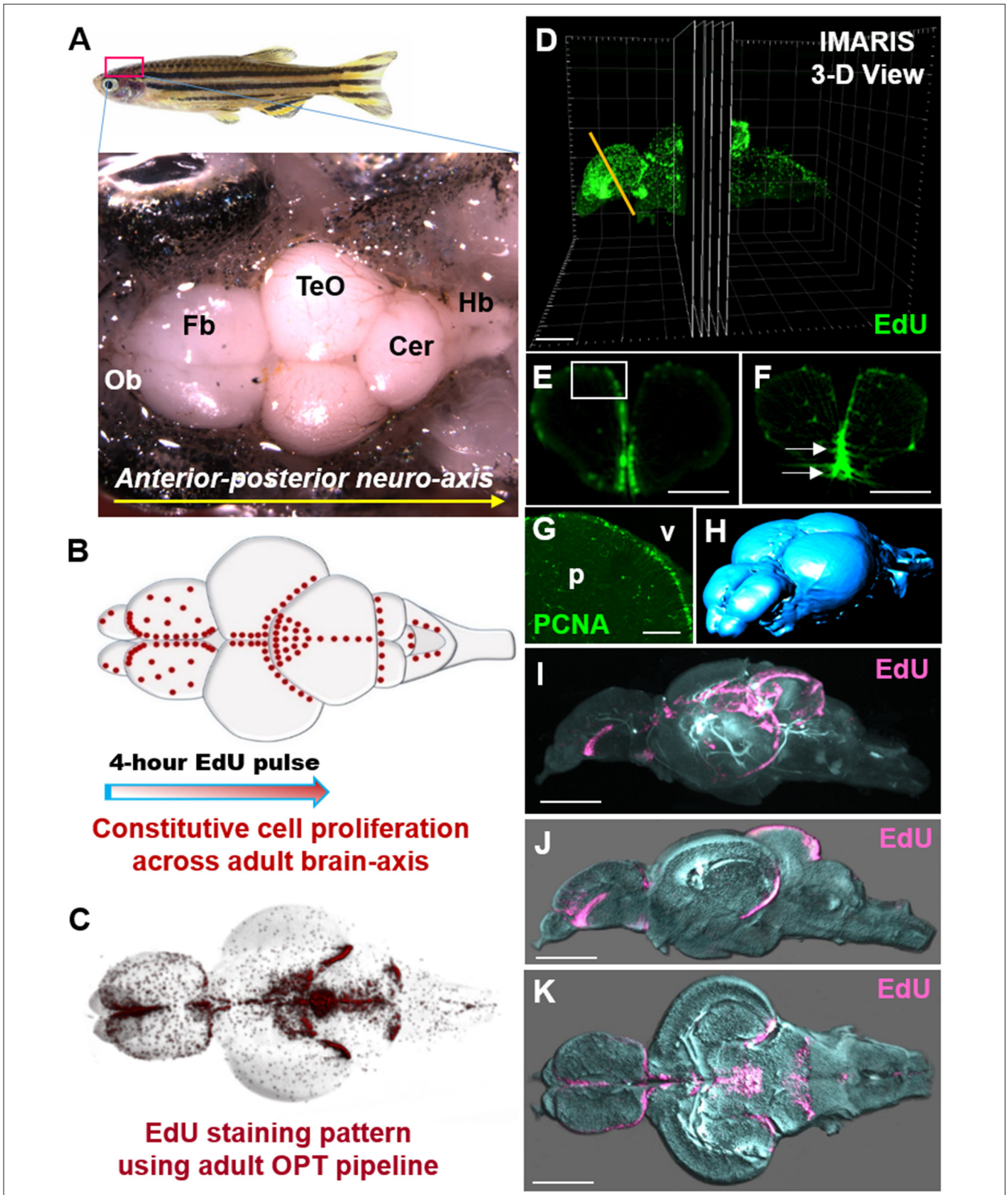

FIGURE 2 | Whole brain EdU labeling and 3-dimensional OPT scanning recapitulates the constitutive pattern of cell proliferation in the adult zebrafish brains. **(A)** Dorsal view of adult zebrafish brain displaying major structures along the A-P neuro-axis. Ob, olfactory bulbs; Fb, forebrain; TeO, optic tectum; Cer, cerebellum; Hb,

(Continued)

FIGURE 2 | hindbrain. **(B)** Schematic dorsal view of adult brain showing the known constitutive pattern (Kaslin et al., 2008) of cell proliferation (red dots) along the brain axis following a 4-h EdU chase. **(C)** Dorsal view of EdU staining using our adult OPT pipeline demonstrating the same labeling pattern across the brain axis as in **(B). (D)** Example of IMARIS 3-D visualization output of an adult EdU injected brain (green) illustrating the ability to visualize or analyse regions of interest in cross-section (or other planes). Yellow line depicts level of telencephalic cross-section shown in **(E,F). (E,F)** Cross-sections through the adult zebrafish telencephalon showing examples of optimal (**E**; near cellular resolution) and suboptimal **(F)** EdU staining (green)/OPT imaging along the periventricular neurogenic niche following data reconstructions. White box in **(E)** denotes dorsal telencephalic domain shown in **(G)**. White arrows in **(F)** show EdU that was over-exposed during scanning, while the slightly fussy image indicates that the post-processing software reconstruction was of poor quality. **(G)** Antibody labeling using Proliferating Cell Nuclear Antigen (PCNA) displaying the homeostatic pattern of cell proliferation at the dorsal telencephalon from cryosectioned, confocal-imaged tissue. Note that labeling is restricted to the stem cell niche adjacent the forebrain ventricle (v) with little to no staining within the parenchyma (p). **(H)** Anterior-dorsal view of iso-surface rendered adult brain (blue) using IMARIS software derived from initial OPT autofluorescence scans of brain contour. **(I–K)** Constitutive brain EdU labeling (pink) across the neuro-axis merged with an autofluorescence scan of brain morphology/volume (pale blue) shown in mid-sagittal **(I,J)** and horizontal **(K)** views. In **(J,K)** images were rendered in IMARIS. Scale bars: **(E,F)** = 300 μm; **(G)** = 150 μm; **(D,I–K)** = 500 μm.

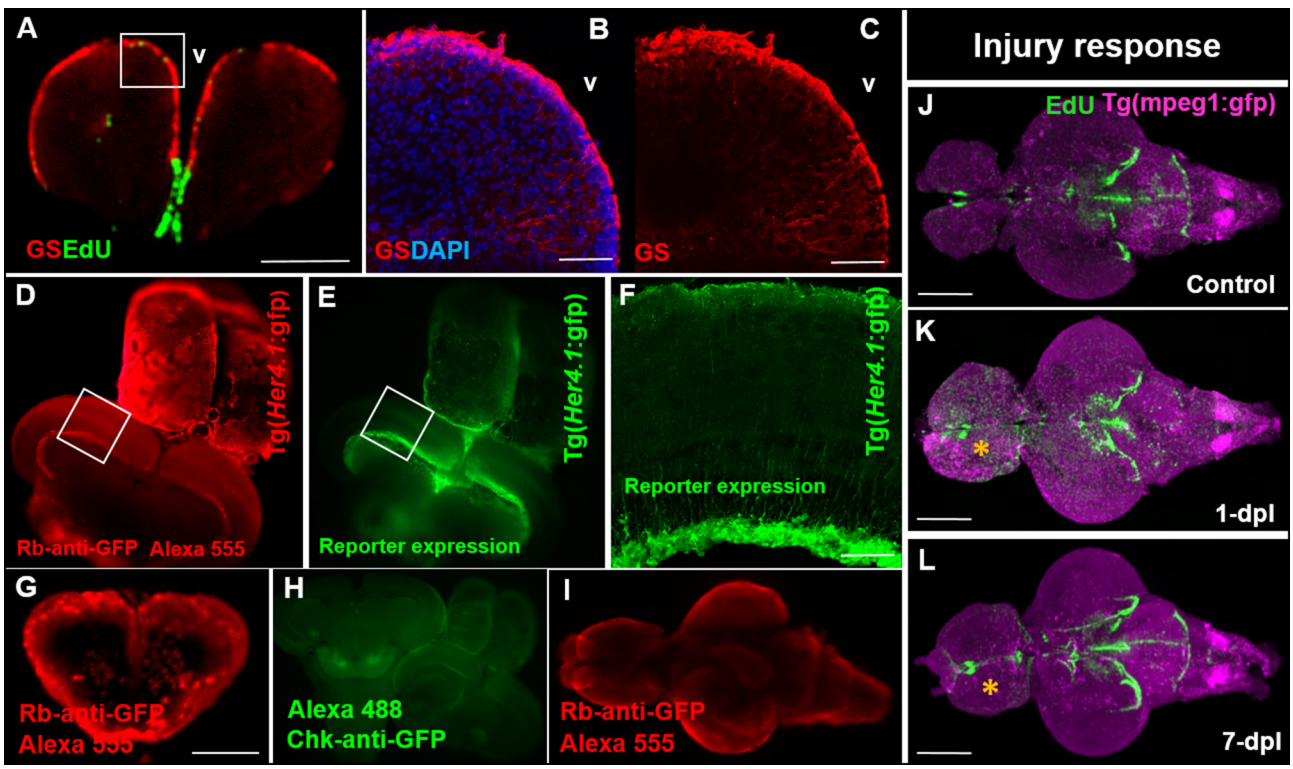

FIGURE 3 | Compatibility of immunohistochemistry with OPT pipeline. **(A)** Successful double-labeling and OPT scanning of EdU (green) and the glial marker, glutamine synthetase (GS; red) in the adult zebrafish forebrain. White box denotes images shown in **(B,C)**. **(B,C)** Co-labeling with DAPI (blue; **B**) and single **(C)** antibody labeling of GS (red) in cryosectioned, confocal-imaged tissue confirming the specificity of GS labeling shown using our OPT pipeline. **(D,E)** Whole brain immunohistochemistry in the adult zebrafish using a rabbit-anti-GFP primary antibody conjugated to Alexa 555 **(D)** recapitulates the same staining pattern seen with the endogenous GFP reporter in the Tg(*Her4.1*:gfp) transgenic line **(E)** prior to dehydration and clearing. White boxes in **(D,E)** depicts location of image displayed in **(F)**. **(F)** GFP-positive staining in the deep quiescent glial layer of the periventricular gray zone of the adult optic tectum shown in cryosectioned, confocal-imaged tissue in the Tg(*Her4.1*:gfp) line mimicking the GFP pattern seen in tissue prepared using our OPT pipeline. **(G–I)** Examples of poor antibody penetration **(G)**, poor immuno-labeling, and **(I)** quenched antibody staining post-OPT imaging using different GFP antibodies. **(J–L)** Adult control brain **(J)** in the Tg(mpeg1:gfp) macrophage line injected with EdU compared with brains post telencephalic lesion (yellow symbol) examined at 1-day post lesion (dpl; **K**) and 7-dpl **(L)** for changes in macrophage distribution (purple) and cell proliferation (green). Scale bars: **A, G** = 300 μm; **B-C** = 150 μm; **F** = 200 μm; **J-K** = 500 μm.

while little staining is observed elsewhere in either telencephalic hemispheres. In the midbrain (Mb) and continuing into the hindbrain (Hb), the observed EdU peaks are a product of a collection of well documented proliferation zones (proliferation zones 7–14). The Mb bin primarily represent proliferation in the hypothalamus, tectum, torus semicircularis and posterior mesencephalic lamina (10–13). The Hb bin primarily represent proliferation in the cerebellum (14). Tracking the forebrain profile of EdU intensity over the first week post-injury shows that at 1-dpl the overall pattern of EdU intensity is elevated along the A-P axis of the forebrain, in particular in the forebrain parenchyma, likely as a consequence of proliferating immune cells (i.e., macrophages, neutrophils) recruited to the site of lesion (**Figure 4C**). Moreover, the EdU profile across all brain segments (i.e., individual points plotted on histograms) of the A-P axis at 1-dpl appear changed as a result of the cumulative

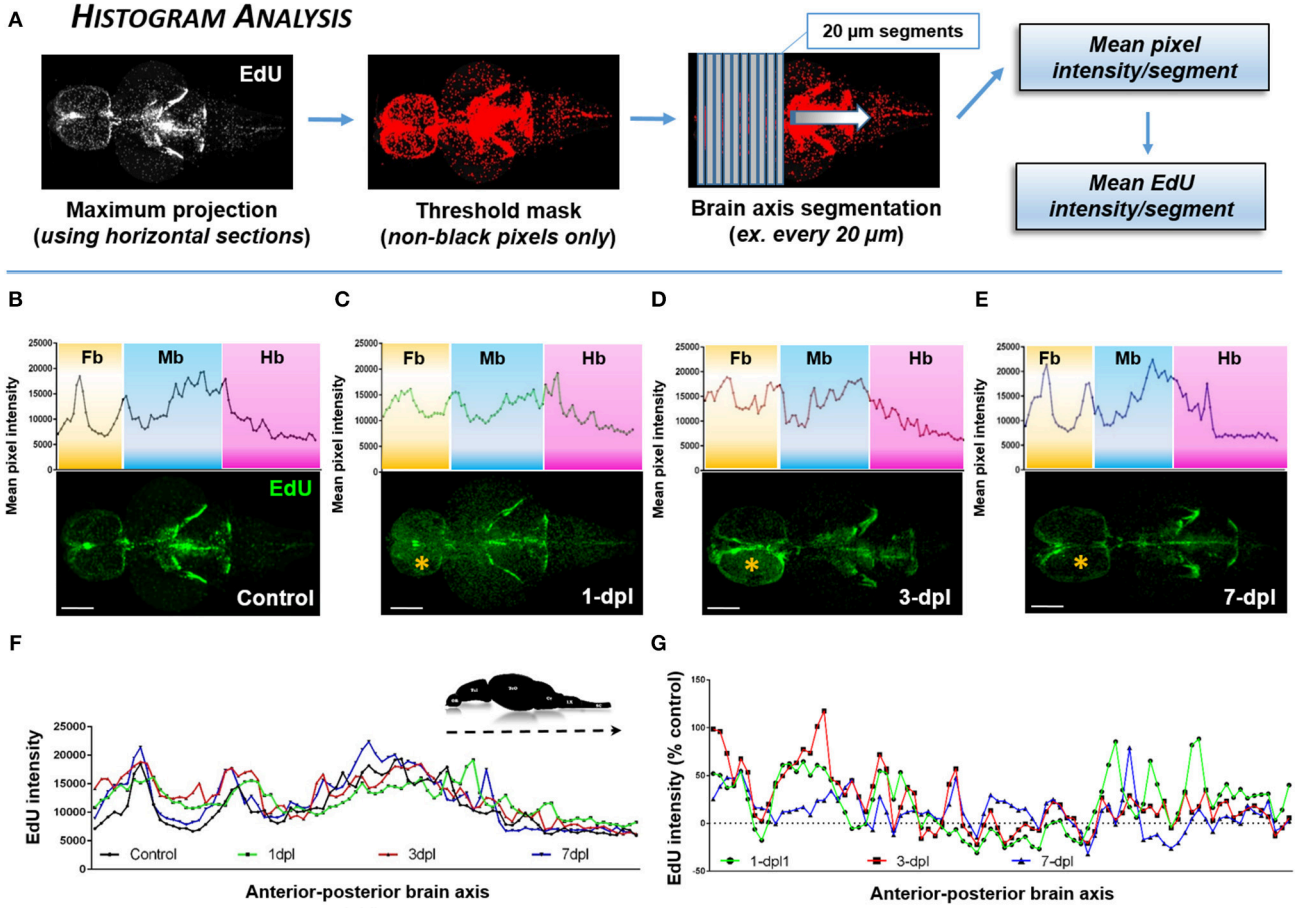

FIGURE 4 | Identifying the proliferative profile across the brain axis following injury using *Histogram Analysis*. **(A)** *Histogram Analysis* workflow using FIJI/IMAGEJ showing a maximum projection derived from horizontal sections and overlayed with a threshold mask to detect only non-black pixels. By segmenting the brain along the A-P axis the mean pixel intensity/segment can be used to represent the mean EdU intensity/segment. **(B–E)** Mean pixel intensity of EdU per segment plotted as a histogram across the brain axis displaying conspicuous peaks in brain regions where greater EdU labeling (green) is present shown in control (**B**; $n = 5$ brains) and 1-dpl (**C**; $n = 4$ brains), 3-dpl (**D**; $n = 4$ brains), and 7-dpl (**E**; $n = 5$ brains) treated animals. The yellow asterisk denotes the lesioned telencephalic hemisphere. Fb, forebrain; Mb, midbrain; Hb, hindbrain. **(F,G)** EdU intensity plotted across the A-P brain axis compared across all groups **(F)** and normalized as the percent change from control **(G)**. Scale bars: **(B–E)** = 500 µm.

difference in EdU intensity staining per segment with injury compared to control levels. By 3-dpl EdU intensity is restricted largely to the lesioned hemisphere (**Figure 4D**; yellow asterisk), whereby at 7-dpl the histogram of forebrain EdU intensity closely resembles the constitutive profile (**Figure 4E**). By plotting all EdU histograms (control, 1-, 3-, 7-dpl) together (**Figure 4F**) or representing the data as the percent change from control (**Figure 4G**), we further show the ability to compared major peaks in cell proliferation for statistical analysis across treatments within a defined range of A-P brain segments of interest using our *Histogram Analysis*.

While quantifying the global pattern of change in EdU across the A-P axis (*Histogram Analysis*) is informative to detect the primary domains of the CNS that respond with damage, more specifically examining the systemic effect of EdU in distinct neuroanatomical structures (Structure Analysis) or niches (Slice Analysis) provides more precise data of how an individual region is modulated. By designing two quantification methods that rely on the voxel size of non-black pixels, our results reveal that using voxel size as a direct readout of EdU volume is a statistically reliable method to compare changes in regions of interest (ROI) between control and lesioned adult brains. Using *Structure Analysis* (**Figure 5A**), where the EdU volume within the z-depth (i.e., multiple slices) of a ROI is analyzed we show that similar to our previous findings in sectioned tissue (Kroehne et al., 2011), a statistical increase in EdU cell proliferation is present at 1-dpl and 3-dpl compared to control in the lesioned hemisphere (**Figures 5B,C**; One-way ANOVA; tukey's *post-hoc* tests for multiple comparisons; $p < 0.05$). Furthermore, we demonstrate for the first time that a similar statistical increase in cell division is present at 1-dpl in the unlesioned telencephalic hemisphere (**Figures 5D,E**), rostral tectum of the midbrain (**Figures 5F,G**), and hindbrain cerebellum (**Figures 5H,I**; One-way ANOVA; tukey's *post-hoc* tests for multiple comparisons; $p < 0.05$), indicating that lesion-induced signals are far-reaching throughout the brain axis and promote structure specific changes

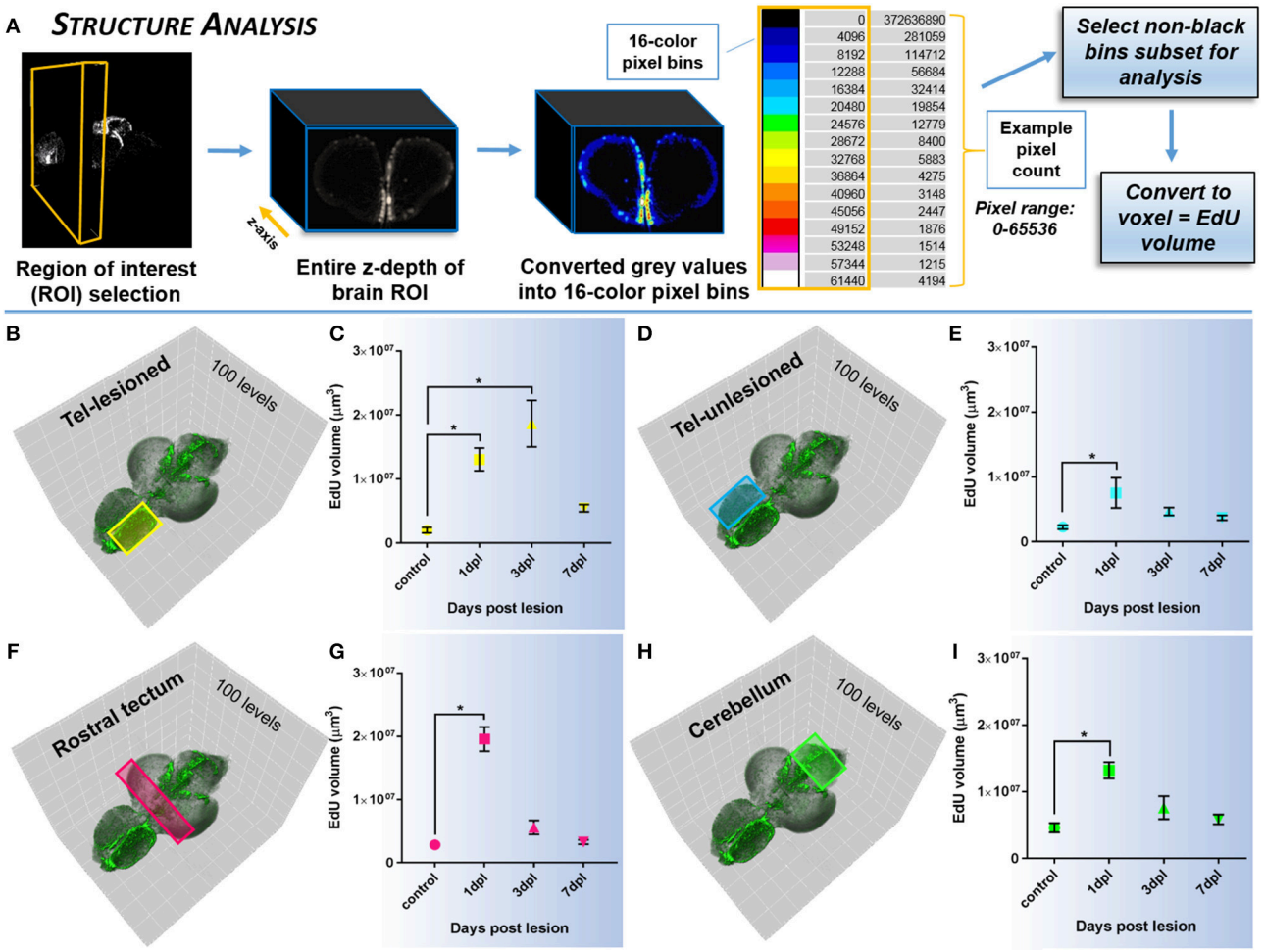

FIGURE 5 | Investigating systemic changes in cell proliferation within major brain subdivisions following brain injury using *Structure Analysis*. **(A)** *Structure Analysis* workflow using FIJI/IMAGEJ showing z-depth of brain region of interest converted from grayscale to 16-color pixel bins to obtain pixel counts/non-black bins for final analysis of EdU volume in voxels. Cross-sectional view shown is from the forebrain telencephalon. The 16-color pixel bins are arranged from cooler to warmer colors, indicating greater pixel intensity values at the upper end of the pixel range. **(B–I)** Proliferative response across four major adult brain structures compared to control in the adult zebrafish brain at 3 time-points (1, 3, 7-dpl) following telencephalic lesion. Brain structures analyzed are indicated by colored rectangles overlayed on 3-D rendered adult zebrafish brains at 3-dpl (EdU, green). For all structures a total of 100 pixel levels through the A-P axis were used for quantification, with *Structure Analysis* performed on all 15 non-black pixel bins. **(B,C)** Lesioned telencephalic hemisphere (yellow; $n = 5$–10 brains/group) displaying a significant increase in EdU volume compared to control at 1-dpl and 3-dpl. **(D–I)** Unlesioned telencephalic hemisphere (**D,E**; blue; $n = 6$–10 brains/group), rostral tectum (**F,G**; pink; $n = 4$–10 brains/group), and cerebellum (**H,I**, green; $n = 4$–10 brains/group) showing a significant increase in EdU volume from control at 1-dpl. *Significance was accepted at $p < 0.05$; One-way ANOVA, Tukey's *post-hoc* test for multiple comparisons.

in cell cycle kinetics. However, applying the same volumetric EdU quantification in 1-pixel thick slice intervals in defined proliferative/neurogenic zones (pink hashed lines) along the A-P axis of the brain using our *Slice Analysis* (**Figure 6A**) exhibited variation in EdU volume within stem cell niches residing in the same structures analyzed previously. We reported significant increases in EdU volume at 3-dpl and 1-dpl in the lesioned (**Figures 6B–G**; yellow circle) and unlesioned (**Figures 6H–M**) telencephalic hemispheres, respectively (One-way ANOVA; tukey's *post-hoc* tests for multiple comparisons; $p < 0.05$), but no change at any time post-injury in the optic tectum (**Figures 6N–S**) and cerebellum (**Figures 6T–Y**) compared to control (One-way ANOVA; tukey's *post-hoc* tests for multiple comparisons; $p > 0.05$). The difference in EdU volume between *Structure Analysis* and *Slice Analysis* likely reflects quantification of both the stem and immune cell response in the former, while during *Slice Analysis* we specifically targeting the neurogenic zones where mostly stem cells reside.

Whole Brain OPT Scanning as a Tool to Understand Stem Cell Niche Development and for Detecting Changes in Brain Morphology

How cell proliferation during early brain growth leads to the adult pattern of proliferative/neurogenic zones remains largely unexplored. Here we show that by taking advantage of the transparency of the larval zebrafish brain for whole brain confocal imaging of EdU (**Figures 7A–C**) and the application

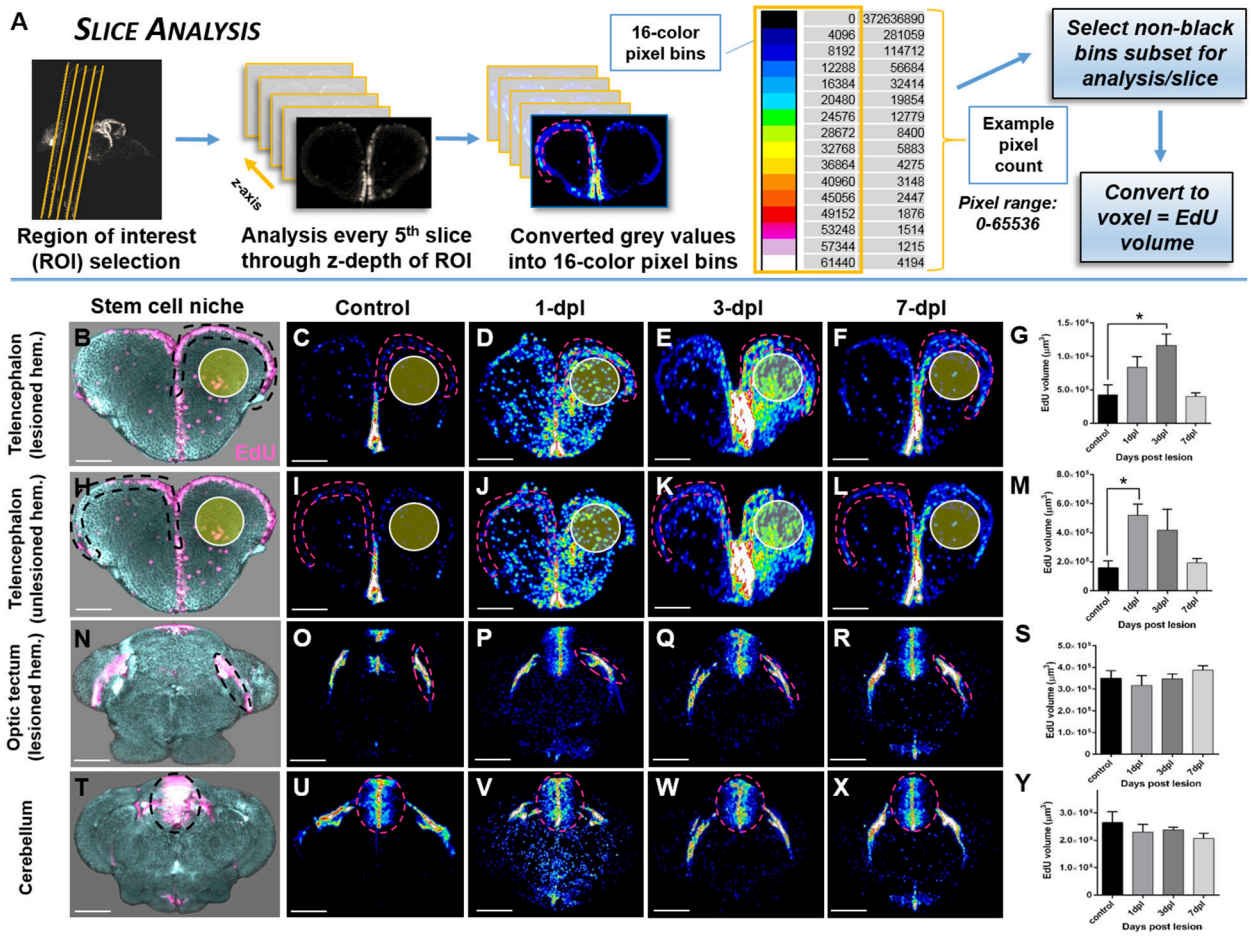

FIGURE 6 | Investigating systemic changes in adult stem cell niche proliferation following brain injury using OPT *Slice Analysis*. **(A)** *Slice Analysis* workflow using FIJI/IMAGEJ showing every 5th pixel slice converted from grayscale to 16-color pixel bins to obtain pixel counts/non-black bins for final analysis of EdU volume in voxels. Cross-sections shown are from the forebrain telencephalon, with pink hashed lines denoting an example sub-region for analysis. The 16-color pixel bins are arranged from cooler to warmer colors, indicating greater pixel intensity values at the upper end of the pixel range. **(B–Y)** Proliferative response across four major adult stem cell niches compared to control in the adult zebrafish brain at 3 time-points (1, 3, 7-dpl) following telencephalic lesion. The site of lesion is denoted by the yellow circle. Hashed lines demarcate the stem cell niche quantified using *Slice Analysis*. **(B,H,N,T)** Representative 3-D rendered images from OPT datasets displaying stem cell niches denoted by EdU staining (pink). All other image panels show maximum projections of representative cross-sections converted to 16-color (FIJI look up table, LUT) for analysis of control and lesioned treatments. For analysis, pixel counts derived from only the first 3 non-black bins were used (i.e., 4,096, 8,192, 12,288). **(B–G)** Lesioned hemisphere (ipsilateral; $n = 5$–8 brains/group) of the pallial stem cell niche showing a significant increase in EdU volume from control at 3-dpl. **(H-M)** Unlesioned (contralateral; $n = 5$–8 brains/group) hemisphere of the pallial stem cell niche showing a significant increase in EdU volume from control at 1-dpl. **(N–S,T–Y)** Both tectal (**N–S**; $n = 4$–10 brains/group) and cerebellar (**T–Y**; $n = 4$–7 brains/group) stem cell niches situated more posterior to the site of injury revealed no significant difference at any of time-points post-lesion. *Significance was accepted at $p < 0.05$; One-way ANOVA, Tukey's *post-hoc* test for multiple comparisons. Scale bars: **(B–F,H–L,N–R,T–X)** = 150 µm.

of our EdU OPT pipeline for the juvenile to senescent brain (**Figures 7D–F**) it is possible to seamlessly track how adult stem cell niches develop, how patterns of cell proliferation change, and assess when cells enter a quiescent state by combining additional markers (data not shown). This approach could be fruitful for comparative studies between other leading teleost models to uncover species-specific differences in stem cell niche development and aging. Additionally, performing the present OPT pipeline in teleost models, such as the medaka, whose brain is comparable in size, offers a novel approach to analyse changes in brain morphology across various inbred strains using autofluorescent scans only (Ishikawa et al., 1999; Spivakov et al., 2014). Results of our OPT scans of three different inbred strains of medaka, H05, HNI, and iCab (**Figures 8A–F**), show that differences in the volume of specific brain structures (**Figures 8G,H**) can be detected and quantified for downstream statistical analysis. Combining this morphological analysis with EdU labeling could further uncover how proliferative patterns are related to the development of smaller or larger brain structures, unveiling how genetic variation regulates brain growth over vertebrate ontogeny.

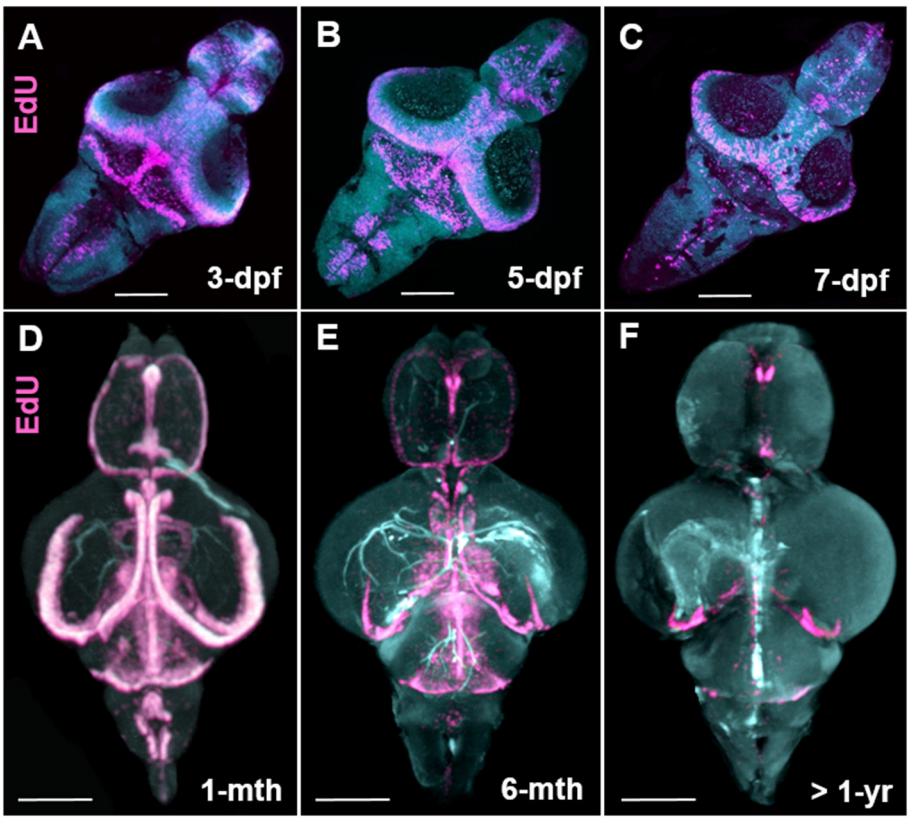

FIGURE 7 | Stem cell niche development over zebrafish ontogeny. **(A–C)** Whole mount EdU (pink) staining and confocal imaging in transparent larvae at 3-, 5-, and 7-dpf visualized in 3-D using IMARIS, displaying the early pattern of cell proliferation throughout the developing zebrafish brain. **(D–F)** Whole mount EdU (pink) staining and OPT scanning in juvenile (**D**), adult (**E**), and senescent (**F**) brains visualized in 3-D using IMARIS, depicting a reduction in constitutive cell proliferation within stem cell niches situated along the A-P brain axis. Dpf, days post fertilization; mth, month; yr, year. Scale bars = 500 μm.

DISCUSSION

Three-dimensional fluorescent macro-imaging of whole organs is becoming commonplace in biology, providing new perspectives on how organs, tissues, and cells develop and respond to trauma or disease (Lupperger et al., 2017; Whitehead et al., 2017). Within the field of neuroscience, the existence of few practical methods to visualize the mature vertebrate brain in a 3-D context has hindered progress in understanding global patterns of change across cell populations following manipulation. The protocol illustrated here provides the neuroscience community with an innovative, simple method to visualize brain-wide patterns of cell proliferation along with brain morphology by taking advantage of the small size of the adult brain of the zebrafish model, the consistency of EdU labeling, and the isotropic nature of Optical Projection Tomography (OPT). Additionally, our OPT pipeline allows for the possibility of combining EdU staining with transgenic reporter lines and/or antibodies. Moreover, we demonstrate that reconstructed datasets can be easily quantified using freeware such as FIJI/IMAGEJ using EdU intensity or volume as output to examine broad patterns of change or within specific neuroanatomical domains of interest. The data can also be used as a building block to create a 3-D atlas and for standardization of expression patterns. Collectively, these features will establish this protocol as a valuable tool in small teleost models such as the zebrafish, to unveil new clues underlying brain-wide stem cell behavior during the regenerative process, new information underpinning systemic cell signaling of stem and immune cell populations, as well as tracking stem cell niche development and changes in brain morphology.

The successful labeling of proliferating stem/progenitor cells in the adult zebrafish brain in the current protocol depends largely on the properties of 5-ethynyl-2′-deoxyuridine (EdU). EdU has evolved as a modern alternative to the use of previous thymidine analogs, 5-bromo-2'-deoxyuridine (BrdU), 5-chloro-2'-deoxyuridine (CldU), and 5-iodo-2'-deoxyuridine (IdU), for labeling active DNA synthesis (*S*-phase) of the cell cycle (Salic and Mitchison, 2008). Moreover, unlike BrdU protocols, EdU labeling does not require DNA denaturation using harsh chemicals such as hydrochloric acid that often degrades tissue (Buck et al., 2008). Rather, EdU staining uses a rapid click-chemistry reaction between an azide (part of staining solution) and an alkyne (bound to EdU), allowing cryosectioned tissue to be labeled at room temperature in <30-min, and in the case of the whole adult zebrafish brain, within 4-days. The small size of the Alexa

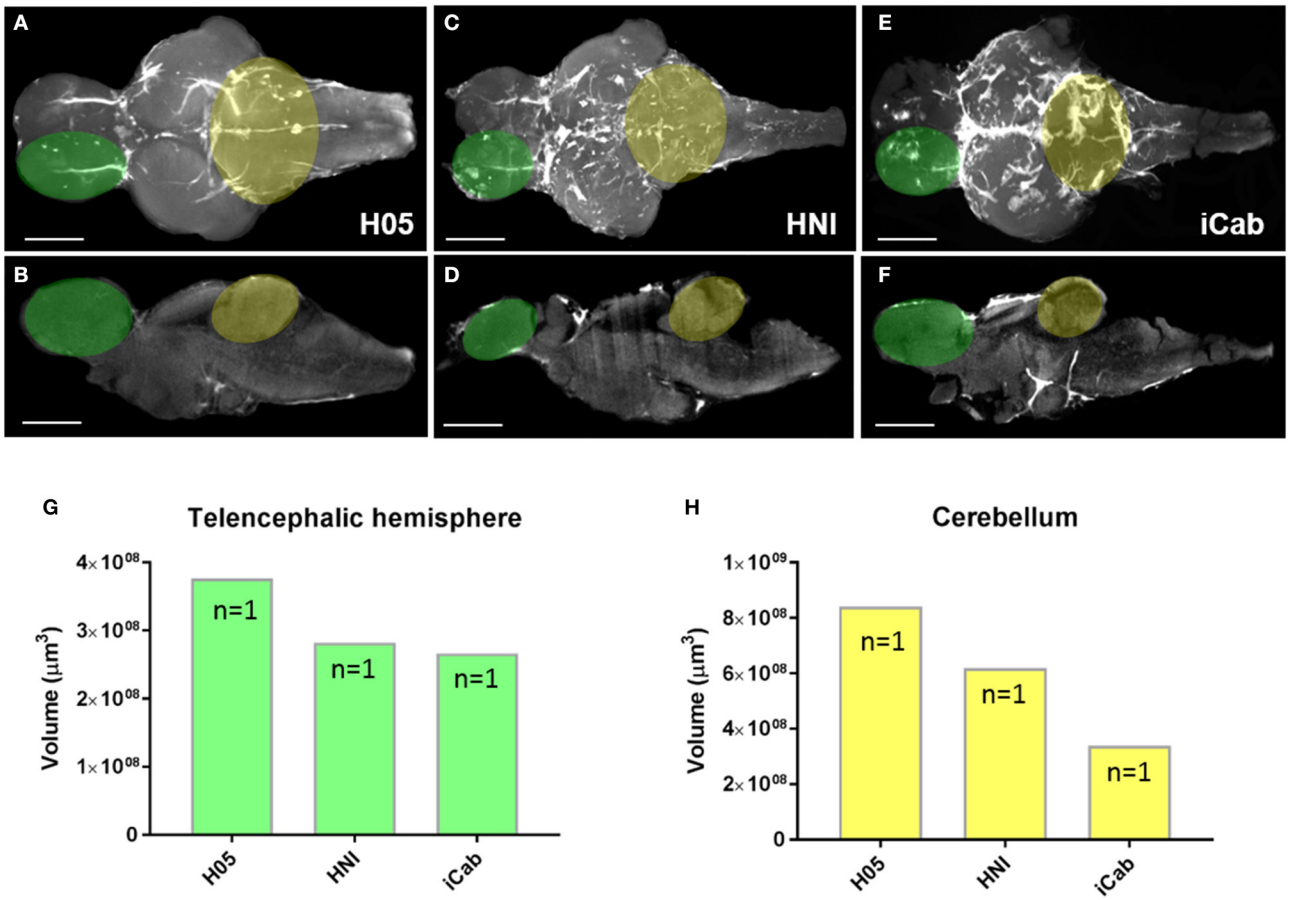

FIGURE 8 | Morphological variation in brain structures across inbred medaka strains. **(A–F)** Adult medaka brains in dorsal and mid-sagittal views from the H05 **(A,B)**, HNI **(C,D)**, and iCab **(E,F)** inbred strains scanned using autofluorescence to investigate morphological variation in the growth/volume of major brain structures. The white region seen on brains depicts autofluorescence of vasculature (H05), or additional pigment left on the brain at the time of imaging (HNI, iCab). Green and yellow overlays on brains denote the neuroanatomical structures used for volume calculations shown in **(G,H)**. **(G,H)** Example volume calculation using IMARIS comparing the size of a single telencephalic hemisphere (**G**, green) and cerebellum (**H**, yellow) across the three inbred medaka strains. Scale bars = 500 µm.

Fluor azide is readily accessible to the DNA, unlike larger anti-BrdU primary antibodies, making it well suited for penetration into thick tissue during the staining process. Importantly, EdU fluorescence is not degraded by methanol dehydration or BABB clearing like many other markers (**Figures 2I–K**), making it ideal for whole brain imaging and resulting in consistent labeling patterns in line with conventional cryosectioned tissue (**Figures 2E,G**).

Effective use of this protocol for sample preparation of zebrafish or other small vertebrates with comparable adult brain size requires attention and expertise at a number of different stages. Proper EdU administration is crucial for visualization of this marker during OPT imaging, and it is most cost effective to inject intraperitoneally as described. However, bath application in EdU can also be considered using the same chase periods presented here. In cases where this protocol is considered in juvenile animals, intraperitoneal microinjection of EdU or bath application must be performed due to the small size of fish. Proceeding EdU chase periods, brain dissection may be one of the more technically challenging steps. Nevertheless, time should be taken to remove the entire brain intact and ensure no debris (i.e., pigment, blood, tissue) remains on the surface before transfer into fixative (**Figures 1C,D**). Debris will impede the passage of light through the sample during OPT imaging, resulting in poor reconstructions and inaccurate analysis.

Without exception, embedding the EdU stained brains in the 6-well plates is the most important step of the protocol. Poor embedding will result in unusable samples even if the EdU labeling appears unspoiled. Thus, it is advisable that when starting this protocol for the first time, only 1–2 brain samples are embedding at a time in low melting agarose (**Figure 1F**). Agarose embedding has long been used in zebrafish research for histology of fixed specimens (ZFIN; Tsao-Wu et al., 1998; Copper et al., 2017) or live *in vivo* confocal imaging of larvae (Kaufmann et al., 2012), and is commonly used during sample preparation for OPT scanning across leading animals models, including but not limited to adult *Drosophila* (McGurk et al., 2007), mouse embryos and kidney (Sharpe et al., 2002; Short et al., 2010), and

human brain tissue (Kerwin et al., 2004). Once the agarose begins to set there is a very narrow window of time to orient brains properly and smoothly without damage. Paramount is that brain samples do not fall to the bottom of the well, as this will place them outside the field of view when OPT imaging. Taking time to observe the samples in the z-plane of the well by looking at the side of the 6-well plate provides a good indication if brain samples are properly oriented. Lastly, before trimming the block always confirm which type of OPT mount will be utilized as this might require modifications to how the block is trimmed. Moreover, applying this protocol to other types of imaging, such as light-sheet microscopy, may necessitate slight deviations.

Those interested in taking advantage of the present protocol should make it common practice to run preliminary experiments and determine experimental parameters for downstream analysis prior to commencing OPT imaging. The importance of this cannot be overlooked, especially if the intensity of EdU is to be a measured output as we show with our *Histogram Analysis* (**Figure 4**). For instance, lesioned brains have considerably greater EdU intensity compared to control levels as a consequence of greater cell proliferation following injury (see **Figures 4C**, **6B–F**). As a result, confirming a consistent level of exposure for both treatments that does not lose data in controls, nor over-expose data in the damaged brains must be done *a priori*. Similar to confocal imaging of immunohistochemical stained tissue, each sample will have slight variations in EdU intensity. Using a sample size of $n = 5$–10 animals in most cases allows for a reliable pattern to be extracted following post-processing.

Whole organ imaging produces large datasets (>1 GB) and often requires specialized quantification tools and powerful software to extract cell counts, staining patterns, or global trends from 3-D tissue. FIJI/IMAGEJ, IMARIS, and MATLAB are some of the more commonly available software programs that can be used to create 2-D or 3-D analysis methods to quantify reconstructed OPT datasets. In this paper we showcase three simple downstream analysis methods we developed exclusively in FIJI/IMAGEJ to examine the A-P profile of EdU intensity (*Histogram Analysis*: **Figure 4**) and EdU volume in large tissue regions of the adult brain (*Structure Analysis*: **Figure 5**) or tightly demarcated adult proliferation zones (*Slice Analysis*: **Figure 6**) following telencephalic lesion. While sophisticated computational methods to normalize 3-D expression data for standardized neuroanatomical maps are emerging in the larval zebrafish following live imaging (Randlett et al., 2015), not surprisingly, few analysis pipelines currently exist to analyze 3-D output derived from the adult zebrafish brain (Lupperger et al., 2017).

Although some modern OPT scanners are capable of single cell resolution, most provide datasets with only near cellular resolution. Undoubtedly this has limitations on how downstream analysis is performed on reconstructed OPT output. Given this, we view our EdU staining OPT pipeline as a starting point to visualize brain-wide trends in cell proliferation under varying conditions to identify neuroanatomical domains of interest that can subsequently be studied at the single cell level using immunohistochemistry, *in situ* hybridization, or electron microscopy on sectioned tissue. Analysis of mouse kidney has previously shown that OPT tissue is compatible with physical sectioning for immunostaining and transmission EM, allowing users to seamlessly move from one technique to the next within a single sample (Combes et al., 2014). Here we illustrate that both EdU intensity and EdU volume are informative and reliable methods to represent and quantify OPT data to investigate systemic changes in the CNS post-injury. In particular, we highlight that EdU volume derived from OPT scans is a statistically detectable readout to compare changes in EdU staining between the uninjured and injured brain.

Our combined *Histogram* and *Structure* analyses bring to light that the systemic response of cell proliferation to forebrain injury is apparent along the entire length of the neuro-axis and peaks at 1-dpl across all structures distal to the lesioned hemisphere (**Figures 4C**, **6B–I**). However, these analyses encompass all cells that have entered a proliferative state, which is known to include a significant population of immune cells that are activated upon injury and present in the tissue parenchyma (Kroehne et al., 2011; Kyritsis et al., 2012; Kaslin et al., 2017). Comparing these findings with the results from our *Slice Analysis*, we observed that lesion-induced signals do not appear to modulate the degree of cell proliferation in the proliferative domains of posteriorly located tectal and cerebellar structures (**Figures 6N–Y**), but rather remains proximal to the lesioned and unlesioned hemisphere (**Figures 6B–M**). The dichotomy in the pattern of change in EdU observed between *Histogram/Structure Analysis* and *Slice Analysis* imply that cues from the lesion site differentially activate populations of adult neural stem cells in stem cell niches positioned along the A-P axis, but trigger global proliferation of leukocytes in the brain parenchyma.

Beyond studies of global changes in EdU following traumatic brain injury, we show that our OPT protocol has merit for uncovering new clues related to stem cell niche development and brain morphology. By combining larval whole brain confocal imaging of EdU (**Figures 7A–C**) with EdU labeling using our OPT pipeline (**Figures 7D–F**) we are now able to visualize the localization of cell proliferation over the full spectrum of zebrafish development into senescence to track the proliferative status of individual life-long proliferation/growth zones. We see this work as a fundamental starting point to transition towards being able to obtain isotropic 3-D data of specific gene expression patterns in the adult CNS that can be used to create standardized brain maps and bridge the gap between embryonic, larval, juvenile and adult shape and morphology. Likewise, coupling whole brain imaging of developing adult stem cell niches with cell-specific markers, methods such as immuno-correlative light and electron microscopy, and niche-specific transcriptomics will be a powerful approach to dissect how distinct niches are constructed and regulated at key developmental milestones. Secondly, we show that our OPT pipeline can readily be adapted to other small experimental fish models, such as the medaka, for comparative studies of brain morphology and cell proliferation (data not shown). Taking advantage of brain autofluorescence that can be imaged during OPT scans, we reveal that this is a tractable method to obtain morphometric scans of brain volume

for quantitative analysis. By directly testing the feasibility of this approach in three inbred strains of medaka (**Figures 8A–F**), we demonstrate that differences in the volume of distinct brain structures can be quantified using IMARIS volumetric algorithms (**Figures 8G,H**). We envision this approach to be highly desirable to the medaka community to progress current knowledge on the genetic basis of brain development as a result of the high tolerance of this species to inbreeding (Kirchmaier et al., 2015).

Optical Projection Tomography was first designed to study gene expression patterns in the developing mouse embryo (Sharpe, 2003). Over the last 15-years OPT has played a pivotal role in answering a diversity of biological questions primarily in rodent models (Vinegoni et al., 2009; Short et al., 2010; Jeansson et al., 2011; Gleave et al., 2012, 2013; Anderson et al., 2013; Combes et al., 2014; Short and Smyth, 2016, 2017), using commercially available or custom built OPT systems (Wong et al., 2013). Here, we have optimized an EdU sample preparation pipeline for the adult zebrafish brain taking advantage of the tomographic imaging of OPT with the aim of expanding our knowledge of adult stem cell behavior following traumatic brain injury. We show that output from OPT scans can be examined quantitatively using FIJI/IMAGEJ to identify systemic changes in cell proliferation post-injury, and that our OPT pipeline would serve as a beneficial imaging tool to track stem cell niche development over ontogeny and study changes in brain morphology. Moving forward we welcome collaborations from members of the teleost community (zebrafish, medaka, or other) and hope this protocol will be of practical use for many laboratories.

AUTHOR CONTRIBUTIONS

The protocol presented here was developed by BL and JK for zebrafish, in collaboration with FL for its application with medaka. BL was responsible for drafting the manuscript and figures with conceptual input from both JK and FL. AD was responsible for EdU staining and larval whole brain confocal imaging in zebrafish. AD and BL performed all revisions to figures and the inclusion of additional data in the manuscript. BL and JK were responsible for the creation of supplementary videos accompanying the manuscript.

FUNDING

This work was supported by an NHMRC project grant (GNT1068411), Monash University Faculty of Medicine and Nursing strategic grant and Operational Infrastructure Support from the Victorian Government. BL was supported by a postdoctoral fellowship from NSERC in Canada.

ACKNOWLEDGMENTS

We thank the laboratory of Prof. I. Smyth in the Department of Anatomy and Developmental Biology at Monash University for the continued use of their Optical Projection Tomography scanner. Kind thanks to G. Lieschke for providing the Tg(mpeg1:gfp) line. We thank Monash Micro Imaging Facility and the FishCore facility for excellent support. Thanks to the staff at the Institute of Toxicology and Genetics, Karlsruhe Institute of Technology, Karlsruhe, Germany for husbandry of medaka strains used in this manuscript.

SUPPLEMENTARY MATERIAL

The Supplementary Material for this article can be found online at: https://www.frontiersin.org/articles/10.3389/fnins.2017.00750/full#supplementary-material

Supplementary Video 1 | Instructional video explaining and demonstrating key steps in whole brain staining, embedding and clearing pipeline for adult zebrafish.

Supplementary Video 2 | OPT scanned and reconstructed adult zebrafish brain following a 4-h EdU pulse displaying the stereotypical pattern of adult stem cell niche proliferation along the anterior-posterior neuro-axis.

Supplementary Video 3 | 3-D reconstructed and rendered adult zebrafish brain showing an overlay of brain volume OPT scanned using autofluorescence from the 488 channel (green) and EdU labeling using the 555 laser (red).

REFERENCES

Adolf, B., Chapouton, P., Lam, C. S., Topp, S., Tannhäuser, B., Strähle, U., et al. (2006). Conserved and acquired features of adult neurogenesis in the zebrafish telencephalon. *Dev. Biol.* 295, 278–293. doi: 10.1016/j.ydbio.2006.03.023

Aguilar-Sanchez, Y., Fainstein, D., Mejia-Alvarez, R., and Escobar, A. L. (2017). Local Field fluorescence microscopy: imaging cellular signals in intact hearts. *J. Vis. Exp.* 121:e55202. doi: 10.3791/55202

Ahnfelt-Rønne, J., Jørgensen, M. C., Hald, J., Madsen, O. D., Serup, P., and Hecksher-Sørensen, J. (2007). An improved method for three-dimensional reconstruction of protein expression patterns in intact mouse and chicken embryos and organs. *J. Histochem. Cytochem.* 55, 925–930. doi: 10.1369/jhc.7A7226.2007

Alunni, A., and Bally-Cuif, L. (2016). A comparative view of regenerative neurogenesis in vertebrates. *Development* 143, 741–753. doi: 10.1242/dev.122796

Anderson, G. A., Wong, M. D., Yang, J., and Henkelman, R. M. (2013). 3D imaging, registration, and analysis of the early mouse embryonic vasculature. *Dev. Dyn.* 242, 527–538. doi: 10.1002/dvdy.23947

Antinucci, P., and Hindges, R. (2016). A crystal-clear zebrafish for *in vivo* imaging. *Sci. Rep.* 6:29490. doi: 10.1038/srep29490

Aswendt, M., Schwarz, M., Abdelmoula, W. M., Dijkstra, J., and Dedeurwaerdere, S. (2017). Whole-brain microscopy meets *in vivo* neuroimaging: techniques, benefits, and limitations. *Mol. Imaging Biol.* 19, 1–9. doi: 10.1007/s11307-016-0988-z

Azaripour, A., Lagerweij, T., Scharfbillig, C., Jadczak, A. E., Willershausen, B., and Van Noorden, C. J. (2016). A survey of clearing techniques for 3D imaging of tissues with special reference to connective tissue. *Prog. Histochem. Cytochem.* 51, 9–23. doi: 10.1016/j.proghi.2016.04.001

Baumgart, E. V., Barbosa, J. S., Bally-Cuif, L., Götz, M., and Ninkovic, J. (2012). Stab wound injury of the zebrafish telencephalon: a model for comparative analysis of reactive gliosis. *Glia* 60, 343–357. doi: 10.1002/glia.22269

Belle, M., Godefroy, D., Couly, G., Malone, S. A., Collier, F., Giacobini, P., et al. (2017). Tridimensional visualization and analysis of early human development. *Cell* 169, 161–173. doi: 10.1016/j.cell.2017.03.008

Belle, M., Godefroy, D., Dominici, C., Heitz-Marchaland, C., Zelina, P., Hellal, F., et al. (2014). A simple method for 3D analysis of immunolabeled

axonal tracts in a transparent nervous system. *Cell Rep*. 9, 1191–1201. doi: 10.1016/j.celrep.2014.10.037

Buck, S. B., Bradford, J., Gee, K. R., Agnew, B. J., Clarke, S. T., and Salic, A. (2008). Detection of S-phase cell cycle progression using 5-ethynyl-2'-deoxyuridine incorporation with click chemistry, an alternative to using 5-bromo-2'-deoxyuridine antibodies. *Biotechniques* 44, 927–929. doi: 10.2144/000112812

Chapouton, P., Jagasia, R., and Bally-Cuif, L. (2007). Adult neurogenesis in non-mammalian vertebrates. *Bioessays* 29, 745–757. doi: 10.1002/bies.20615

Chung, K., and Deisseroth, K. (2013). CLARITY for mapping the nervous system. *Nat. Methods* 10, 508–513. doi: 10.1038/nmeth.2481

Combes, A. N., Short, K. M., Lefevre, J., Hamilton, N. A., Little, M. H., and Smyth, I. M. (2014). An integrated pipeline for the multidimensional analysis of branching morphogenesis. *Nat. Protoc*. 9, 2859–2879. doi: 10.1038/nprot.2014.193

Copper, J. E., Budgeon, L. R., Foutz, C. A., van Rossum, D. B., Vanselow, D. J., Hublev, M. J., et al. (2017). Comparative analysis of fixation and embedding techniques for optimized histological preparation of zebrafish. *Comp. Biochem. Physiol. C Toxicol. Pharmacol.* doi: 10.1016/j.cbpc.2017.11.003. [Epub ahead of print].

Ellett, F., Pase, L., Hayman, J. W., Andrianopoulos, A., and Lieschke, G. J. (2011). mpeg1 promoter transgenes direct macrophage-lineage expression in zebrafish. *Blood* 117, e49–e56. doi: 10.1182/blood-2010-10-314120

Epp, J. R., Niibori, Y., Liz Hsiang, H. L., Mercaldo, V., Deisseroth, K., Josselyn, S. A., et al. (2015). Optimization of CLARITY for clearing whole-brain and other intact organs. *eNeuro* 2:e0022-15. doi: 10.1523/ENEURO.0022-15.2015

Ganz, J., Kaslin, J., Hochmann, S., Freudenreich, D., and Brand, M. (2010). Heterogeneity and fgf dependence of adult neural progenitors in the zebrafish telencephalon. *Glia* 58, 1345–1363. doi: 10.1002/glia.21012

Ghosh, S., and Hui, S. P. (2016). Regeneration of zebrafish CNS: adult neurogenesis. *Neural Plast.* 2016:5815439. doi: 10.1155/2016/5815439

Gleave, J. A., Lerch, J. P., Henkelman, R. M., and Nieman, B. J. (2013). A method for 3D immunostaining and optical imaging of the mouse brain demonstrated in neural progenitor cells. *PLoS ONE* 8:e72039. doi: 10.1371/journal.pone.0072039

Gleave, J. A., Wong, M. D., Dazai, J., Altaf, M., Henkelman, R. M., Lerch, J. P., et al. (2012). Neuroanatomical phenotyping of the mouse brain with three-dimensional autofluorescence imaging. *Physiol. Genomics* 44, 778–785. doi: 10.1152/physiolgenomics.00055.2012

Grandel, H., Kaslin, J., Ganz, J., Wenzel, I., and Brand, M. (2006). Neural stem cells and neurogenesis in the adult zebrafish brain: origin, proliferation dynamics, migration and cell fate. *Dev. Biol.* 295, 263–277. doi: 10.1016/j.ydbio.2006.03.040

Ishikawa, Y., Yoshimoto, M., Yamamoto, N., and Ito, H. (1999). Different brain morphologies from different genotypes in a single teleost species, the medaka (*Oryzias latipes*). *Brain Behav. Evol*. 53, 2–9.

Jeansson, M., Anderson, G., Li, C., Kerjaschki, D., Henkelman, M., and Quaggin, S. E. (2011). Angiopoietin-1 is essential in mouse vasculature during development and in response to injury. *J. Clin. Invest.* 121, 2278–2289. doi: 10.1172/JCI46322

Kaslin, J., Ganz, J., and Brand, M. (2008). Proliferation, neurogenesis and regeneration in the non-mammalian vertebrate brain. *Philos. Trans. R. Soc. Lond. B Biol. Sci*. 363, 101–122. doi: 10.1098/rstb.2006.2015

Kaslin, J., Kroehne, V., Ganz, J., Hans, S., and Brand, M. (2017). Distinct roles of neuroepithelial-like and radial glia-like progenitor cells in cerebellar regeneration. *Development* 144, 1462–1571. doi: 10.1242/dev.144907

Kaufmann, A., Mickoleit, M., Weber, M., and Huisken, J. (2012). Multilayer mounting enables long-term imaging of zebrafish development in a light sheet microscope. *Development* 139, 3242–3247. doi: 10.1242/dev.082586

Keller, P. J., Schmidt, A. D., Santella, A., Khairy, K., Bao, Z., Wittbrodt, J., et al. (2010). Fast, high-contrast imaging of animal development with scanned light sheet-based structured-illumination microscopy. *Nat. Methods* 7, 637–642. doi: 10.1038/nmeth.1476

Kerwin, J., Scott, M., Sharpe, J., Puelles, L., Robson, S. C., Martinez-de-la-Torre, M., et al. (2004). 3 dimensional modelling of early human brain development using optical projection tomography. *BMC Neurosci*. 5:27. doi: 10.1186/1471-2202-5-27

Kirchmaier, S., Naruse, K., Wittbrodt, J., and Loosli, F. (2015). The genomic and genetic toolbox of the teleost medaka (*Oryzias latipes*). *Genetics* 199, 905–918. doi: 10.1534/genetics.114.173849

Kishimoto, N., Shimizu, K., and Sawamoto, K. (2012). Neuronal regeneration in a zebrafish model of adult brain injury. *Dis. Model. Mech.* 5, 200–209. doi: 10.1242/dmm.007336

Kizil, C., Kaslin, J., Kroehne, V., and Brand, M. (2012). Adult neurogenesis and brain regeneration in zebrafish. *Dev. Neurobiol*. 72, 429–461. doi: 10.1002/dneu.20918

Kolesová, H., Capek, M., Radochová, B., Janáček, J., and Sedmera, D. (2016). Comparison of different tissue clearing methods and 3D imaging techniques for visualization of GFP-expressing mouse embryos and embryonic hearts. *Histochem. Cell Biol*. 146, 141–152. doi: 10.1007/s00418-016-1441-8

Kroehne, V., Freudenreich, D., Hans, S., Kaslin, J., and Brand, M. (2011). Regeneration of the adult zebrafish brain from neurogenic radial glial-type progenitors. *Development* 138, 4831–4841. doi: 10.1242/dev.072587

Kromm, D., Thumberger, T., and Wittbrodt, J. (2016). An eye on light-sheet microscopy. *Methods Cell Biol*. 133, 105–123. doi: 10.1016/bs.mcb.2016.01.001

Kyritsis, N., Kizil, C., Zocher, S., Kroehne, V., Kaslin, J., Freudenreich, D., et al. (2012). Acute inflammation initiates the regenerative response in the adult zebrafish brain. *Science* 338, 1353–1356. doi: 10.1126/science.1228773

Lindsey, B. W., Darabie, A., and Tropepe, V. (2012). The cellular composition of neurogenic periventricular zones in the adult zebrafish forebrain. *J. Comp. Neurol.* 520, 2275–2316. doi: 10.1002/cne.23065

Lindsey, B. W., Di Donato, S., Kaslin, J., and Tropepe, V. (2014). Sensory-specific modulation of adult neurogenesis in sensory structures is associated with the type of stem cell present in the neurogenic niche of the zebrafish brain. *Eur. J. Neurosci.* 40, 3591–3607. doi: 10.1111/ejn.12729

Lindsey, B. W., and Kaslin, J. (2017). Optical projection tomography as a novel method to visualize and quantitate whole-brain patterns of cell proliferation in the adult zebrafish brain. *Zebrafish* 14, 574–577. doi: 10.1089/zeb.2017.1418

Lindsey, B. W., and Tropepe, V. (2014). Changes in the social environment induce neurogenic plasticity predominantly in niches residing in sensory structures of the zebrafish brain independently of cortisol levels. *Dev. Neurobiol*. 74, 1053–1077. doi: 10.1002/dneu.22183

Lloyd-Lewis, B., Davis, F. M., Harris, O. B., Hitchcock, J. R., Lourenco, F. C., Pasche, M., et al. (2016). Imaging the mammary gland and mammary tumours in 3D: optical tissue clearing and immunofluorescence methods. *Breast Cancer Res*. 18:127. doi: 10.1186/s13058-016-0754-9

Lupperger, V., Buggenthin, F., Chapouton, P., and Marr, C. (2017). Image analysis of neural stem cell division patterns in the zebrafish brain. *Cytometry Part A*. doi: 10.1002/cyto.a.23260. [Epub ahead of print].

McGowan, J. W., and Bidwell, G. L. III. (2016). The use of *ex vivo* whole-organ imaging and quantitative tissue histology to determine the bio-distribution of fluorescently labeled molecules. *J. Vis. Exp*. 118:e54987. doi: 10.3791/54987

McGurk, L., Morrison, H., Keegan, L. P., Sharpe, J., and O'Connell, M. A. (2007). Three-dimensional imaging of *Drosophila melonagaster*. *PLoS ONE* 2:e834. doi: 10.1371/journal.pone.0000834

Miller, C. E., Thompson, R. P., Bigelow, M. R., Gittinger, G., Trusk, T. C., and Sedmera, D. (2005). Confocal imaging of the embryonic heart: how deep? *Microsc. Microanal*. 11, 216–223. doi: 10.1017/S1431927605050464

Ode, K. L., and Ueda, H. R. (2015). Seeing the forest and trees: whole-body and whole-brain imaging for circadian biology. *Diabetes Obes. Metab.* 17(Suppl. 1), 47–54. doi: 10.1111/dom.12511

Pan, C., Cai, R., Quacquarelli, F. P., Ghasemigharagoz, A., Lourbopoulos, A., Matryba, P., et al. (2016). Shrinkage-mediated imaging of entire organs and organisms using uDISCO. *Nat. Methods* 113, 859–867. doi: 10.1038/nmeth.3964

Parra, S. G., Vesuna, S. S., Murray, T. A., and Levene, M. J. (2012). Multiphoton microscopy of cleared mouse brain expressing YFP. *J. Vis. Exp.* 23:e3848. doi: 10.3791/3848

Randlett, O., Wee, C. L., Naumann, E. A., Nnaemeka, O., Schoppik, D., Fitzgerald, J. E., et al. (2015). Whole-brain activity mapping onto a zebrafish brain atlas. *Nat. Methods* 12, 1039–1046. doi: 10.1038/nmeth.3581

Renier, N., Wu, Z., Simon, D. J., Yang, J., Ariel, P., and Tessier-Lavigne, M. (2014). iDISCO: a simple rapid method to immunolabel large tissue samples for volume imaging. *Cell* 159, 896–910. doi: 10.1016/j.cell.2014.10.010

Salic, A., and Mitchison, T. J. (2008). A chemical method for fast and sensitive detection of DNA synthesis *in vivo*. *Proc. Natl. Acad. Sci. U.S.A*. 105, 2415–2420. doi: 10.1073/pnas.0712168105

Sharpe, J. (2003). Optical projection tomography as a new tool for studying embryo anatomy. *J. Anat.* 202, 175–181. doi: 10.1046/j.1469-7580.2003.00155.x

Sharpe, J., Ahlgren, U., Perry, P., Hill, B., Ross, A., Hecksher-Sorensen, J., et al. (2002). Optical projection tomography as a tool for 3D microscopy and gene expression studies. *Science* 296, 541–545. doi: 10.1126/science.1068206

Short, K. M., Hodson, M. J., and Smyth, I. M. (2010). Tomographic quantification of branching morphogenesis and renal development. *Kidney Int.* 77, 1132–1139. doi: 10.1038/ki.2010.42

Short, K. M., and Smyth, I. M. (2016). The contribution of branching morphogenesis to kidney development and disease. *Nat. Rev. Nephrol.* 12, 754–767. doi: 10.1038/nrneph.2016.157

Short, K. M., and Smyth, I. M. (2017). Imaging, analysis, and interpreting branching morphogenesis in the developing kidney. *Results Probl. Cell Differ.* 60, 233–256. doi: 10.1007/978-3-319-51436-9_9

Song, E., Seo, H., Choe, K., Hwang, Y., Ahn, J., Ahn, S., et al. (2015). Optical clearing based cellular-level 3D visualization of intact lymph node cortex. *Biomed. Opt. Express* 6, 4154–4164. doi: 10.1364/BOE.6.004154

Spivakov, M., Auer, T. O., Peravali, R., Dunham, I., Dolle, D., Fujiyama, A., et al. (2014). Genomic and phenotypic characterization of a wild medaka population: towards the establishment of an isogenic population genetic resource in fish. *G3* 4, 433–445. doi: 10.1534/g3.113.008722

Susaki, E. A., Tainaka, K., Perrin, D., Kishino, F., Tawara, T., Watanabe, T. M., et al. (2014). Whole-brain imaging with single-cell resolution using chemical cocktails and computational analysis. *Cell* 157, 726–739. doi: 10.1016/j.cell.2014.03.042

Susaki, E. A., Tainaka, K., Perrin, D., Yukinaga, H., Kuno, A., and Ueda, H. R. (2015). Advanced CUBIC protocols for whole-brain and whole-body clearing and imaging. *Nat. Protoc.* 10, 1709–1727. doi: 10.1038/nprot.2015.085

Susaki, E. A., and Ueda, H. R. (2016). Whole-body and whole-organ clearing and imaging techniques with single-cell resolution: toward organism-level systems biology in mammals. *Cell Chem. Biol.* 23, 137–157. doi: 10.1016/j.chembiol.2015.11.009

Than-Trong, E., and Bally-Cuif, L. (2015). Radial glia and neural progenitors in the adult zebrafish central nervous system. *Glia* 63, 1406–1428. doi: 10.1002/glia.22856

Tsao-Wu, G. S., Weber, C. H., Budgeon, L. R., and Cheng, K. C. (1998). Agarose-embedded tissue arrays for histologic and genetic analysis. *Biotechniques* 25, 614–618.

Vigouroux, R. J., Belle, M., and Chédotal, A. (2017). Neuroscience in the third dimension: shedding new light on the brain with tissue clearing. *Mol. Brain.* 10:33. doi: 10.1186/s13041-017-0314-y.

Vinegoni, C., Razansky, D., Figueiredo, J. L., Fexon, L., Pivovarov, M., Nahrendorf, M., et al. (2009). Born normalization for fluorescence optical projection tomography for whole heart imaging. *J. Vis. Exp.* 2:e1389. doi: 10.3791/1389

White, R. M., Sessa, A., Burke, C., Bowman, T., LeBlanc, J., Ceol, C., et al. (2008). Transparent adult zebrafish as a tool for *in vivo* transplantation analysis. *Cell Stem Cell* 2, 183–189. doi: 10.1016/j.stem.2007.11.002

Whitehead, L. W., McArthur, K., Geoghegan, N. D., and Rogers, K. L. (2017). The reinvention of twentieth century microscopy for 3-dimensional imaging. *Immunol. Cell Biol.* 95, 520–524. doi: 10.1038/icb.2017.36

Wong, M. D., Dazai, J., Walls, J. R., Gale, N. W., and Henkelman, R. M. (2013). Design and implementation of a custom built optical projection tomography system. *PLoS ONE* 8:e73491. doi: 10.1371/journal.pone.0073491

Yang, B., Treweek, J. B., Kulkarni, R. P., Deverman, B. E., Chen, C.-K., Lubeck, E., et al. (2014). Single-cell phenotyping within transparent intact tissue through whole-body clearing. *Cell* 158, 945–958. doi: 10.1016/j.cell.2014.07.017

Zucker, R. M. (2006). Whole insect and mammalian embryo imaging with confocal microscopy: morphology and apoptosis. *Cytometry A* 69, 1143–1152. doi: 10.1002/cyto.a.20343

Conflict of Interest Statement: The authors declare that the research was conducted in the absence of any commercial or financial relationships that could be construed as a potential conflict of interest.

The reviewer GRM and handling Editor declared their shared affiliation.

frontiers in Neuroscience

REVIEW
published: 23 October 2017
doi: 10.3389/fnins.2017.00570

Adult Neurogenesis in Sheep: Characterization and Contribution to Reproduction and Behavior

Frederic Lévy, Martine Batailler, Maryse Meurisse and Martine Migaud*

Institut National de la Recherche Agronomique, UMR85, Centre National de la Recherche Scientifique, UMR7247, Université F. Rabelais, IFCE, Physiologie de la Reproduction et des Comportements, Nouzilly, France

Sheep have many advantages to study neurogenesis in comparison to the well-known rodent models. Their development and life expectancy are relatively long and they possess a gyrencephalic brain. Sheep are also seasonal breeders, a characteristic that allows studying the involvement of hypothalamic neurogenesis in the control of seasonal reproduction. Sheep are also able to individually recognize their conspecifics and develop selective and lasting bonds. Adult olfactory neurogenesis could be adapted to social behavior by supporting recognition of conspecifics. The present review reveals the distinctive features of the hippocampal, olfactory, and hypothalamic neurogenesis in sheep. In particular, the organization of the subventricular zone and the dynamic of neuronal maturation differs from that of rodents. In addition, we show that various physiological conditions, such as seasonal reproduction, gestation, and lactation differently modulate these three neurogenic niches. Last, we discuss recent evidence indicating that hypothalamic neurogenesis acts as an important regulator of the seasonal control of reproduction and that olfactory neurogenesis could be involved in odor processing in the context of maternal behavior.

Keywords: hypothalamus, hippocampus, olfactory bulb, photoperiod, maternal behavior, neuroblasts, seasonal reproduction, neurogenic niche

OPEN ACCESS

Edited by:
Irmgard Amrein,
University of Zurich, Switzerland

Reviewed by:
Anne Didier,
Claude Bernard University Lyon 1, France
Krishna Vadodaria,
Salk Institute for Biological Studies, United States

****Correspondence:***
Frederic Lévy
frederic.levy@inra.fr

Specialty section:
This article was submitted to Neurogenesis, a section of the journal Frontiers in Neuroscience

Received: *16 June 2017*
Accepted: *28 September 2017*
Published: *23 October 2017*

Citation:
Lévy F, Batailler M, Meurisse M and Migaud M (2017) Adult Neurogenesis in Sheep: Characterization and Contribution to Reproduction and Behavior. Front. Neurosci. 11:570. doi: 10.3389/fnins.2017.00570

INTRODUCTION

A majority of invertebrates and vertebrates species show a continuous addition of neurons throughout life. Neurogenesis occurring in species with long development and life span (e.g., carnivores, ungulates, and primate) is far much less documented than in rodents. However, the timing of generation, migration, and differentiation of new neurons have been reported to differ according to lifespan and life history (Amrein et al., 2011). These differences are not surprising when one considers that neurogenesis is part of the plastic changes allowing adaptation to functional demands that differ according to species.

Sheep are an interesting species for studying neurogenesis for several reasons. Its development (puberty at 6–8 months) and its life expectancy (10–12 years) are rather long in comparison to rodents and differences in life span could influence the rate of neuronal maturation in adulthood. Sheep possess a gyrencephalic brain, a cortex with a laterally expanded folded pial surface similar to non-human and human primates, and adult neurogenesis could differ from a lissencephalic brain with a smooth cortical surface, like rodents, since major developmental differences exists between both types of brain (Fietz et al., 2010). It is hypothesized that brain expansion accompanied

by gyrification and topographical complexity leads to dramatic differences in the migration and maturation rates of newborn neurons (Paredes et al., 2016). Sheep is also a seasonal breeder, unlike the majority of laboratory rodents, and these seasonal changes are under the control of the hypothalamic region. Because this region has also the capacity to produce adult-born neurons (see below), the ovine model allows one to study the role of such plasticity in the regulation of seasonal reproduction. Species such as sheep that live under different complexity of social organization and in a more natural environment than laboratory rodents would extend our knowledge of the functional significance of adult neurogenesis in social contexts (Gheusi et al., 2009). Sheep are highly social and develop selective and stable bonds. In this species, odors play a key role in individual recognition of conspecifics either in male-female or mother-young interactions (Keller and Lévy, 2012). Thus, sheep offer a unique opportunity to understand how adult olfactory neurogenesis, one of the numerous forms of brain plasticity constitutes an adaptive response to social behavior by favoring recognition of conspecifics.

The aim of this review is to point out recent findings on the characterization of olfactory, hippocampal, and hypothalamic neurogenic niches in sheep (**Figure 1A**). In addition, their regulation by physiological status and social interactions are considered and the possible functional relevance of these different forms of adult neurogenesis is discussed in the context of seasonal regulation and social interactions.

CHARACTERIZATION OF OLFACTORY, HIPPOCAMPAL, AND HYPOTHALAMIC NEUROGENIC NICHES

Olfactory Neurogenesis

SVZ Organization and Migration Pathway

As in rodents and primates, adult neural stem cells in sheep are located in the subventricular zone (SVZ) and produce neurogenic and gliogenic precursors (**Figure 1C**). These precursors migrate toward the main olfactory bulb (MOB) forming a pathway called the rostral migratory stream (RMS; for an extended review, see Doetsch et al., 1999a; Gil-Perotin et al., 2009; Brus et al., 2010; Sawamoto et al., 2011). In a study establishing the origin of adult-born neurons in the MOB, an AAV5-eGFP was injected in the SVZ (Brus et al., 2013). AAV5-eGFP labeled cells were observed in the MOB when the injection site was located in the SVZ, but not when located posterior at the level of the corpus callosum. This result indicates a similar distribution of neural stem cells between ovine and rodents SVZ (Luskin, 1993). In addition, the SVZ is expanded to the sheep MOB because their lateral ventricle extends up to the MOB, as is the case in rabbits (Luzzati et al., 2003; Brus et al., 2013). Like rabbits and primates, chains of neuroblasts in the anterior SVZ are immersed within an astrocytic meshwork. The presence of a hypocellular layer separating chains of neuroblasts from the ependymal layer resembles the SVZ composition in bovines (Rodriguez-Perez et al., 2003) and primates (Quinones-Hinojosa et al., 2006; Gil-Perotin et al., 2009). Thus, in sheep, from the SVZ up to the MOB a migratory pathway is found along the lateral ventricle from the SVZ to the ventricle of MOB (Brus et al., 2013).

Cells, labeled by injection of an AAV5-eGFP into the SVZ, and found in the periventricular layer of the MOB show an undifferentiated phenotype at 2 months of age. They are mostly Sox2+, a marker of proliferating precursor cells and of glial-like cells; they show a simple dendritic arborization. Likewise, 1-day-old bromodeoxyuridine+ (BrdU) cells are observed in the periventricular layer of the MOB and are co-labeled with Ki-67, an endogenous mitotic marker (Kee et al., 2002). These cells are co-labeled with GFAP, which is a marker for astrocytes and neural stem/progenitor cells (Chojnacki et al., 2009), further suggesting the existence of a neurogenic niche within the MOB (Doetsch et al., 1999b; Brus et al., 2010). Similarly, neuroblasts, evidenced by DCX labeling, are also found in the periventricular layer with a round or fusiform shape and short processes, whereas deeper in the granular cell layer of the MOB, neuroblasts are more mature and display multiple processes (**Figure 1B**). Thus, a continuous zone of neural progenitors exists along from the lateral ventricle to the rostral extreme of the MOB ventricle. This characteristic was confirmed by Low et al.'s (2013) study and resembles the human RMS (Curtis et al., 2007). Thus, in sheep, the periventricular layer of the MOB could also constitute a pool of cells that could supply new neurons that migrate to the granular layer. However, cell proliferation rate in the MOB is much lower than in the SVZ. Interestingly, the MOB of mice (Gritti et al., 2002), macaque monkeys (Kornack and Rakic, 2001), and humans (Pagano et al., 2000; Bedard and Parent, 2004) also contains neural progenitors. The ability of stem cells isolated from the MOB to produce neurospheres is weaker than those from the SVZ, though (Gritti et al., 2002). Hence, in some species, the periventricular layer of the MOB could be neurogenic but its activity may be relatively minor.

Dynamics of Maturation

Although adult neurogenesis is well-conserved in mammals, some features differ between species. In addition to the organization of the SVZ, the dynamic of neurogenesis appear to vary between short-lived and long-lived mammals (Amrein, 2015). For instance, in the MOB of rodents, the far majority of newborn neurons are observed within 15 days after BrdU injections and are fully mature 15 days later (Petreanu and Alvarez-Buylla, 2002; Winner et al., 2002; Brown et al., 2003; Imayoshi et al., 2008). By contrast, in the macaque, only a very small population of BrdU positive cells is found even at 3 months post-injection in the granular cell layer (Kornack and Rakic, 2001). In female sheep, using BrdU injections in combination with maturation markers, noticeable differences in the dynamic of neuronal maturation are found in comparison to rodent adult neurogenesis (Brus et al., 2013; **Figure 2**). For instance, in sheep no variation of BrdU cell density is observed across time except a decrease at 8-month post-injection, suggesting a slow process of apoptosis over this period, in contrast to rodents in which half of the newborn cells die within the first month after birth (Alvarez-Buylla et al., 2001; Lemasson et al., 2005). Very few neuroblasts (BrdU+/DCX+ cells) are found at 1 month after BrdU injections in the granular layer of the

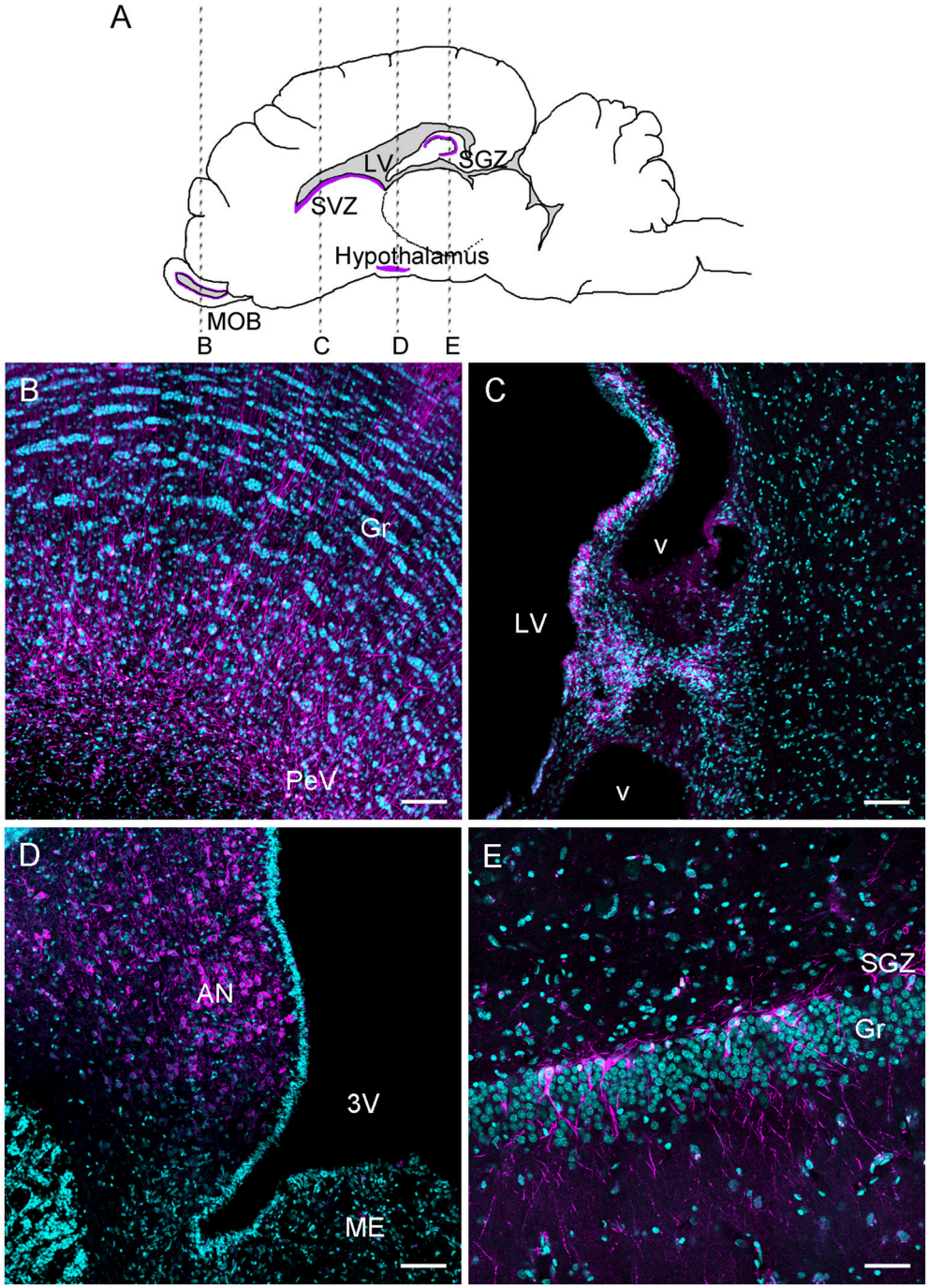

FIGURE 1 | Schematic drawing of a sagittal ewe brain representing rostro-caudal levels of B, C, D, E photomicrographs **(A)**; DCX immunoreactive cells and fibers (magenta) in the main olfactory bulb **(B)**, subventricular zone **(C)**, hypothalamus **(D)**, and dentate gyrus of the hippocampus **(E)**. The sections were counterstained with Hoechst (cyan). AN, arcuate nucleus; Gr, granular layer; LV, lateral ventricle; 3V, third ventricle; ME, median eminence; PeV, periventricular zone; SGZ, subgranular zone; SVZ, subventricular zone; v, blood vessel. Scale bar: 100 μm.

sheep MOB. This population peaks at 3-month and decreases slowly up to 8 months after BrdU injections. No mature neurons (BrdU+/NeuN+ cells) are observed before 3 months post-injections and the highest proportion of new neurons is found 8 months after BrdU injections. These new cells could be activated because they express immediate early genes indicating their functional integration into the granular cell layer. In addition, a substantial proportion of immature cells, evidenced by Sox2

labeling, is found both in the periventricular and granular layers, again supporting the hypothesis of the presence of stem cells that could differentiate according to physiological challenges.

Hippocampal Neurogenesis

Evidence for a Neurogenic Niche

It is currently clear that the dentate gyrus (DG) of the hippocampus is a neurogenic niche for the majority of the mammalian species investigated so far (for a brief overview, see Vadodaria and Gage, 2014; for an extended review, see Amrein, 2015). In Merino ewes, Hawken et al. (2009) reported for the first time the existence of cell proliferation in the DG using BrdU immunohistochemistry. A more detailed study shows in Ile-de-France ewes that 1 day-old BrdU + cells are indeed present in the DG and that their density is highest in the subgranular layer (SGZ) than in the granular layer (**Figure 1E**; Brus et al., 2010). A confocal analysis reveals that almost the entire population of these cells also expresses Ki-67, and half of the BrdU+ cell population co-localizes with GFAP. In addition, a significant population of Sox2+ cells is present in the subgranular layer of the DG. Unexpectedly, a high percentage of these cells are found for up to 8 months (Brus et al., 2010), suggesting that a pool of presumed stem cells continues to generate new neurons over a long time, as has been reported in mice (Ninkovic and Gotz, 2007). Cell proliferation in the DG was also evidenced in another domestic breed of sheep, Romney/Suffolk ewes (Low et al., 2013), and in a feral breed of sheep (Hazlerigg et al., 2013), the Soay sheep. However, in the Soay breed, a very low rate (2 cells/mm^2) was found in comparison to the domestic breed (30 cells/mm^2 in Brus et al.'s (2010) study) albeit despite the dose of BrdU injected in that study being three-fold. Whether this difference is due to disparities in methodology or to breed differences remain unknown.

Dynamics of Maturation

Similar to what is observed in the MOB, neuronal maturation in the DG takes a longer time in sheep than in rodents. In the DG of rodents, the majority of neuroblasts is observed at 7 days after BrdU injection and this population declines by 30 days (Brown et al., 2003; Kempermann et al., 2003; Steiner et al., 2004; McDonald and Wojtowicz, 2005; Suh et al., 2007). In sheep, the proportion of neuroblasts peaks at 1 month and stays fairly stable up to 8 months post-injection (**Figure 2**; Brus et al., 2013). A similar timing of maturation of the neuroblasts is reported in the macaque monkey (Kohler et al., 2011). As for the mature neurons, in rodents they are detected at 10 days post-injection and their number increases up to 1-month survival time (Cameron et al., 1993; Brown et al., 2003; Steiner et al., 2004; McDonald and Wojtowicz, 2005; Suh et al., 2007). In sheep, a low proportion of DCX+ or NeuN+ cells is observed at 1 month BrdU post-injection and the proportion of mature neurons peaks at 4 months survival time (Brus et al., 2013). Similarly, in primates, very few mature neurons are found at 1-month survival time and are the most numerous at 6-months survival time (Kohler et al., 2011; Sawamoto et al., 2011).

In both the MOB and the DG, <50% of the BrdU+ cells turn into mature neurons even at 8 months post-injections, in contrast to mice and rats in which the majority of BrdU+ cells become neurons (Petreanu and Alvarez-Buylla, 2002; Winner et al., 2002; Suh et al., 2007; Imayoshi et al., 2008). In summary, olfactory and hippocampal neurogenesis in sheep are characterized by delayed neuronal maturation, similar to primates (Kohler et al., 2011). However, one cannot exclude that the production of neurons by progenitor cells is reduced in comparison to rodents, as was shown in primates (Tonchev and Yamashima, 2006). Although the mechanisms underlying differences in the length of maturation between species remain to be determined, a parsimonious hypothesis could be related to differences in their life spans.

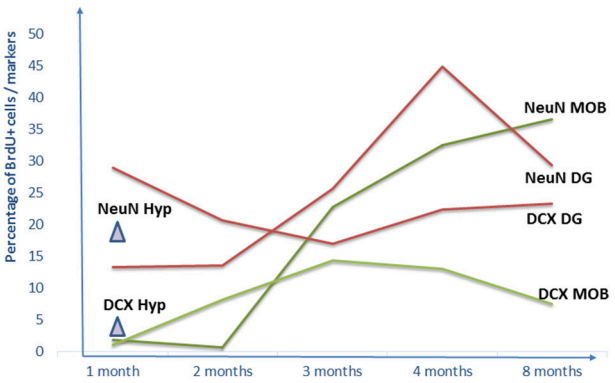

FIGURE 2 | Dynamics of adult neurogenesis in the main olfactory bulb, the dentate gyrus of the hippocampus and the hypothalamus. Results are expressed as percentage of BrdU+ cells per markers for NeuN+ and DCX+ at 1, 2, 3, 4, and 8-month BrdU post-injections. No data are available after 1-month post-injection for the hypothalamus. DG, dentate gyrus; Hyp, hypothalamus; MOB, main olfactory bulb.

Hypothalamic Neurogenesis

Historic

Fifteen years ago, the neurogenic activity observed in the mammalian brain was thought to be limited to the two defined regions described above. However, numerous pieces of evidence indicate that other brain regions retained the capacity to produce adult-born neurons under physiological conditions. Indeed the existence of new neurons has been revealed in the hypothalamus (Kokoeva et al., 2005; Xu et al., 2005; Migaud et al., 2010), the amygdala (Bernier et al., 2002; Luzzati et al., 2003; Akbari et al., 2007; Ahmed et al., 2008), the striatum (Bedard et al., 2002, 2006; Emsley et al., 2005), the piriform and prefrontaly cortices (Bernier et al., 2002; Pekcec et al., 2006; Staffend et al., 2014) as well as more caudally in the substantia nigra (Zhao and Janson Lang, 2009) and the midbrain raphe nuclei (Holschbach and Lonstein, 2017).

Among these structures the hypothalamus has received much attention (reviews: Migaud et al., 2010; Lee and Blackshaw, 2012, although its level of constitutive neurogenesis seems lower than in the two well-documented neurogenic regions (Lee and Blackshaw, 2012). Constitutive hypothalamic neurogenesis has been proven to occur in many species of mammals, including mice (Kokoeva et al., 2005, 2007; Lee et al., 2012; Li et al.,

2012; Werner et al., 2012; review in Lee and Blackshaw, 2012), rats (Pencea et al., 2001; Xu et al., 2005; Pérez-Martín et al., 2010), voles (Fowler et al., 2005), hamsters (Huang et al., 1998; Mohr and Sisk, 2013), and sheep (Migaud et al., 2010, 2011; Batailler et al., 2014, 2016; **Figure 3**), indicating that structural plasticity involving *de novo* cell genesis is an evolutionary conserved process possibly taking place in humans as well (Dahiya et al., 2011; Batailler et al., 2014). The hypothalamus is limited anteriorly and posteriorly by the optic chiasm and the mammillary bodies, respectively, whereas the optic tract constitutes its lateral perimeter. This small ventral brain region is symmetrically located between the third ventricle and contains numerous distinct nuclei (**Figure 3**). Constant hypothalamic neurogenic sites have been located in the subependymal zone of the third ventricle of the arcuate nucleus and the median eminence (ME; Kokoeva et al., 2005; Yuan and Arias-Carrion, 2011; Cheng, 2013). This neurogenesis process may be involved in hypothalamic regulatory mechanisms, including in the control of energy balance and in the regulation of reproductive physiology.

Hypothalamic Cell Proliferation

There are now numerous pieces of evidence indicating that new neurons can be formed outside the SGZ and the SVZ, in niches located in other structures of the adult brain. The presence of cells having incorporated the proliferation marker BrdU in the adult hypothalamus was first reported in 2001 in the rat (Pencea et al., 2001). These authors showed for the first time a proliferative activity outside the neurogenic niches and demonstrated that the number of cells in proliferation increased after brain-derived neurotrophic factor (BDNF) infusion. Few years later, a more comprehensive study, revealed the presence of neural progenitor cells (NPCs) located in the ependymal layer of the adult third ventricle, including tanycytes-derived NPCs (Xu et al., 2005). From then, it was shown that hypothalamic cell proliferation occurs constitutively without conspicuous contribution of external signals (Huang et al., 1998; Pencea et al., 2001; Fowler et al., 2002; Kokoeva et al., 2005; Xu et al., 2005; Pérez-Martín et al., 2010; Migaud et al., 2011; Mohr and Sisk, 2013) regardless of the concentration of the proliferation marker used, the route of administration, or the species being studied.

In sheep, constitutive cell proliferation in the whole hypothalamus is detected 24 h after a single intravenous (i.v.) BrdU injection (Migaud et al., 2010, 2011) and substantial proliferative activity is observed in the hypothalamus of Ile-de-France ewe (i.e., ∼400 BrdU+ nuclei per hypothalamic section). BrdU+ nuclei are often seenas contacting cell pairs, which is a characteristic of recent or ongoing mitotic activity (Migaud et al., 2011). Similarly, in the male Soay sheep, dividing cells are detected in the hypothalamus following two consecutive i.v. injections of BrdU. Mitotic cells have been detected in the three distinct hypothalamic regions the ependymal cell layer, the median eminence and a region covering the tanycyte projection zone (Hazlerigg et al., 2013). More recently, the use of proliferating cell nuclear antigen (PCNA) a cell proliferation marker confirms ongoing hypothalamic new cell generation in the arcuate nucleus and the ME of adult sheep (Batailler et al., 2014). However, no BrdU+ cells are detected in the

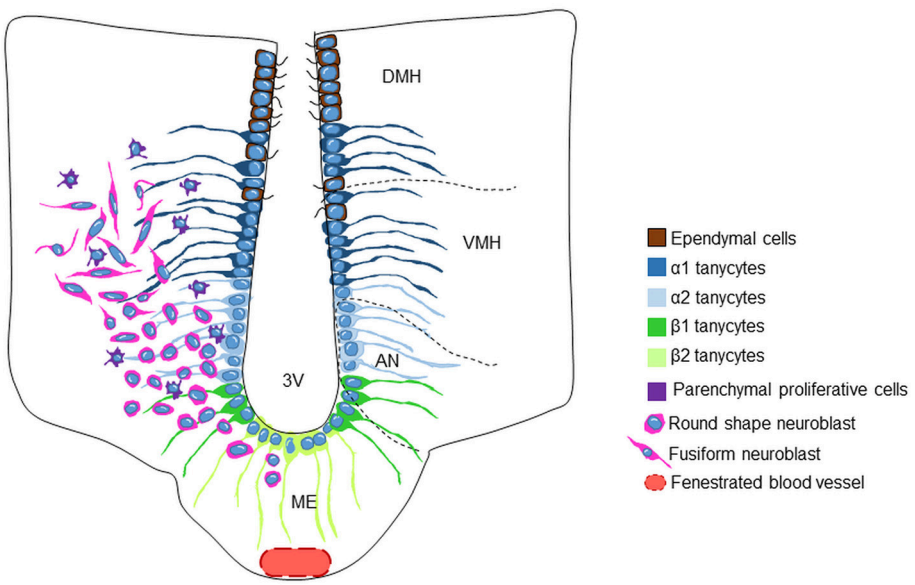

FIGURE 3 | Schematic representation of the tanycytic/stem cell populations in the adult sheep hypothalamic neurogenic niche. The third ventricle (3V) wall is composed of ciliated ependymal cells and four different populations of tanycytes. The medial part of the 3V contains α1-and α2-tanycytes that contact the VMN and the ARN nuclei, respectively. The ventral part of the 3V wall (median eminence) contains β1- and β2-tanycytes, the latter residing on the floor of the 3V. β2-tanycytes are in contact with the hypothalamic-pituitary portal system through fenestrated blood vessels. The round shaped neuroblasts are located in the AN and become more fusiform when they reach the VMH. Progenitor cells are detected throughout the VMH and AN parenchyma. DMH, dorsomedial hypothalamus; VMH, ventromedial hypothalamus; AN, arcuate nucleus; 3V, 3rd ventricle; ME, median eminence.

hypothalamus of female Merino sheep (Hawken et al., 2009). These inconsistencies could be attributed to the differences in the technical procedures used, including the protocol for BrdU immunodetection (e.g., different primary antisera concentrations of HCl used).

Fate of the Hypothalamic Newborn Cells

The hypothalamic mitotic cells in sheep adopt a neuronal phenotype as revealed by the high number of immature neurons that express DCX (Batailler et al., 2014; Migaud et al., 2015; **Figure 1D**). Among the cohort of immature neurons, a subset appear to go through maturation, as demonstrated by the colocalization of DCX with markers of more mature neurons, such as human neuronal protein C and D (HuC/D). More specifically, 1 month following BrdU administration, around 17% of the hypothalamic BrdU+ cells expressed the mature neuronal marker NeuN, confirming the existence of a neurogenic process in the adult sheep hypothalamus (Migaud et al., 2011). In contrasting, in Soay rams, the hypothalamic BrdU-positive cells did not seem to adopt a neuronal phenotype, but rather, 10% of the mitotic cells located in the ME showed morphological features consistent with microglia as they co-express the pan-leukocytic marker CD45 (Hazlerigg et al., 2013). The phenotype of the remaining 90% BrdU positive cells remain unknown. The reason for this discrepancy is not clear, but one hypothesis could be that the maturation process was delayed due to the photoperiodic protocol used, leading to a delayed expression of the marker for mature neurons.

However, in rodent species, the neuronal commitment of the hypothalamic newborn cells was generally verified and between 10 and 37% of the total BrdU-positive cells were found to co-express the neuronal marker. The number of hypothalamic newborn neurons is, therefore, much lower than in the two canonical niches, the SVZ and SGZ. The existence of constitutive hypothalamic neurogenesis at a low rate of neurogenesis was established in rodent models using genetic fate mapping techniques (Lee et al., 2012; Li et al., 2012; Haan et al., 2013; Robins et al., 2013a). By these approaches, the phenotype of the adult born hypothalamic neurons was determined by their expression of peptides relevant for metabolism and feeding control, including neuropeptide-Y (NPY), proopiomelanocortin (POMC; Kokoeva et al., 2005; Li et al., 2012; Haan et al., 2013), and agouti-related protein (AgRP; Pierce and Xu, 2010). In sheep, subsets of hypothalamic neuroblasts also developed specific hypothalamic phenotypes such as NPY (Batailler et al., 2014). In addition, hypothalamic new-born neurons were shown to express estrogen receptor (ER)α, in female mice (Bless et al., 2016) and in ewes (Batailler et al., 2014) indicative of a putative role for these newborn (ER)α cells in the modulation of reproductive behavior (Musatov et al., 2006; Gao and Horvath, 2008).

The sheep hypothalamus appears to be also gliogenic because 70% of the new cells differentiated into S100B+ and GFAP+ astrocytes. However, similarly to what is described in the rat model, no new cells become oligodendrocytes (Steiner et al., 2004). Yet, in mice, Kokoeva et al. (2005) reported the capacity of the hypothalamic adult born cells to produce oligodendrocytes using APC another oligodendrocytic marker. Whether these results reveal difference between species in the time course of glial differentiation requires clarification. Interestingly, adult hypothalamic neurogenesis is notably influenced by various external stimuli, including season (Migaud et al., 2010, 2011, 2015, see below for details), diet (for a review, see Yon et al., 2013), exercise (Niwa et al., 2015) and the social environment (Fowler et al., 2002), which could also explain inconsistencies in the number of newborn neurons detected depending on the study.

The Hypothalamic Neurogenic Niche

In contrast with the two main documented niches the SVZ and the SGZ, little is known about the hypothalamic neurogenic niche, and most of our knowledge is inferred from rodent studies. Three cell layers were identified in the adult third ventricle wall: multiciliated cubic ependymal cells, astrocytic subependyma and non-ciliated cells known as tanycytes extending their long cell processes into the hypothalamic parenchyma (Flament-Durand and Brion, 1985). This subset of specialized ependymoglial cells retaining the morphological features of embryonic radial glia cells contact the cerebrospinal fluid. This configuration is generally reminiscent of the generalstructural organization of the SVZ of the lateral ventricle, although the hypothalamic region lined by the tanycytes lacks an identifiable subventricular zone, like the one lining the walls of the lateral ventricles (Doetsch et al., 1997; Alvarez-Buylla et al., 2002).

Four types of hypothalamic tanycytes have been distinguished regarding based on their location within the ventricular wall and gene expression profile (**Figure 3**). The α1- and α2-tanycytes reside at the level of the ventromedial nuclei and the arcuate nuclei respectively. β1-tanycytes are located in the lateral part of the infundibulum. Finally, β2-tanycytes are positioned in the floor of the third ventricle (Rodriguez et al., 2005). Interestingly, in contrast to other hypothalamic regions, the ME lies outside of the blood-brain barrier, and is therefore a circumventricular organ (Miyata, 2015). Consequently, tanycytes located in the ME are responsive to the hormones, growth factors and nutritional substances transported by the blood and conversely, the tanycytic cell bodies lining the third ventricular wall are exposed to the molecular signals conveyed by the cerebrospinal fluid.

All the tanycyte populations express proteins that are typical for NSC/precursor cells, including Sox2 (Lee et al., 2012; Li et al., 2012), Nestin (Wei et al., 2002), vimentin (Bolborea and Dale, 2013), doublecortin-like protein (DCL; Saaltink et al., 2012), and Alpha-tanycytes express GFAP and the astrocyte-specific glutamate transporter (GLAST) like the SVZ B1 type cells, whereas β tanycytes and a small portion of α tanycytes express Fibroblast growth factor 10 (FGF-10; Li et al., 2012; Robins et al., 2013a), a growth factor implicated in regulating the formation of cortical radial glial cells (Sahara and O'Leary, 2009).

In the sheep hypothalamus, numerous nuclei expressing Sox2 are found in the ependymal or subependymal layers. In addition, almost all cells lining the walls of the third ventricule express the intermediate filament vimentin and most vimentin positive cells, if not all, also strongly coexpressed GFAP in their long processes, producing a staining pattern similar to that previously described in other species, particularly in rodents (Prevot, 2002; Kameda

et al., 2003; Baroncini et al., 2007; Langlet et al., 2013). In both the ME and the arcuate nucleus, cells immunoreactive for the three stem cell markers Sox2, GFAP, and Vimentin, are therefore principally distributed in the ependymal and subependymal cell layers lining the third ventricle. The existence of a neurogenic niche in the sheep hypothalamus was further evidenced by the typical tanycyte morphology of the cells lining the third ventricular wall expressing both nestin and Sox2.

The identity of the tanycyte subtypes representing the rodent hypothalamic NSCs is still a matter of debate. Some lineage tracing experiments have revealed that α2-tanycytes have the potential to be the hypothalamic NSCs (Robins et al., 2013a), since the proliferation of α-tanycyte is promoted by FGF2 (Robins et al., 2013a) and the insulin-like growth factor (IGF; Pérez-Martín et al., 2010). In addition, they are the only subtype capable of forming neurospheres and they can give rise to β1-tanycytes. Alternatively, several other studies using different lineage tracing mice models have shown that β-tanycytes are the major sources of progenitor cells in the hypothalamus of young adult mice (Bolborea and Dale, 2013; Haan et al., 2013). More specifically, β2 cells are highly proliferative and neurogenic in young animals (Lee et al., 2012, 2014). Due to our large mammalian model, it is hardly conceivable to develop such intersectional genetic approaches in order to identify the tanycyte(s) subtypes incriminated. However, the recent introduction of the "CRISPR-cas9" technology (Hsu et al., 2014) and the potential regulatory programmable schemes employed in the future to provide temporal control for these reagents (Guha et al., 2017) will be useful to modify the genome, regardless of the mammalian species. These strategies will undoubtedly participate in our understanding of neurogenesis mechanisms in large mammalian species like sheep.

While tanycytes surely constitute a major class of NSCs of the hypothalamic neurogenic niche, a subset of Sox2 expressing cells also showing a proliferative activity has been detected in the hypothalamic parenchyma in sheep (Migaud et al., 2011; Batailler et al., 2014) and in rodents (Kokoeva et al., 2005; Li et al., 2012; Robins et al., 2013b). Whether these cells contribute to the neurogenic process and to hypothalamic physiological functions is currently unknown.

In sheep, numerous DCX-positive immature neurons are observed in the arcuate nucleus, likely originating from the germinative zones lining the ventral part of the third ventricle (Batailler et al., 2014). The morphology of the DCX-positive cells changes whether they are close to or distant from the third ventricle cavity. DCX-positive cells near the third ventricle show a rather round shape with no processes, typical of very immature neuroblasts. Conversely, DCX-positive cells found in the parenchyma of the ventromedial hypothalamus show fusiform perikarya and lengthened processes, some of the characteristics of migrating cells undergoing maturation (**Figure 3**; Batailler et al., 2014). One hypothesis is that neuroblasts located in the subependymal niche may spread toward neighboring hypothalamic nuclei and form a migratory path (Batailler et al., 2014), as it has been suggested in rodents (Haan et al., 2013). One way to test this hypothesis would be to label progenitors with iron oxide particles and detect their putative migration by means of magnetic resonance imaging.

In contrast, a very different pattern of DCX labeling was found in the mouse hypothalamus (Kokoeva et al., 2007; Batailler et al., 2014), with only low-intensity labeled cells detected in the arcuate nucleus and moderate to high levels of labeled fibers in the ME. This was true in both sexes, excluding an effect of the estrous cycle. Likely differences in the function of these DCX-positive cells between species may be the reason for this discrepancy.

The flow of adult rodent hypothalamic neurogenesis is promoted by numerous growth factors, including IGF-1 (Pérez-Martín et al., 2010; Chaker et al., 2016), BDNF (Pencea et al., 2001), ciliary neurotrophic factor (CNTF; Kokoeva et al., 2005), FGF, and epidermal growth factor (Xu et al., 2005; Pierce and Xu, 2010, reviewed in Sousa-Ferreira et al., 2014). Additionally, a recent study also reported an enhancement of the hypothalamic proliferating activity in aged mice by gonadotropin releasing hormone (Zhang et al., 2013). As with the DG and the SVZ, the rate of hypothalamic proliferation may be affected by exogenous factors. For example, in the highly social prairie vole male exposure enhances cell proliferation in the female hypothalamus and the amygdala when compared to socially isolated animals (Fowler et al., 2002). Voluntary exercise may also enhance hypothalamic cell turnover in rats (Niwa et al., 2015).

PHYSIOLOGICAL REGULATION OF NEUROGENESIS

Seasonal Regulation

In seasonal species, photoperiod is a critical environmental cue required for the seasonal programming of reproductive and metabolic functions, an adaptive strategy to cope with the annual fluctuations in climate, temperature, and food availability. The influence of seasons and photoperiod on adult cell proliferation and neurogenesis, mainly in the two canonical niches, has been extensively studied in a broad range of mammalian seasonal species including Golden (Huang et al., 1998) and F1B (Smith et al., 2001) hamsters, deer mice (Perrot-Sinal et al., 1998), white footed mice (Walton et al., 2012), meadow voles (Galea and McEwen, 1999; Galea et al., 1999; Ormerod and Galea, 2003), Richardson's ground squirrel (Burger et al., 2013), eastern gray squirrels (Lavenex et al., 2000), shrew (Bartkowska et al., 2008), and sheep (Migaud et al., 2010, 2011; Hazlerigg et al., 2013).

Seasonal changes in cell proliferation have been detected in the DG of adult female meadow voles (Galea and McEwen, 1999; Galea et al., 1999). In this species, females show higher levels of cell proliferation than males and higher levels during the non-breeding than during the breeding period (Galea and McEwen, 1999; Ormerod and Galea, 2003). In the DG of the golden hamster, a two-fold increase in the number of dividing cells has been found after a transition from long days to short days (Huang et al., 1998). Photoperiod also affects cell proliferation in DG of the Richardson's ground squirrel (Burger et al., 2013), the Soay ram (Hazlerigg et al., 2013), and the shrew (Bartkowska et al., 2008). In contrast, some studies failed to detect cell proliferation

changes in male meadow voles (Ormerod and Galea, 2003) or in squirrels (Lavenex et al., 2000).

The olfactory neurogenic niche is also influenced by photoperiodic changes. In short day exposure, Syrian hamsters show an increased rate of neurogenesis in the MOB (Huang et al., 1998). In white-footed mice, an increase in new neurons in the caudal olfactory bulb resulting from short day exposure is linked with changes in behavioral responses to the urine of conspecific males (Walton et al., 2012), suggesting that olfactory neurogenesis may be a mechanism underlying photoperiodic variations in social interactions. In contrast, in two species of photoperiodic shrews, short day exposure induces a reduction in SVZ proliferation and neurogenesis (Bartkowska et al., 2008). In the sheep SVZ, no cell proliferation changes are observed across the seasons (Migaud et al., 2011). All these data indicate species-specific effects of the photoperiod on the neurogenesis in the SGZ and the SVZ.

By contrast, only a few studies have examined the influence of season on adult hypothalamic neurogenesis. In Syrian hamsters, a transition from long to short days increases cell proliferation (Huang et al., 1998). In Siberian hamster tanycytes, the expression of the transcript for nestin, an intermediate filament protein used as a neural stem cell marker (Kronenberg et al., 2003; for review see Wiese et al., 2004), is down-regulated during short-day photoperiod exposure (Barrett et al., 2006; Ebling and Barrett, 2008).

In Ile-de-France ewes, the proliferative capacity of the hypothalamus is seasonally regulated (Migaud et al., 2010, 2011). Significantly more new hypothalamic cells are generated, independent of sex steroids, during the short days (corresponding to the period of sexual activity in this species) compared with the long days (coinciding with the period of sexual inactivity; Migaud et al., 2011). However, in Soay rams, no clear seasonal variation is observed in the level of cell proliferation, whatever the hypothalamic region considered (Hazlerigg et al., 2013). The reason for this discrepancy is unknown but might depend on differences in the immunohistochemical procedure, or in the photoperiodic treatment provided. Nevertheless, a higher density of DCX-expressing neurons is found in the arcuate nucleus and the ME (Batailler et al., 2014), the most neurogenic region of the hypothalamus (Lee et al., 2013), during the stimulatory short photoperiod compared with the inhibitory long photoperiod. These data suggest that seasonal regulation of neurogenesis might be a common regulatory mechanism among adult seasonal mammals.

Regulation by Physiological Status and Social Interactions

The different processes of neurogenesis, mainly production, maturation, and survival are also under the control of various internal factors (Lledo et al., 2006). Many studies have shown that the estrous cycle, pregnancy, and parturition regulate hippocampal and olfactory neurogenesis in laboratory rodents (for review: Pawluski et al., 2009; Lévy et al., 2011). In sheep, physiological changes associated with parturition influence cell proliferation in the DG and the MOB. Mothers permanently separated from their newborn lambs immediately after parturition show a decrease in cell proliferation, evidenced by BrdU labeling, in the MOB and in the sub-granular zone of the DG compared to non-separated ewes (Brus et al., 2010). In a follow-up study, using Ki67 as a marker of proliferation, a similar decrease in proliferation was found in both the MOB and the DG of parturient ewes in comparison to non-pregnant females (Brus et al., 2014).

This down-regulation could be the consequence of the change in circulating steroids occurring at parturition. In the female rat, a regime of ovarian steroids that mimicks the fluctuations occurring at birth, decreases cell proliferation in the DG (Tanapat et al., 2005; Pawluski et al., 2009). The increased cortisol levels at parturition also decreases cell proliferation in the DG (Tanapat et al., 1999; Darnaudery et al., 2007). In sheep, both oestradiol and cortisol could be involved in the decreased cell proliferation in the DG and in the MOB. Interestingly, estrogen and glucocorticoid receptors are found in both structures (Morimoto et al., 1996; Shughrue et al., 1997; Sah et al., 2005). This down-regulation is not observed in the SVZ, suggesting that olfactory cell proliferation could be differently regulated according to the brain region. Supporting this view, the SVZ lacks estrogen and glucocorticoid receptors (Shughrue et al., 1997; Shughrue and Merchenthaler, 2000) and cortisol treatment differentially affects the DG and the SVZ, reducing neural production in the DG but sparing it in the SVZ (Siopi et al., 2016).

Regulation of cell survival by parturition differs from that of cell proliferation because changes in survival are found only for the DG but not for the MOB. Survival is reduced by parturition as indicated by the finding that mothers separated from their young at parturition show a down-regulation of BrdU+/NeuN+ cells (Brus et al., 2014). Cortisol release at parturition could be involved, as well as other endocrine factors as oxytocin (Leuner et al., 2012). By contrast, no change in the number of neuroblasts is found in these parturient ewes, suggesting differential regulation according to the maturity stage, which has been reported for the effects of corticosterone in the DG of mice (Gonzalez-Perez et al., 2011; Lussier et al., 2013).

Not only can endocrine changes regulate neurogenesis, but social factors can also affect cell proliferation and survival (Gheusi et al., 2009; Holmes, 2016). In sheep, a reproductive cycle can be induced in anoestrus females when exposed to males (Martin et al., 1986), which doubles the rate of cell proliferation in the DG (Hawken et al., 2009). In addition, in sheep maternal behavior at parturition depends on olfactory attraction toward amniotic fluids that cover the newborn lamb (Lévy et al., 2004; Poindron et al., 2007; Lévy and Keller, 2009). These cues render the newborn lamb attractive and stimulate its licking by the mother, thus inducing maternal behavior. Moreover, ewes are able to discriminate their own young from an alien lamb by learning its olfactory signature within 2 h after parturition (Lévy et al., 2004; Lévy and Keller, 2009). This learning is accompanied with neurochemical changes occurring in the MOB (Lévy et al., 1993; Lévy and Keller, 2009). Olfactory neurogenesis could also contribute to the onset of maternal behavior and associated learning, and altered neurogenesis during the establishment of

maternal behavior support this hypothesis. Brus et al. (2010) show that decreased cell proliferation occurs in the SVZ, but not in the DG, in ewes that remain with their lambs for the first 2 days after parturition when compared to ewes separated from them. However, SVZ cell proliferation is not affected in ewes mating with a male, and thus appears to be specific to interactions with the young. Consistent with these findings, the survival of neuroblasts in the MOB is also reduced in ewes interacting with their lamb but maturation of the remaining neuroblasts is heightened (Brus et al., 2014). Interactions with young and associated olfactory learning rather than parturition are responsible for these modifications because they are prevented by separating ewes from their lambs at parturition. Numerous studies report that olfactory experience sculpts newborn neurons (for review: Lazarini and Lledo, 2011), with nostril closure decreasing (Saghatelyan et al., 2005) and odor enrichment increasing the arborization complexity of newborn granule cells (Livneh and Mizrahi, 2011). In the context of motherhood, olfactory exposure to pups induces changes in structural synaptic plasticity of newly born olfactory neurons in mice (Kopel et al., 2012; Belnoue et al., 2016). Although, the functional relevance of the plasticity occurring in the MOB of sheep remains to be determined, one can hypothesize that the decrease in the number of neuroblasts would reduce cell competition and consequently increases their maturation, allowing them to be integrated in the neural network involved in learning. In support to this proposition, neural network models of hippocampal neurogenesis show that high levels of cell proliferation are have negative effects on the stability of neural activity and consequently for learning (Lehmann et al., 2005; Butz et al., 2006). Another modeling study indicates that an increase in cell proliferation causes a reduction in the amount of synaptic rewiring which is not beneficial for learning (Butz et al., 2008). Whether these findings can be applied for olfactory neurogenesis remains to be determined.

FUNCTIONAL RELEVANCE OF NEUROGENESIS

Hypothalamic Neurogenesis

The hypothalamus is an essential homeostatic regulator of many physiological and behavioral processes, such as reproduction, feeding, growth, metabolism, body temperature, and circadian rhythms (Saper and Lowell, 2014). Some of the important roles of this structure are to integrate sensory inputs with hormonal and peripheral signals, to control pituitary hormone secretions and regulate the downstream major biological functions. Evidence for adult hypothalamic neurogenesis raises the issue of its functional role that is still in its early exploratory phases. Because of the key role plays by the hypothalamus in metabolism and food intake, the significance of hypothalamic neurogenesis in these functions has been the most explored so far. In mice, hypothalamic newborn neurons acquire the identities and the functional phenotypes related to the control of energy homeostasis, including NPY or POMC (Kokoeva et al., 2005; McNay et al., 2012; Gouaze et al., 2013). In addition, some of these new neurons are responsive to fasting and leptin (Kokoeva et al., 2005; Pierce and Xu, 2010; Haan et al., 2013). Several recent studies show that diet can regulate adult hypothalamic neurogenesis, although the results are equivocal. Opposing effects of high fat diet on neurogenesis and body weight are reported depending on the ages and sexes of the animals tested, as well as the duration of the diet and the targeted hypothalamic area (Lee et al., 2012; Li et al., 2012). In mice, the loss of weight induced by the administration of the CNTF is suppressed when administered concomitantly with the cytosine arabinoside (Ara-C), an antimitotic drug, which blocks hypothalamic cell proliferation indicating a role of hypothalamic neurogenesis in weight regulation (Kokoeva et al., 2005).

The hypothalamus is also the integrative center that regulates reproduction, and newly formed hypothalamic cells express ERα (Batailler et al., 2014; Bless et al., 2016), a receptor involved in many aspects of both male and female reproduction (Ogawa et al., 1998; Emmen and Korach, 2003). In sheep, to explore the role of hypothalamic neurogenesis in the seasonal control of reproductive function, Ara-C was administered into the third ventricle for 30 days during the peak of hypothalamic cell proliferation (Batailler et al., submitted). This treatment induced a notable 75% decrease in hypothalamic neurogenesis assessed by the density of DCX-positive cells. This decrease resulted in an advance of the entry in seasonal anoestrus and a similar advance in the re-entry in sexual activity the following season. Interestingly, in our experimental conditions, none of the animals showed altered body weight. These data draw a strong interaction between new neuron production and the seasonal adaptation of neuroendocrine networks, with hypothalamic neurogenesis being likely involved in the functional adaptation of the brain to the changing environmental conditions. The precise identification of the phenotype and the destinations of the newborn neurons will give insights to the molecular pathways involved in these processes.

Olfactory Neurogenesis

In mammals, only a few studies have looked at changes in social behavior induced by reducing or blocking neurogenesis (Holmes, 2016). In sheep, the functional relevance of neurogenesis has been examined in the context of maternal behavior by testing the hypothesis that increased activation of newborn neurons after exposure to lambs is behaviourally relevant. By pairing neurogenic markers with markers of neural activity, activation of olfactory newborn neurons have been compared between mothers exposed either to their own lamb, an unfamiliar lamb, or to an adult conspecific (Corona et al., 2016). Exposure to either both lambs increases the percentage of neuroblasts activated in the granular layer of the MOB compared to exposure to an unfamiliar ewe, indicating that the preferential activation is not seen for any social odors but is specific to lamb odors. By contrast, newborn neurons in the DG do not show any activation in response to any of the odors.

Hence, newborn neurons of the MOB could participate to the processing of olfactory cues responsible for maternal attraction to any newborn lambs at parturition. However, these olfactory adult-born neurons fail to differentiate between familiar and

unfamiliar lamb exposure, so another pool of newborn neurons of distinct ages could be involved in recognition of the familiar lamb.

To further understand the functional relevance of olfactory neurogenesis disruption of neurogenesis was performed and its consequences on maternal behavior was assessed. To prevent adult olfactory neurogenesis in parturient sheep mothers, infusion of Ara-C into the SVZ for 1 month during pregnancy was performed and the consequences on maternal behavior and recognition of the familiar lamb assessed during early postpartum period (Corona et al., submitted). Ara-C infusion led to a 70% reduction in olfactory neurogenesis, evidenced by DCX labeling, sparing hippocampal neurogenesis. The impairment of olfactory neurogenesis was found to reduce maternal vocalizations in the presence of the familiar lamb at parturition and during selectivity tests. However, all the ewes are maternal and selective for their own lamb. These relatively minor effects on mothering could be related to limitations of the method used for blocking neurogenesis. Although the levels of olfactory neurogenesis are dramatically reduced by Ara-C infusion, it is possible that the remaining olfactory newborn neurons are sufficient to sustain maternal behavior and olfactory recognition of the familiar lamb. Similarly, in mice infusion of an anti-mitotic agent into the SVZ induces little disturbance of maternal behavior (Larsen and Grattan, 2010) and irradiation of the SVZ does not alter either maternal behavior or dams' ability to discriminate familiar pups from alien pups (Feierstein et al., 2010). However, genetic manipulations inducing continuous inhibition of neurogenesis during pregnancy and postpartum disrupts nursing (Sakamoto et al., 2011). Therefore, a more extended ablation of olfactory neurogenesis would be helpful to assess the role of olfactory neurogenesis in motherhood of sheep.

CONCLUSION AND FUTURE DIRECTIONS

The generation of new neurons in the adult mammalian brain, long thought to be non-existent, is now widely established although the issue of human olfactory neurogenesis is still under debate (Curtis et al., 2007; Bergmann et al., 2012). Over the last few decades, studies performed in rodents have led to considerable improvements in our understanding of this phenomenon. However, as shown in the present review, the cellular and molecular machinery and the functional mechanisms behind how this process influences adult brain circuits may differ qualitatively and quantitatively between species according to their brain features, lifespan, physiological, and behavioral burdens (**Table 1**). These differences between species stress the importance of analyzing the neurogenic process in multiple different model systems. Overall, this review highlights sheep as an appropriate model to investigate the role of adult neurogenesis during individual recognition/discrimination and in neuroendocrine behaviors related to reproduction, although further experiments are needed to explore in depth the neural circuits underlying these relationships as well as the physiological underpinnings involved.

Similar to laboratory rodents, studies performed in sheep have demonstrated the existence of neurogenic niches in the SVZ, the SGZ, and the hypothalamus. In contrast, the cellular composition and the morphological organization of the sheep SVZ and the hypothalamus differ from that of rodents (**Table 1**). Furthermore, a longer maturation time frame is observed for newborn neurons in sheep compared with rodents. These latter features appear to share similarities with the non-human primate brain. In addition, a comparable pattern of distribution of neuroblasts is reported in sheep and human hypothalamus, but both different from the murine hypothalamus (Batailler et al., 2014). Thus, sheep could be a suitable alternative model to primates to gain insights into the function of adult neurogenesis for therapeutics in humans. Currently, no data are available on the time required for the full neuronal maturation of the newborn neurons in our species and further investigation is necessary to compare the timing of differentiation of the new neurons in humans and in non-human primates or sheep.

TABLE 1 | Comparative organization of the three neurogenic niches the SVZ, SGZ, and the hypothalamic neurogenic niche (Hyp) in five mammalian species.

	SVZ					SGZ		Hyp		
	PPCs	**Hypocellular Gap**	**RMS**	**Migration rates**	**Neurogenic olfactory ventricle**	**PPCs**	**Adult born GCs**	**PPCs**	**DCX+ Neuroblasts**	**Adult born neurons**
Rodents	++	0	+	3–7 days in mice 10–12 days in rats	0	++	+	++	±	POMC, NPY, AgRP
Rabbit	++	+	+	ND	+	ND	ND	ND	ND	ND
NHP	++	+	+	2–3 months	0	++	+	ND	ND	ND
Sheep	++	+	+	1 month	+	+	+	++	++	NPY
Adult Human	+	0	0	ND	0	++	++	ND	ND	ND

NHP, Non-human primates; PPCs, proliferative progenitor cells; RMS, rostral migratory stream; ++, strong presence; +, presence; ±, weak presence; 0, absence; ND, Not determined. POMC, Pro-Opiomelanocortin. NPY, Neuropeptide Y; AgRP, Agouti related Peptide. Rodents, Lois and Alvarez-Buylla, 1994; Kokoeva et al., 2005; Pierce and Xu, 2010; Lee et al., 2012; Haan et al., 2013; Rabbits, Bonfanti and Ponti, 2008; Larriva-Sahd, 2014; NHP, Gil-Perotin et al., 2009; Sawamoto et al., 2011; Wang et al., 2011; Sheep, Migaud et al., 2011; Brus et al., 2013; Batailler et al., 2014. Adult human, Quinones-Hinojosa et al., 2006; Butz et al., 2008; Sanai et al., 2011; Spalding et al., 2013.

Increasing our knowledge on the existence of newly formed neurons in humans will also require the development of advanced imaging techniques. In some regards, sheep are already considered as an important developing model for translational imaging procedures (Forschler et al., 2007; van der Bom et al., 2013; Beuing et al., 2014) and in support of that the ovine brain template and corresponding tissue probability maps have very recently been generated and made available (Ella and Keller, 2015; Nitzsche et al., 2015). In our sheep, a magnetic resonance imaging study is currently being undertaken to label progenitors with iron oxide particles to detect their migration. The implementation of neuroimaging procedures enabling the study of neurogenesis in an appropriate animal model, such as sheep, will very likely lead to the development of translational experiments performed in normal and pathological human brains.

AUTHOR CONTRIBUTIONS

FL, MB, MMe, and MMi wrote and edited the manuscript. MB and MMe drew the figures.

ACKNOWLEDGMENTS

MMi work's was funded by the French National Research Agency (Agence Nationale pour la Recherche: SeasoNRG ANR-09-JCJC-0049-01 and HypNeurogen ANR-16-CE37-0006-01) and FL's work was funded by French National Research Agency (PLASTMATBEHAV ANR12-BSV7-0017). This work has benefited from the facilities and expertise of the cellular imaging platform (PIC), UMR PRC, INRA Centre Val de Loire, France. We thank Prof. J. Lonstein for his kind revision of the manuscript.

REFERENCES

Ahmed, E. I., Zehr, J. L., Schulz, K. M., Lorenz, B. H., DonCarlos, L. L., and Sisk, C. L. (2008). Pubertal hormones modulate the addition of new cells to sexually dimorphic brain regions. *Nat Neurosci.* 11, 995–997. doi: 10.1038/nn.2178

Akbari, E. M., Chatterjee, D., Lévy, F., and Fleming, A. S. (2007). Experience-dependent cell survival in the maternal rat brain. *Behav. Neurosci.* 121, 1001–1011. doi: 10.1037/0735-7044.121.5.1001

Alvarez-Buylla, A., Garcia-Verdugo, J. M., and Tramontin, A. D. (2001). A unified hypothesis on the lineage of neural stem cells. *Nat. Rev. Neurosci.* 2, 287–293. doi: 10.1038/35067582

Alvarez-Buylla, A., Seri, B., and Doetsch, F. (2002). Identification of neural stem cells in the adult vertebrate brain. *Brain Res. Bull.* 57, 751–758. doi: 10.1016/S0361-9230(01)00770-5

Amrein, I. (2015). Adult hippocampal neurogenesis in natural populations of mammals. *Cold Spring Harb. Perspect. Biol.* 7:a021295. doi: 10.1101/cshperspect.a021295

Amrein, I., Isler, K., and Lipp, H. P. (2011). Comparing adult hippocampal neurogenesis in mammalian species and orders: influence of chronological age and life history stage. *Eur. J. Neurosci.* 34, 978–987. doi: 10.1111/j.1460-9568.2011.07804.x

Baroncini, M., Allet, C., Leroy, D., Beauvillain, J. C., Francke, J. P., and Prevot, V. (2007). Morphological evidence for direct interaction between gonadotrophin-releasing hormone neurones and astroglial cells in the human hypothalamus. *J. Neuroendocrinol.* 19, 691–702. doi: 10.1111/j.1365-2826.2007.01576.x

Barrett, P., Ivanova, E., Graham, E. S., Ross, A. W., Wilson, D., Ple, H., et al. (2006). Photoperiodic regulation of cellular retinol binding protein, CRBP1 [corrected] and nestin in tanycytes of the third ventricle ependymal layer of the Siberian hamster. *J. Endocrinol.* 191, 687–698. doi: 10.1677/joe.1.06929

Bartkowska, K., Djavadian, R. L., Taylor, J. R., and Turlejski, K. (2008). Generation recruitment and death of brain cells throughout the life cycle of Sorex shrews (Lipotyphla). *Eur. J. Neurosci.* 27, 1710–1721. doi: 10.1111/j.1460-9568.2008.06133.x

Batailler, M., Derouet, L., Butruille, L., and Migaud, M. (2016). Sensitivity to the photoperiod and potential migratory features of neuroblasts in the adult sheep hypothalamus. *Brain Struct. Funct.* 221, 3301–3314. doi: 10.1007/s00429-015-1101-0

Batailler, M., Droguerre, M., Baroncini, M., Fontaine, C., Prevot, V., and Migaud, M. (2014). DCX-expressing cells in the vicinity of the hypothalamic neurogenic niche: a comparative study between mouse, sheep, and human tissues. *J. Comp. Neurol.* 522, 1966–1985. doi: 10.1002/cne.23514

Bedard, A., and Parent, A. (2004). Evidence of newly generated neurons in the human olfactory bulb. *Dev. Brain Res.* 151, 159–168. doi: 10.1016/j.devbrainres.2004.03.021

Bedard, A., Cossette, M., Levesque, M., and Parent, A. (2002). Proliferating cells can differentiate into neurons in the striatum of normal adult monkey. *Neurosci. Lett.* 328, 213–216. doi: 10.1016/S0304-3940(02)00530-X

Bedard, A., Gravel, C., and Parent, A. (2006). Chemical characterization of newly generated neurons in the striatum of adult primates. *Exp. Brain Res.* 170, 501–512. doi: 10.1007/s00221-005-0233-5

Belnoue, L., Malvaut, S., Ladeveze, E., Abrous, D. N., and Koehl, M. (2016). Plasticity in the olfactory bulb of the maternal mouse is prevented by gestational stress. *Sci. Rep.* 6:37615. doi: 10.1038/srep37615

Bergmann, O., Liebl, J., Bernard, S., Alkass, K., Yeung, M. S. Y., Steier, P., et al. (2012). The age of olfactory bulb neurons in humans. *Neuron* 74, 634–639. doi: 10.1016/j.neuron.2012.03.030

Bernier, P. J., Bédard, A., Vinet, J., Lévesque, M., and Parent, A. (2002). Newly generated neurons in the amygdala and adjoining cortex of adult primates. *Proc. Natl. Acad. Sci. U.S.A.* 99 , 11464–11469. doi: 10.1073/pnas.172403999

Beuing, O., Boese, A., Kyriakou, Y., Deuerling-Zengh, Y., Jollenbeck, B., Scherlach, C., et al. (2014). A novel technique for the measurement of CBF and CBV with robot-arm-mounted flat panel CT in a large-animal model. *AJNR Am. J. Neuroradiol.* 35, 1740–1745. doi: 10.3174/ajnr.A3973

Bless, E. P., Yang, J., Acharya, K. D., Nettles, S. A., Vassoler, F. M., Byrnes, E. M., et al. (2016). Adult neurogenesis in the female mouse hypothalamus: estradiol and high-fat diet alter the generation of newborn neurons expressing estrogen receptor alpha. *eNeuro* 3:eNeuro-0027. doi: 10.1523/ENEURO.0027-16.2016

Bolborea, M., and Dale, N. (2013). Hypothalamic tanycytes: potential roles in the control of feeding and energy balance. *Trends Neurosci.* 36, 91–100. doi: 10.1016/j.tins.2012.12.008

Bonfanti, L., and Ponti, G. (2008). Adult mammalian neurogenesis and the New Zealand white rabbit. *Vet. J.* 175, 310–331. doi: 10.1016/j.tvjl.2007.01.023

Brown, J. P., Couillard-Despres, S., Cooper-Kuhn, C. M., Winkler, J., Aigner, L., and Kuhn, H. G. (2003). Transient expression of doublecortin during adult neurogenesis. *J. Comp. Neurol.* 467, 1–10. doi: 10.1002/cne.10874

Brus, M., Meurisse, M., Franceschini, I., Keller, M., and Lévy, F. (2010). Evidence for cell proliferation in the sheep brain and its down-regulation by parturition and interactions with the young. *Horm. Behav.* 58, 737–746. doi: 10.1016/j.yhbeh.2010.07.006

Brus, M., Meurisse, M., Gheusi, G., Keller, M., Lledo, P. M., and Lévy, F. (2013). Dynamics of olfactory and hippocampal neurogenesis in adult sheep. *J. Comp. Neurol.* 521, 169–188. doi: 10.1002/cne.23169

Brus, M., Meurisse, M., Keller, M., and Lévy, F. (2014). Interactions with the young down-regulate adult olfactory neurogenesis and enhance the maturation of olfactory neuroblasts in sheep mothers. *Front. Behav. Neurosci.* 8:53. doi: 10.3389/fnbeh.2014.00053

Burger, D. K., Saucier, J. M., Iwaniuk, A. N., and Saucier, D. M. (2013). Seasonal and sex differences in the hippocampus of a wild rodent. *Behav. Brain Res.* 236, 131–138. doi: 10.1016/j.bbr.2012.08.044

Butz, M., Lehmann, K., Dammasch, I. E., and Teuchert-Noodt, G. (2006). A theoretical network model to analyse neurogenesis and synaptogenesis in the dentate gyrus. *Neural Netw.* 19, 1490–1505. doi: 10.1016/j.neunet.2006.07.007

Butz, M., Teuchert-Noodt, G., Grafen, K., and van Ooyen, A. (2008). Inverse relationship between adult hippocampal cell proliferation and synaptic rewiring in the dentate gyrus. *Hippocampus*, 18, 879–898. doi: 10.1002/hipo.20445

Cameron, H. A., Woolley, C. S., McEwen, B. S., and Gould, E. (1993). Differentiation of newly born neurons and glia in the dentate gyrus of the adult rat. *Neuroscience* 56, 337–344. doi: 10.1016/0306-4522(93)90335-D

Chaker, Z., George, C., Petrovska, M., Caron, J. B., Lacube, P., Caille, I., et al. (2016). Hypothalamic neurogenesis persists in the aging brain and is controlled by energy-sensing IGF-I pathway. *Neurobiol. Aging* 41, 64–72. doi: 10.1016/j.neurobiolaging.2016.02.008

Cheng, M. F. (2013). Hypothalamic neurogenesis in the adult brain. *Front. Neuroendocrinol.* 34, 167–178. doi: 10.1016/j.yfrne.2013.05.001

Chojnacki, A. K., Mak, G. K., and Weiss, S. (2009). Identity crisis for adult periventricular neural stem cells: subventricular zone astrocytes, ependymal cells or both? *Nat. Rev. Neurosci.* 10, 153–163. doi: 10.1038/nrn2571

Corona, R., Meurisse, M., Cornilleau, F., Moussu, C., Keller, M., and Levy, F. (2016). Exposure to young preferentially activates adult-born neurons in the main olfactory bulb of sheep mothers. *Brain Struct Funct.* 222, 1219–1229. doi: 10.1007/s00429-016-1272-3

Curtis, M. A., Kam, M., Nannmark, U., Anderson, M. F., Axell, M. Z., Wikkelso, C., et al. (2007). Human neuroblasts migrate to the olfactory bulb via a lateral ventricular extension. *Science* 315, 1243–1249. doi: 10.1126/science.1136281

Dahiya, S., Lee, D. Y., and Gutmann, D. H. (2011). Comparative characterization of the human and mouse third ventricle germinal zones. *J. Neuropathol. Exp. Neurol.* 70, 622–633. doi: 10.1097/NEN.0b013e31822200aa

Darnaudery, M., Perez-Martin, M., Del Favero, F., Gomez-Roldan, C., Garcia-Segura, L. M., and MacCari, S. (2007). Early motherhood in rats is associated with a modification of hippocampal function. *Psychoneuroendocrinology* 32, 803–812. doi: 10.1016/j.psyneuen.2007.05.012

Doetsch, F., Caille, I., Lim, D. A., Garcia-Verdugo, J. M., and Alvarez-Buylla, A. (1999a). Subventricular zone astrocytes are neural stem cells in the adult mammalian brain. *Cell* 97, 703–716. doi: 10.1016/S0092-8674(00)80783-7

Doetsch, F., Garcia-Verdugo, J. M., and Alvarez-Buylla, A. (1997). Cellular composition and three-dimensional organization of the subventricular germinal zone in the adult mammalian brain. *J. Neurosci.* 17, 5046–5061.

Doetsch, F., Garcia-Verdugo, J. M., and Alvarez-Buylla, A. (1999b). Regeneration of a germinal layer in the adult mammalian brain. *Proc. Natl. Acad. Sci. U.S.A.* 96, 11619–11624. doi: 10.1073/pnas.96.20.11619

Ebling, F. J., and Barrett, P. (2008). The regulation of seasonal changes in food intake and body weight. *J. Neuroendocrinol.* 20, 827–833. doi: 10.1111/j.1365-2826.2008.01721.x

Ella, A., and Keller, M. (2015). Construction of an MRI 3D high resolution sheep brain template. *Magn Reson. Imaging* 33, 1329–1337. doi: 10.1016/j.mri.2015.09.001

Emmen, J. M., and Korach, K. S. (2003). Estrogen receptor knockout mice: phenotypes in the female reproductive tract. *Gynecol. Endocrinol.* 17, 169–176. doi: 10.1080/gye.17.2.169.176

Emsley, J. G., Mitchell, B. D., Kempermann, G., and MacKlis, J. D. (2005). Adult neurogenesis and repair of the adult CNS with neural progenitors, precursors, and stem cells. *Prog. Neurobiol.* 75, 321–341. doi: 10.1016/j.pneurobio.2005.04.002

Feierstein, C. E., Lazarini, F., Wagner, S., Gabellec, M. M., de Chaumont, F., Olivo-Marin, J. C., et al. (2010). Disruption of adult neurogenesis in the olfactory bulb affects social interaction but not maternal behavior. *Front. Behav. Neurosci.* 4:176. doi: 10.3389/fnbeh.2010.00176

Fietz, S. A., Kelava, I., Vogt, J., Wilsch-Brauninger, M., Stenzel, D., Fish, J. L., et al. (2010). OSVZ progenitors of human and ferret neocortex are epithelial-like and expand by integrin signaling. *Nat. Neurosci.* 13, 690–699. doi: 10.1038/nn.2553

Flament-Durand, J., and Brion, J. P. (1985). Tanycytes: morphology and functions: a review. *Int. Rev. Cytol.* 96, 121–155. doi: 10.1016/S0074-7696(08)60596-3

Forschler, A., Boltze, J., Waldmin, D., Gille, U., and Zimmer, C. (2007). [MRI of experimental focal cerebral ischemia in sheep]. *Rofo* 179, 516–524. doi: 10.1055/s-2007-962977

Fowler, C. D., Johnson, F., and Wang, Z. (2005). Estrogen regulation of cell proliferation and distribution of estrogen receptor-alpha in the brains of adult female prairie and meadow voles. *J. Comp. Neurol.* 489, 166–179. doi: 10.1002/cne.20638

Fowler, C. D., Liu, Y., Ouimet, C., and Wang, Z. (2002). The effects of social environment on adult neurogenesis in the female prairie vole. *J. Neurobiol.* 51, 115–128. doi: 10.1002/neu.10042

Galea, L. A., and McEwen, B. S. (1999). Sex and seasonal differences in the rate of cell proliferation in the dentate gyrus of adult wild meadow voles. *Neuroscience* 89, 955–964. doi: 10.1016/S0306-4522(98)00345-5

Galea, L. A., Perrot-Sinal, T. S., Kavaliers, M., and Ossenkopp, K. P. (1999). Relations of hippocampal volume and dentate gyrus width to gonadal hormone levels in male and female meadow voles. *Brain Res. Bull.* 821, 383–391. doi: 10.1016/S0006-8993(99)01100-2

Gao, Q., and Horvath, T. L. (2008). Cross-talk between estrogen and leptin signaling in the hypothalamus. *Am. J. Physiol. Endocrinol. Metab.* 294, E817–826. doi: 10.1152/ajpendo.00733.2007

Gheusi, G., Ortega-Perez, I., Murray, K., and Lledo, P. M. (2009). A niche for adult neurogenesis in social behavior. *Behav. Brain Res.* 200, 315–322. doi: 10.1016/j.bbr.2009.02.006

Gil-Perotin, S., Duran-Moreno, M., Belzunegui, S., Luquin, M. R., and Garcia-Verdugo, J. M. (2009). Ultrastructure of the subventricular zone in Macaca fascicularis and evidence of a mouse-like migratory stream. *J. Comp. Neurol.* 514, 533–554. doi: 10.1002/cne.22026

Gonzalez-Perez, O., Chavez-Casillas, O., Jauregui-Huerta, F., Lopez-Virgen, V., Guzman-Muniz, J., Moy-Lopez, N., et al. (2011). Stress by noise produces differential effects on the proliferation rate of radial astrocytes and survival of neuroblasts in the adult subgranular zone. *Neurosci. Res.* 70, 243–250. doi: 10.1016/j.neures.2011.03.013

Gouaze, A., Brenachot, X., Rigault, C., Krezymon, A., Rauch, C., Nedelec, E., et al. (2013). Cerebral cell renewal in adult mice controls the onset of obesity. *PLoS ONE* 8:e72029. doi: 10.1371/journal.pone.0072029

Gritti, A., Vescovi, A. L., and Galli, R. (2002). Adult neural stem cells: plasticity and developmental potential. *J. Physiol. Paris* 96, 81–90. doi: 10.1016/S0928-4257(01)00083-3

Guha, T. K., Wai, A., and Hausner, G. (2017). Programmable genome editing tools and their regulation for efficient genome engineering. *Comput. Struct. Biotechnol. J.* 15, 146–160. doi: 10.1016/j.csbj.2016.12.006

Haan, N., Goodman, T., Najdi-Samiei, A., Stratford, C. M., Rice, R., El Agha, E., et al. (2013). Fgf10-expressing tanycytes add new neurons to the appetite/energy-balance regulating centers of the postnatal and adult hypothalamus. *J. Neurosci.* 33, 6170–6180. doi: 10.1523/JNEUROSCI.2437-12.2013

Hawken, P. A., Jorre, T. J., Rodger, J., Esmaili, T., Blache, D., and Martin, G. B. (2009). Rapid induction of cell proliferation in the adult female ungulate brain (*Ovis aries*) associated with activation of the reproductive axis by exposure to unfamiliar males. *Biol. Reprod.* 80, 1146–1151. doi: 10.1095/biolreprod.108.075341

Hazlerigg, D. G., Wyse, C. A., Dardente, H., Hanon, E. A., and Lincoln, G. A. (2013). Photoperiodic variation in CD45-positive cells and cell proliferation in the mediobasal hypothalamus of the Soay sheep. *Chronobiol. Int.* 30, 548–558. doi: 10.3109/07420528.2012.754450

Holmes, M. M. (2016). Social regulation of adult neurogenesis: a comparative approach. *Front. Neuroendocrinol.* 41, 59–70. doi: 10.1016/j.yfrne.2016.02.001

Holschbach, M. A., and Lonstein, J. S. (2017). Motherhood and infant contact regulate neuroplasticity in the serotonergic midbrain dorsal raphe. *Psychoneuroendocrinology* 76, 97–106. doi: 10.1016/j.psyneuen.2016.10.023

Hsu, P. D., Lander, E. S., and Zhang, F. (2014). Development and applications of CRISPR-Cas9 for genome engineering. *Cell* 157, 1262–1278. doi: 10.1016/j.cell.2014.05.010

Huang, L., DeVries, G. J., and Bittman, E. L. (1998). Photoperiod regulates neuronal bromodeoxyuridine labeling in the brain of a seasonally breeding mammal. *J. Neurobiol.* 36, 410–420. doi: 10.1002/(SICI)1097-4695(19980905)36:3<410::AID-NEU8>3.0.CO;2-Z

Imayoshi, I., Sakamoto, M., Ohtsuka, T., Takao, K., Miyakawa, T., Yamaguchi, M., et al. (2008). Roles of continuous neurogenesis in the structural and functional integrity of the adult forebrain. *Nat. Neurosci.* 11, 1153–1161. doi: 10.1038/nn.2185

Kameda, Y., Arai, Y., and Nishimaki, T. (2003). Ultrastructural localization of vimentin immunoreactivity and gene expression in tanycytes and their alterations in hamsters kept under different photoperiods. *Cell Tissue Res.* 314, 251–262. doi: 10.1007/s00441-003-0789-y

Kee, N., Sivalingam, S., Boonstra, R., and Wojtowicz, J. M. (2002). The utility of Ki-67 and BrdU as proliferative markers of adult neurogenesis. *J. Neurosci. Methods* 115, 97–105. doi: 10.1016/S0165-0270(02)00007-9

Keller, M., and Lévy, F. (2012). The main but not the accessory olfactory system is involved in the processing of socially relevant chemosignals in ungulates. *Front. Neuroanat.* 6:39. doi: 10.3389/fnana.2012.00039

Kempermann, G., Gast, D., Kronenberg, G., Yamaguchi, M., and Gage, F. H. (2003). Early determination and long-term persistence of adult-generated new neurons in the hippocampus of mice. *Development* 130, 391–399. doi: 10.1242/dev.00203

Kohler, S. J., Williams, N. I., Stanton, G. B., Cameron, J. L., and Greenough, W. T. (2011). Maturation time of new granule cells in the dentate gyrus of adult macaque monkeys exceeds six months. *Proc. Natl. Acad. Sci. U.S.A.* 108, 10326–10331. doi: 10.1073/pnas.1017099108

Kokoeva, M. V., Yin, H., and Flier, J. S. (2005). Neurogenesis in the hypothalamus of adult mice: potential role in energy balance. *Science* 310, 679–683. doi: 10.1126/science.1115360

Kokoeva, M. V., Yin, H., and Flier, J. S. (2007). Evidence for constitutive neural cell proliferation in the adult murine hypothalamus. *J. Comp. Neurol.* 505, 209–220. doi: 10.1002/cne.21492

Kopel, H., Schechtman, E., Groysman, M., and Mizrahi, A. (2012). Enhanced synaptic integration of adult-born neurons in the olfactory bulb of lactating mothers. *J. Neurosci.* 32, 7519–7527. doi: 10.1523/JNEUROSCI.6354-11.2012

Kornack, D. R., and Rakic, P. (2001). The generation, migration, and differentiation of olfactory neurons in the adult primate brain. *Proc. Natl. Acad. Sci. U.S.A.* 98, 4752–4757. doi: 10.1073/pnas.081074998

Kronenberg, G., Reuter, K., Steiner, B., Brandt, M. D., Jessberger, S., Yamaguchi, M., et al. (2003). Subpopulations of proliferating cells of the adult hippocampus respond differently to physiologic neurogenic stimuli. *J. Comp. Neurol.* 467, 455–463. doi: 10.1002/cne.10945

Langlet, F., Levin, B. E., Luquet, S., Mazzone, M., Messina, A., Dunn-Meynell, A. A., et al. (2013). Tanycytic VEGF-A boosts blood-hypothalamus barrier plasticity and access of metabolic signals to the arcuate nucleus in response to fasting. *Cell Metabol.* 17, 607–617. doi: 10.1016/j.cmet.2013.03.004

Larriva-Sahd, J. (2014). Structural variation and interactions among astrocytes of the rostral migratory stream and olfactory bulb: II. Golgi and electron microscopic study of the adult rat. *Neurosci. Res.* 89, 10–30. doi: 10.1016/j.neures.2014.08.011

Larsen, C. M., and Grattan, D. R. (2010). Prolactin-induced mitogenesis in the subventricular zone of the maternal brain during early pregnancy is essential for normal postpartum behavioral responses in the mother. *Endocrinology* 151, 3805–3814. doi: 10.1210/en.2009-1385

Lavenex, P., Steele, M. A., and Jacobs, L. F. (2000). The seasonal pattern of cell proliferation and neuron number in the dentate gyrus of wild adult eastern grey squirrels. *Eur. J. Neurosci.* 12, 643–648. doi: 10.1046/j.1460-9568.2000.00949.x

Lazarini, F., and Lledo, P.-M. (2011). Is adult neurogenesis essential for olfaction? *Trends Neurosci.* 34, 20–30. doi: 10.1016/j.tins.2010.09.006

Lee, D. A., and Blackshaw, S. (2012). Functional implications of hypothalamic neurogenesis in the adult mammalian brain. *Int. J. Dev. Neurosci.* 30, 615–621. doi: 10.1016/j.ijdevneu.2012.07.003

Lee, D. A., Bedont, J. L., Pak, T., Wang, H., Song, J., Miranda-Angulo, A., et al. (2012). Tanycytes of the hypothalamic median eminence form a diet-responsive neurogenic niche. *Nat. Neurosci.* 15, 700–702. doi: 10.1038/nn.3079

Lee, D. A., Salvatierra, J., Velarde, E., Wong, J., Ford, E. C., and Blackshaw, S. (2013). Functional interrogation of adult hypothalamic neurogenesis with focal radiological inhibition. *J. Vis. Exp.* 81:e50716. doi: 10.3791/50716

Lee, D. A., Yoo, S., Pak, T., Salvatierra, J., Velarde, E., Aja, S., et al. (2014). Dietary and sex-specific factors regulate hypothalamic neurogenesis in young adult mice. *Front. Neurosci.* 8:157. doi: 10.3389/fnins.2014.00157

Lehmann, K., Butz, M., and Teuchert-Noodt, G. (2005). Offer and demand: proliferation and survival of neurons in the dentate gyrus. *Eur. J. Neurosci.* 21, 3205–3216. doi: 10.1111/j.1460-9568.2005.04156.x

Lemasson, M., Saghatelyan, A., Olivo-Marin, J. C., and Lledo, P. M. (2005). Neonatal and adult neurogenesis provide two distinct populations of newborn neurons to the mouse olfactory bulb. *J. Neurosci.* 25, 6816–6825. doi: 10.1523/JNEUROSCI.1114-05.2005

Leuner, B., Caponiti, J. M., and Gould, E. (2012). Oxytocin stimulates adult neurogenesis even under conditions of stress and elevated glucocorticoids. *Hippocampus* 22, 861–868. doi: 10.1002/hipo.20947

Lévy, F., and Keller, M. (2009). Olfactory mediation of maternal behavior in selected mammalian species. *Behav. Brain Res.* 200, 336–345. doi: 10.1016/j.bbr.2008.12.017

Lévy, F., Gheusi, G., and Keller, M. (2011). Plasticity of the parental brain: a case for neurogenesis. *J. Neuroendocrinol.* 23, 984–993. doi: 10.1111/j.1365-2826.2011.02203.x

Lévy, F., Guevara-Guzman, R., Hinton, M. R., Kendrick, K. M., and Keverne, E. B. (1993). Effects of parturition and maternal experience on noradrenaline and acetylcholine release in the olfactory bulb of sheep. *Behav. Neurosci.* 107, 662–668. doi: 10.1037/0735-7044.107.4.662

Lévy, F., Keller, M., and Poindron, P. (2004). Olfactory regulation of maternal behavior in mammals. *Horm. Behav.* 46, 284–302. doi: 10.1016/j.yhbeh.2004.02.005

Li, J., Tang, Y., and Cai, D. (2012). IKKbeta/NF-kappaB disrupts adult hypothalamic neural stem cells to mediate a neurodegenerative mechanism of dietary obesity and pre-diabetes. *Nat. Cell Biol.* 14, 999–1012. doi: 10.1038/ncb2562

Livneh, Y., and Mizrahi, A. (2011). Experience-dependent plasticity of mature adult-born neurons. *Nat. Neurosci.* 15, 26–28. doi: 10.1038/nn.2980

Lledo, P. M., Alonso, M., and Grubb, M. S. (2006). Adult neurogenesis and functional plasticity in neuronal circuits. *Nat. Rev. Neurosci.* 7, 179–193. doi: 10.1038/nrn1867

Lois, C., and Alvarez-Buylla, A. (1994). Long-distance neuronal migration in the adult mammalian brain. *Science* 264, 1145–1148. doi: 10.1126/science.8178174

Low, V. F., Faull, R. L., Bennet, L., Gunn, A. J., and Curtis, M. A. (2013). Neurogenesis and progenitor cell distribution in the subgranular zone and subventricular zone of the adult sheep brain. *Neuroscience* 244, 173–187. doi: 10.1016/j.neuroscience.2013.04.006

Luskin, M. B. (1993). Restricted proliferation and migration of postnatally generated neurons derived from the forebrain subventricular zone. *Neuron* 11, 173–189. doi: 10.1016/0896-6273(93)90281-U

Lussier, A. L., Lebedeva, K., Fenton, E. Y., Guskjolen, A., Caruncho, H. J., and Kalynchuk, L. E. (2013). The progressive development of depression-like behavior in corticosterone-treated rats is paralleled by slowed granule cell maturation and decreased reelin expression in the adult dentate gyrus. *Neuropharmacology* 71, 174–183. doi: 10.1016/j.neuropharm.2013.04.012

Luzzati, F., Peretto, P., Aimar, P., Ponti, G., Fasolo, A., and Bonfanti, L. (2003). Glia-independent chains of neuroblasts through the subcortical parenchyma of the adult rabbit brain. *Proc. Natl. Acad. Sci. U.S.A.* 100, 13036–13041. doi: 10.1073/pnas.1735482100

Martin, G., Oldham, C., Cognié, Y., and Pearce, D. (1986). The physiological responses of anovulatory ewes to the introduction of rams: a review. *Livestock Prod. Sci.* 15, 219–247. doi: 10.1016/0301-6226(86)90031-X

McDonald, H. Y., and Wojtowicz, J. M. (2005). Dynamics of neurogenesis in the dentate gyrus of adult rats. *Neurosci. Lett.* 385, 70–75. doi: 10.1016/j.neulet.2005.05.022

McNay, D. E., Briançon, N., Kokoeva, M. V., Maratos-Flier, E., and Flier, J. S. (2012). Remodeling of the arcuate nucleus energy-balance circuit is inhibited in obese mice. *J. Clin. Invest.* 122, 142–152. doi: 10.1172/JCI43134

Migaud, M., Batailler, M., Pillon, D., Franceschini, I., and Malpaux, B. (2011). Seasonal changes in cell proliferation in the adult sheep brain and pars tuberalis. *J. Biol. Rhythms* 26, 486–496. doi: 10.1177/0748730411420062

Migaud, M., Batailler, M., Segura, S., Duittoz, A., Franceschini, I., and Pillon, D. (2010). Emerging new sites for adult neurogenesis in the mammalian brain: a comparative study between the hypothalamus and the classical neurogenic zones. *Eur. J. Neurosci.* 32, 2042–2052. doi: 10.1111/j.1460-9568.2010.07521.x

Migaud, M., Butrille, L., and Batailler, M. (2015). Seasonal regulation of structural plasticity and neurogenesis in the adult mammalian brain:

focus on the sheep hypothalamus. *Front. Neuroendocrinol.* 37, 146–157. doi: 10.1016/j.yfrne.2014.11.004

Miyata, S. (2015). New aspects in fenestrated capillary and tissue dynamics in the sensory circumventricular organs of adult brains. *Front. Neurosci.* 9:390. doi: 10.3389/fnins.2015.00390

Mohr, M. A., and Sisk, C. L. (2013). Pubertally born neurons and glia are functionally integrated into limbic and hypothalamic circuits of the male Syrian hamster. *Proc. Natl. Acad. Sci. U.S.A.* 110, 4792–4797. doi: 10.1073/pnas.1219443110

Morimoto, M., Morita, N., Ozawa, H., Yokoyama, K., and Kawata, M. (1996). Distribution of glucocorticoid receptor immunoreactivity and mRNA in the rat brain: an immunohistochemical and *in situ* hybridization study. *Neurosci. Res.* 26, 235–269. doi: 10.1016/S0168-0102(96)01105-4

Musatov, S., Chen, W., Pfaff, D. W., Kaplitt, M. G., and Ogawa, S. (2006). RNAi-mediated silencing of estrogen receptor in the ventromedial nucleus of hypothalamus abolishes female sexual behaviors. *Proc. Natl. Acad. Sci. U.S.A.* 103, 10456–10460. doi: 10.1073/pnas.0603045103

Ninkovic, J., and Gotz, M. (2007). Signaling in adult neurogenesis: from stem cell niche to neuronal networks. *Curr. Opin. Neurobiol.* 17, 338–344. doi: 10.1016/j.conb.2007.04.006

Nitzsche, B., Frey, S., Collins, L. D., Seeger, J., Lobsien, D., Dreyer, A., et al. (2015). A stereotaxic, population-averaged T1w ovine brain atlas including cerebral morphology and tissue volumes. *Front Neuroanat.* 9:69. doi: 10.3389/fnana.2015.00069

Niwa, A., Nishibori, M., Hamasaki, S., Kobori, T., Liu, K., Wake, H., et al. (2015). Voluntary exercise induces neurogenesis in the hypothalamus and ependymal lining of the third ventricle. *Brain Struct. Funct.* 221, 1653–1666. doi: 10.1007/s00429-015-0995-x

Ogawa, S., Eng, V., Taylor, J., Lubahn, D. B., Korach, K. S., and Pfaff, D. W. (1998). Roles of estrogen receptor-alpha gene expression in reproduction-related behaviors in female mice. *Endocrinology* 139, 5070–5081. doi: 10.1210/endo.139.12.6357

Ormerod, B. K., and Galea, L. A. (2003). Reproductive status influences the survival of new cells in the dentate gyrus of adult male meadow voles. *Neurosci. Lett.* 346, 25–28. doi: 10.1016/S0304-3940(03)00546-9

Pagano, S. F., Impagnatiello, F., Girelli, M., Cova, L., Grioni, E., Onofri, M., et al. (2000). Isolation and characterization of neural stem cells from the adult human olfactory bulb. *Stem Cells* 18, 295–300. doi: 10.1634/stemcells.18-4-295

Paredes, M. F., Sorrells, S. F., Garcia-Verdugo, J. M., and Alvarez-Buylla, A. (2016). Brain size and limits to adult neurogenesis. *J.Comp. Neurol.* 524, 646–664. doi: 10.1002/cne.23896

Pawluski, J. L., Brummelte, S., Barha, C. K., Crozier, T. M., and Galea, L. A. M. (2009). Effects of steroid hormones on neurogenesis in the hippocampus of the adult female rodent during the estrous cycle, pregnancy, lactation and aging. *Front. Neuroendocrinol.* 30, 343–357. doi: 10.1016/j.yfrne.2009.03.007

Pekcec, A., Loscher, W., and Potschka, H. (2006). Neurogenesis in the adult rat piriform cortex. *Neuroreport* 17, 571–574. doi: 10.1097/00001756-200604240-00003

Pencea, V., Bingaman, K. D., Wiegand, S. J., and Luskin, M. B. (2001). Infusion of brain-derived neurotrophic factor into the lateral ventricle of the adult rat leads to new neurons in the parenchyma of the striatum, septum, thalamus, and hypothalamus. *J. Neurosci.* 21, 6706–6717.

Pérez-Martín, M., Cifuentes, M., Grondona, J. M., López-Avalos, M. D., Gómez-Pinedo, U., García-Verdugo, J. M., et al. (2010). IGF-I stimulates neurogenesis in the hypothalamus of adult rats. *Eur. J. Neurosci.* 31, 1533–1548. doi: 10.1111/j.1460-9568.2010.07220.x

Perrot-Sinal, T. S., Kavaliers, M., and Ossenkopp, K. P. (1998). Spatial learning and hippocampal volume in male deer mice: relations to age, testosterone and adrenal gland weight. *Neuroscience* 86, 1089–1099. doi: 10.1016/S0306-4522(98)00131-6

Petreanu, L., and Alvarez-Buylla, A. (2002). Maturation and death of adult-born olfactory bulb granule neurons: role of olfaction. *J. Neurosci.* 22, 6106–6113.

Pierce, A. A., and Xu, A. W. (2010). *De novo* neurogenesis in adult hypothalamus as a compensatory mechanism to regulate energy balance. *J. Neurosci.* 30, 723–730. doi: 10.1523/JNEUROSCI.2479-09.2010

Poindron, P., Lévy, F., and Keller, M. (2007). Maternal responsiveness and maternal selectivity in domestic sheep and goats: the two facets of maternal attachment. *Dev. Psychobiol.* 49, 54–70. doi: 10.1002/dev.20192

Prevot, V. (2002). Glial-neuronal-endothelial interactions are involved in the control of GnRH secretion. *J. Neuroendocrinol.* 14, 247–255. doi: 10.1046/j.0007-1331.2001.00772.x

Quinones-Hinojosa, A., Sanai, N., Soriano-Navarro, M., Gonzalez-Perez, O., Mirzadeh, Z., Gil-Perotin, S., et al. (2006). Cellular composition and cytoarchitecture of the adult human subventricular zone: a niche of neural stem cells. *J. Comp. Neurol.* 494, 415–434. doi: 10.1002/cne.20798

Robins, S. C., Stewart, I., McNay, D. E., Taylor, V., Giachino, C., Goetz, M., et al. (2013a). α-Tanycytes of the adult hypothalamic third ventricle include distinct populations of FGF-responsive neural progenitors. *Nat. Commun.* 4:2049. doi: 10.1038/ncomms3049

Robins, S. C., Trudel, E., Rotondi, O., Liu, X., Djogo, T., Kryzskaya, D., et al. (2013b). Evidence for NG2-glia derived, adult-born functional neurons in the hypothalamus. *PLoS ONE* 8:e78236. doi: 10.1371/journal.pone.0078236

Rodriguez, E. M., Blazquez, J. L., Pastor, F. E., Pelaez, B., Pena, P., Peruzzo, B., et al. (2005). Hypothalamic tanycytes: a key component of brain-endocrine interaction. *Int. Rev. Cytol.* 247, 89–164. doi: 10.1016/S0074-7696(05)47003-5

Rodriguez-Perez, L. M., Perez-Martin, M., Jimenez, A. J., and Fernandez-Llebrez, P. (2003). Immunocytochemical characterisation of the wall of the bovine lateral ventricle. *Cell Tissue Res.* 314, 325–335. doi: 10.1007/s00441-003-0794-1

Saaltink, D. J., Havik, B., Verissimo, C. S., Lucassen, P. J., and Vreugdenhil, E. (2012). Doublecortin and doublecortin-like are expressed in overlapping and non-overlapping neuronal cell population: implications for neurogenesis. *J. Comp. Neurol.* 520, 2805–2823. doi: 10.1002/cne.23144

Saghatelyan, A., Roux, P., Migliore, M., Rochefort, C., Desmaisons, D., Charneau, P., et al. (2005). Activity-dependent adjustments of the inhibitory network in the olfactory bulb following early postnatal deprivation. *Neuron* 46, 103–116. doi: 10.1016/j.neuron.2005.02.016

Sah, R., Pritchard, L. M., Richtand, N. M., Ahlbrand, R., Eaton, K., Sallee, F. R., et al. (2005). Expression of the glucocorticoid-induced receptor mRNA in rat brain. *Neuroscience* 133, 281–292. doi: 10.1016/j.neuroscience.2005.01.066

Sahara, S., and O'Leary, D. D. (2009). Fgf10 regulates transition period of cortical stem cell differentiation to radial glia controlling generation of neurons and basal progenitors. *Neuron* 63, 48–62. doi: 10.1016/j.neuron.2009.06.006

Sakamoto, M., Imayoshi, I., Ohtsuka, T., Yamaguchi, M., Mori, K., and Kageyama, R. (2011). Continuous neurogenesis in the adult forebrain is required for innate olfactory responses. *Proc. Natl. Acad. Sci. U.S.A.* 108, 8479–8484. doi: 10.1073/pnas.1018782108

Sanai, N., Nguyen, T., Ihrie, R. A., Mirzadeh, Z., Tsai, H. H., Wong, M., et al. (2011). Corridors of migrating neurons in the human brain and their decline during infancy. *Nature* 478, 382–386. doi: 10.1038/nature10487

Saper, C. B., and Lowell, B. B. (2014). The hypothalamus. *Curr. Biol.* 24, R1111–R1116. doi: 10.1016/j.cub.2014.10.023

Sawamoto, K., Hirota, Y., Alfaro-Cervello, C., Soriano-Navarro, M., He, X. P., Hayakawa-Yano, Y., et al. (2011). Cellular composition and organization of the subventricular zone and rostral migratory stream in the adult and neonatal common marmoset brain. *J. Comp. Neurol.* 519, 690–713. doi: 10.1002/cne.22543

Shughrue, P. J., and Merchenthaler, I. (2000). Estrogen is more than just a "sex hormone": novel sites for estrogen action in the hippocampus and cerebral cortex. *Front. Neuroendocrinol.* 21, 95–101. doi: 10.1006/frne.1999.0190

Shughrue, P., Scrimo, P., Lane, M., Askew, R., and Merchenthaler, I. (1997). The distribution of estrogen receptor-beta mRNA in forebrain regions of the estrogen receptor-alpha knockout mouse. *Endocrinology* 138, 5649–5652. doi: 10.1210/endo.138.12.5712

Siopi, E., Denizet, M., Gabellec, M. M., de Chaumont, F., Olivo-Marin, J. C., Guilloux, J. P., et al. (2016). Anxiety- and depression-like states lead to pronounced olfactory deficits and impaired adult neurogenesis in mice. *J. Neurosci.* 36, 518–531. doi: 10.1523/JNEUROSCI.2817-15.2016

Smith, D., Pedro-Botet, J., Cantuti-Castelvetri, I., Shukitt-Hale, B., Schaefer, E. J., Joseph, J., et al. (2001). Influence of photoperiod, laboratory caging and aging on plasma lipid response to an atherogenic diet among F1B hamsters. *Int. J. Neurosci.* 106, 185–194. doi: 10.3109/00207450109149748

Sousa-Ferreira, L., de Almeida, L. P., and Cavadas, C. (2014). Role of hypothalamic neurogenesis in feeding regulation. *Trends Endocrinol. Metab.* 25, 80–88. doi: 10.1016/j.tem.2013.10.005

Spalding, K. L., Bergmann, O., Alkass, K., Bernard, S., Salehpour, M., Huttner, H. B., et al. (2013). Dynamics of hippocampal neurogenesis in adult humans. *Cell* 153, 1219–1227. doi: 10.1016/j.cell.2013.05.002

Staffend, N. A., Mohr, M. A., DonCarlos, L. L., and Sisk, C. L. (2014). A decrease in the addition of new cells in the nucleus accumbens and prefrontal cortex between puberty and adulthood in male rats. *Dev. Neurobiol.* 74, 633–642. doi: 10.1002/dneu.22160

Steiner, B., Kronenberg, G., Jessberger, S., Brandt, M. D., Reuter, K., and Kempermann, G. (2004). Differential regulation of gliogenesis in the context of adult hippocampal neurogenesis in mice. *Glia* 46, 41–52. doi: 10.1002/glia.10337

Suh, H., Consiglio, A., Ray, J., Sawai, T., D'Amour, K. A., and Gage, F. H. (2007). *In vivo* fate analysis reveals the multipotent and self-renewal capacities of Sox2(+) neural stem cells in the adult hippocampus. *Cell Stem Cell* 1, 515–528. doi: 10.1016/j.stem.2007.09.002

Tanapat, P., Hastings, N. B., and Gould, E. (2005). Ovarian steroids influence cell proliferation in the dentate gyrus of the adult female rat in a dose- and time-dependent manner. *J. Comp. Neurol.* 481, 252–265. doi: 10.1002/cne.20385

Tanapat, P., Hastings, N. B., Reeves, A. J., and Gould, E. (1999). Estrogen stimulates a transient increase in the number of new neurons in the dentate gyrus of the adult female rat. *J. Neurosci.* 19, 5792–5801.

Tonchev, A. B., and Yamashima, T. (2006). Differential neurogenic potential of progenitor cells in dentate gyrus and CA1 sector of the postischemic adult monkey hippocampus. *Exp. Neurol.* 198, 101–113. doi: 10.1016/j.expneurol.2005.11.022

Vadodaria, K. C., and Gage, F. H. (2014). SnapShot: adult hippocampal neurogenesis. *Cell* 156, 1114–1114. doi: 10.1016/j.cell.2014.02.029

van der Bom, I. M., Moser, R. P., Gao, G., Mondo, E., O'Connell, D., Gounis, M. J., et al. (2013). Finding the striatum in sheep: use of a multi-modal guided approach for convection enhanced delivery. *J. Huntingtons Dis.* 2, 41–45. doi: 10.3233/JHD-130053

Walton, J. C., Pyter, L. M., Weil, Z. M., and Nelson, R. J. (2012). Photoperiod mediated changes in olfactory bulb neurogenesis and olfactory behavior in male white-footed mice (*Peromyscus leucopus*). *PLoS ONE* 7:e42743. doi: 10.1371/journal.pone.0042743

Wang, C., Liu, F., Liu, Y. Y., Zhao, C. H., You, Y., Wang, L., et al. (2011). Identification and characterization of neuroblasts in the subventricular zone and rostral migratory stream of the adult human brain. *Cell Res.* 21, 1534–1550. doi: 10.1038/cr.2011.83

Wei, L. C., Shi, M., Chen, L. W., Cao, R., Zhang, P., and Chan, Y. S. (2002). Nestin-containing cells express glial fibrillary acidic protein in the proliferative regions of central nervous system of postnatal developing and adult mice. *Brain Res. Dev. Brain Res.* 139, 9–17. doi: 10.1016/S0165-3806(02)00509-6

Werner, L., Müller-Fielitz, H., Ritzal, M., Werner, T., Rossner, M., and Schwaninger, M. (2012). Involvement of doublecortin-expressing cells in the arcuate nucleus in body weight regulation. *Endocrinology* 153, 2655–2664. doi: 10.1210/en.2011-1760

Wiese, C., Rolletschek, A., Kania, G., Blyszczuk, P., Tarasov, K. V., Tarasova, Y., et al. (2004). Nestin expression–a property of multi-lineage progenitor cells? *Cell. Mol. Life Sci.* 61, 2510–2522. doi: 10.1007/s00018-004-4144-6

Winner, B., Cooper-Kuhn, C. M., Aigner, R., Winkler, J., and Kuhn, H. G. (2002). Long-term survival and cell death of newly generated neurons in the adult rat olfactory bulb. *Eur. J. Neurosci.* 16, 1681–1689. doi: 10.1046/j.1460-9568.2002.02238.x

Xu, Y., Tamamaki, N., Noda, T., Kimura, K., Itokazu, Y., Matsumoto, N., et al. (2005). Neurogenesis in the ependymal layer of the adult rat 3rd ventricle. *Exp. Neurol.* 192, 251–264. doi: 10.1016/j.expneurol.2004.12.021

Yon, M. A., Mauger, S. L., and Pickavance, L. C. (2013). Relationships between dietary macronutrients and adult neurogenesis in the regulation of energy metabolism. *Br. J. Nutr.* 109, 1573–1589. doi: 10.1017/S000711451200579X

Yuan, T. F., and Arias-Carrion, O. (2011). Adult neurogenesis in the hypothalamus: evidence, functions, and implications. *CNS Neurol. Disord. Drug Targets* 10, 433–439. doi: 10.2174/187152711795563985

Zhang, G., Li, J., Purkayastha, S., Tang, Y., Zhang, H., Yin, Y., et al. (2013). Hypothalamic programming of systemic ageing involving IKK-beta, NF-kappaB and GnRH. *Nature* 497, 211–216. doi: 10.1038/nature12143

Zhao, M., and Janson Lang, A. M. (2009). Bromodeoxyuridine infused into the cerebral ventricle of adult mice labels nigral neurons under physiological conditions–a method to detect newborn nerve cells in regions with a low rate of neurogenesis. *J. Neurosci. Methods* 184, 327–331. doi: 10.1016/j.jneumeth.2009.08.007

Conflict of Interest Statement: The authors declare that the research was conducted in the absence of any commercial or financial relationships that could be construed as a potential conflict of interest.

frontiers in Neuroscience

ORIGINAL RESEARCH
published: 17 August 2017
doi: 10.3389/fnins.2017.00437

Cell Proliferation, Migration, and Neurogenesis in the Adult Brain of the Pulse Type Weakly Electric Fish, *Gymnotus omarorum*

Valentina Olivera-Pasilio[1,2,3], *Moira Lasserre*[1] and *María E. Castelló*[1,3]*

[1] *Desarrollo y Evolución Neural, Departamento de Neurociencias Integrativas y Computacionales, Instituto de Investigaciones Biológicas Clemente Estable, Ministerio de Educación y Cultura, Montevideo, Uruguay,* [2] *Departamento de Histología y Embriología, Facultad de Medicina, Universidad de la República, Montevideo, Uruguay,* [3] *IIBE "Histología de Sistemas Sensoriales", Unidad Asociada F. de Medicina, Montevideo, Uruguay*

OPEN ACCESS

Edited by:
Irmgard Amrein,
University of Zurich, Switzerland

Reviewed by:
Jan Kaslin,
Australian Regenerative Medicine Institute (ARMI), Australia
Krishna Vadodaria,
Salk Institute for Biological Studies, United States
Satoshi Ogawa,
Monash University Malaysia, Malaysia

***Correspondence:**
María E. Castelló
mcastello@iibce.edu.uy;
maritacastello@gmail.com

Specialty section:
This article was submitted to Neurogenesis, a section of the journal Frontiers in Neuroscience

Received: *06 April 2017*
Accepted: *17 July 2017*
Published: *17 August 2017*

Citation:
Olivera-Pasilio V, Lasserre M and Castelló ME (2017) Cell Proliferation, Migration, and Neurogenesis in the Adult Brain of the Pulse Type Weakly Electric Fish, Gymnotus omarorum. Front. Neurosci. 11:437. doi: 10.3389/fnins.2017.00437

Adult neurogenesis, an essential mechanism of brain plasticity, enables brain development along postnatal life, constant addition of new neurons, neuronal turnover, and/or regeneration. It is amply distributed but negatively modulated during development and along evolution. Widespread cell proliferation, high neurogenic, and regenerative capacities are considered characteristics of teleost brains during adulthood. These anamniotes are promising models to depict factors that modulate cell proliferation, migration, and neurogenesis, and might be intervened to promote brain plasticity in mammals. Nevertheless, the migration path of derived cells to their final destination was not studied in various teleosts, including most weakly electric fish. In this group adult brain morphology is attributed to sensory specialization, involving the concerted evolution of peripheral electroreceptors and electric organs, encompassed by the evolution of neural networks involved in electrosensory information processing. In wave type gymnotids adult brain morphology is proposed to result from lifelong region specific cell proliferation and neurogenesis. Consistently, pulse type weakly electric gymnotids and mormyrids show widespread distribution of proliferation zones that persists in adulthood, but their neurogenic potential is still unknown. Here we studied the migration process and differentiation of newborn cells into the neuronal phenotype in the pulse type gymnotid *Gymnotus omarorum*. Pulse labeling of S-phase cells with 5-Chloro-2′-deoxyuridine thymidine followed by 1 to 180 day survivals evidenced long distance migration of newborn cells from the rostralmost telencephalic ventricle to the olfactory bulb, and between layers of all cerebellar divisions. Shorter migration appeared in the tectum opticum and torus semicircularis. In many brain regions, derived cells expressed early neuronal markers doublecortin (chase: 1–30 days) and HuC/HuD (chase: 7–180 days). Some newborn cells expressed the mature neuronal marker tyrosine hydroxylase in the subpallium (chase: 90 days) and olfactory bulb (chase: 180 days), indicating the acquisition of a mature neuronal phenotype. Long term CldU labeled newborn cells of the granular layer of the corpus cerebelli were also retrogradely labeled "*in vivo*," suggesting

their insertion into the neural networks. These findings evidence the neurogenic capacity of telencephalic, mesencephalic, and rhombencephalic brain proliferation zones in *G. omarorum,* supporting the phylogenetic conserved feature of adult neurogenesis and its functional significance.

Keywords: cerebellum, olfactory bulb, tectum opticum, CldU, doublecortin, HuC/HuD, tyrosine hydroxylase, retrograde tracing

INTRODUCTION

Neurogenesis is the main mechanism of adult brain plasticity that enables the continuation of brain development, the constant addition of new neurons and/or the neuronal turnover (Barker et al., 2011; Alunni and Bally-Cuif, 2016). It has been demonstrated in a wide range of animals, from cnidarians to mammals, including humans (Altman, 1963, 1969; Altman and Das, 1965; Sullivan et al., 2007; Galliot and Quiquand, 2011). Neurogenesis is progressively restricted during animal development and negatively modulated along evolution. Its spatial distribution remains widespread in all brain divisions of adult anamniotes, particularly in teleost fish (Cayre et al., 2002; Lindsey and Tropepe, 2006; Kaslin et al., 2008; Barker et al., 2011; Grandel and Brand, 2013). However, it is almost confined to two zones in the telencephalon of adult mammals (Ma et al., 2008; Altman, 2011; Vadodaria and Gage, 2014).

Soon after the discovery of adult neurogenesis in mammals by Altman (Altman, 1962, 1963; Altman and Das, 1965, 1966) the widespread distribution of cell proliferation in the brain of adult teleost was evidenced by tritiated thymidine (3H-thymidine) labeling (*Brachydanio rerio*: Rahmann, 1968; *Lebistes reticulatus*: Richter and Kranz, 1970). In spite of ultrastructural evidences of adult neurogenesis in mammals (Kaplan and Hinds, 1977), the field of cell proliferation and neurogenesis in both amniotes and anamniotes resumed after a 20 years hindrance (Gross, 2000). Even though the spatial distribution of proliferation zones was since then evidenced in several teleost, numerous taxa remain underexplored. One of the earliest and most thoroughly studied anamniotes is the wave type weakly electric gymnotid *Apteronotus leptorhynchus*, which is considered a classical biological model in the field. Weakly electric fish are also good models for the study of brain evolution sub-serving variations in animal behavior (Albert et al., 1998). The peculiar adult brain morphology of weakly electric fish is associated to the relevance of the electrosensory modality for these fish lifestyle (Evans, 1940; Bennett, 1971; Hodos and Butler, 1997; Kotrschal et al., 1998; Meek and Nieuwenhuys, 1998; Ito et al., 2007; Shumway, 2008). It results from the differential growth of portions of the neural tube that progressively differentiate into brain vesicles followed by the subsequent formation and differential growth of brain structures derived from the alar plate, as shown in wave (Leyhausen et al., 1987; Lannoo et al., 1990) and pulse (Iribarne and Castelló, 2014) gymnotids, and pulse mormyrids (Haugedé-Carré et al., 1977, 1979; Radmilovich et al., 2016). The maintenance of adult brain morphology as fish body grows indefinitely depends in turn on heterogeneous cell proliferation and neurogenesis. Thus, neurogenesis can be considered as a plastic mechanism to maintain the "proper mass" of neural tissue controlling particular functions (Jerisson, 1973) or for the "matching" between peripheral elements and brain processing power (Zupanc, 2006, 2008, 2011), contributing to the functional specialization (Grandel et al., 2006). Brain proliferation zones also persist in adulthood in *G. omarorum* (Olivera-Pasilio et al., 2014) and *Brachyhypopomus gauderio* (Dunlap et al., 2011) showing overall similarities with their distribution in *A. leptorhynchus* (Zupanc and Horschke, 1995; Zupanc, 2006, 2008).

Adult *G. omarorum* newborn cells appear to differ in their pace of migration (Olivera-Pasilio et al., 2014). Newborn cells show long distance displacement at the rostral part of the telencephalon, suggesting a migration process similar to what occurs in amniotes (Altman, 1969; Lim et al., 2008) including humans (Wang et al., 2011) and birds (Goldman and Nottebohm, 1983; Nottebohm, 2002; Barnea and Pravosudov, 2011), and anamniotes (*Danio rerio*: Adolf et al., 2006; Kishimoto et al., 2011). Other brain region of comparative interest are the cerebellum (Cb), the dorsal, ventral, and posterior subdivisions of the dorsolateral zone of the dorsal telencephalon (considered homologous of the amniote hippocampus; Zupanc, 2006) and the tectum opticum (TeO). Newborn cells originated from these proliferation zones also display long range and/or relatively fast migration, as evidenced by the almost complete displacement of derived cells between cerebellar layers after a 30 days chase (Olivera-Pasilio et al., 2014). The location, as well as shape and appearance of the nuclei suggest that newborn cells are in the process of differentiation as shown in other teleost (Zupanc et al., 1996, 2005; Kaslin et al., 2009; Delgado and Schmachtenberg, 2011; Teles et al., 2012).

In this manuscript, we further analyze in adult *G. omarorum* the migration process of derived cells by pursuing their location from the proliferation zones to their final destination. We also studied the differentiation of newborn cells into the neuronal phenotype by demonstrating the co-localization of long-term thymidine analog labeling and expression of early neuronal markers doublecortin (DCX) and HuC/HuD or the mature neuronal marker tyrosine hydroxylase (TH). We found evidences of neurogenesis in several brain regions of the telencephalon, mesencephalon, and rhombencephalon. We further evidenced the insertion of newborn cells into neural circuits by the demonstration of long term thymidine analog labeling and "*in vivo*" retrogradely labeling of cerebellar granular cells. These findings contribute to support the widespread distribution of brain proliferation zones and their neurogenic capacity in teleost.

MATERIALS AND METHODS

General Procedures

Animals

Thirteen adult specimens of *G. omarorum* (Richer-de-Forges et al., 2009; 8 males, 2 females and 3 of non-determined sex; weight: 6.26 ± 2.94; total fish length: 12.23 ± 2.04 mean ± SD) were collected from Laguna del Cisne, Uruguay (latitude 35°50 S, longitude 55°08 W). According to the measured length of the specimens, which is about half of the maximal length (Richer-de-Forges et al., 2009), we estimate that most of the fish used in this study have already reached the adult period, corresponding to the first gonadal maturation, at the age of 1 year (Balon, 1975; Barbieri and Cruz, 1983).

Macroscopic gonadal morphology was confirmed in 10 of the specimens studied. Animals were kept in individual tanks on a 12 h:12 h light: dark cycle and daily fed with *Tubifex tubifex*. Water conductivity was adjusted to 200 μs and temperature maintained at 20–25°C.

Anesthesia

All procedures were performed in accordance to the guidelines of CHEA (Comisión Honoraria de Experimentación Animal, ordinance number: 4332-99, Universidad de la República). Experiments were approved by the Animal Ethics Committee of the Instituto de Investigaciones Biológicas Clemente Estable (protocol number 010/09/2011).

For the application of Neurobiotin tracer (Vector Laboratories, Burlingame, CA, USA) in the corpus cerebelli (CCb), animals were anesthetized by immersion in 3-aminobenzoic acid ethyl ester (MS-222, Sigma-Aldrich, St Louis, MO, USA, at a dose of 120 mg/l) maintained by gill perfusion of the same anesthetic solution during surgery.

For transcardial fixation, fish were deeply anesthetized by immersion in MS-222 (500 mg/l, Sigma-Aldrich) followed by gill perfusion of the same anesthetic solution.

Fixation and Tissue Sectioning

Animals were first perfused with 20–30 ml of saline (0.7% NaCl solution) in order to wash blood out from the circulatory system, followed by 10% paraformaldehyde (Sigma-Aldrich) dissolved in phosphate buffer 0.1 M, pH 7.4 (PB; Carlo Erba, Val de Reuil, France). Brains were dissected out and post fixed in the same fixative solution for 24 h at 4°C. After embedding the brains in a gelatin/albumin (Sigma-Aldrich) mixture denatured with glutaraldehyde (Sigma-Aldrich), frontal serial sections (60 μm) were obtained with a vibratome (Leica VT1000S, Wetzlar, Germany) and serially collected in 24 or 48 multiwell plates.

In many cases, sections from most brain regions were processed in parallel, though we focused on certain rostral-caudal levels. At these levels, long distance and/or high pace of migration of newborn cells were previously evidenced (Olivera-Pasilio et al., 2014): the medial (L1) and caudal region (L2) of OB, corresponding to plates 1 of *Gymnotus carapo* atlas (Corrêa et al., 1998) and plate 38 of *A. lepthorhynchyus* atlas (Maler et al., 1991); the rostral region of the subpallium (L3) that corresponds to plates 2 and 32 of the mentioned atlases, respectively; the medial region and caudal pole of the midbrain TeO and torus semicircularis (TS; L4, and L5), the rostral pole of the rhombencephalic corpus cerebelli (CCb; L5), and the caudal pole of the rhombencephalic electrosensory lateral line lobe (ELL; L6; **Figure 1**).

Histological Analysis of the Brain of *G. omarorum*

To reveal the structural organization of the brain regions under analysis, mainly those where newborn neurons migrate, some sections were counterstained with DAPI (Sigma) or ToPro3 (Molecular Probes, Grand Island, NY, USA) after immunohistochemistry. Also, serial sections of control animals ($N = 2$) were counterstained with fluorescent Nissl staining using Neuro Trace® (Molecular Probes) as described below (Supplementary Figure 1) and βIII-tubulin, HuC/HuD or tyrosine hydroxylase (TH; Supplementary Figure 2). For fluorescent Nissl counterstaining, free floating brain sections of a control animal were stained with Neuro Trace® at 1/150 dilution in PB for 20 min at room temperature and rinsed in PB with 0.1% Triton X-100 (10 min) followed by PB (3 × 5 min). For ToPro3 counterstaining, brain sections were immersed in ToPro3 for 10 min at a 1/4,000 dilution, followed by rinsing in PB (3 × 5 min). All sections were mounted in a sealing and anti-fading coverslipping solution containing polyvinyl alcohol (PVA, Sigma) and 1,4 diazabicyclo [2.2.2]octane (DABCO, Sigma) and prepared according Peterson lab protocol (http://neurorenew.com/wp-content/uploads/2014/12/pva2.pdf).

Specific Procedures

In order to evidence the migration and/or differentiation of newborn cells into the neuronal phenotype, we labeled derived cells using two protocols of thymidine analog administration. Then, we demonstrated their differentiation into the neuronal phenotype by demonstration of analog retention by CldU immunohistochemistry combined with immunohistochemical demonstration of neuronal markers' expression or labeling with neuronal tracers.

Thymidine Analog Labeling

Proliferating cells were labeled with 2.3 mg/ml 5-Chloro-2′-deoxyuridine thymidine (CldU, Sigma-Aldrich) dissolved in 0.7% sodium chloride, and administered i.p. at 20 μl/g of body weight, according to two procedures: (1) pulse administration: a single injection followed by post-thymidine analog survivals of 1 ($N = 3$), 7 ($N = 2$), or 30 days ($N = 3$); and (2) sequential administration: four daily injections followed by survivals of 90 ($N = 2$) or 180 days ($N = 1$).

In vivo Neuronal Tracer Administration

To reveal the differentiation of cerebellar newborn cells into the neuronal phenotype, Neurobiotin tracer (Vector Laboratories, Inc., Burlingame, CA, USA) was applied *in vivo* at the molecular layer of the Cb, 86 or 176 days after repetitive CldU administration. Animals were anesthetized and the soft tissue over the rostralmost portion of the sagittal suture was carefully removed with the tip of a scalpel (Supplementary Figure 3A). Then, a small perpendicular and superficial incision was made in

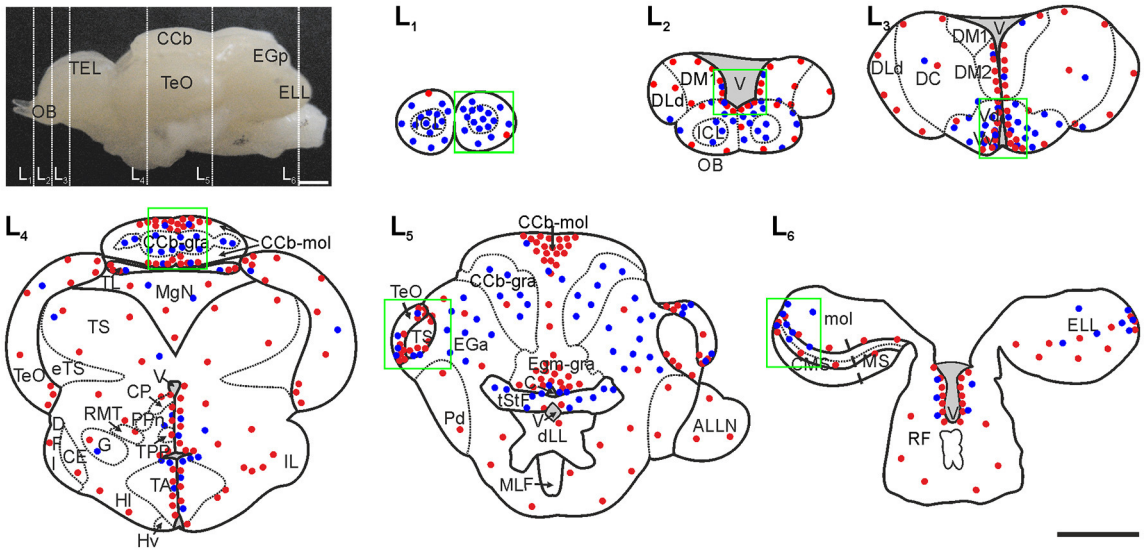

FIGURE 1 | Spatial-temporal distribution of brain labeled cells in adult *G. omarorum* after short (1 day) and long (30 days) survivals following CldU administration. Labeled cells are qualitatively represented by red and blue dots (after chases of 1 day and 30 days, respectively) in the schematic diagrams of frontal sections (L1–L6) corresponding to the planes indicated by the dotted lines over the lateral view of the brain. Regions of interest of this work are indicated by the green squares. Modified from Olivera-Pasilio et al. (2014). CCb-mol, Cerebellum, molecular layer; CCb, Corpus cerebelli; CP, Central-posterior nucleus; CMS, Centromedial segment; DFI, Nucleus diffusus lateralis of the inferior lobe; EGa, EGa-gra, Eminentia granularis pars anterior, granular layer; ELL, Electrosensory lateral line lobe; eTS, Torus semicircularis efferents; Hv, Hypothalamus ventralis; ICL, Internal cell layer; IL, Inferior lobe; DM1, Dorsomedial telencephalon; DLd, Dorsolateral telencephalon, dorsal subdivision; DM1, Dorsomedial telencephalon, subdivision 1; DM2, Dorsomedial telencephalon, subdivision 2; MgN, Magnocellular mesencephalic nucleus; MS, Medial segment; mol, Molecular layer (ELL); PPn, Prepacemaker nucleus; RF, Reticular formation; TA, Nucleus tuberis anterior; TEL, Telencephalon; TeO, Tectum Opticum; TL, Torus longitudinalis; TPP, Periventricular nucleus of the posterior tuberculum; tStF, Tractus stratum fibrosum; V, Ventricle; Vd, Ventral telencephalon, dorsal subdivision; Vv, Ventral telencephalon, ventral subdivision. Scale bars: 1 mm.

order to disrupt this portion of the sagittal suture and expose the dorsal surface of the rostral portion of CCb. After slightly cutting the cerebellar surface, crystals of Neurobiotin were applied with the tip of a needle (Supplementary Figure 3B). Finally, the wound was sealed with Histoacryl® (B. Braun Aesculap AG, Tuttligen, Germany), animals were allowed to recover from anesthesia and returned to their tanks.

Double Immunohistochemistry (CldU Label Retention and Neuronal Markers' Expression)

To break double-stranded DNA into single strands and expose the proliferation marker CldU to the antibodies, free floating tissue sections were first incubated in 2 N HCl (Baker, Phillipsburg, N.J. USA) in PB containing 0.3% Triton X-100 (Baker; PB-T) for 50 min at room temperature, followed by rinsing in PB (3 × 10 min). Then, sections were incubated for 1–2 days at 4°C in rat anti BrdU-CldU antibody (Accurate Chemical & Scientific Corporation, Westbury, NY, USA) at a dilution of 1:500 in PB-T, along with other primary antibody [rabbit anti doublecortin (Abcam, Cambridge, MA, USA) at 1/2,000 dilution, mouse anti HuC/HuD (Molecular Probes, Eugene, OR, USA) at 1:200 dilution, or rabbit anti TH (ThermoScientific, Waltham, MA USA) at 1/800 dilution]. Sections were rinsed in PB (3 × 10 min) and incubated in a mixture of donkey anti rat Cy5 secondary antibody (Jackson Immuno Research, West Grove, PA, USA) at 1:1,000 dilution and goat anti mouse Alexa 488 (Jackson Immuno Research) at 1:1,000 dilution in PB-T, for 90 min at room temperature. After rinsing in PB (3 × 10 min), sections were mounted in PVA/DABCO cover slipping solution. Negative controls involved the omission of CldU or of primary antibodies incubation; both controls resulted in no detectable staining (data not shown).

Simultaneous Demonstration of CldU Label Retention and Neuronal Tracer Labeling

In order to evidence the co-localization of CldU and Neurobiotin, sections were first pretreated in HCl and incubated in rat anti BrdU-CldU as described above. After rinsing in PB (3 × 10 min), sections were incubated during 90 min in donkey anti rat Cy5 at 1:1,000 dilution, together with streptavidin Cy3 (VECTOR) at a 1:500 dilution in PB-T. Sections were finally rinsed in PB (3 × 10 min) and mounted in PVA-DABCO coverslipping solution for immunofluorescence.

Image Acquisition and Processing

Most sections were imaged on a confocal system consisting of an Olympus BX61 microscope equipped with a FV300 confocal module and four lasers lines (405, 488, 543, and 633 nm) and the following objectives: 4x: UPlanFLN 0,13AN, 10x: UplanSAPO 0,40AN, 20x: UPlanFI 0,50AN, 40x: UPlanFI 0.75AN, and 60x: Plan ApoN 1,42AN objectives of the Confocal Microscopy Facility (IIBCE). Others were imaged on a Leica TCS SP5 II microscope equipped with four lasers lines (405, argon multiline

458, 476, 488, and 514 nm, and HeNe 543 and 633 nm), and HC PL FLUOTAR 5x/0.15, HC PL APO 20x/0.70 CS, HCX PL APO 40x/1.25-0.75 Oil, HCX PL APO 63x/1.40-0.60 Oil, HCX PL APO 63x/1.20 W CORR, and PL APO 100x/1.40-0.70 Oil CS objectives of the Confocal Microscopy Unit (Facultad de Medicina, UdelaR).

Acquisition settings were adjusted to ensure the completely dynamic range detection. Images of confocal planes were sequentially scanned with each laser line. Fifteen confocal planes, every 2 μm, were acquired in sections of levels L1–L3. For levels L4–L6, 15, 20, 25 to 30 confocal planes, every 0.5 or 1 μm were acquired. Post-processing of images was limited to small changes in the distribution histogram or background subtraction (Fiji Rolling ball radius: 50 pixels) in most cases.

Co-expression of markers was confirmed by orthogonal projections in the X-Z and Y-Z planes of the z-stacks at X-Y position of presumptive co-localization and/or visualization of the images corresponding to each channel of a single plane separately along with their overlay.

We used the same nomenclature and abbreviations as previously (Maler et al., 1991; Zupanc et al., 1996; Corrêa et al., 1998; Meek and Nieuwenhuys, 1998; Olivera-Pasilio et al., 2014).

Quantification

To quantify the amount of labeled cells per section in levels L1–L3, we constructed 3-D models of the sections from serial 2D low power confocal microphotographs with BioVis3D (R) as detailed in Iribarne and Castelló (2014). The boundaries of the olfactory bulb (OB), and internal cell layer were drawn and the location of every labeled nucleus was indicated in each plane of the 3D reconstruction with the tool "dot sets." The spatial distribution of labeled nuclei was evidenced by making transparent the constructed models.

We also used BioVis3D to determine the location of labeled nuclei in the x and y axes. First, we established the crossing of the mid-line and dorsal border of the OB as the origin of the x and y axes (red lines in Supplementary Figure 1). Then, lines extending from each nucleus to the x and y axes (green and blue lines in Supplementary Figure 1) were drawn and their length was calculated by the software. The resulting values were normalized by the width and height of each region of interest at each studied level to calculate the relative distance of every nucleus.

For every level (L1–L3) of each chase duration (1, 7, and 30 days), the mean and standard deviation of the total amount of labeled nuclei per section were calculated. We also quantified the amount of labeled nuclei within and outside the internal cell layer of L1 and L2 (Supplementary Figures 4A,B), and within and outside the ventricular proliferation zone adjacent to the ventral and dorsal subdivisions of the ventral telencephalon of L3 (Supplementary Figure 4C).

Differentiation into the neuronal phenotype by demonstration of the expression of neuronal markers (HuC/HuD or TH) or retrograde Neurobiotin labeling of long term CldU label retaining newborn cells was quantified with the aid of Fiji-ImageJ Point tool. In z stacks of the brain regions of interest, CldU+ nuclei, and double labeled CldU+/HuC/HuD+, CldU+/TH+, or CldU/Neurobiotin cells were marked in selected equally spaced confocal planes to avoid over counting. The total amount of each class was registered and the percentages of CldU+ cells that expressed neuronal markers or were labeled with Neurobiotin were calculated.

Statistical Analysis

We analyzed variations in the amount of CldU labeled cells per section using One-way ANOVA or Mann-Whitney *U*-test, after determining the variance of the samples with Kolmogorov-Smirnov test. Differences among groups were considered significant when $p < 0.05$.

RESULTS

Spatial Distribution of Brain Proliferation Zones

We first analyzed the spatial distribution of brain proliferation zones in adult *G. omarorum* as a reference to depict the migration and/or differentiation of newborn cells. The spatial distribution of CldU labeled cells after a short survival (1 day) following the administration of a pulse of CldU (red dots in **Figure 1**) reproduced previous findings (Olivera-Pasilio et al., 2014). Briefly, most proliferating cells populated ventricular proliferation zones at the lining of the telencephalic (L2, L3, **Figure 1**), mesencephalic, diencephalic (L4, L5, **Figure 1**), and rhombencephalic (L6, **Figure 1**) ventricles. Outstanding: clusters of proliferating cells were found in all cerebellar divisions (L4, L5, **Figure 1**) and in the lateral-caudal pole of the ELL (L6, **Figure 1**). This spatial pattern allowed us to depict the boundaries of proliferation zones that were used as a reference to determine whether derived cells persist within the proliferation zones or migrate toward other regions or sub-regions at longer survival times (7–180 days).

Migration of Newborn Cells

Some labeled cells remained within the proliferation zones after post CldU survival times between 7 and 180 days. Conversely, most of the CldU labeled cells were located at increasingly greater distances from the proliferation zones boundaries, according to the survival duration. This shift is exemplified in **Figure 1** for survivals of 1 and 30 days (red and blue dots in **Figure 1**). The abundance of migrating newborn cells and the locations that they reached as a result of the migration varied among proliferation zones. In this work we focused on the brain regions where the migration process was more salient: the rostral telencephalon and OB, the TeO, the TS, and the Cb.

Olfactory Bulb and Rostral Telencephalon

The sessile OB of *G. omarorum* shares the histoarchitecture of teleost's OB (Byrd and Brunjes, 1995; Kermen et al., 2013), consisting of a round core of small and densely packed cells, the internal cell layer (ICL) surrounded by three concentric diffuse layers: the external cell layer (ECL), the glomerular layer (GL), and the outer primary olfactory fiber layer (POFL) adjacent to the OB's surface (L1 and L2 in Supplementary Figure 1).

One day after a pulse of CldU, labeled cells were rare in the OB. Few and scattered proliferating cells were located at any of

the layers of the rostral and medial part of the OB (red dots in L1 and L2, **Figure 1**: double arrows in AL1 and AL2, **Figure 2**; red dots in AL1 and AL2, **Figure 3A**). Conversely, densely packed CldU labeled cells were found at the lining of the most rostral portion of the telencephalic ventricle, nearby the caudal OB and the rostral region of the ventral (Vv) and dorsal (Vd) subdivisions of the subpallium. There, proliferating cells formed an extended ventricular proliferation zone (zone 1b, Olivera-Pasilio et al., 2014; red dots lining the ventricle at the zones indicated by the green rectangles in L2 and L3, **Figures 1**, **3A**; arrows in AL2 and AL3, **Figure 2**). This rostral-caudal gradient in the amount of proliferating cells was confirmed quantitatively as the number of proliferating cells in the rostral and caudal part of the OB was significantly lower than in the rostral portion of the subpallium 1 day after CldU administration (**Figure 3B**).

Seven days after CldU administration, proliferating cells were also located predominantly at ventricular proliferation zones in the caudal portion of the OB and rostral subpallium (BL1–L3, **Figure 2**). Only few CldU labeled nuclei were placed throughout the OB layers or the subpallium. The number of labeled cells increased in all levels at this chase duration, but only significantly at L3. The rostral-caudal gradient was preserved but steeper (**Figure 3B**).

Thirty days after CldU administration, some proliferating cells remained within the boundaries of the proliferation zone 1b adjacent to the caudal OB (CL2, **Figure 2**) and rostral subpallium (CL3, **Figure 2**). Unlike shorter chases, some CldU labeled nuclei were located at considerable distances from the rostral region of the proliferation zone 1b, reaching the ICL of caudal and, in a less extent, rostral OB (CL2 and CL1, **Figure 2**). The amount of CldU labeled cells in L1 and L2 increased up to 2.4 and 3.7 times the values found 1 day after CldU administration, respectively. However, only L1 showed significant differences in the amount of CldU labeled cells between both chases. Conversely, the amount of CldU labeled cells decreased significantly in L3 from 7 to 30 days (**Figure 3B**). Few CldU labeled nuclei were found lateral to the caudal zone of 1b (adjacent to the subpallium), reaching Vd, Vv, MOTF, and medial zone of FB (CL3, **Figure 2**).

CldU label retaining cells spilled out the boundaries of the ICL of the caudal OB at a 90 day chase (**Figure 2**, EL2) whereas most labeled cells remain within the ICL boundaries of the ICL of the rostral OB (**Figure 2**, EL1). At 180 day chase the spilled out of labeled cells from the ICL of the rostral OB to the surrounding layer was evident (**Figure 2**, FL1).

The amount of CldU label retaining cells in the lateral zone of the subpallium increased considerably 90 and 180 day after CldU administration. At 90 days newborn cells predominate in the ventral zone, whereas at 180 days were distributed along all the dorso-ventral extension of the subpallium.

Cerebellum

All the divisions of the Cb of *G. omarorum* (CCb, valvula cerebelli -VCb, and caudal lobe, including the eminentia granularis anterior -EGa- and posterior -EGp-), are organized in three layers, molecular, ganglionic, and granular, as exemplified in Supplementary Figure 5A. The ganglionic layer consists of Purkinje and eurydendroid cells. Eurydendroid cells, which are the origin of Cb efferents, are not aggregated in nuclei unlike other vertebrates (Finger, 1978).

Remarkable migrations processes both for the abundance of migrating cells as well as for their final destination, were detected in all cerebellar divisions as previously described (Olivera-Pasilio et al., 2014). Proliferation zones were circumscribed to a single cerebellar layer or even a region within a single cerebellar layer (red dots in L4 and L5, **Figure 1**).

The proliferation zone of the CCb, evidenced by the distribution of proliferating cells at 1 day chase, occupied the medial zone of its molecular layer (CCb-mol; red dots in L4, **Figure 1**). Thirty days after CldU administration, derived cells were mainly found at the granular layer of CCb (CCb-gra; blue dots in L4, **Figure 1**). However, scarce and intensely labeled CldU cells remained within the proliferation zone's boundaries.

In the VCb a conspicuous proliferation zone occupied all the extension of the molecular layer (VCb-mol). Proliferating cells were more densely packed near the dorsal-medial region of VCb-mol and migrating cells were sparsely and homogeneously found in all the extension of the granular layer (VCb-gra).

The proliferation zone of the caudal lobe of the Cb occupied the granular layer of the medial granular eminence (EGm-gra) while derived cells were located at the granular layer of the posterior granular eminence (EGp-gra) as shown in Olivera-Pasilio et al. (2014).

Tectum Opticum

The TeO is a multimodal integration center which is interconnected with the torus longitudinalis forming a Cb-like structure (Bell, 2002). In *G. omarorum*, it is a hollow hemispheric shaped structure. It has a cortical histoarchitecture and consists of seven cellular and fibrillary alternating layers (Supplementary Figure 5B; Meek and Nieuwenhuys, 1998). Proliferating cells were located at the dorsal-medial and ventral-lateral border of the caudal pole of TeO, forming a horseshoe shaped ribbon-like proliferation zone. One day after CldU administration, proliferating cells were distributed in all TeO layers (red dots in L4 and L5, **Figure 1**), though appeared to be more densely packed in deeper layers as the stratum periventriculare (SPV). At longer chases, CldU label cells occupied more superficial layers of TeO, also extending beyond the proliferation zones' boundaries in the rostral direction (blue dots in L4 and L5, **Figure 1**).

One hundred eighty days after CldU administration, derived cells were located ∼100 μm away from the dorsal region of the proliferation zone at rostral levels of the caudal TeO. These long labeled retaining cells were grouped mainly at the SPV and SAC layers, and less frequently reached the SGC (L5, **Figure 1**).

Torus Semicircularis

The TS of *G. omarorum* is a spherical protrusion of the mesencephalic tegmentum beneath the TeO. It is a layered structure which receives octavolateral inputs from rhombencephalic primary brain centers (Meek and Nieuwenhuys, 1998). One day after CldU administration proliferating cells were located at the medial and lateral borders

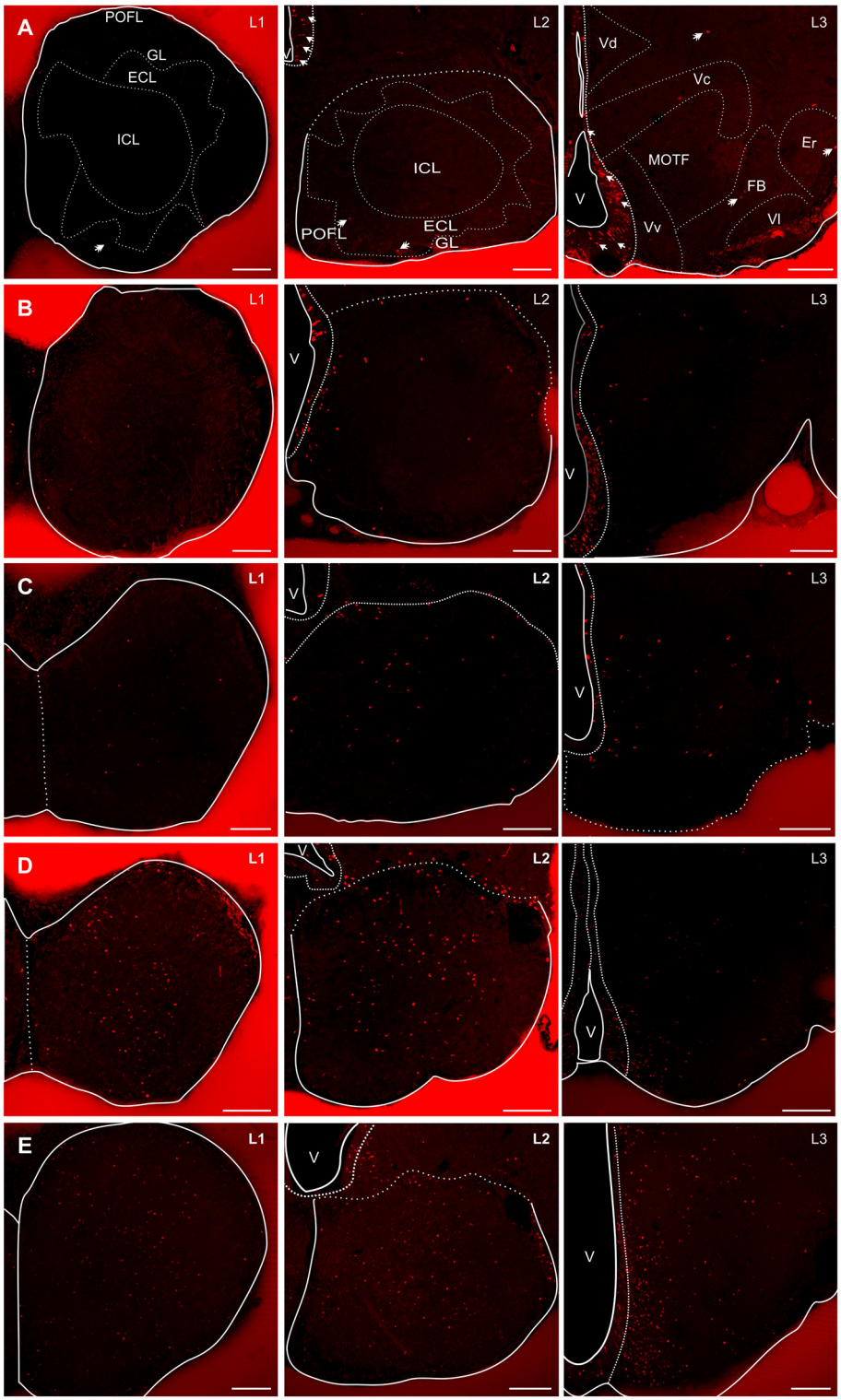

FIGURE 2 | Spatial-temporal distribution of proliferating cells and derived cells in the rostral (L1) and caudal (L2) regions of the OB, and rostral subpallium (L3) in *G. omarorum*. Images correspond to microphotographs of frontal sections of the brains of animals treated with a single **(A–C)** or four daily doses **(D,E)** of CldU followed by 1 **(A)**, 7 **(B)**, 30 **(C)**, 90 **(D)**, and 180 **(E)** days of survival. The OB is almost devoid of CldU+ cells after short survivals (**A** L1, L2). Conversely, the lining of the rostral portion of the telencephalic ventricle, adjacent to the subpallium was populated by densely packed CldU labeled cells, conforming a clear proliferation zone (arrows in **A** L2, L3). From 1 to 30 days CldU+ cells appeared within the nerve tissue at progressively greater distances from the proliferation zones at L2 and L3. At longer

(Continued)

FIGURE 2 | Continued
chases (90 and 180 days), CldU+ cells also populate the rostral OB, and appeared to increase in number in L1–L3. ECL, External cell layer; Er, Rostral entopeduncular nucleus; FB, Forebrain bundle; GL, granular layer; ICL, Internal cell layer; MOTF, medial olfactory terminal field; POFL, V, Ventricle; Vc, Ventral telencephalon, central subdivision Vl, Ventral telencephalon, lateral subdivision. Scale bars: 100 μm.

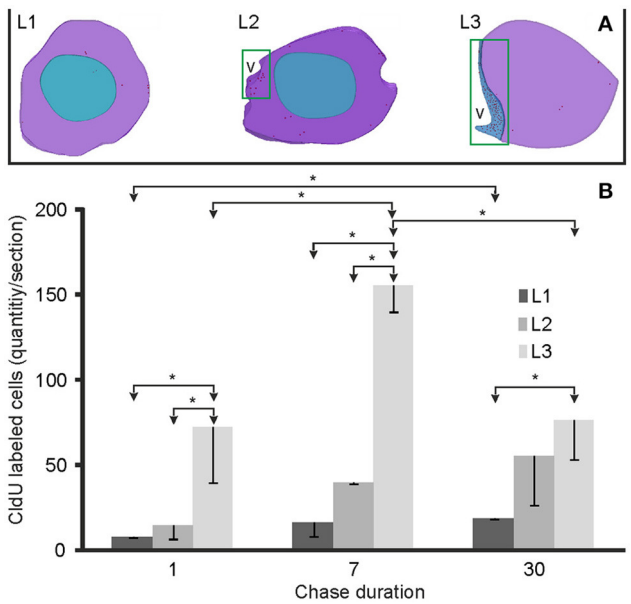

FIGURE 3 | Spatial-temporal distribution and quantification of proliferating and derived cells within the rostral telencephalon. **(A)** The location of proliferating cells is represented by red dots in the 3D reconstructions of rostral (L1) and caudal (L2) olfactory bulb and rostral subpallium (L3). Proliferation zones were located at the ventricular lining indicated by green rectangles in L2 and L3. **(B)** Bar plots of the amount of labeled cells per section at the three levels studied (L1–L3) following 1 ($N = 3$), 7 ($N = 2$), and 30 ($N = 3$) days after the administration of a pulse of CldU. Values are expressed as the mean and standard deviation of the total amount of labeled cells per section. * <0.05, One-way ANOVA.

of the caudal pole of TS (red dots in L5, **Figure 1**), forming a ring-shaped proliferation zone. At longer chases derived cells appeared diffusely distributed at the caudal pole of TS (blue dots in L5, **Figure 1**).

Electrosensory Lateral Line Lobe

The ELL is the primary relay nucleus of electrosensory pathways. It is a layered cerebellum-like structure (Supplementary Figure 5C; Meek and Nieuwenhuys, 1998) in which principal cells project to contralateral rhombencephalic and mesencephalic structures (praeminentialis nucleus and TS) which project back to the ELL, either directly or indirectly through Cb. At 1 day chase duration, proliferating cells were mainly located at the lateral-caudal border of cellular layers of ELL, and showed a medial-lateral and rostral-caudal gradient (red dots in L6, **Figure 1**). At longer chases, ELL CldU label retaining cells were extensively and diffusely distributed (blue dots in L6, **Figure 1**).

Neuronal Differentiation and Insertion into Neuronal Circuits

With the aim of studying neuronal differentiation and neurogenic capacity of *G. omarorum* adult brain proliferation zones, we analyzed the expression of neuronal markers, including the early neuronal markers DCX, and HuC/HuD or markers of further differentiation into the neuronal phenotype as tyrosine hydroxylase (TH), in CldU label retaining cells after post thymidine analog administration chases ranging from 7 to 180 days. We also assessed the insertion of newborn neurons into pre-existing neural circuits of the CCb by "*in vivo*" retrograde labeling of granule cell after Neurobiotin administration at the molecular layer of CCb.

Neuronal Differentiation in the Olfactory Bulb and Rostral Telencephalon Evidenced by Co-localization of CldU and HuC/HuD, DCX, or TH

One day after thymidine analog administration, DCX labeled a net of processes beneath the ventricular proliferation zone adjacent to the medial and dorsal-medial zone of the telencephalic proliferation zone 1b (inset, Supplementary Figure 6A). We only found CldU-DCX double labeled cells adjacent to the ventral region of this proliferation zone (Supplementary Figure 6B) as evidenced by the overlay of CldU and DCX signals corresponding to a single confocal plane (Supplementary Figure 6C) or by orthogonal projections of a z stack (Supplementary Figure 6D). At this chase duration, we did not find CldU-DCX or CldU-HuC/HuD double labeled cells in any other brain region.

Seven days after CldU administration, some cells at the ventral part of the subventricular zone of the rostral subpallium were CldU-HuC/HuD double labeled (**Figure 4**), but not at the rostral or caudal zones of the OB. Unexpectedly, we did not find any CldU-DCX double labeled cell at this chase duration.

After a 30 day chase, CldU label retaining cells expressed HuC/HuD at the ICL of the caudal OB (**Figure 5A**) and the ventral region of the subventricular zone of the rostral subpallium (**Figure 5B**). CldU-HuC/HuD double labeled cells' nuclei were round and the chromatin either densely (**Figure 5A**) or loosely (**Figure 5B**) packed. Some newborn CldU labeled cells with fusiform shape and elongated nuclei with densely packed chromatin also express DCX (**Figures 5C,D**).

Double labeled CldU-HuC/HuD cells were found at the ICL (**Figure 6A**) and the dorso-medial zone (**Figure 6B**) of the rostral OB 90 days after CldU administration. All CldU-HuC/HuD double-labeled cells had ovoid to round nuclei surrounded by a thin cytoplasm without evident cellular processes. At 90 days CldU-HuC/HuD double-labeled were also found at L3 (**Figure 6C**).

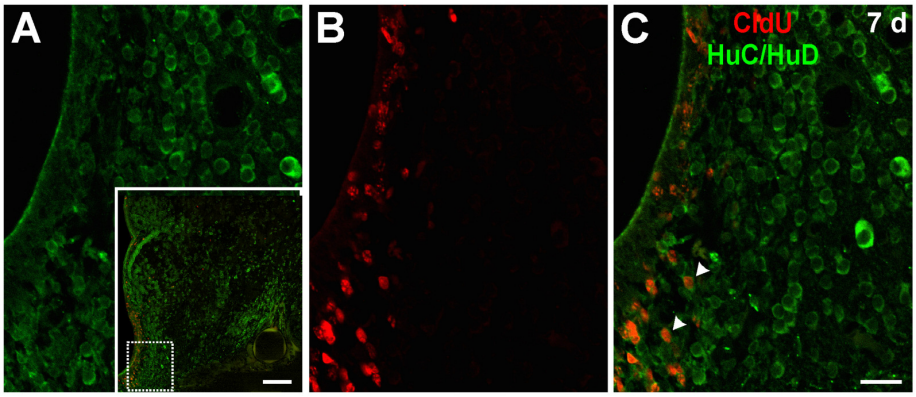

FIGURE 4 | Neuronal differentiation in the subpallium at 7 days after the administration of a pulse of CldU demonstrated by co-localization with HuC/HuD. **(A)** Confocal microphotographs of the ventricular lining at the region of the rostral subpallium indicated by the rectangle in the panoramic view (inset). HuC/HuD and CldU labeling are shown in green and red channels in the microphotographs of a single plane shown in **(A,B)**, respectively. The overlay of both channels is shown in **(C)**. Arrowheads indicate CldU labeled retaining cells also expressing the neuronal marker HuC/HuD. Scale bars: (inset) 100 μm; **(A–C)** 20 μm.

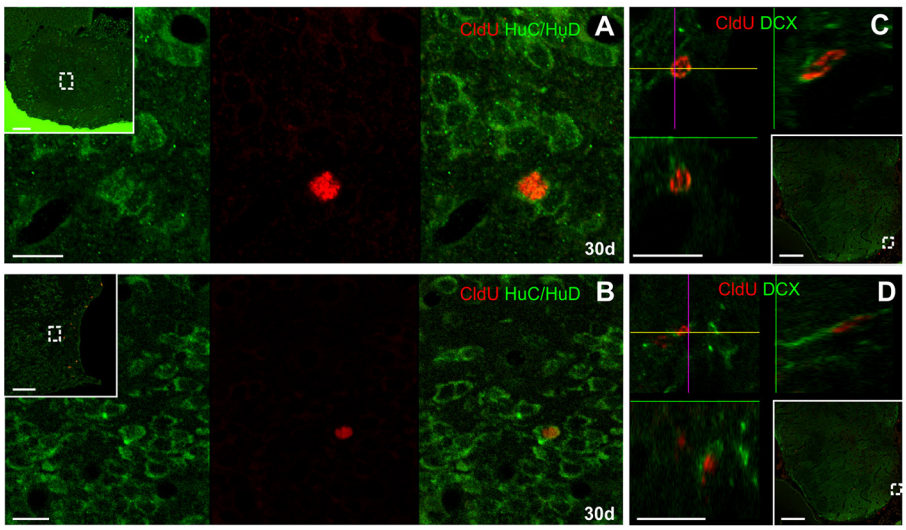

FIGURE 5 | Neuronal differentiation in the olfactory bulb and rostral subpallium at 30 days after the administration of a pulse of CldU demonstrated by co-localization with HuC/HuD and DXC. **(A,B)** Confocal microphotographs of the caudal OB and rostral subpallium at the regions containing double labeled cells indicated by the dotted squares in the panoramic views (insets), respectively. HuC/HuD and CldU labeling are shown in green (left) and red (middle) channels; the right image corresponds to the overlays of both channels. **(C,D)** *x-z* and *y-z* orthogonal projection of stacks of 35 confocal planes scanned every 0.5 μm at the lines crossing at the cell of interest, confirming the co-localization of CldU and DCX in the rostral subpallium at the positions indicated by the dotted rectangles in the panoramic views (insets). Scale bars: **(A,B)** 10 μm; **(C,D)** 5 μm; insets, 100 μm.

At 90 days, double labeled CldU-DCX cells were only found at the dorsal-medial zone of the rostral level of OB (data not shown).

At this chase duration CldU labeled cells also express TH at the ventricular or sub ventricular zone of the rostral subpallium (**Figure 7**). Some of these cells showed a thin cytoplasmic halo without cellular processes (**Figures 7A,A′**) whereas others had more expanded cytoplasm from which thin and short cellular processes with few branching points emerge (**Figure 7B**, arrowheads in **Figure 7B′**).

One hundred eighty days after CldU administration, double labeled CldU-TH cells were found in the rostral subpallium, far from the proliferation zone (**Figure 8**), and at both, caudal (**Figure 9**) and rostral (**Figure 10**) levels of the OB. Some newborn cells had an ovoid nucleus surrounded by a thin cytoplasmic halo without cellular processes, as those found lateral to the subpallial proliferation zone (**Figures 8B,C**). Many double labeled cells showed a larger cytoplasmic halo from which two or three relatively thick cellular processes emerged from opposite regions of the cell body. These cells resembling bipolar or multipolar neurons

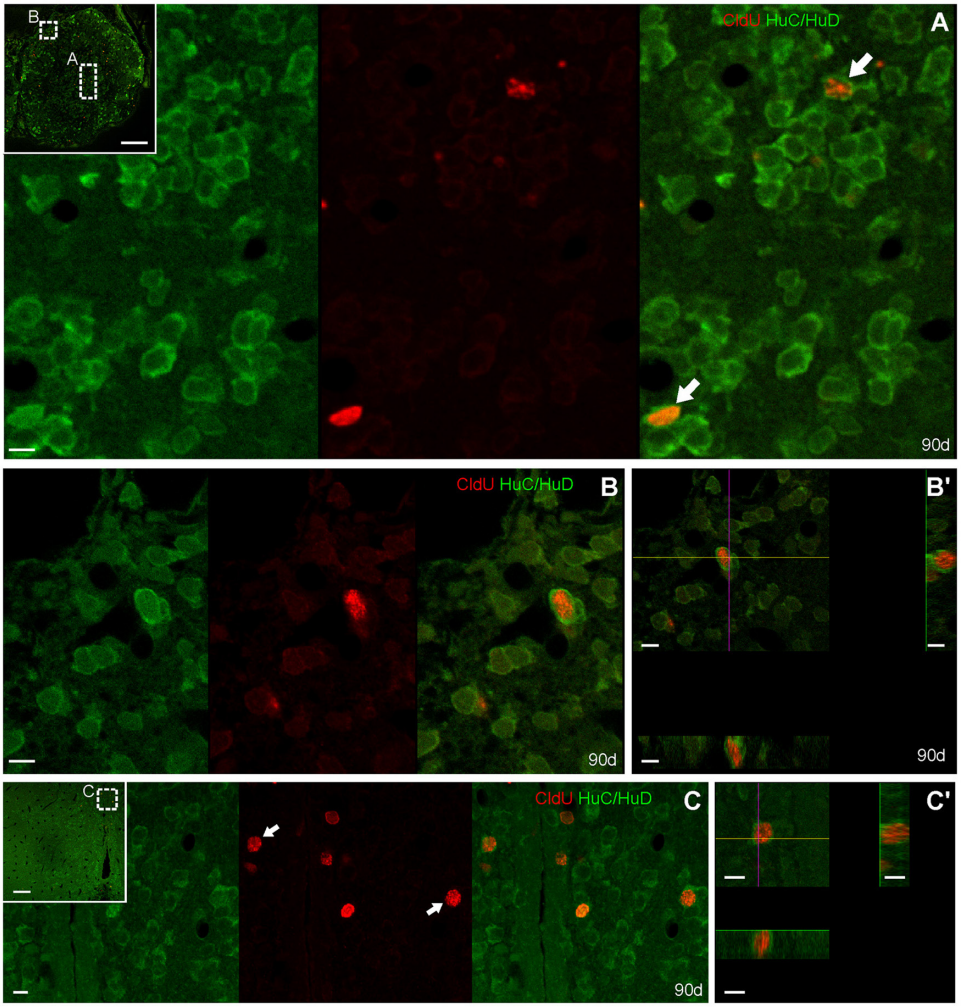

FIGURE 6 | Neuronal differentiation in the olfactory bulb and rostral subpallium at 90 days after four daily injections of CldU demonstrated by co-localization with HuC/HuD. Confocal microphotographs of the olfactory bulb **(A,B,B′)** and the rostral subpallium **(C,C′)** at the level indicated by the dotted rectangles in the panoramic view (insets) to evidence double labeled cells. HuC/HuD and CldU labeling are shown in green and red channels of single scans, respectively. Co-localization is confirmed by the overlay of both channels, or by the *x-z* and *y-z* orthogonal projections of stacks obtained from 19 planes, every 0.5 μm **(B′)**, or 15 planes, every 0.5 μm **(C′)**.

were located at the ICL of caudal (**Figures 9B,B′,C,C′**, **Supplementary Video 1**) and rostral (**Figures 10C,C′,C″**) OB. In other cells at the ICL of the rostral OB, a relatively large nucleus occupied an asymmetric location respect to a very thin cytoplasmic halo, resembling migrating neuroblasts (**Figures 10A,B**). All double labeled CldU-TH cells were intermingled with cells with single labeled CldU+ nuclei or TH+ cytoplasm.

According to the quantitative analysis, almost 0.5% of long term CldU retaining new born cells at the lateral regions of the subpallium (L3) expressed the mature neuronal marker TH+ after a 180 day chase. The fraction of CldU labeled cells that also expressed TH reached almost 1% and more than 1.5% of the total amount of CldU labeled cells at the caudal (L2) rostral (L1; **Table 1**).

Neuronal Differentiation in the Corpus Cerebelli and Cerebellum-Like Structures Evidenced by Co-localization of CldU and HuC/HuD

After a short thymidine analog survival (7 days), we did not find HuC/HuD expression in CldU labeled cells. However, longer survivals (30, 90, and 180 days) allowed us to evidence the differentiation of derived cells into neurons in the CCb and other Cb-like structures.

Corpus cerebelli

We did not find CldU-DCX double labeled cells in CCb-mol 1 or 7 days after CldU administration, even though DCX processes were abundant at the CCb-mol (running parallel to the cerebellar surface in the medial-lateral direction) and the Purkinje cells' layer (running parallel to the cerebellar surface in the rostral-caudal direction; Supplementary Figure 7).

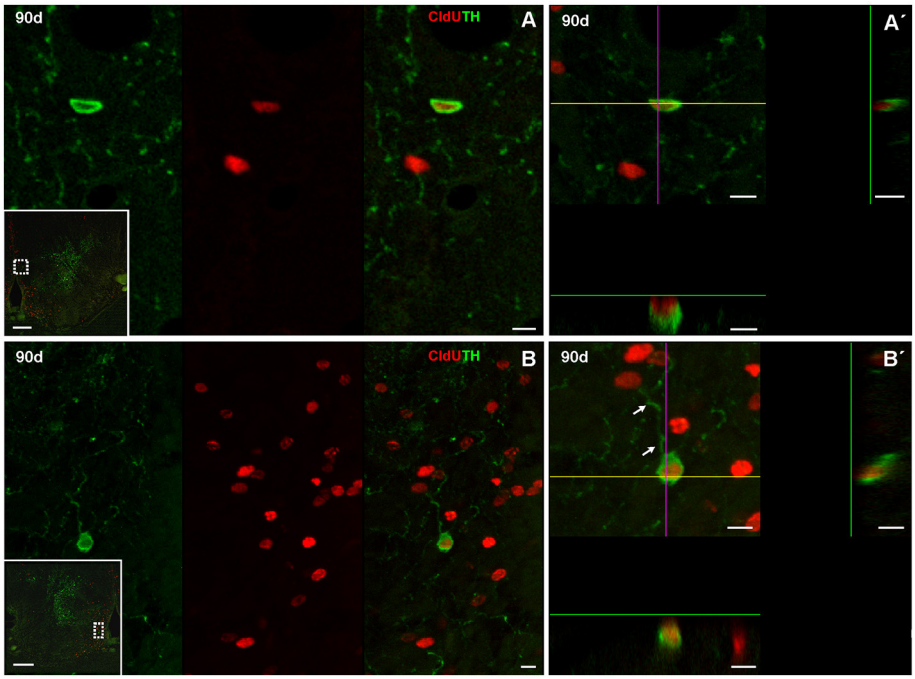

FIGURE 7 | Neuronal differentiation in the rostral subpallium at 90 days after after four daily injections of CldU demonstrated by co-localization with TH. **(A,B)** Confocal microphotographs of the subpallium at the regions indicated by the dotted rectangles in the panoramic views (insets). Co-localization is demonstrated by TH and CldU labeling of a single confocal plane and the overlay of both images **(A,B)**. Co-localization is also confirmed by the *x-z* and *y-z* orthogonal projections of 16 confocal planes, every 0.5 μm **(A′)** or 45 confocal planes, every 0.5 μm **(B′)**. Arrows indicate neuronal processes of a newborn neuron. Scale bars: **(A,B)** 20 μm; **(A′,B′)** 5 μm; insets 100 μm.

Thirty days after CldU administration, scarce CldU labeled cells at the CCb-gra also expressed HuC/HuD (**Figure 11A**). These double labeled cells were small, with an ovoid or polygonal nucleus and granular CldU labeling of varied intensity, surrounded by a thin polygonal cytoplasmic halo (**Figure 11B**). Double labeled cells were intermingled with a myriad of HuC/HuD+ cells of the CCb-gra.

Double-labeled CldU-HuC/HuD cells with similar labeling characteristics were found at the CCb-gra 90 (**Figures 11C,C′**) and 180 days (data not shown) after CldU administration.

Purkinje and/or eurydendroid cells show a marked expression of HuC/HuD but did not showed co-localization with CldU at any of the chases studied.

Tectum opticum and torus semicircularis

Similar to the CCb, we did not find double labeled CldU-DCX newborn cells in the TeO at any of the chases studied, even though bundles of DCX processes were abundant beneath the dorsal-medial tectal proliferation zone (Supplementary Figure 8).

Ninety days after CldU administration, long term label retaining cells also expressed HuC/HuD at the deeper layers of the caudal pole of the TeO (**Figure 12**). Double labeled cells were found in all dorsal-ventral extension of the stratum periventriculare (SPV), and in lesser density at the boundaries between stratum album centrale (SAC) and stratum griseum centrale (SGC). Most double labeled cells had round to ovoid nucleus surrounded by a thick cytoplasmic halo without cellular processes (**Figures 12A–D**). Likewise, CldU label retaining cells also expressing HuC/HuD with round morphology were found at the ventral region of the TS. Double labeled cells showed a round morphology (**Figures 12E,F**).

One hundred eighty days after CldU administration, derived cells were mainly grouped at the SPV and SAC layers at about 100 μm from the rostral portion of the dorsal-medial region of the TeO proliferation zone (asterisk in **Figure 13A**). Some of these cells expressed HuC/HuD (arrows in **Figures 13A–C**). Conversely, most of CldU labeled were not displaced from the ventro-lateral region of the tectal proliferation zone (arrow in **Figure 13D**); few others were located quite far from it (double arrows in **Figures 13D,E**). Some of these long term CldU label retaining cells also expressed HuC/HuD (**Figure 13E**).

In the ventral region of the TS, long term CldU labeled cells were distributed in and extended zone with numerous double CldU-HuC/HuD labeled cells (**Figures 13D,F,G**).

Electrosensory lateral line lobe

Unlike other brain regions, very scarce CldU long-term label retaining cells were found at the caudal region of the ELL 90 (**Figures 14A,B**) or 180 (**Figure 14C**) days after CldU administration. Some of these cells with a thin fusiform to ovoid cytoplasmic

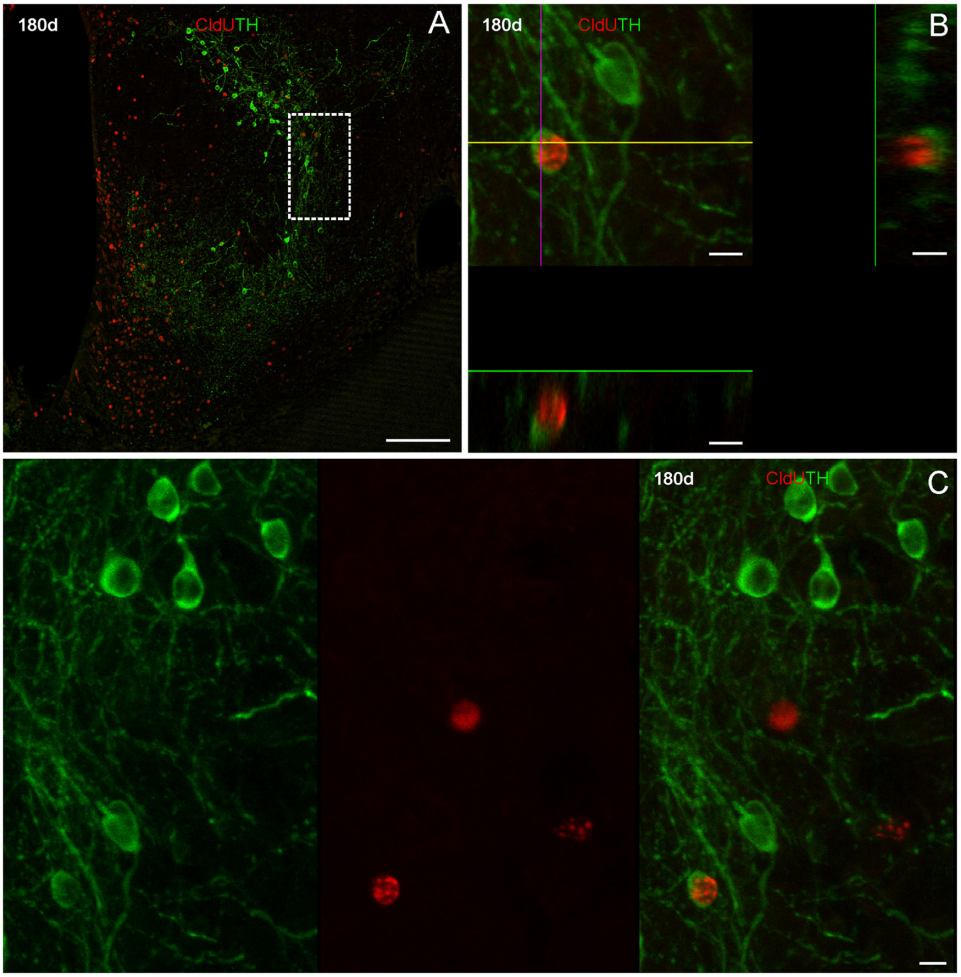

FIGURE 8 | Neuronal differentiation in the rostral subpallium at 180 days after four daily injections of CldU demonstrated by co-localization with TH. **(A)** Maximal intensity projection of 15 confocal planes taken every 2 μm at the rostral subpallium. **(B)** *x-z* and *y-z* orthogonal projection of 25 confocal planes, every 2 μm, confirming the co-localization of CldU and TH in a cell at the region indicated by the dotted rectangle in **(A)**. **(C)** Co-localization of TH and CldU is also confirmed by the overlay of the sequentially acquired channels of a single plane. Scale bars **(A)** 100 μm; **(B,C)** 5 μm.

halo were located at the GCL, near the boundaries with adjacent layers, also expressing HuC/HuD (**Figures 14 A′,A″,B′,C′,C″**).

Considering the quantitative data from all the analyzed brain regions (OB, TeO, TS and CCb), 50% of long term CldU retaining new born cells expressed HuC/HuD 90 days after CldU administration (range: TS: 33,33—CCb: 57,14). The fraction of double labeled cells increased up to almost 80% in the TS and TeO after 180 day chase (**Table 1**).

Neuronal Differentiation in the CCb Evidenced by CldU and Neurobiotin

Repetitive CldU administration allowed the long term retention of CldU in numerous cells at the CCb-gra, both 90 (**Figure 15A**) and 180 days (**Figure 15B**) after thymidine analog administration. These derived cells probably correspond to granule cells, both because of their location, as well as the shape and size of their nuclei. Cortical application of Neurobiotin labeled many cells with small round, ovoid, or polygonal soma, at the CCb-gra at both chase durations, even far from the site of tracer application. Note that the site of injection is not visible in the topographic images of **Figures 15A,B**, and thus is located more than 200 μm from the soma of the Neurobiotin labeled cells. This indicates that the tracer was incorporated into the axons or end terminals of the labeled cells at the CCb-mol and retrogradely transported up to the cell's soma and perisomatic dendrites at the CCb-gra. This, as well as the known histoarchitectural organization of the Cb, further supports the identification of these cells as granule cells. Many long term CldU retaining cells were labeled with Neurobiotin (**Figures 15A′,B′,B″**, **Supplementary Video 2**), indicating that the newborn cells acquired the mature granular morphology in 90 days. Also indicates that these newborn granule cells very probably were incorporated into

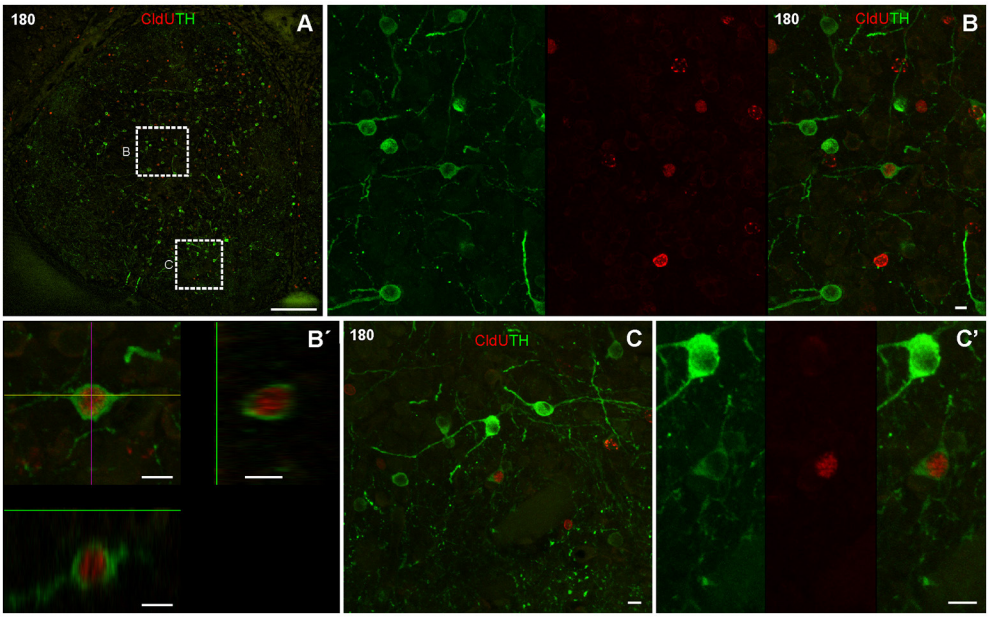

FIGURE 9 | Neuronal differentiation in the caudal olfactory bulb at 180 days after four daily injections of CldU demonstrated by colocalization with TH. **(A)** Topographic confocal image of a frontal section of the caudal olfactory bulb. The rectangles indicate the locations at which higher power confocal images were acquired **(B,B′,C,C′)**. Images corresponding to both channels of a single confocal plane and the overlay at the regions indicated by the dotted rectangles in **(A)** are shown in **(B,C′)**. **(B')** x-z and y-z orthogonal projection of 22 confocal planes, every 1 μm, confirming the colocalization of CldU and TH in the same cell as in **(B)**. Scale bars: **(A)** 50 μm; **(B–C')** 5 μm.

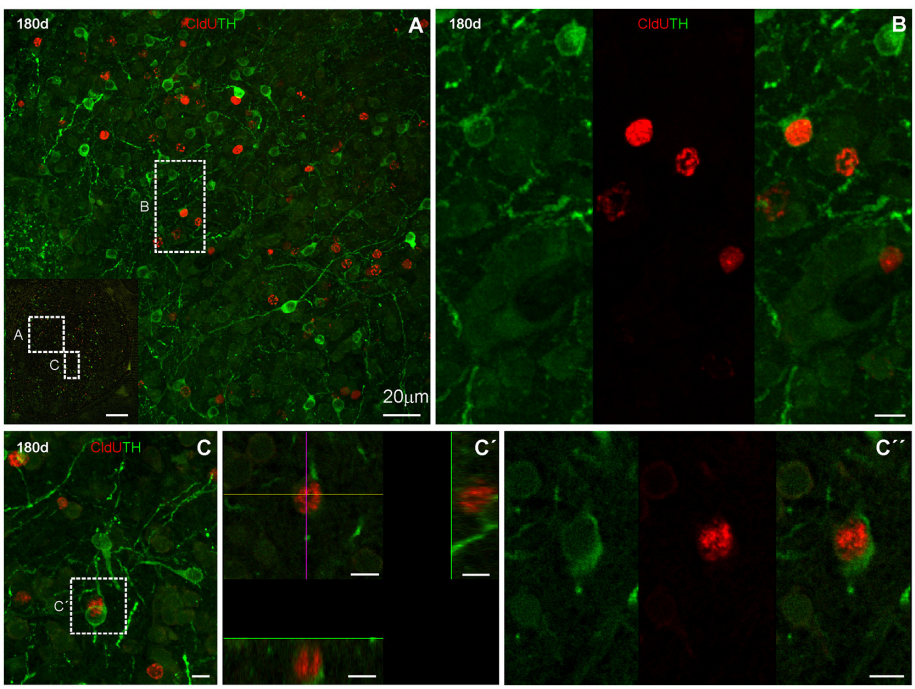

FIGURE 10 | Neuronal differentiation in the rostral olfactory bulb at 180 days after four daily injections of CldU demonstrated by co-localization with TH. Microphotograph at the region of the rostral OB indicated by the rectangle in the inset in **(A)**. **(B)** Higher power images of both channels and the overlay of the region containing a cell of interest at the region indicated by the dotted square in the inset in **(A)**. **(C)** Maximal intensity projection of a stack of 17 confocal planes, every 0.5 μm. The rectangle indicates the location of a cell which co-localization was demonstrated by *x-z* and *y-z* orthogonal projections of the same stack **(C′)** as well as each channel and overlay of the sequentially acquired channels of a single plane **(C′′)**. Scale bars: **(A)** 20 μm; (**B**, Inset in **A**) 100 μm; **(B,C′′)** 5 μm.

TABLE 1 | Quantitative analysis of neuronal differentiation in the brain of adult *G. omarorum*.

	Brain region	90 days				180 days			
		CldU+	Double	%	*N*	CldU+	Double	%	*N*
TH	OB (L1)	n.d.	n.d.	n.d.		434	7	1.61	1
	OB (L2)	n.d.	n.d.	n.d.		317	3	0.94	1
	Subpallim (L3)	419	2	0.47	1	n.d.	n.d.	n.d.	1
HuC/HuD	OB (L1)	51	26	50.98	1	n.d.	n.d.	n.d.	
	TeO (L4)	n.d.	n.d.	n.d.		519	403	77.65	2
	TeO (L5)	88	43	48.86	1	n.d.	n.d.	n.d.	
	TS (L4)	n.d.	n.d.	n.d.		142	124	87.32	1
	TS(L5)	18	54	33.33	1	354	253	71.46	2
	CCb (L4)	140	80	57.14	1	n.d.	n.d.	n.d.	
Nb	CCb (L4)	727	6	0.82	1	373	34	9.11	1

Newborn cells retaining CldU after 90 or 180 days chases and co-expressing CldU and tyrosine hydroxylase (TH) or HuC/HuD, and newborn cells retaining CldU after 90 or 180 days chases and retrogradely labeled with Neurobiotin (Nb) were quantified in 1–4 z stacks of sections corresponding to the studied levels (intermediate olfactory bulb, OB; L1, caudal OB, L5 subpallium; L3, intermediate and, caudal tectum opticum (TeO, L4, and L5); intermediate and caudal torus semicircularis (TS, L4, and L5), and rostral corpus cerebelli (CCb, L5) of four specimens of G. omarorum. Results are expressed as the total amount of CldU labeled cells (CldU+), double labeled cells (Double), and as the fraction of long term CldU label retaining cells that also express one of the neuronal markers or were retrogradely labeled with Neurobiotin (%).

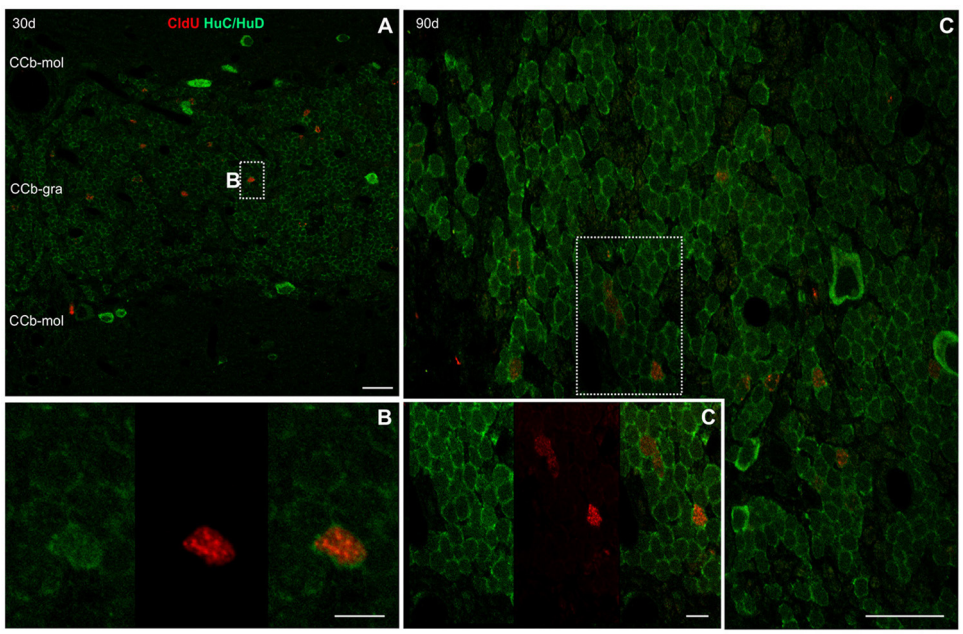

FIGURE 11 | Neuronal differentiation in the corpus cerebelli at 30, 90, and, 180 days after four daily injections of CldU demonstrated by co-localization with HuC/HuD. **(A)** Low power microphotograph at the region of the corpus cerebelli. The dotted rectangle indicates location of a double labeled cell, as illustrated by the microphotographs of each channel and the overlay **(B)** in the inset in **(A)**. **(C)** Higher power image of a stack of 25 confocal planes, every 0.5 μm. The rectangle indicates the location of a cell which co-localization was demonstrated by the *x-z* and *y-z* orthogonal projections of the same stack **(C')** as well as each channel and overlay of a single plane **(C'')**. Scale bars: **(A)** 20 μm; (**B**, Inset in **A**) 100 μm; **(B,C")** 5 μm.

the local cerebellar circuit and might be already functional. Conversely, Purkinje cells were also labeled with Neurobiotin but not CldU.

The fraction of CldU CCb-gra labeled cells that were retrogradely labeled represented almost 1% and more than 9% after chase durations of 90 and 180 days, respectively (**Table 1**).

DISCUSSION

Adult neurogenesis, whether involved in protracted postnatal development of parts of the brain, the persistent addition of new neurons (constitutive neurogenesis), cellular turnover, or the regeneration after injury (Grandel and Brand, 2013) is a widespread process in the animal kingdom, from the most

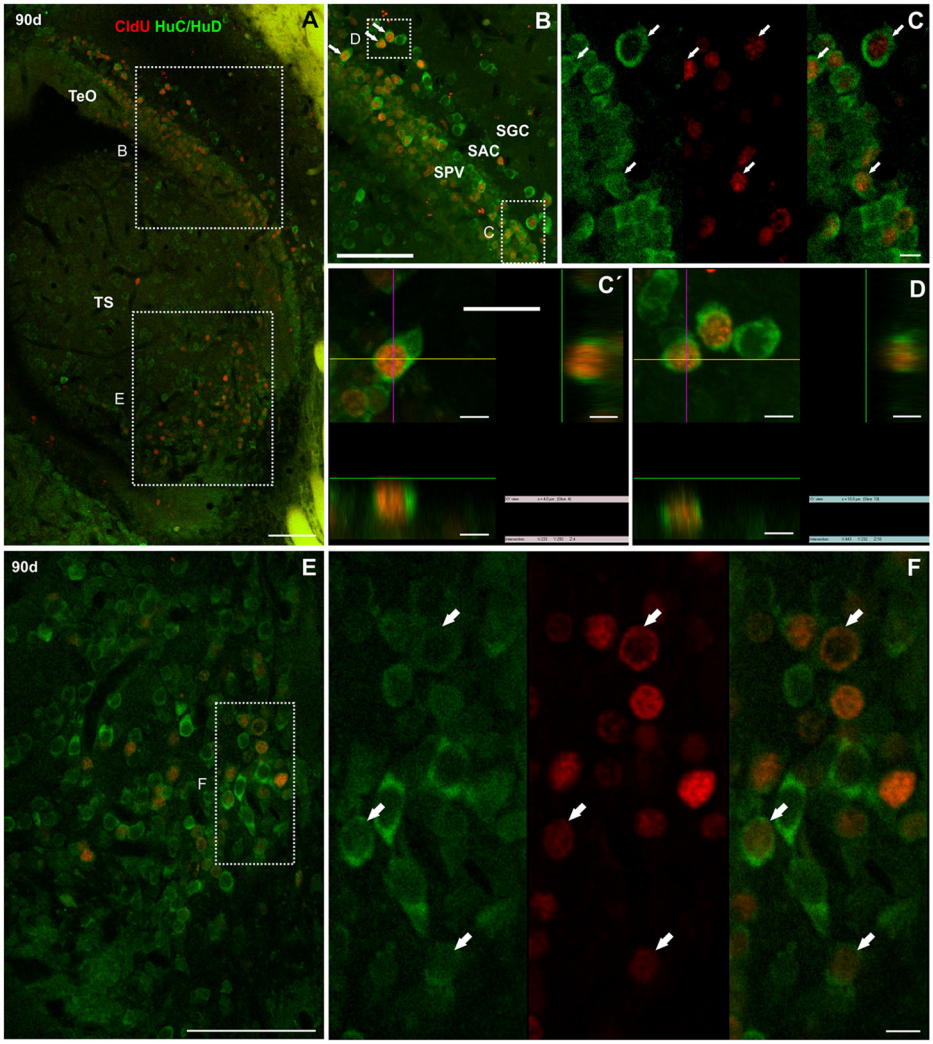

FIGURE 12 | Neuronal differentiation in the tectum opticum and torus semicircularis at 90 and 180 days after four daily injections of CldU demonstrated by co-localization with HuC/HuD. **(A)** Maximal intensity projections of confocal microphotographs of a *z* stack (20 μm, every 0.5 μm) at the caudal pole of the tectum opticum (TeO) and torus semicircularis (TS). The dotted rectangles indicate location of two regions of interest observed at higher magnification in **(B,E)**. Double labeling of tectal cells **(B,C,C′,D)** was confirmed by the microphotograph of each channel and of the overlay **(C)** as well as the *x-z* and *y-z* projection of two stacks **(C′,D)**. Double labeling of toral cells is demonstrated in **(F)** by microphotographs of each channel and of the overlay of the region indicated by the dotted rectangle in **(E)**. Scale bars: **(A,B,E)** 50 μm; **(C,C′,D,F)** 5 μm.

primitive species in which the nervous system first evolved to diverse vertebrate radiations.

Though adult cell proliferation was studied in teleost (Rahmann, 1968) soon after the discovery of adult neurogenesis in mammals by Altman (1962), only few species of the numerous teleostean radiation have been studied. Even fewer are the teleost species in which adult neurogenesis was demonstrated. Remarkably, proliferating cells give place to newborn neurons in a period as short as 24 h after BrdU administration in several brain regions (OB, TEL, TO, TL, and Cb) of *Austrolebias* (Fernández et al., 2011; Rosillo et al., 2016), probably related to the short duration of their life cycle. In all other studied teleost species, longer chases are necessary for the demonstration of neurogenesis: 3 days in the dorsal telencephalon of *D. rerio* (Adolf et al., 2006), 7 days in the TEL, TeO, and Cb of *N. furzeri* (Terzibasi et al., 2012), 15 days in the OB and TEL of *D. rerio* (Adolf et al., 2006). Almost 50% of the total amount of proliferating cells differentiates into neurons at 270–744 days chases in *D. rerio* (Zupanc et al., 2005; Hinsch and Zupanc, 2007) though a great variation among brain regions exists. A high and variable proportion of adult brain cells expressing HuC/HuD in *O. mossambicus* was demonstrated 100 days after BrdU administration (Teles et al., 2012).

G. omarorum brain develops rostro-caudally; as morphogenesis develops, the widespread distribution of larval brain proliferating cells is progressively reduced but persist in several ventricular and extraventricular proliferation

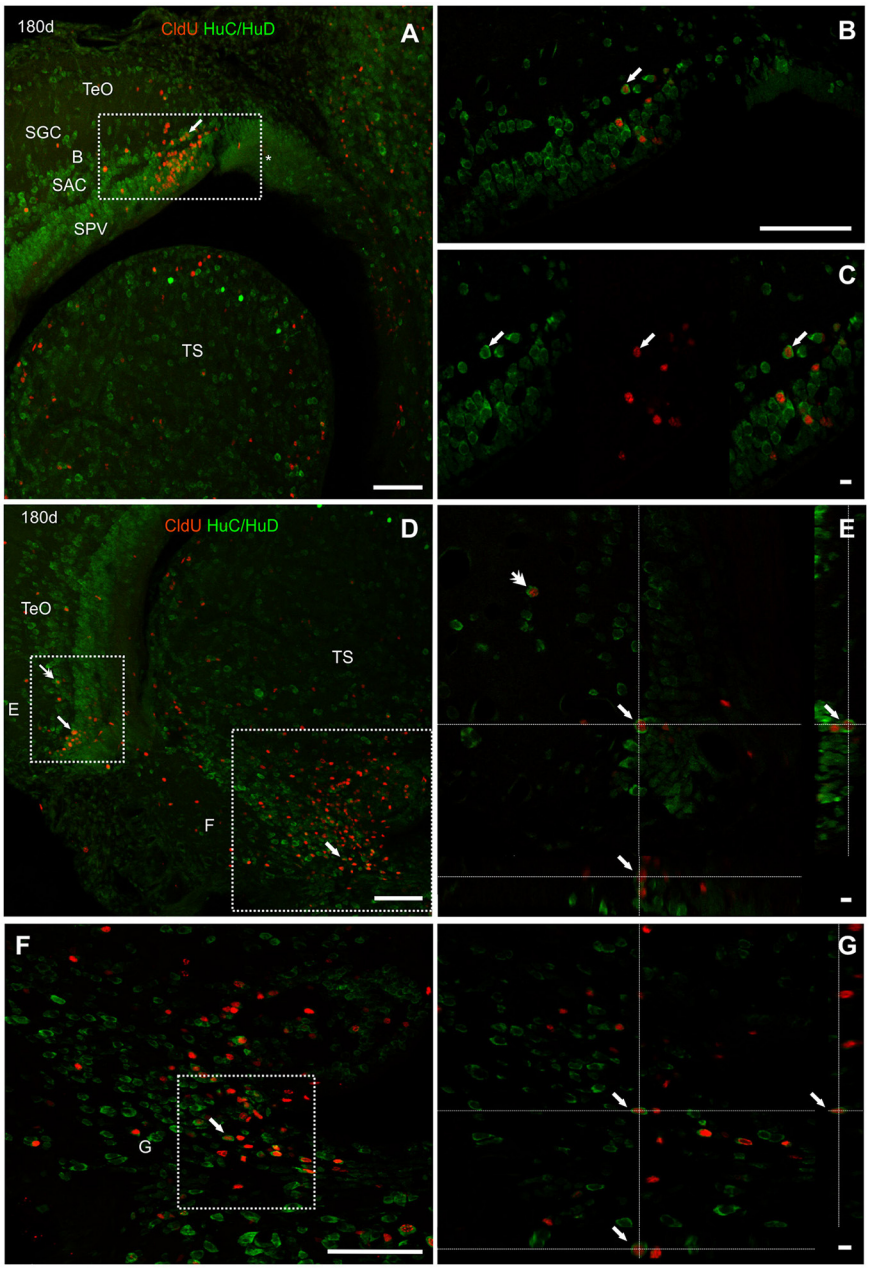

FIGURE 13 | Neuronal differentiation in the intermediate region of the optic tectum and torus semicircularis at 90 and 180 days after four daily injections of CldU demonstrated by co-localization with HuC/HuD. **(A,B)** Low power microphotographs at the dorsal-medial and ventral-lateral border of the tectum opticum (TeO) and dorsal region of the torus semicircularis **(TS),** rostral to the caudal pole**.** The dotted rectangles indicate the location of three regions of interest observed at higher magnification in **(B,E,F),** respectively. Double labeling of tectal cells **(B,C,E)** and toral newborn cells **(F,G)** was confirmed by the overlay of each channel **(C)** and *xy* and *zy* orthogonal projections a stacks. Scale bars: **(A**,**B**,**D**,**F)** 20 μm; (**B**, Inset in **A** and **D**) 100 μm; **(C**,**E**,**G)** 5 μm.

zones up to adulthood (Iribarne and Castelló, 2014; Olivera-Pasilio et al., 2014). In the present work we deepened the study of the migration process (particularly at the rostral telencephalon and OB), and demonstrate the differentiation into the neuronal phenotype of newborn cells generated in telencephalic, mesencephalic, and rhombencephalic proliferation zones.

Adult *G. omarorum* Brain Proliferation Zones are the Source of Long-Range Migratory Streams

According to the chase and the brain region, newborn cells were found close to the proliferation zones from where they originate or at increasing distances from their boundaries. At 7–180 days survivals after CldU administration we evidenced wide-ranging

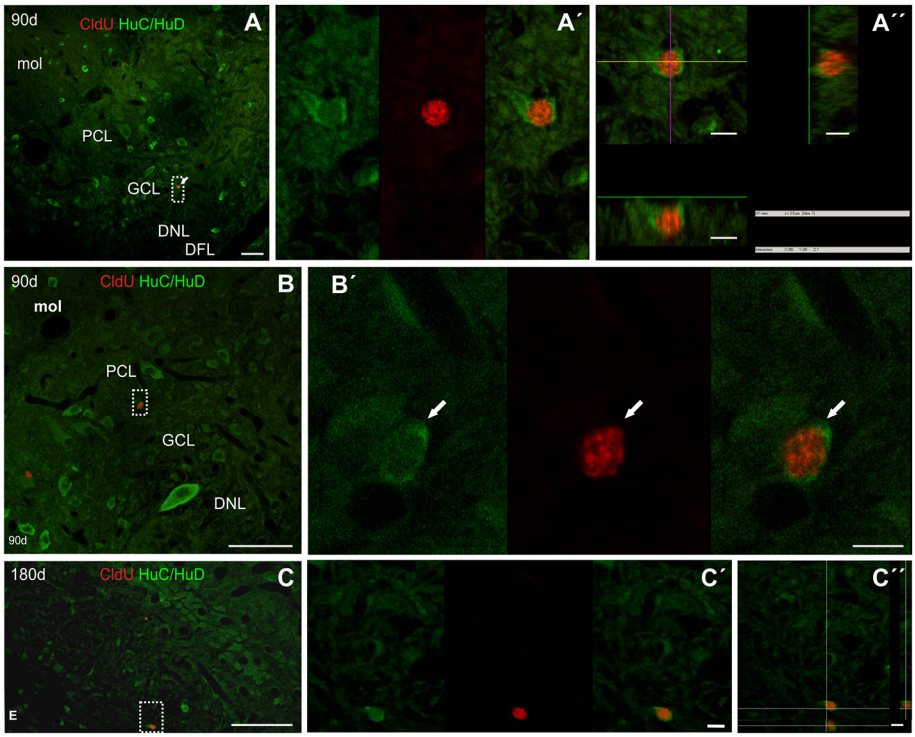

FIGURE 14 | Neuronal differentiation in the caudal pole of the electrosensory lateral line lobe at 90 and 180 days after four daily injections of CldU demonstrated by co-localization with HuC/HuD. **(A–C)** Low power microphotographs of frontal sections at the lateral-caudal border of the electrosensory lateral line lobe. The dotted rectangles indicate the location of double labeled CldU-HuC/HuD newborn cells as evidenced by the overlays of sequentially acquired images **(A′–C′)** and orthogonal projections of stacks **(A′′,C′′)**. DNL, deep neuropile layer of ELL; DFL, deep fiber layer of ELL; GCL, granular cell layer of ELL; PCL, pyramidal cell layer of ELL; mol, molecular layer of ELL. Scale bars: **(A–C)** 50 μm; **(A′,A′′,B′,C′,C′′)** 5 μm.

migrating cells with thin and elongated nuclei (usually intensely stained with CldU) surrounded by thin elongated cellular process of diverse lengths, typical characteristics of migrating neuroblasts. Other cells had round to ovoid nuclei, with granular or diffuse CldU staining, indicative of cells that already reached their final location.

No proliferation zone was found at the rostral region of *G. omarorum* OB. Despite that, the OB was progressively populated by CldU labeled cells at chase durations from 7 to 180 days.

Considering that the nearest proliferation zone was found at the ventricular lining of the rostralmost region of the telencephalic ventricle (adjacent to the caudal portion of OB and the rostral portion of the subpallium), we inferred that this is the main source of OB newborn cells. Taking into account the location of CldU labeled nuclei at the three telencephalic levels studied as a function of chase duration, we propose a three-step migration process. First, a medial-lateral migration from the proliferation 1b to adjacent regions of the subpallium and caudal OB; second, a caudal-rostral migration along the ICL and the dorsal-medial zone of the caudal and rostral OB; finally, a radial migration to populate other layers of caudal and rostral levels of OB. This resembles the rostral migratory stream from the telencephalic ventricle to the OB described in mammals.

Even though the rostral migratory stream was first demonstrated in mammals (Altman, 1969), a similar mechanism of cell proliferation at the wall of the telencephalic ventricle and collective cellular migration was also demonstrated in birds (Goldman and Nottebohm, 1983; Nottebohm, 2002; Barnea and Pravosudov, 2011), and only recently identified in *D. rerio* (Adolf et al., 2006; Grandel et al., 2006; Pellegrini et al., 2007), and supported by *ex vivo* imaging by Kishimoto et al. (2011). The generality of this process among teleost was suggested by Olivera-Pasilio et al. (2014) and supported by Lasserre (2014) in the phylogenetically close teleost *G. omarorum* and by Rosillo et al. (2016) in *Austrolebias charrua*, a Cyprinodontiforme phylogenetically very distant from the former teleosts. Consistently, here we showed that the ICL and dorsal-medial zone of the OB of *G. omarorum* contains rostral-caudally oriented cellular processes that are reactive to DCX. This microtubule associated protein is expressed by migrating neuroblasts during development (Francis et al., 1999) up to adulthood in the telencephalon of mammals (Gleeson et al., 1999; Lim et al., 2008; including the rostral migratory stream on humans, Wang et al., 2011), and birds (Boseret et al., 1997). In our knowledge DCX was only demonstrated in the telencephalon and mesencephalon the teleost, *Nothobranchius furzeri* (Terzibasi et al., 2012).

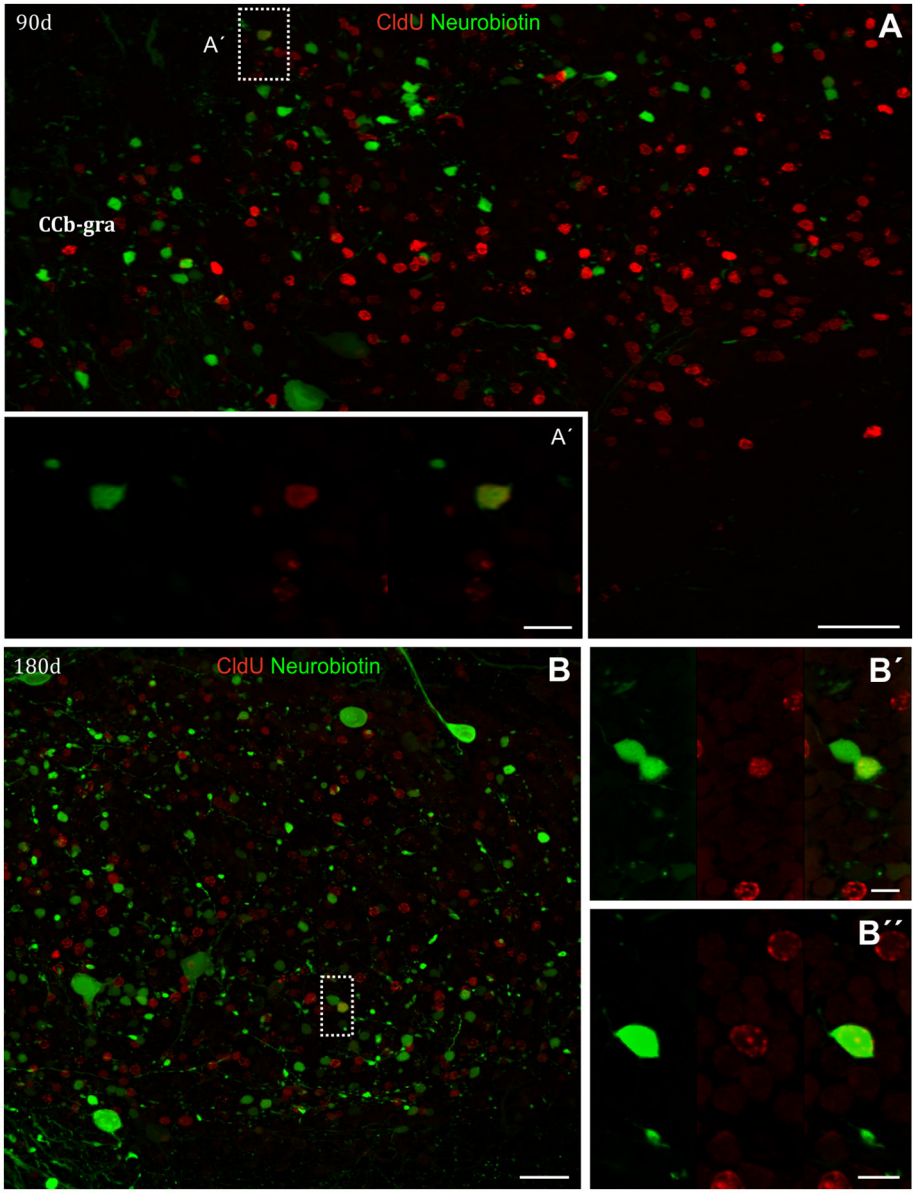

FIGURE 15 | Neuronal differentiation in the corpus cerebelli at 90 and 180 days after four daily injections of CldU demonstrated by co-localization retrogradely transported Neurobiotin. **(A,B)** Low power microphotograph of frontal sections at the corpus cerebelli (CCb). The dotted rectangles indicate the location of double labeled newborn cells nearby the boundary between molecular (CCb-mol) and granular (CCb-gra) layer of the CCb **(A)**, or within CCb-gra **(B)**. The double labeling was confirmed at higher magnification by the microphotographs of each channel and the overlays **(A′,B′,B′′)** as well as by the 3-D visualization as shown in the **Supplementary Video 2**. Scale bars: **(A)** = 20 μm; (**B**, Inset in **A**) = 100 μm; **(A′,B′,B′′)** = 5 μm.

Nevertheless, other authors demonstrated local proliferation zones at superficial layers of the OB in *C. auratus*, *Barbus meridionalis*, *Cyprinus carpio,* and *Salmo gardneri* (Alonso et al., 1989), *Oreochromis mossambicus* (Teles et al., 2012), *A. leptorhynchus* (Zupanc and Horschke, 1995), and *D. rerio* (Zupanc et al., 2005) and local migration between layers of the OB.

Our results also support a simultaneous process of radial migration of newborn cells from the proliferation zone nearby rostral subpallium and caudal OB to the surrounding subpallial cell masses, as indicated by the distribution of CldU labeled nuclei (Supplementary Figure 3), similar to the findings of Grandel et al. (2006) in *D. rerio*.

Other outstanding proliferation and migration processes occurred in the Cb of adult *G. omarorum* as newborn cells migrated along relatively large distances in all cerebellar divisions (CCb, VCb, and EG) as they relocate from one cerebellar layer to another. There, the migration process involved an almost

complete shift of newborn cells between cerebellar layers in a period of 30 days after CldU administration, as previously shown in the Cb of this (Olivera-Pasilio, 2014) and other teleost species (*A. leptorhynchus*: Zupanc et al., 1996; *D rerio*: Zupanc et al., 2005; Kaslin et al., 2009; *C. auratus*: Delgado and Schmachtenberg, 2011; *O. mossambicus*: Teles et al., 2012; and *M. rume*: Radmilovich et al., 2016). According to the distribution of DCX cellular process in the CCb of *G. omarorum*, the migration process of new born cells may involve displacements in the medial-lateral direction along the CCb-mol (as shown by Kaslin et al., 2009), as well as in the rostral-caudal direction in the ganglionic layer, not described previously.

Shorter range or less numerous migration processes were found in other mesencephalic (TeO and OT) and rhombencephalic brain regions (ELL) involved in multimodal and electrosensory information processing. The migration process of newborn cells in the TeO of *G. omarorum* appeared to occur mainly from the caudal pole of the tectal proliferation zone toward almost all tectal layers as well as from the dorso-medial edge of more rostral zones of the tectal proliferation zone. This involves both the addition of newborn cells to the dorso-medial edge to the tectal proliferation zone, and the displacement of older cells to adjacent caudal parts of the TeO in the ventro-lateral direction as demonstrated in *O. latipes* (Alunni et al., 2010), *C. auratus* (Raymond and Easter, 1983) and *D. rerio* (Ito et al., 2010), and *N. furzeri* (Terzibasi et al., 2012). Consistently, a net of DCX process lies beneath *G. omarorum* dorsal-medial tectal proliferation zone.

Neurogenic Potential of Adult *G. omarorum* Brain Proliferation Zones

After long term chases, the nuclei of most derived cells lost the typical appearance of migrating cells as they reached their target brain regions. Nuclei acquired a rounded shape with heterogeneous distribution of loosely and densely packed chromatin, frequently showing a carriage wheel arrangement of compacted chromatin, as evidenced by thymidine analog labeling. This indicates that these cells are already in the process of cell differentiation that was confirmed by the demonstration of the expression of early or mature neuronal markers, or the retrograde transport of Neurobiotin by long term CldU label retaining cells.

Even though at short chases (1 or 7 days) some derived cells had the aspect of migrating neuroblasts; most of these cells do not express the early neuronal marker DCX, with the exception of few cells nearby the ventral zone of the telencephalic proliferation zone 1b, similar to *N. furzeri* (Terzibasi et al., 2012). Conversely, 7 days were sufficient for the expression of HuC/HuD by CldU label retaining cells nearby the subpallial proliferation zone, indicating their differentiation into the neuronal phenotype. Some newborn cells nearby the ventricular surface of the subpallial proliferation zone express DCX at a chase duration of 30 days, a slightly longer time interval than observed in mammal hippocampus (Kempermann et al., 2008) and *N. furzeri* (Terzibasi et al., 2012). This and their morphology indicate that they correspond to migrating neuroblasts. At this chase, other newborn neurons expressing HuC/HuD were located laterally to the subpallial proliferation zone, or rostrally, at the ICL of caudal OB. Longer chases were required for newborn neurons expressing HuC/HuD to reach the ICL of the rostral OB, supporting a long-range migration from the telencephalic ventricle. Strikingly, CldU-HuC/HuD double labeled cells reached more than 50% of newborn migrated cells 90 days after CldU administration. To our knowledge, this has not been reported before, since most of previous studies combining HuC/HuD and thymidine analog retention to demonstrate the differentiation into the neuronal phenotype in the OB failed, either to identify cells expressing HuC/HuD (Zupanc et al., 2005) or the co-localization of HuC/HuD and the thymidine analog (Adolf et al., 2006), or find very few double labeled cells (Grandel et al., 2006). Only the quantitative results of Hinsch and Zupanc (2007) support a 30% fraction of BrdU labeled cells also expressing HuC/HuD after chases between 446 and 656 days.

On the other hand, Alonso et al. (1989) not only found a proliferation zone in the wall of the telencephalic ventricle or ventricular recess but also another at the outer limiting glial membrane and the olfactory nerve fiber layer of *C. auratus*, *B. meridionalis*, *C. carpio,* and *Salmo gairdneri*. Superficial proliferation zones at the primary olfactory fiber layer and/or the glomerular layer of the OB were also found in other teleost (*O. mossambicus*: Teles et al., 2012; *A. leptorhynchus*: Zupanc and Horschke, 1995; *D. rerio*: Zupanc et al., 2005) that give rise to newborn cells that migrate toward the inner cell layers. Only in *O. mossambicus* it was shown a high proportion of newborn cells originated from the superficial proliferation zone of the OB expressing HuC/HuD (Teles et al., 2012). All these findings suggest that there are marked interspecific differences in the site of generation, the paths of migration and fate of newborn cells.

A step forward in the process of neuronal differentiation was evidenced by the expression of a more cell specific neuronal marker: TH, the key step-limiting enzyme of the catecholamine synthesis pathway. TH first co-localize with CldU at a chase of 90 days in newborn neurons located within or nearby the subpallial proliferation zone. At 180 chase duration (similar to CldU-HuC/HuD double labeled cells), CldU-TH cells were found further away from the proliferation zones, both in the medial lateral direction (reaching the MOTF and Vc) and in the rostral caudal direction (reaching the ICL of caudal and rostral OB). This is coincident with the results of Grandel et al. (2006) and Adolf et al. (2006) in *D. rerio*, though in *G. omarorum* it was not a rare finding. Conversely, according to our quantitative data, newborn catecholaminergic neurons reached 0,5% of migrated newborn neurons of the subpallium 90 days after CldU administration, a figure that was duplicated and triplicated at caudal and intermediate regions of the OB at the longest chase studied (180 days). The population of newborn catecholaminergic neurons was not homogeneous, but showed morphological characteristics corresponding to different steps in the process of cell maturation (from migrating neuroblasts to multipolar granular cells). According to the morphology and location, double labeled CldU-TH newborn cells of the OB of *G. omarorum* correspond to granule cells of the ICL as shown in other teleosts (*Dicentrarchus labrax*: Batten et al.,

1993; *D. rerio*: Byrd and Brunjes, 1995; and *Solea senegalensis*: Rodríguez-Gómez et al., 2000). However, this is not coincident with the distribution of catecholaminergic neurons in the OB of *A. leptorhynchus* (Sas et al., 1990), *D. rerio* (Adolf et al., 2006), and *D. labrax* (Sébert et al., 2008) as in these species TH positive cells are almost absent in the ICL and more abundant in outer layers.

According to our results and, it takes 30 days for newborn cells of the CCb-gra to express the early neuronal marker HuC/HuD, indicating their differentiation into granule cells. This is similar to *D. rerio* but either much longer (Grandel et al., 2006) or shorter (Kaslin et al., 2009) chase durations were reported, or even absence of double labeling of CCb-gra newborn cells even at very long chase durations (Zupanc et al., 2005). Conversely, in *Austrolebias*, a 1 day chase is enough for co-localization of BrdU and HuC/HuD (Fernández et al., 2011). These differences may be due to variations in the sensitivity of immunohistochemical procedures, or in the process of cell differentiation because of differences in the durations of life span as argued before.

More than half of newborn CCb-gra cells express HuC/HuD in *G. omarorum* at 90 day chase duration, a value that amply surpass the fraction of CCb new born cells in *D. rerio* at 446–656 day chases (2,4%, according to the numbers of BrdU and BrdU-HuC/HuD double labeled cells reported by Hinsch and Zupanc, 2007).

HuC/HuD is also expressed by tectal and toral newborn neurons but requiring longer chases (90–180 days). In *D. rerio*, double labeled BrdU-HuC/HuD newborn neurons were found nearby the proliferation zone of the TeO (Zupanc et al., 2005; Grandel et al., 2006). The cortical organization of the TeO and the distribution of newborn neurons in almost all its width, suggest the coordinated migration of cohorts of newborn cells of various phenotypes. The fraction of TeO double labeled cells here found in adult *G. omarorum* also largely exceeds the values in *D. rerio* according to the quantitative results reported in Hinsch and Zupanc (2007).

We also found newborn double labeled CldU-HuC/HuD neurons in the ELL, though they show weak HuC/HuD immunoreactivity. To our knowledge, the generation of new neurons (by demonstration of HuC/HuD expression in thymidine analog retaining cells) has not been reported neither in the TS nor the ELL of teleosts. It is interesting to note that all these brain regions are involved in sensory information processing, particularly of electrosensory information.

To identify the neuronal phenotype of newborn neurons, we draw upon the combination of repetitive thymidine analog labeling and "*in vivo*" neuronal tracing to retrogradely label cerebellar and ELL granule cells. This approach rendered a high proportion of granule cells retrogradely labeled, even at distances of more than 200 microns of the site of Neurobiotin application, as well as a high proportion of long term CldU retaining granule cells. These facts probably favored the identification of several double labeled CldU-Neurobiotin granule cells, indicating that these cells already acquired a mature phenotype with axonal projections to the CCb-mol. Similar, though quantitatively much less frequent results were obtained in *A. leptorhynchus* (Zupanc et al., 1996) and *D. rerio* (Zupanc et al., 2005) by "*ex vivo*" retrograde labeling of granule cells with dextran-fluorescein. We did not identify double labeling of any of the other Cb cell types. Finally, unlike the CCb, we did not observe double labeled CldU-Neurobiotin granule cells in the ELL, even though Neurobiotin application to the lateral line nerve rendered abundant trans-synaptic labeled granule cells (data not shown).

In summary, the results of this work confirm the spatial distribution of adult *G. omarorum* brain proliferation zones, and the migration paths of newborn cells from the proliferation zones to their final locations, particularly at the rostral telencephalon, TeO, TS, and CCb. Our results are compatible with a rostral migratory stream of newborn cells from a proliferation zone at the rostralmost end of the telencephalic ventricle toward the rostral and caudal OB. We also demonstrate widespread and relatively frequent neurogenesis in the telencephalon (subpallium and OB), mesencephalon (TeO and TS), and rhombencephalon (CCb and ELL) of adult *G. omarorum*. These findings contribute to support the widespread distribution of brain proliferation zones and their neurogenic capacity in *G. omarorum*, an animal model suitable to assess the functional significance, as well as comparative analysis of adult neurogenesis. Our results also contribute to support the phylogenetically conserved feature of adult neurogenesis. Considering the rough similarity in distribution of brain proliferation zones among teleost species studied up to date, the differences in the neurogenic capacity between the same regions among teleosts suggest differences in the intrinsic/extrinsic factors modulating both cell proliferation and neurogenesis, which is the topic of ongoing research.

AUTHOR CONTRIBUTIONS

MC, ML, and VO made substantial contributions to the conception or design of the work; and/or the acquisition, analysis, and interpretation of data for the work; MC and VO drafted the work. Final approval of the version to be published was done by VO and MC.

FUNDING

This work was partially supported by Agencia Nacional de Investigación e Innovación (Research Grants # FCE_2009_1_2246; FCE_3_2011_1_6168 and ANII fellowship #INI_X_2012_1_4392 to ML), and Programa para el desarrollo de Ciencias Básicas (PEDECIBA).

ACKNOWLEDGMENTS

The authors thank Ranch Los Mojinetes (Laguna del Sauce, Maldonado, Uruguay) for cooperating with this investigation by allowing and assisting with the exploration of the Laguna del Sauce northern coast. The authors also thank to Neurochemistry

Department at IIBCE for the generously provide of anti-TH primary AB. We also acknowledge Dr. Milka Radmilovich for helpful reading of the manuscript and fruitful comments and suggestions.

SUPPLEMENTARY MATERIAL

The Supplementary Material for this article can be found online at: http://journal.frontiersin.org/article/10.3389/fnins.2017.00437/full#supplementary-material

Supplementary Video 1 | Newborn neuron in the olfactory bulb of adult *G. omarorum*. The video corresponds to an animation obtained with Fluoview from a stack of confocal images obtained from a frontal section of the caudal OB processed for the immunohistochemical detection of tyrosine hydroxilase (green) and CldU (red). The stack consisted in 13 confocal planes, acquired in sequential mode, every 1 μm. Note in the center of the animation a double labeled newborn neuron, corresponding to the cell shown in **Figure 10C**, as well as other single labeled TH+ or CldU+ cells. Online available at: https://figshare.com/s/0fab179fd0e1e6356371.

Supplementary Video 2 | Newborn neuron in the corpus cerebelli of adult *G. omarorum*. The video corresponds to an animation obtained with Fluoview from a stack of confocal images obtained from a frontal section of the corpus cerebelli (CCb) processed for the immunohistochemical detection CldU (red) and histochemical demonstration of Neurobiotin (green). Note in the right of the animation a double labeled newborn neuron, corresponding to the cell shown in **Figure 15B**, as well as other single labeled Neurobiotin+ or CldU+ cells. Online available at: https://figshare.com/s/af3f18ae8aea51d80b27.

REFERENCES

Adolf, B., Chapouton, P., Lam, C. S., Topp, S., Tannhäuser, B., Strähle, U., et al. (2006). Conserved and acquired features of adult neurogenesis in the zebrafish telencephalon. *Dev. Biol.* 295, 278–293. doi: 10.1016/j.ydbio.2006.03.023

Albert, J., Lannoo, M., and Yuri, T. (1998). Testing hypotheses of neural evolution in gymotiform electric fishes using phylogenetic character data. *Evolution* 52, 1760–1860.

Alonso, J. R., Lara, J., Vecino, E., Cove-as, R., and Aijón, J. (1989). Cell proliferation in the olfactory bulb of adult freshwater teleosts. *J. Anat.* 163, 155–163.

Altman, J. (1962). Are new neurons formed in the brains of adult mammals? *Science* 135, 1127–1128. doi: 10.1126/science.135.3509.1127

Altman, J. (1963). Autoradiographic investigation of cell proliferation in the brains of rats and cats. *Anat. Rec.* 145, 573–591. doi: 10.1002/ar.1091450409

Altman, J. (1969). Autoradiographic and histological studies of postnatal neurogenesis. IV. Cell proliferation and migration in the anterior forebrain, with special reference to persisting neurogenesis in the olfactory bulb. *J. Comp. Neurol.* 137, 433–457. doi: 10.1002/cne.901370404

Altman, J. (2011). "The discovery of adult mammalian neurogenesis," in *Neurogenesis in the Adult Brain I*, eds T. Seki, K. Sawamoto, J. M. Parent, and A. Alvarez-Buylla (Tokyo: Springer Japan), 3–46.

Altman, J., and Das, G. (1965). Autoradiographic and histological evidence of postnatal hippocampal neurogenesis in rats. *J. Comp. Neurol.* 124, 319–335. doi: 10.1002/cne.901240303

Altman, J., and Das, G. D. (1966). Autoradiographic and histological studies of postnatal neurogenesis. I. A longitudinal investigation of the kinetics, migration and transformation of cells incorporating tritiated thymidine in neonate rats, with special reference to postnatal neurogenesis. *J. Comp. Neurol.* 126, 337–389.

Alunni, A. and Bally-Cuif, L. (2016). A comparative view of regenerative neurogenesis in vertebrates. *Development* 1, 741–753. doi: 10.1242/dev.122796

Alunni, A., Hermel, J.-M., Heuzé, A., Bourrat, F., Jamen, F., and Joly, J.-S. (2010). Evidence for neural stem cells in the medaka optic tectum proliferation zones. *Dev. Neurobiol.* 70, 693–713. doi: 10.1002/dneu.20799

Balon, E. K. (1975). Terminology of intervals in fish development. *J. Fish. Res. Board Can.* 32, 1663–1670. doi: 10.1139/f75-196

Barbieri, G., and Cruz, M. (1983). Growth and first sexual maturation size of *Gymnotus carapo* (Linnaeus, 1758) in the Lobo reservoir (state of Sao Paulo, Brazil) (pisces, gymnotidae). *Rev. Hydrobiol. Trop.* 16, 195–201.

Barker, J. M., Boonstra, R., and Wojtowicz, J. M. (2011). From pattern to purpose: how comparative studies contribute to understanding the function of adult neurogenesis. *Eur. J. Neurosci.* 34, 963–977. doi: 10.1111/j.1460-9568.2011.07823.x

Barnea, A., and Pravosudov, V. (2011). Birds as a model to study adult neurogenesis: bridging evolutionary, comparative and neuroethological approaches. *Eur. J. Neurosci.* 34, 884–907. doi: 10.1111/j.1460-9568.2011.07851.x

Batten, T. F. C., Berry, P. A., Maqbool, A., Moons, L., and Vandesande, F. (1993). Immunolocalization of catecholamine enzymes, serotonin, dopamine and L-dopa in the brain of *Dicentrarchus labrax* (Teleostei). *Brain Res. Bull.* 31, 233–252. doi: 10.1016/0361-9230(93)90214-V

Bell, C. C. (2002). Evolution of cerebellum-like structures. *Brain. Behav. Evol.* 59, 312–326. doi: 10.1159/000063567

Bennett, M. V. L. (1971). "Electric organs," in *Fish Physiology,* eds W. S. Hoar and D. J. Randall (London: Academic Press), 347–491.

Boseret, G. F., Ball, G. F., and Balthazart, J. (1997). The microtubule-associated protein doublecortin is broadly expressed in the telencephalon of adult canaries. *J. Chem. Neuroanat.* 33, 140–154. doi: 10.1016/j.jchemneu.2007.02.002

Byrd, C. A., and Brunjes, P. C. (1995). Organization of the olfactory system in the adult zebrafish: histological, immunohistochemical, and quantitative analysis. *J. Comp. Neurol.* 358, 247–259. doi: 10.1002/cne.903580207

Cayre, M., Malaterre, J., Scotto-Lomassese, S., Strambi, C., and Strambi, A. (2002). The common properties of neurogenesis in the adult brain: from invertebrates to vertebrates. *Comp. Biochem. Physiol. B Biochem. Mol. Biol.* 132, 1–15. doi: 10.1016/S1096-4959(01)00525-5

Corrêa, S. A., Corrêa, F. M., and Hoffmann, A. (1998). Stereotaxic atlas of the telencephalon of the weakly electric fish *Gymnotus carapo*. *J. Neurosci. Methods* 84, 93–100. doi: 10.1016/S0165-0270(98)00098-3

Delgado, L. M., and Schmachtenberg, O. (2011). Neurogenesis in the adult goldfish cerebellum. *Anat. Rec.* 294, 11–15. doi: 10.1002/ar.21291

Dunlap, K. D., Silva, A. C., and Chung, M. (2011). Environmental complexity, seasonality and brain cell proliferation in a weakly electric fish, *Brachyhypopomus gauderio*. *J. Exp. Biol.* 214, 794–805. doi: 10.1242/jeb.051037

Evans, H. M. (1940). *Brain and Body Fish. A Study of Brain Pattern in Relation to Hunting and Feeding in Fish.* Norwich: London and Norwich Press.

Fernández, A. S., Rosillo, J. C., Casanova, G., and Olivera-Bravo, S. (2011). Proliferation zones in the brain of adult fish *Austrolebias* (Cyprinodontiform: Rivulidae): a comparative study. *Neuroscience* 189, 12–24. doi: 10.1016/j.neuroscience.2011.05.063

Finger, T. E. (1978). Efferent neurons of the teleost cerebellum. *Brain Res.* 153, 608–614. doi: 10.1016/0006-8993(78)90346-3

Francis, F., Koulakoff, A., Boucher, D., Chafey, P., Schaar, B., Vinet, M. C., et al. (1999). Doublecortin is a developmentally regulated, microtubule-associated protein expressed in migrating and differentiating neurons. *Neuron* 23, 247–256. doi: 10.1016/S0896-6273(00)80777-1

Galliot, B., and Quiquand, M. (2011). A two-step process in the emergence of neurogenesis. *Eur. J Neurosci.* 34, 847–862. doi: 10.1111/j.1460-9568.2011.07829.x

Gleeson, J. G., Lin, P. T., Flanagan, L. A., and Walsh, C. A. (1999). Doublecortin is a microtubule-associated protein and is expressed widely by migrating neurons. *Neuron* 23, 257–271. doi: 10.1016/S0896-6273(00)80778-3

Goldman, S. A., and Nottebohm, F. (1983). Neuronal production, migration, and differentiation in a vocal control nucleus of the adult female canary brain. *Proc. Natl. Acad. Sci. U.S.A.* 80, 2390–2394. doi: 10.1073/pnas.80.8.2390

Grandel, H., and Brand, M. (2013). Comparative aspects of adult neural stem cell activity in vertebrates. *Dev. Genes Evol.* 223, 131–147. doi: 10.1007/s00427-012-0425-5

Grandel, H., Kaslin, J., Ganz, J., Wenzel, I., and Brand, M. (2006). Neural stem cells and neurogenesis in the adult zebrafish brain: origin, proliferation dynamics, migration and cell fate. *Dev. Biol.* 295, 263–277. doi: 10.1016/j.ydbio.2006.03.040

Gross, C. G. (2000). Neurogenesis in the adult brain: death of a dogma. *Nat. Rev. Neurosci.* 1, 67–73. doi: 10.1038/35036235

Haugedé-Carré, F., Kirschbaum, F., and Szabo, T. (1977). On the development of the gigantocerebellum in the mormyrid fish *Pollimyrus (Marcusenius) isidori*. *Neurosci. Lett.* 6, 209–213. doi: 10.1016/0304-3940(77)90020-9

Haugedé-Carré, F., Szabo, T., and Kirschbaum, F. (1979). Development of the gigantocerebellum of the weakly electric fish *Pollimyrus*. *J. Physiol. Paris* 75, 381–395.

Hinsch, K., and Zupanc, G. K. H. (2007). Generation and long-term persistence of new neurons in the adult zebrafish brain: a quantitative analysis. *Neuroscience* 146, 679–696. doi: 10.1016/j.neuroscience.2007.01.071

Hodos, W., and Butler, B. (1997). Evolution of sensory pathways in vertebrates. *Brain Behav. Evol.* 50, 189–197. doi: 10.1159/000113333

Iribarne, L., and Castelló, M. E. (2014). Postnatal cell proliferation in the brain of the weakly electric fish *Gymnotus omarorum*. *J. Physiol. Paris* 108, 47–60. doi: 10.1016/j.jphysparis.2014.05.001

Ito, H., Ishikawa, Y., Yoshimoto, M., and Yamamoto, N. (2007). Diversity of brain morphology in teleosts: brain and ecological niche. *Brain. Behav. Evol.* 69, 76–86. doi: 10.1159/000095196

Ito, Y., Tanaka, H., Okamoto, H., and Ohshima, T. (2010). Characterization of neural stem cells and their progeny in the adult zebrafish optic tectum. *Dev. Biol.* 342, 26–38. doi: 10.1016/j.ydbio.2010.03.008

Jerisson, H. J. (1973). *Evolution of the Brain and Intelligence*. London: Academic Press, Inc. (London) Ltd.

Kaplan, M. S., and Hinds, J. (1977). Neurogenesis in the adult rat: electron microscopic analysis of light radioautographs. *Science* 197, 1092–1094. doi: 10.1126/science.887941

Kaslin, J., Ganz, J., and Brand, M. (2008). Proliferation, neurogenesis and regeneration in the non-mammalian vertebrate brain. *Philos. Trans. R. Soc. Lond. B Biol. Sci.* 363, 101–122. doi: 10.1098/rstb.2006.2015

Kaslin, J., Ganz, J., and Geffarth, M. (2009). Stem cells in the adult zebrafish cerebellum: initiation and maintenance of a novel stem cell niche. *J. Neurosci.* 29, 6142–6153. doi: 10.1523/JNEUROSCI.0072-09.2009

Kempermann, G., Song, H., and Gage, F. H. (2008). "Neurogenesis in the adult hippocampus," in *Adult Neurogenesis*, eds F. H. Gage, G. Kempermann, and H. Song (New York, NY: Cold Spring Harbor Laboratory Press), 159–174. doi: 10.1101/087969784.52.159

Kermen, F., Franco, L. M., Wyatt, C., and Yaksi, E. (2013). Neural circuits mediating olfactory-driven behavior in fish. *Front. Neural Circuits* 7:62. doi: 10.3389/fncir.2013.00062

Kishimoto, N., Alfaro-Cervello, C., Shimizu, K., Asakawa, K., Urasaki, A., Nonaka, S., et al. (2011). Migration of neuronal precursors from the telencephalic ventricular zone into the olfactory bulb in adult zebrafish. *J. Comp. Neurol.* 519, 3549–3565. doi: 10.1002/cne.22722

Kotrschal, K., Van Staaden, M., and Huber, R. (1998). Fish brains: evolution and environmental relationships. *Rev. Fish Biol. Fish.* 8, 373–408. doi: 10.1023/A:1008839605380

Lannoo, M. J., Vischer, H. A., and Maler, L. (1990). Development of the electrosensory nervous system of Eigenmannia (gymnotiformes): II. The electrosensory lateral line lobe, midbrain, and cerebellum. *J. Comp. Neurol.* 294, 37–58. doi: 10.1002/cne.902940105

Lasserre, M. (2014). *Evaluación de la Capacidad Neurogénica Adulta en el Telencéfalo de Gymnotus omarorum*. Dissertation/undergraduate thesis, Universidad de la República, Montevideo.

Leyhausen, C., Kirschbaum, F., Szabo, T., and Erdelen, M. (1987). Differential growth in the brain of the weakly electric fish, *Apteronotus leptorhynchus* (Gymnotiformes), during ontogenesis (Part 1 of 2). *Brain Behav.* 30, 230–248. doi: 10.1159/000118648

Lim, D. A., Huang, Y., and Alvarez-Buylla, A. (2008). "Adult subventricular zone and olfactory bulb neurogenesis," in *Adult Neurogenesis*, eds F. H. Gage, G. Kempermann, and H. Song (New York, NY: Cold Spring Harbor Laboratory Press), 175–206.

Lindsey, B. W., and Tropepe, V. (2006). A comparative framework for understanding the biological principles of adult neurogenesis. *Prog. Neurobiol.* 80, 281–307. doi: 10.1016/j.pneurobio.2006.11.007

Ma, D., Ming, G., Gage, F. H., and Song, H. (2008). "Neurogenic niches in the adult mammalian brain," in *Adult Neurogenesis*, eds F. H. Gage, G. Kempermann, and H. Song (New York, NY: Cold Spring Harbor Laboratory Press), 207–255.

Maler, L., Sas, E., Johnston, S., and Ellis, W. (1991). An atlas of the brain of the electric fish *Apteronotus leptorhynchus*. *J. Chem. Neuroanat.* 4, 1–38. doi: 10.1016/0891-0618(91)90030-G

Meek, J., and Nieuwenhuys, R. (1998). "Holosteans and teleosts," in *The Central Nervous System of Vertebrates*, eds R. H. Nieuwenhuys, J. ten Donkelaar, and C, Nicholson (Berlin: Springer), 759–938.

Nottebohm, F. (2002). Why are some neurons replaced in adult brain? *J. Neurosci.* 22, 624–628. doi: 10.1016/so361-9230(02)00750-5

Olivera-Pasilio, V., Peterson, D. A., and Castelló, M. E. (2014). Spatial distribution and cellular composition of adult brain proliferative zones in the teleost, *Gymnotus omarorum*. *Front. Neuroanat.* 8:83. doi: 10.3389/fnana.2014.00088

Olivera-Pasilio, V. (2014). *Distribución Espacial, Composición Celular y Capacidad Neurogénica de las Zonas Proliferativas del Cerebro de Gymnotus omarorum en la Vida Posnatal*. Dissertation/masters'thesis, Universidad de la República, Montevideo.

Pellegrini, E., Mouriec, K., Anglade, I., Menuet, A., Le Page, Y., Gueguen, M.-M., et al. (2007), Identification of aromatase-positive radial glial cells as progenitor cells in the ventricular layer of the forebrain in zebrafish. *J. Comp. Neurol.* 501, 150–167. doi: 10.1002/cne.21222

Radmilovich, M., Barreiro, I., Iribarne, L., Grant, K., Kirschbaum, F., and Castelló, M. E. (2016). Post-hatching brain morphogenesis and cell proliferation in the pulse-type mormyrid *Mormyrus rume proboscirostris*. *J. Physiol. Paris* 110, 245–258. doi: 10.1016/j.jphysparis.2016.11.007

Rahmann, H. (1968). Autoradiographische Untersuchüngen zum DNs-Stoffwechsel (Mitose-Häufigkeit) im ZNS von Brachydanio rerio HAM: BUCH. (Cyprinidae, Pisces). *J. Hirnforsc.* 10, 279–284.

Raymond, P., and Easter, S. (1983). Postembryonic growth of the optic tectum in goldfish. I. Location of germinal cells and numbers of neurons produced. *J. Neurosci.* 5, 1077–1091.

Richer-de-Forges, M., Crampton, W. G. R., and Albert, J. S. (2009). A new species of Gymnotus (Gymnotiformes, Gymnotidae) from Uruguay: description of a model species in neurophysiological research. *Copeia* 3, 538–544. doi: 10.1643/CI-07-103

Richter, W., and Kranz, D. (1970). Die Abhängigkeit der DNS-synthese in den matrixzonen des mesencephalons vom lebensalter der versuchstiere (*Lebistes reticulatus* – Teleostei): autoradiographische untersuchungen. *Z Mikrosk Anat. Forsch* 82, 76–92.

Rodríguez-Gómez, F. J., Rendön-Unceta, M. C., Sarasquete, C., and Mu-oz-Cueto, J. A. (2000). Localization of tyrosine hydroxylase-immunoreactivity in the brain of the Senegalese sole, Solea senegalensis. *J. Chem. Neuroanat.* 19, 17–32. doi: 10.1016/S0891-0618(00)00047-8

Rosillo, J. C., Torres, M., Olivera-Bravo, S., Casanova, G., García-Verdugo, J. M., and Fernández, A. S. (2016). Telencephalic-olfactory bulb ventricle wall organization in *Austrolebias charrua*: cytoarchitecture, proliferation dynamics, neurogenesis and migration. *Neuroscience* 12, 63–80. doi: 10.1016/j.neuroscience.2016.08.045

Sas, E., Maler, L., and Tinner, B. (1990). Catecholaminergic systems in the brain of a gymnotiform teleost fish: an immunohistochemical study. *J. Comp. Neurol.* 292, 127–162. doi: 10.1002/cne.902920109

Sébert, M. E., Weltzien, F. A., Moisan, C., Pasqualini, C., and Dufour, S. (2008). Dopaminergic systems in the European eel: characterization, brain distribution, and potential role in migration and reproduction. *Hydrobiología* 602, 27–46. doi: 10.1007/s10750-008-9288-1

Shumway, C. A. (2008). Habitat complexity, brain, and behavior. *Brain. Behav. Evol.* 72, 123–*34*. doi: 10.1159/000151472

Sullivan, J. M., Benton, J. L., Sandeman, D. C., and Beltz, B. S. (2007). Adult neurogenesis: a common strategy across diverse species. *J. Comp. Neurol.* 500, 574–584. doi: 10.1002/cne.21187

Teles, M. C., Sîrbulescu, R. F., Wellbrock, U. M., Oliveira, R. F., and Zupanc, G. K. H. (2012). Adult neurogenesis in the brain of the Mozambique tilapia, *Oreochromis mossambicus*. *J. Comp. Physiol. A Neuroethol. Sens. Neural. Behav. Physiol.* 198, 427–449. doi: 10.1007/s00359-012-0721-6

Terzibasi, E. T., Baumgart, M., Battistoni, G., and Cellerino, A. (2012). Adult neurogenesis in the short-lived teleost *Nothobranchius furzeri*: localization of neurogenic niches, molecular characterization and effects of aging. *Aging Cell* 11, 241–251. doi: 10.1111/j.1474-9726.2011.00781.x

Vadodaria, K. C., and Gage, F. H. (2014). SnapShot: adult hippocampal neurogenesis. *Cell* 156, 1114.e1. doi: 10.1016/j.cell.2014.02.029

Wang, C., Liu, F., Liu, Y. Y., Zhao, C. H., You, Y., Wang, L., et al. (2011). Identification and characterization of neuroblasts in the subventricular zone and rostral migratory stream of the adult human brain. *Cell Res.* 21, 1534–1550. doi: 10.1038/cr.2011.83

Zupanc, G. (2008). "Adult neurogenesis in teleosts fish," in *Adult Neurogenesis,* eds F. Gage, G. Kempermann, and H. Song (New York, NY: Cold Spring Harbor Laboratory Press), 571–592.

Zupanc, G., and Horschke, I. (1995). Proliferation zones in the brain of adult gymnotiform fish: a quantitative mapping study. *J. Comp. Neurol.* 353, 213–233. doi: 10.1002/cne.903530205

Zupanc, G. K. H. (2006). Neurogenesis and neuronal regeneration in the adult fish brain. *J. Comp. Physiol. A Neuroethol. Sens. Neural. Behav. Physiol.* 192, 649–670. doi: 10.1007/s00359-006-0104-y

Zupanc, G. K. H. (2011). "Adult neurogenesis in teleost fish," in *Neurogenesis in the Adult Brain I*, eds T. Seki, K. Sawamoto, J. M. Parent, and A. Alvarez-Buylla (Tokyo: Springer Japan), 137–168.

Zupanc, G. K. H., Hinsch, K., and Gage, F. H. (2005). Proliferation, migration, neuronal differentiation, and long-term survival of new cells in the adult zebrafish brain. *J. Comp. Neurol.* 488, 290–319. doi: 10.1002/cne.20571

Zupanc, G. K., Horschke, I., Ott, R., and Rascher, G. B. (1996). Postembryonic development of the cerebellum in gymnotiform fish. *J. Comp. Neurol.* 370, 443–464. doi: 10.1002/(SICI)1096-9861(19960708)370:4<443::AID-CNE3>3.0.CO;2-4

Conflict of Interest Statement: The authors declare that the research was conducted in the absence of any commercial or financial relationships that could be construed as a potential conflict of interest.

frontiers in Neuroscience

ORIGINAL RESEARCH
published: 05 October 2018
doi: 10.3389/fnins.2018.00706

Comparing Adult Hippocampal Neurogenesis Across Species: Translating Time to Predict the Tempo in Humans

Christine J. Charvet[1,2] *and Barbara L. Finlay*[2]*

[1] Department of Psychology, Delaware State University, Dover, DE, United States, [2] Laboratory of Behavioral and Evolutionary Neuroscience, Department of Psychology, Cornell University, Ithaca, NY, United States

Comparison of neurodevelopmental sequences between species whose initial period of brain organization may vary from 100 days to 1,000 days, and whose progress is intrinsically non-linear presents large challenges in normalization. Comparing adult timelines when lifespans stretch from 1 year to 75 years, when underlying cellular mechanisms under scrutiny do not scale similarly, presents challenges to simple detection and comparison. The question of adult hippocampal neurogenesis has generated numerous controversies regarding its simple presence or absence in humans versus rodents, whether it is best described as the tail of a distribution centered on early neural development, or is several distinct processes. In addition, adult neurogenesis may have substantially changed in evolutionary time in different taxonomic groups. Here, we extend and adapt a model of the cross-species transformation of early neurodevelopmental events which presently reaches up to the equivalent of the third human postnatal year for 18 mammalian species (www.translatingtime.net) to address questions relevant to hippocampal neurogenesis, which permit extending the database to adolescence or perhaps to the whole lifespan. We acquired quantitative data delimiting the envelope of hippocampal neurogenesis from cell cycle markers (i.e., Ki67 and DCX) and RNA sequencing data for two primates (macaque and humans) and two rodents (rat and mouse). To improve species coverage in primates, we gathered the same data from marmosets (*Callithrix jacchus*), but additionally gathered data on a number of developmental milestones to find equivalent developmental time points between marmosets and other species. When all species are so modeled, and represented in a common time frame, the envelopes of hippocampal neurogenesis are essentially superimposable. Early developmental events involving the olfactory and limbic system start and conclude possibly slightly early in primates than rodents, and we find a comparable early conclusion of primate hippocampal neurogenesis (as assessed by the relative number of Ki67 cells) suggesting a plateau to low levels at approximately 2 years of age in humans. Marmosets show equivalent patterns within neurodevelopment, but unlike macaque and humans may have wholesale delay in the initiation of neurodevelopment processes previously observed in some precocial mammals such as the guinea pig and multiple large ungulates.

Keywords: hippocampus, neurogenesis, adult, human, rodent, monkey, Ki67, allometry

OPEN ACCESS

Edited by:
Luca Bonfanti,
Università degli Studi di Torino, Italy

Reviewed by:
Joshua Breunig,
Cedars-Sinai Medical Center, United States
Hidenori Tabata,
Aichi Human Service Center, Japan
Myriam Cayre,
UMR7288 Institut de Biologie du Développement de Marseille (IBDM), France

***Correspondence:**
Barbara L. Finlay
blf2@cornell.edu

Specialty section:
This article was submitted to Neurogenesis, a section of the journal Frontiers in Neuroscience

Received: *01 June 2018*
Accepted: *18 September 2018*
Published: *05 October 2018*

Citation:
Charvet CJ and Finlay BL (2018) Comparing Adult Hippocampal Neurogenesis Across Species: Translating Time to Predict the Tempo in Humans. Front. Neurosci. 12:706. doi: 10.3389/fnins.2018.00706

INTRODUCTION

The following paper, a contribution to the collection "Adult Neurogenesis: beyond rats and mice," is a hybrid of two components. At its core is an empirical contribution to the literature on hippocampal neurogenesis, comparing late neurogenesis in two rodents and three primates, using evidence from cell cycle markers. We have informed that analysis with the "Translating Time" project[1], where we have gathered evidence about the relative progress of neurodevelopmental events from the first birthdays of mature neurons until increasingly later ages across 18 mammalian species. We will argue that any claim that onset, offset or duration of a developmental process, or an adult brain feature produced by such a process, is "unique," or even "specialized" in humans or any other species or taxonomic group is absolutely dependent on a proper allometric comparison, such as made possible by the "Translating time" modeling work, or other similar analyses. A comparison of a developmental feature of the brain of a particular rodent to particular primate species is not such an analysis, and will systematically mislead researchers.

The second component is a discussion of the problems and opportunities of developmental allometric analyses across mammals, which we present in this introduction. We include a review and exposition of basic allometric claims and procedures as they apply to brain mass and developmental duration in general, as well as the progress of neurogenesis targeted in this paper. We will describe some of the quantitative misunderstandings that typically arise from moving between the exponential functions used in allometric analyses, and the linear functions used in basic measurements of cell number and volume in developmental cell biology. The immediately following expanded introduction concerns the motivation, history, and methodology necessary to understand methods of analysis in developmental allometry.

The Purpose and Methodology of Allometric Comparison

Prior Work on Developmental Allometry

In order to limit the need to contrast statistical methodologies of successive papers within the text, the following description of species, neural structures, developmental span, and mathematical models employed in this research project follows, including immediately relevant work of several other laboratories. First, the current database for the "Translating Time" model with tables of species, structures and sources, a description of the current model, and a utility to translate or predict a developmental equivalent day between any two species in the model can be found at www.translatingtime.org (Clancy et al., 2007). The initial comparison of neurogenetic schedules in rhesus monkey, cat, four rodents and a marsupial, extending from onset of neurogenesis to approximately birth in the monkey, using principal components analysis, is described in Finlay and Darlington (1995) and an extended discussion of statistical considerations, principally phylogenetic covariation can be found in Finlay et al. (2001). Darlington et al. (1999) and Clancy et al. (2000) bring the number of species to nine eutherian (placental) mammals including humans and six metatherians (marsupials), principally using regression analyses. Clancy et al. (2001) extend the neurodevelopmental events past neurogenesis to include synaptogenesis, cell death, ocular dominance columns and the like, using regression and the general linear model (see also Clancy et al., 2007; Finlay and Clancy, 2008). The relationship of individual variability to between-species variability is discussed in Finlay et al. (2011), and specifically in humans in Charvet et al. (2013). The current iterative model deriving the "event scale" of maturation developed in Workman et al. (2013) brings the number of mammalian species to 18, the number of developmental events to 271, including myelination, volume change, and early behavioral events, extending to human-equivalent of the third postnatal year. Particularly relevant to the present paper, patterns in the neural maturation of altricial versus precocial species are contrasted. A demonstration of the problems arising from a failure to account for allometric concerns can be found in "Human exceptionalism" (Finlay and Workman, 2013). Early behavioral development and related neuroplasticity are integrated with translating time in Finlay and Uchiyama (2017), and finally, evolution of life histories, including events like weaning and menopause in Hawkes and Finlay (2018). Readers are directed to the early work of Passingham (1985), and Garwicz et al. (2009), who use similar methods to examine early independent ambulation, as well as that of Halley's studies of the growth of initial primordia and brain across a wide range of mammals (Halley, 2016, 2017). More recently, the advent of single cell RNA sequencing provides an exciting opportunity to investigate developmental trajectories of neural subpopulations across species (Habib et al., 2017; Iacono et al., 2017; Fan et al., 2018; Zhong et al., 2018). We here broaden the maturational range of neurodevelopmental ages of studies in our database to capture late stages of hippocampal neurogenesis across species.

Allometry of Brain and Brain Parts

The general form of scaling of neural mass or neuron numbers in any brain region compared to the whole brain, has been studied for many years (Jerison, 1973; Gould, 1975; Fleagle, 1985). Overall consensus exists about general features of brain and body scaling, though subject to the normal continuing debate about optimal ways to quantify statistical variation in large and complex datasets (Finlay et al., 2001; Freckleton et al., 2002). We will take the particular example of cross-species comparisons of the volume and number of neurons in the neocortex, and particularly the frontal cortex (the allometric study of the brain), to introduce the related and less familiar topic of scaling of developmental duration across species, which we term developmental allometry.

If scaling of neocortical volume (or "isocortex") is the focus for consideration, the fact that the human brain has a disproportionately large cortex compared to primates and most other mammals is quite "obvious" – for example, the human cortex comprises over 80% of its total brain mass, compared to around 20% in shrews and rodents (Finlay and Darlington, 1995). The correct empirical observation of the apparently

[1] http://www.translatingtime.org

disproportionate size of the cortex along with its persistent misinterpretation is the prototypical example of a problem we will call "human exceptionalism" (Finlay and Workman, 2013). The disproportionate volume of the human neocortex suggested to multiple researchers alike – anthropologists, embryologists, neuroscientists and psychologists – that it must be the result of special selection compared to the rest of the brain. Since the cortex was thus thought to be the subject of selection within the brain, every cognitive alteration or adaptation in evidence in humans has typically been typically credited to its superior computational prowess. But it's not necessarily so. Although we have an unusually large brain, our cortex is the size it should be for a brain of our absolute size when cross-species cortex volume or cell numbers are represented on logarithmic scales (Jerison, 1973; Hofman, 1989; Finlay and Darlington, 1995; Kaas and Herculano-Houzel, 2017).

Linear Scales, Logarithmic Scales, and the Allometric Equation

A "proper" comparison of variations across species of different sizes and developmental durations requires care (this section is abridged from Hawkes and Finlay, 2018 to which the reader is directed for a more extensive discussion). Even with "all else equal" in such factors as a species' niche, number of brain components, sex and age, still, the laws of geometry, and of physics and chemistry, impose lawful changes in both form and process with increase in brain mass. The intrinsic geometry of physical relationships results in variable allometric relationships (e.g., doubling the volume of a sphere only increases its radius by 1.26 times). After such geometric constants are understood, any two structures or processes changing in size or duration across species could show non-linear scaling relationships, scale linearly, or might show no predictable scaling, depending on the mechanisms or functions that are relevant. For example, the divisions, doubling and redoubling of stem cell pools are best described by non-linear equations. Some features change linearly: for example, if multiplied by the appropriate constant, cross-sectional diagrams of mice and rat eyes are superimposable even though the rat's eye is twice as big, as both are solving a linear optical problem with the same materials (Remtulla and Hallet, 1985). Some features do not scale at all with brain mass (considering mammals only here), such as the diameter of the cell bodies of neurons, the time to complete the first generation of a mature neuron, or the duration of action potentials. Such variable geometrical and biological scaling relations can coexist for different aspects of the same structure. Finally, datasets of interest often have underlying geometries that can mislead graphical comparisons. Consider a typical Mercator projection of the earth's landmasses, where the continents of Africa and Greenland appear approximately equal in size, but when measured in its correct spherical coordinates, Africa is more than 10 times larger than Greenland.

Allometries are conventionally represented as scaling relationships. If the relationship between two features that correlate with each other in size, say 'x' and 'y,' is represented as $y = kx^a$ where 'k' is some constant, and the exponent 'a' represents the rate at which 'y' changes with respect to a change in 'x.' If exponent 'a' is more or less than 1 then a change in 'y' is associated with a geometrical change in 'x.' Such geometrical or exponential relationships can be plotted and visualized as linear ones by logarithmic transformation: $\log y = a\log x + \log k$. In such log plots, the exponent 'a' now appears as the slope of the increase in 'y' with respect to x. Using this representation of cortex mass relative to the whole brain on a logarithmic scale, it is clear that the human neocortex is exactly the size it "should" be (**Figure 1**). The human brain is absolutely large compared to other primates, but given this large brain, each part falls onto its "expected" position, from hindbrain to cortex (Hofman, 1989). The cortex has "positive allometry" with respect to the rest of the brain, its slope greater than one, which is the "linear scaling reference" of **Figure 1**. Inevitably, therefore, with different brain components each increasing in mass at different rates, larger mammalian brains become "disproportionately" composed of cortex. The exact exponent of cortical positive allometry might vary with whether neurons, all cells, surface area or volume is measured, and shows some taxon-specific differences, but none reduce the positive exponent to one or less (a sampling of a large literature: Jerison, 1973, 1989; Hofman, 1989; Herculano-Houzel et al., 2007; Reep et al., 2007; Charvet et al., 2013).

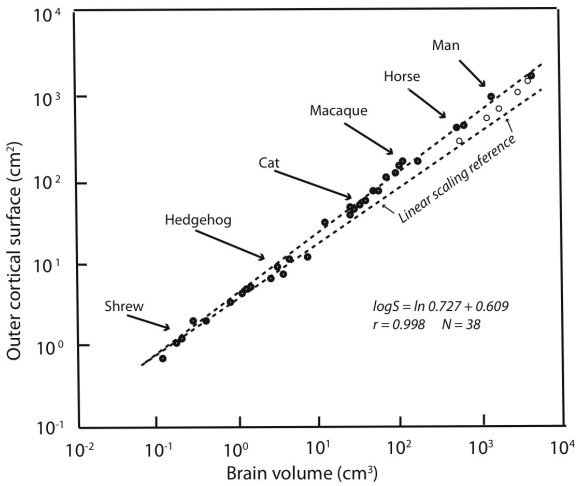

FIGURE 1 | Redrawn from Figure 2 of Hofman (1989). Outer cortical surface area is plotted as a function of brain volume on a logarithmic scale. The slope of the standard major axis is 0.727 ± 0.009. The dashed line represents the scaling of the cortical surface area according to a two-thirds power relation (the necessary geometric similarity of plotting an area against a volume if both increase linearly). Dolphins and whales are indicated by circles.

Because of the regular, predictable relationships of the relative sizes of brain parts at all absolute brain volumes, lacking other information, our large cortex cannot be attributed to special selection for that feature, as it comes "for free" with selection on the whole brain, or in fact, could arise by leverage by selection on any part of the brain (Finlay and Darlington, 1995). It is interesting, to be sure, that over evolutionary time that the cortex, and the cerebellum are the two brain regions where disproportionate neuron number, volume and

energy consumption are routinely allocated (Finlay et al., 2011). Comparison of relative cortical and cerebellar volume between any two mammals of different brain size will reveal this feature, not only comparison of the human brain with all others. The most telling evidence is that those several mammalian brains which are absolutely larger in mass than the human brain, including several cetaceans and ungulates, continue the allometric equation of the cortex, so that they have proportionately even more cortex than humans do (**Figure 1**).

The Evolutionary Question at Issue: The Case of the Prefrontal Cortex

Questions involving allometric scaling are in no way historical debates as a similar controversy is ongoing about whether a specific region of cortex, the prefrontal cortex, is "allometrically unexpected" in humans (Sherwood and Smaers, 2013). Just as the cortex has a particular exponent of enlargement with respect to the rest of the brain, every cortical area (e.g., prefrontal, primary visual) has its own exponent (or slope in the log-transformed equation) showing its change in relative volume compared to overall cortex volume. Both the prefrontal and parietal cortex regions have an exponent that is larger than the cortex's overall exponent, showing a positive allometry (Jerison, 1997). The issue under debate is whether the frontal cortex in humans is larger still than would be expected from its already high positive allometry (Semendeferi et al., 2002; Barton and Venditti, 2013; Chaplin et al., 2013; Passingham and Smaers, 2014). As before, however, when we discussed preferential allocation of "excess" neural mass for cortex and cerebellum versus the rest of the brain, it is interesting that it is frontal and parietal cortex that are preferentially enlarged in the cortical sheet when brains increase in volume across mammals.

Why should these researchers care about this issue? If researchers claim a region's volume is "allometrically unexpected" in humans, they are claiming that it must have been the target of selection, typically because of special importance of the function ascribed to that brain region in that species. In the case of the frontal cortex, the cognitive features usually evoked are cognitive control, the ability to choose reasonable behavioral solutions from competing possibilities, or to evaluate choices with respect to goals distant in space or time. Thus, the claim that the frontal cortex is allometrically unexpected in humans is a claim that humans have been selected on a behavioral feature like cognitive control, which in turn is improved with the relative volume of frontal cortex. Structures that change their volume according to regular, cross-species allometric rules, however, even if they look disproportionate on a linear scale, require no special explanation. If the entire brain has been under special selection for larger size in any species, every single change in the proportionality of its parts is generated by its change in size. We'll make no ruling on this claim, except to note that the deviation in human frontal cortex volume, if it exists, is small enough to make it susceptible to relatively minor differences in methodology between research groups.

It remains interesting and important that brains enlarge in particular ways, and that predictable patterns of reorganization, both behavioral and computational, are associated with cortical enlargement (Finlay and Uchiyama, 2017). Mammals with large brains are certain to show evidence of a disproportionate contribution of frontal cortex (Passingham and Smaers, 2014). Allometric regularities in structural scaling, whether in the cortex, or in the hippocampus we will soon be discussing, require that we investigate coordinated mechanisms *outside* the structures of interest, and should make us skeptical of causal accounts that depend on selection on hypothesized special adaptations of the particular species of animal.

An important mechanism of volumes and neuron number coordination in several cases studied so far appears to be the coordinated control of duration of neurogenesis, as applied to every part of mammalian brains (e.g., Finlay and Darlington, 1995; Dyer et al., 2009; Cahalane et al., 2014; Charvet and Finlay, 2014). As the duration of hippocampal neurogenesis is the subject of the empirical component of this paper, we will now turn to issues in the allometry of development.

The Allometry of Developmental Duration: Basic Requirements

The Need for Data From Multiple Species: Why Attempts to "Norm" Measurements Between Only Two Species Will Be Ineffective

The formal properties of "allometrically expected" changes in mass also apply to translations of developmental time from one species to another. The appropriate coordinate system to represent time translations will depend on the data to be represented, and the representation desired. The relationship of developmental timing between species cannot be presumed to be best represented on a linear scale. In order to fairly compare developmental durations between animals, enough data must be collected from a number of relevant species to support generating an allometric equation with credible confidence intervals for its slope and intercept. For example, taking a first example from volume allometry, if you hypothesized that special selection in humans for language ability resulted in a comparatively larger Broca's area, it is necessary to show that the size of Broca's area in humans exceeds its expected allometric position compared to Broca's area in other primates (Schoenemann, 2006). A "control structure" such as primary visual cortex, a subcortical structure, or the rest of the brain cannot be used to "normalize" the volume of Broca's area, as allometric relationships in brain volumes can be expected to be non-linear. Broca's area will be disproportionately large in humans versus rhesus monkeys, but it will also be disproportionately large in rhesus monkeys versus marmosets, or in horses versus sheep, where relative language competence will not apply. If Broca's area has positive allometry compared to visual cortex, every contrast of a large and small mammalian brain will *always* show disproportionate volume increase in Broca's area in the larger brain. Similarly, the question of whether hippocampal neurogenesis and maturation is unusually early or late in humans depends on whether the timing of hippocampal maturation deviates from its expected developmental allometry.

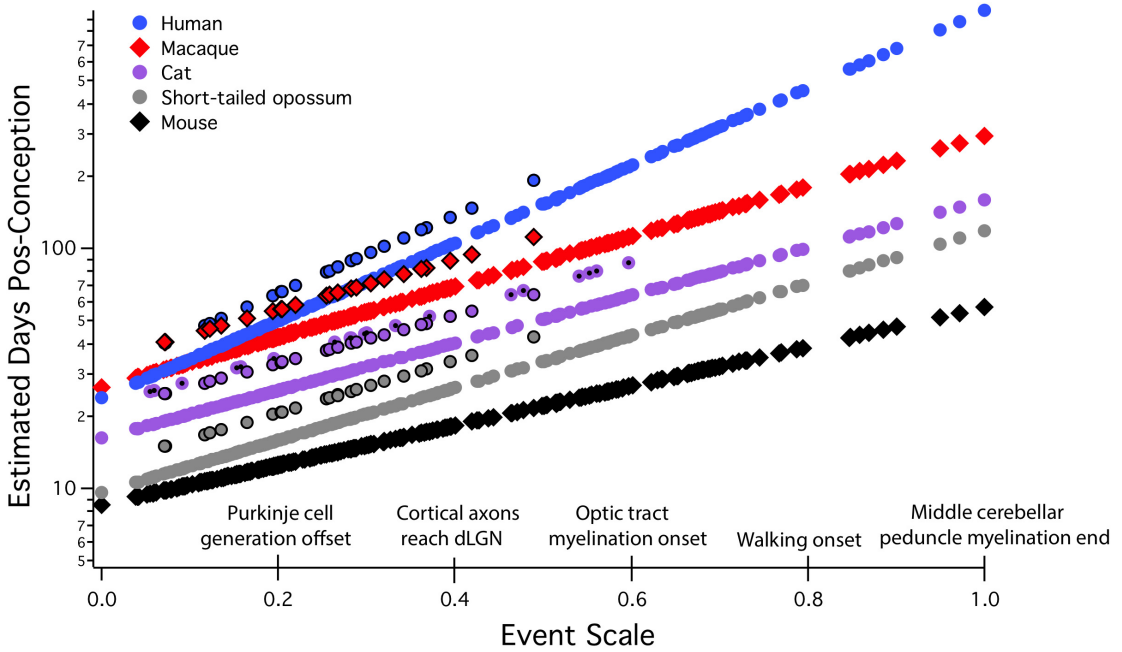

FIGURE 2 | Predicted developmental schedules for human (blue circle), macaque (red diamonds), cat (purple circle), short-tailed opossum (gray circle), and mouse (black diamonds), selected from 18 species to illustrate the full range of developmental durations. This figure is modified from Workman et al. (2013). In this graph, the event scale is the *x*-axis, to which we have added a subset of the 271 events that were observed. The event scale is a common ordering of developmental events across all species and ranges from 0 to 1. The *y*-axis is the estimated date of occurrence of each event in each species from conception (log scale). To determine when a particular event would be predicted to occur in any species from this graph, using the name of the event on the event scale, find where it intersects the regression line for that particular species. The *y*-axis value will be the predicted PC day for that event/species combination. In future graphical representations of the event scale, the event scale value for any named event can be found in **Supplementary Table S1**. Also represented on this graph are interaction terms for corticogenesis and retinogenesis, with interaction terms always associated with individual species. The parallel lines for a subset of events in four of the species (black bordered circles for human, macaque, cat, and possum) represent delays in cortical neurogenesis with respect to their time of occurrence in the rodent and rabbit. In the cat, a second parallel line can be seen representing the delay of retinal neurogenesis relative to the timing of other transformations (purple circle with a black dot). dLGN, dorsal lateral geniculate nucleus.

Inappropriate norming procedures applied to developmental timing questions will produce the identical errors to those produced by inappropriately norming allometric comparisons of volume. You cannot, for example, compare the time from birth to adolescence in chimpanzees versus humans, see that the duration is longer in humans, and conclude that humans have been specially selected for a longer childhood. The duration may be entirely predictable from the time required to generate a large brain, intrinsic correlation with longevity or some other superordinate feature of life history. The "translating time" database was collected, in part, to be able to understand such comparisons in a larger cross-species context. A major surprise of this work was the extreme regularity of neural development in mammals, which in addition to the interest of the regularity alone, gives us a reliable set of brain-based benchmarks to understand the relative maturation of each species with respect to life-history events like birth or weaning (Hawkes and Finlay, 2018).

Setting Zero, or Onset of Neurodevelopment: Birth Is Not a Reliable Indicator of Brain Maturation

All allometric equations have a slope and an intercept, but in developmental allometry, the intercept often suggests a real-world developmental meaning, for example, the onset of neurogenesis, conception, or birth. Even though a real-world event like conception may appear to be a likely candidate for "zero" in an allometric equation, this must be mathematically determined, not stipulated. In "translating time," the best fit for "day zero" to the empirically measured neuroembryological data first proved to be a point located between conception and first production of mature neurons, possibly implantation (Finlay and Darlington, 1995; Finlay et al., 2001; Workman et al., 2013). Although birth is often chosen as a natural zero in anthropological work, and especially for research on late hippocampal neurogenesis to be discussed here, for the good theoretical reason that it marks the beginning of the independent life of the organism, and for the practical reason that prenatal measurements often hard to come by, still, this choice can be very misleading when attempting to compare developmental schedules (**Figure 2**). We will explain the derivation of the axes and the maturational progress represented on this graph in more detail in the next section, but for the moment, the *x* scale, the "event scale" is a multivariate measure of overall maturational state of the nervous system, with the generation of the first neurons near "0," with "1" corresponding to about 2 years postnatal in humans, with embryological features

like achievement of 80% of adult brain volume and variable progress of myelination. The *y*-axis is post-conception days of development on a linear scale – on a log scale, the allometric equation of each curve plotted would become a straight line (**Figure 3**). Post-conception days are plotted on a linear scale in this graph to emphasize the extreme divergences in absolute days to maturity in the species plotted here.

We have stressed the importance of two basic features of developmental allometric analysis critical for interpreting the presence or absence of "postnatal" or "adult neurogenesis." The first is obtaining developmental data from enough species to generate reliable allometric equations, and the second is locating a true "zero" from which to scale maturational events in the same equations. The Translating Time database and model can supply both necessities. Exploring "postnatal" neurogenesis in the hippocampus will be reporting on very different phenomena if mice, precocial guinea pigs, or humans are compared.

A Brief Review of Our Specific Methodology for Comparing Neurodevelopmental Sequences Across Species

Over the past 20 years, a database and methodology to compare the progress of neural development across species have been elaborated (see footnote 1). The multiple statistical considerations leading to this representation can be found in the series of papers detailed in the first section, and a full description of the model in Workman et al. (2013). The original purpose of this work was to describe a mammalian "Bauplan" for neural development, and thus identify deviations from this plan that might mark taxon- or species-specific alterations corresponding to evolutionary adaptations, which is exactly how we will employ it for to examine the hippocampal data we have collected. The present model includes 18 species, and 271 "events" of mixed type, including neurogenesis in particular structures or cell classes (e.g., Layer 4 of striate cortex; Purkinje cells in the cerebellum; onset of synaptogenesis in a thalamic nucleus; emergence of some minimal behavioral reactivity, and transitions capturing continuous processes such as increases in brain volume or myelination).

The model from Workman et al. (2013) is reproduced in **Figure 2**, and extends to a maturational stage equal to approximately 2 years postnatal in humans. Only events in brain and some early behavioral capacities are included to model the event scale and each species' regression line – no measures of body or organ maturation or volume, or interactional, life history events like birth or weaning are included in this version. The "event scale," which is the best order and interval relationship of the 271 distinct neurodevelopmental events in the 18 species, is fit iteratively to all the data, (*x*-axis, **Figure 2**). The speed of progress of each individual species through these events is given as a regression equation, in days on a log scale (*y*-axis; compare the linear scale in **Figure 2** of the same functions). It is more typical to plot time on the *x*-axis in developmental studies, and it is important to remember this difference in representation. Days are on the *y*-axis because we are interested in duration as a function of maturational state. For example, for species with different sized brains, how long will it take them to reach equivalent maturational states? The differences in each species' slope show differences in maturational rate, with steeper slopes meaning slower progress through maturational stages in absolute time: the mouse takes only about 30 days to execute its 271 neurodevelopmental events, while the human takes 1,000 days, as humans generate greater numbers of neurons and volumes of connectivity per event.

The fit of model results to empirically measured results is astonishingly close, 0.9929, which reflects an extreme, and initially unexpected conservation of developmental sequences in mammals. Only two interaction terms are necessary to produce taxon-specific differences in these data so far, which are the black-circled points floating above the larger number of points of the corresponding color. The first term corresponds to an extension in corticogenesis in primates, some marsupial species and carnivores (n.b: this can be equally well represented as an advance in initiation and termination of neurogenesis in the "rest of the brain" –Clancy et al., 2001; Workman et al., 2013; Charvet et al., 2017a,b). The second represents a delay in neurogenesis in the retina of the nocturnal cat and ferret (also owl monkey, Dyer et al., 2009). Extensions in cortical neurogenesis produce a disproportionate expansion of cortical and, in particular, upper layer neuron numbers in primates (Cahalane et al., 2014; Charvet et al., 2015, 2017a,b), and a greater number of rods and rod-associated neurons in carnivores and owl monkeys.

Birth can intersect quite different developmental events in different species

As noted earlier, birth may occur at a wide range of stages in neural development in different species. For example, cortical and cerebellar neurogenesis is ongoing at birth in some rodents, but in primates, both are largely concluded at that time. No obvious inflections, halts or accelerations near birth can be found in basic central nervous system construction. There is one event, a whole-brain surge of synaptogenesis, which appears to just antedate either birth or burrow exit in the four mammals studied to date instead of conforming the otherwise monolithic neurodevelopment program (reviewed in Finlay and Uchiyama, 2017).

Other evidence for regular mammalian neurodevelopment

Empirical support for the surprising claim of an extremely conserved mammalian neurodevelopmental schedule can be found in several independent sources. Mammalian brains continue to grow after birth, and Passingham (1985) first noted that if the volume of the brain at birth is plotted against gestation length for an eclectic set of eutherian mammals, including rats, pigs and dolphins (log transformed), a straight line results, suggesting brain mass is produced generally at the same rates in all species, smaller brains simply ceasing their growth earlier (Passingham, 1985). Halley (2016, 2017), in a much larger and more closely measured data set of changes in brain volume post-conception, recently confirmed the same notion. We have also successfully modeled the development of neuron number in the cortex combining information on kinetics of neurogenesis with adult neuron numbers in multiple species (Charvet and Finlay, 2014; Cahalane et al., 2014).

Other observations of single maturational phenomena give other insights, and underline further unexpected consequences of this conserved neurodevelopmental rate.

Two surprising findings about precocial animals

In mammals, the onset of walking is predicted by neural maturation (which is conserved) but not birth or any known niche variable. The time of the first unsupported step is highly predictable from a developmental allometric equation derived from adult brain mass, including one interaction term slightly accelerating the time of first step for those species with a plantigrade standing position (Garwicz et al., 2009), which fits seamlessly into the translating time model. This monolithic nature of the neurodevelopmental program, and its close correlation with brain size puts an interesting constraint on precocial mammals. Relatively large-brained, precocial ungulates like sheep and elk, who must be ready to run just after birth, accomplished this evolutionarily by extending gestation and delaying birth in their large offspring to match conserved parameters of brain development. They do not selectively advance the general rate of brain maturation nor push forward the maturation of circuitry closely associated with ambulation apart from the rest of the brain, which might seem to be a less stressful solution.

A related peculiarity can be seen in precocial species with relatively small brains such as the guinea pig and spiny mouse, that are born looking and moving quite mature, furred, and with sensory systems functional. While it might seem a reasonable strategy to make the most of every possible second for brain maturation available *in utero* in precocial species, to allow fine tuning of the coordinated behavior required immediately after birth, the conserved pace of brain maturation seems to rule this out. Since these animals must also produce large, mature bodies, which appear to require more time than the brain, the onset of neural development as marked by the first postmitotic neurons is substantially *delayed,* not stretched to fill the available time, allowing somatic maturation a head start (Workman et al., 2013). We will discuss whether a similar situation is present in marmosets, born with some precocial features.

Applying "Translating Time" to the Question of Late Hippocampal Neurogenesis

The first reports of neurogenesis in adult humans and other mammals produced much excitement, in that it contradicted the central dogma that no new neurons, are generated in adulthood and offered a possible avenue for brain rehabilitation and repair. At first, the presence of new neurons was reported widely throughout the forebrain, but in time, unambiguous neurogenesis was finally limited to two locations, the hippocampus and the olfactory bulb via the "rostral migratory stream," mostly from work in rodents, but with confirmation in humans (Ming and Song, 2005). Recently, however, the existence of significant adult hippocampal neurogenesis has been questioned (Dennis et al., 2016; Andreae, 2018; Kempermann et al., 2018; Lee and Thuret, 2018; Sorrells et al., 2018). A report by Sorrells et al. (2018) concluded that neurogenesis in the human hippocampal dentate gyrus drops to undetectable levels during childhood, suggesting that human hippocampal neurogenesis is unlike that of other mammals (Knoth et al., 2010). A concurrent study (Boldrini et al., 2018) also investigated adult neurogenesis in the human hippocampus (14–79 years of age) and contradicts the first study. Using quite similar methodologies, the second group argued that adult hippocampal neurogenesis is in fact present throughout the lifespan. In such cases of contradiction, consultation with the animal model literature is of major help. A problem that has plagued this work is the absence of a robust and reliable way to compare time courses of events in different species. Adult hippocampal neurogenesis of any species could represent the tail end of a normal embryonic period of neurogenesis, or a truly indeterminate phenomenon, as is seen in virtually all non-mammalian vertebrates, or perhaps a targeted rekindling of neurogenesis for a particular purpose in adulthood. Because of the methodological similarity of the two studies, it may not be possible to rule in favor of one or the other on reported evidence, but a better idea of where errors might lie is a natural outcome of quantitative developmental modeling.

Specific Objectives 1: Extending the Translating Time Model and Representing Species on a Common Scale

As we described previously, mammalian species vary in the length of both neural and somatic development, the positioning of birth with respect to neural maturation, and the relative length of neurogenesis in different structures. Comparing humans to macaques and mice, human neurodevelopment is much longer (duration correlating close with brain volume, as does the duration of lifespan). Humans are born at a slightly earlier stage of neural maturation than macaques, and at much later stage than rats and mice. Rhesus monkeys and humans also curtail neurogenesis in limbic structures relatively earlier than rodents (Workman et al., 2013), corresponding to the fact that as limbic structures are systematically relatively smaller (that is, scale with a smaller exponent) in primates compared to rodents (Reep et al., 2007). The translating time model at present does not have good data representation for late developmental stages to allow close comparisons in adulthood. We are therefore adding new data, and one new species to extend the model farther into the lifespan, but without any substantive change in its basic structure. We find appropriately transformed envelopes of neurogenesis across species to be very similar, and continuous.

Specific Objectives 2: Closer Examination of Human Hippocampal Neurogenesis and the Problems of Detecting Non-scaling Cellular Events in a Non-linearly Scaling Lifespan

We consider the allometric nature of developmental schedules in humans to identify how hippocampal neurogenesis should vary if the duration of hippocampal neurogenesis in humans is similar to that of rodents. Further, the ability to align timetables allows us to investigate an intrinsic problem of detecting a

cellular signal in scaling situations, which is that organismal variables of size and duration show robust scaling, but cellular phenomena like action potentials, the length of the cell cycle and so forth rarely do. A rat may expect to live around 700 days post-adolescence, while an approximate comparable human figure is 25,000 days. If the cellular processes associated with an occasion of neurogenesis are transitory, and almost certainly do not scale with lifespan, the probability of simple detection falls radically in the long lifespan. We will discuss this aspect of scaling both as a methodological problem, and as a question about the importance of extremely low-probability events.

MATERIALS AND METHODS

Species and Sources

In order to extend the current neurodevelopmental model to later developmental stages, we added some additional data on the timing of developmental milestones in two rodent species (i.e., rats and mice), and three primate species (i.e., macaques, marmosets, and humans). "Developmental events" capture rapid transformations, such as onset of neurogenesis, any other process, or arbitrary divisions of continuous processes into epochs (e.g., 20%, 40%, 60%, and 80% of a structure's adult volume). Examples of developmental events include birth-dating of cell types, synaptogenesis, myelination, changes in protein and RNA expression. The new types of data added were those capturing temporal changes in cell proliferation from markers (i.e., DCX and Ki67) in the hippocampus. We only include developmental events present in at least two species, and at least one rodent species.

We identified variation in proliferative and newly born neuron numbers over the course of prenatal and postnatal development in primates and in rodents. More specifically, we collected previously published data where the number of Ki67+ (proliferative) and newly born (DCX+) cells relative to the total number of hippocampal granule cells was quantified at several stages of development in rodents and in primates. We defined as epochs when Ki67+ cells decline to 2%, 0.7%, 0.5%, 0.3%, 0.2%, and 0.1% of total granule cells in primates and rodents. We also identified when the number of DCX+ cells reach 3, 2.5, 2, 1.5, 1, and 0.5% of total granule cells in rodents and in primates. To do so, we fit a linear regression between the natural-logged values of age and the relative number of cell markers to compare the duration of the decline in late hippocampal neurogenesis between primates and rodents (**Figure 3**). We only selected age ranges in which there is a sharp decline in the relative number of Ki67 and DCX+ cells over time as assessed on a natural-log scale. This permits fitting a linear regression through the data for each species (**Figure 3**). These data are from Merrill et al. (2003), Rao et al. (2006), Ben Abdallah et al. (2010), Jabès et al. (2010), Amrein et al. (2011), Amrein et al. (2015), and Hochgerner et al. (2018). For rats, we considered the number of Ki67+ and DCX+ cells from Rao et al. (2006) and total granule cell numbers from Merrill et al. (2003). We consider studies that normalize the total number of proliferative and immature cells relative to total granule cells rather than those that consider the number of proliferative and immature neurons per mm^2 of tissue.

We consider developmental transitions as the emergence of "plateaus" in the expression of multiple genes in single structures. We identified such plateaus in RNA expression from RNA sequencing data of bulk from the hippocampus in both species (Iacono et al., 2017). We identified when expressed genes reach a plateau in their expression across 14,417 orthologous genes as defined by the mouse genome database (Smith et al., 2018). We used a non-linear model with the software package R (easynls, model 3). Only orthologous expressed genes were considered. Age ranges were constrained to vary between 101 and 999 days in humans (n = 10) and between P1 to P30 in mice (n = 15) to compare roughly equivalent developmental time windows across these two species. We used normalized RNA sequencing expression made available by the Allen brain Institute. RNA expression from mice hippocampi was obtained from Iacono et al. (2017) (GEO: GSE79380). We selected only those models with p-values of coefficients less than 0.05 in humans and mice. This resulted in 34 genes in which plateaus were identified in both species. We averaged the age in which plateaus in RNA expression were identified in both species and include these data as one developmental event.

Developmental Timing in Marmosets

We gathered available data on the timing of early neurodevelopmental events for the marmoset as we had done for other species. We matched our previously collected database on developmental event definitions, principally using anatomical changes from structural MRI scans (Hikishima et al., 2013), spatiotemporal changes in gene expression, as well as anatomical transformations from the literature. Examples of developmental events include morphological events such as first observation of retinal axons in the optic stalk, or when neurofilament heavy polypeptide (NEFH) expression emerges in the cortex. Because the marmoset is increasingly used as a model organism, we expect this inclusion to be useful past this study alone. To compute the timing of developmental events from MRIs, we noted the earliest age in which a event had occurred and the latest age in which the event had not yet occurred, as we had done previously (Charvet and Striedter, 2010; Workman et al., 2013). In total, we include 29 events for marmosets (**Supplementary Table S1**).

Statistical Analyses

We include 213 developmental events from Workman et al. (2013) and Charvet et al. (2017b), eliminating events capturing the timing of cortical neurogenesis because cortical neurogenesis is extended in primates compared with rodents. We only included developmental events present in at least two of the species. Of the 213 events, 47 represented events or stages in limbic system development, including neurogenesis timing as well as the emergence of axonal pathways of limbic structures. We added 22 developmental events, 14 of which that capture the decline in late hippocampal neurogenesis (six Ki67, eight DCx; **Figure 3**).

A new 0–1 "event scale" was fit linearly to span this extended range, by subtracting the timing of each developmental

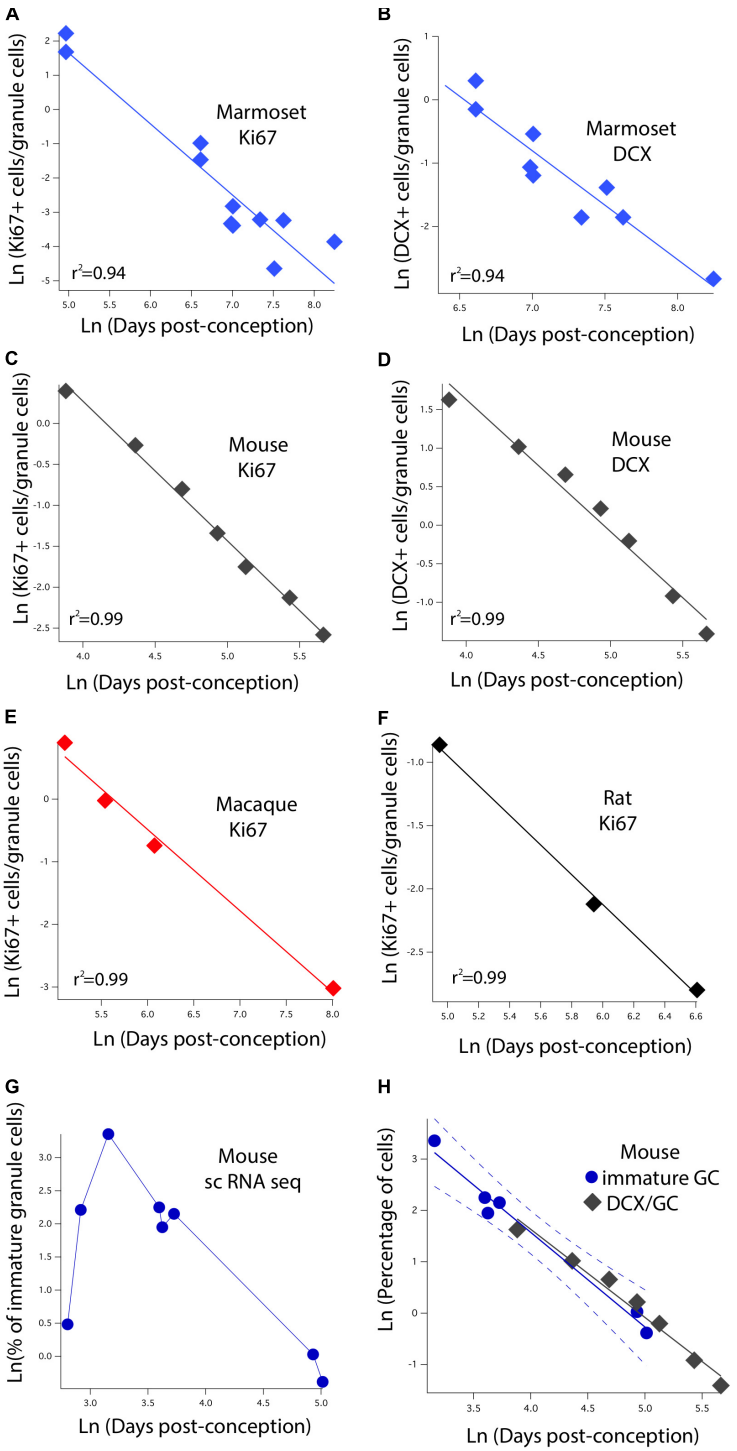

FIGURE 3 | The natural-logged values of DCX+ and Ki67+ cell numbers relative to hippocampal granule cell numbers are plotted against the natural-logged values of age in days post-conception in **(A,B)** marmosets, **(C,D)** mice, **(E)** macaques, and **(F)** rats. We performed a linear regression through these values to identify when the relative number of Ki67+ cells reaches 0.7, 0.5, 0.3, 0.2, and 0.1% of the total granule cell population. We also identify when DCX cell numbers reach 3, 2.5, 2, and 1.5% of the total granule cell population. With the exception of the marmoset, the relative number of DCX+ and Ki67+ to total granule cells were averaged at each age. **(G)** We use single cell RNA-seq to compute the number of immature granule cells relative to hippocampal neurons over the course of prenatal and postnatal development in mice. **(H)** Such an analysis shows that DCX+/granule cell numbers of mice fall within the 99% confidence intervals generated from single cell RNA-seq data. These findings demonstrate strong concordance between methods. Data are from Merrill et al. (2003), Rao et al. (2006), Ben Abdallah et al. (2010), Jabès et al. (2010), and Amrein et al. (2011, 2015). Data from single cell RNA-seq are from Hochgerner et al. (2018). Regressions were generated with software package IGOR.

event from the earliest event and divided these values by the difference between the latest event and the earliest event. We fit a linear regression through log-transformed values for each species against the event scale. We use the fitted values from the regression of human developmental event timing versus the event scale to predict the timing of late stages of human hippocampal neurogenesis timing. We omitted developmental events capturing cortical neurogenesis because a subset of cortical cell types are generated later than expected in primates (Clancy et al., 2001; Charvet et al., 2017a,b), which may increase error when predicting the duration of hippocampal neurogenesis across species.

We tested whether hippocampal neurogenesis occurs earlier than expected given the timing of other developmental events. We fit a linear model with the event scale as a continuous variable and developmental event timing as the response variable. To test whether limbic structures undergo neurogenesis earlier than expected relative to the timing of other events, we classified neurogenetic events as limbic or non-limbic. We tested whether the "limbic factor" as well as the interaction between the event scale and the "limbic factor" would account for a significant percentage of the variance.

Single Cell RNA Sequencing to Identify Adult Hippocampal Neurogenesis

Because adult neurogenesis has recently been disputed in humans (Sorrells et al., 2018), we investigated whether adult neurogenesis could be observed from single cell RNA sequencing data extracted from the human hippocampus and prefrontal cortex aged 40–65 (Habib et al., 2017). We computed the relative number of cells expressing neural progenitor markers (DCX+, SOX2+, DPYSL3+) relative to the number of cells expressing PROX1+ in humans. We select PROX1 as a marker for granule cells because it is expressed by hippocampal granule cells but not by other cell types in the cortex. That is, the expression of PROX1 from bulk samples is higher in the hippocampus than in other cortical regions (**Supplementary Figure S1A**). PROX1 is expressed by hippocampal granule cells but not by isocortical cells (**Supplementary Figure S1B**). We selected SOX2, DCX, and DPYSL3 (aka TUC-4) because they are markers of immature neurons (Ngwenya et al., 2006; Cipriani et al., 2018). We considered PROX1 to be expressed if the gene count was greater than 0. To identify whether DCX+, SOX2+, and DPYSL3+ collocate with PROX1+ cells above chance level, we randomly reassigned PROX1 expression to different neuronal types 1,000 times. We then computed the number of DCX+, SOX2+, and DPYSL3+ cells relative to the number of PROX1+ cells. We assess whether the relative number of DCX+, SOX2+, and DPYSL3+ falls above the 95% confidence intervals generated from 1,000 permutations. Such an analysis permits investigating whether the number of immature neurons is present above chance level. Because we are focused on whether new neurons are generated in the adult hippocampus, we do not include cells belonging to clusters previously identified as glial, astrocytic, microglia, and endothelial. Data are from DroNc-Seq generated by Habib et al. (2017).

RESULTS

Initial Characterization of Late Hippocampal Neurogenesis

The initial step is to characterize how the number of dividing progenitors (Ki67+ cells) and immature neurons (DCX+) relative to granule cell numbers vary with post-conceptional day. **Figures 3A,C,E,F** show the measured values of Ki67+ cells expressed as a percent of total granule cells versus days post-conception for the marmoset, mouse, macaque, and rat. Frames B and D show DCX+ labeled granule cells for marmoset and mouse only, again as a percent of total granule cells. Both scales are natural log scales, and the durations spanned vary considerably, from approximately 50 to 250 days post-conception in the mouse, versus approximately 150 to 3,000 days postnatal in macaque and marmoset. This enables calculating when the percentage of Ki67+ to total granule cells reach 2%, 0.7%, 0.5%, 0.3%, 0.2%, and 0.1%, and when the percentage of DCX+ to total granule cells reach 3%, 2.5%, 2%, 1.5%, 1%, and 0.5% in each species. The range for each species was constrained so that the natural-logged values of the relative number of Ki67+ and DCX+ to total granule cells systematically decline with age. This approach permitted fitting a linear regression through the data.

Addition of Declining Hippocampal Neurogenesis Values Into the Overall Maturational Event Scale

In **Figure 3**, hippocampal neurogenesis indicators are described with relation to post-conception day in each species, but we would like to know how the decline in hippocampal neurogenesis relates to the common progress of brain maturation across species. Two ways of presenting "translating time" data can be used. In **Figure 4A**, the new data on late hippocampal neurogenesis for marmoset, macaque, and mouse, and the single rat point are plotted against the common "event scale." This type of data representation is optimal for visualizing overall slope and intercept similarities and differences between multiple species. As expected, the species with long early neurodevelopment periods show longer periods of adult hippocampal neurogenesis. No truncations, breaks or sudden accelerations in any particular species are in evidence, though there are interesting differences in the maturational path in marmosets versus macaques we will address subsequently.

It is also possible to use the translating time scale to express the events of one species in the time frame of a second species, "translate" the approximately 130 modeled days of the macaque to the 50 days of a mouse, which facilitates close comparisons of delay or advance of any class of events between the selected species (**Figures 4B,C**). For example, comparing nocturnal to diurnal mammals, the rods and other rod-related cells of the retina are generated later in nocturnal mammals, which would be visible in graphs like **Figures 4B,C** as an elevation of rod-related points (nocturnal animals on the *y*-axis) (Dyer et al., 2009; Workman et al., 2013). In this case, we look for a difference in the implied intercept or slope of the "late hippocampal neurogenesis" points to determine if they show any signs of systematic variation

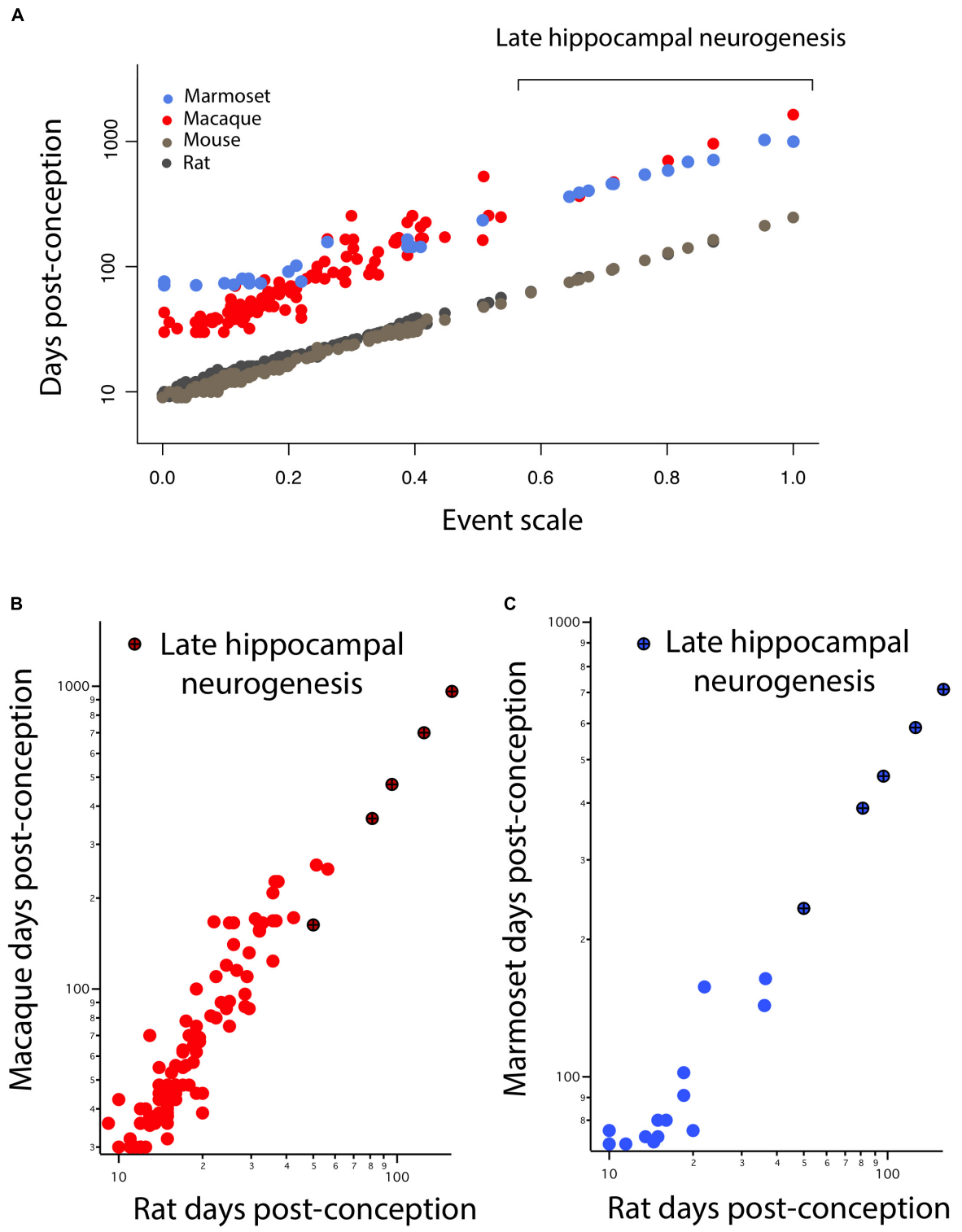

FIGURE 4 | (A) The timing of developmental events is plotted against an event scale in macaques, marmosets, rats, and mice. The timing of hippocampal neurogenesis was extrapolated from regressions capturing the decline in the number of DCX and Ki67+ cells relative to hippocampal granule cell numbers in primates and rodents. The timing of developmental events in macaques **(B)** and marmosets **(C)** are plotted against those in rats. **(B,C)** Developmental time points capturing late stages of hippocampal neurogenesis are highlighted (x).

from the common developmental scaling function. No such differences are apparent.

Marmoset Developmental Timing

Early in development, equivalent events in marmosets occur later than in macaques (**Figure 4A**). At later time points, equivalent events occur earlier in marmosets than in macaques. A linear model with the event scale as a continuous variable and the logged values of developmental event timing as the predictor shows that the slope is lower in marmosets ($y = 1.27x + 1.73$, slope $SE = 0.037$, intercept $SE = 0.02$, $R^2 = 0.976$, $p < 2.2e\text{-}16$) than it is in macaques ($y = 1.89x + 1.44$, slope $SE = 0.056$, intercept $SE = 0.016$, $R^2 = 0.903$; $p < 2.2e\text{-}16$). In other words, marmosets initiate neural development late with respect to conception, close to day 90 compared to day 35 in macaques, but then progress through developmental events faster than macaques, producing a smaller brain by the end of neural development. The consequence of this late, accelerated developmental trajectory is that hippocampal neurogenesis wanes earlier in marmosets than in macaques. This is similar to the pattern previously observed in precocial mammals like guinea pigs, spiny mouse, and sheep (Workman et al., 2013) where neural development is delayed with respect to conception later, but once initiated, proceeds at a faster rate than in a number of altricial species. Equivalent developmental ages between marmosets and other species (i.e., mouse, rat, macaque, and human) are listed in **Supplementary Table S2**.

Somewhat Earlier Termination of Limbic Neurogenesis in the Macaque

The large sample size in macaques allows us to test whether limbic neurogenesis occurs earlier relative to the timing of other events in macaques (**Figure 5**). To that end, we fit a linear model with the logged values of developmental event timing as the predictor, the event scale as a continuous variable and a discrete categorical variable that classifies neurogenetic events as limbic or not. We also tested whether the interaction between the "limbic" factor and the event scale accounts for a significant percentage of the variance. The fitted model accounts for a significant percentage of the variance in developmental event timing for macaques ($F = 416.7$; $R^2 = 0.91$). The limbic factor is not significant ($F = 2.065$; $p = 0.15$) but the interaction between the limbic factor and the event scale is significant for macaques ($F = 11.92$; $p < 0.05$). These data demonstrate that the slope of the natural-logged values of late hippocampal neurogenesis versus the event scale is lower than expected in macaques considering the timing of other developmental events. In other words, hippocampal neurogenesis may cease slightly earlier than expected in macaques compared with rodents.

Hippocampal Neurogenesis in Humans

For humans, a linear regression of the timing of reported developmental milestones versus the event scale computed for humans by the translating time model (Workman et al., 2013) is plotted for the reduced dataset we used in this model, as a visual check and demonstration of the predictability of human data points, in **Figure 6A**. No new data are introduced in **Figure 6A**; its intention is only to show the baseline variability against which we might introduce and compare other data ($y = 2.44x + 1.53$; slope $SE = 0.12$; intercept $SE = 0.04$, $R^2 = 0.85$, $p < 2.2e\text{-}16$). We then extrapolated predicted values from the linear model to see how late stages of hippocampal neurogenesis should vary if the timing of hippocampal neurogenesis were conserved across humans and mice (solid lines, **Figures 6B,C**) According to these predictions from mice, human hippocampal neurogenesis as assessed from the relative number of Ki67+ and DCX+ cells should drop sharply between prenatal stages up until to 8–26 years of age and subsequently remain relatively invariant at later time points (**Figure 6B**). More specifically, the percentage of Ki67+ to total granule cells should drop up until about 8–26 years of age (post-conception day 3,000 to 10,000; **Figure 6**) and remain relatively invariant thereafter. Similarly, the relative number of DCX+ to total granule cells should drop from birth to about 8–26 years of age (post-conception day 3,000 to 10,000; **Figure 6C**).

On these predicted functions, we overlay the number of DCX+ and Ki67+ cells compared to total granule cells as reported by Boldrini et al. (2018). Our predictions are very generally consistent with those of Boldrini et al. (2018), in that we predict that both markers should remain relatively invariant from 8 to 26 years of age onward, but the added data do appear

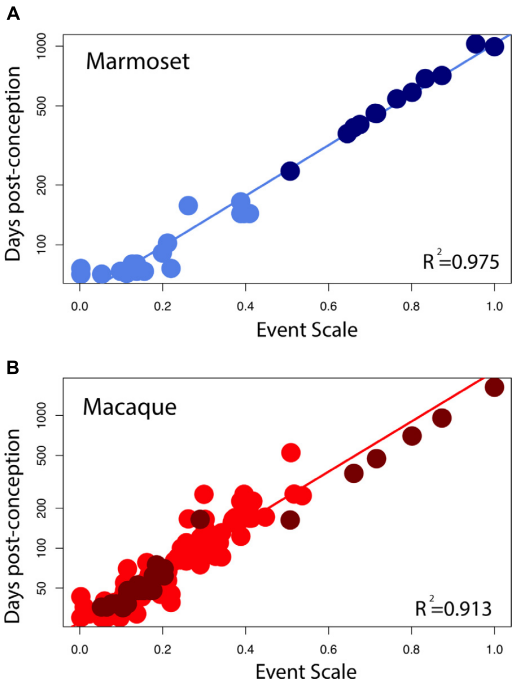

FIGURE 5 | Developmental milestones are plotted against the event scale in marmosets **(A)** and macaques **(B)**. Milestones that capture the timing of limbic neurogenesis are in dark blue (marmosets) and in dark red (macaque). We fit a linear regression through the logged values of the timing of developmental milestones against the event scale. Late hippocampal neurogenesis consistently falls below the regression. In other words, late hippocampal neurogenesis may occur earlier than expected given the timing of most developmental milestones in macaques.

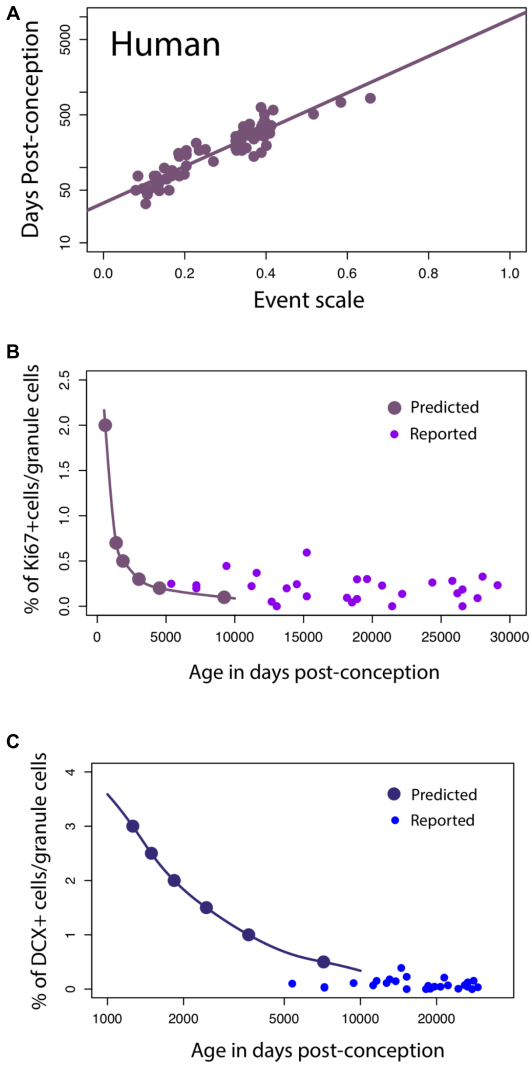

FIGURE 6 | (A) The timing of developmental milestones in humans are plotted against the event scale. We fit a regression through the timing of developmental transformations against age in days post-conception. We use this regression to predict the decline in late hippocampal neurogenesis in humans. **(B,C)** The number of Ki67+ **(B)** and DCX+ **(C)** cells relative to the total granule cell population is predicted to decline sharply during childhood in humans.

more variable, and the Ki67+ cell numbers higher than would be expected. Other data potentially addressing this timetable, that of Sorrells et al. (2018), could not be plotted against this representation because number of proliferative cells/mm^2 was assessed rather than relative to the total granule cell numbers determined in the rodent studies.

To investigate whether hippocampal neurogenesis timing in humans should deviate from that of rodents, we compare temporal changes in DCX expression in humans and mice. These data offer a slightly different perspective on the temporal pattern of late stages of hippocampal neurogenesis between species. We first note similarities between DCX RNA expression and the relative number of immature hippocampal granule cells assayed from single cell RNA sequencing data (**Supplementary Figure S2**). A qualitative investigation of DCX expression from multiple datasets in mice suggests that RNA sequencing from bulk data mirrors the temporal changes in the relative number of immature granule cells. As the relative number of granule cells declines in mice, DCX expression from bulk samples also declines sharply. At roughly 38–50 days post-conception, the relative number of immature granule cells varies relatively compared to earlier time points. That is, DCX expression is relatively invariant from 1 to 4 months of age in mice. In humans, DCX expression also decreases from prenatal time points up until around post-conception 316 (50 days after birth) and subsequently remains relatively invariant. According to the translating time model, 38–50 days post-conception in mice is roughly equivalent to 445–700 days post-conception in humans. In other words, the end in the abrupt decline in DCX expression might occur slightly earlier than expected in humans.

Because the presence of hippocampal neurogenesis has recently been questioned, we investigate whether hippocampal neurogenesis can be observed from single cell RNA sequencing obtained from the human hippocampus and prefrontal cortex (**Figure 7A**). We compare the number of cells expressing DPYSL3, DCX, and SOX2 relative to the number of PROX1 cells (**Figures 7B–E**). PROX1 is used as a marker of hippocampal granule cells and its expression is observed in previously identified excitatory hippocampal granule cells (cluster 8) and GABAergic cells (cluster 7). We computed the number of DCX+, SOX2+, and DPYSL3+ cells relative to the number of PROX1+ cells. We assess whether these values lie above chance level by comparing these values to those generated by permutation-based significance thresholds. Such an analysis shows that the SOX2+ and DPYSL3+ cell numbers relative to PROX1+ cell numbers occurs above the 99% confidence intervals of distributions generated from permutations (**Figures 7F–H**). However, the number of DCX+ to PROX1+ cells falls within the 99% confidence intervals generated from permutations. These findings suggest that human hippocampal neurogenesis is present at low but detectable numbers in the adult human brain but that DCX expression may drop to such low levels in adulthood that human hippocampal neurogenesis may be difficult to conclusively identify with DCX RNA expression.

DISCUSSION

Late Hippocampal Neurogenesis as an Extension of Development

When the dates and magnitudes of the long tail of declining late hippocampal neurogenesis are represented on the common maturational scale of the translating time procedure, it is clear that these events are continuous with early hippocampal neurogenesis, with little or no convincing evidence or hints of breaks or inflections. The translation of a maturational state to a particular duration of development is consistent with the normal translation seen in smaller versus larger brains.

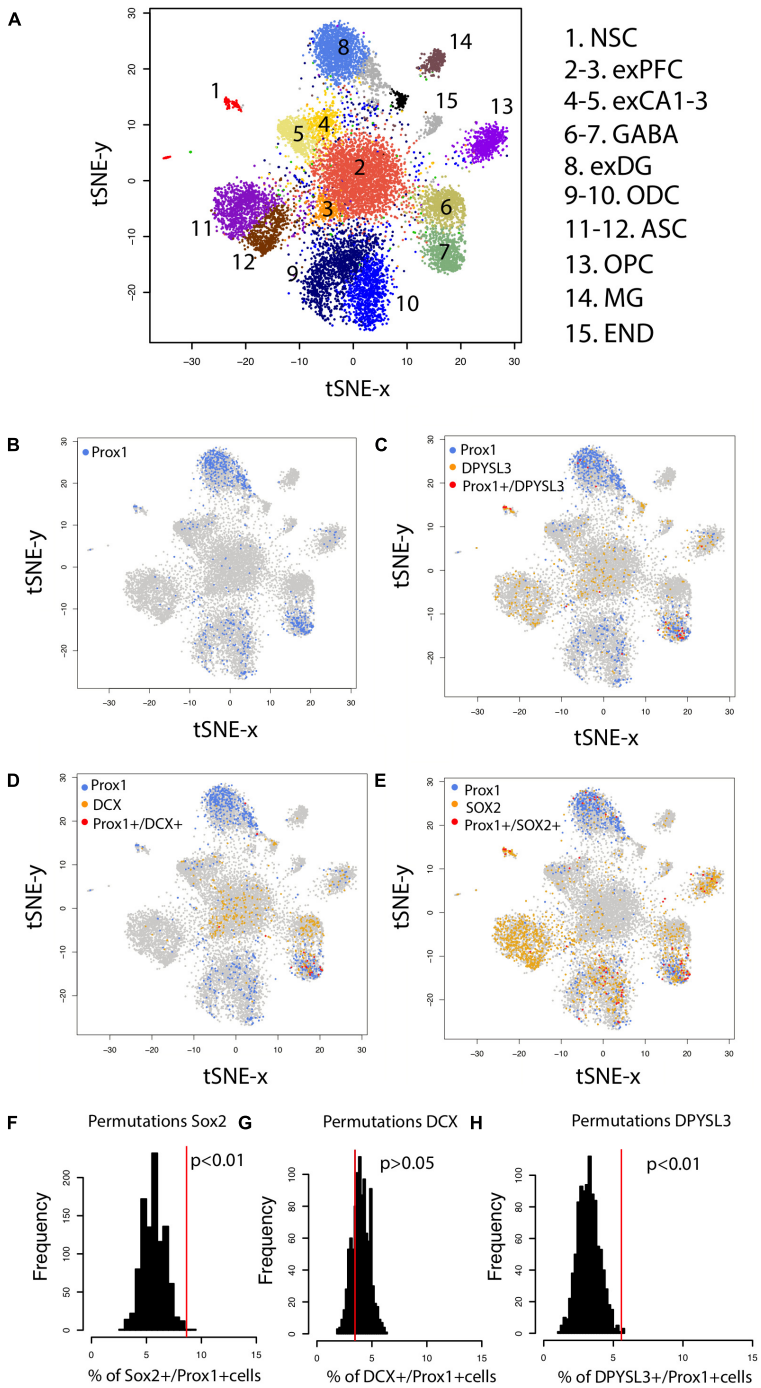

FIGURE 7 | (A) t_SNE plots of RNA expression from single cells extracted from the hippocampus and the prefrontal cortex of the human brain identifies clusters of cell populations. **(B)** PROX1 is used as a marker of hippocampal granule cells and its expression is observed in previously identified excitatory hippocampal granule cells (cluster 8) and GABAergic cells (cluster 7). **(C)** PROX1 co-localizes with genes expressed by immature neurons [**(D)** DPYSL3 **(E)** DCX **(F)** SOX2], which suggests that new granule cells are born in the human hippocampus. To identify whether DCX+, SOX2+, and DPYSL3+ collocate with PROX1+ cells above chance level, we randomly reassigned PROX1 expression to different neuronal types 1,000 times. We then extracted the number of DCX+, SOX2+, and DPYSL3+ cells relative to the number of PROX1+ cells 1,000 times **(F–H)**. Such an analysis shows that the SOX2+ **(F)** and DPYSL3+ **(H)** cell numbers relative to PROX1+ cell numbers occurs above the 99% confidence intervals generated from permutations. However, the number of DCX+ to PROX1+ cells falls within the 99% confidence intervals generated from permutations **(G)**. We removed cells belonging to clusters 9–15 from the analyses because they are identified as glia, astrocytic, microglia, and endothelial cell populations. We omit these cell types because our analysis is focused on identifying whether neurons rather than glial and endothelial cells are generated in the adult hippocampus. Data and identified clusters are from DroNc-Seq generated by Habib et al. (2017). Abbreviations: NSC, neural stem cells; exPFC, excitatory neurons in the prefrontal cortex; exCA1-3, excitatory neurons in CA1-3; exDG, excitatory neurons in dentate gyrus; ODC, oligodendrocytes; ASC, astrocytes; OPC, oligodendrocyte progenitors; MG, microglia; END, endothelial cells.

A structural correlate of duration of neurogenesis in the embryonic brain lends additional support to the conclusion that late hippocampal neurogenesis is an aspect of developmental neurogenesis in the brain. The embryonic brain first appears as a plate, with its caudal-to-rostral dimension comprised of repeating segments, the familiar spinal segments which undergo relatively little reorganization from embryo to adult, rhombomeres to the level of the midbrain (Lumsden and Krumlauf, 1996), and prosomeres in the telencephalon (Puelles et al., 2013; Albuixech-Crespo et al., 2017). The rhombomeric and prosomeric segments have repeating structural similarities, but undergo prolonged neurogenesis compared to the spinal cord, producing major changes in their appearance due to simple mass of neurons and neuronal migration. Important for the present purposes, the basal-to-alar dimension of the original neural plate is also a gradient in neurogenesis duration, shortest medially and longest laterally corresponding to, but not completely accounting for the number of neurons in each segment derived from each germinal position (Finlay et al., 1998; Workman et al., 2013). At the most lateral margin of the most anterior segments that produce the pallium, we find the zones that generate the olfactory bulb, the hippocampus, and the neocortex. This region collectively generates neurons for the longest duration, the first two continuing to add neurons well past the early developmental period. Thus, extended neurogenesis is a feature of the embryonic origin of the hippocampus, not a feature applied to an unpredictable location.

Limitations of the Database

Several caveats are in order, some about the translating time approach in general, and some about the particular procedures we used to incorporate this atypical corpus of data. While the translating time database is presently the only source integrating multiple aspects of developmental information over a large number of species, from a phylogenetic perspective, those species are anything but systematically or randomly chosen, featuring a large number of rodents and marsupials, relatively few primates, with the first New World primate appearing with this article, few large ungulates or carnivores and no cetaceans. As additions of new taxonomic groups or functionally defined groups, such as the precocial mammals in Workman et al. (2013) typically reveal new ways that neural development can be altered, blanket statements about "mammalian" neurogenesis should be avoided. So far, however, a few generalities can be made. Neurogenesis can begin very rapidly after the completion of the early germinal tissue, or it can be delayed while other tissues begin proliferation as is seen in some precocial mammals, but it always moves *en bloc*, and we have never observed breaks introduced into the overall sequence, as none were observed in this analysis. The onset and offset of neurogenesis in identified groups can be shifted, most frequently seen for the limbic versus neocortex shift described earlier, a neural variation extending back to sharks and rays (Finlay and Darlington, 1995; Reep et al., 2007; Yopak et al., 2010). Finally, while duration of neurogenesis is a very important aspect of brain evolution, it is important to keep in mind it is not the only source of variation, with medial–lateral axis location, for example, only accounting for about 50% of the variance in neuron number (Finlay et al., 1998).

We estimated the relative timing of the decline in hippocampal neurogenesis not by a complete recomputation of the model to include the new observations, but rather by extrapolating the former model, duration extending almost by a factor of 2 in mice and more in the larger species, a substantial amount. It is possible that this procedure could mis-estimate the slope of the decline fairly substantially, but it seemed reasonable to attempt a first description. We did note that macaques appeared to begin initial hippocampal neurogenesis slightly earlier and end earlier than expected given the timing of surrounding, non-hippocampal events. Ideally, other late developmental events should be used to anchor these observations, at which point the overall model will be recalculated, but defined points become harder to identify in later development. Continued reduction of neuron density in most structures in later development as well as spatiotemporal changes in RNA expression are potential candidates, but these approaches have rarely been employed systematically across a broad range of species.

Developmental Timing in Marmosets

The inclusion of marmosets in the present study was intended to allow better comparisons between primate species, particularly because information on late hippocampal neurogenesis was available for it. We were somewhat thwarted in this enterprise, however, because we did not observe the simple translation for production of a smaller brain expected from the pattern laid out in rhesus macaques. Rather, early developmental events were delayed with respect to conception, then maturation proceeded rapidly, consistent with the marmoset's smaller brain, and finally, late developmental events occurred earlier than predicted. A delay followed by rapid maturation was a pattern we had observed before, however, in precocial rodents and ungulates (Workman et al., 2013). Why the rate of neural development does not simply slow to take advantage of the extra time *in utero* is unclear. We have not yet observed any case of slowing of rate of neural production in eutherian mammals, although marsupials generate neural tissue at a slower rate overall (Darlington et al., 1999). Marmosets do have small brains compared to macaques, and perhaps to have time to generate the body, it is necessary to delay the onset of generation of the brain, to avoid producing a post-mature brain while still *in utero* if no change in its rate of development is possible. In a prior study of retinal neurogenesis in the owl monkey, *Aotus*, compared to the capuchin monkey *Cebus apella*, we had notice that gestational lengths were longer than we had anticipated from earlier work in Old World monkeys (Dyer et al., 2009). The reason for this potential difference in life history parameters will require more observations in the marmoset, and other New World monkeys as well.

The Timing of Late Stages of Human Hippocampal Neurogenesis and the Problems of Detecting Rare Events

We used the timing of developmental transformation across non-human mammalian species to predict the timing of late stages of hippocampal neurogenesis in humans. If the timing

of hippocampal neurogenesis is conserved across humans, marmosets, and rodents, hippocampal neurogenesis as assessed from the relative number of DCX+ and Ki67+ to total granule cells should drop sharply up until 8–26 years of age and remain low and invariant at later time points. Sorrells et al. (2018) showed that the relative number of Ki67+ and DCX+ cells drop sharply during childhood up until 7–13 years of age, consistent with our predictions in humans. The question is whether human hippocampal neurogenesis ends earlier than expected given the developmental allometries of late developmental events. It is presently difficult to determine whether human hippocampal neurogenesis does indeed deviate from predictions generated from rodents. However, the work of Boldrini et al. (2018), using similar techniques demonstrates low and invariant human hippocampal neurogenesis between the ages of 14 and 79 years, but a markedly higher incidence than the prior studies.

We found inconsistent evidence for late hippocampal neurogenesis in humans within our own study. Our analysis of RNA sequences from single cells showed that the relative number of immature neurons to PROX1 (i.e., a marker of granule cells) were observed at greater than chance levels in adult humans. However, the relative number of DCX+/PROX1 is unusually low and fell below chance levels as assessed from our permutation-based significance thresholds. Whether DCX expression is expressed at high enough levels for it to be reliably detected in the adult human brain is unclear. Although the number of potential confounds to detection of immature neurons are many, including retention of immature neuron morphology in displaced populations until adulthood (Piumatti et al., 2018); unusual levels of genetic variation (Kaushal et al., 2003) as well as all of the problems of processing human tissue, developmental scaling plays a role as well.

As mentioned at the outset of this discussion, different components of the same tissue may scale in altogether different ways with respect to brain size and developmental duration. As a rule of thumb, with the usual number of exceptions, cell-based properties do not scale with brain size or developmental duration. As cells essentially depend on diffusion for many critical metabolic factors, in at least one plane of section, neuron diameter cannot scale with brain size (long axons, but not fat ones, are acceptable). Oxidative metabolism, action potentials and most other cellular processes ignore animal mass. How about the cell cycle? The cell cycles of initial neurogenesis take similar amounts of time in small and large brains (Takahashi et al., 1994; Charvet and Striedter, 2008). The duration of the cell cycle becomes longer and longer as maturation proceeds, not by uniform elongation of every part, but particularly the quiescent period; in addition, fewer and fewer cells contribute to the cell cycle (Takahashi et al., 1994; Kornack and Rakic, 1998; Charvet and Striedter, 2008). We have claimed, though, that the termination of hippocampal neurogenesis looks quite similar in its overall envelope across the rodents, monkeys and the human we measured. This is with respect to these animals' maturational state, however, not their age in days. A back-of-napkin calculation of the duration of equivalent maturational periods from early "childhood" to death would be about 700 days for rats and about 25,000 days for a human. The initial spatial densities for Ki67 and DCX+ are roughly similar (**Figure 3**). It seems unlikely that generating a neuron would require 36 times longer in humans, or that the features of a young neuron would persist a similar long duration. On the other hand, the migration and integration of new neurons into circuits has been reported to take very much longer in adults, exceeding 6 months (Kohler et al., 2011). Thus, an empirical question remains, as it is unclear if these patterns represent a maintained state, or a transitory event. If they are time-limited events, the chance of registering such an event in the slice of time caught by a brain slice will be radically different in short- and long-lived mammals, and comparisons must take these basic scaling features into account.

AUTHOR CONTRIBUTIONS

BF and CC designed the study, analyzed the data, and wrote the study. Both authors read and approved the manuscript.

FUNDING

This work was supported by an NIH 1F32HD067011-01A1 fellowship to CC as well as an NSF grant, and by research chair support from the W. R. Kenan Jr. Charitable Trust to BF.

ACKNOWLEDGMENTS

RNA sequencing data from human hippocampi were taken from the Allen Institute Website, which are supported by the NIH Contract HHSN-271-2008-00047-C to the Allen Institute for Brain Science. The opinions in this article are not necessarily those of the NIH. We thank Dr. Marnin Wolfe for helpful statistical discussions.

SUPPLEMENTARY MATERIAL

The Supplementary Material for this article can be found online at: https://www.frontiersin.org/articles/10.3389/fnins.2018.00706/full#supplementary-material

FIGURE S1 | PROX1 is more strongly expressed in the hippocampus than in other regions and is a marker of granule cells. **(A)** PROX1 expression from RNA-seq data from humans between 19 and 40 years of age is greater in the hippocampus than in prefrontal cortical regions. An ANOVA followed by a TUKEY HSD test shows that PROX1 is significantly more expressed in the hippocampus compared with prefrontal cortical regions in humans (ANOVA, TUKEY HSD, $p < 0.01$). **(B)** *In situ* hybridization through a sagittal and coronal section of mouse brain at post-natal day 56 and 24 months of age shows that Prox1 is strongly expressed in granule cells of the hippocampus but not in the isocortex. Abbreviations: HIP, hippocampus; dPFC, dorsal prefrontal cortex; vPFC, ventral prefrontal cortex; aPFC, anterior cingulate cortex; oPFC, orbital frontal cortex; ISO, isocortex. These data are from the Allen Brain Atlas.

FIGURE S2 | (A) Normalized DCX expression from bulk hippocampal samples and the number of immature granule cells as assessed from single cell RNA sequencing data in mice are plotted against the age in days post-conception in mice. We see strong concordance between RNA expression from bulk samples and the relative number of immature granule cells. DCX expression steadily declines with the relative number of immature granule cells. After 150 days of age, the number of immature granule cells as well as DCX expression level off. **(B)** In humans, DCX expression falls abruptly until 1,000 days of post-conception.

TABLE S1 | Developmental event timing data-set.

TABLE S2 | Predicted developmental time points between marmosets, and other species.

REFERENCES

Albuixech-Crespo, B., López-Blanch, L., Burguera, D., Maeso, I., Sánchez-Arrones, L., and Moreno-Bravo, J. A. (2017). Molecular regionalization of the developing amphioxus neural tube challenges major partitions of the vertebrate brain. *PLoS Biol.* 15:e2001573. doi: 10.1371/journal.pbio.2001573

Amrein, I., Isler, K., and Lipp, H. P. (2011). Comparing adult hippocampal neurogenesis in mammalian species and orders: influence of chronological age and life history stage. *Eur. J. Neurosci.* 34, 978–987. doi: 10.1111/j.1460-9568.2011.07804.x

Amrein, I., Nosswitz, M., Slomianka, L., van Dijk, R. M., Engler, S., and Klaus, F. (2015). Septo-temporal distribution and lineage progression of hippocampal neurogenesis in a primate (*Callithrix jacchus*) in comparison to mice. *Front. Neuroanat.* 9:85. doi: 10.3389/fnana.2015.00085

Andreae, L. C. (2018). Adult neurogenesis in humans: dogma overturned, again and again? *Sci. Trans. Med.* 10:eaat3893.

Barton, R. A., and Venditti, C. (2013). Human frontal lobes are not relatively large. *Proc. Natl. Acad. Sci. U.S.A.* 110, 9001–9006. doi: 10.1073/pnas.1215723110

Ben Abdallah, N. M., Slomianka, L., Vyssotski, A. L., and Lipp, H. P. (2010). Early age-related changes in adult hippocampal neurogenesis in C57 mice. *Neurobiol. Aging* 31, 151–161. doi: 10.1016/j.neurobiolaging.2008.03.002

Boldrini, M., Fulmore, C. A., Tartt, A. N., Simeon, L. R., Pavlova, I., and Poposka, V. (2018). Human hippocampal neurogenesis persists throughout aging. *Cell Stem Cell.* 22, 589.e5–599.e5. doi: 10.1016/j.stem.2018.03.015

Cahalane, D., Charvet, C. J., and Finlay, B. L. (2014). Modeling local and cross-species neuron number variations in the cerebral cortex as arising from a common mechanism. *Proc. Natl. Acad. Sci. U.S.A.* 111, 17642–17647. doi: 10.1073/pnas.1409271111

Chaplin, T. A., Yu, H.-H., Soares, J. G., Gatass, R., and Rosa, M. G. P. (2013). A conserved pattern of differential expansion of cortical areas in simian primates. *J. Neurosci.* 33, 15120–15125. doi: 10.1523/JNEUROSCI.2909-13.2013

Charvet, C. J., Cahalane, D. J., and Finlay, B. L. (2015). Systematic, cross-cortex variation in neuron numbers in rodents and primates. *Cereb. Cortex* 25, 147–160. doi: 10.1093/cercor/bht214

Charvet, C. J., Darlington, R. B., and Finlay, B. L. (2013). Variation in human brains may facilitate evolutionary change toward a limited range of phenotypes. *Brain Behav. Evol.* 81, 74–85. doi: 10.1159/000345940

Charvet, C. J., and Finlay, B. L. (2014). Evo-devo and the primate isocortex: the central organizing role of intrinsic gradients of neurogenesis. *Brain Behav. Evol.* 84, 81–92. doi: 10.1159/000365181

Charvet, C. J., Hof, P. R., Raghanti, M. A., Kouwe, A. J., Sherwood, C. C., and Takahashi, E. (2017a). Combining diffusion magnetic resonance tractography with stereology highlights increased cross-cortical integration in primates. *J. Comp. Neurol.* 525, 1075–1093. doi: 10.1002/cne.24115

Charvet, C. J., Šimić, G., Kostović, I., Knezović, V., Vukšić, M., Leko, M. B., et al. (2017b). Coevolution in the timing of GABAergic and pyramidal neuron maturation in primates. *Proc. R. Soc. B* 284:20171169. doi: 10.1098/rspb.2017.1169

Charvet, C. J., and Striedter, G. F. (2008). Developmental species differences in brain cell cycle rates between northern bobwhite quail (*Colinus virginianus*) and parakeets (*Melopsittacus undulatus*): implications for mosaic brain evolution. *Brain Behav. Evol.* 72, 295–306. doi: 10.1159/000184744

Charvet, C. J., and Striedter, G. F. (2010). Bigger brains cycle faster before neurogenesis begins: a comparison of brain development between chickens and bobwhite quail. *Proc. R. Soc. B* 277, 3469–3475. doi: 10.1098/rspb.2010.0811

Cipriani, S., Ferrer, I., Aronica, E., Kovacs, G. G., Verney, C., and Nardelli, J. (2018). Hippocampal radial Glial subtypes and their neurogenic potential in human fetuses and Healthy and Alzheimer's Disease Adults. *Cereb. Cortex* 28, 2458–2478. doi: 10.1093/cercor/bhy096

Clancy, B., Darlington, R. B., and Finlay, B. L. (2000). The course of human events: predicting the timing of primate neural development. *Dev. Sci.* 3, 57–66. doi: 10.1111/1467-7687.00100

Clancy, B., Darlington, R. B., and Finlay, B. L. (2001). Translating developmental time across mammalian species. *Neuroscience* 105, 7–17. doi: 10.1016/S0306-4522(01)00171-3

Clancy, B., Kersh, B., Hyde, J., Anand, K. J. S., Darlington, R. B., and Finlay, B. L. (2007). Web-based method for translating neurodevelopment from laboratory species to humans. *Neuroinformatics* 5, 79–94. doi: 10.1385/NI:5:1:79

Darlington, R. B., Dunlop, S. A., and Finlay, B. L. (1999). Neural development in metatherian and eutherian mammals: variation and constraint. *J. Comp. Neurol.* 411, 359–368. doi: 10.1002/(SICI)1096-9861(19990830)411:3<359::AID-CNE1>3.0.CO;2-J

Dennis, C. V., Suh, L. S., Rodriguez, M. L., Kril, J. J., and Sutherland, G. T. (2016). Human adult neurogenesis across the ages: an immunohistochemical study. *Neuropathol. Appl. Neurobiol.* 42, 621–638. doi: 10.1111/nan.12337

Dyer, M. A., Martins, R., da Silva Filho, M., Muniz, J. A., Silveira, L. C. L., Cepko, C., et al. (2009). Developmental sources of conservation and variation in the evolution of the primate eye. *Proc. Natl. Acad. Sci. U.S.A.* 106, 8963–8968. doi: 10.1073/pnas.0901484106

Fan, X., Dong, J., Zhong, S., Wei, Y., Wu, Q., and Yan, L. (2018). Spatial transcriptomic survey of human embryonic cerebral cortex by single-cell RNA-seq analysis. *Cell Res.* 28, 730–745. doi: 10.1038/s41422-018-0053-3

Finlay, B. L., and Clancy, B. (2008). *Chronology of the Development of the Mouse Visual System. Eye, Retina and Visual System of the Mouse*, eds L. Chalupa and R. W. Williams (Cambridge, MA: MIT Press), 257–265.

Finlay, B. L., and Darlington, R. B. (1995). Linked regularities in the development and evolution of mammalian brains. *Science* 268, 1578–1584. doi: 10.1126/science.7777856

Finlay, B. L., Darlington, R. D., and Nicastro, N. (2001). Developmental structure of brain evolution. *Behav. Brain Sci.* 24, 263–308. doi: 10.1017/S0140525X01003958

Finlay, B. L., Hersman, M. N., and Darlington, R. B. (1998). Patterns of vertebrate neurogenesis and the paths of vertebrate evolution. *Brain Behav. Evol.* 52, 232–242. doi: 10.1159/000006566

Finlay, B. L., Hinz, F., and Darlington, R. B. (2011). Mapping behavioral evolution onto brain evolution: the strategic roles of conserved organization in individuals and species. *Philos. Trans. R. Soc. B* 366, 2111–2123. doi: 10.1098/rstb.2010.0344

Finlay, B. L., and Uchiyama, R. (2017). "The timing of brain maturation, early experience, and the human social niche," in *Evolution of Nervous Systems 2e*, Vol. 3, ed. J. Kaas (Oxford: Elsevier), 123–148.

Finlay, B. L., and Workman, A. J. (2013). Human exceptionalism. *Trends Cogn. Sci.* 17, 199–201. doi: 10.1016/j.tics.2013.03.00

Fleagle, J. G. (1985). "Size and adaptation in primates," in *The Lesser Apes: Evolutionary and Behavioral Biology*, eds H. Preuschoft, D. Chivers, W. Brockelman, and N. Creel (Edinburgh: Edinburgh University Press), 1–19.

Freckleton, R. P., Harvey, P. H., and Pagel, M. (2002). Phylogenetic analysis and comparative data: a test and review of evidence. *Am. Nat.* 160, 712–726. doi: 10.1086/343873

Garwicz, M., Christiansen, M., and Psouni, E. (2009). A unifying model for timing of walking onset in humans and other mammals. *Proc. Natl. Acad. Sci. U.S.A.* 106, 21889–21893. doi: 10.1073/pnas.0905777106

Gould, S. J. (1975). Allometry in primates, with emphasis on scaling and the evolution of the brain. *Contrib. Primatol.* 5, 244–292.

Habib, N., Avraham-Davidi, I., Basu, A., Burks, T., Shekhar, K., and Hofree, M. (2017). Massively parallel single-nucleus RNA-seq with DroNc-seq. *Nat. Methods* 14, 955–958. doi: 10.1038/nmeth.4407

Halley, A. C. (2016). Prenatal brain-body allometry in mammals. *Brain Behav. Evol.* 88, 14–24. doi: 10.1159/000447254

Halley, A. C. (2017). Minimal variation in eutherian brain growth rates during fetal neurogenesis. *Proc. Roy. Soc. B* 284:20170219. doi: 10.1098/rspb.2017.0219

Hawkes, K., and Finlay, B. L. (2018). Mammalian brain development and the evolution of our grandmothering life history. *Physiol. Behav.* 193, 55–68. doi: 10.1016/j.physbeh.2018.01.013

Herculano-Houzel, S., Collins, C. E., Wong, P., and Kaas, J. H. (2007). Cellular scaling rules for primate brains. *Proc. Natl. Acad. Sci. U.S.A.* 104, 3562–3567. doi: 10.1073/pnas.0611396104

Hikishima, K., Sawada, K., Murayama, A. Y., Komaki, Y., Kawai, K., and Sato, N. (2013). Atlas of the developing brain of the marmoset monkey constructed using magnetic resonance histology. *Neuroscience* 230, 102–113. doi: 10.1016/j.neuroscience.2012.09.053

Hochgerner, H., Zeisel, A., Lönnerberg, P., and Linnarsson, S. (2018). Conserved properties of dentate gyrus neurogenesis across postnatal development revealed by single-cell RNA sequencing. *Nat. Neurosci.* 21, 290–299. doi: 10.1038/s41593-017-0056-2

Hofman, M. A. (1989). On the evolution and geometry of the brain in mammals. *Prog. Neurobiol.* 32, 137–158. doi: 10.1016/0301-0082(89)90013-0

Iacono, G., Benevento, M., Dubos, A., Herault, Y., Bokhoven, H., Kasri, N. N., et al. (2017). Integrated transcriptional analysis unveils the dynamics of cellular differentiation in the developing mouse hippocampus. *Sci. Rep.* 7:18073. doi: 10.1038/s41598-017-18287-w

Jabès, A., Lavenex, P. B., Amaral, D. G., and Lavenex, P. (2010). Quantitative analysis of postnatal neurogenesis and neuron number in the macaque monkey dentate gyrus. *Eur. J. Neurosci.* 31, 273–285. doi: 10.1111/j.1460-9568.2009.07061.x

Jerison, H. J. (1973). *Evolution of the Brain and Intelligence*. New York, NY: Academic Press.

Jerison, H. J. (1989). *Brain Size and the Evolution of Mind. The 59th James Arthur Lecture on the Evolution of the Human Brain*. New York, NY: American Museum of Natural History, 1–99.

Jerison, H. J. (1997). "Evolution of prefrontal cortex," in *Development of the Prefrontal Cortex: Evolution, Neurobiology and Behavior*, eds N. A. Krasnegor, G. R. Lyon, and P. S. Goldman-Rakic (Baltimore, MA: Brooks Publishing Co.), 9–26.

Kaas, J. H., and Herculano-Houzel, S. (2017). "What makes the human brain special: key features of brain and neocortex," in *The Physics of the Mind and Brain Disorders. Springer Series in Cognitive and Neural Systems*, Vol. 11, eds I. Opris and M. Casanova (Cham: Springer).

Kaushal, D., Contos, J. J., Treuner, K., Yang, A. H., Kingsbury, M. A., Rehen, S. K., et al. (2003). Alteration of gene expression by chromosome loss in the postnatal mouse brain. *J. Neurosci.* 23, 5599–5606. doi: 10.1523/JNEUROSCI.23-13-05599.2003

Kempermann, G., Gage, F. H., Aigner, L., Song, H., Curtis, M. A., and Thuret, S. (2018). Human adult neurogenesis: evidence and remaining questions. *Cell Stem Cell* 23, 25–30. doi: 10.1016/j.stem.2018.04.004

Knoth, R., Singec, I., Ditter, M., Pantazis, G., Capetian, P., and Meyer, R. P. (2010). Murine features of neurogenesis in the human hippocampus across the lifespan from 0 to 100 years. *PLoS One* 5:e8809. doi: 10.1371/journal.pone.0008809

Kohler, S. J., Williams, N. I., Stanton, G. B., Cameron, J. L., and Greenough, W. T. (2011). Maturation time of new granule cells in the dentate gyrus of adult macaque monkeys exceeds six months. *Proc. Natl. Acad. Sci. U.S.A.* 108, 10326–10331. doi: 10.1073/pnas.1017099108

Kornack, D. R., and Rakic, P. (1998). Changes in cell-cycle kinetics during the development and evolution of primate neocortex. *Proc. Natl. Acad. Sci. U.S.A.* 95, 1242–1246. doi: 10.1073/pnas.95.3.1242

Lee, H., and Thuret, S. (2018). Adult human hippocampal neurogenesis: controversy and evidence. *Trends Mol. Med.* 24, 521–522. doi: 10.1016/j.molmed.2018.04.002

Lumsden, A., and Krumlauf, R. (1996). Patterning the vertebrate neuraxis. *Science* 274, 1109–1115. doi: 10.1126/science.274.5290.1109

Merrill, D. A., Karim, R., Darraq, M., Chiba, A. A., and Tuszynski, M. H. (2003). Hippocampal cell genesis does not correlate with spatial learning ability in aged rats. *J. Comp. Neurol.* 459, 201–207. doi: 10.1002/cne.10616

Ming, G.-L., and Song, H. (2005). Adult neurogenesis in the mammalian central nervous system. *Ann. Rev. Neurosci.* 28, 223–250. doi: 10.1146/annurev.neuro.28.051804.101459

Ngwenya, L. B., Peters, A., and Rosene, D. L. (2006). Maturational sequence of newly generated neurons in the dentate gyrus of the young adult rhesus monkey. *J. Comp. Neurol.* 498, 204–216. doi: 10.1002/cne.21045

Passingham, R. E. (1985). Rates of brain development in mammals including man. *Brain Behav. Evol.* 26, 167–175. doi: 10.1159/000118773

Passingham, R. E., and Smaers, J. B. (2014). Is the prefrontal cortex especially enlarged in the human brain allometric relations and remapping factors. *Brain Behav. Evol.* 84, 156–166. doi: 10.1159/000365183

Piumatti, M., Palazzo, O., La Rosa, C., Crociara, P., Parolisi, R., and Luzzati, F. (2018). Non-newly generated, "immature" neurons in the sheep brain are not restricted to cerebral cortex. *J. Neurosci.* 38, 826–842. doi: 10.1523/JNEUROSCI.1781-17.2017

Puelles, L., Harrison, M., Paxinos, G., and Watson, C. (2013). A developmental ontology for the mammalian brain based on the prosomeric model. *Trends Neurosci.* 36, 570–578. doi: 10.1016/j.tins.2013.06.004

Rao, M. S., Hattiangady, B., and Shetty, A. K. (2006). The window and mechanisms of major age-related decline in the production of new neurons within the dentate gyrus of the hippocampus. *Aging Cell* 6, 545–558. doi: 10.1111/j.1474-9726.2006.00243.x

Reep, R., Darlington, R. B., and Finlay, B. L. (2007). The limbic system in mammalian brain evolution. *Brain Behav. Evol.* 70, 57–70. doi: 10.1159/000101491

Remtulla, S., and Hallet, P. E. (1985). A schematic eye for the mouse and comparisons with the rat. *Vis. Res.* 25, 21–31. doi: 10.1016/0042-6989(85)90076-8

Schoenemann, P. T. (2006). Evolution of the size and functional areas of the human brain. *Annu. Rev. Anthropol.* 35, 379–406. doi: 10.1146/annurev.anthro.35.081705.123210

Semendeferi, K., Lu, A., Schenker, N., and Damasio, H. (2002). Humans and great apes share a large frontal cortex. *Nat. Neurosci.* 5, 272–276. doi: 10.1038/nn814

Sherwood, C. C., and Smaers, J. B. (2013). What's the fuss over human frontal lobe evolution? *Trends Cogn. Sci.* 17, 432–433. doi: 10.1016/j.tics.2013.06.008

Smith, C. L., Blake, J. A., and Kadin, J. A. (2018). Mouse Genome Database (MGD)-2018: knowledgebase for the laboratory mouse. *Nucleic Acids Res.* 46, D836–D842. doi: 10.1093/nar/gkx1006

Sorrells, S. F., Paredes, M. F., Cebrian-Silla, A., Sandoval, K., Qi, D., and Kelley, K. W. (2018). Human hippocampal neurogenesis drops sharply in children to undetectable levels in adults. *Nature* 555, 377–381. doi: 10.1038/nature25975

Takahashi, T., Nowakowski, R. S., and Caviness, V. S. (1994). Mode of cell proliferation in the developing mouse neocortex. *Proc. Natl. Acad. Sci. U.S.A.* 91, 375–379. doi: 10.1073/pnas.91.1.375

Workman, A. D., Charvet, C. J., Clancy, B., Darlington, R. B., and Finlay, B. L. (2013). Modeling transformations of neurodevelopmental sequences across mammalian species. *J. Neurosci.* 33, 7368–7383. doi: 10.1523/JNEUROSCI.5746-12.2013

Yopak, K., Lisney, T., Collin, S. E., Montgomery, J., Darlington, R. B., and Finlay, B. L. (2010). Brain scaling from sharks to primates: a highly conserved vertebrate pattern. *Proc. Natl. Acad. Sci. U.S.A.* 107, 12946–12951. doi: 10.1073/pnas.1002195107

Zhong, S., Zhang, S., Fan, X., Wu, Q., Yan, L., and Dong, J. (2018). A single-cell RNA-seq survey of the developmental landscape of the human prefrontal cortex. *Nature* 555, 524–528. doi: 10.1038/nature25980

Conflict of Interest Statement: The authors declare that the research was conducted in the absence of any commercial or financial relationships that could be construed as a potential conflict of interest.

frontiers in Neuroscience

ORIGINAL RESEARCH
published: 19 December 2017
doi: 10.3389/fnins.2017.00719

Effects of Strain and Species on the Septo-Temporal Distribution of Adult Neurogenesis in Rodents

Franziska Wiget[1], *R. Maarten van Dijk*[1,2], *Estelle R. Louet*[1], *Lutz Slomianka*[1,3] *and Irmgard Amrein*[1,3]*

[1] Division of Functional Neuroanatomy, Institute of Anatomy, University of Zurich, Zurich, Switzerland, [2] Institute of Pharmacology, Toxicology and Pharmacy, Ludwig-Maximilian-University, Munich, Germany, [3] Department of Health Sciences and Technology, ETH Zurich, Zurich, Switzerland

The functional septo-temporal (dorso-ventral) differentiation of the hippocampus is accompanied by gradients of adult hippocampal neurogenesis (AHN) in laboratory rodents. An extensive septal AHN in laboratory mice suggests an emphasis on a relation of AHN to tasks that also depend on the septal hippocampus. Domestication experiments indicate that AHN dynamics along the longitudinal axis are subject to selective pressure, questioning if the septal emphasis of AHN in laboratory mice is a rule applying to rodents in general. In this study, we used C57BL/6 and DBA2/Crl mice, wild-derived F1 house mice and wild-captured wood mice and bank voles to look for evidence of strain and species specific septo-temporal differences in AHN. We confirmed the septal > temporal gradient in C57BL/6 mice, but in the wild species, AHN was low septally and high temporally. Emphasis on the temporal hippocampus was particularly strong for doublecortin positive (DCX+) young neurons and more pronounced in bank voles than in wood mice. The temporal shift was stronger in female wood mice than in males, while we did not see sex differences in bank voles. AHN was overall low in DBA and F1 house mice, but they exhibited the same inversed gradient as wood mice and bank voles. DCX+ young neurons were usually confined to the subgranular zone and deep granule cell layer. This pattern was seen in all animals in the septal and intermediate dentate gyrus. In bank voles and wood mice however, the majority of temporal DCX+ cells were radially dispersed throughout the granule cell layer. Some but not all of the septo-temporal differences were accompanied by changes in the DCX+/Ki67+ cell ratios, suggesting that new neuron numbers can be regulated by both proliferation or the time course of maturation and survival of young neurons. Some of the septo-temporal differences we observe have also been found in laboratory rodents after the experimental manipulation of the molecular mechanisms that control AHN. Adaptations of AHN under natural conditions may operate on these or similar mechanisms, adjusting neurogenesis to the requirements of hippocampal function.

Keywords: doublecortin, Ki67, *Apodemus sylvaticus*, *Myodes glareolus*, *Mus domesticus*

OPEN ACCESS

Edited by:
Paolo Peretto,
Università degli Studi di Torino, Italy

Reviewed by:
Martine Migaud,
INRA CNRS UMR7247, France
María Llorens Martín,
Universidad Autonoma de Madrid, Spain

***Correspondence:**
Irmgard Amrein
irmgard.amrein@hest.ethz.ch

Specialty section:
This article was submitted to Neurogenesis, a section of the journal Frontiers in Neuroscience

Received: *16 October 2017*
Accepted: *08 December 2017*
Published: *19 December 2017*

Citation:
Wiget F, van Dijk RM, Louet ER, Slomianka L and Amrein I (2017) Effects of Strain and Species on the Septo-Temporal Distribution of Adult Neurogenesis in Rodents. Front. Neurosci. 11:719. doi: 10.3389/fnins.2017.00719

INTRODUCTION

There has been a long-standing interest in differences between the septal and temporal hippocampus, which are expressed by specific behavioral effects after septal or temporal lesions (e.g., Hughes, 1965; Moser et al., 1995), differences in the relative abundance of cell types (e.g., Gaarskjaer, 1978; Jinno and Kosaka, 2006), or efferent and afferent connections (Ishizuka et al., 1990; Agster and Burwell, 2013; Prasad and Chudasama, 2013). Such differences were typically thought to reflect gradual changes along an anatomical and functional septo-temporal continuum. Recently, detailed genomic studies (Thompson et al., 2008; Dong et al., 2009; Cembrowski et al., 2016a,b) suggest a functional differentiation within hippocampal principal cell populations (reviewed by Fanselow and Dong, 2010; Strange et al., 2014), which may subserve different functions in different septo-temporal segments. The septal hippocampus has been associated with cognition (Moser et al., 1995; Bannerman et al., 1999; Kjelstrup et al., 2008; Reichel et al., 2017). The intermediate hippocampus has been proposed to integrate the septally mediated visuospatial information with the motivational behavioral control for precise place learning which is translated into behavior (Bast, 2007; Bast et al., 2009; Barker et al., 2017). The interconnection of the temporal hippocampus with the amygdala (Felix-Ortiz et al., 2013) and its control of the HPA-axis (Herman et al., 1995; Lowry, 2002; Belujon and Grace, 2015) emphasizes its role in stress coping and anxiety-related behaviors (Fanselow and Dong, 2010).

In view of the functional differentiation of the hippocampal formation itself, it is not surprising that septo-temporal differences are also observed in one of the phenomena that it hosts—adult hippocampal neurogenesis (AHN). In most species that have been investigated, AHN is higher in the septal than in the temporal dentate gyrus (Uchida et al., 2005; Jinno, 2011b; Snyder et al., 2012; Amrein et al., 2015; Lowe et al., 2015). Interestingly, domestication selectively increases the number and distribution of doublecortin-positive neuroblasts and differentiating young neurons in the temporal dentate gyrus of foxes, a species in which temporal AHN is also higher than septal AHN (Huang et al., 2015). We have recently shown that AHN is a strong differentiator between rodent species (van Dijk et al., 2016a), in which the extent of AHN may relate to factors as diverse as habitat conditions (Cavegn et al., 2013) or social status (Oosthuizen and Amrein, 2016). The differentiation by AHN between species living under different natural conditions strongly implies an adaptive value. Considering the ontogenetic plasticity of AHN in response to experimental manipulation of the external or internal environment, it seems reasonable to expect that septo-temporal gradients in baseline AHN may be affected as well. Such gradients can become phylogenetically fixed if they are adaptive to the environment that represents a species niche. In this context, defining species-specific septo-temporal profiles for AHN in wild and laboratory-bred rodents may pinpoint, in which functional domain of the hippocampus one ought to look for the adaptive value of AHN.

Our data have, so far, been equivocal with regard to septo-temporal phylogenetic effects. While we did see such effects associated with domestication in foxes (Huang et al., 2015), we also found rather similar septo-temporal distributions of proliferating cells and differentiating young neurons in a comparison of C57BL/6 mice with New World monkeys (Amrein et al., 2015). In the present study, we therefore focused on two wild rodent species, which we previously found to differ from each other (Amrein et al., 2004a,b), that is bank voles (*Myodes glareolus*) and long-tailed wood mice (*Apodemus sylvaticus*). We also used F1 offspring of wild-captured house mice (*Mus domesticus*) to study if domestication may impact septo-temporal features of AHN in mice. Large differences in AHN were seen between different strains of laboratory mice (Kempermann et al., 1997; Hayes and Nowakowski, 2002; Kempermann and Gage, 2002b). We included C57BL/6 and DBA strains to compare them to the wild species and their wild-derived house mouse conspecifics. In DBA mice, far fewer new neurons are generated than in C57BL/6 mice (Kempermann et al., 2006; van Dijk et al., 2016b), and AHN reacts differently to experimental interference (Overall et al., 2013). Such strain differences may also extend to septo-temporal differences in AHN. For all mice, proliferation and neuronal differentiation were studied using Ki67 and doublecortin (DCX) as markers for proliferation and neuronal differentiation. To facilitate comparisons at different septo-temporal levels in different strains and species, these markers were applied to sections of extracted and physically extended hippocampi.

MATERIALS AND METHODS

Animals

Eighty four rodents of different strains and species were investigated (**Table 1**). C57BL/6, DBA2/Crl and house mice were 4.5–5.5 month old, while the age of wild trapped mice was unknown. All experimental work was conducted under the permits #26394 (laboratory and house mice) and #27034 (wild mice) of the Canton of Zürich veterinary office.

Trapping and Housing

Wild bank voles and wood mice were trapped at three locations (Zürich, Rifferswil, Trüllikon) in the canton of Zürich, Switzerland. Baited Sherman traps were set along hedges and scrubs from late afternoon to 4 h into darkness, traps were checked at 2–3 h intervals. Under isoflurane anesthesia, trapped animals were implanted subcutaneously with identification transponders (Planet ID GmbH, Germany) in the dorsal neck region, checked for health, gender, and signs of pregnancy, and treated against ectoparasites (Stronghold 15 mg, Selamectin, one drop). Animals were then single housed for 3 weeks. During this period, animals were fed *ad libitum* with anti-endoparasitic mouse food (Ivermectin, Kliba SA, Switzerland). Afterwards, animals were grouped according to species and sex. Groups of maximal nine adult animals were housed in a set of two to four tube-connected cages. All cages contained ample bedding and nesting material (tissue, hay, cardboard boxes) and *ad libitum* access to commercial mouse food and water. Group housed laboratory and house mice were kept in the same animal facility as wild mice. Lighting conditions corresponded to the

TABLE 1 | Study animals.

Species/strain	Number/sex	Source	Body weight (g)	Brain weight (g)
C57BL/6	16 female	Charles River Laboratories, Germany	24.9 ± 2.0	0.48 ± 0.02
DBA2/Crl	16 female	Charles River Laboratories, Germany	24.3 ± 1.7	0.41 ± 0.01
House mouse *(Mus domesticus)*	13 female	Department of Evolutionary Biology and Environmental Studies, University of Zürich: F1 of wild trapped animals	24.5 ± 3.5	0.47 ± 0.04
Long-tailed wood mouse *(Apodemus sylvaticus)*	8 female	Wild trapped	*f* : 24.4 ± 3.9	*f* : 0.58 ± 0.03
	8 male		*m* : 28.3 ± 4.1	*m* : 0.59 ± 0.04
Bank vole *(Myodes glareolus)*	12 female	Wild trapped	*f* : 21.1 ± 3.4	*f* : 0.54 ± 0.06
	11 male		*m* : 24.3 ± 3.4	*m* : 0.52 ± 0.03

natural light cycle in late summer (light on 07:00–19:00). All mice underwent the same behavioral testing in IntelliCages (Galsworthy et al., 2005) for 31 days before perfusion. Analysis of the behavioral tests is ongoing.

Perfusion and Dissection

Animals were deeply anesthetized with pentobarbital-Na intraperitoneally (50 mg/kg body weight) and perfused transcardially with 1% paraformaldehyde (PFA) solution containing 15% picric acid. Hippocampi were dissected, straightened and post-fixed in 4% PFA in this position for 5 h as described before (Amrein et al., 2015). The left and right hippocampi of each animal were randomly assigned to further processing.

Gelatin Embedding

For immunohistochemistry, one hippocampus of each animal was transferred into 20% glycerol in 0.1M phosphate-buffered saline (PBS, pH = 7.2) for cryoprotection overnight at 4°C. A gelatin matrix was used for tissue embedding as described in Smiley and Bleiwas (2012). Gelatin-egg albumin solution in 0.9% NaCl was prepared and mixed with 37% formaldehyde as hardener of the matrix. A 2.5M lysine solution and 25% glutaraldehyde at a ratio of 1:1 served as a cross-linking reagent. Mixed solution was poured as a base layer into embedding forms, four hippocampi were placed under the surface of the base layer. After setting of the base layer, a top layer of gelatin matrix was added. The hardened gelatin blocks were immersed in 20% glycerol. 40 µm sections were cut on a sliding microtom (HM 430, Thermo Fisher Scientific, Waltham, MA) equipped with a freezing stage. Sections were cut perpendicular to the hippocampal longitudinal (septo-temporal) axis and collected in 10 series. One series was collected in PBS in well plates and mounted in correct anatomical order (reference series). These sections were Giemsa stained (Iñiguez et al., 1985) (Giemsa stock solution 1.09204.1000. Merck, Darmstadt, Germany). Nine series were stored in cryoprotective solution (CPS) at −20°C until further processing.

Immunohistochemistry

We used the endogenous proliferation marker Ki67 (Starborg et al., 1996; Cuylen et al., 2016; Sobecki et al., 2016) and the young neuron marker doublecortin (DCX; Matsuo et al., 1998). Test sections of all species and strains were used to titrate antibody concentrations that generated optimal signal-to-noise ratios and a saturated signal for the strongest stained cells. Every tenth section (one series) of each hippocampus was processed free-floating. Sections were rinsed in Tris-Triton (Tris-buffered saline (TBS), pH = 7.4 with 0.05% Triton). For epitope retrieval, sections were heat-treated for 45 min at 90°C in citrate buffer (Dako REAL, Glostrup, Denmark) diluted 1:10 in distilled water. Pre-incubation was done for 1 h in 2% normal horse serum (NHS) for Ki67 and 2% normal rabbit serum (NRS) for DCX in Tris-Triton with 0.2% Triton. Incubation with primary antibody in pre-incubation buffer followed over night at 4°C (Ki67: monoclonal mouse-anti-Ki67, BD Pharming, 1:1,000–1:3,000; DCX: polyclonal goat-anti-DCX, Santa Cruz, 1:4,000–1:8,000; for DBA mice in addition monoclonal mouse-anti-DCX, Santa Cruz, 1:50, and polyclonal rabbit-anti-DCX, Abcam, 1:1,000 were used). Thereafter, rinsed sections were incubated in biotinylated secondary antibody (all Vectastain Elite kits, Vector Laboratories, Burlingame, CA, USA, 1:1,000) diluted in TBS, 2% serum and 0.1% bovine serum albumin (BSA). Incubation in avidin-biotin-peroxidase complex (Vectastain Elite kits) was followed by staining with diaminobenzidine and H_2O_2 (Sigmafast™, D4418-50SET, Sigma-Aldrich, Steinheim, Germany) in distilled water. Mounted sections were embedded with Mowiol 4-88 (Ki67) diluted in glycerol and PBS (v/v) in a ratio of 1:3 (Sigma-Aldrich, Steinheim, Germany), or counterstained with hematoxylin solution (DCX) (Sigma-Aldrich, Steinheim, Germany) and embedded with Eukitt.

Cell Quantification

Quantification of the two markers Ki67 and DCX was performed applying design-based stereological methods (West et al., 1991, for stereology-specific parameters see **Table 2**). The investigations were carried out using the StereoInvestigator software v10.50 (MBF Bioscience, Williston, Vermont, USA) on a Zeiss Axio Imager 2 microscope, and blinded with regard to mouse identity, strain and species.

For the estimation of the total number of DCX-positive cells (DCX+), the optical fractionator of the StereoInvestigator software was used (West et al., 1991). Every tenth section was analyzed (section sampling fraction (ssf) = 1/10). Step sizes between sampling locations were determined using data from estimates of the area of the region of interest in pilot animals. Counting frame sizes (see **Table 2**) that returned, on

TABLE 2 | Total estimated cell numbers (unilateral) and associated stereological parameters.

Species/strain	Mean	Min	Max	*SD*	Mean CE = 0	CE^2/CV^2	Counting frame, μm (X, Y)	Sampling grid, μm(X, Y)	Disector height, μm	Evaluation interval	Mean sections analyzed
DCX											
C57BL/6	5,954	4,087	9,750	1,250	0.09	0.19	45 × 45	75 × 75	40	10	14
DBA	1,418	660	3,070	638	0.07	0.02	Exhaustive counts		40	10	14
House mouse	3,192	1,028	8,111	1,708	0.13	0.06	45 × 45	75 × 75	40	10	13
Wood mouse	12,480	4,849	20,445	5,043	0.07	0.03	55 × 55	85 × 85	40	10	18
Bank vole	10,956	2,069	17,149	4,139	0.07	0.03	55 × 55	85 × 85	40	10	20
Ki67											
C57BL/6	3,811	2,550	6,180	820	0.06	0.08	Exhaustive counts		40	10	14
DBA	1,211	900	1,780	208	0.09	0.28			40	10	14
House mouse	1,752	780	2,780	599	0.08	0.06			40	10	13
Wood mouse	10,839	2,260	24,490	5,648	0.04	0.01			40	10	19
Bank vole	5,011	1,270	11,410	2,309	0.04	0.01			40	10	20

average, more than one count from the sampling locations were determined by trials of differently sized frames. Cells were counted in the anatomically ordered sections using a 63× oil immersion objective (Zeiss, Plan-Apochromat/1.4 oil DIC). Nuclei of DCX+ cells were counted throughout the entire section thickness of 40 μm. To avoid oversampling, DCX+ cells that had their counterstained nucleus in focus in the focal plane that first touched the uppermost surface of the section were not counted. Following Disector counting rules (Sterio, 1984; West et al., 1991), only the nuclei of DCX+ cells that appeared in focus in the subsequent focal planes were included into the counts. We found DCX+ cells not only in the subgranular layer, but in some animals also within the granule cell layer. In eight randomly chosen animals, DCX+ cells in the subgranular layer were assessed separately from more superficial DCX+ cells between granule cells. Estimation of total cell number (N) for DCX+ cells was calculated using the following formula: $N = \sum Q^- \cdot \frac{1}{asf} \cdot \frac{1}{ssf}$, where $\sum Q^-$ is the total number of counted cells. The area sampling fraction (asf) is calculated from the area of a counting frame, divided by the area associated with every step in x- and y direction ($\frac{a(counting\ frame)}{a(x,y\ step)}$).

Ki67-positive (Ki67+) proliferating cells in the subgranular layer of the dentate gyrus were counted exhaustively using a 63× oil immersion objective (Zeiss, Plan-Apochromat/1.4 oil DIC), again excluding Ki67+ nuclei that appeared in focus in the uppermost focal plane of a section. The anatomical order of the sections was determined by comparison of the sections with the reference series. Estimates of total Ki67+ cell number per hippocampus were calculated by multiplying the total counts by the section sampling fraction (ssf) of 10.

Definition of the Septal, Intermediate and Temporal Part of the Hippocampus

Acquisition of cell numbers were performed in the dissected and straightened hippocampi. Data of Ki67+ and DCX+ cells in each section in the correct anatomical order from septal to temporal were standardized for all animals into 12 virtual sections (bins) as described by Amrein et al. (2015). In short, raw data from each real section was divided into 12 sub-bins, corresponding to the desired number of virtual sections. Cell numbers for each virtual section was generated by successively pooling the cell numbers of these sub-bins. The number of pooled sub-bins corresponded to the number of the real sections available for an animal.

The division into equally sized septal, intermediate and temporal subdivision of the hippocampus was then applied on these 12 virtual sections. One third representing the septal (virtual sections 1–4), one third representing the intermediate (virtual sections 5–8) and one third representing the temporal (virtual sections 9–12) subdivisions of the hippocampus were used for graphical presentation and analysis.

Statistical Analysis

To assess estimate precision, the Coefficient of Error (*CE*) was calculated (Gundersen et al., 1999; Slomianka and West, 2005) for cell counts.

Statistical analyses and graphics were compiled using R software (version 3.3.2). The standardized data of Ki67+ and DCX+ cells within the septal, intermediate and temporal subdivision were used. To account for age-related differences between and within species and strains, values in the virtual sections were recalculated as the percentage of the total estimated cell number for each animal. Nested two-way ANOVA with gender as covariate was used to test for species/strain-specific differences in the relative distribution of Ki67+ and DCX+ cells in the three septo-temporal subdivisions. Tukey *post-hoc* analyses were performed when the main effect was found to be significant. Within species, the distribution of DCX+ cells and gender related differences was tested using a nested one-way ANOVA.

RESULTS

Species-Specific Rates of AHN

Estimates of the total numbers of proliferating cells and young neurons were not statistically tested between species and strains, as the age of wild trapped animals was not assessed. The numerical data obtained (**Table 2**) do however confirm previously found species and strain differences. Wild house mice

showed lower AHN than laboratory C57BL/6 (Klaus et al., 2012). Bank voles, lower in cell proliferation when compared to wood mice, had high numbers of DCX+ cells. This observation has been made previously in the comparison of bank voles with yellow-necked wood mice (Amrein et al., 2004b; van Dijk et al., 2016a), and may be due to attenuated cell death observed in this species (Amrein et al., 2004a). Proliferation in DBA laboratory mice was equal to previously reported data in this strain and at this age (van Dijk et al., 2016b), however DCX counts were unexpectedly lower. Repeating the estimates using three different DCX antibodies yielded similar results.

Differences in Septo-Temporal AHN Gradients

We observed striking differences in the distribution of proliferating Ki67+ cells and young neurons (DCX+ cells) along the septo-temporal axis in the five rodent species and strains (**Figure 1**). While C57BL/6 showed an emphasis on neurogenesis in the septal subdivision, all other rodent species had more neurogenesis toward the temporal hippocampus. Statistical comparisons on standardized data revealed a significant main effect for species and strains in the distribution of DCX+ cells (**Figure 2A**) along the hippocampal axis [$F_{(4, 77)} = 11.36$, $p < 0.0001$]. Furthermore, a strong interaction was found for species/strains and septo-temporal subdivisions [$F_{(8, 154)} = 9.05$, $p < 0.0001$]. *Post-hoc* comparison in the septal subdivision showed C57BL/6 to have higher DCX values than all other species (comparison wood mouse $p = 0.004$; bank vole, house mouse and DBA all < 0.0001), while DBA, bank voles, wood mice and house mice did not differ from each other. In the intermediate subdivision, bank voles showed higher DCX values than C57BL/6, DBA and house mice ($p = 0.029$, 0.01, and 0.004, respectively), the difference to wood mice did not reach significance ($p = 0.07$). All other pairwise comparisons were non-significant in the intermediate subdivision. C57BL/6 differ again in the temporal subdivision, by having significantly lower DCX values than all other species (wood mouse $p = 0.049$, bank vole 0.024, DBA and house mouse $p < 0.0001$). No further significant species differences were found in the temporal subdivision. We found no overall effect of species and strains in the distribution of Ki67+ cells (**Figure 2B**) along the septo-temporal axis [$F_{(4, 77)} = 1.52$, $p = 0.21$]. Interaction between species/strains and septo-temporal subdivision however was significant [$F_{(8, 154)} = 7.46$, $p < 0.0001$]. Within the septal

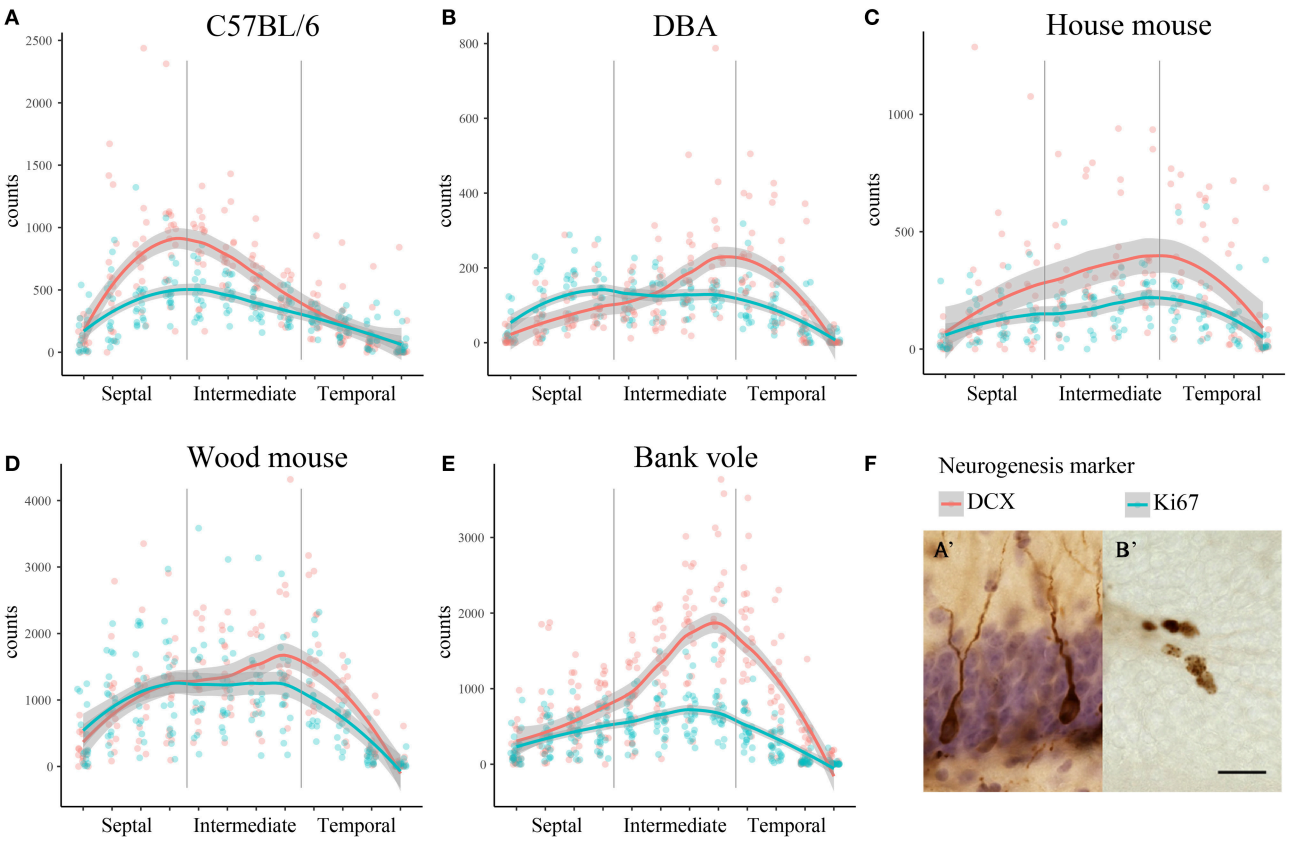

FIGURE 1 | Distribution of neurogenesis-related absolute cell counts along the septo-temporal axis. Neurogenesis assessment in dissected, straightened hippocampi in laboratory C57BL/6 **(A)** follows a general septal>temporal gradient, whereas DBA **(B)**, house mice **(C)**, wood mice **(D)**, and bank voles **(E)** show a septal<temporal gradient for young neurons (DCX), and, except for DBA, also for cell proliferation (Ki67). Raw data of cell counts were re-distributed into 12 virtual sections to allow direct comparisons within and between species/strains, gray areas indicate 95% confidence intervals. **(F)** Shows representative images of hematoxylin-counterstained DCX+ young neurons **(A')** and Ki67+ cells **(B')** in the subgranular layer of the dentate gyrus. Scale bar = 20 μm.

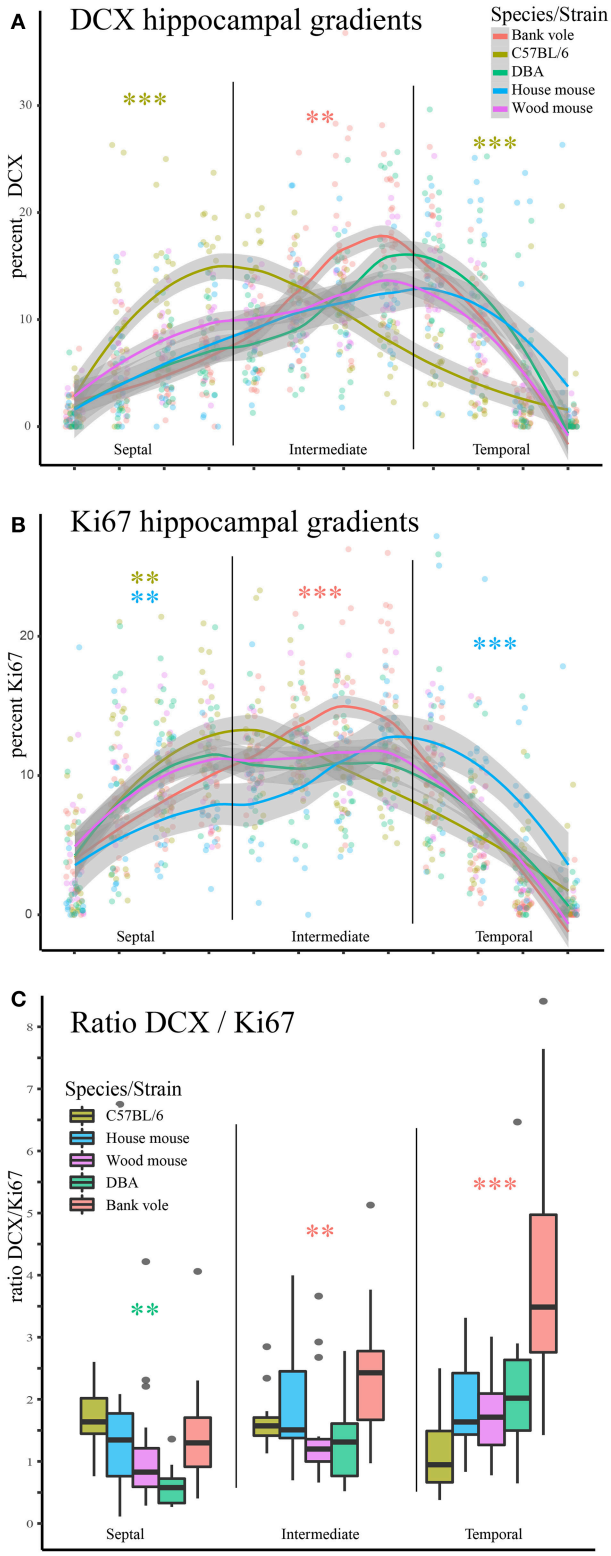

FIGURE 2 | Opposite neurogenesis gradient in laboratory C57BL/6. Values of young neurons and proliferating cells were re-calculated as percentage for each animal to allow statistical comparisons. **(A)** C57BL/6 is distinct from other species and strains in the septal subdivision with significantly more young *(Continued)*

FIGURE 2 | neurons than all other species (all $p < 0.01$) and significantly fewer young neurons in the temporal subdivision (all comparisons $p < 0.05$). In the intermediate hippocampus, bank voles have higher DCX values than C57BL/6, DBA and house mice. **(B)** Septo-temporal distribution of proliferating cells is overall more similar, however, in the septal subdivision the extremes are represented by C57BL/6 (high) and house mice (low), which are significantly different from DBA, bank voles and wood mice. In the intermediate hippocampus, bank voles score higher than all other species ($p = 0.002$ to < 0.0001). In the temporal subdivision house mice have more proliferating cells than all other species ($p = 0.006$ to < 0.0001). As a proxy for young neuron survival, the ratio of DCX+ cells to Ki67+ cells is presented in **(C)**, separately for the three hippocampal subdivision. Survival rate is lowest in DBA in the septal subdivision. Bank voles score higher in survival rate than DBA and wood mice in the intermediate ($p < 0.01$). In the temporal subdivision, neuronal survival in bank voles excels all other species values ($p < 0.001$). $^*p < 0.05$, $^{**}p < 0.01$, and $^{***}p < 0.001$; color-coding corresponds to the species/strain showing the difference, for exact values see results.

subdivision, C57BL/6 showed higher Ki67 values compared to bank voles and house mice ($p = 0.04$ and $p = 0.004$). House mice on the other hand have significantly fewer Ki67+ cells than DBA and wood mice ($p = 0.005$ and 0.02). In the intermediate subdivision, bank voles had higher Ki67 values than all other species ($p = 0.002$ to < 0.0001). In the temporal subdivision, house mice differed from all other species in having the highest Ki67 values ($p = 0.006$ to < 0.0001). All animals had more DCX+ and Ki67+ cells in the intermediate part than in the septal or temporal subdivision (**Table 3**).

Differences in the DCX/Ki67 Ratio

As a proxy for young neuron survival, we also assessed the ratios of DCX+ cells to Ki67+ cells (**Figure 2C**). Overall, there are significant differences between strains and species [$F_{(4, 77)} = 9.51$, $p < 0.0001$] and an interaction between strain/species differences in the DCX/Ki67 ratio in the hippocampal subdivisions [$F_{(8, 154)} = 10.97$, $p < 0.0001$]. *Post-hoc* comparison for the septal subdivision suggests a lower survival rate in DBA compared to bank voles, house mice and C56BL/6 ($p = 0.041$, 0.028, and 0.006 respectively). In the intermediate subdivision, bank voles have a higher DCX/Ki67 ratio than wood mice and DBA ($p = 0.009$ and 0.003). Temporally, the DCX/Ki67 ratio of bank voles exceeded that of all other species (all $p < 0.0001$). All other comparisons did not show significant differences.

Radial Position of DCX+ Cells in Wild Mice

Among all 84 quantified animals, some animals showed widely scattered DCX+ cells along the radial axis of the dentate gyrus. DCX+ cells were found in the subgranular zone (SGZ, **Figures 3A,A'**) and in the dentate granule cell layer proper (GCL, **Figures 3B,B'**). Eight animals with this phenotype were randomly selected when animal identity was still blinded, and DCX+ cells were assessed separately in the SGZ and GCL. Out of the five investigated species, the selected animals exhibiting this phenotype were exclusively either wood mice or bank voles. The binomial probability of the sample to only contain wood mice and bank voles ($n = 39$) if this trait was distributed at random in all species and strains ($n = 84$) would be $(39/84)^8 = 0.002$. Overall, we found in these two species a significant main effect

TABLE 3 | Percentage of neurogenesis-related cells in the three hippocampal subdivision.

Species/strain	DCX			Ki67		
	Septal (%)	Intermediate (%)	Temporal (%)	Septal (%)	Intermediate (%)	Temporal (%)
C57BL/6	40	46	14	37	44	19
DBA	20	44	36	36	42	22
House mouse	19	43	38	24	42	34
Wood mouse	22	48	30	33	46	21
Bank vole	15	56	29	26	58	16

of the radial axis distribution of DCX+ cells [$F_{(2, 14)} = 17.8$, $p < 0.001$] and a significant interaction between the radial distribution of young neurons and hippocampal subdivision ($p < 0.0001$). *Post-hoc* tests revealed that DCX+ cells in the SGZ predominate in the septal [$F_{(1, 14)} = 50.7$, $p < 0.001$] and intermediate [$F_{(1, 14)} = 14.7$, $p = 0.002$] subdivision, while in the temporal subdivision DCX+ cells found in the GCL proper are more common [$F_{(1, 14)} = 36.2$, $p < 0.001$, **Figure 3C**]. With the caveats of small samples and unequal group sizes, there was no difference between the two wood mice and six bank voles within this sample (data not shown).

Sex-Related Differentiation along the Septo-Temporal Axis in Wood Mice

In wood mice and bank voles, animals of both sexes were available, and gender differences in distribution of proliferating and differentiating cells were tested for. The percentage of DCX+ young neurons did show a gender effect in wood mice for the distribution along the septo-temporal axis [$F_{(1, 14)} = 9.91$, $p = 0.007$, **Figure 4A**], and an interaction of gender with septo-temporal subdivisions [$F_{(2, 28)} = 3.87$, $p = 0.033$]. *Post-hoc* tests revealed that in the septal subdivision, female wood mice have lower DCX values then males ($p = 0.03$), the intermediate subdivisions did not differ ($p = 0.62$), and in the temporal subdivision females had higher DCX values ($p = 0.0499$). The percentage of Ki67+ cells did not show a gender effect [$F_{(1, 14)} = 2.44$, $p = 0.14$] in wood mice. We also found no gender × subdivision interaction for Ki67 [$F_{(2, 28)} = 0.875$, $p = 0.43$]. Likewise, bank vole female and males did not differ in the distribution of Ki67+ cells along the septo-temporal axis [$F_{(1, 21)} = 0.046$, $p = 0.83$], and there was also no gender x subdivision interaction [$F_{(2, 42)} = 1.48$, $p = 0.24$]. Gender differences for DCX in bank voles were absent as well [$F_{(1, 21)} = 0.45$, $p = 0.51$, **Figure 4B**]. Neither could interactions between gender and septo-temporal subdivisions be found in bank voles [$F_{(2, 42)} = 1.42$, $p = 0.25$].

DISCUSSION

Opposing Septo-Temporal Gradients of Hippocampal Neurogenesis in Closely Related Rodents

Structural and functional specificity along the longitudinal axis of the hippocampus have been reported repeatedly (Fanselow and Dong, 2010; Kesner, 2013; Poppenk et al., 2013; Strange et al., 2014), with gradients of adult hippocampal neurogenesis (AHN) fitting well into this framework (Wu et al., 2015). The age related decline of AHN (Ben Abdallah et al., 2010; Amrein et al., 2011) has septo-temporally different effects on the relative densities of progenitor cell populations and a larger overall effect in the temporal dentate gyrus (Jinno, 2011a). The maturation of septally generated cells is faster than that of temporally generated ones (Piatti et al., 2011; Snyder et al., 2012), which, in turn, can be selectively accelerated by voluntary exercise (Piatti et al., 2011). Ritalin (Lagace et al., 2006), seizures (Ferland et al., 2002; Häussler et al., 2012) or GABA-receptor blockade (Felice et al., 2012) increase AHN more temporally than septally. Unpredictable stress results in a larger temporal decrease in AHN (Tanti et al., 2012), while acute stress appears to increase septal AHN (Kirby et al., 2013). Rats that display learned helplessness after inescapable shocks show a decrease of septal AHN, whereas AHN is not affected in rats that do not display this behavior (Ho and Wang, 2010). Behavioral effects specific to the ablation of AHN in the septal or temporal dentate gyrus have also been found (Wu and Hen, 2014). Different septo-temporal effects may be explained by the distribution of progenitors with septo-temporally differing stimulus sensitivities (Jhaveri et al., 2015) or suppressed activity of temporal stem cells (Sun et al., 2015).

Reports in rats, mice, gerbils and primates support a septal > temporal gradient for neurogenesis (Dawirs et al., 1998; Teuchert-Noodt et al., 2000; Snyder et al., 2009b, 2012; Jinno, 2011b; Amrein et al., 2015; Bekiari et al., 2015). Our data on C57BL/6 follow the same pattern. Neurogenesis is high septally and lowest in the temporal dentate gyrus. However, we observe the opposite gradient in DBA, house mice, wood mice and bank voles, in which neurogenesis is higher temporally than septally. The shift toward a higher temporal AHN is more pronounced in female wood mice as compared to male wood mice. The inverted gradient in these species is, to some extent, apparent in proliferation, neuronal differentiation and the ratio of DCX/Ki67 positive cells. As observed before in a larger and phylogenetically more diverse sample of species (Amrein et al., 2011), cell proliferation is less variable across species. It also appears more restricted with respect to a septo-temporal differentiation, as we found no main effect in the distribution of Ki67-positive cells between species. The largest differences between strains and species are observed for DCX+ young neurons. This cell population may either modulate local network circuitry or regulate hippocampus-dependent behaviors

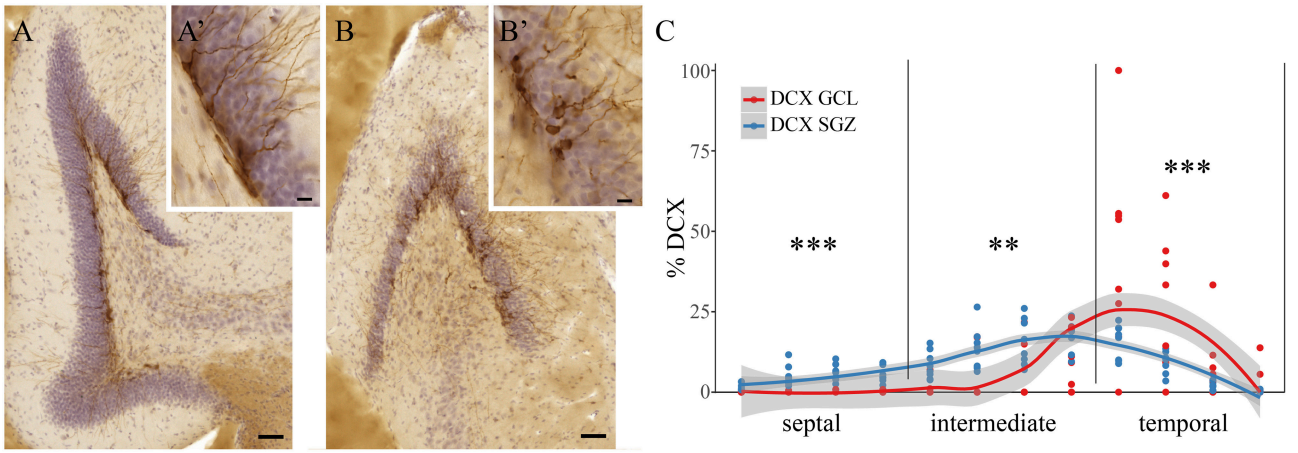

FIGURE 3 | Radial location of DCX positive cells in bank voles and wood mice. DCX+ cells in wild rodents are not only found in the subgranular zone (SGZ, **A,A'**), but are found dispersed throughout the granular cell layer (GCL, **B,B'**). Quantitative assessment of DCX+ cells in the SGZ vs. those cells within the GCL reveals differences along the septo-temporal axis **(C)**. While DCX+ cells in the SGZ predominate in the septal and intermediate hippocampus, significantly more DCX+ cells are found within the granule cell layer in the temporal subdivision. Scale bare **(A,B)** = 50 μm; **(A',B')** = 10 μm. $^{**}p < 0.01$, and $^{***}p < 0.001$; for exact values see results.

attributed to the septal or temporal hippocampus (Wu et al., 2015) according to species-specific needs. In particular, bank voles show a strong emphasis on a contribution of young neurons in the temporal hippocampal function. This is likely due to an increased or extended survival of young neurons in the temporal dentate gyrus.

Neurogenesis and the Hippocampal Longitudinal Axis

Gene expression studies (Thompson et al., 2008) do indicate a division into three domains, while behavioral (Moser and Moser, 1998) and electrophysiological studies (Patel et al., 2012, 2013) demarcate a temporal third from the (combined) septal-intermediate two-thirds (summarized in Strange et al., 2014). A smooth long-axis gradient as described for hippocampal connectivity (Amaral and Witter, 1989; Witter, 1993) and place field sizes (Kjelstrup et al., 2008) could have been a possible approach to analysis as well. Our partition of the hippocampus into equally sized subdivisions (septal, intermediate and temporal) is somewhat arbitrary, but roughly corresponds to the divisions that have been suggested and is independent of anatomical landmarks that may depend on the orientation of the sections when the hippocampus is cut *in situ*. Tanti and Belzung (2013) have previously emphasized the problems associated with comparisons of experimental outcomes that arise from variable *in situ* demarcations between septal and temporal hippocampus. Our approach to analyze dissected hippocampi cut perpendicular to their long axis allowed for comparisons between species with similar body sizes but different brain and hippocampal sizes with minimal data distortion. This approach has also been used previously to overcome the ambiguities of other definitions (Gaarskjaer, 1978; Rapp and Amaral, 1988; Jinno and Kosaka, 2006; Snyder et al., 2009b; Amrein et al., 2015; Sun et al., 2015). We took care to present the data in graphs visualizing the entire longitudinal axis. Beyond a septo-temporal differentiation, our data also indicate that neurogenesis shows few differences between strains or species in an intermediate subdivision and that this subdivision harbors the highest percentages of proliferating cells and young neurons in all species, accounting for ∼50% of all Ki67+ and DCX+ cells. Research in gradients has focused primarily on the septal and/or temporal pole, either by investigating septal and temporal parts, or by dividing the hippocampus into two areas (Wu et al., 2015). To our knowledge, neurogenesis has not been experimentally manipulated selectively in the intermediate hippocampus. fMRI recordings of the optogenetically stimulated intermediate hippocampus (Weitz et al., 2015) indicate a special role of this hippocampal subdivision by its widespread yet distinct cortical and subcortical network activation. Specific inactivation of the intermediate hippocampus by lesions or pharmacogenetic deactivation in rats shows that the intermediate hippocampus is necessary for spatial components of episodic memory (Barker et al., 2017) and sufficient to translate rapid place learning into a behavioral response (Bast et al., 2009). Our finding of high neurogenesis in the intermediate hippocampus in all species and strains further emphasizes the importance of this subdivision in the context of AHN.

Tame and Wild

Defensive behavior, independent of prior experience, and adequate unconditioned fear responses in rats rely on an intact temporal hippocampus (Kjelstrup et al., 2002). There is a large body of evidence that a stress response is mediated by projections from the temporal subiculum to the basolateral amygdala and dorsomedial hypothalamus (reviewed by Lowry, 2002; Belujon and Grace, 2015). It should be pointed out here that the behavior of wild rodents brought into the laboratory is radically different from that of laboratory strains. Wild rodents do everything to avoid human contact and take painful defensive measures if it

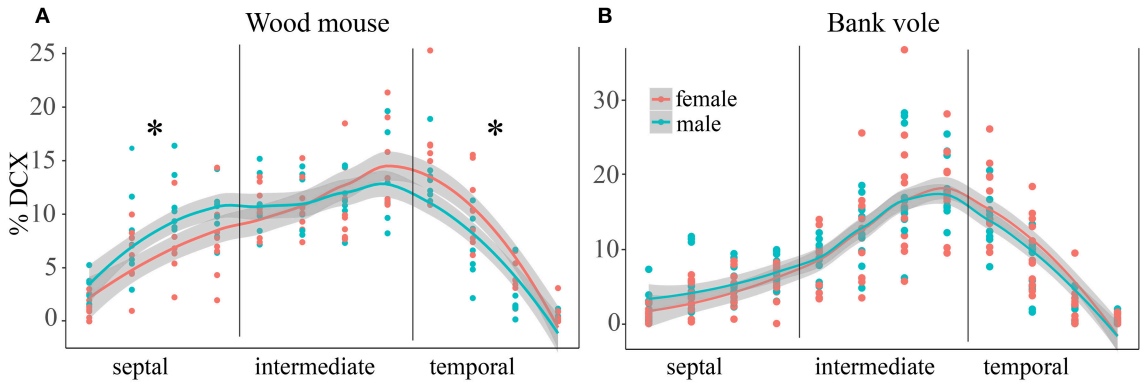

FIGURE 4 | Sex differences in DCX+ cells in wood mice along the hippocampal axis. The septal < temporal gradient in DCX+ cell distribution is more pronounced in female wood mice **(A)** as compared to males. Septally, they have lower values than males, while temporally females DCX+ values exceed those of males. In bank voles **(B)**, males and females do not differ with regard to DCX+ cell distribution along the septo-temporal axis. *$p < 0.05$; for exact values see results.

cannot be avoided. They are very skillful jumpers and will leap out of the cages for safety if given the smallest opportunity. Such behaviors are adaptive in the natural environment of wild mice, but selective pressures that result from the environment (e.g., predation) have been absent or even been replaced by selection for docility in the laboratory (Goto et al., 2013). The behavior of the F1 generation of wild house mice used here was indeed still very "wild-type" like. Differences in behavior should therefore be reflected in differences of temporal hippocampal function, and such differences apparently encompass a higher number of temporal generated young neurons in wild rodents used in this study. The unexpected wild-type-like temporal AHN in DBA mice may support this idea. Although poorer performers than C57BL/6 in many hippocampal-dependent spatial learning tasks (Ammassari-Teule et al., 1992; Jones et al., 2001), they show a better passive avoidance learning, which, in contrast to C57BL/6 mice, is not impaired by septal NMDA receptor antagonist infusion (Mineur et al., 2007; Baarendse et al., 2008). They also show less freezing in fear conditioning tasks than C57BL/6 mice (Baarendse et al., 2008) that is not altered by chronic mild stress (Mineur et al., 2007).

DCX/Ki67 Ratio, Cell Maturation and Survival

Changes in the ratio between DCX+ and Ki67+ cell numbers may be generated by at least three different mechanisms. The duration of expressions of DCX or Ki67 in the cells may change. Ki67 is expressed during S, G2, and M phases of the cell cycle, but only late during G1. Considering the short duration of G1 in cycling progenitors (Lewis, 1978; Nowakowski et al., 1989; Overall et al., 2016), changes in Ki67 expression during G1 could not generate the DCX/Ki67 ratio differences seen in bank voles. Instead, there is evidence for differences between laboratory rats and mice in the rate of young neuron maturation (Snyder et al., 2009a). Furthermore, delayed maturation and extended expression of markers of young neurons has been described in other species (Amrein and Slomianka, 2010; Brus et al., 2013), including primates (Ngwenya et al., 2008, 2015; Kohler et al., 2011; Amrein et al., 2015). Differences in the speed of maturation of young neurons, depending on septo-temporal location, have also been reported in laboratory rodents (Piatti et al., 2011; Snyder et al., 2012). On this background, the high DCX/Ki67 ratio in the intermediate and, even more so, in the temporal dentate gyrus of bank voles suggest to us an extended period in which DCX is expressed in bank voles. In that a large fraction of newly generated neurons dies before expressing markers of adult neurons (Dayer et al., 2003; Kempermann et al., 2003), which coincides with the shut-down of DCX expression (Brown et al., 2003), the extended period of maturation may also represent an extended period of survival. An alternative explanation of differences in the DCX/Ki67 ratio would be differences between strains or species in the number of cells that will have either neuronal or glial fates (Kempermann and Gage, 2002a,b), although heritable traits have been found to account for only little of the differences in gliogenesis between strains (Kempermann et al., 2006). Our material does not allow the assessment of this possibility.

Changes in the Distribution along the Radial Axis

In wild wood mice and bank voles, our data suggest septo-temporal differences in the distance that DCX+ cells migrate along the radial axis, with DCX+ cells preferentially found in the SGZ in the septal and intermediate subdivision, and more DCX+ cells within the granule cell layer proper in the temporal hippocampus. In laboratory rodents, there is only a modest migration of newborn neurons into the dentate granule cell layer during the first week after their formation (Kempermann et al., 2003) and most of the newborn cells remain at the base or in the lower one-third of the granule cell layer. Both in sheep and monkeys, in which newly generated neurons retain immature characteristics far longer than in rodent, there is at least statistical evidence for a migration of new neurons into the granule cell layer (Kohler et al., 2011; Brus et al., 2013). Unfortunately, the illustrations provided do not allow a comparison with our observations in wood mice and bank voles.

While a prolonged period of migration may result in differences in radial positioning, genetic control of cell migration can also generate a distribution of newborn cell reminiscent of that seen in the temporal dentate gyrus of wood mice and bank voles (Namba et al., 2011; Teixeira et al., 2012; Schafer et al., 2015; Woodbury et al., 2015). In the case of miR-155 overexpression, this seems possible even though the survival of newborn cells is reduced (Woodbury et al., 2015). We cannot address which of these factors may be responsible for the radial distribution of newborn cells in wood mice and bank voles. However, these mice show that natural selection may operate on these or similar mechanisms to generate what must be believed to be adaptive species differences.

CONCLUDING REMARKS

The variability in AHN in terms of absolute cell numbers, their septo-temporal distributions, ratios between proliferating and maturing cells between rodent species may be surprising and bewildering. It is less surprising when one considers the role that AHN may play in differentiating hippocampal function across taxonomic units. Within a larger sample of rodent species, we found that AHN is a far better differentiator between species than other hippocampal principal cell populations (van Dijk et al., 2016a). It is only equaled by variation in hilar cell numbers, which, like newborn neurons, are involved in the control of information flow through the dentate gyrus. Septo-temporal differences in AHN and differential septo-temporal effects of experimental manipulations suggest that AHN participates in the anatomical and functional septo-temporal differentiation of the hippocampus (Sahay and Hen, 2007; Glasper et al., 2012; Tanti and Belzung, 2013; Jinno, 2016). Considering the power of AHN to differentiate between species, a species-specific septo-temporal modulation of AHN turns from surprise to expectation. Much could be said about the relative vices and virtues of working with laboratory or wild rodents. Without the countless studies performed in laboratory animals, our observation would be phenomenology without plausible mechanisms. On the other hand, observations in wild animals may turn what we perceive as anatomical aberrations and functional deficits after the experimental manipulations of these mechanisms into substrates of adaptive onto- and phylogenetic changes.

AUTHOR CONTRIBUTIONS

IA, RMvD and LS planned experiments. FW, EL, RMvD and IA conducted experiments FW, LS and IA wrote the manuscript.

FUNDING

IA and RMvD were funded by the EMDO foundation, Zurich.

ACKNOWLEDGMENTS

Special thanks goes to Prof. Barbara König for providing the wild house mice, and to Elisabeth Jakob, Rifferswil and Silvana Ressegatti, Zürich, for their help in trapping mice. We also thank Sonìa Matos for expert technical assistance. This work was supported by a grant of the EMDO Stiftung, Zurich, to RMvD and IA.

REFERENCES

Agster, K. L., and Burwell, R. D. (2013). Hippocampal and subicular efferents and afferents of the perirhinal, postrhinal, and entorhinal cortices of the rat. *Behav. Brain Res.* 254, 50–64. doi: 10.1016/j.bbr.2013.07.005

Amaral, D. G., and Witter, M. P. (1989). The three-dimensional organization of the hippocampal formation: a review of anatomical data. *Neuroscience* 31, 571–591. doi: 10.1016/0306-4522(89)90424-7

Ammassari-Teule, M., Fagioli, S., and Rossi-Arnaud, C. (1992). Genotype-dependent involvement of limbic areas in spatial learning and postlesion recovery. *Physiol. Behav.* 52, 505–510. doi: 10.1016/0031-9384(92)90338-3

Amrein, I., Isler, K., and Lipp, H.-P. (2011). Comparing adult hippocampal neurogenesis in mammalian species and orders: influence of chronological age and life history stage. *Eur. J. Neurosci.* 34, 978–987. doi: 10.1111/j.1460-9568.2011.07804.x

Amrein, I., Nosswitz, M., Slomianka, L., van Dijk, R. M., Engler, S., Klaus, F., et al. (2015). Septo-temporal distribution and lineage progression of hippocampal neurogenesis in a primate (*Callithrix jacchus*) in comparison to mice. *Front. Neuroanat.* 9:85. doi: 10.3389/fnana.2015.00085

Amrein, I., and Slomianka, L. (2010). A morphologically distinct granule cell type in the dentate gyrus of the red fox correlates with adult hippocampal neurogenesis. *Brain Res.* 1328, 12–24. doi: 10.1016/j.brainres.2010.02.075

Amrein, I., Slomianka, L., and Lipp, H. P. (2004a). Granule cell number, cell death and cell proliferation in the dentate gyrus of wild-living rodents. *Eur. J. Neurosci.* 20, 3342–3350. doi: 10.1111/j.1460-9568.2004.03795.x

Amrein, I., Slomianka, L., Poletaeva, I. I, Bologova, N. V., and Lipp, H. P. (2004b). Marked species and age-dependent differences in cell proliferation and neurogenesis in the hippocampus of wild-living rodents. *Hippocampus* 14, 1000–1010. doi: 10.1002/hipo.20018

Baarendse, P. J., van Grootheest, G., Jansen, R. F., Pieneman, A. W., Ögren, S. O., and Verhage, M. (2008). Differential involvement of the dorsal hippocampus in passive avoidance in C57bl/6J and DBA/2J mice. *Hippocampus* 18, 11–19. doi: 10.1002/hipo.20356

Bannerman, D. M., Yee, B. K., Good, M. A., Heupel, M. J., Iversen, S. D., and Rawlins, J. N. P. (1999). Double dissociation of function within the hippocampus: a comparison of dorsal, ventral, and complete hippocampal cytotoxic lesions. *Behav. Neurosci.* 113, 1170–1188. doi: 10.1037/0735-7044.113.6.1170

Barker, G. R., Banks, P. J., Scott, H., Ralph, G. S., Mitrophanous, K. A., Wong, L. F., et al. (2017). Separate elements of episodic memory subserved by distinct hippocampal-prefrontal connections. *Nat. Neurosci.* 20, 242–250. doi: 10.1038/nn.4472

Bast, T. (2007). Toward an integrative perspective on hippocampal function: from the rapid encoding of experience to adaptive behavior. *Rev. Neurosci.* 18, 253–281. doi: 10.1515/REVNEURO.2007.18.3-4.253

Bast, T., Wilson, I. A., Witter, M. P., and Morris, R. G. M. (2009). From rapid place learning to behavioral performance: a key role for the intermediate hippocampus. *PLoS Biol.* 7:e1000089. doi: 10.1371/journal.pbio.1000089

Bekiari, C., Giannakopoulou, A., Siskos, N., Grivas, I., Tsingotjidou, A., Michaloudi, H., et al. (2015). Neurogenesis in the septal and temporal part of the adult rat dentate gyrus. *Hippocampus* 25, 511–523. doi: 10.1002/hipo.22388

Belujon, P., and Grace, A. A. (2015). Regulation of dopamine system responsivity and its adaptive and pathological response to stress. *Proc. Biol. Sci.* 282:20142516. doi: 10.1098/rspb.2014.2516

Ben Abdallah, N. M., Slomianka, L., Vyssotski, A. L., and Lipp, H.-P. (2010). Early age-related changes in adult hippocampal neurogenesis in C57 mice. *Neurobiol. Aging* 31, 151–161. doi: 10.1016/j.neurobiolaging.2008.03.002

Brown, J. P., Couillard-Després, S., Cooper-Kuhn, C. M., Winkler, J., Aigner, L., and Kuhn, H. G. (2003). Transient expression of doublecortin during adult neurogenesis. *J. Comp. Neurol.* 467, 1–10. doi: 10.1002/cne.10874

Brus, M., Meurisse, M., Gheusi, G., Keller, M., Lledo, P. M., and Lévy, F. (2013). Dynamics of olfactory and hippocampal neurogenesis in adult sheep. *J. Comp. Neurol.* 521, 169–188. doi: 10.1002/cne.23169

Cavegn, N., van Dijk, R. M., Menges, D., Brettschneider, H., Phalanndwa, M., Chimimba, C. T., et al. (2013). Habitat-specific shaping of proliferation and neuronal differentiation in adult hippocampal neurogenesis of wild rodents. *Front. Neurosci.* 7:59. doi: 10.3389/fnins.2013.00059

Cembrowski, M. S., Bachman, J. L., Wang, L., Sugino, K., Shields, B. C., and Spruston, N. (2016a). Spatial gene-expression gradients underlie prominent heterogeneity of CA1 pyramidal neurons. *Neuron* 89, 351–368. doi: 10.1016/j.neuron.2015.12.013

Cembrowski, M. S., Wang, L., Sugino, K., Shields, B. C., and Spruston, N. (2016b). Hipposeq: a comprehensive RNA-seq database of gene expression in hippocampal principal neurons. *Elife* 5:e14997. doi: 10.7554/eLife.14997

Cuylen, S., Blaukopf, C., Politi, A. Z., Müller-Reichert, T., Neumann, B., Poser, I., et al. (2016). Ki-67 acts as a biological surfactant to disperse mitotic chromosomes. *Nature* 535, 308–312. doi: 10.1038/nature18610

Dawirs, R. R., Hildebrandt, K., and Teuchert-Noodt, G. (1998). Adult treatment with haloperidol increases dentate granule cell proliferation in the gerbil hippocampus. *J. Neural Transm. (Vienna)* 105, 317–327. doi: 10.1007/s007020050061

Dayer, A. G., Ford, A. A., Cleaver, K. M., Yassaee, M., and Cameron, H. A. (2003). Short-term and long-term survival of new neurons in the rat dentate gyrus. *J. Comp. Neurol.* 460, 563–572. doi: 10.1002/cne.10675

Dong, H. W., Swanson, L. W., Chen, L., Fanselow, M. S., and Toga, A. W. (2009). Genomic-anatomic evidence for distinct functional domains in hippocampal field CA1. *Proc. Natl. Acad. Sci. U.S.A.* 106, 11794–11799. doi: 10.1073/pnas.0812608106

Fanselow, M. S., and Dong, H.-W. (2010). Are the dorsal and ventral hippocampus functionally distinct structures? *Neuron* 65, 7–19. doi: 10.1016/j.neuron.2009.11.031

Felice, D., O'leary, O. F., Pizzo, R. C., and Cryan, J. F. (2012). Blockade of the GABAB receptor increases neurogenesis in the ventral but not dorsal adult hippocampus: relevance to antidepressant action. *Neuropharmacology* 63, 1380–1388. doi: 10.1016/j.neuropharm.2012.06.066

Felix-Ortiz, A. C., Beyeler, A., Seo, C., Leppla, C. A., Wildes, C. P., and Tye, K. M. (2013). BLA to vHPC inputs modulate anxiety-related behaviors. *Neuron* 79, 658–664. doi: 10.1016/j.neuron.2013.06.016

Ferland, R. J., Gross, R. A., and Applegate, C. D. (2002). Differences in hippocampal mitotic activity within the dorsal and ventral hippocampus following flurothyl seizures in mice. *Neurosci. Lett.* 332, 131–135. doi: 10.1016/S0304-3940(02)00808-X

Gaarskjaer, F. B. (1978). Organization of the mossy fiber system of the rat studied in extended hippocampi I. terminal area related to the number of granule and pyramidal cells. *J. Comp. Neurol.* 178, 49–72. doi: 10.1002/cne.901780104

Galsworthy, M. J., Amrein, I., Kuptsov, P. A., Poletaeva, I. I., Zinn, P., Rau, A., et al. (2005). A comparison of wild-caught wood mice and bank voles in the Intellicage: assessing exploration, daily activity patterns and place learning paradigms. *Behav. Brain Res.* 157, 211–217. doi: 10.1016/j.bbr.2004.06.021

Glasper, E. R., Schoenfeld, T. J., and Gould, E. (2012). Adult neurogenesis: optimizing hippocampal function to suit the environment. *Behav. Brain Res.* 227, 380–383. doi: 10.1016/j.bbr.2011.05.013

Goto, T., Tanave, A., Moriwaki, K., Shiroishi, T., and Koide, T. (2013). Selection for reluctance to avoid humans during the domestication of mice. *Genes Brain Behav.* 12, 760–770. doi: 10.1111/gbb.12088

Gundersen, H. J., Jensen, E. B., Kiêu, K., and Nielsen, J. (1999). The efficiency of systematic sampling in stereology – reconsidered. *J. Microsc.* 193, 199–211. doi: 10.1046/j.1365-2818.1999.00457.x

Häussler, U., Bielefeld, L., Froriep, U. P., Wolfart, J., and Haas, C. A. (2012). Septotemporal position in the hippocampal formation determines epileptic and neurogenic activity in temporal lobe epilepsy. *Cereb. Cortex* 22, 26–36. doi: 10.1093/cercor/bhr054

Hayes, N. L., and Nowakowski, R. S. (2002). Dynamics of cell proliferation in the adult dentate gyrus of two inbred strains of mice. *Brain Res. Dev. Brain Res.* 134, 77–85. doi: 10.1016/S0165-3806(01)00324-8

Herman, J. P., Cullinan, W. E., Morano, M. I., Akil, H., and Watson, S. J. (1995). Contribution of the ventral subiculum to inhibitory regulation of the hypothalamo-pituitary-adrenocortical axis. *J. Neuroendocrinol.* 7, 475–482. doi: 10.1111/j.1365-2826.1995.tb00784.x

Ho, Y. C., and Wang, S. (2010). Adult neurogenesis is reduced in the dorsal hippocampus of rats displaying learned helplessness behavior. *Neuroscience* 171, 153–161. doi: 10.1016/j.neuroscience.2010.08.062

Huang, S., Slomianka, L., Farmer, A. J., Kharlamova, A., Gulevich, R. G., Herbeck, Y. E., et al. (2015). Selection for tameness, a key behavioral trait of domestication, increases adult hippocampal neurogenesis in foxes. *Hippocampus* 25, 963–975. doi: 10.1002/hipo.22420

Hughes, K. R. (1965). Dorsal and ventral hippocampus lesions and maze learning: influence of preoperative environment. *Can. J. Psychol.* 19, 325–332. doi: 10.1037/h0082915

Iñiguez, C., Gayoso, M. J., and Carreres, J. (1985). A versatile and simple method for staining nervous tissue using Giemsa dye. *J. Neurosci. Methods* 13, 77–86. doi: 10.1016/0165-0270(85)90045-7

Ishizuka, N., Weber, J., and Amaral, D. G. (1990). Organization of intrahippocampal projections originating from CA3 pyramidal cells in the rat. *J. Comp. Neurol.* 295, 580–623. doi: 10.1002/cne.902950407

Jhaveri, D. J., O'keeffe, I., Robinson, G. J., Zhao, Q. Y., Zhang, Z. H., Nink, V., et al. (2015). Purification of neural precursor cells reveals the presence of distinct, stimulus-specific subpopulations of quiescent precursors in the adult mouse hippocampus. *J. Neurosci.* 35, 8132–8144. doi: 10.1523/JNEUROSCI.0504-15.2015

Jinno, S. (2011a). Decline in adult neurogenesis during aging follows a topographic pattern in the mouse hippocampus. *J. Comp. Neurol.* 519, 451–466. doi: 10.1002/cne.22527

Jinno, S. (2011b). Topographic differences in adult neurogenesis in the mouse hippocampus: a stereology-based study using endogenous markers. *Hippocampus* 21, 467–480. doi: 10.1002/hipo.20762

Jinno, S. (2016). Aging affects new cell production in the adult hippocampus: a quantitative anatomic review. *J. Chem. Neuroanat.* 76, 65–72. doi: 10.1016/j.jchemneu.2015.10.009

Jinno, S., and Kosaka, T. (2006). Cellular architecture of the mouse hippocampus: a quantitative aspect of chemically defined GABAergic neurons with stereology. *Neurosci. Res.* 56, 229–245. doi: 10.1016/j.neures.2006.07.007

Jones, M. W., Peckham, H. M., Errington, M. L., Bliss, T. V. P., and Routtenberg, A. (2001). Synaptic plasticity in the hippocampus of awake C57BL/6 and DBA/2 mice: interstrain differences and parallels with behavior. *Hippocampus* 11, 391–396. doi: 10.1002/hipo.1053

Kempermann, G., Chesler, E. J., Lu, L., Williams, R. W., and Gage, F. H. (2006). Natural variation and genetic covariance in adult hippocampal neurogenesis. *Proc. Natl. Acad. Sci. U.S.A.* 103, 780–785. doi: 10.1073/pnas.0510291103

Kempermann, G., and Gage, F. H. (2002a). Genetic determinants of adult hippocampal neurogenesis correlate with acquisition, but not probe trial performance, in the water maze task. *Eur. J. Neurosci.* 16, 129–136. doi: 10.1046/j.1460-9568.2002.02042.x

Kempermann, G., and Gage, F. H. (2002b). Genetic influence on phenotypic differentiation in adult hippocampal neurogenesis. *Brain Res. Dev. Brain Res.* 134, 1–12. doi: 10.1016/S0165-3806(01)00224-3

Kempermann, G., Gast, D., Kronenberg, G., Yamaguchi, M., and Gage, F. H. (2003). Early determination and long-term persistence of adult-generated new neurons in the hippocampus of mice. *Development* 130, 391–399. doi: 10.1242/dev.00203

Kempermann, G., Kuhn, H. G., and Gage, F. H. (1997). Genetic influence on neurogenesis in the dentate gyrus of adult mice. *Proc. Natl. Acad. Sci. U.S.A.* 94, 10409–10414. doi: 10.1073/pnas.94.19.10409

Kesner, R. P. (2013). An analysis of the dentate gyrus function. *Behav. Brain Res.* 254, 1–7. doi: 10.1016/j.bbr.2013.01.012

Kirby, E. D., Muroy, S. E., Sun, W. G., Covarrubias, D., Leong, M. J., Barchas, L. A., et al. (2013). Acute stress enhances adult rat hippocampal neurogenesis and activation of newborn neurons via secreted astrocytic FGF2. *Elife* 2:e00362. doi: 10.7554/eLife.00362

Kjelstrup, K. B., Solstad, T., Brun, V. H., Hafting, T., Leutgeb, S., Witter, M. P., et al. (2008). Finite scale of spatial representation in the hippocampus. *Science* 321, 140–143. doi: 10.1126/science.1157086

Kjelstrup, K. G., Tuvnes, F. A., Steffenach, H.-A., Murison, R., Moser, E. I., and Moser, M.-B. (2002). Reduced fear expression after lesions of the ventral hippocampus. *Proc. Natl. Acad. Sci. U.S.A.* 99, 10825–10830. doi: 10.1073/pnas.152112399

Klaus, F., Hauser, T., Lindholm, A. K., Cameron, H. A., Slomianka, L., Lipp, H.-P., et al. (2012). Different regulation of adult hippocampal neurogenesis in Western house mice (Mus musculus domesticus) and C57BL/6 mice. *Behav. Brain Res.* 227, 340–347. doi: 10.1016/j.bbr.2011.07.026

Kohler, S. J., Williams, N. I., Stanton, G. B., Cameron, J. L., and Greenough, W. T. (2011). Maturation time of new granule cells in the dentate gyrus of adult macaque monkeys exceeds six months. *Proc. Natl. Acad. Sci. U.S.A.* 108, 10326–10331. doi: 10.1073/pnas.1017099108

Lagace, D. C., Yee, J. K., Bolaños, C. A., and Eisch, A. J. (2006). Juvenile administration of methylphenidate attenuates adult hippocampal neurogenesis. *Biol. Psychiatry* 60, 1121–1130. doi: 10.1016/j.biopsych.2006.04.009

Lewis, P. D. (1978). Kinetics of cell proliferation in the postnatal rat dentate gyrus. *Neuropathol. Appl. Neurobiol.* 4, 191–195. doi: 10.1111/j.1365-2990.1978.tb00536.x

Lowe, A., Dalton, M., Sidhu, K., Sachdev, P., Reynolds, B., and Valenzuela, M. (2015). Neurogenesis and precursor cell differences in the dorsal and ventral adult canine hippocampus. *Neurosci. Lett.* 593, 107–113. doi: 10.1016/j.neulet.2015.03.017

Lowry, C. A. (2002). Functional subsets of serotonergic neurones: implications for control of the hypothalamic-pituitary-adrenal axis. *J. Neuroendocrinol.* 14, 911–923. doi: 10.1046/j.1365-2826.2002.00861.x

Matsuo, N., Kawamoto, S., Matsubara, K., and Okubo, K. (1998). Cloning and developmental expression of the murine homolog of doublecortin. *Biochem. Biophys. Res. Commun.* 252, 571–576. doi: 10.1006/bbrc.1998.9698

Mineur, Y. S., Belzung, C., and Crusio, W. E. (2007). Functional implications of decreases in neurogenesis following chronic mild stress in mice. *Neuroscience* 150, 251–259. doi: 10.1016/j.neuroscience.2007.09.045

Moser, M. B., and Moser, E. I. (1998). Functional differentiation in the hippocampus. *Hippocampus* 8, 608–619. doi: 10.1002/(SICI)1098-1063(1998)8:6<608::AID-HIPO3>3.0.CO;2-7

Moser, M. B., Moser, E. I., Forrest, E., Andersen, P., and Morris, R. G. (1995). Spatial learning with a minislab in the dorsal hippocampus. *Proc. Natl. Acad. Sci. U.S.A.* 92, 9697–9701. doi: 10.1073/pnas.92.21.9697

Namba, T., Ming, G.-L., Song, H., Waga, C., Enomoto, A., Kaibuchi, K., et al. (2011). NMDA receptor regulates migration of newly generated neurons in the adult hippocampus via Disrupted-In-Schizophrenia 1 (DISC1). *J. Neurochem.* 118, 34–44. doi: 10.1111/j.1471-4159.2011.07282.x

Ngwenya, L. B., Heyworth, N. C., Shwe, Y., Moore, T., and Rosene, D. L. (2015). Age-related changes in dentate gyrus cell numbers, neurogenesis, and associations with cognitive impairments in the rhesus monkey. *Front. Syst. Neurosci.* 9:102. doi: 10.3389/fnsys.2015.00102

Ngwenya, L. B., Rosene, D. L., and Peters, A. (2008). An ultrastructural characterization of the newly generated cells in the adult monkey dentate gyrus. *Hippocampus* 18, 210–220. doi: 10.1002/hipo.20384

Nowakowski, R. S., Lewin, S. B., and Miller, M. W. (1989). Bromodeoxyuridine immunohistochemical determination of the lenghts of the cell cycle and the DNA-synthetic phase for an anatomically defined population. *J. Neurocytol.* 18, 311–318. doi: 10.1007/BF01190834

Oosthuizen, M. K., and Amrein, I. (2016). Trading new neurons for status: adult hippocampal neurogenesis in eusocial Damaraland mole-rats. *Neuroscience* 324, 227–237. doi: 10.1016/j.neuroscience.2016.03.020

Overall, R. W., Walker, T. L., Fischer, T. J., Brandt, M. D., and Kempermann, G. (2016). Different mechanisms must be considered to explain the increase in hippocampal neural precursor cell proliferation by physical activity. *Front. Neurosci.* 10:362. doi: 10.3389/fnins.2016.00362

Overall, R. W., Walker, T. L., Leiter, O., Lenke, S., Ruhwald, S., and Kempermann, G. (2013). Delayed and transient increase of adult hippocampal neurogenesis by physical exercise in DBA/2 mice. *PLoS ONE* 8:e83797. doi: 10.1371/journal.pone.0083797

Patel, J., Fujisawa, S., Berényi, A., Royer, S., and Buzsáki, G. (2012). Traveling theta waves along the entire septotemporal axis of the hippocampus. *Neuron* 75, 410–417. doi: 10.1016/j.neuron.2012.07.015

Patel, J., Schomburg, E. W., Berényi, A., Fujisawa, S., and Buzsáki, G. (2013). Local generation and propagation of ripples along the septotemporal axis of the hippocampus. *J. Neurosci.* 33, 17029–17041. doi: 10.1523/JNEUROSCI.2036-13.2013

Piatti, V. C., Davies-Sala, M. G., Espósito, M. S., Mongiat, L. A., Trinchero, M. F., and Schinder, A. F. (2011). The timing for neuronal maturation in the adult hippocampus is modulated by local network activity. *J. Neurosci.* 31, 7715–7728. doi: 10.1523/JNEUROSCI.1380-11.2011

Poppenk, J., Evensmoen, H. R., Moscovitch, M., and Nadel, L. (2013). Long-axis specialization of the human hippocampus. *Trends Cogn. Sci.* 17, 230–240. doi: 10.1016/j.tics.2013.03.005

Prasad, J. A., and Chudasama, Y. (2013). Viral tracing identifies parallel disynaptic pathways to the hippocampus. *J. Neurosci.* 33, 8494–8503. doi: 10.1523/JNEUROSCI.5072-12.2013

Rapp, P. R., and Amaral, D. G. (1988). The time of origin of somatostatin-immunoreactive neurons in the rat hippocampal formation. *Brain Res.* 41, 231–239. doi: 10.1016/0165-3806(88)90185-X

Reichel, J. M., Bedenk, B. T., Czisch, M., and Wotjak, C. T. (2017). Age-related cognitive decline coincides with accelerated volume loss of the dorsal but not ventral hippocampus in mice. *Hippocampus* 27, 28–35. doi: 10.1002/hipo.22668

Sahay, A., and Hen, R. (2007). Adult hippocampal neurogenesis in depression. *Nat. Neurosci.* 10, 1110–1115. doi: 10.1038/nn1969

Schafer, S. T., Han, J., Pena, M., von Bohlen Und Halbach, O., Peters, J., and Gage, F. H. (2015). The Wnt adaptor protein ATP6AP2 regulates multiple stages of adult hippocampal neurogenesis. *J. Neurosci.* 35, 4983–4998. doi: 10.1523/JNEUROSCI.4130-14.2015

Slomianka, L., and West, M. J. (2005). Estimators of the precision of stereological estimates: an example based on the CA1 pyramidal cell layer of rats. *Neuroscience* 136, 757–767. doi: 10.1016/j.neuroscience.2005.06.086

Smiley, J. F., and Bleiwas, C. (2012). Embedding matrix for simultaneous processing of multiple histological samples. *J. Neurosci. Methods* 209, 195–198. doi: 10.1016/j.jneumeth.2012.06.005

Snyder, J. S., Choe, J. S., Clifford, M. A., Jeurling, S. I., Hurley, P., Brown, A., et al. (2009a). Adult-born hippocampal neurons are more numerous, faster maturing, and more involved in behavior in rats than in mice. *J. Neurosci.* 29, 14484–14495. doi: 10.1523/JNEUROSCI.1768-09.2009

Snyder, J. S., Ferrante, S. C., and Cameron, H. A. (2012). Late maturation of adult-born neurons in the temporal dentate gyrus. *PLoS ONE* 7:e48757. doi: 10.1371/journal.pone.0048757

Snyder, J. S., Radik, R., Wojtowicz, J. M., and Cameron, H. A. (2009b). Anatomical gradients of adult neurogenesis and activity: young neurons in the ventral dentate gyrus are activated by water maze training. *Hippocampus* 19, 360–370. doi: 10.1002/hipo.20525

Sobecki, M., Mrouj, K., Camasses, A., Parisis, N., Nicolas, E., Llères, D., et al. (2016). The cell proliferation antigen Ki-67 organises heterochromatin. *Elife* 5:e13722. doi: 10.7554/eLife.13722

Starborg, M., Gell, K., Brundell, E., and Höög, C. (1996). The murine Ki-67 cell proliferation antigen accumulates in the nucleolar and heterochromatic regions of interphase cells and at the periphery of the mitotic chromosomes in a process essential for cell cycle progression. *J. Cell Sci.* 109, 143–153.

Sterio, D. C. (1984). The unbiased estimation of number and sizes of arbitrary particles using the disector. *J. Microsc.* 134, 127–136. doi: 10.1111/j.1365-2818.1984.tb02501.x

Strange, B. A., Witter, M. P., Lein, E. S., and Moser, E. I. (2014). Functional organization of the hippocampal longitudinal axis. *Nat. Rev. Neurosci.* 15, 655–669. doi: 10.1038/nrn3785

Sun, J., Bonaguidi, M. A., Jun, H., Guo, J. U., Sun, G. J., Will, B., et al. (2015). A septo-temporal molecular gradient of sfrp3 in the dentate gyrus differentially regulates quiescent adult hippocampal neural stem cell activation. *Mol. Brain* 8:52. doi: 10.1186/s13041-015-0143-9

Tanti, A., and Belzung, C. (2013). Neurogenesis along the septo-temporal axis of the hippocampus: are depression and the action of antidepressants region-specific? *Neuroscience* 252, 234–252. doi: 10.1016/j.neuroscience.2013.08.017

Tanti, A., Rainer, Q., Minier, F., Surget, A., and Belzung, C. (2012). Differential environmental regulation of neurogenesis along the septo-temporal axis of the hippocampus. *Neuropharmacology* 63, 374–384. doi: 10.1016/j.neuropharm.2012.04.022

Teixeira, C. M., Kron, M. M., Masachs, N., Zhang, H., Lagace, D. C., Martinez, A., et al. (2012). Cell-autonomous inactivation of the Reelin pathway impairs adult neurogenesis in the hippocampus. *J. Neurosci.* 32, 12051–12065. doi: 10.1523/JNEUROSCI.1857-12.2012

Teuchert-Noodt, G., Dawirs, R. R., and Hildebrandt, K. (2000). Adult treatment with methamphetamine transiently decreases dentate granule cell proliferation in the gerbil hippocampus. *J. Neural Transm. (Vienna)* 107, 133–143. doi: 10.1007/s007020050012

Thompson, C. L., Pathak, S. D., Jeromin, A., Ng, L. L., Macpherson, C. R., Mortrud, M. T., et al. (2008). Genomic anatomy of the hippocampus. *Neuron* 60, 1010–1021. doi: 10.1016/j.neuron.2008.12.008

Uchida, K., Nakamura, S., Kobayashi, T., and Machida, T. (2005). Topographic analysis of cell proliferation in the hippocampus of the adult mouse. *Neuroreport* 16, 2033–2036. doi: 10.1097/00001756-200512190-00013

van Dijk, R. M., Huang, S.-H., Slomianka, L., and Amrein, I. (2016a). Taxonomic separation of hippocampal networks: principal cell populations and adult neurogenesis. *Front. Neuroanatomy* 10:22. doi: 10.3389/fnana.2016.00022

van Dijk, R. M., Lazic, S. E., Slomianka, L., Wolfer, D. P., and Amrein, I. (2016b). Large-scale phenotyping links adult hippocampal neurogenesis to the reaction to novelty. *Hippocampus* 26, 646–657. doi: 10.1002/hipo.22548

Weitz, A. J., Fang, Z., Lee, H. J., Fisher, R. S., Smith, W. C., Choy, M., et al. (2015). Optogenetic fMRI reveals distinct, frequency-dependent networks recruited by dorsal and intermediate hippocampus stimulations. *Neuroimage* 107, 229–241. doi: 10.1016/j.neuroimage.2014.10.039

West, M. J., Slomianka, L., and Gundersen, H. J. (1991). Unbiased stereological estimation of the total number of neurons in the subdivisions of the rat hippocampus using the optical fractionator. *Anat. Rec.* 231, 482–497. doi: 10.1002/ar.1092310411

Witter, M. P. (1993). Organization of the entorhinal-hippocampal system: a review of current anatomical data. *Hippocampus* 3, 33–44.

Woodbury, M. E., Freilich, R. W., Cheng, C. J., Asai, H., Ikezu, S., Boucher, J. D., et al. (2015). miR-155 is essential for inflammation-induced hippocampal neurogenic dysfunction. *J. Neurosci.* 35, 9764–9781. doi: 10.1523/JNEUROSCI.4790-14.2015

Wu, M. V., and Hen, R. (2014). Functional dissociation of adult-born neurons along the dorsoventral axis of the dentate gyrus. *Hippocampus* 24, 751–761. doi: 10.1002/hipo.22265

Wu, M. V., Sahay, A., Duman, R. S., and Hen, R. (2015). Functional differentiation of adult-born neurons along the septotemporal axis of the dentate gyrus. *Cold Spring Harb. Perspect. Biol.* 7:a018978. doi: 10.1101/cshperspect.a018978

Conflict of Interest Statement: The authors declare that the research was conducted in the absence of any commercial or financial relationships that could be construed as a potential conflict of interest.

frontiers in Neuroscience

OPINION
published: 21 July 2017
doi: 10.3389/fnins.2017.00420

Evolutionary Shaping of Adult Hippocampal Neurogenesis in Mammals–Cognitive Gain or Developmental Priming of Personality Traits?

Hans-Peter Lipp [1, 2, 3]*

[1] Institute of Evolutionary Medicine, University of Zurich, Zurich, Switzerland, [2] Institute of Anatomy, University of Zurich, Zurich, Switzerland, [3] Department of Physiology, School of Laboratory Medicine, University of Kwazulu-Natal, Durban, South Africa

Keywords: adult neurogenesis, natural selection, evolution, hippocampal functions, cognition, comparative, personality, genetic assimilation

Adult hippocampal neurogenesis (AHN) in mammals peaks in early postnatal/juvenile periods and is strongly down-regulated thereafter. Depending on species, it may disappear rapidly in adult individuals, or persist at very low levels for a lifetime. Commonly, higher levels of AHN in mammals are thought to provide mental flexibility allowing for adapting to new ecological niches. But why does natural selection not prevent down-regulation of AHN, and why should a rudimentary proliferation rate in humans provide reproductive fitness even for aged individuals? The problem is compounded by species-specific behavioral manifestations of hippocampal functions that depend on brain size and ecological niches. Moreover, in laboratory rodents, proliferation levels of AHN and behavioral covariates appear unpredictable and context-sensitive. Conversely, one might ask why evolutionary mechanisms tolerate in nearly all mammals a certain level of early postnatal or subadult AHN. Specifically, the hypothesis of cognitive flexibility appears odd in species in which AHN is massively reduced in early infancy such as in humans. I suggest that early but not late AHN plays a hidden role in developing randomly different epigenetic personality traits in local populations. Such traits may counteract or enhance natural selection of the underlying genetic architecture—a process known as genetic assimilation.

OPEN ACCESS

Edited by:
Vincent Tropepe,
University of Toronto, Canada

Reviewed by:
Troy Ghashghaei,
North Carolina State University, United States

***Correspondence:**
Hans-Peter Lipp
hplipp@anatom.uzh.ch

Specialty section:
This article was submitted to Neurogenesis, a section of the journal Frontiers in Neuroscience

Received: *15 March 2017*
Accepted: *05 July 2017*
Published: *21 July 2017*

Citation:
Lipp H-P (2017) Evolutionary Shaping of Adult Hippocampal Neurogenesis in Mammals–Cognitive Gain or Developmental Priming of Personality Traits?. Front. Neurosci. 11:420. doi: 10.3389/fnins.2017.00420

In mammals, protracted neurogenesis occurs in subventrical zones (SVZ) from which neuroblasts migrate rostrally to the olfactory bulb (rostral migratory stream, RMS) and from a secondary proliferation zone in the dentate gyrus, the subgranular zone (SGZ). The ongoing postnatal proliferation there is denoted as "adult" hippocampal neurogenesis (AHN). Molecular markers for migration and differentiation are often not correlated with basic levels of AHN in many species. For example, doublecortin (DCX) is a reasonable proxy for estimating proliferation rates in mice and rats. In other species such markers persist for long periods after the cessation of proliferation or appear even generated *de novo* (Amrein, 2015; Penz et al., 2015; Lipp and Bonfanti, 2016). Therefore, AHN and its potential relation to natural selection will refer here to simple proliferation only. After all, it is the dogma-breaking role of persisting neurogenesis that dominates the public view of AHN.

THE MAIN PROBLEMS

The evolutionary role of AHN in mammals is not understood. The most straightforward explanation shared by many has been offered by Kempermann (2012, 2016) who claims that AHN is an evolutionary recent addition since it is linked with the mammalian hippocampus, which itself is unique for mammals. As the human hippocampus is mediating

complex forms of memory, the putative beneficial role of AHN for human memory is extrapolated from rodent studies to humans and to other mammalian species. Thus, cognitive flexibility originating from AHN should provide mammalian species with superior abilities for adapting to new environments. This view bears some problems, namely the role of the hippocampus in mammalian behavior, the different levels of AHN in various species, the differential down-regulation of AHN across species, and the process of natural selection in small populations.

DOES NATURAL SELECTION ACT ON BEHAVIORAL TRAITS DEPENDING ON AHN?

To answer this, one would need to know what behaviors and abilities are clearly correlated with hippocampal structural traits including AHN. Perhaps surprisingly, the situation is not clear since even laboratory rodents show a bewildering variety of hippocampus-dependent behaviors, mostly ignored by AHN research. For one, they include natural behaviors such as food burrowing and nest building (Deacon et al., 2002), and social behavior (Ely et al., 1976). Better known are many learning paradigms including simple two-way avoidance (Lipp et al., 1989) and cognitive behaviors such as spatial navigation and pattern separation.

Why is such diversity not known for humans? The human hippocampus interacts chiefly with higher-order association cortex mostly lacking in rodents (**Figures 1A,B**), see also Dong (2008). In addition, the rodent hippocampus integrates less "cognitive" input with subcortical limbic structures (**Figures 1B,D**). In both species (**Figures 1C,D**), the hippocampal loops form the ultimate associative cortex. However, in rodents this structure must also handle functions relegated to specialized cortex regions in humans (Bergmann et al., 2016), being therefore multifunctional. Furthermore, the rodent hippocampus blends hypothalamic and basal forebrain activity into input/output loops connecting to fronto-limbic cortical areas. Thus, the hippocampus is likely to be involved in modulation of many species-typical behaviors. The prevailing uncritical bidirectional extrapolation from human hippocampal functions to rodents and *vice versa* has led to some ill-founded views.

For example, many researchers and editors believe now that AHN is specifically critical for complex tests involving pattern separation, the human ability to memorize fine-grained differences in spatial or contextual environments (Sahay et al., 2011). Yet the behavioral evidence for this conclusion is shaky as it was obtained in mice exposing them to test situations requiring gradually recognizing subtle differences in spatial arrangements of threatening situations. But small rodents cannot afford to discriminate subtleties of threats such as the color and size of a cat and must react immediately. Obviously, AHN-dependent pattern separation is useful for survival of rodents only if it works at once, and this demonstration is still lacking.

CAN VARIABLE STRUCTURAL TRAITS IN GRANULE CELLS AND MOSSY FIBERS MEDIATE BEHAVIOR AND BEING TARGETED BY NATURAL SELECTION?

The extent of the so-called intra/infrapyramidal mossy fiber projection (IIP-MF) correlates genetically and individually with behavioral traits, not all of them being considered as "hippocampal" (Lipp et al., 1989). Variations of IIP-MF in mice co-vary positively with predictability of ongoing behaviors, and respond rapidly to selective breeding and natural selection (Lipp and Wolfer, 1995, 2002, 2013). Therefore, developmental variations in the distribution of the granule cell axons can predict behavioral traits of adults.

On the other hand, it is difficult to find in rodents consistent correlations between individual numbers of newly generated neurons and individual behaviors. A likely reason is that the extent of the IIP-MF is determined during the first postnatal days of rodent pups, and remains rather stable during adulthood. Conversely, AHN in rodents is extremely sensitive to environmental changes, activity and stress levels, and appears influenced by about 190 genes (Kempermann et al., 2006). It also changes strongly during life history as explained below. Thus, functional relations between AHN and behaviors in mice and rats are masked by excessive temporal variability of the structural substrate, possible interactions with learning, and by the multi-functionality of the rodent hippocampus. This may explain the huge number of behavioral AHN studies with discordant results (Lipp and Bonfanti, 2016). Exceptions with more predictable outcome are some naturalistic behaviors. Genetic suppression of AHN resulted in impairments of species-typical behaviors and sucrose preference in mice (Jedynak et al., 2012) and rats (Snyder et al., 2016). Studies of individual correlations showed positive correlations of AHN levels with sucrose preference (Hu et al., 2016), and with roaming in large enclosures (Freund et al., 2013). Conversely, reactions to novelty correlated negatively with the number of proliferating neurons (van Dijk et al., 2016). But even for species-typical behaviors, their relation to AHN appears unpredictable. Yet natural selection requires that behavioral phenotype and genotype should be strongly linked. It is thus difficult to see how natural selection could act on cognitive or species-typical behaviors linked unpredictably to AHN, and even more difficult to imagine selective pressure on increased AHN in species in which it is already sparse early in life.

AHN IS STRONGLY DOWN-REGULATED BUT IS BOTTOMING OUT AFTER TWO YEARS, INDEPENDENT OF SPECIES

AHN diminishes with age, initially considered as a normal aging process. However, studies in mice showed that AHN is exponentially decreasing after 7 weeks of age till about 4 months—during peak conditions for reproduction—and leveling off afterwards (Ben Abdallah et al., 2010). A strong decline during the first year of life has now been documented repeatedly for humans (Knoth et al., 2010; Dennis et al., 2016, 2017).

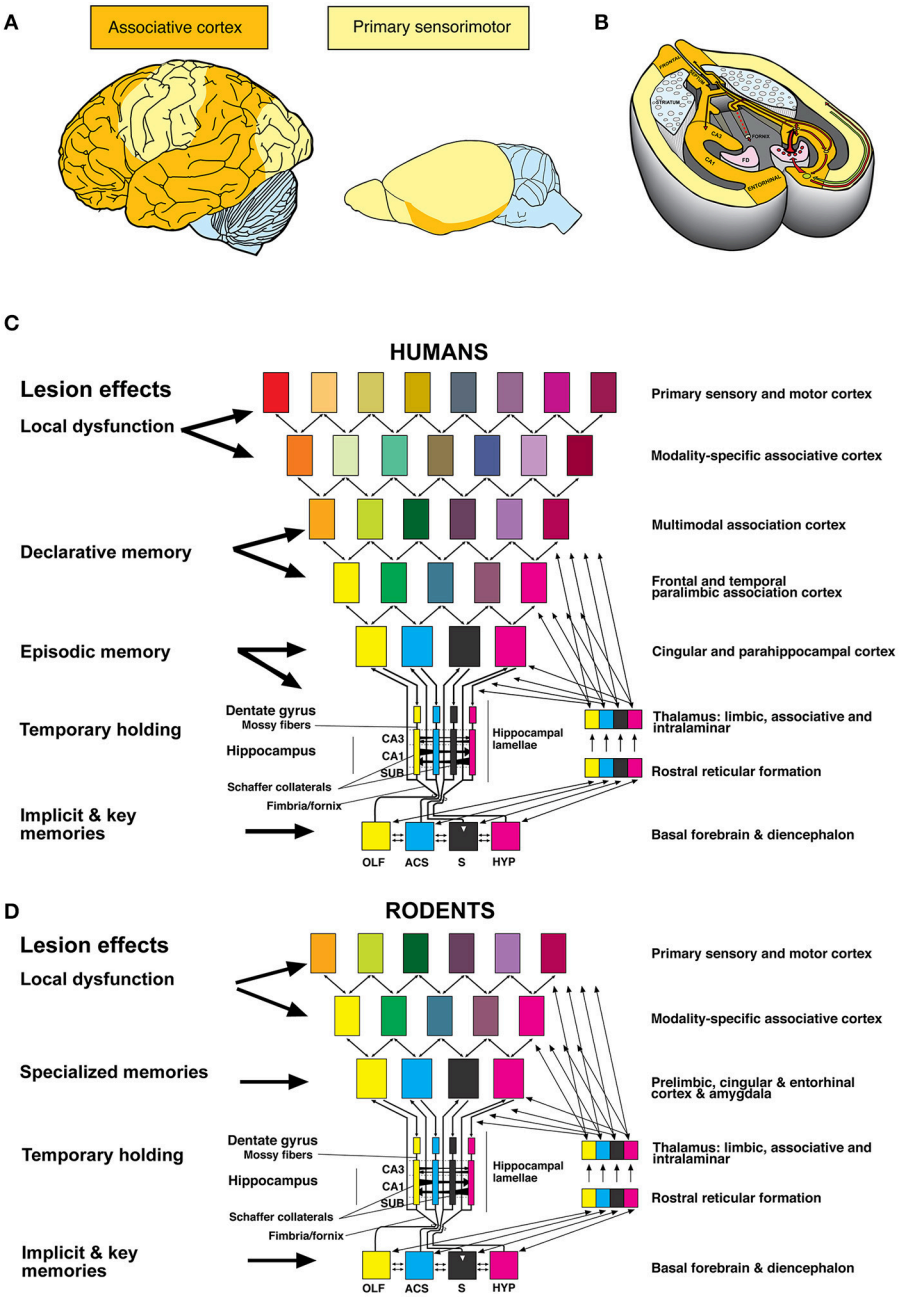

FIGURE 1 | (A) Proportions of associative and sensori-motor association cortex differ in humans and rodents, see also (Dong, 2008). **(B)** Associative cortex in rodents is formed mostly by the hippocampal formation. **(C)** Human hippocampal loops receive reduced columnar activity patterns from cortex areas, aligning them to parallel ("trisynaptic") loops that permit transformation of input/out patterns by Schaffer collaterals in CA3 and CA1. Different colors of rectangles indicate a progressive reduction of cortical activity pattern for representation in the hippocampal formation (Lipp, 2015). **(D)** Corresponding view in rodents in which the input to the hippocampal loop system originates chiefly from non-associative cortex regions but also from subcortical structures. Random dispersal of newly born cells in the dentate gyrus may prime the early postnatal development into different behavioral phenotypes and personalities.

Weissleder et al. (2016) have reported a further decrease from years 21 till 91, yet starting from a low level. Other markers of proliferative activity in the human hippocampus did not show an age-dependent decline. Thus it makes sense to distinguish early vs. late AHN.

The belief in a functional role of AHN in aged humans is supported solely by a widely cited study by Spalding et al. (2013) even though it remains controversial among experts. Using the decay of radioactive C14 in human hippocampi, they calculated daily turnover rates of 700 cells per day among 20 millions

granule cells. However, they miscalculated proliferation levels in mice and concluded—widely cited also—that AHN in 40 year-old humans is comparable in proliferation levels to correspondingly aged mice (for details see Lipp and Bonfanti, 2016).

In comparative terms, the work of Amrein et al. (2011) has shown that strong down-regulation of AHN occurs in many species regardless of life span and ecological conditions. A bottom in proliferative activity is reached in both mice and men after about 2 years, and AHN is continuing at minimal rates independent of the life span of the species. These findings make cross-species comparability of AHN and life history questionable.

For example, we had hypothesized that the decay of AHN in humans might follow a much slower pace, bottoming out at the age of about 30 years (Amrein and Lipp, 2009). This view might have explained some typical transitions in human life history such as the emergence of long-term memory at the expense of short-term memory in children (Yim et al., 2013; Akers et al., 2014). Likewise, it would have fitted the transition from exuberant and reckless juvenile behavior to cautious adult behavior—a characteristic of the maturation of the hippocampus as postulated by Altman et al. (1973). The general idea was that the input-output patterns of the hippocampal formation between the loops crossing the hippocampal formation (**Figures 1C,D**) would initially be kept malleable by the AHN-dependent production of juvenile excitable granule cells. The down-regulation of AHN would then entail a fixation of input-output relations associated with acquired and species-typical behaviors optimal for a given environment. This concept would make sense in species in which the initial reduction of AHN covers pre- and post-puberty and early adulthood such as in mice or rats. In these species, the altered hippocampal physiology might be of evolutionary adaptive value. Therefore, natural selection might favor strong early AHN followed by a period of fixing behavioral traits. However, in humans the decay period falls into a time window with reduced behavioral expression and cognitive abilities. Moreover, it is accompanied by an enormous (non-proliferative) growth of dendrites and connections in the forebrain. This raises the question whether early peaking of AHN and down-regulation with late bottoming-out is useful for humans at all.

WHY IS LATE HUMAN AHN NOT ENHANCED BY NATURAL SELECTION?

The most parsimonious answer is that continuing low-level AHN does not matter at all, assuming that the addition of 700 new cells per day (if this can be proved) has a negligible impact on adult on human hippocampal functions. Nowadays, this view has become almost heretical. But one might rightly ask why a putative beneficial structural trait has been curtailed in humans and not increased by natural selection. At present there is no answer. A conceptually related question is why natural selection has (regrettably) not increased the intelligence quotient in humans from an average of 100 to one of 140 points. Obviously, reproductive fitness—a benchmark of evolution—is not strongly correlated with cognitive abilities. Its reproductive advantage is counteracted by competing traits such as physical attractiveness and, among males, physical strength and aggression, not infrequently at the disadvantage of courting academics. For human AHN, the reasons are less obvious. Possibly, the emergence of highly excitable young neurons may interfere with the orchestrated development of other granule cell functions (Drew et al., 2016), or it is even impairing normal cognitive function (Walton et al., 2012). Alternatively, hippocampal functionality and granule cell excitability is regulated by other mechanisms than simple proliferation. Whatever reasons, it would seem that AHN in humans is suppressed early in ontogeny, in parallel with neurogenesis in the SVZ, probably also in other primate species (Lipp and Bonfanti, 2016). It is thus difficult to see why natural selection should preserve a small and dwindling cell population in the human dentate gyrus. This would require showing that late human AHN has a clearly beneficial effect on reproductive fitness or is advantageous for the survival of the group members.

BUT WHY IS EARLY POSTNATAL AHN MAINTAINED EVEN IN HUMANS?

On the other hand, comparative analysis across mammals (Amrein, 2015; Patzke et al., 2015) suggests that an initial level of AHN is maintained in most species, at least in those in which age-dependency could be investigated. Differences between orders and species emerge primarily in the time course of the decay within a span of 2 years, and in the molecular differentiation of the newly generated cells (Amrein, 2015). Up to now, a coherent picture of how species differences in AHN relate to ecological conditions must remain speculative, chiefly because of low sample sizes and problems in quantifying age levels. However, the typical time course of AHN in mammals must provide some variable advantages in terms of natural selection, perhaps more in short-living rodents than in primates and other species.

EARLY HIPPOCAMPAL NEUROGENESIS MAY PRIME RANDOMLY THE DEVELOPMENT OF PERSONALITY TRAITS

The problem in humans is to find a useful function for early postnatal neurogenesis during a period of reduced cognition. This function ought to provide a target for natural selection in adults in order to maintain this developmental trait. One might argue that hippocampal neurogenesis in such an early postnatal stage could help in organizing the development of forebrain circuitry underlying cognitive processing, e.g., the emergence of language. But this should have consequences for adult behavior many years later. Yet it remains questionable whether individual differences in language development do have an impact on evolutionary relevant adult behavior.

On the other hand, personality traits such as risk-taking behavior or food preferences must have been obvious targets for rapid natural selection during human evolution, specifically in small populations. In larger populations, genetic variation balances competing traits, permitting rapid natural selection of carriers fitting into a changed environment. However, in smaller groups natural selection, for example for timidity, might rapidly eliminate genetic variation supporting risk-taking behavior. This can reduce the ability of genetically adapting to new environments suddenly favoring risk-takers.

Loss of evolutionary plasticity due to natural selection is a common problem for small populations in many species. A possible mechanism counteracting such processes is the early development of personality traits in absence of genetic variation. The unpredictable occurrence of correlations between AHN and personality traits in isogenic rodents suggests that such personality traits emerge randomly. For example, sucrose preference shows strong genetic variability in mice and humans (Reed et al., 1997). Yet testing inbred mice for sucrose preference shows often a minority of individuals with initial taste neophobia, indicating that this long-lasting trait can develop purely epigenetically, remaining correlated in rats with individual levels of AHN (Hu et al., 2016). Sweet preference is an adaptive trait that seemingly deserves to be naturally selected, fixing it rapidly genetically. However, this might be fatal for a population as soon as sucrose becomes associated with toxins. But if there are epigenetic traits for taste neophobia, these individuals will not be eliminated rapidly and natural selection might start selecting alleles promoting taste neophobia, a process known as genetic assimilation (Renn and Schumer, 2013).

This idea is in line with recent findings of an elegant study using a chemogenetic approach to inactivate selectively perinatally and postnatally born olfactory neurons in mice (Muthusamy et al., 2017). They found that perinatally born neurons were controlling innate fear responses to predator odor, while neurons born 6 weeks later appeared to control the acquisition of novel appetitive odors. Thus, newly added neurons may prime novel preferences without erasing critical responses for survival. A second example is the individual propensity for roaming, often taken as a measure for risk-taking behavior. Again, individual correlations between levels of AHN and "exploratory" activities have been reported for inbred mice (Freund et al., 2013; van Dijk et al., 2016). Therefore, developmental randomization of behavioral traits by means of AHN at very early ages might predict later gustatory and olfactory preferences, plus roaming activity, not only in mice but also in humans. After all, from 110,000 years ago humans had to survive evolutionary critical bottlenecks by switching to a mussel diet (Marean, 2016)—certainly not the preferred food of most primates. Likewise, the presence of roamers and non-roamers in a population helps to find new habitats. Thus, the evolutionary gain of AHN in most mammalian species including humans might not be cognition but regulating the degree of genetic assimilation of behavioral traits of fundamental importance for adaptation to new habitats.

AUTHOR CONTRIBUTIONS

The author confirms being the sole contributor of this work and approved it for publication.

FUNDING

Writing of this paper was supported by intramural funds of the University of Zurich.

ACKNOWLEDGMENTS

I thank Irmgard Amrein and David Wolfer for critical reading, and Irina Lipp for administrative support.

REFERENCES

Akers, K. G., Martinez-Canabal, A., Restivo, L., Yiu, A. P., De Cristofaro, A., Hsiang, H. L., et al. (2014). Hippocampal neurogenesis regulates forgetting during adulthood and infancy. *Science* 344, 598–602. doi: 10.1126/science.1248903

Altman, J., Brunner, R. L., and Bayer, S. A. (1973). The hippocampus and behavioral maturation. *Behav. Biol.* 8, 557–596. doi: 10.1016/S0091-6773(73)80144-0

Amrein, I. (2015). Adult hippocampal neurogenesis in natural populations of mammals. *Cold Spring Harb. Perspect. Biol.* 7, 1–19. doi: 10.1101/cshperspect.a021295

Amrein, I., Isler, K., and Lipp, H. P. (2011). Comparing adult hippocampal neurogenesis in mammalian species and orders: influence of chronological age and life history stage. *Eur. J. Neurosci.* 34, 978–987. doi: 10.1111/j.1460-9568.2011.07804.x

Amrein, I., and Lipp, H. P. (2009). Adult hippocampal neurogenesis of mammals: evolution and life history. *Biol. Lett.* 5, 141–144. doi: 10.1098/rsbl.2008.0511

Ben Abdallah, N. M., Slomianka, L., Vyssotski, A. L., and Lipp, H. P. (2010). Early age-related changes in adult hippocampal neurogenesis in C57 mice. *Neurobiol. Aging* 31, 151–161. doi: 10.1016/j.neurobiolaging.2008.03.002

Bergmann, E., Zur, G., Bershadsky, G., and Kahn, I. (2016). The organization of mouse and human cortico-hippocampal networks estimated by intrinsic functional connectivity. *Cereb. Cortex* 26, 4497–4512. doi: 10.1093/cercor/bhw327

Deacon, R. M., Croucher, A., and Rawlins, J. N. (2002). Hippocampal cytotoxic lesion effects on species-typical behaviours in mice. *Behav. Brain Res.* 132, 203–213. doi: 10.1016/S0166-4328(01)00401-6

Dennis, C. V., Suh, L. S., Rodriguez, M. L., Kril, J. J., and Sutherland, G. T. (2016). Human adult neurogenesis across the ages: an immunohistochemical study. *Neuropathol. Appl. Neurobiol.* 42, 621–638. doi: 10.1111/nan.12337

Dennis, C. V., Suh, L. S., Rodriguez, M. L., Kril, J. J., and Sutherland, G. T. (2017). Response to: comment on "Human adult neurogenesis across the ages: an immunohistochemical study." *Neuropathol. Appl. Neurobiol.* 43, 452–454. doi: 10.1111/nan.12394

Dong, H. W. (2008). *The Allen Reference Atlas: A Digital Color Brain Atlas of the C57Bl/6J Male Mouse*. Hoboken: John Wiley & Sons.

Drew, L. J., Kheirbek, M. A., Luna, V. M., Denny, C. A., Cloidt, M. A., Wu, M. V., et al. (2016). Activation of local inhibitory circuits in the dentate gyrus by adult-born neurons. *Hippocampus* 26, 763–778. doi: 10.1002/hipo.22557

Ely, D., Greene, E. G., and Henry, J. P. (1976). Minicomputer monitored social behavior of mice with hippocampus lesions. *Behav. Biol.* 16, 1–29. doi: 10.1016/S0091-6773(76)91082-8

Freund, J., Brandmaier, A. M., Lewejohann, L., Kirste, I., Kritzler, M., Kruger, A., et al. (2013). Emergence of individuality in genetically identical mice. *Science* 340, 756–759. doi: 10.1126/science.1235294

Hu, P., Wang, Y., Liu, J., Meng, F. T., Qi, X. R., Chen, L., et al. (2016). Chronic retinoic acid treatment suppresses adult hippocampal neurogenesis, in close correlation with depressive-like behavior. *Hippocampus* 26, 911–923. doi: 10.1002/hipo.22574

Jedynak, P., Jaholkowski, P., Wozniak, G., Sandi, C., Kaczmarek, L., and Filipkowski, R. K. (2012). Lack of cyclin D2 impairing adult brain neurogenesis alters hippocampal-dependent behavioral tasks without reducing learning ability. *Behav. Brain Res.* 227, 159–166. doi: 10.1016/j.bbr.2011.11.007

Kempermann, G. (2012). New neurons for 'survival of the fittest'. *Nat. Rev. Neurosci.* 13, 727–736. doi: 10.1038/nrn3319

Kempermann, G. (2016). Adult neurogenesis: an evolutionary perspective. *Cold Spring Harb. Perspect. Biol.* 8:a018986. doi: 10.1101/cshperspect.a018986

Kempermann, G., Chesler, E. J., Lu, L., Williams, R. W., and Gage, F. H. (2006). Natural variation and genetic covariance in adult hippocampal neurogenesis. *Proc. Natl. Acad. Sci. U.S.A.* 103, 780–785. doi: 10.1073/pnas.0510291103

Knoth, R., Singec, I., Ditter, M., Pantazis, G., Capetian, P., Meyer, R. P., et al. (2010). Murine features of neurogenesis in the human hippocampus across the lifespan from 0 to 100 years. *PLoS ONE* 5:e8809. doi: 10.1371/journal.pone.0008809

Lipp, H.-P. (2015). Über die Organisation des Gedächtnisses: ein neurobiologisches Modell zum Verständnis der unbewussten Erinnerung. *Psychotherapiewissenschaft* 5, 24–32.

Lipp, H. P., and Bonfanti, L. (2016). Adult neurogenesis in mammals: variations and confusions. *Brain Behav. Evol.* 87, 205–221. doi: 10.1159/000446905

Lipp, H. P., Schwegler, H., Crusio, W. E., Wolfer, D. P., Leisinger-Trigona, M. C., Heimrich, B., et al. (1989). Using genetically-defined rodent strains for the identification of hippocampal traits relevant for two-way avoidance behavior: a non-invasive approach. *Experientia* 45, 845–859. doi: 10.1007/BF01954059

Lipp, H.-P., and Wolfer, D. P. (1995). "New paths towards old dreams: microphrenology or the study of intact brains in intact worlds," in *Behavioural Brain Research in Naturalistic and Semi-Naturalistic Settings: Possibilities and Perspectives*, eds E. Alleva, A. Fasolo, H.-P. Lipp, L. Nadel, and L. Ricceri (Dordrecht: Kluwer), 1–39.

Lipp, H.-P., and Wolfer, D. P. (2002). Big brains for bad genes: non-mental correlates of encephalization. *Evol. Anthropol.* 11, 126–131. doi: 10.1002/evan.10074

Lipp, H.-P., and Wolfer, D. P. (2013). "Natural neurobiology and behavior of the mouse: relevance for behavioral studies in the laboratory," in *Behavioral Genetics of the Mouse. Vol. 1, Genetics of Behavioral Phenotypes*, eds W. E. Crusio, F. Sluyter, R. T. Gerlai, and S. Pietropaola (New York, NY: Cambridge University Press), 5–16.

Marean, C. W. (2016). The transition to foraging for dense and predictable resources and its impact on the evolution of modern humans. *Philos. Trans. R. Soc. Lond. B. Biol. Sci.* 371:20150239. doi: 10.1098/rstb.2015.0239

Muthusamy, N., Zhang, X., Johnson, C. A., Yadav, P. N., and Ghashghaei, H. T. (2017). Developmentally defined forebrain circuits regulate appetitive and aversive olfactory learning. *Nat. Neurosci.* 20, 20–23. doi: 10.1038/nn.4452

Patzke, N., Spocter, M. A., Karlsson, K. A. E., Bertelsen, M. F., Haagensen, M., Chawana, R., et al. (2015). In contrast to many other mammals, cetaceans have relatively small hippocampi that appear to lack adult neurogenesis. *Brain Struct. Funct.* 220, 361–383. doi: 10.1007/s00429-013-0660-1

Penz, O. K., Fuzik, J., Kurek, A. B., Romanov, R., Larson, J., Park, T. J., et al. (2015). Protracted brain development in a rodent model of extreme longevity. *Sci. Rep.* 5:11592. doi: 10.1038/srep11592

Reed, D. R., Bachmanov, A. A., Beauchamp, G. K., Tordoff, M. G., and Price, R. A. (1997). Heritable variation in food preferences and their contribution to obesity. *Behav. Genet.* 27, 373–387. doi: 10.1023/A:1025692031673

Renn, S. C. P., and Schumer, M. E. (2013). Genetic accommodation and behavioural evolution: insights from genomic studies. *Anim. Behav.* 85, 1012–1022. doi: 10.1016/j.anbehav.2013.02.012

Sahay, A., Scobie, K. N., Hill, A. S., O'Carroll, C. M., Kheirbek, M. A., Burghardt, N. S., et al. (2011). Increasing adult hippocampal neurogenesis is sufficient to improve pattern separation. *Nature* 472, 466–470. doi: 10.1038/nature 09817

Snyder, J. S., Grigereit, L., Russo, A., Seib, D. R., Brewer, M., Pickel, J., et al. (2016). A transgenic rat for specifically inhibiting adult neurogenesis. *eNeuro* 3:ENEURO.0064-16.2016. doi: 10.1523/ENEURO.0064-16.2016

Spalding, K. L., Bergmann, O., Alkass, K., Bernard, S., Salehpour, M., Huttner, H. B., et al. (2013). Dynamics of hippocampal neurogenesis in adult humans. *Cell* 153, 1219–1227. doi: 10.1016/j.cell.2013.05.002

van Dijk, R. M., Lazic, S. E., Slomianka, L., Wolfer, D. P., and Amrein, I. (2016). Large-scale phenotyping links adult hippocampal neurogenesis to the reaction to novelty. *Hippocampus* 26, 646–657. doi: 10.1002/hipo.22548

Walton, N. M., Zhou, Y., Kogan, J. H., Shin, R., Webster, M., Gross, A. K., et al. (2012). Detection of an immature dentate gyrus feature in human schizophrenia/bipolar patients. *Transl. Psychiatry* 2:e135. doi: 10.1038/tp.2012.56

Weissleder, C., Fung, S. J., Wong, M. W., Barry, G., Double, K. L., Halliday, G. M., et al. (2016). Decline in proliferation and immature neuron markers in the human subependymal zone during aging: relationship to EGF- and FGF-related transcripts. *Front. Aging Neurosci.* 8:274. doi: 10.3389/fnagi.2016. 00274

Yim, H., Dennis, S. J., and Sloutsky, V. M. (2013). The development of episodic memory: items, contexts, and relations. *Psychol. Sci.* 24, 2163–2172. doi: 10.1177/0956797613487385

Conflict of Interest Statement: The author declares that the research was conducted in the absence of any commercial or financial relationships that could be construed as a potential conflict of interest.

frontiers in Neuroscience

ORIGINAL RESEARCH
published: 27 March 2017
doi: 10.3389/fnins.2017.00139

Exploring the Relationship between Brain Plasticity, Migratory Lifestyle, and Social Structure in Birds

Shay Barkan[1], *Yoram Yom-Tov*[1] *and Anat Barnea*[2]*

[1] *Department of Zoology, Tel-Aviv University, Tel-Aviv, Israel,* [2] *Department of Natural and Life Sciences, The Open University of Israel, Ra'anana, Israel*

Studies in Passerines have found that migrating species recruit more new neurons into brain regions that process spatial information, compared with resident species. This was explained by the greater exposure of migrants to spatial information, indicating that this phenomenon enables enhanced navigational abilities. The aim of the current study was to test this hypothesis in another order—the Columbiformes – using two closely-related dove species—the migrant turtle-dove (*Streptopelia turtur*) and the resident laughing dove (*S. senegalensis*), during spring, summer, and autumn. Wild birds were caught, treated with BrdU, and sacrificed 5 weeks later. New neurons were recorded in the hyperpallium apicale, hippocampus and nidopallium caudolaterale regions. We found that in doves, unlike passerines, neuronal recruitment was lower in brains of the migratory species compared with the resident one. This might be due to the high sociality of doves, which forage and migrate in flocks, and therefore can rely on communal spatial knowledge that might enable a reduction in individual navigation efforts. This, in turn, might enable reduced levels of neuronal recruitment. Additionally, we found that unlike in passerines, seasonality does not affect neuronal recruitment in doves. This might be due to their non-territorial and explorative behavior, which exposes them to substantial spatial information all year round. Finally, we discuss the differences in neuronal recruitment between Columbiformes and Passeriformes and their possible evolutionary explanations. Our study emphasizes the need to further investigate this phenomenon in other avian orders and in additional species.

Keywords: bird migration, brain plasticity, hippocampus, hyperpallium apicale, new neuronal recruitment, nidopallium caudolaterale

OPEN ACCESS

Edited by:
Irmgard Amrein,
University of Zurich, Switzerland

Reviewed by:
Dina Kea Noanoa Dechmann,
Max Planck Institute for Ornithology (MPG), Germany
Loreta Medina,
University of Lleida, Spain

***Correspondence:**
Anat Barnea
anatba@openu.ac.il

Specialty section:
This article was submitted to Neurogenesis, a section of the journal Frontiers in Neuroscience

Received: *02 November 2016*
Accepted: *07 March 2017*
Published: *27 March 2017*

Citation:
Barkan S, Yom-Tov Y and Barnea A (2017) Exploring the Relationship between Brain Plasticity, Migratory Lifestyle, and Social Structure in Birds. Front. Neurosci. 11:139. doi: 10.3389/fnins.2017.00139

INTRODUCTION

The phenomenon of new neuronal recruitment in the adult avian brain has been extensively studied during the last few decades. Many of these studies have indicated a relationship between the amount of new neuronal recruitment and the amount of new information that the brain has to acquire, for example during song learning and production, social interactions, and food hoarding (reviewed in Barnea and Pravosudov, 2011). However, so far, only a few studies have investigated whether a relationship exists between new neuronal recruitment and migratory behavior as the latter exposes migrating birds to more spatial changes than resident ones. For example, LaDage et al. (2011) showed that migratory adult white-crowned sparrows (*Zonotrichia leucophrys gambelii*) recruit more new hippocampal neurons than their residential subspecies (*Z. l. nuttalli*). More

recently, we extended this examination (Barkan et al., 2014), looking at two brain regions known to be involved in processing spatial information—the hippocampus (HC) and the nidopallium caudolaterale (NCL), and compared new neuronal recruitment in these regions between two closely-related species—the migratory reed warbler (*Acrocephalus scirpaceus*) and the residential clamorous warbler (*A. stentoreus*). Similarly to LaDage et al. (2011), our study, which was carried out under semi-natural conditions, found more new neurons in both the HC and NCL of the migrant species, compared to the resident one. We suggested that this phenomenon enables the enhanced navigational abilities that are required for the migratory lifestyle.

Most of the studies on new neuronal recruitment in birds have focused on passerine species. Hence, in the current study we aimed to extend the investigation via another avian order—the Columbiformes—and more specifically, in relation to migratory behavior, by comparing migrant and resident species. In this avian order, many studies have used homing pigeons (*Columba livia domestica*), a species with supreme navigational abilities (Papi et al., 1989; Wallraff, 1996, 2001; Odetti et al., 2003; Bingman et al., 2004, 2005; Biro et al., 2007; Jorge et al., 2010; Mehlhorn et al., 2010). These studies indicated that homing pigeons rely on several external cues for orientation and navigation, such as visual landmarks, sun compass, magnetic fields, olfactory cues and more. Motivation and experience were also found to be important for successful homing (reviewed by Mehlhorn and Rehkamper, 2009). In this respect, experience must include learning and memory mechanisms in order to improve navigation abilities and maintain cognitive maps (inherited or acquired by experience). These mechanisms have been suggested as a tool for spatial orientation of long-distance migration in birds (Wiltschko and Wiltschko, 1999). However, to the best of our knowledge, no study has yet examined whether a relationship exist between migratory behavior and new neuronal recruitment in brains of non-passerine species. The only study that recorded neuronal recruitment in Columbiformes used ring doves (*Streptoplia risoria*), and found an overall age-related decline of neuronal recruitment in the forebrain, and primarily in the nidopallium caudal and hyperstriatum regions (Ling et al., 1997).

Accordingly, we aimed to extend our previous study (Barkan et al., 2014) and investigate whether the positive correlation that we had found in passerines, between migratory lifestyle and neuronal recruitment, exists also in non-passerine species. If so, we hypothesized that, as in passerines, new neuronal recruitment into relevant brain regions will be more pronounced in migrant species that travel long-distances twice a year, than in resident ones. In addition, we sought to determine whether differences in neuronal recruitment, if found, would follow a seasonal pattern that will correlate with the migration periods. More specifically, we predicted that neuronal recruitment will increase during or prior to the migrating seasons (spring and autumn), in comparison to summer, the non-migrating season. However, we are aware of possible alternative hypotheses, because others have found, for example in bats, no indication of a correlation between neurogenesis and phylogenetic relationships, foraging behavior, habitat, or diet (Amrein et al., 2007). Such studies argue that the widely accepted notion that neurogenesis has an important role in spatial abilities has to be considered carefully (Amrein and Lipp, 2009).

In order to test our hypothesis, we focused our attention on three brain regions: the HC, NCL, and hyperpallium apicale (HA). The roles of the HC and NCL in processing spatial information were described in our previous study (Barkan et al., 2014; and see also the recent review by Herold et al., 2015). The third brain region, HA, is part of the Wulst, a brain region considered to be homologous to the mammalian visual cortex, although some of its structures evolved independently in birds and mammals (Medina and Reiner, 2000). The Wulst has been suggested to be involved in sun-compass-guided behavior (Budzynski et al., 2002) and in learning or acquisition of familiar landmark navigation (reviewed by Bingman et al., 1998) in homing pigeons. Another function that had been suggested for the HA, together with cluster N neurons, is in assisting in orientated magnetic-compass-guided behavior in nocturnal migrants (Mouritsen et al., 2005). The assumption is that through this pathway birds are able to perceive the geomagnetic field and follow it to navigate in the dark (Heyers et al., 2007; Zapka et al., 2009).

We used two species from the Columbiformes order: the laughing dove (*Streptopelia senegalensis*) and the turtle dove (*S. turtur*). These species were chosen because they are closely related and similar in their behavioral ecology, but the former is resident in Israel while the latter is a migratory species. Their similar behavioral ecology is expressed in both species occupying a wide range of Mediterranean habitats, including agricultural areas and well-vegetated plains. Both species are granivorous, but laughing doves tend to inhabit urban areas and their outskirts, whereas turtle doves prefer semi-open landscapes with trees, orchards or citrus groves (Shirihai et al., 1996). In Israel, laughing doves breed from February to July and their nesting sites vary greatly, from tree-tops to house windowsills, with a minimum of 100 m between nests. Turtle doves breed from April to mid-September and, unlike laughing doves, tend to nest in close proximity to each other, only a few meters apart. Breeding populations arrive in Israel from Africa during spring (mid-March to mid-June) and remain until the end of autumn (mid-September to mid-October), when they gather in large pre-migration flocks and then depart for their winter quarters (Shirihai et al., 1996). Turtle doves winter mainly in northern and central Africa, although on rare occasions they have been recorded as far south as Botswana and South Africa (Cramp and Perrins, 1994; Lepage, 2014; Barkan et al., 2016). In both species we recorded, in spring, summer, and autumn, the number of new neurons in the three brain regions that are thought to be relevant for the processing of spatial information—the HA, HC, and NCL. We hypothesized that, similar to our previous findings in passerines (Barkan et al., 2014), new neuronal recruitment in these brain regions would be higher in the migrant turtle dove than in the resident laughing dove, and that this pattern will correlate with the migration seasons.

MATERIALS AND METHODS

Experimental Design

Turtle doves and laughing doves were collected under the Israel Nature and National Parks Protection Authority permit (2005/24706). The study was approved by the Tel-Aviv University Institutional Animal Care and Use Committee (permit L-06-008) and was carried out in accordance with its regulations and guidelines regarding the care and use of animals for experimental procedures. Birds were caught at three times during the year: February to mid-April (spring), June to mid-July (summer), September to mid-November (autumn), and **Table 1** presents the sample sizes for each species, season, sex and age. Turtle doves were caught in the Beit She'an valley (35°31′E; 32°24′N) using mist nets, and laughing doves were caught by using 1*1*1 m trap cages built with one directional corridor entrance, and lured with food bait in the Zoological Gardens at Tel-Aviv University (34°48′E; 32°6′N). Upon capture, birds were banded with plastic colored rings (A.C. Hughes LTD., UK) and weighed to the nearest 0.5 g using a 300 g spring scale (Pesola AG, Switzerland). In addition, birds were aged according to plumage and iris color (Shirihai et al., 1996; personal knowledge), and transferred to outdoor aviaries in the Botanical Gardens of Tel-Aviv University. Each bird was held individually and injected, on three consecutive days, into the pectoral muscle with 10 μl/g body mass of 5-bromo-2-deoxyuridine (BrdU; SigmaUltra, Sigma, diluted 10 mg/ml in sterile water). BrdU is a cellular birth-date marker and our doses were similar to those previously used to study adult neurogenesis in birds (Wang et al., 2002; Pytte et al., 2007; Adar et al., 2008). Birds were kept in their aviaries for 5 weeks, to allow enough time for neurons born at the time of treatment to migrate to their final destination and undergo final anatomical differentiation (Alvarez-Buylla et al., 1988; Kirn et al., 1999). Aviaries were 3*2.5*1 m in size and spaced 1 m apart. The walls of the aviaries were covered halfway up with burlap and the roof was of opaque plastic, to allow visual and auditory contact between individuals, while at the same time providing some isolation, to reduce possible stress. Birds were exposed to natural illumination (10.1–14.7 h of light/day) and temperature (ranging between 12 and 30°C seasonally). Food and water were provided *ad libitum* and consisted of sorghum, milled corn, wheat seeds, crushed eggs, and mineral stones (Redstone,Versele-Laga, Belgium). As an indirect measure of the general health of the birds, we weighed each individual upon capture, then 3 days and 3 weeks later, and on the day of perfusion.

TABLE 1 | Sample sizes, divided by species, seasons, and ages.

Species	Season	Adults		Juveniles		Total
		Males	Females	Males	Females	
Laughing dove	Summer	1	3	1	4	9
(resident)	Autumn	4	2	3	2	11
	Spring	5	4	1		10
Turtle dove	Summer	6	2		2	10
(migrant)	Autumn	1				1
	Spring	6	2	2		10

Histology and Immunohistochemistry

Birds were killed with an overdose of anesthesia (0.06 ml of ketalar diluted 10 times followed by 0.06 ml of xylazine per gr/body mass) and fixed with an intracardiac perfusion with saline (0.9% NaCl) followed by 4% paraformaldehyde in 0.1 M phosphate buffer (PB; pH 7.4). Sex was determined by gonadal inspection, brains were removed, weighed, transferred into PB in 4°C, and then within 1–4 days they were dehydrated in alcohols, embedded in polyethylene glycol, blocked and cut transversely to 6 μm thick sections. Every 20th section (intervals of 120 μm between sections) was mounted on slides (Superfrost/PLUS), using a solution of 0.1% BSA (albumin bovine, minimum 98%) in PBS. Sections were incubated for 10 min in 0.01 M citrate buffer (pH 5.6–6) at 90–95°C to denature the DNA (to make BrdU more accessible to the antibody), washed in PB for 5 min, and incubated for 2 min in weak pepsin (pepsin stock; Sigma, 2.5% in PBS 1M) diluted 1:19 in 0.1N HCl at room temperature (RT). After washing (PB, 3 times, 5 min each), sections were incubated in 3% H_2O_2 in PB for 20 min and then washed with PB twice, 5 min each. Blocking of non-specific binding sites was done by incubating the sections for 1 h in blocking buffer (PB containing 10% normal horse serum and 0.3% Triton X-100). Then, sections were incubated for 48 h at 4°C, with primary antibodies: rat anti-BrdU IgG2a (Serotec; diluted 1:200) and neuronal specific antibody, anti-HuC/HuD mouse IgG2b, monoclonal 16A11 (Invitrogen; diluted 1:200). Then sections were washed and incubated for 2 h at RT with the secondary antibodies: F(ab)2 donkey anti-rat IgG-Cy3 (Jackson ImmunoResearch; diluted 1:200), which stains BrdU cells with fluorescent red and Alexa Flour 488 donkey anti mouse IgG (H+L; Invitrogen; diluted 1:200) which stains neurons with fluorescent green. Then, sections were washed 3 times for 5 min each with PB, coverslipped with Aqua-Poly/Mount glue (Polysciences), and kept in the dark at 4°C until mapping.

Brain Regions, Mapping, and Quantification

We focused our attention on three brain regions: the hyperpallium apicale (HA), hippocampal complex (HC), and nidopallium caudolaterale (NCL) (**Figure 1A**). The borders of the brain regions and anatomical positions noted below were defined according to the atlas of the pigeon brain (Karten and Hodos, 1967). We do not know whether pigeons (on which the landmarks were based) and our investigated dove species have proportionally identical brain regions on the rostral-caudal plane. Therefore, in our mapping we wanted to ensure that: (1) our sampling does not extend outside the borders of the region that we mapped; and (2) we avoid overlapping or inclusion of part of another brain region that we sampled. To achieve these goals, we used a conservative approach, so that all the sections that we mapped, in each brain region, were well within it, and did not reach its outmost caudal or rostral extents as identified in the atlas of the pigeon brain. This method resulted in the fact

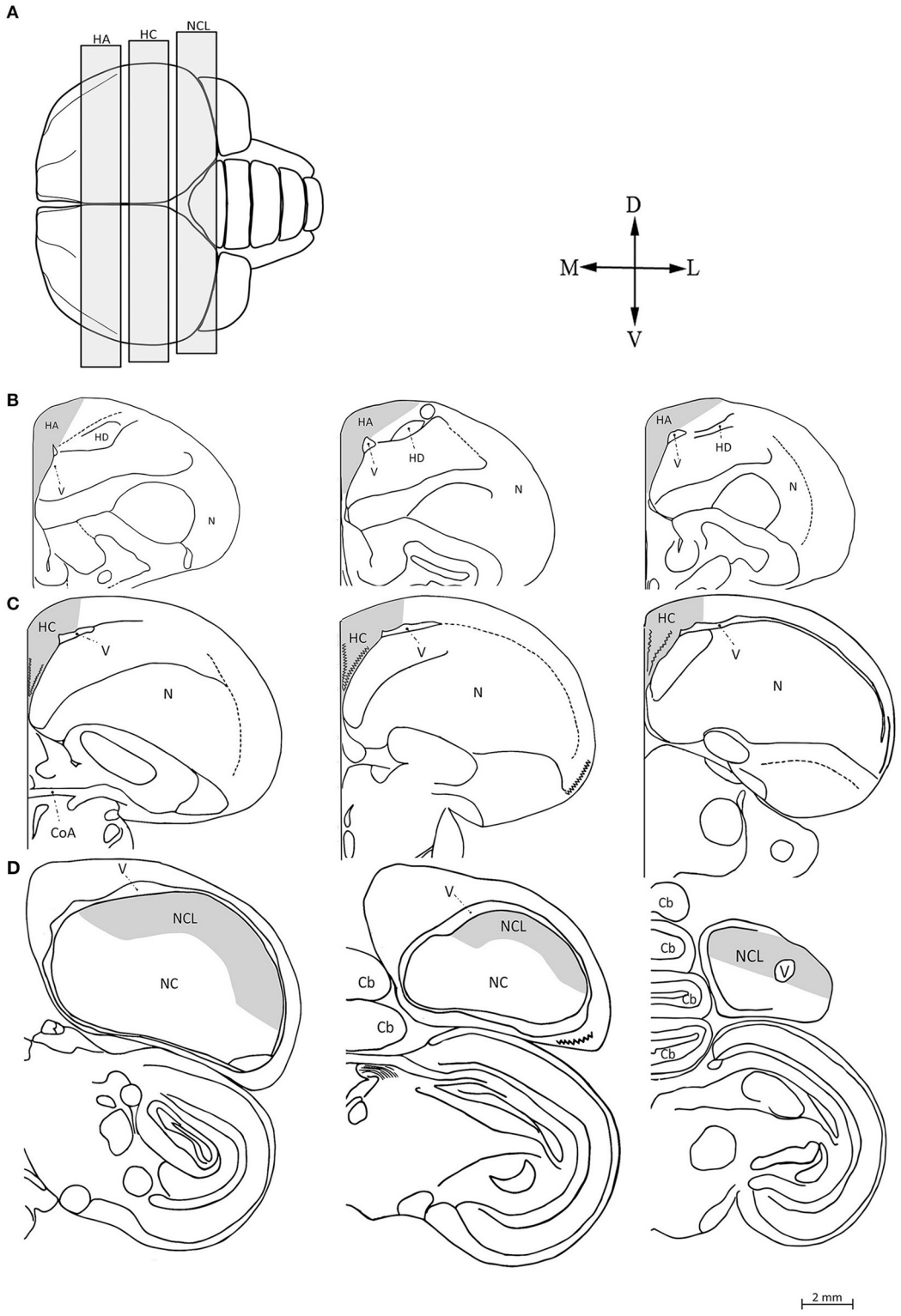

FIGURE 1 | Schematic views of the three investigated brain regions. (A) Top view of the brain: rostral is to the left, caudal is to the right. We indicate the range within which frontal sections were taken from the hyperpallium apicale (HA), hippocampal complex (HC), and nidopallium caudolaterale (NCL). Seven sections were sampled along the rostro-caudal axis of each brain region (for details, see text), three of which are shown here: the most rostral, the middle, and the most caudal (from left to right), in HA **(B)**, HC **(C)**, and NCL **(D)**. Abbreviations: Cerebellum (Cb), Commissura anterior (CoA), Hyperpallium Dorsal (HD), Nidopallium (N), Nidopallium caudale (NC), Lateral ventricle (V). Orientations: Dorsal (D), Lateral (L), Ventral (V), and Medial (M). Adapted from Karten and Hodos (1967).

that we did not map the whole region rostral-caudally, but on the other hand it ensured that we mapped only sections that are within this region, and also that these sections do not include parts of another brain region that we sampled. For more specific descriptions, see below.

Accordingly, within each region we defined the rostal and caudal sections that we sampled, and between them we sampled additional ones. Ideally, one would want to sample as many sections as possible, but given the number of birds involved and time limitations, we conducted preliminary mapping on one brain, to determine how many sections we need to map in order to representative results. Therefore, in this brain we mapped about 10 sections per region, and then compared the results that were obtained from these 10 sections to results that we got by including, each time, one less section in our calculations (i.e., by including nine sections, then eight sections, and so on). Based on this preliminary mapping test we settled for total of seven sections per region, which is similar and sometimes even more than the number of sections that we used in previous studies that investigated the same brain regions (e.g., Adar et al., 2008; Barkan et al., 2014). These sections were at fixed and constant anatomical locations across the rostro-caudal axis, so that in all brains, each of the seven sampled sections were exactly in the same rostral-caudal position (with an overall average interval of 240 μm between each pair of sections).

Hyperpallium Apicale (HA)

The atlas of the pigeon brain defines the rostral-caudal extents of the HA as A14.50 and A7.50, respectively. Therefore, following our conservative approach that is described above, we restricted our sampling so that it was well within the HA, as follows: The most rostral section corresponded to level A9.5 in the atlas of the pigeon brain and the most caudal section was defined 500 μm rostrally to the CoA, corresponding to level A8.25 in the same atlas (**Figure 1B**). By doing so we ensured that we sampled well within the HA, and in addition do not include parts of the HC (which, according to the atlas, its most rostral extent is A8.00, while we started sampling the HA even more rostrally than that). In each section, the ventral boundary was defined by the wall of the lateral ventricle, the medial boundary by the midline, and the dorsal one by the surface of the brain. The lateral boundary was indistinguishable by our staining methods and was therefore defined arbitrarily, as follows: in the rostral sections (#1–4) we drew a line between the dorsal tip of the lateral ventricle and the dorsal surface of the brain at 30° relative to the midline (**Figure 2A**). The same method was applied in the caudal sections (#5–7), but at 60° relative to the midline (**Figure 2B**).

Hippocampal Complex (HC)

The atlas of the pigeon brain defines the rostral-caudal extents of the HC as A8.00 and A3.25, respectively. According to the same conservative approach that we mentioned above, our sampling of HC was restricted as follows: The most rostral section was defined by the presence of the commissura anterior (CoA), and corresponded to level A7.75 in the atlas of the pigeon brain (**Figure 1C**). The most caudal section of the HC corresponded to level A6.25 in that atlas. The ventral, dorsal, and medial

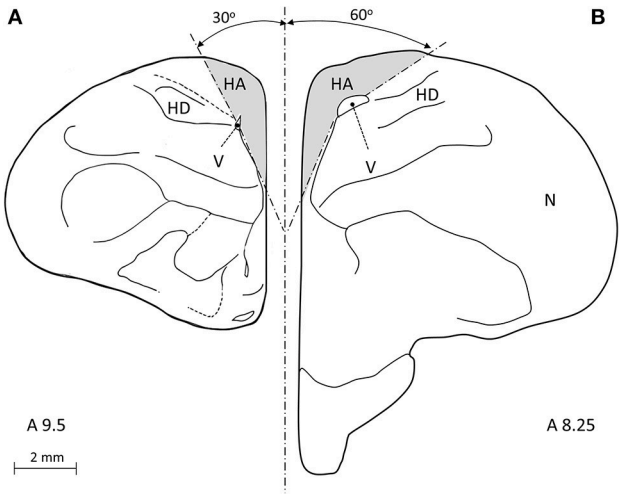

FIGURE 2 | A frontal view of a pigeon brain (adapted from Karten and Hodos, 1967), is used to illustrate our definition of the lateral boundary of the hyperpallium apicale (HA). (A) In rostral sections (#1–4) we drew an arbitrary line from the dorsal tip of the lateral ventricle (V) to the dorsal surface of the brain at 30° relative to the midline. **(B)** In caudal sections (#5–7) we applied the same method but at 60° relative to the midline.

boundaries in each section were defined according to previously defined criteria (Barnea and Nottebohm, 1994; Barnea et al., 2006).

Nidopallium Caudolaterale (NCL)

The most caudal section corresponded to level A3.0 in the atlas of the pigeon brain. The most rostral section corresponded to level A4.5 in the atlas, and was defined according to the lateral ventricle along the dorsal part of the brain (**Figure 1D**). The ventral boundary was indistinguishable by our staining methods and was therefore determined according to the dopaminergic innervation recorded in pigeons by Waldmann and Gunturkun (1993). Since brains of laughing doves and turtle doves differ in size from the pigeon brain, we followed the method described in Barkan et al. (2014) to determine the ventral boundary relative to that in the pigeon brain.

Mapping

We used a computerized brain-mapping system (Stereo Investigator; MicroBrightField Inc.) to draw boundaries of the HA, HC, and NCL, in each section sampled, mark the position of each labeled neuron, count neurons and quantify other neuronal parameters, as described below. All sections of all the brains were mapped and analyzed by only one person (SB). Mapping of all the brains was always done blind in relation to season and age. However, due to overall differences in brain sizes between the two species, in some sections the person who did the mapping could identify the species by the size of the section. Ling et al. (1997) found that new neurons are distributed in dove's forebrain without clustering in any particular pattern, and therefore we focused only on the left brain hemisphere. Each of the sampled sections was completely scanned, using a 63X objective and the Stereo-Investigator meander scan probe.

Our immunohistochemistry protocol yielded neurons that were stained fluorescent green (with anti-HuC/HuD), and nuclei of new neurons that were stained fluorescent red (with anti-BrdU). Therefore, cells with co-localization of green cytoplasm and a red fluorescent nucleus were identified as new neurons (**Figure 3**). Accordingly, in each section, we recorded the location of all $BrdU^+$ neurons and counted them. To validate co-localization of the two markers, we used a confocal microscope to examine several dozens of such neurons, from the investigated species and from the examined brain regions (**Figure 4**).

Neuronal Densities and Nuclear Diameters of Neurons

We also measured nuclear diameters of all $BrdU^+$ neurons. From the knowledge of section thickness (6 μm) and mean nuclear diameter of labeled neurons in a certain brain region, using the Abercrombie stereological correction equation (Guillery and Herrup, 1997) we could estimate the number of new neurons per mm^3 in each section. Data from all mapped sections for each brain region were averaged so that each region was represented by a single estimated number of $BrdU^+$ neurons per mm^3.

In each brain region we also sampled the nuclear diameters of total neurons ($BrdU^+$ and unlabeled ones) and estimated their density per mm^3. This was done in a section that was positioned midway between sections #3 and #4, in order to avoid fluorescence decay in the sections that were used for mapping. In this section, all neurons were counted in 12–18 sampling squares (100 × 100 μm each), randomly chosen by the mapping software, using the fractionator probe. All neurons that were observed within each square or touched two of its boundaries were counted, while neurons that touched the two other boundaries were excluded. In every other sampling square, we also measured the diameters of all neurons. As explained above, these data allowed us to estimate the total number of neurons per mm^3 in each of the investigated brain regions.

Statistical Analysis

Our data contained four independent fixed variables: migration strategy (migrant, resident); brain region (HA, HC, NCL); season (spring, summer, autumn); age (adult, juvenile). Due to small sample sizes, sex differences were not examined and, therefore, both sexes were pooled. The numbers and percentages of new neurons/mm^3 that were counted and calculated at seven sections in each brain region were averaged, giving one value for each brain region per bird (depended variables). We could directly compare the number of $BrdU^+$ neurons/mm^3 between species, because densities of total neurons ($BrdU^+$ and unlabeled ones) for each brain region were similar between the two species. Accordingly, the results are presented as number of $BrdU^+$ neurons/mm^3. In addition, to allow comparisons with other species in previous studies (ours, as well as from other laboratories), we also calculated and present the percentages of $BrdU^+$ neurons out of total neurons/mm^3.

Effects of the four independent variables on the number and percentage of new neurons/mm^3 were analyzed by Generalized Linear Mixed Model (GLMM) analysis. This model was chosen because it can deal with gamma-distributed data, as was the case in our study. Total neuronal density and nuclear diameter were tested against the same four independent variables by linear mixed model (MIXED). Model goodness of fit was tested by Akaike information criterion (AIC). Interactions between any of the tested variables are indicated only if they were found to be significant. Significant differences were followed by Bonferroni *post-hoc* comparison, adjusted with multiple comparisons correction. Brain and body mass were log transformed before analysis and tested with one way ANOVA. Tests were performed at 0.05 level of significance (IBM Corp, 2012; SPSS Version 20, Armonk, NY). Results are presented as means (±SE) and sample sizes are provided in brackets.

RESULTS

Number of New Neurons Per mm^3

Overall we found more new neurons in brains of laughing doves than in those of turtle doves [GLMM, $F_{(1, 144)} = 11.6$, $P = 0.001$]. A correlation between species and season [GLMM, $F_{(2, 144)} = 3.5$, $P = 0.033$] revealed that laughing dove have significantly higher values than turtle dove in autumn and in summer [*post-hoc*, $P = 0.07$; $P = 0.017$; respectively; **Figure 5**], while at

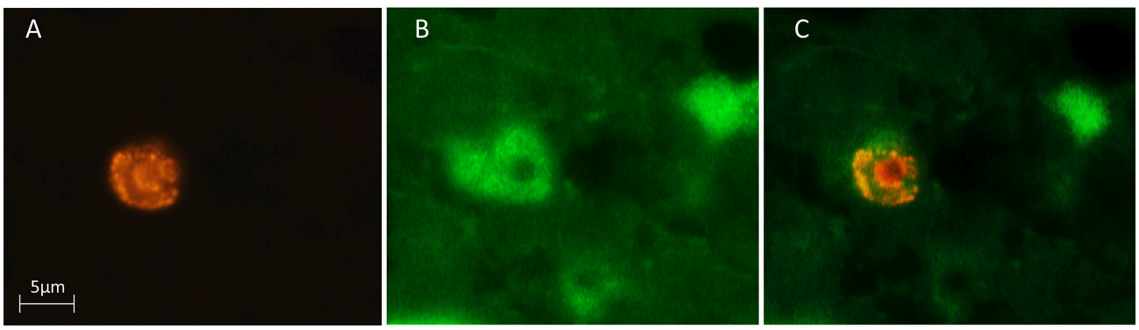

FIGURE 3 | Three microphotographs of the same field, showing a newly-formed neuron in the hyperpallium apicale (HA) of a turtle dove. BrdU-labeled cells were identified with a rhodamine filter **(A)** and Hu-labeled neurons were identified with a FITC filter **(B)**. Double-labeled neurons were identified by alternating between these two filters and by using a dual FITC-rhodamine filter to show co-localization of the two markers **(C)**.

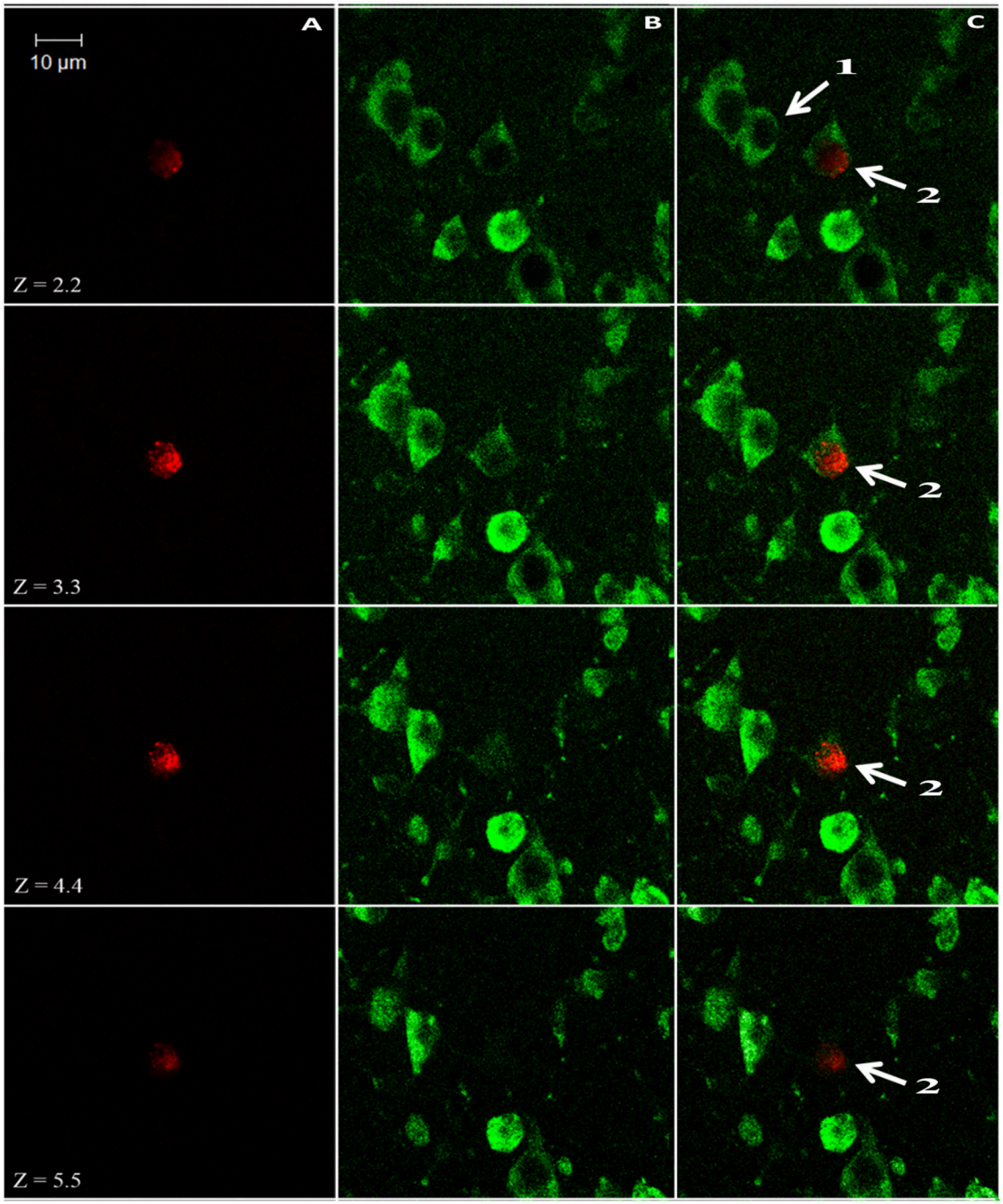

FIGURE 4 | Z-stack images from the nidopallium caudolaterale (NCL) of a laughing dove (*Streptopelia senegalensis*), under a confocal microscope. Neurons display only green cytoplasm (labeled with the endogenous marker HU; e.g., cell 1), whereas new neurons also display red nuclei (labeled with the birth-date exogenous marker BrdU; cell 2); these two markers have to co-localize within the same cell along several Z-positions to validate its identification as new neuron. Images were collected at 1.1-lm intervals. **(A)** Red 543-nm wavelength frame. **(B)** Green 488-nm wavelength frame. **(C)** Combined red and green wavelengths.

spring no differences were found between the species. Overall, no significant differences were found between ages, seasons and brain regions. Within each species no differences were found between seasons or brain regions.

Percentage of New Neurons Per mm^3

We found higher percentages of new neurons in brains of laughing doves than in those of turtle doves [GLMM, $F_{(1,\ 144)} = 23.3$, $P < 0.001$]. A correlation between species and season

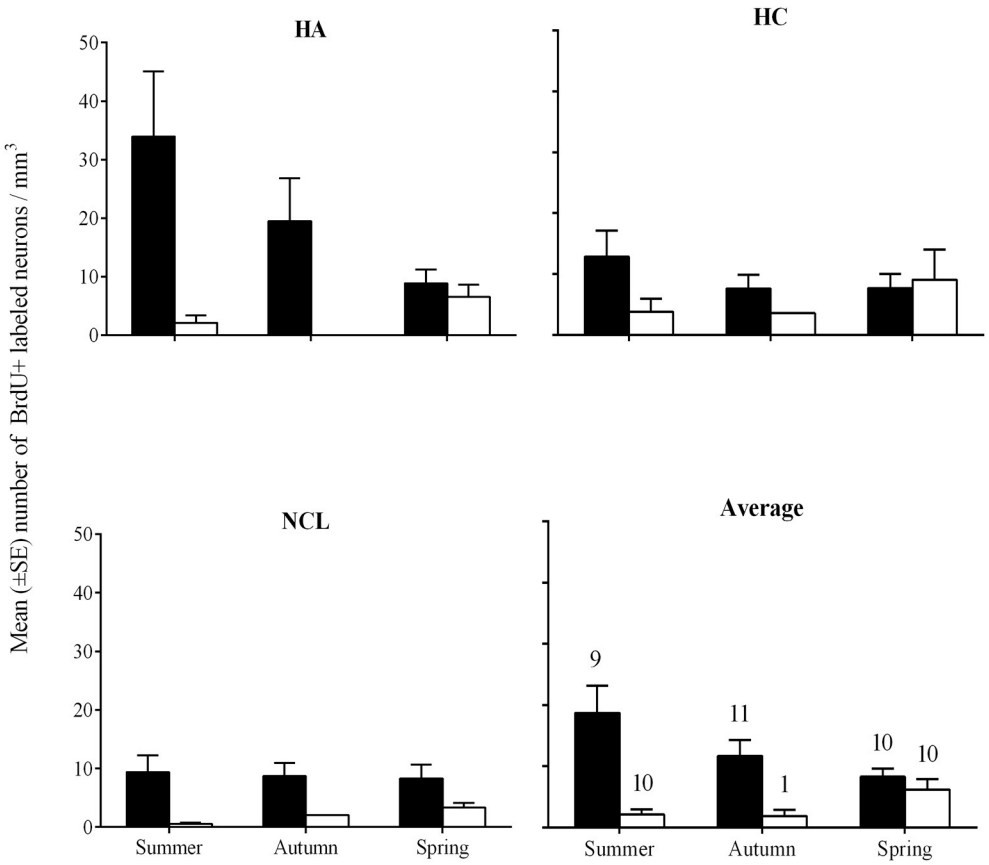

FIGURE 5 | Mean number (±SE) of new neurons per mm^3 in the hippocampal complex (HC), hyperpallium apicale (HA), nidopallium caudolaterale (NCL), and the average of the three brain regions (Average), by species and seasons. Laughing dove: black bars; Turtle dove: empty bars. Sample sizes that are indicated in the Average figure also apply to the three other figures.

[GLMM, $F_{(2,\ 144)} = 9.64$, $P < 0.001$] revealed that laughing dove have higher neuronal recruitment than turtle dove at autumn and summer while at spring no differences were found between the two species (*post-hoc*, $P = 0.003$; $P = 0.005$; respectively; **Figure 6**). Overall, significant differences were also found between ages, in both species, with higher values in young individuals than in older ones [GLMM, $F_{(1,\ 144)} = 5.1$; $P = 0.026$; 0.018 ± 0.001; 0.007 ± 0.001; respectively]. However, due to sample size limitations, we could not test correlations between age and the other variables (seasons, brain regions). No difference was found between the brain regions. Within each species no differences were found between seasons or brain regions.

Estimated Densities of Total (BrdU$^+$ and Non-labeled) Neurons Per mm^3

No differences were found between species, season, or age, and pooled data per region, for each species, are presented in **Table 2**. Significant differences were found between all three brain regions [MIXED, $F_{(2,\ 146)} = 48.2$, $P < 0.001$], with highest neuronal density in the NCL, intermediate in the HA and lowest in the HC (for all comparisons $P < 0.001$).

Estimated Nuclear Diameters of New and Total Neurons

Due to the relatively low number of new (only BrdU$^+$ labeled) neurons found in a given brain region, no statistical comparisons were conducted regarding their nuclear diameters between species, brain regions, seasons, or ages. Pooled data per region, in each species, are presented in **Table 2**. Total (BrdU$^+$ and non-labeled) neuronal nuclear diameters were larger in juveniles than in adults [*t*-test, $t_{(1,\ 149)} = 2.76$; $P = 0.006$; 10 ± 0.2 ($N = 3{,}893$); 9.28 ± 0.15 ($N = 9{,}528$); respectively]. However, for simplicity, in the following comparisons we pooled both age categories and the results for each species are presented in **Table 2**. No differences were found between the two species in total neuronal nuclear diameter. Brain region comparison found significant differences, with largest neuronal nuclear diameters in the HC, intermediate ones in the HA and smallest in the NCL [MIXED, $F_{(2,\ 145)} = 44.1$, $P < 0.001$; *Post-hoc* for all comparisons, $P < 0.001$; 10.7 ± 0.2 ($N = 3{,}912$); 9.2 ± 0.16 ($N = 4{,}229$); 8.5 ± 0.16 ($N = 5{,}280$) respectively].

Body and Brain Mass

For both turtle doves and laughing doves, no seasonal differences were found in body mass [128.2 g $\pm$ 3.46 ($N = 20$); 115.3 g $\pm$

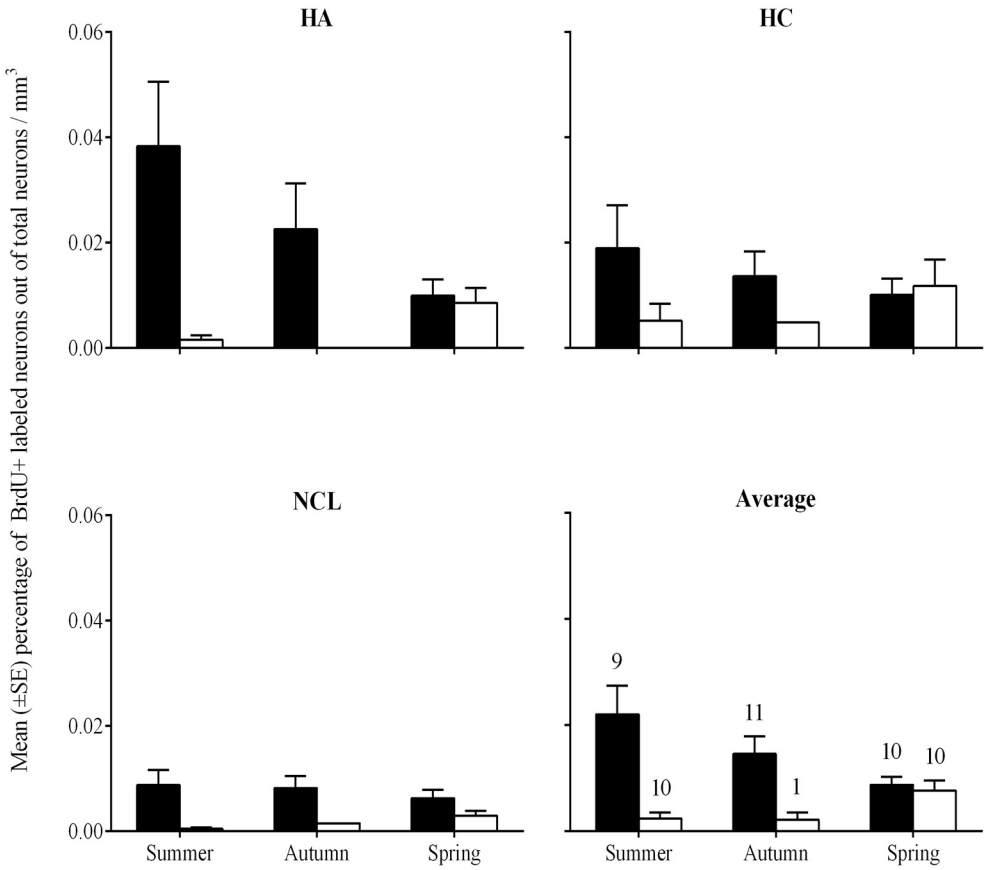

FIGURE 6 | Mean percentage (±SE) of new neurons per mm^3 in the hippocampal complex (HC), hyperpallium apicale (HA), nidopallium caudolaterale (NCL), and the average of the three brain regions (Average), by species and seasons. Laughing dove: black bars; Turtle dove: empty bars. Sample sizes that are indicated in the Average figure also apply to the three other figures.

2.88 ($N = 19$); respectively]. During the 5 weeks of captivity, birds' mean body mass decreased only by 1–4.5% of their initial mass and no difference in percentage of body mass loss was found between the species. Similarly, for both species, no seasonal differences were found in brain mass [1.2 g ± 0.01 ($N = 20$); 1.1 g ± 0.02 ($N = 19$); respectively]. Age comparison of brain mass revealed no differences in laughing doves and was not compared in turtle doves due to sample size limitation.

DISCUSSION

Neuronal Recruitment and Sociality

Our previous study (Barkan et al., 2014), which focused on passerine species, supported our hypothesis of a positive relation between migratory lifestyle and new neuronal recruitment in brain regions that are known to process spatial information. An earlier study by others (LaDage et al., 2011) also supports this notion. However, our present study, which used non-passerines from the Columbiformes order, found an opposite outcome, of overall higher neuronal recruitment in relevant brain regions of the resident laughing dove than in those of the migratory turtle dove.

The contesting results found between doves and passerines are mainly due to the differences in levels of neuronal recruitment between the migratory species, whereas the resident ones exhibit similar levels, and **Figure 7** demonstrates these patterns. We suggest that the differences in neuronal recruitment between the migrating species might be due to their different social structure, with reed warblers being less social than turtle doves. For example, during the breeding season pairs of reed warblers establish separate territories and nest dozens of meters apart from their neighbors (Catchpole, 1972). Similarly, during migration, they move as a wave of individuals, with no apparent organized flocks (Dewolfe et al., 1973; Evans and Heiser, 2004a). Turtle doves, in contrast, are social birds, tending to nest in dense groups only a few meters apart from each other (Shirihai et al., 1996), and migrate in organized flocks (Ash, 1977; personal observation). Hence, could social structure explain the amount of new neuronal recruitment that we found in our studies?

Several studies have focused on the role of sociality in decision-making in migratory birds. For example, homing pigeons form group flights in order to increase their vigilance and reduce predation risk (Gould, 2006). Group flights have also been suggested to improve the birds' navigation as a

TABLE 2 | Mean (±SE) densities and nuclear diameters of total (new and old) and only new neurons, in brains of laughing doves (residents) and turtle doves (migrants). Pooled data from all seasons are presented by brain region. In brackets for densities—the number of brains sampled; in brackets for diameters—the number of neurons sampled.

Species	Brain region	Density of total neurons per mm^3	Nuclear diameter of total neurons (μm)	Nuclear diameter of new neurons (μm)
Laughing dove	HA	96,364 ± 4,376 (29)	9.4 ± 0.17 (2,365)	9.0 ± 0.43 (231)
	HC	73,061 ± 4,288 (39)	10.7 ± 0.26 (2,225)	8.5 ± 0.57 (71)
	NCL	122,051 ± 5,438 (30)	8.8 ± 0.16 (3,062)	9.2 ± 0.37 (1,116)
Turtle dove	HA	104,127 ± 7,395 (21)	8.9 ± 0.3 (1,864)	9.6 ± 0.75 (27)
	HC	77,153 ± 4,619 (20)	10.6 ± 0.35 (1,657)	8.1 ± 0.73 (20)
	NCL	143,146 ± 8,851 (21)	8.1 ± 0.33 (2,218)	8.1 ± 0.41 (181)

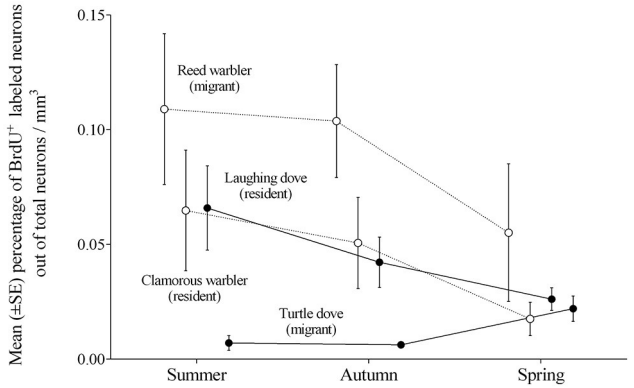

FIGURE 7 | Mean percentages (±SE) of new neurons per mm^3 by seasons, combined from the hippocampal complex (HC), hyperpallium apicale (HA), and nidopallium caudolaterale (NCL), in brains of two warblers species (empty circles; the migrant Reed warbler and the resident Clamorous warbler; Barkan et al., 2014), and two dove species (filled circles; the migrant Turtle dove and the resident Laughing dove; current study).

consequence of the "many wrongs" principle: The pooling of information from many inaccurate compasses yields a single more accurate compass (Simons, 2004). In addition, it had been shown that when conflicts occur between migrating individuals in a group of pigeons, the submissive individuals tend to follow the dominant leaders (Biro et al., 2006; Gould, 2006; Nagy et al., 2010; Flack et al., 2013). Moreover, simulation models of group flights have demonstrated that a few individuals with strong directional preferences can lead large groups of less-well-informed individuals without losing group structure. The model predicted that as group size increases, fewer leaders are needed in order to obtain great accuracy (Couzin et al., 2005). Taken together, these studies suggest that group migration not only improves navigation accuracy compared to solitary migration, but also reduces the navigational efforts invested by each individual in the group. This could, in turn, reduce spatial demands and result in lower levels of neuronal recruitment, as we found in our migrating turtle doves. We are obviously aware that our suggestion that sociality during migration reduces spatial demands has to be tested. This can be done in a future study that will test the spatial memory of these two species.

Another future direction that might be worthwhile taken is in regard to the HC, which is composed of several sub-regions: V-field (that is considered comparable to the dentate gyrus); DM (dorsalmedial); and DL (dorsalateral) (reviewed in Barnea and Pravosudov, 2011, and see also more recent publications, e.g., Abellán et al., 2014; Striedter, 2016). If the counting of new neurons will be adjusted according to these sub-regions, then we might obtain more accurate information regarding levels of neuronal recruitment in the different parts of the HC of migrant vs. non-migrant doves. In addition, it is worth noting that the relationship we suggest, between low neuronal recruitment and high sociality, might be restricted to those brain regions that are known to process spatial orientation tasks. In this study we did not map brain regions which are not involved in spatial tasks. However, in another avian species (zebra finches; *Taeniopygia guttata*), it has been found that in such brain regions (e.g., HVC, Area X, and nidopallium caudale (NC), social complexity increases neuronal recruitment (Lipkind et al., 2002). This was explained by the involvement of these regions in auditory processes and vocal communication, skills that are required in social interactions. Hence, our suggestion is that sociality might have a differential effect on neuronal recruitment in different brain regions, depending on the function of these regions and their contribution to the organism's ability to adjust to different situations.

We realize that other factors might explain the contesting results that we found between doves (this study) and warblers (Barkan et al., 2014), rather than different navigation needs. For example, foraging behavior: granivorous species, such as doves, are not territorial, while most insectivours species, such as warblers, are (Shirihai et al., 1996). Therefore, migrating doves do not need to establish, memorize, and defend territories in order to ensure food supply. Another factor that might explain this opposite outcome between doves and warblers is the fact that doves, which are social and live in groups, can spend less time searching for predators and hence can invest more time foraging, compared with solitary species as the warblers. These differences between doves and warblers exist both in their wintering grounds, as well as in stopover sites en route, and might result in reduced spatial needs in migrating doves, that is manifested by lower neuronal recruitment, compared with migrating warblers. However, because to date only few studies investigated the possible relation between neurogenesis and animal migration, it is needless to say that one has to be cautious when discussing the results. Further research on more species has to be carried out before we can reach reliable conclusions and extract generalizations.

Neuronal Recruitment and Seasonality

Several studies revealed a relationship between seasonal behaviors—such as food hoarding (Barnea and Nottebohm, 1994; Patel et al., 1997; Hoshooley and Sherry, 2007; Sherry

and Hoshooley, 2010), or song production (Kirn et al., 1991; Alvarez-Buylla and Kirn, 1997)—and seasonal increase in neuronal recruitment. These studies suggested that neuronal recruitment peaks at times of the years when information load peaks. However, testing interactions between behavior and neuronal recruitment is challenging, because it is easy to confound correlation and causation, but difficult to determine the direction of the casual relationships (Brenowitz and Larson, 2015). Do seasonal changes (day length, temperature) cause changes in behavior, which, in turn, cause changes in brain nuclei that are associated with this behavior? Or is the causation opposite (Brenowitz, 2008), so that seasonal environmental changes cause changes in brain nuclei, which, in turn, cause changes in behavior? In relation to singing behavior in seasonal species, Brenowitz (2008) presents evidence for the latter suggestion, arguing that seasonal changes in the song nuclei are predominantly regulated by hormones, and that the subsequent changes in song play a secondary role in reinforcing neuronal changes. Another suggestion is that, in relation to the seasonal food-storing behavior, seasonal changes in the HC may be a consequence of the behavior itself (Herold et al., 2015; Sherry and MacDougall-Shackleton, 2015). Hence, there is still a debate about the factors that control changes in neurogenesis and further examples are needed to draw generalizations.

Our previous work (Barkan et al., 2014) also found seasonal changes in neuronal recruitment in brains of warblers, in regions that are known to process spatial information, where fewer new neurons were recruited in spring compared to other seasons. We interpreted this as being that in spring, when the birds settle in small breeding territories, they require fewer spatial skills, and this might conduce to a reduction in neuronal recruitment, as reflected in a decrease in new neurons, compared to other seasons, when the birds expand their home-range or migrate. However, unlike warblers, in the present study, in both dove species, we found no seasonal changes in neuronal recruitment.

A possible explanation for the different seasonal patterns of neuronal recruitment between doves and warblers could relate to their different territory sizes and the amount of exploration that these species exhibit during the breeding season. Warblers, which are insectivorous (Schluter, 1984), are highly territorial during the breeding season, occupy small territories (average of 332 m^2 for reed warblers and ∼800 m^2 for clamorous warblers), and spend much time defending them from intruders (Catchpole, 1972; Fazili, 2014). Doves in contrast, are granivorous and rely on patchy food, are less territorial and tend to flock for food searching (Davies, 1976; Schluter, 1984; Shirihai et al., 1996; Temple, 2004). For example, in our study area, doves nested densely in grapefruit orchards and foraged in large flocks in wheat fields, a few hundred meters to several kilometers distant from their nests (Browne and Aebischer, 2003; personal observations). Hence, it can be assumed that doves, which are more explorative than warblers during the breeding season, are exposed to heavier loads of spatial information, and therefore their neuronal recruitment levels in spring, which are similar to those in the other seasons, might serve to facilitate this explorative behavior.

We are aware of the need to be cautious when suggesting that differences in spatial use due to diet and sociality might affect neuronal recruitment. For example, it could be that our captive conditions, although similar for both species, caused them differential stress, because they differ in their natural history and therefore might react differently to captivity. Laughing doves are more urban and more associated with humans, whereas turtle doves prefer open land and normally avoid human presence. Hence, it could be that the latter were more stressed than the laughing doves. Studies in mammals indicated that stress has an inhibiting effect on neurogenesis (reviewed by Mirescu and Gould, 2006). If stress plays a similar role in birds, it could be argued that the reduced neuronal recruitment in brains of turtle doves, compared to laughing doves, is a consequence of captivity. We cannot rule out completely this possibility, because we did not measure levels of stress hormones. This could be tested in a future experiment with a similar set-up, in which glucocorticoid levels will be tested, to assess possible differences in the stress of the two species. Nevertheless, in our current study, the fact that both species lost similar percentages of body mass during captivity might indicate that stress was not a significant concern. In addition, the weight loss was relatively small, much lower than the 10% that is usually accepted as a stress indication, and also much lower than the weight loss of the migrant warblers (average of 9.3%), in which we found higher neuronal recruitment than in the resident ones, although the later lost only 4.7% in average, of their initial body weight (Barkan et al., 2014). Taken together, this evidence indicates that stress might not be a significant concern.

Another factor that should be kept in mind when discussing the different patterns of neuronal recruitment between passerines and non-passerines in relation to migratory behavior, is that Columbiformes and Passeriformes became evolutionally separated over ∼85 million years ago (Jetz et al., 2012). Therefore, it could be that over the course of this long period their brain structures and neuronal mechanisms were shaped under different evolutionary pressures rather than migratory or residency lifestyles. Further study is thus needed in order to test our suggested hypothesis.

Neuronal Recruitment and Age

Previous studies in birds and mammals have revealed a general decline in neuronal recruitment with age, which is explained as a consequence of the post-natal brain growth and maturation attained in adulthood (reviewed by Barnea and Pravosudov, 2011). This trend was reported in several passerines species (Alvarez-Buylla et al., 1994; Barnea and Nottebohm, 1996; DeWulf and Bottjer, 2002; Pytte et al., 2007; LaDage et al., 2011; Barkan et al., 2014), but in non-passerines there has been only one study (Ling et al., 1997), which reported a similar pattern in the NC of ring doves. According to that study, at the age of 3 months ring doves recruited on average 0.14% of new neurons per mm^2 in their NC, declining to 0.02% at the age of 6–8 years. We found a similar age effect (between juveniles and adults), in both species, when calculating percentages of new neurons out of the total. However, due to sample size limitations we could not further correlate age with other factors such as seasons or brain regions, comparisons that could add interesting insights upon neuronal recruitment in the aging avian brain.

Neuronal Recruitment in Columbiformes and Passeriformes

In both bird orders neuronal recruitment occurs in the HA (current study; Hoshooley et al., 2005), HC (current study; Barnea and Nottebohm, 1994), Medial striatum (former named Lobus parolfactorius - LPO; Alvarez-Buylla et al., 1994; Ling et al., 1997), NC (Ling et al., 1997; Barkan et al., 2007) and NCL (current study; Barkan et al., 2014). However, other brain regions exhibit neuronal recruitment in one of the two above orders, but are less developed or absent in the other. For example, HVC, which is an important nucleus in the brain pathway that controls song production and exhibits seasonal new neuronal recruitment in Passerines (Kirn et al., 1994; Rasika et al., 1994; Alvarez-Buylla and Kirn, 1997; Balthazart et al., 2008), is absent in Columbiformes. Similarly, evidence indicates that pigeons use olfactory cues for navigation and have relatively developed olfactory lobes (reviewd by Mehlhorn and Rehkamper, 2009), while most Passerines are assumed to have a poor sense of smell (Cobb, 1968; Evans and Heiser, 2004b). Thus, it would be interesting to compare neuronal recruitment in the olfactory lobes of Passerines and Columbiformes.

Total Neuronal Densities

Unlike passerines such as white-crowned sparrows (LaDage et al., 2011), juncos (*Junco hyemalis*; Cristol et al., 2003), or warblers (Barkan et al., 2014), in which migrant birds' brains had higher densities of total neurons than resident birds' brains, no such difference was found in the present study in doves. From this finding, combined with the higher neuronal recruitment found in the brains of laughing doves, we can assume that a faster neuronal turnover occurs in this resident species compared to that in brains of the migrating turtle doves. If this is so, then neurons in the brains of laughing doves survive for a shorter time than neurons in the brains of turtle doves. Barnea et al. (2006) suggested that "if neurons store information which is acquired by experience, then one form of time representation would be how long neurons that encode information will survive, because when these neurons are replaced, any information they might have stored will be probably lost." According to this notion, the rate of neuronal turnover might regulate memory duration, so that slower turnover results in more prolonged memory in turtle doves and shorter memory in laughing doves. Longer memory duration could be beneficial to migrating birds by enabling them to store orientation information for a longer period. Differences in memory duration were demonstrated for example in migrating garden warblers, which were able to remember feeding sites for up to 12 months, compared to resident Sardinian warblers that remembered such sites for only 2 weeks (Mettke-Hofmann and Gwinner, 2003).

OVERVIEW

In the current study we found that in two dove species, unlike passerines, new neuronal recruitment was lower in the brains of a migrating species compared with a resident one. We suggest that this could be due to the high sociality of these doves, which forage and migrate in flocks, and therefore can rely on the communal spatial knowledge that is acquired by the flock and might reduce individual navigation efforts. This, in turn, might enable reduced levels of neuronal recruitment in brain regions that process spatial information. In addition, we found that, unlike in several passerine species, seasonality does not affect neuronal recruitment in these two dove species. We suggest that the similar amount of neuronal recruitment that we observed in the brains of the doves throughout the year might be due to their non-territorial and explorative behavior, which exposes them to substantial loads of spatial information all year round. We also found an age effect on neuronal recruitment, which is in line with previous studies in other avian species.

Our current findings are novel in shedding light on neuronal recruitment in brains of two species from the Columbiformes, an order that been hardly studied to date in this respect. Moreover, we looked at three brain regions that are known to process spatial information—the HC, HA, and NCL. Consequently, we discuss the differences in neuronal recruitment patterns that we observed between doves (the present study) and warblers (Barkan et al., 2014), and their possible evolutionary explanations. We suggest that the hypothesis, confirmed in previous studies, that neuronal recruitment in relevant brain regions is expected to be higher in migratory species, might not hold true in all cases. Nevertheless, the idea in principle that the need for more spatial information correlates with higher recruitment hold true, but it can depend on various aspects of the general biology of the species under study, such as sociality, amount of territoriality, foraging patterns, and levels of predation risks. Hence, the findings from our study suggest that variability might exist among different avian orders in patterns of brain plasticity, and emphasizes the importance of further investigation of this phenomenon in other avian orders and in more species, for a better understanding of its role in different lifestyles. This is in line with the growing acknowledgment regarding the remarkable cognitive abilities of birds and their usefulness as a comparative model in order to study the translation of nervous system organization into representations of space that can support navigation and memory (see review by Herold et al., 2015).

AUTHOR CONTRIBUTIONS

AB, YY, and SB conceived this work, SB conducted the experiments, all authors wrote the paper and contributed to ideas.

FUNDING

This study was supported by The National Institute for Psychobiology in Israel and The Research Fund of The Open University of Israel.

ACKNOWLEDGMENTS

We thank Kobi Merom for assisting in field work and bird banding, Ido Izhaki and Shai Meiri for statistical advice, Naomi Paz for editing the paper and the two reviewers whose comments significantly improved this manuscript. We declare no conflict of interests.

REFERENCES

Abellán, A., Desfilis, E., and Medina, L. (2014). Combinatorial expression of Lef1, Lhx2, Lhx5, Lhx9, Lmo3, Lmo4, and Prox1 helps to identify comparable subdivisions in the developing hippocampal formation of mouse and chicken. *Front. Neuroanat.* 8:59. doi: 10.3389/fnana.2014.00059

Adar, E., Nottebohm, F., and Barnea, A. (2008). The relationship between nature of social change, age, and position of new neurons and their survival in adult zebra finch brain. *J. Neurosci.* 28, 5394–5400. doi: 10.1523/JNEUROSCI.5706-07.2008

Alvarez-Buylla, A., and Kirn, J. R. (1997). Birth, migration, incorporation, and death of vocal control neurons in adult songbirds. *J. Neurobiol.* 33, 585–601. doi: 10.1002/(SICI)1097-4695(19971105)33:5<585::AID-NEU7>3.0.CO;2-0

Alvarez-Buylla, A., Ling, C. Y., and Yu, W. S. (1994). Contribution of neurons born during embryonic, juvenile, and adult life to the brain of adult canaries - regional specificity and delayed birth of neurons in the song-control nuclei. *J. Comp. Neurol.* 347, 233–248. doi: 10.1002/cne.903470207

Alvarez-Buylla, A., Theelen, M., and Nottebohm, F. (1988). Mapping of radial glia and of a new cell type in adult canary brain. *J. Neurosci.* 8, 2707–2712.

Amrein, I., Dechmann, D. K., Winter, Y., and Lipp, H. P. (2007). Absent or low rate of adult neurogenesis in the hippocampus of bats (Chiroptera). *PLoS ONE* 2:e455. doi: 10.1371/journal.pone.0000455

Amrein, I., and Lipp, H. P. (2009). Adult hippocampal neurogenesis of mammals: evolution and life history. *Biol. Lett.* 5, 141–144. doi: 10.1098/rsbl.2008.0511

Ash, J. S. (1977). Turtle-dove migration in southern Europe, middle-East and North-Africa. *British Birds* 70, 504–506.

Balthazart, J., Boseret, G., Konkle, A., Hurley, L. L., and Ball, G. F. (2008). Doublecortin as a marker of adult neuroplasticity in the canary song control nucleus HVC. *Eur. J. Neurosci.* 27, 801–817. doi: 10.1111/j.1460-9568.2008.06059.x

Barkan, S., Ayali, A., Nottebohm, F., and Barnea, A. (2007). Neuronal recruitment in adult zebra finch brain during a reproductive cycle. *Dev. Neurobiol.* 67, 687–701. doi: 10.1002/dneu.20379

Barkan, S., Roll, U., Yom-Tov, Y., Wassenaar, L. I., and Barnea, A. (2016). Possible linkage between neuronal recruitment and flight distance in migratory birds. *Sci. Rep.* 6:21983. doi: 10.1038/srep21983

Barkan, S., Yom-Tov, Y., and Barnea, A. (2014). A possible relation between new neuronal recruitment and migratory behavior in Acrocephalus warblers. *Dev. Neurobiol.* 74, 1194–1209. doi: 10.1002/dneu.22198

Barnea, A., Mishal, A., and Nottebohm, F. (2006). Social and spatial changes induce multiple survival regimes for new neurons in two regions of the adult brain: an anatomical representation of time? *Behav. Brain Res.* 167, 63–74. doi: 10.1016/j.bbr.2005.08.018

Barnea, A., and Nottebohm, F. (1994). Seasonal recruitment of hippocampal-neurons in adult free- ranging black-capped chickadees. *Proc. Natl. Acad. Sci. U.S.A.* 91, 11217–11221. doi: 10.1073/pnas.91.23.11217

Barnea, A., and Nottebohm, F. (1996). Recruitment and replacement of hippocampal neurons in young and adult chickadees: an addition to the theory of hippocampal learning. *Proc. Natl. Acad. Sci. U.S.A.* 93, 714–718. doi: 10.1073/pnas.93.2.714

Barnea, A., and Pravosudov, V. (2011). Birds as a model to study adult neurogenesis: bridging evolutionary, comparative and neuroethological approaches. *Eur. J. Neurosci.* 34, 884–907. doi: 10.1111/j.1460-9568.2011.07851.x

Bingman, V. P., El Agbani, M. A., Benazzouz, B., and Gagliardo, A. (2004). Initial orientation of homing pigeons on the Atlantic coast of Morocco is affected by a strong Preferred Compass Direction (PCD). *Ital. J. Zool.* 71, 325–328. doi: 10.1080/11250000409356590

Bingman, V. P., Gagliardo, A., Hough, G. E., Ioale, P., Kahn, M. C., and Siegel, J. J. (2005). The avian hippocampus, homing in pigeons and the memory representation of large-scale space. *Integr. Comp. Biol.* 45, 555–564. doi: 10.1093/icb/45.3.555

Bingman, V. P., Riters, L. V., Strasser, R., and Gagliardo, A. (1998). "Neuroethology of avian navigation," in *Animal Cognition in Nature*, eds R. P. Balda, I. M. Pepperberg, and A. C. Kamil (San Diego, CA: Academic Press), 201–226.

Biro, D., Freeman, R., Meade, J., Roberts, S., and Guilford, T. (2007). Pigeons combine compass and landmark guidance in familiar route navigation. *Proc. Natl. Acad. Sci. U.S.A.* 104, 7471–7476. doi: 10.1073/pnas.0701575104

Biro, D., Sumpter, D. J. T., Meade, J., and Guilford, T. (2006). From compromise to leadership in pigeon homing. *Curr. Biol.* 16, 2123–2128. doi: 10.1016/j.cub.2006.08.087

Brenowitz, E. A. (2008). *Plasticity of the Song Control System in Adult Birds*. New York, NY: Cambridge University Press.

Brenowitz, E. A., and Larson, T. A. (2015). Neurogenesis in the adult avian song-control system. *Cold Spring Harb. Perspect. Biol.* 7:a019000. doi: 10.1101/cshperspect.a019000

Browne, S. J., and Aebischer, N. J. (2003). Habitat use, foraging ecology and diet of turtle doves *Streptopelia turtur* in Britain. *Ibis* 145, 572–582. doi: 10.1046/j.1474-919X.2003.00185.x

Budzynski, C. A., Gagliardo, A., Ioale, P., and Bingman, V. P. (2002). Participation of the homing pigeon thalamofugal visual pathway in sun-compass associative learning. *Eur. J. Neurosci.* 15, 197–210. doi: 10.1046/j.0953-816x.2001.01833.x

Catchpole, C. K. (1972). A comparative study of territory in the reed warbler (*Acrocephalus scirpaceus*) and sedge warbler (*A. schoenobaenus). J. Zool.* 166, 213–231. doi: 10.1111/j.1469-7998.1972.tb04086.x

Cobb, S. (1968). The size of the olfactory bulb in 108 species of birds. *Auk* 85, 55–61. doi: 10.2307/4083624

Couzin, I. D., Krause, J., Franks, N. R., and Levin, S. A. (2005). Effective leadership and decision-making in animal groups on the move. *Nature* 433, 513–516. doi: 10.1038/nature03236

Cramp, S., and Perrins, C. M. (1994). *The Birds of the Western Palearctic*. Oxford: Oxford University Press.

Cristol, D. A., Reynolds, E. B., Leclerc, J. E., Donner, A. H., Farabaugh, C. S., and Ziegenfus, C. W. S. (2003). Migratory dark-eyed juncos, *Junco hyemalis*, have better spatial memory and denser hippocampal neurons than nonmigratory conspecifics. *Anim. Behav.* 66, 317–328. doi: 10.1006/anbe.2003.2194

Davies, N. B. (1976). Food, flocking and territorial behaviour of the pied wagtail (*Motacilla alba yarrellii Gould*) in winter. *J. Anim. Ecol.* 45, 235–253. doi: 10.2307/3777

Dewolfe, B. B., West, G. C., and Peyton, L. J. (1973). Spring migration of gambels sparrows through Southern Yukon Territory. *Condor* 75, 43–59. doi: 10.2307/1366534

DeWulf, V., and Bottjer, S. W. (2002). Age and sex differences in mitotic activity within the zebra finch telencephalon. *J. Neurosci.* 22, 4080–4094.

Evans, H. E., and Heiser, J. B. (2004a). "Birds on the move: flight and migration," in *Cornell Lab of Ornithology Handbook of Bird Biology*, *2nd Edn.*, eds S. Podulka, R. W. Rohrbaugh, and R. Bonney (Ithaca, NY: Princeton University Press), 5–99.

Evans, H. E., and Heiser, J. B. (2004b). "What's inside: anatomy and physiology," in *Cornell Lab of Ornithology Handbook of Bird Biology*, *2nd Edn.*, eds S. Podulka, R. W. Rohrbaugh, and R. Bonney (Ithaca, NY: Princeton University Press), 1–161.

Fazili, M. F. (2014). Pairing behavior and territoriality in Indian great reed warbler (*Acrocephalus stentoreus brunnescens*, Jerdon) at lake Wular. *J. Global Biosci.* 3, 562–568.

Flack, A., Freeman, R., Guilford, T., and Biro, D. (2013). Pairs of pigeons act as behavioural units during route learning and co-navigational leadership conflicts. *J. Exp. Biol.* 216, 1434–1438. doi: 10.1242/jeb.082800

Gould, J. L. (2006). Homing behavior: decisions, dominance and democracy. *Curr. Biol.* 16, R920–R921. doi: 10.1016/j.cub.2006.09.051

Guillery, R. W., and Herrup, K. (1997). Quantification without pontification. *J. Comp. Neurol.* 386, 2–7. doi: 10.1002/(SICI)1096-9861(19970915)386:1<2::AID-CNE2>3.0.CO;2-6

Herold, C., Coppola, V. J., and Bingman, V. P. (2015). The maturation of research into the avian hippocampal formation: recent discoveries from one of the nature's foremost navigators. *Hippocampus* 25, 1193–1211. doi: 10.1002/hipo.22463

Heyers, D., Manns, M., Luksch, H., Gunturkun, O., and Mouritsen, H. (2007). A visual pathway links brain structures active during magnetic compass orientation in migratory birds. *PLoS ONE* 2:e937. doi: 10.1371/journal.pone.0000937

Hoshooley, J. S., Phillmore, L. S., and MacDougall-Shackleton, S. A. (2005). An examination of avian hippocampal neurogenesis in relationship to photoperiod. *Neuroreport* 16, 987–991. doi: 10.1097/00001756-200506210-00021

Hoshooley, J. S., and Sherry, D. F. (2007). Greater hippocampal neuronal recruitment in food-storing than in non-food-storing birds. *Dev. Neurobiol.* 67, 406–414. doi: 10.1002/dneu.20316

IBM Corp. (2012). *IBM SPSS Statistics for Windows, Version 21.0*. Armonk, NY: IBM Corp.

Jetz, W., Thomas, G. H., Joy, J. B., Hartmann, K., and Mooers, A. O. (2012). The global diversity of birds in space and time. *Nature* 491, 444–448. doi: 10.1038/nature11631

Jorge, P. E., Marques, P. A. M., and Phillips, J. B. (2010). Activational effects of odours on avian navigation. *Proc. Biol. Sci.* 277, 45–49. doi: 10.1098/rspb.2009.1521

Karten, H. J., and Hodos, W. (1967). *A Stereotaxic Atlas of the Brain of the Pigeon (Columba livia)*. Baltimore, MD: The Johns Hopkins Press.

Kirn, J. R., AlvarezBuylla, A., and Nottebohm, F. (1991). Production and survival of projection neurons in a forebrain vocal center of adult male canaries. *J. Neurosci.* 11, 1756–1762.

Kirn, J. R., Fishman, Y., Sasportas, K., Alvarez-Buylla, A., and Nottebohm, F. (1999). Fate of new neurons in adult canary high vocal center during the first 30 days after their formation. *J. Comp. Neurol.* 411, 487–494. doi: 10.1002/(SICI)1096-9861(19990830)411:3<487::AID-CNE10>3.0.CO;2-M

Kirn, J., O'Loughlin, B., Kasparian, S., and Nottebohm, F. (1994). Cell-death and neuronal recruitment in the high vocal center of adult male Canaries are temporally related to changes in song. *Proc. Natl. Acad. Sci. U.S.A.* 91, 7844–7848. doi: 10.1073/pnas.91.17.7844

LaDage, L. D., Roth, T. C., and Pravosudov, V. V. (2011). Hippocampal neurogenesis is associated with migratory behaviour in adult but not juvenile sparrows (*Zonotrichia leucophrys* ssp.). *Proc. Biol. Sci.* 278, 138–143. doi: 10.1098/rspb.2010.0861

Lepage, D. (2014). *AviBase: The World Bird Database. Hosted by Bird Studies Canada*. Available online at: http://avibase.bsc-eoc.org

Ling, C. Y., Zuo, M. X., Alvarez-Buylla, A., and Cheng, M. F. (1997). Neurogenesis in juvenile and adult ring doves. *J. Comp. Neurol.* 379, 300–312. doi: 10.1002/(SICI)1096-9861(19970310)379:2<300::AID-CNE10>3.0.CO;2-T

Lipkind, D., Nottebohm, F., Rado, R., and Barnea, A. (2002). Social change affects the survival of new neurons in the forebrain of adult songbirds. *Behav. Brain Res.* 133, 31–43. doi: 10.1016/S0166-4328(01)00416-8

Medina, L., and Reiner, A. (2000). Do birds possess homologues of mammalian primary visual, somatosensory and motor cortices? *Trends Neurosci.* 23, 1–12. doi: 10.1016/S0166-2236(99)01486-1

Mehlhorn, J., Haastert, B., and Rehkamper, G. (2010). Asymmetry of different brain structures in homing pigeons with and without navigational experience. *J. Exp. Biol.* 213, 2219–2224. doi: 10.1242/jeb.043208

Mehlhorn, J., and Rehkamper, G. (2009). Neurobiology of the homing pigeon-a review. *Naturwissenschaften* 96, 1011–1025. doi: 10.1007/s00114-009-0560-7

Mettke-Hofmann, C., and Gwinner, E. (2003). Long-term memory for a life on the move. *Proc. Natl. Acad. Sci. U.S.A.* 100, 5863–5866. doi: 10.1073/pnas.1037505100

Mirescu, C., and Gould, E. (2006). Stress and adult neurogenesis. *Hippocampus* 16, 233–238. doi: 10.1002/hipo.20155

Mouritsen, H., Feenders, G., Liedvogel, M., Wada, K., and Jarvis, E. D. (2005). Night-vision brain area in migratory songbirds. *Proc. Natl. Acad. Sci. U.S.A.* 102, 8339–8344. doi: 10.1073/pnas.0409575102

Nagy, M., Ákos, Z., Biro, D., and Vicsek, T. (2010). Hierarchical group dynamics in pigeon flocks. *Nature* 464, 890–893. doi: 10.1038/nature08891

Odetti, F., Ioale, P., and Gagliardo, A. (2003). Development of the navigational map in homing pigeons: effects of flight experience on orientation performance. *Anim. Behav.* 66, 1093–1099. doi: 10.1006/anbe.2003.2293

Papi, F., Gagliardo, A., Fiaschi, V., and Dallantonia, P. (1989). Pigeon homing - does early experience determine what cues are used to navigate. *Ethology* 82, 208–215. doi: 10.1111/j.1439-0310.1989.tb00500.x

Patel, S. N., Clayton, N. S., and Krebs, J. R. (1997). Spatial learning induces neurogenesis in the avian brain. *Behav. Brain Res.* 89, 115–128. doi: 10.1016/S0166-4328(97)00051-X

Pytte, C. L., Gerson, M., Miller, J., and Kirn, J. R. (2007). Increasing stereotypy in adult zebra finch song correlates with a declining rate of adult neurogenesis. *Dev. Neurobiol.* 67, 1699–1720. doi: 10.1002/dneu.20520

Rasika, S., Nottebohm, F., and AlvarezBuylla, A. (1994). Testosterone increases the recruitment and/or survival of new high vocal center neurons in adult female Canaries. *Proc. Natl. Acad. Sci. U.S.A.* 91, 7854–7858. doi: 10.1073/pnas.91.17.7854

Schluter, D. (1984). Feeding correlates of breeding and social organization in two Galápagos finches. *Auk* 110, 59–68.

Sherry, D. F., and Hoshooley, J. S. (2010). Seasonal hippocampal plasticity in food-storing birds. *Philos. Trans. R. Soc B-Biol. Sci.* 365, 933–943. doi: 10.1098/rstb.2009.0220

Sherry, D. F., and MacDougall-Shackleton, S. A. (2015). Seasonal change in the avian hippocampus. *Front. Neuroendocrinol.* 37, 158–167. doi: 10.1016/j.yfrne.2014.11.008

Shirihai, H., Dovrat, E., Christie, D. A., Harris, A., and Cottridge, D. (1996). *The Birds of Israel*. London: Academic Press.

Simons, A. M. (2004). Many wrongs: the advantage of group navigation. *Trends Ecol. Evol.* 19, 453–455. doi: 10.1016/j.tree.2004.07.001

Striedter, F. G. (2016). Evolution of the hippocampus in reptiles and birds. *J. Comp. Neurol.* 254, 496–517. doi: 10.1002/cne.23803

Temple, S. A. (2004). "Individuals, populations and communities: the ecology of birds," in *Cornell Lab of Ornithology Handbook of Bird Biology,* eds S. Podulka, R.W. Rohrbaugh, and R. Bonney. (Ithaca, NY: Princeton University Press), 1–134.

Waldmann, C., and Gunturkun, O. (1993). The dopaminergic innervation of the pigeon caudolaterale forebrain - immunocytochemical evidence for a prefrontal cortex in birds. *Brain Res.* 600, 225–234. doi: 10.1016/0006-8993(93)91377-5

Wallraff, H. G. (1996). Seven theses on pigeon homing deduced from empirical findings. *J. Exp. Biol.* 199, 105–111.

Wallraff, H. G. (2001). Navigation by homing pigeons: updated perspective. *Ethol. Ecol. Evol.* 13, 1–48. doi: 10.1080/08927014.2001.9522786

Wang, N. G., Hurley, P., Pytte, C., and Kirn, J. R. (2002). Vocal control neuron incorporation decreases with age in the adult zebra Finch. *J. Neurosci.* 22, 10864–10870.

Wiltschko, R., and Wiltschko, W. (1999). The orientation system of birds - II. Homing and navigation. *J. Ornithol.* 140, 129–164. doi: 10.1007/BF01653595

Zapka, M., Heyers, D., Hein, C. M., Engels, S., Schneider, N. L., Hans, J., et al. (2009). Visual but not trigeminal mediation of magnetic compass information in a migratory bird. *Nature* 461, 1274–1277. doi: 10.1038/nature08528

Conflict of Interest Statement: The authors declare that the research was conducted in the absence of any commercial or financial relationships that could be construed as a potential conflict of interest.

frontiers in Neuroscience

REVIEW
published: 07 December 2017
doi: 10.3389/fnins.2017.00662

From Blood to Brain: Adult-Born Neurons in the Crayfish Brain Are the Progeny of Cells Generated by the Immune System

Barbara S. Beltz and Jeanne L. Benton*

Neuroscience Program, Wellesley College, Wellesley, MA, United States

New neurons continue to be born and integrated into the brains of adult decapod crustaceans. Evidence in crayfish indicates that the 1st-generation neural precursors that generate these adult-born neurons originate in the immune system and travel to the neurogenic niche via the circulatory system. These precursors are attracted to the niche, become integrated amongst niche cells, and undergo mitosis within a few days; both daughters of this division migrate away from the niche toward the brain clusters where they will divide again and differentiate into neurons. In the crustacean brain, the rate of neuronal production is highly sensitive to serotonin (5-hydroxytryptamine, 5-HT) levels. These effects are lineage-dependent, as serotonin's influence is limited to late 2nd-generation neural precursors and their progeny. Experiments indicate that serotonin regulates adult neurogenesis in the crustacean brain by multiple mechanisms: via direct effects of serotonin released from brain neurons into the hemolymph or by local release onto target cells, or by indirect influences via a serotonin-mediated release of agents from other regions, such as hormones from the sinus gland and cytokines from hematopoietic tissues. Evidence in crayfish also indicates that serotonin mediates the attraction of neural precursors generated by the immune system to the neurogenic niche. Thus, studies in the crustacean brain have revealed multiple roles for this monoamine in adult neurogenesis, and identified several pathways by which serotonin influences the generation of new neurons.

Keywords: serotonin, 5-HT, adult neurogenesis, immune system, dorsal giant neuron, neurogenic niche

OPEN ACCESS

Edited by:
Luca Bonfanti,
Università degli Studi di Torino, Italy

Reviewed by:
Alice Powers,
Stony Brook University, United States
Jan Kaslin,
Australian Regenerative Medicine Institute (ARMI), Australia

****Correspondence:***
Barbara S. Beltz
bbeltz@wellesley.edu

Specialty section:
This article was submitted to Neurogenesis, a section of the journal Frontiers in Neuroscience

Received: *02 August 2017*
Accepted: *13 November 2017*
Published: *07 December 2017*

Citation:
Beltz BS and Benton JL (2017) From Blood to Brain: Adult-Born Neurons in the Crayfish Brain Are the Progeny of Cells Generated by the Immune System. Front. Neurosci. 11:662. doi: 10.3389/fnins.2017.00662

INTRODUCTION

When the embryonic precursor cells die during late embryonic life, neural proliferation stops in most areas of the decapod crustacean brain (Harzsch, 2003; Sintoni et al., 2012). Exceptions to this are in the central olfactory and higher order processing pathways, where mitotic activity and the integration of new interneurons continue throughout life (Schmidt, 1997; Schmidt and Demuth, 1998; Harzsch et al., 1999; Schmidt and Harzch, 1999). The source of these adult-born neurons remained a mystery for many years, until the discovery of a neurogenic niche containing the 1st-generation neural precursors (Song et al., 2007; Sullivan et al., 2007a); these niche precursors generate a lineage of cells whose final progeny differentiate into neurons (Sullivan and Beltz, 2005b). However, the mystery deepened once again when it was discovered that the 1st-generation precursors do not self-renew

(Benton et al., 2011). Calculations of cell-cycle time and counts of the niche precursor population showed that without self-renewal, the small pool of 1st-generation neural precursors should be rapidly depleted. But the niche is never exhausted and adult-born neurons continue to be produced throughout the long lives of these animals, leading to the conclusion that the neural precursors in the niche must be replenished from a source elsewhere in the animal. This paper reviews the intense hunt for the source of these cells, which ultimately led to the immune system and the identification of a specific type of circulating blood cell (hemocyte) that is attracted to the neurogenic niche, where these go through their first division as neural precursors; their daughters migrate along streams arising from the niche, finally arriving at brain cell clusters containing interneurons in the olfactory pathway. Ultimately, these cells undergo at least two more divisions over 1–2 weeks, before the progeny differentiate into neurons.

Serotonin has long been known to regulate neuronal proliferation in the embryonic and adult brains of crustaceans (Benton et al., 1997, 2008), as in vertebrate brains (Brezun and Daszuta, 1999, 2000; Banasr et al., 2004; Lledo et al., 2006). In crayfish, serotonin is involved in multiple functions contributing to adult neurogenesis, including the attraction of immune cells to the niche (Benton et al., 2011) and the timing of cell divisions in the neural precursor lineage (Zhang et al., 2011). One major source of serotonin in the brains of crustaceans is the dorsal giant neuron (DGN). Tests in which the DGN was electrically stimulated have shown that serotonin released from this neuron directly alters the rate of adult neurogenesis in the crayfish brain. Further, by activating a cytokine pathway, serotonin is emerging as a critical link between the immune and nervous systems.

ADULT NEUROGENESIS IN THE DECAPOD CRUSTACEAN BRAIN

The Neural Precursor Lineage in the Adult Brain Has Been Identified

Most neurons in the decapod brain are born during embryonic development and are the descendants of large precursor cells, the neuroblasts (for review see Harzsch, 2003). Neuroblasts are active during embryonic development, dividing asymmetrically, generating specific neural lineages before dying during the period around hatching (Sintoni et al., 2012). Therefore, neural proliferation in most regions of the decapod brain ends during late embryonic or early postembryonic development. However, the cell cycle resumes after hatching in the local (Cluster 9) and projection (Cluster 10) neuron clusters located in the midbrain (deutocerebrum) (**Figure 1**; Harzsch et al., 1999; Schmidt and Harzch, 1999); the production of these adult-born neurons and the roles of serotonin in this process will be the focus of this review. Neurons in these clusters innervate the primary olfactory processing areas (olfactory lobes; OLs) and higher-order processing areas (accessory lobes; ALs) that integrate olfactory, visual and mechanosensory information. Life-long neurogenesis is also found in the clusters of olfactory sensory neurons in the antennules (Steullet et al., 2000; Sullivan and Beltz, 2005a; Tadesse et al., 2011) and among neurons in the visual pathway (Sullivan and Beltz, 2005b).

The production of new midbrain neurons has been demonstrated in sexually mature adults in several decapod groups (Schmidt and Demuth, 1998; Schmidt and Harzch, 1999), suggesting that adult neurogenesis is a general feature of the decapod brain. However, evidence for the differentiation of newly born cells into neurons expressing the appropriate transmitters has been obtained only for crayfish (Astacida; Sullivan and Beltz, 2005b) and spiny lobsters (Achelata; Schmidt, 2001). It has been proposed that the neural precursors supporting adult neurogenesis in the spiny lobster *Panulirus argus* may be self-renewing neuroblasts that survived after embryonic life (Schmidt and Derby, 2011), but direct tests of this hypothesis have not yet been conducted. However, the precursor cell lineage producing adult-born neurons in the midbrain of the crayfish *Procambarus clarkii* has been identified (**Figure 1**). The 1st-generation neural precursors are located in two neurogenic niches lying on the ventral surface of the brain, just beneath the sheath (Song et al., 2007; Sullivan et al., 2007a). The niche cells are immunoreactive for glutamine synthetase (GS), an enzyme that converts glutamate to glutamine, and which is also a marker of astrocytes (Anlauf and Derouiche, 2013) and radial glial-like cells including neural stem cells in the CNS of fish (Wen et al., 2008, 2009). When the crayfish brain and niche are labeled with antibodies for GS, the neurogenic cells in the brains of adult crayfish are revealed (**Figures 2A,B**; Sullivan et al., 2007a). As in mammals, the neurogenic niches supporting adult neurogenesis in the crayfish brain are intimately associated with the vasculature, as these lie on blood vessels that communicate with the niche via a vascular connection (**Figure 2C**) (Sullivan et al., 2007a; Chaves da Silva et al., 2012). This vascular cavity contains amorphous non-cellular material that reacts with alcian blue and periodic acid-Schiff (Bazin, 1969), suggesting a glycidic substance (Chaves da Silva et al., 2012).

The vast majority of cells in the niche are bipolar, with long processes that project from the niche to either Cluster 9 or 10 and short processes that terminate at the vascular cavity (**Figure 2D**). When the 1st-generation neural precursors in the niche divide, their daughters (2nd-generation neural precursors) migrate along these processes to Cluster 9 or 10, forming streams that deliver the niche descendants to the brain cell clusters. Thus, niche cells in the crustacean brain appear to function as precursor and support cells; it is now thought that these may represent two distinct cell types. The 2nd-generation neural precursor cells require 5–7 days to migrate along the streams (Benton et al., 2011). After reaching the proliferation zones in Cluster 9 or 10, they divide again, their progeny differentiating into interneurons innervating the olfactory and/or accessory lobes (Sullivan and Beltz, 2005b; Sullivan et al., 2007a,b). A wave of cell death culls the newborn cells during the first 2 weeks after birth, but by 4 weeks the surviving cells have begun to express neurotransmitters that are typical of local (Cluster 9) and projection (Cluster 10) neurons in the olfactory pathway (Kim et al., 2014).

Many of the events underlying the production of neurons in the adult crayfish brain are reminiscent of adult neurogenesis in the mammalian brain, suggesting that these processes may

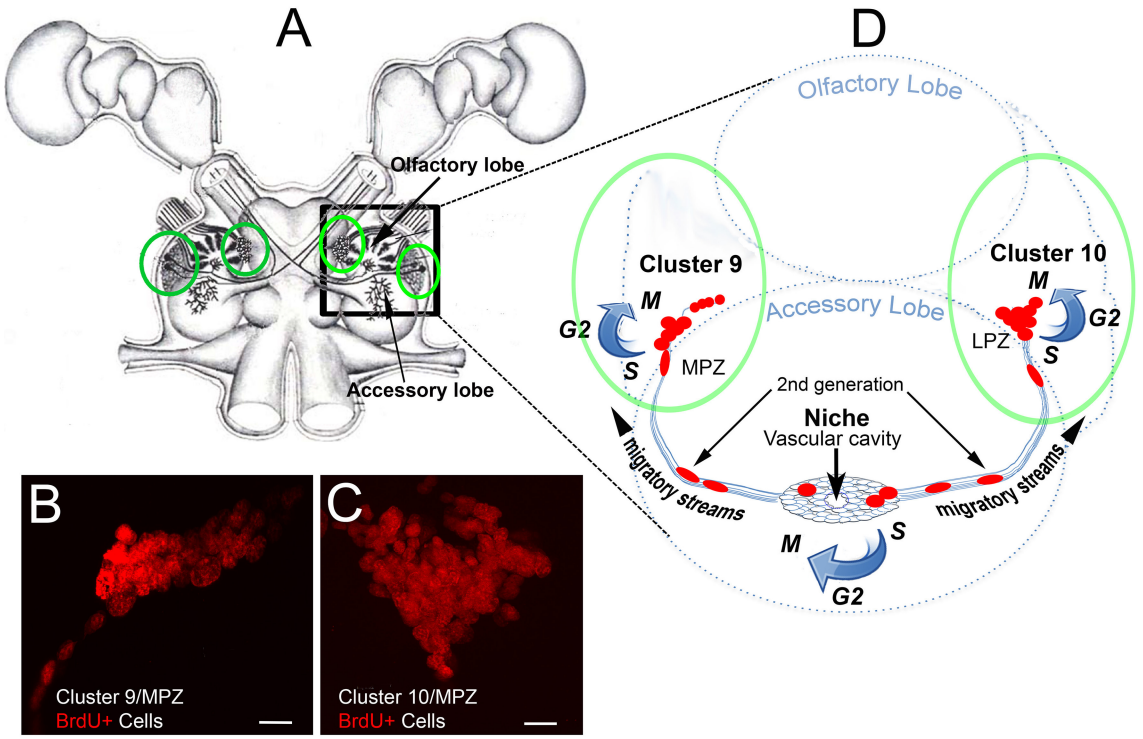

FIGURE 1 | The cellular machinery producing adult-born neurons in the crayfish brain**. (A)** Drawing of the eureptantian (crayfish/lobster) brain including the eyes and optic ganglia of the lateral protocerebrum, and showing the locations of the cell body clusters and neuropils in the brain (supraesophageal ganglion). Bilateral soma clusters 9 and 10 (circled in green, **(A)** are locations where neurogenesis persists in the adult brain, shown with bromodeoxyuridine labeling (red) of S-phase cells in **(B,C)**. These cell clusters lie beside two neuropil regions in the deutocerebrum, the olfactory (OL) and accessory (AL) lobes, shown diagrammatically in **(D)** (right hemibrain). The neurogenic niche lies on the ventral surface of the accessory lobes, just beneath the membrane ensheathing the brain. The niche contains bipolar cells that have short processes that project to the rim of a vascular cavity, and long processes that form migratory streams extending to Clusters 9 or 10, along which the daughters of 1st-generation neural precursors in the niche migrate. Scale bars: **(A,B)**, 20 μm.

be grounded in common ancestral mechanisms that have been retained in a phylogenetically broad group of species, or, alternatively, that reflect convergence on common mechanisms (Sullivan et al., 2007a). These similarities include the presence of vascularized niches that house the neural precursors and the directed migration of their descendants, conservation in molecular pathways underlying neuronal differentiation, and extensive parallels in the environmental and endogenous factors that regulate adult neurogenesis (Beltz et al., 2011; Brenneis et al., 2017). However, there also are important differences that distinguish adult neurogenesis in crayfish. For example, in contrast to the coexistence of several precursor cell generations in the mammalian neurogenic niche, the generations of cells in the neural precursor lineage in crayfish are compartmentalized: the 1st -generation precursors in the crayfish niche are separated from their progeny in the migratory streams (2nd-generation precursors), which in turn are segregated from their descendants in the proliferation zones associated with Clusters 9 and 10 (3rd-generation and later precursors). As a result, the lineage relationships among the precursors are clear and changes in the numbers of cells in each generation are easily assessed (e.g., Zhang et al., 2011).

First-Generation Neural Precursors in the Crayfish Brain Are Not Self-Renewing

Unlike embryonic neural stem cells (neuroblasts) in crustaceans, the 1st-generation precursors that support adult neurogenesis undergo morphologically symmetrical divisions (Zhang et al., 2009). Pulse-chase double-nucleoside labeling allows the separate detection of two different nucleosides (5-bromo-2′-deoxyuridine [BrdU] and 5-ethynyl-2′-deoxyuridine [EdU]), which are incorporated into cells that are synthesizing DNA during S phase of the cell cycle. BrdU (presented first) is not retained in the 1st-generation precursors, and is replaced with EdU (presented 3-7 days later) in niche cells (**Figure 3**). Rapid division and dilution of the BrdU label cannot explain the absence of nucleoside retention by the precursor cells in the niche, because the cell cycle of the 1st-generation precursors is relatively long [~48 h; (Benton et al., 2011)]. Thus, because the 1st-generation neural precursors in the crayfish neurogenic niche do not retain BrdU or EdU, we have concluded that these are not self-renewing and that both daughters of a niche cell division enter the streams; this is supported by the observation of pairs of labeled cells migrating together in the streams proximal to the niche. However, in spite of this apparent lack of self-renewal capacity among the

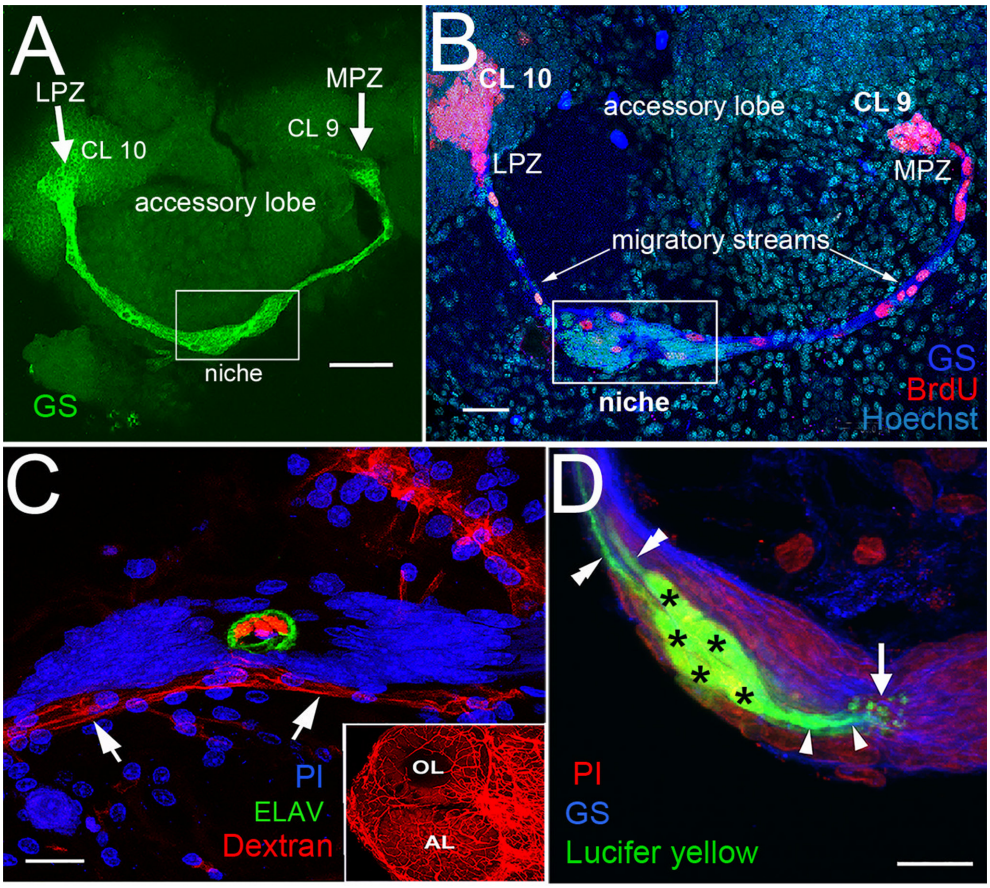

FIGURE 2 | The proliferative system maintaining adult neurogenesis in the crayfish (*Procambarus clarkii*) brain. **(A)** The lateral (LPZ) and medial (MPZ) proliferation zones are contacted by the processes of a population of cells immunoreactive to GS (green) whose somata are located in a neurogenic niche (white box) on the ventral surface of the brain. **(B)** Left side of the brain of *P. clarkii* labeled immunocytochemically for the S-phase marker BrdU (red). Labeled cells are found in the LPZ contiguous with Cluster 10 (CL 10) and in the MPZ near Cluster 9 (CL 9). The two zones are linked by a chain of labeled cells in a migratory stream that originates in the boxed region labeled "niche." Labeling for glutamine synthetase (blue), BrdU (red), and Hoechst (cyan) is shown. **(C)** The vascular connection to the cavity in the center of the niche was demonstrated by injecting dextran tetramethylrhodamine dye into the cerebral artery. The cavity, outlined by its reactivity to an antibody to *ELAV* (green), contains the dextran dye (red), which is also contained within a larger blood vessel that lies beneath the niche (arrows). PI (blue) labeling of the niche cell nuclei is also shown. Inset: dextran-filled vasculature in the olfactory (OL) and accessory (AL) lobes on the left side of the brain. **(D)** Niche cells (green), labeled by intracellular injection of Lucifer yellow, have short processes (arrowheads) projecting to the vascular cavity (arrow) and longer fibers (double arrowheads) that fasciculate to form the tracts projecting to the LPZ and MPZ, along which the daughters of the niche cells (2nd-generation neural precursors) migrate. Glutamine synthetase (GS), blue; propidium iodide (PI), red. Scale bars: **(A)**, 100 μm; **(B)**, 30 μm; **(C,D)**, 20 μm (A, C and D from Sullivan et al., 2007a).

1st-generation neural precursors, these cells are never depleted and neurons continue to be generated throughout the long lives of these animals. It therefore follows that cells generated elsewhere in the organism must be replenishing the pool of 1st-generation neural precursors in the niche (Zhang et al., 2009).

The existence of an extrinsic source of neural precursors was confirmed by experiments in which groups of adult crayfish were injected once with BrdU; nucleoside labeling of 1st-generation precursors in the niche was then documented daily for 1 week and at intervals until 21 days after injection. We anticipated that 1st-generation precursors in the niche that are in S phase during the BrdU exposure would label with BrdU, as would proliferating cells in other tissues, including those that produce neural precursors. However, we hypothesized that neural precursor cells from extrinsic sources would require time after BrdU incorporation to complete their lineages and travel to the niche. Therefore, we expected that cells from an external source would arrive at the niche after a delay. Indeed, BrdU labeling among 1st-generation neural precursors in the niche was observed reliably on days 1–4 following exposure (**Figure 4**). No BrdU+ cells were found in the niche on days 5–7 following BrdU exposure. We attributed this "gap" in labeling to the fact that BrdU has a ∼2 day clearing time in crayfish (Benton et al., 2011), and thus after this period BrdU would no longer be available. Further, cells instrinsic to the niche that had incorporated BrdU during the initial exposure would have divided and migrated into the streams, as these cells have an 18–24 h cell cycle time (Benton et al., 2011). However, on days 8–14 following BrdU injection, intensely labeled cells were once again observed in

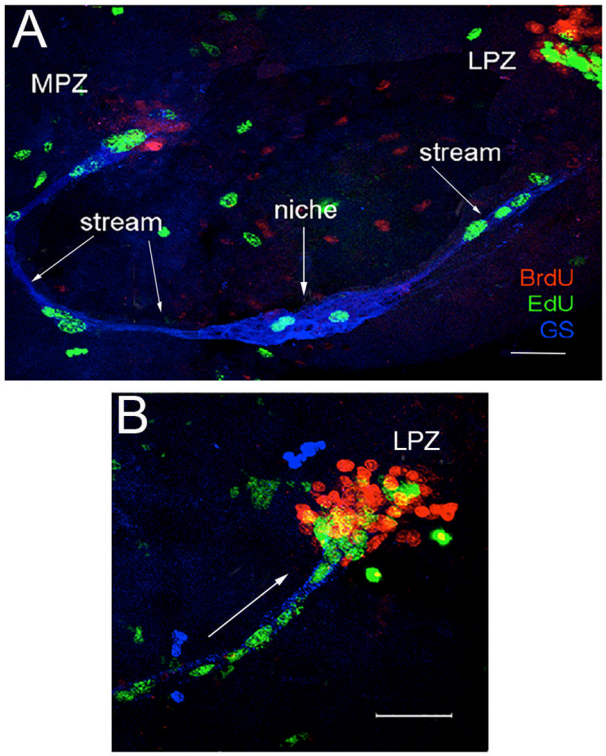

FIGURE 3 | Double-nucleoside labeling demonstrates that the niche cells are not self-renewing. Crayfish were incubated for 24 h in BrdU (red), then maintained in pond water for 7 days. Six hours before sacrifice, they were treated with EdU (green). Brains also were labeled immunocytochemically for glutamine synthetase (blue) to reveal the niche and streams. **(A)** BrdU+ cells were found only in the proliferation zones (MPZ and LPZ), not in the niche. Only EdU labels S-phase cells in the niche, showing that niche cells do not retain BrdU, and thus that divisions are not self-renewing. These labeling patterns also demonstrate that migration is unidirectional, away from the niche. **(B)** Higher magnification image of the LPZ. Arrow in B indicates the direction of neural precursor cell migration. Scale bars: **(A)**, 100 μm; **(B)**, 50 μm. Adapted from Benton et al. (2014).

the niche. As BrdU was no longer available, we concluded that this delayed labeling of niche cells must be due to cells that traveled to the niche that had incorporated BrdU while in their source tissue (Benton et al., 2014). These data also suggest a "just-in-time" replenishment in which neural precursors arrive at the niche and rapidly divide; their daughters then migrate to brain clusters 9 and 10. This experiment therefore supports the existence of an extrinsic source that replenishes neural precursors in the niche, and also indicates that the non-mitotic cells in the niche may be a distinct cell type that serves a supporting role. Consistent with this interpretation, four morphologically distinct niche cell types have been described, with Type 1 cells by far the most numerous. These bipolar cells have long processes that extend to either Cluster 9 or 10, forming the streams along which the 2nd-generation neural precursors migrate. They also have short processes with microvillar extensions that contact the vascular cavity, and junctional complexes between adjacent cells; these features suggest a role in regulating transport and communication between the vasculature and the niche cells (Chaves da Silva et al., 2012). Beyond their morphological characteristics, we know very little about the other three niche cell types.

Identifying the source(s) of the 1st-generation neural precursors has been the priority in our recent work. *In vitro* studies were conducted in which cells were isolated from several different types of tissues. These were labeled with CellTrackerTM Green CMFDA (CTG; Invitrogen), a fluorescent marker, and were then incubated at 18°C with freshly dissected, desheathed crayfish brains and their associated neurogenic niches. After 6 h, the distribution of labeled cells in each culture dish was recorded. Most cell types were distributed evenly in the culture dishes and showed no affinity for the brains or niches (e.g., cells extracted from green gland, hepatopancreas and hematopoietic tissues). In contrast, hemocytes (blood cells) expressed a strong affinity for the niche; these were observed in the vascular cavity or among the niche cells in 77% of cultures. In addition, many of the CTG-labeled cells were immunoreactive for glutamine synthetase, which is a marker of all niche cells in *P. clarkii*. These *in vitro* studies thus provided the first direct evidence that the immune system might be the source of neural precursor cells.

The Immune System Generates Neural Precursors Supporting Adult Neurogenesis

The next goal of our work was to explore the relationship between adult neurogenesis and the immune system, and to test the *in vivo* competence of hemocytes as precursors of adult-born neurons in the crustacean brain. Invertebrates do not generate adaptive immune responses, as they do not have oxygen-carrying erythrocytes or blood cells of the lymphoid lineage. However, these organisms do have a sophisticated innate immune system in which hemocytes play a dominant role, participating in both innate immunity and blood clotting (Lin and Söderhäll, 2011). Freshwater crayfish contain discrete hematopoietic tissues (Noonin et al., 2012; Chaves da Silva et al., 2013) that generate three morphologically distinct types of circulating hemocytes (hyaline, semi-granular and granular cells; Chaga et al., 1995) throughout an animal's long lifetime (up to 20 years in some species). Hemocytes are synthesized and partly differentiated through two main cell lineage pathways in the hematopoietic tissues, but the final development into functional hemocytes takes place after release into the circulation (Söderhäll et al., 2003; Wu et al., 2008). The crustacean immune system also generates prokineticin-family cytokines; these "astakines" promote the proliferation and release of hemocytes from hematopoietic tissues (Söderhäll et al., 2005; Lin et al., 2010). In vertebrate species, prokineticins play roles in circadian regulation, angiogenesis and neurogenesis; adult neurogenesis in the olfactory bulb requires prokineticin 2 (Ng et al., 2005).

Our first experiments exploring the relationship between the immune system and adult neurogenesis in crayfish assessed whether total hemocyte counts (THC) were correlated with the number of cells in the neurogenic niche. THC was manipulated either by ablating part of the hematopoietic tissue to reduce

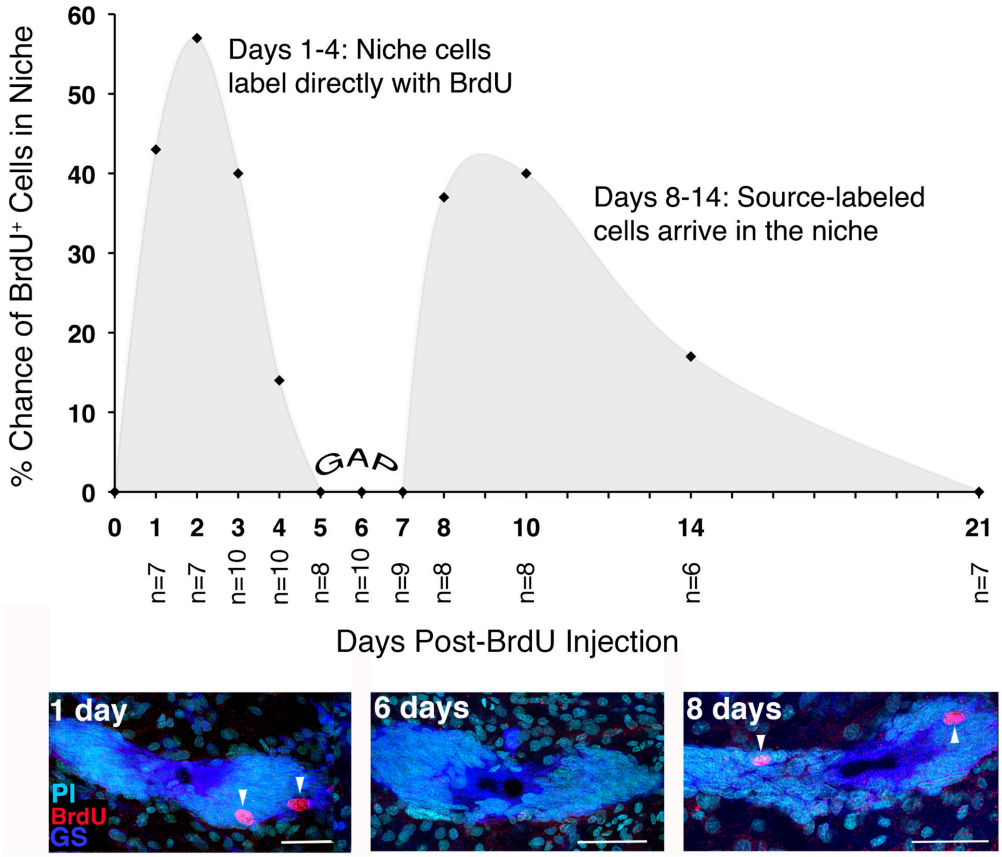

FIGURE 4 | Actively proliferating (BrdU+) cells in the neurogenic niche have a bimodal temporal distribution. BrdU+ cells were quantified in the niches of crayfish that were sacrificed daily for 1 week after BrdU injection, and at intervals thereafter for 21 days. The probability of observing BrdU+ cells in the niche was then plotted for each of the sampling days. BrdU+ cells were observed in the niche on days 1–4 following injection (shown in the day 1 image below graph). On days 5–7, the niches contained no BrdU+ cells (GAP). However, between days 8 and 14 after injection, BrdU+ cells were once again observed in the niche. Adapted from Benton et al. (2014). Scale bar: 50 μm.

THC, or by injecting the crustacean cytokine astakine 1 (AST1) into crayfish to increase THC. AST1 selectively promotes the proliferation and release of semi-granular hemocytes in the crayfish *P. leniusculus* (Lin et al., 2010) and in *P. clarkii* (Benton et al., 2014, 2017). The THC manipulation studies demonstrated a close relationship between the system producing adult-born neurons in the brain and the innate immune system of *P. clarkii*. First, the immune system regulates the neural precursor lineage by releasing AST1, which promotes hemocyte release from hematopoietic tissues (**Figure 5A**), thus raising THC. Second, THC and the number of cells in the neurogenic niche are positively correlated; manipulating the levels of circulating hemocytes results in highly predictable changes in the niche, with AST1 raising and hematopoietic tissue ablations reducing niche cell numbers (and THC). Further, the reduced niche cell numbers that result after partial hematopoietic tissue ablation can be rescued by injecting recombinant AST1 (r-AST1) prior to sacrifice (**Figure 5B**; Benton et al., 2014). Finally, r-AST1 increases the number of BrdU-labeled cells in the niche and streams, suggesting an effect on cell cycle time. These results demonstrate that the immune system regulates the neurogenic niche dynamically and implicates semi-granular hemocytes in this process, because AST1 specifically regulates the release of this blood cell type and also is capable of rescuing the reduction in niche cell counts after hematopoietic tissue ablations.

Adoptive transfer methods were then used to ask whether hemocytes labeled with EdU in donor crayfish would be attracted to the niche in recipient crayfish, as they were *in vitro*. Despite the fact that labeled donor cells represented less than 1% of circulating hemocytes in the recipients, EdU+ cells were nevertheless found in the neurogenic niches of recipient crayfish within a few days of transfer (**Figure 6**; Benton et al., 2014). Over a period of several days following hemocyte transfer, EdU+ cells were observed in both the migratory streams and in Clusters 9 and 10 in the brain, where adult-born neurons normally differentiate. And, by 7 weeks following hemocyte transfers, EdU+ cells in these cell clusters expressed transmitter substances typical of cells in these regions (**Figure 6**). These studies therefore showed that cells circulating in the hemolymph can become neural precursors when transferred directly to recipient crayfish

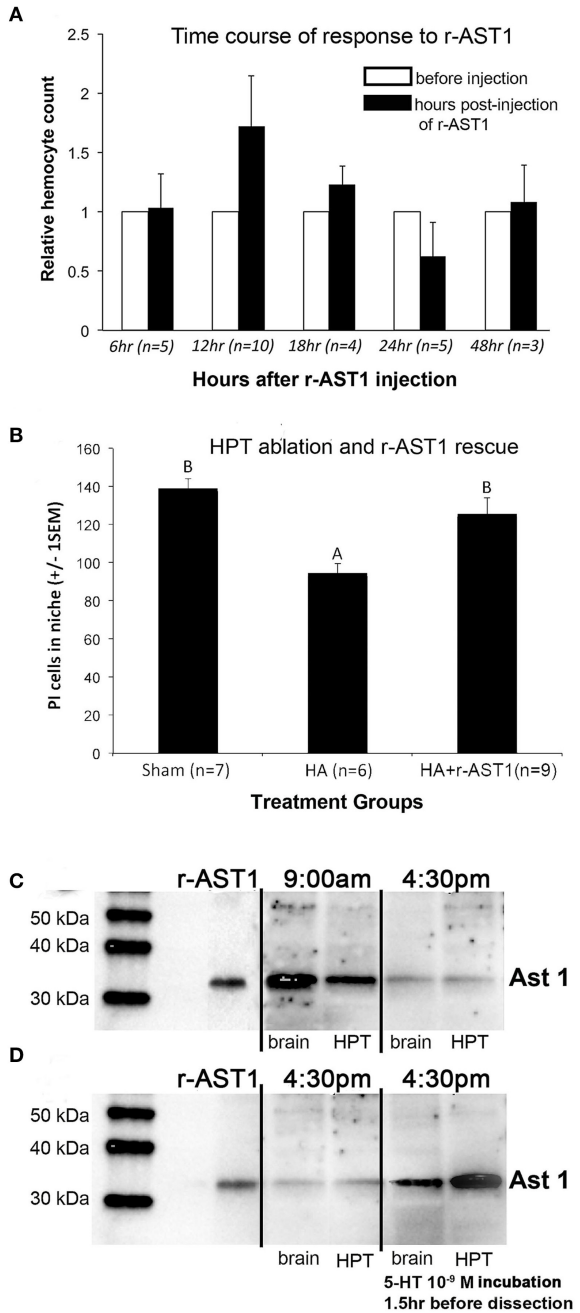

FIGURE 5 | Astakine 1: Effects on hemocyte release and the neurogenic niche, and regulation by time of day and serotonin. **(A)** Time course of release of hemocytes after r-AST1 injection into *P. clarkii*. The relative hemocyte count was calculated as the total hemocyte count (THC) at each time point divided by THC prior to r-AST1 injection. The greatest release of hemocytes occurs 12 h after r-AST1 injection ($p = 0.0002$). **(B)** Crayfish in which hematopoietic tissues were partially ablated (HA) have a significantly lower total number of niche cells (propidium iodide [PI]-labeled) compared to shams (ANOVA, $F = 2.19$, $p < 0.002$). Injection of r-AST1 into HA crayfish 48 h prior to sacrifice (HA+r-AST1) restores the niche cell counts to sham values. **(C)** Western blot of *P. clarkii* AST1 and *P. leniusculus* r-AST1 at 9 a.m. and 4:30 p.m., showing that AST1 expression varies depending on time of day, with higher expression in the morning as previously reported for *P. leniusculus* (Watthanasurorot et al., 2011). **(D)** After serotonin (10^{-9} M) incubation, the 4:30 p.m. expression of AST1 increases. A, B published in Benton et al. (2014).

(Benton et al., 2014). Additional adoptive transfer experiments in which specific hemocyte types were tested have shown that semi-granular hemocytes are the only circulating cell type that is attracted to the niche, strongly implicating these as the cells that replenish the pool of neural precursors in the niche (Cockey et al., 2015; Benton et al., 2017).

Labeled cells harvested from other tissues that are adoptively transferred using the same methods do not result in labeling of cells in the niche, migratory streams or brain cell clusters, suggesting that the attraction of hemocytes to the neurogenic niche is specific and not a general property of all transferred cell types. In addition, transferred hemocytes are not incorporated into other rapidly proliferating tissues such as hepatopancreas or hematopoietic tissue, also indicating that the interaction of donor hemocytes with the niche results from a selective affinity between these tissues. Our experiments therefore suggest that circulating blood cells, specifically the semi-granular hemocytes, are able to become neural precursors, and that these cells and their descendants successfully navigate the many challenges involved in attraction to the niche, migration along the streams, neural differentiation and survival. Further, the generation of neural precursors by the innate immune system challenges the canonical view that ectodermal tissues are the sole source of neurons in the brain.

SEROTONIN REGULATES ADULT NEUROGENESIS

The generation of adult-born neurons in the decapod crustacean brain is highly regulated. Modulatory factors include the living conditions (i.e., enriched vs. deprived environments) (Sandeman and Sandeman, 2000; Ayub et al., 2011), hormonal cycles (Harrison et al., 2001), diet (Beltz et al., 2007), seasonality (Hansen and Schmidt, 2001), the day/night cycle (Goergen et al., 2002), nitric oxide (Benton et al., 2007) and serotonin (Benton et al., 2008; Zhang et al., 2011). As described below, serotonin works at multiple levels to influence neurogenesis: by regulating the expression of the cytokine astakine, which in turn promotes the differentiation and release of semi-granular hemocytes from hematopoietic tissues; as a mediator of hemocyte attraction to the neurogenic niche; and as a cell cycle regulator acting directly on specific neural precursor generations. However, as is clear from the variety of environmental and intrinsic factors that influence the generation of new neurons, the regulation of adult neurogenesis is a complex process involving actions of multiple modulators working in concert. Therefore, although serotonin's roles are highlighted here, these influences will be integrated in the living organism with the actions of the many other regulatory agents in play at a given time.

The adult-born neurons in Clusters 9 and 10 project to the olfactory and accessory lobes, which receive a dense serotonergic innervation, much of which is contributed by the dorsal giant neurons (DGNs). Experiments in embryonic lobsters demonstrated that when serotonin is depleted, the growth and maturation of the olfactory and accessory lobes are selectively delayed compared to these regions in the brains of embryos

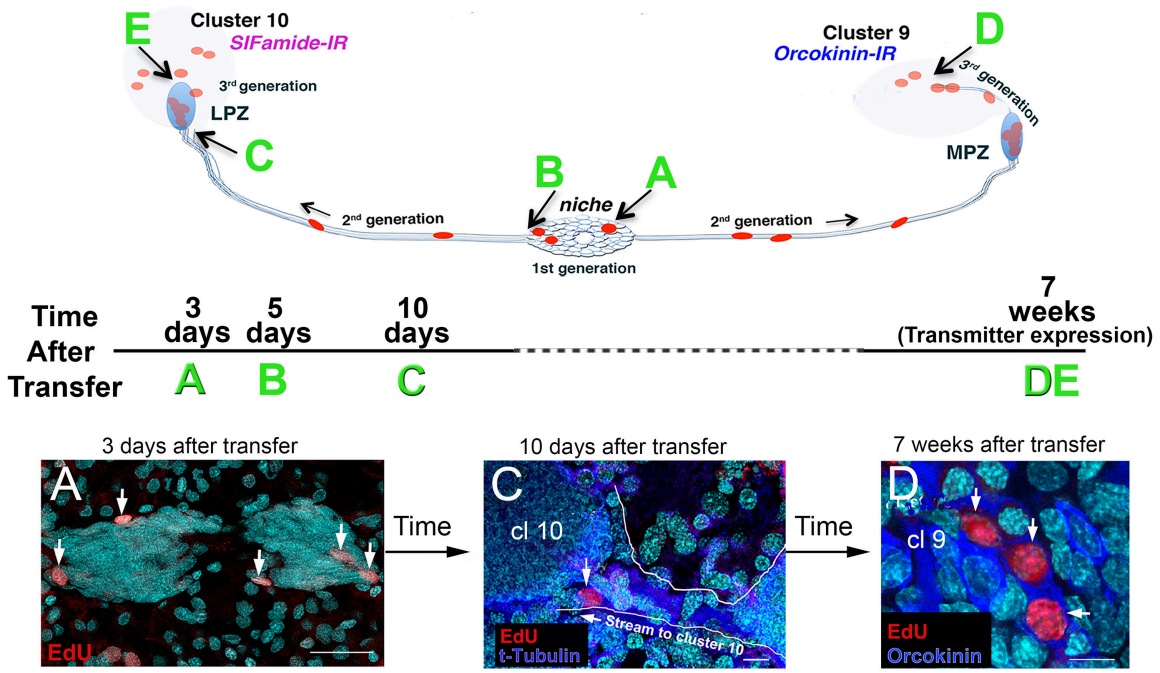

FIGURE 6 | EdU+ cells were observed in the niche, streams, and in Clusters 9 and 10 of recipient crayfish after adoptive transfer of EdU+ hemocytes from donor animals**.** The schematic diagrams illustrate (top) the locations of the EdU+ cells that were observed following adoptive transfers, and (middle) the experimental timeline for each sample (time after transfer, **A–E**), and (bottom) images from *P. clarkii* **(A,D)** and *P. leniusculus* **(C)**. All samples in these images **(A,C,D)** were labeled with the nuclear marker Hoechst 33342 (cyan). **(A)** Three days after adoptive transfer of hemocytes, EdU+ cells (red) were observed in the niche. **(C)** Ten days after hemocyte transfer, cells were observed in the distal ends of the streams, near Clusters 9 and 10 (arrow). Immunoreactivity for tyrosinated tubulin (blue) highlights the migratory stream, which is also outlined in white. **(D)** Seven weeks after adoptive transfer of hemocytes from donor to recipient crayfish, EdU+ cells (red) were observed in cell Clusters 9 and 10. Some of these cells in Cluster 9 express orcokinin, a peptide transmitter used by many Cluster 9 cells. Examples of cell labeling at B (5 days, in the niche) and at E (7 weeks, in Cluster 10) are not shown (but see Benton et al., 2014). Scale bars: **(A)**, 40 μm; **(C)**, 10 μm; **(D)**, 10 μm. Adapted from Benton et al. (2014).

with normal serotonin levels (Benton et al., 1997). Subsequent studies demonstrated that this retarded development is due to a failure of Cluster 9 and 10 neurons to branch and grow into the olfactory and accessory lobes (Sullivan et al., 2000), and to reduced proliferation and survival of neurons in both cell clusters (Beltz et al., 2001; Benton and Beltz, 2001). Thus, serotonin influences both neurogenesis and neuronal differentiation in the embryonic brain.

Regulation of Adult Neurogenesis by Serotonin

Serotonin also is a potent regulator of neurogenesis in the adult crustacean brain, acting directly to increase proliferation in the neurogenic lineage at low levels (10^{-9}–10^{-10} M), or indirectly suppressing neurogenesis by a serotonin-mediated release of hormones from the sinus gland, which requires higher concentrations (10^{-4} M) of the monoamine (Benton et al., 2008, 2011). The neurogenic niche does not appear to receive neural innervation, although serotonergic fibers have been reported in the proliferation zone of Cluster 10 (Beltz et al., 2001). In addition, both the niche and BrdU-labeled cells in the proliferation zone of Cluster 10 lie close to or directly adjacent to blood vessels (Sullivan et al., 2007a; Sandeman et al., 2009). Together, these features suggest that the serotonergic stimulation of neurogenesis may be mediated by serotonin that is circulating at low levels in the hemolymph.

While there may be multiple origins of circulating serotonin, one major source is the DGNs. These very large neurons have massive projections that infiltrate each and every glomerulus in the olfactory and accessory lobes (**Figure 7**; Sandeman and Sandeman, 1994; Sandeman D. et al., 1995; Sandeman R. E. et al., 1995). These structural characteristics suggest that the DGNs are sensory integrators, with the potential to receive olfactory, visual and mechanosensory information, and to influence processing in these regions. In addition, these giant neurons also release serotonin into the hemolymph (Sandeman et al., 2009). We therefore tested the hypothesis that the serotonergic DGN regulates adult neurogenesis by examining the influence of DGN stimulation on BrdU incorporation into cells in the proliferation zone of Cluster 10, an area known to be sensitive to serotonin levels (Benton et al., 2008), and where the final divisions of neural precursors take place prior to differentiation into projection neurons.

Adult neurogenesis continues in dissected, perfused crayfish (*Cherax destructor*) brain preparations, although at a slower rate than *in vivo*; however, 10^{-9} M serotonin added to the perfusate bathing the brain restores the rate of neurogenesis to

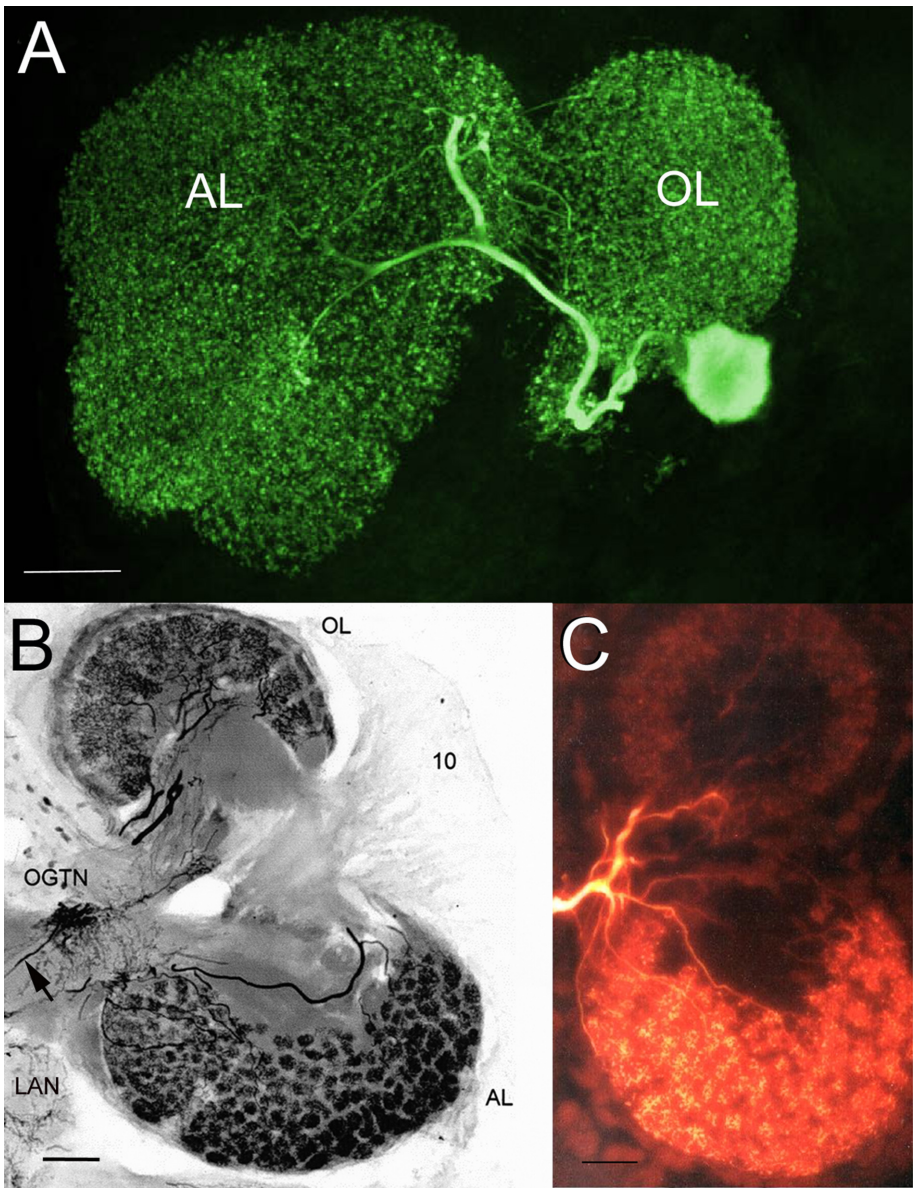

FIGURE 7 | The serotonergic dorsal giant neuron (DGN) innervates each and every glomerulus in the olfactory and accessory lobes. **(A)** Stacked confocal image of a neurobiotin-filled DGN in a lobster (*Homarus americanus*) embryo, revealing the massive projections of the DGN within the olfactory and accessory lobes. **(B)** Photomicrograph of a thick section (100 μm) of the right side of the adult brain of the Australian crayfish *Cherax destructor* immunolabeled for serotonin. The DGN is the only serotonergic neuron that projects to the AL, but shares its projection into the OL with at least two other serotonergic midbrain neurons. The large cell body of the DGN is dorsal and out of the section plane, but the thin primary neurite that connects it with the olfactory globular tract neuropil (OGTN) before it projects into the OL and AL is observed (arrow). 10, Cluster 10 cell bodies; LAN, lateral antennular neuropil. **(C)** Neurobiotin injection of the DGN in an adult *C. destructor* brain illustrating the projections of this neuron to virtually all glomeruli in the OL and AL. Scale bars: **(A)**, 50 μm; **(B,C)**, 100 μm. Adapted from Beltz and Sandeman (2003).

in vivo levels (Sandeman et al., 2009). Therefore, a dissected brain preparation was used to depolarize or hyperpolarize the serotonergic DGN on one side of the brain, while using the contralateral unstimulated side as the paired control; after a 6-h stimulation period and perfusion of the brain with BrdU, brains were fixed and the numbers of BrdU-labeled cells in Cluster 10 on each side of the brain were counted. Stimulation and the generation of action potentials in the DGN on one side of the brain was correlated with an increase in BrdU incorporation into cells in Cluster 10 on that side compared to the unstimulated side. Hyperpolarization of the DGN, on the other hand, was associated with a small decrease in the number of BrdU-labeled cells on the stimulated relative to the control side of the brain. High-performance liquid chromatography (HPLC) was used to measure serotonin levels in the perfusate of stimulated brains; serotonin levels increase

roughly10-fold, confirming that serotonin is released when the DGN is active. Further, perfusate levels of serotonin collected during stimulation ranged from 10^{-11}–10^{-13} M; factoring in the added dilution in the perfusate following serotonin release implies values at the sites of neural proliferation that are optimal for increasing the rate of neurogenesis (10^{-9}–10^{-10} M) (Benton et al., 2008). These data suggest that suprathreshold excitation of the DGN results in a non-synaptic release of serotonin into the vascular system, which carries the amine to the proliferation zones associated with Clusters 9 and 10. Serotonin in these regions may accelerate the cell cycle progress of neural precursors, increasing the rate of cells entering S phase, and thus the numbers of cells labeled with BrdU (Sandeman et al., 2009). The interpretation of the decrease in BrdU labeling following hyperpolarization of the DGN is less apparent. However, the perfusate in these brain preparations contained detectable levels of serotonin even when there was no DGN stimulation, perhaps suggesting an ongoing release of serotonin at very low levels. Hyperpolarization of the DGN might therefore reduce this release, leading to decreases in cell proliferation. These studies therefore suggest that one role of the DGNs in crayfish (and related decapods), is to regulate adult neurogenesis according to the sensory information that is collected and analyzed in the olfactory lobes and further integrated with visual and mechanosensory information in the accessory lobes.

The Influence of Serotonin Is Lineage-Dependent

Serotonin (10^{-9} M) does not alter the rate of BrdU incorporation into neural precursors in the neurogenic niche or proximal migratory streams of *P. clarkii*, but does increase the rate of BrdU uptake into cells in Clusters 9 and 10 where final divisions and differentiation occur. These data indicate that the cell cycle of the 1st- and early 2nd-generation neural precursors are not sensitive to this monoamine. However, the total number of cells composing the niche increases, suggesting that this group of cells is expanding due to the addition of cells from outside the niche, rather than by proliferation of the resident cell population (Benton et al., 2011; Zhang et al., 2011).

Serotonin receptors (5-$HT_{1\alpha}$ and 5-$HT_{2\beta}$) that are homologous to mammalian subtypes 1A and 2B have been identified and cloned from several crustacean species, including *P. clarkii,* and antibodies raised against conserved regions of the orthologous molecules (Clark et al., 2004; Sosa et al., 2004; Spitzer et al., 2008). Because our BrdU incorporation data (Zhang et al., 2011) indicated lineage-dependent influences of serotonin, we tested this possibility by exploiting the spatial separation of the neural precursor cell generations. *In situ* hybridization with antisense riboprobes specific for 5-$HT_{1\alpha}$ and 5-$HT_{2\beta}$ receptors revealed strong expression of these mRNAs in several brain regions, including cell clusters 9 and 10. Further, antibodies specific for these receptor subtypes do not bind to the 1st-generation neural precursors in the niche or their daughters as they exit into the migratory streams, but do label the 2nd-generation precursors as they approach the proliferation zones of cell clusters 9 and 10. Experiments using the 5-$HT_{1\alpha}$ specific agonist quipazine maleate salt (QMS) increases the number of BrdU-labeled cells in Cluster 10, and the 5-$HT_{2\beta}$ antagonist methiothepin mesylate salt (MMS) suppresses neurogenesis in this region, suggesting the involvement of these receptor subtypes in serotonin's effects. However, these pharmacological agents do not alter the rate of BrdU incorporation into the 1st-generation precursors in the niche or their 2nd-generation daughters in the streams proximal to the niche. These studies therefore show that serotonin's influence on adult neurogenesis in the crayfish brain is limited to the late 2nd-generation precursors and their descendants. The conclusion that serotonergic effects are exerted directly on specific generations of neural precursors is reinforced by the distribution of 5-$HT_{1\alpha}$ and 5-$HT_{2\beta}$ mRNAs and proteins in the later generations of the neural precursor lineage. Taken together, these results indicate that serotonin exerts lineage-dependent effects on adult neurogenesis that are mediated by specific receptor subtypes (Zhang et al., 2011).

Serotonin Promotes the Attraction of Circulating Neural Precursors to the Niche

The adoptive transfer experiments described above suggest that the attraction between hemocytes and the niche is highly selective. What is the nature of this attraction? The first clue came from the co-culture experiments in which brains and their associated niches were incubated for 6 h with cells that had been dissociated from several tissue types. As discussed above, only hemocytes showed a significant attraction for the niche *in vitro* (Benton et al., 2011). These studies also probed the basis for this affinity, and showed that hemocyte attraction was severely reduced by the crustacean 5-$HT_{2\beta}$ receptor antagonist methiothepin mesylate salt (MMS; 10^{-8} M) or by treating crayfish with parachlorophenylalanine (PCPA; an inhibitor of serotonin synthesis) prior to dissecting brains for co-cultures. Although somewhat counter-intuitive, the attraction of hemocytes for the niche also was eliminated if serotonin (10^{-9} M) was introduced into the culture medium, suggesting that the presence of serotonin abolished the natural affinity of hemocytes for the niche. Our interpretation of this result is that serotonin added to the culture medium may destroy or mask a serotonergic signaling gradient associated with the niche (Benton et al., 2011). Finally, serotonin immunoreactivity is localized in the rim of the vascular cavity (the "crown"; **Figure 8**) in the niche, and hemocytes strongly express the crustacean 5-$HT_{1\alpha}$, as well as 5-$HT_{2\beta}$ receptors, albeit more weakly (**Figure 9**) (Benton et al., 2011). Based on these several lines of evidence, we have concluded that serotonin is involved in attracting hemocytes to the niche, building on an extensive history of serotonin as a chemoattractant in the nervous system [reviewed in (Daubert and Condron, 2010)] and the vascular system (Duerschmied et al., 2013; Kang et al., 2013).

The origin of serotonin labeling in the "crown" is still unknown. None of the four cell types in the niche (Chaves da Silva et al., 2012) labels immunocytochemically for serotonin

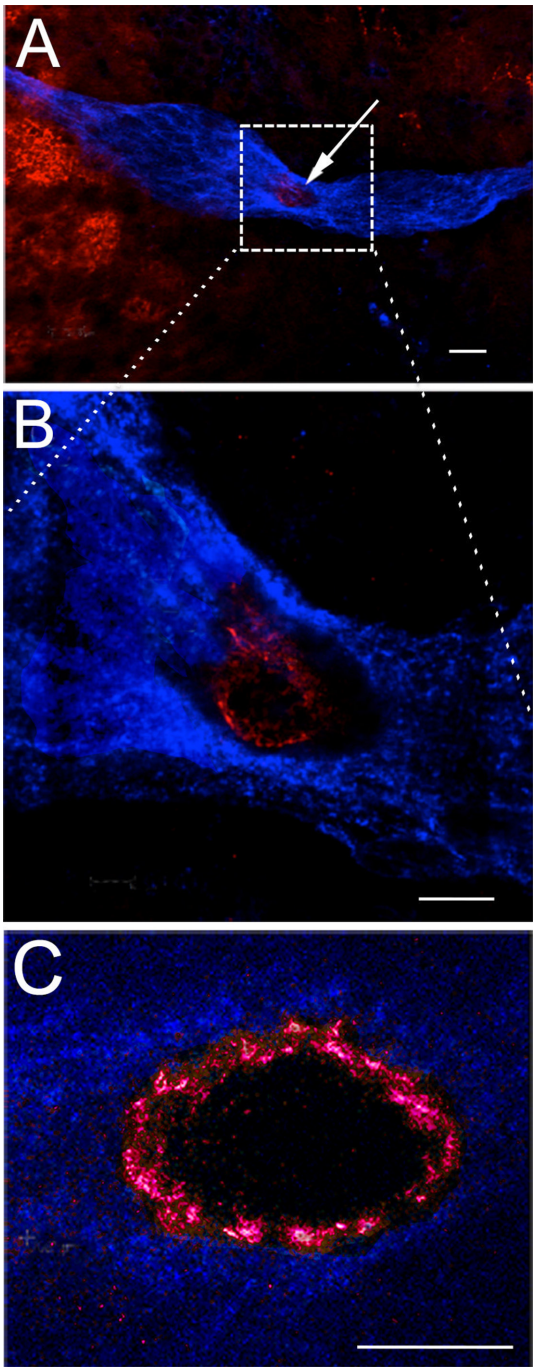

FIGURE 8 | Serotonin is localized in the rim of the vascular cavity**.** The neurogenic niche in *P. clarkii*, labeled immunocytochemically for glutamine synthetase (blue) and serotonin (red). The vascular cavity is outlined by a rim of serotonin labeling, most clearly seen in **(C)**. The additional serotonin labeling observed in **(A)** to the left of the niche is localized in neural terminals in the accessory lobe. **(A,B)** were contributed by V. Quinan. Scale bars: **(A)**, 20 μm; **(B)**, 10 μm; **(C)**, 10 μm.

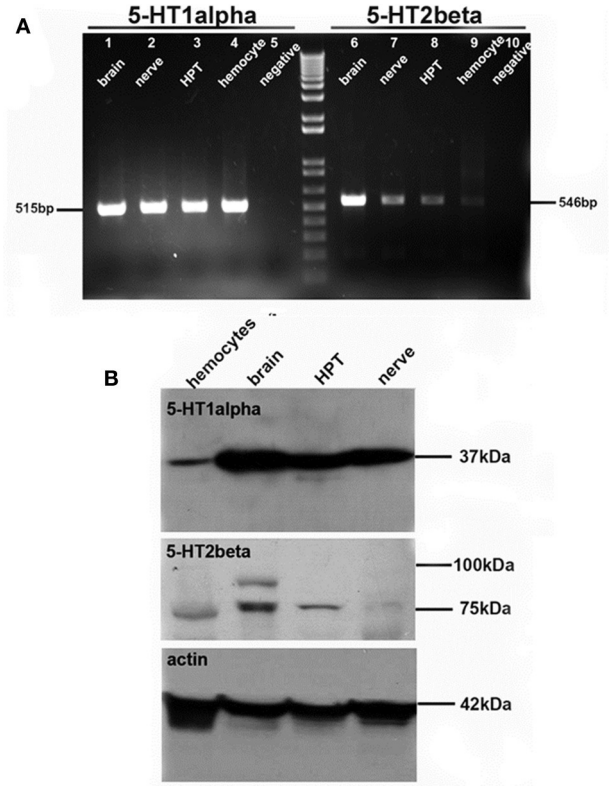

FIGURE 9 | Serotonin receptor subtypes are expressed in hemocytes and brain. **(A)** RT-PCR reveals the expression of 5-HT1α (left) and 5-HT2β (right) receptor subtype mRNAs in brain (lanes 1, 6), nerve (lanes 2, 7), hematopoietic tissue (HPT, lanes 3, 8), hemocytes (lanes 4, 9) and the negative control (lanes 5, 10). **(B)** Western blot for 5-HT1α (top) and 5-HT2β (middle) receptor proteins, with actin control (bottom). Adapted from Benton et al. (2011).

or its rate-limiting enzyme, tryptophan hydroxylase; the niche cells are thus are not considered "serotonergic." However, no innervation of the niche has yet been discovered that could explain this labeling. We are currently testing the hypothesis that the serotonin immunoreactivity that encircles the vascular cavity results from "borrowed transmitter" taken up through serotonin transporters from the hemolymph and into the terminals of type 1 niche cells. This hypothetical mechanism could provide a means by which serotonin released into the circulation by the DGN could directly influence serotonin levels in the "crown," and thereby alter the attraction of hemocytes for the niche.

FUTURE DIRECTIONS

Next-Generation Sequencing

In order to characterize the cellular lineage that produces adult-born neurons, we have generated transcriptome data for *P. clarkii* tissues by next-generation sequencing. Genes and members of gene families that are known to play key roles in arthropod neurogenesis and neural and glial differentiation have been identified in the transcriptome. Among these sequences are *SoxB*, *Achaete-Scute-Complex* and *Snail* transcription factors, *Prospero*, *Elav* and *Repo*. *In situ* hybridization for these mRNAs is being combined with *in vivo* cell proliferation studies, to examine the distribution of gene expression for these markers

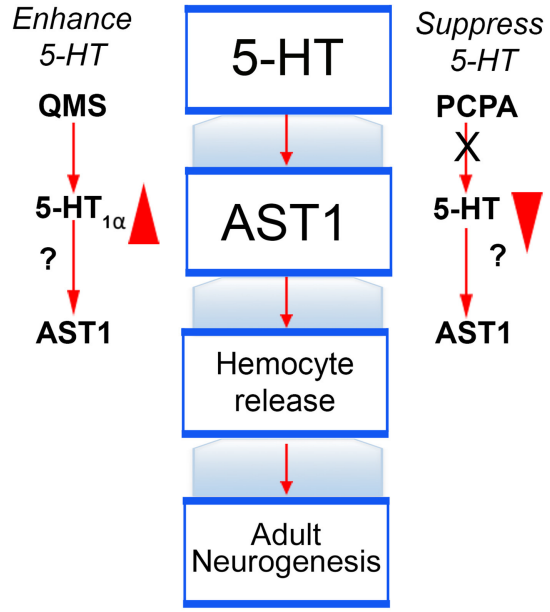

FIGURE 10 | Testing serotonin as a link between the nervous and immune systems**.** Our working model describing serotonin's role in adult neurogenesis includes stimulating the expression of AST1, which in turn promotes the release of semi-granular hemocytes and accelerates the rate of adult neurogenesis. These relationships will be further tested using agents that enhance or suppress serotonin's action (e.g., quizapine maleate salt [QMS] and PCPA, respectively). While the influence of these compounds on adult neurogenesis in crayfish is known, it has not yet been determined if these effects are mediated by AST1, or result from direct influences of serotonin.

in both the embryonic and adult nervous systems (Brenneis et al., 2017). Further, these probes will be used to examine the differentiation of adoptively transferred hemocytes, to determine whether the lineage of cells produced by hemocytes expresses markers comparable to the natural neurogenic lineage in crayfish. The molecular differentiation of neural precursors and neurons generated in the adult brain will be compared with the spatiotemporal progression of these markers during embryonic neurogenesis. Our ultimate goal is to unravel the genetic network governing the proposed neural differentiation of hemocytes in the procambarid brain.

Serotonin: A Link between the Immune and Nervous Systems?

Studies in the lab of Irene Söderhäll (Uppsala University, Sweden) and by us (**Figures 5C,D**) have shown that the expression of AST1, the crustacean cytokine that promotes the differentiation and release of semi-granular hemocytes from hematopoietic tissues (Lin et al., 2010, 2011; Cockey et al., 2015), is regulated by serotonin. This association between serotonin and AST1 may suggest a coordinated regulation of the immune and nervous systems, such that hemocyte release is controlled, at least in part, by an agent synthesized and released by the nervous system. Serotonin has potent influences on the rate of neurogenesis, and this may speak not only to its direct effect on the cell cycle, but also to controlling access to neural precursors. For these reasons, we are exploring the connections between serotonin, astakine and adult neurogenesis, to learn how the immune and nervous systems may be influenced by neural agents that alter immune function and by immune agents that alter neurogenesis.

The linkage between serotonin, AST1, hemocyte release and adult neurogenesis will be further explored by, for example, manipulating serotonergic activity with the 5-$HT_{1\alpha}$ specific agonist QMS (**Figure 10**, left) or depressing the serotonin pathway using the tryptophan hydroxylase inhibitor PCPA (**Figure 10**, right). Studies using these agents were described above and have been published (Zhang et al., 2011), but their influence on AST1 has not yet been explored; future experiments will fill this gap in our knowledge. Further, RNA interference (RNAi) has been used successfully in the Söderhäll lab (Lin et al., 2010, 2011) to silence AST1 in hematopoietic tissues *in vivo*, which resulted in low hemocyte counts following injection of lipopolysaccharide (LPS) into crayfish; LPS injection normally causes the release of hemocytes and high hemocyte counts. These studies ultimately led to the discovery of an AST1-dependent molecule, crustacean hematopoietic factor (CHF), which is an anti-apoptotic agent. Thus, AST1 promotes the proliferation, release and survival (via CHF) of semi-granular hemocytes. The sequence for *P. clarkii* AST1 has been identified in our transcriptome data, and confirmed by PCR on *P. clarkii* cDNA and subsequent cloning. Knock-down of AST1 will provide a means of separating direct effects of serotonin on adult neurogenesis from those that are mediated by AST1 expression. Overall, these studies will connect our past work on the serotonergic control of adult neurogenesis in crustaceans with cytokine regulation of these processes.

Finally, to better understand the relationship between the immune system and adult neurogenesis, we also are testing whether cells released from immune tissues can be biased toward a neural fate by treatment with a variety of agents, including serotonin, astakine and homogenates of various brain regions. To begin, we have asked whether these agents increase the attraction of cells to the neurogenic niche *in vitro*. Preliminary studies have shown that cultured immune cells treated with homogenate made from the accessory lobes in the brain adopted a more differentiated morphology and also had an enhanced attraction to the niche *in vitro* (Benton et al., 2017). Using adoptive transfer methods, future experiments will examine whether immune cells biased by accessory lobe homogenate are capable of progressing through the neural precursor lineage and whether they express appropriate markers of neural differentiation, finally producing mature neurons. If so, the active agent(s) in the accessory lobe homogenate that promotes the neural biasing of immune cells will be explored and identified.

CONCLUSIONS

The studies reviewed here indicate that the immune and nervous systems work together to generate adult-born neurons in the crustacean brain. Serotonin is one agent that has a potent influence over adult neurogenesis by promoting proliferation

in the neural precursor lineage. Serotonin may also serve as a pivotal link between the nervous and immune systems by influencing AST1 expression and by attracting hemocytes to the neurogenic niche. Our future studies will further define the connections between the immune system and adult neurogenesis, and will explore the role that serotonin plays in mediating this relationship.

AUTHOR CONTRIBUTIONS

BB composed the first draft of this review, which was read critically and edited by JB.

FUNDING

This work was supported by grants: NSF IOS #0091092, IOS #0344448, IOS #1121345, IOS #1456918, IOS #1656103; NIH R01MH67157. A Maren Fellowship awarded by the Mt. Desert Island Biological Laboratory, as well as Brachman Hoffman and Staley Fellowships from Wellesley College, also contributed to these studies.

ACKNOWLEDGMENTS

The studies described in this review have spanned 25 years in the Beltz Lab at Wellesley College. We therefore wish to acknowledge the following students, postdoctoral fellows and colleagues for their many contributions to the projects highlighted in this review: Silvana Allodi, Neishay Ayub, Leslie Bagay, Kara Banson, Georg Brenneis, Paula Chaves da Silva, Emily Cockey, Anushree Dugar, Maria Genco, Erin Goergen, Steffen Harzsch, Simone Helluy, Rachel Kery, Youngmi Faith Kim, Colleen Kirkhart, Emmy Li, Mike Mellon, Julie Miller, Chadanat Noonin, Zehra Omer, Adriane Otopalik, Jody Platto, Virginia Quinan, Kristina Ramos, Maureen Ruchhoeft, David Sandeman, Renate Sandeman, Silvia Sintoni, Irene Söderhäll, Jeremy Sullivan, and Yi Zhang. The authors also recognize Pat Carey and Val LePage for the care of animals used in these studies.

REFERENCES

Anlauf, E., and Derouiche, A. (2013). Glutamine synthetase as an astrocytic marker: its cell type and vesicle localization. *Front. Endocrinol.* 4:144. doi: 10.3389/fendo.2013.00144

Ayub, N., Benton, J. L., Zhang, Y., and Beltz, B. S. (2011). Environmental enrichment influences neuronal stem cells in the adult crayfish brain. *Dev. Neurobiol.* 71, 351–361. doi: 10.1002/dneu.20864

Banasr, M., Hery, M., Printemps, R., and Daszuta, A. (2004). Serotonin-induced increases in adult cell proliferation and neurogenesis are mediated through different and common 5-HT receptor subtypes in the dentate gyrus and the subventricular zone. *Neuropsychopharmacology* 29, 450–460. doi: 10.1038/sj.npp.1300320

Bazin, F. (1969). *L'organe deutocérébral chez les Crustacés Décapodes Reptantia In Laboratoire de Biologie Animale et du Laboratoire Maritime.* Caen: University of Caen Normandy.

Beltz, B. S., and Sandeman, D. C. (2003). Regulation of life-long neurogenesis in the decapod crustacean brain. *Arthropod. Struct. Dev.* 32, 39–60. doi: 10.1016/S1467-8039(03)00038-0

Beltz, B. S., Benton, J. L., and Sullivan, J. M. (2001). Transient uptake of serotonin by newborn olfactory projection neurons. *Proc. Natl. Acad. Sci. U.S.A.* 98, 12730–12735. doi: 10.1073/pnas.231471298

Beltz, B. S., Tlusty, M. F., Benton, J. L., and Sandeman, D. C. (2007). Omega-3 fatty acids upregulate adult neurogenesis. *Neurosci. Lett.* 415, 154–158. doi: 10.1016/j.neulet.2007.01.010

Beltz, B. S., Zhang, Y., Benton, J. L., and Sandeman, D. C. (2011). Adult neurogenesis in the decapod crustacean brain: a hematopoietic connection? *Eur. J. Neurosci.* 34, 870–883. doi: 10.1111/j.1460-9568.2011.07802.x

Benton, J. L., Banson, K. M., and Beltz, B. S. (2017). The immune system and adult neurogenesis in a crustacean brain: semi-granular hemocytes are neural precursors [Abstract 31.20]. *Soc. Neurosci.*

Benton, J. L., Goergen, E. M., Rogan, S. C., and Beltz, B. S. (2008). Hormonal and synaptic influences of serotonin on adult neurogenesis. *Gen. Comp. Endocrinol.* 158, 183–190. doi: 10.1016/j.ygcen.2008.07.016

Benton, J. L., Kery, R., Li, J., Noonin, C., Söderhäll, I., and Beltz, B. S. (2014). Cells from the immune system generate adult-born neurons in crayfish. *Dev. Cell* 30, 322–333. doi: 10.1016/j.devcel.2014.06.016

Benton, J. L., Sandeman, D. C., and Beltz, B. S. (2007). Nitric oxide in the crustacean brain: regulation of neurogenesis and morphogenesis in the developing olfactory pathway. *Dev. Dyn.* 236, 3047–3060. doi: 10.1002/dvdy.21340

Benton, J. L., Zhang, Y., Kirkhart, C. R., Sandeman, D. C., and Beltz, B. S. (2011). Primary neuronal precursors in adult crayfish brain: replenishment from a non-neuronal source. *BMC Neurosci.* 12:53. doi: 10.1186/1471-2202-12-53

Benton, J., and Beltz, B. (2001). Effects of serotonin depletion on local interneurons in the developing olfactory pathway of lobsters. *J. Neurobiol.* 46, 193–205. doi: 10.1002/1097-4695(20010215)46:3<193::AID-NEU1002>3.0.CO;2-8

Benton, J., Huber, R., Ruchhoeft, M., Helluy, S., and Beltz, B. (1997). Serotonin depletion by 5,7-dihydroxytryptamine alters deutocerebral development in the lobster, Homarus americanus. *J. Neurobiol.* 33, 357–373. doi: 10.1002/(SICI)1097-4695(199710)33:4<357::AID-NEU2>3.0.CO;2-9

Brenneis, G., Schwentner, M., Benton, J. L., and Beltz, B. S. (2017). First insights into the genetic network underlying embryonic and adult neurogenesis in procambarid crayfish – using gene expression studies to document the differentiation of hemocytes into neurons during life-long neurogenesis [Abstract 31.21]. *Soc. Neurosci.*

Brezun, J. M., and Daszuta, A. (1999). Depletion in serotonin decreases neurogenesis in the dentate gyrus and the subventricular zone of adult rats. *Neuroscience* 89, 999–1002. doi: 10.1016/S0306-4522(98)00693-9

Brezun, J. M., and Daszuta, A. (2000). Serotonin may stimulate granule cell proliferation in the adult hippocampus, as observed in rats grafted with foetal raphe neurons. *Eur. J. Neurosci.* 12, 391–396. doi: 10.1046/j.1460-9568.2000.00932.x

Chaga, O., Lignell, M., and Söderhäll, K. (1995). The haemopoietic cells of the freshwater crayfish, *Pacifastacus leniusculus*. *Anim. Biol.* 4, 59–70.

Chaves da Silva, P. G., Benton, J. L., Beltz, B. S., and Allodi, S. (2012). Adult neurogenesis: ultrastructure of a neurogenic niche and neurovascular relationships. *PLoS ONE* 7:e39267. doi: 10.1371/journal.pone.0039267

Chaves da Silva, P. G., Benton, J. L., Sandeman, D. C., and Beltz, B. S. (2013). Adult neurogenesis in the crayfish brain: the hematopoietic anterior proliferation center has direct access to the brain and stem cell niche. *Stem Cells Dev.* 22, 1027–1041. doi: 10.1089/scd.2012.0583

Clark, M. C., Dever, T. E., Dever, J. J., Xu, P., Rehder, V., Sosa, M. A., et al. (2004). Arthropod 5-HT2 receptors: a neurohormonal receptor in decapod crustaceans that displays agonist independent activity resulting from an evolutionary alteration to the DRY motif. *J. Neurosci.* 24, 3421–3435. doi: 10.1523/JNEUROSCI.0062-04.2004

Cockey, E., Li, J., Benton, J. L., and Beltz, B. S. (2015). Cytokine regulation of adult neurogenesis: the immune system provides neuronal precursors for adult neurogenesis. *Soc. Neurosci. Abstr.* 289.15.

Daubert, E. A., and Condron, B. G. (2010). Serotonin: a regulator of neuronal morphology and circuitry. *Trends Neurosci.* 33, 424–434. doi: 10.1016/j.tins.2010.05.005

Duerschmied, D., Suidan, G. L., Demers, M., Herr, N., Carbo, C., Brill, A., et al. (2013). Platelet serotonin promotes the recruitment of neutrophils to sites of acute inflammation in mice. *Blood* 121, 1008–1015. doi: 10.1182/blood-2012-06-437392

Goergen, E. M., Bagay, L. A., Rehm, K., Benton, J. L., and Beltz, B. S. (2002). Circadian control of neurogenesis. *J. Neurobiol.* 53, 90–95. doi: 10.1002/neu.10095

Hansen, A., and Schmidt, M. (2001). Neurogenesis in the central olfactory pathway of the adult shore crab *Carcinus maenas* is controlled by sensory afferents. *J. Comp. Neurol.* 441, 223–233. doi: 10.1002/cne.1408

Harrison, P. J., Cate, H. S., Swanson, E. S., and Derby, C. D. (2001). Postembryonic proliferation in the spiny lobster antennular epithelium: rate of genesis of olfactory receptor neurons is dependent on molt stage. *J. Neurobiol.* 47, 51–66. doi: 10.1002/neu.1015

Harzsch, S. (2003). Ontogeny of the ventral nerve cord in malacostracan crustaceans: a common plan for neuronal development in Crustacea, Hexapoda and other Arthropoda? *Arthropod. Struct. Dev.* 32, 17–37. doi: 10.1016/S1467-8039(03)00008-2

Harzsch, S., Miller, J., Benton, J., and Beltz, B. (1999). From embryo to adult: persistent neurogenesis and apoptotic cell death shape the lobster deutocerebrum. *J. Neurosci.* 19, 3472–3485.

Kang, B. N., Ha, S. G., Bahaie, N. S., Hosseinkhani, M. R., Ge, X. N., Blumenthal, M. N., et al. (2013). Regulation of serotonin-induced trafficking and migration of eosinophils. *PLoS ONE* 8:e54840. doi: 10.1371/journal.pone.0054840

Kim, Y. F., Sandeman, D. C., Benton, J. L., and Beltz, B. S. (2014). Birth, survival and differentiation of neurons in an adult crustacean brain. *Dev. Neurobiol.* 74, 602–615. doi: 10.1002/dneu.22156

Lin, X., and Söderhäll, I. (2011). Crustacean hematopoiesis and the astakine cytokines. *Blood* 117, 6417–6424. doi: 10.1182/blood-2010-11-320614

Lin, X., Novotny, M., Söderhäll, K., and Söderhäll, I. (2010). Ancient cytokines, the role of astakines as hematopoietic growth factors. *J. Biol. Chem.* 285, 28577–28586. doi: 10.1074/jbc.M110.138560

Lin, X., Söderhäll, K., and Söderhäll, I. (2011). Invertebrate hematopoiesis: an astakine-dependent novel hematopoietic factor. *J. Immunol.* 186, 2073–2079. doi: 10.4049/jimmunol.1001229

Lledo, P. M., Alonso, M., and Grubb, M. S. (2006). Adult neurogenesis and functional plasticity in neuronal circuits. *Nat. Rev. Neurosci.* 7, 179–193. doi: 10.1038/nrn1867

Ng, K. L., Li, J. D., Cheng, M. Y., Leslie, F. M., Lee, A. G., and Zhou, Q. Y. (2005). Dependence of olfactory bulb neurogenesis on prokineticin 2 signaling. *Science* 308, 1923–1927. doi: 10.1126/science.1112103

Noonin, C., Lin, X., Jiravanichpaisal, P., Söderhäll, K., and Söderhäll, I. (2012). Invertebrate hematopoiesis: an anterior proliferation center as a link between the hematopoietic tissue and the brain. *Stem Cells Dev.* 21, 3173–3186. doi: 10.1089/scd.2012.0077

Sandeman, D. C., and Sandeman, R. E. (1994). Electrical responses and synaptic connections of giant serotonin-immunoreactive neurons in crayfish olfactory and accessory lobes. *J. Comp. Neurol.* 341, 130–144. doi: 10.1002/cne.903410111

Sandeman, D. C., Benton, J. L., and Beltz, B. S. (2009). An identified serotonergic neuron regulates adult neurogenesis in the crustacean brain. *Dev. Neurobiol.* 69, 530–545. doi: 10.1002/dneu.20722

Sandeman , D., Beltz, B., and Sandeman, R. (1995). Crayfish brain interneurons that converge with serotonin giant cells in accessory lobe glomeruli. *J. Comp. Neurol.* 352, 263–279. doi: 10.1002/cne.903520209

Sandeman, R. E., Watson, A. H., and Sandeman, D. C. (1995). Ultrastructure of the synaptic terminals of the dorsal giant serotonin-IR neuron and deutocerebral commissure interneurons in the accessory and olfactory lobes of the crayfish. *J. Comp. Neurol.* 361, 617–632. doi: 10.1002/cne.903610406

Sandeman, R., and Sandeman, D. (2000). "Impoverished" and "enriched" living conditions influence the proliferation and survival of neurons in crayfish brain. *J. Neurobiol.* 45, 215–226. doi: 10.1002/1097-4695(200012)45:4<215::AID-NEU3>3.0.CO;2-X

Schmidt, M. (1997). Continuous neurogenesis in the olfactory brain of adult shore crabs, *Carcinus maenas*. *Brain Res.* 762, 131–143. doi: 10.1016/S0006-8993(97)00376-4

Schmidt, M. (2001). Neuronal differentiation and long-term survival of newly generated cells in the olfactory midbrain of the adult spiny lobster, *Panulirus argus*. *J. Neurobiol.* 48, 181–203. doi: 10.1002/neu.1050

Schmidt, M., and Demuth, S. (1998). Neurogenesis in the central olfactory pathway of adult decapod crustaceans. *Ann. N.Y. Acad. Sci.* 855, 277–280. doi: 10.1111/j.1749-6632.1998.tb10583.x

Schmidt, M., and Derby, C. D. (2011). Cytoarchitecture and ultrastructure of neural stem cell niches and neurogenic complexes maintaining adult neurogenesis in the olfactory midbrain of spiny lobsters, *Panulirus argus*. *J. Comp. Neurol.* 519, 2283–2319. doi: 10.1002/cne.22657

Schmidt, M., and Harzch, S. (1999). Comparative analysis of neurogenesis in the central olfactory pathway of adult decapod crustaceans by *in vivo* BrdU labeling. *Biol. Bull.* 196, 127–136. doi: 10.2307/1542558

Sintoni, S., Benton, J. L., Beltz, B. S., Hansson, B. S., and Harzsch, S. (2012). Neurogenesis in the central olfactory pathway of adult decapod crustaceans: development of the neurogenic niche in the brains of procambarid crayfish. *Neural Dev.* 7:1. doi: 10.1186/1749-8104-7-1

Söderhäll, I., Bangyeekhun, E., Mayo, S., and Söderhäll, K. (2003). Hemocyte production and maturation in an invertebrate animal; proliferation and gene expression in hematopoietic stem cells of *Pacifastacus leniusculus*. *Dev. Comp. Immunol.* 27, 661–672. doi: 10.1016/S0145-305X(03)00039-9

Söderhäll, I., Kim, Y. A., Jiravanichpaisal, P., Lee, S. Y., and Söderhäll, K. (2005). An ancient role for a prokineticin domain in invertebrate hematopoiesis. *J. Immunol.* 174, 6153–6160. doi: 10.4049/jimmunol.174.10.6153

Song, C. K., Johnstone, L. M., Schmidt, M., Derby, C. D., and Edwards, D. H. (2007). Social domination increases neuronal survival in the brain of juvenile crayfish *Procambarus clarkii*. *J. Exp. Biol.* 210, 1311–1324. doi: 10.1242/jeb.02758

Sosa, M. A., Spitzer, N., Edwards, D. H., and Baro, D. J. (2004). A crustacean serotonin receptor: cloning and distribution in the thoracic ganglia of crayfish and freshwater prawn. *J. Comp. Neurol.* 473, 526–537. doi: 10.1002/cne.20092

Spitzer, N., Edwards, D. H., and Baro, D. J. (2008). Conservation of structure, signaling and pharmacology between two serotonin receptor subtypes from decapod crustaceans, *Panulirus interruptus* and *Procambarus clarkii*. *J. Exp. Biol.* 211, 92–105. doi: 10.1242/jeb.012450

Steullet, P., Cate, H. S., and Derby, C. D. (2000). A spatiotemporal wave of turnover and functional maturation of olfactory receptor neurons in the spiny lobster *Panulirus argus*. *J. Neurosci.* 20, 3282–3294.

Sullivan, J. M., and Beltz, B. S. (2005a). Integration and segregation of inputs to higher-order neuropils of the crayfish brain. *J. Comp. Neurol.* 481, 118–126. doi: 10.1002/cne.20346

Sullivan, J. M., and Beltz, B. S. (2005b). Newborn cells in the adult crayfish brain differentiate into distinct neuronal types. *J. Neurobiol.* 65, 157–170. doi: 10.1002/neu.20195

Sullivan, J. M., Benton, J. L., and Beltz, B. S. (2000). Serotonin depletion *in vivo* inhibits the branching of olfactory projection neurons in the lobster deutocerebrum. *J. Neurosci.* 20, 7716–7721.

Sullivan, J. M., Benton, J. L., Sandeman, D. C., and Beltz, B. S. (2007a). Adult neurogenesis: a common strategy across diverse species. *J. Comp. Neurol.* 500, 574–584. doi: 10.1002/cne.21187

Sullivan, J. M., Sandeman, D. C., Benton, J. L., and Beltz, B. S. (2007b). Adult neurogenesis and cell cycle regulation in the crustacean olfactory pathway: from glial precursors to differentiated neurons. *J. Mol. Hist.* 38, 527–542. doi: 10.1007/s10735-007-9112-7

Tadesse, T., Schmidt, M., Walthall, W. W., Tai, P. C., and Derby, C. D. (2011). Distribution and function of splash, an achaete-scute homolog in the adult olfactory organ of the Caribbean spiny lobster *Panulirus argus*. *Dev. Neurobiol.* 71, 316–335. doi: 10.1002/dneu.20862

Watthanasurorot, A., Söderhäll, K., Jiravanichpaisal, P., and Soderhall, I. (2011). An ancient cytokine, astakine, mediates circadian regulation of invertebrate hematopoiesis. *Cell. Mol. Life Sci.* 68, 315–323. doi: 10.1007/s00018-010-0458-8

Wen, C. M., Cheng, Y. H., Huang, Y. F., and Wang, C. S. (2008). Isolation and characterization of a neural progenitor cell line from tilapia

brain. *Comp. Biochem. Physiol. A Mol. Integr. Physiol.* 149, 167–180. doi: 10.1016/j.cbpa.2007.11.005

Wen, C. M., Huang, J. Y., Ciou, J. H., Kao, Y. L., and Cheng, Y. H. (2009). Immunochemical and molecular characterization of GBC4 as a tanycyte-like cell line derived from grouper brain. *Comp. Biochem. Physiol. A Mol. Integr. Physiol.* 153, 191–201. doi: 10.1016/j.cbpa.2009.02.017

Wu, C., Söderhäll, I., Kim, Y.-A., Liu, H., and Söderhäll, K. (2008). Hemocyte-lineage marker proteins in a crustacean, the freshwater crayfish, *Pacifastacus leniusculus*. *Proteomics* 8, 4226–4235. doi: 10.1002/pmic.200800177

Zhang, Y., Allodi, S., Sandeman, D. C., and Beltz, B. S. (2009). Adult neurogenesis in the crayfish brain: proliferation, migration, and possible origin of precursor cells. *Dev. Neurobiol.* 69, 415–436. doi: 10.1002/dneu.20717

Zhang, Y., Benton, J. L., and Beltz, B. S. (2011). 5-HT receptors mediate lineage-dependent effects of serotonin on adult neurogenesis in *Procambarus clarkii*. *Neural Dev.* 6:2. doi: 10.1186/1749-8104-6-2

Conflict of Interest Statement: The authors declare that the research was conducted in the absence of any commercial or financial relationships that could be construed as a potential conflict of interest.

frontiers in Neuroscience

PERSPECTIVE
published: 30 October 2017
doi: 10.3389/fnins.2017.00602

From Mice to Mole-Rats: Species-Specific Modulation of Adult Hippocampal Neurogenesis

*Maria K. Oosthuizen**

Department of Zoology and Entomology, University of Pretoria, Pretoria, South Africa

Rodent populations living in their natural environments have very diverse ecological and life history profiles that may differ substantially from that of conventional laboratory rodents. Free-living rodents show species-specific neurogenesis that are dependent on their unique biology and ecology. This perspective aims to illustrate the benefit of studying wild rodent species in conjunction with laboratory rodents. African mole-rats are discussed in terms of habitat complexity, social structures, and longevity. African mole-rats are a group of subterranean rodents, endemic to Africa, that show major differences in both intrinsic and extrinsic traits compared to the classical rodent models. Mole-rats exhibit a spectrum of sociality within a single family, ranging from solitary to eusocial. This continuum of sociality provides a platform for comparative testing of hypotheses. Indeed, species differences are apparent both in learning ability and hippocampal neurogenesis. In addition, social mole-rat species display a reproductive division of labor that also results in differential hippocampal neurogenesis, independent of age, offering further scope for comparison. In conclusion, it is evident that neurogenesis studies on conventional laboratory rodents are not necessarily representative, specifically because of a lack of diversity in life histories, uniform habitats, and low genetic variability. The observed level of adult neurogenesis in the dentate gyrus is the result of an intricate balance between many contributing factors, which appear to be specific to distinct groups of animals. The ultimate understanding of the functional and adaptive role of adult neurogenesis will involve research on both laboratory animals and natural rodent populations.

Keywords: African mole-rats, breeding, laboratory rodents, neurogenesis, non-breeding, social, solitary

OPEN ACCESS

Edited by:
Luca Bonfanti,
Università degli Studi di Torino, Italy

Reviewed by:
Philippe Vullioud,
University of Cambridge, United Kingdom
Joshua Breunig,
Cedars-Sinai Medical Center, United States

***Correspondence:**
Maria K. Oosthuizen
moosthuizen@zoology.up.ac.za

Specialty section:
This article was submitted to Neurogenesis, a section of the journal Frontiers in Neuroscience

Received: *19 January 2017*
Accepted: *16 October 2017*
Published: *30 October 2017*

Citation:
Oosthuizen MK (2017) From Mice to Mole-Rats: Species-Specific Modulation of Adult Hippocampal Neurogenesis. Front. Neurosci. 11:602. doi: 10.3389/fnins.2017.00602

INTRODUCTION

It is widely accepted that adult neurogenesis is restricted to two neurogenic regions in the mammalian brain, the subventricular zone of the lateral ventricles and the subgranular zone of the hippocampus (Gage, 2000). Adult hippocampal neurogenesis (AHN) is a dynamic process that has been implicated in hippocampus dependent cognitive functions and both positive and negative regulators of AHN have been described (Aimone et al., 2014). However, the majority of our knowledge originates from studies performed on a few laboratory species that are highly inbred and are maintained in stable laboratory conditions (Kempermann, 2012). Intrinsic and extrinsic traits of wild rodents that were not raised in the laboratory, may differ significantly from that of conventional laboratory animals in factors such as genetic variability, social structure, habitat

complexity, and longevity, all of which can influence AHN (Kuhn et al., 1996; Kempermann et al., 1997a; Kozorovitskiy and Gould, 2004). Hence, the main drivers of AHN may interact in diverse and unpredictable ways to produce opposite patterns of AHN in wild rodents compared to conventional laboratory rodents, or the drivers may be altogether different.

Since laboratory rodents are frequently used as models for disease-related medical research, it is imperative to understand their limitations and appreciate that life history may influence experimental results. Although the functional significance of AHN may overlap in diverse taxonomic groups, the adaptive value thereof may differ considerably across taxa. Indeed, substantial differences in the extent and magnitude of neurogenesis between mice and humans have been revealed (Jessberger and Gage, 2014). Hence, the investigation of species other than conventional laboratory animals with different traits may provide a useful comparative framework to investigate the adaptive advantage of AHN.

The aim of this work is to highlight that both intrinsic and extrinsic traits of non-conventional rodent species can deviate significantly from that of conventional laboratory animals, and may affect the modulation of AHN very differently depending on species specific requirements. A relevant example is the African mole-rats, a group of subterranean rodents, endemic to Africa. African mole-rats are rodent moles that belong to the family Bathyergidae, which differ radically from laboratory rodents in a number of contexts such as environmental niche, social structures, behavior, and longevity (**Figure 1**). These factors will be compared between laboratory rodents and mole-rats to provide a perspective on differences in the adaptive value of neurogenesis in the two groups of rodents.

NEUROGENESIS IN CONVENTIONAL LABORATORY RODENT MODELS

Adult hippocampal neurogenesis (AHN) has been extensively studied in laboratory rodents, both in the context of basal and experimentally manipulated levels of AHN. Both positive and negative regulators of neurogenesis have been identified, some factors are context dependent and may serve as positive, and negative regulators. The factors mentioned below is by no means a complete survey of all potential regulators, merely ones deemed relevant for the ensuing discussion.

Habitat Complexity

Laboratory animals frequently live in a relatively constant habitat, lacking many of the external factors that can influence their biology. Several studies have demonstrated increased AHN in laboratory rodents in response to enriched environments (Kempermann et al., 1997b, 1998; Nillson et al., 1999; Brown et al., 2003). Habitat complexity increases the need for behavioral flexibility (Amrein, 2015), thus free-living rodent species living in very complex habitats have been shown to exhibit much higher neurogenesis compared to animals that inhabit less complex habitats (Amrein et al., 2007; Garthe et al., 2009; Cavegn et al., 2013).

Social Environment

The social environment of laboratory animals can exert both positive and negative effects on neurogenesis, depending on the circumstances. Laboratory rodents such as mice and rats are typically communal species and social interactions have been shown to significantly affect the regulation of adult neurogenesis in the hippocampus (Fowler et al., 2008; Lieberwirth and Wang, 2012). Social status can influence the rate of neurogenesis where, in laboratory rodents, animals with a higher status typically show more neurogenesis than the ones with a lower social status (Gould et al., 1997, 1998; Kozorovitskiy and Gould, 2004; Thomas et al., 2007; Wu et al., 2014). Variation in estrogen levels may be the underlying mechanism responsible for differences in AHN between dominant and subordinate animals. Dominant animals typically have a higher probability of breeding, and breeding individuals usually exhibit higher levels of estrogen. Estrogen has been shown to play a role in proliferation, the survival as well as the activation of the new neurons (Fowler et al., 2008). Following ovariectomy, AHN was reduced but this could be reversed by estrogen replacement (Tanapat et al., 1999). Cell proliferation in the dentate gyrus (DG) of the hippocampus of laboratory rat females also fluctuates according to the estrous cycle, with higher cell proliferation when more estrogen is present (Tanapat et al., 1999).

Stress hormones can have positive or negative effects on AHN, depending on the type of stressor and whether the stress is acute or chronic (Schoenfeld and Gould, 2012). High levels of corticosterone in response to social isolation causes a reduction in neurogenesis and also decreases performance in other behavioral tests (Stranahan et al., 2006). This effect seems to be larger in females compared to males (Westenbroek et al., 2004). In contrast, exercise (running) induces lower levels of corticosterone and is associated with an increase in AHN (Stranahan et al., 2006).

Age

Age is commonly viewed as a potent negative regulator of AHN since there is a dramatic decline in neurogenesis that appears to be age related in most mammals investigated, laboratory rodents included (Kuhn et al., 1996; Amrein et al., 2004; Ben Abdallah et al., 2010). This downregulation of neurogenesis is not correlated with the environment or other species-specific traits such as longevity or developmental strategy (Amrein et al., 2004). Technically, this decrease occurs relatively early in life, after which the level of neurogenesis remains relatively stable.

Cognitive Activity

A vast number of studies suggest a link between learning, memory, and adult neurogenesis. Initial studies showed that learning increases hippocampal neurogenesis (Gould et al., 1999a,b) which accordingly enhances spatial memory (Snyder et al., 2005; Winocur et al., 2006). In turn, learning impairments are associated with a reduction in hippocampal neurogenesis (Lemaire et al., 2000). However, more recent evidence suggests that this is highly species and context dependent and the results are not always consistent (Dobrossy et al., 2003; Jaholkowski et al., 2009; Groves et al., 2013; Duarte-Guterman et al., 2015).

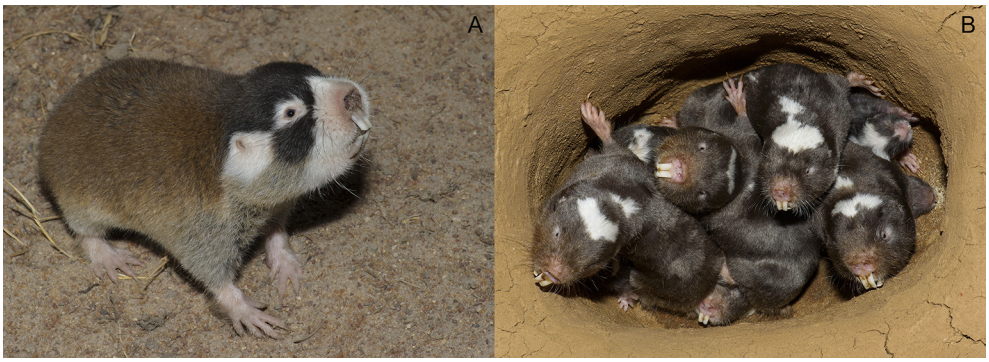

FIGURE 1 | (A) Solitary Cape mole-rat. **(B)** A colony of social Damaraland mole-rats.

In some cases, neurogenesis has no effect on spatial memory at all (Groves et al., 2013). The mixed results may be attributed to the type of behavioral tests performed or the history and age of the animals, or a combination of factors.

COMPARING LABORATORY MODELS WITH THE MOLE-RAT MODEL

Some factors that can influence AHN in rodents exhibit parallel features in laboratory rodent models and the mole-rat model, with the difference that it occurs naturally in mole-rats but are human induced in laboratory rodents. Other factors are distinctly different for the two models.

Habitat Complexity

Habitat complexity, or the lack thereof, can influence AHN in rodents depending on the need for behavioral flexibility (Amrein, 2015). Laboratory rodents have probably adapted to their relatively uniform and confined laboratory habitat over many generations in captivity, with accompanying alterations in behavioral needs (Toth et al., 2011). Although in a different spatial context, the sealed burrow systems of mole-rats is devoid of light and lack many other sensory cues available to aboveground living rodents (Burda et al., 1990). Mole-rats thus present a model that naturally inhabits a uniform environment. In addition, even the simplistic environment of mole-rats shows interspecific variation in terms of length and complexity of the tunnels, depending on the social structure of the species, presenting opportunity for comparisons.

Social Structure

Laboratory mice and rats are generally classified as social and polygamous but the social structure is not rigidly fixed (Lund, 1975; Hedrich, 2012). As a taxonomic group, mole-rats show much more diverse and complex social organizations compared to laboratory animals. Bathyergids exhibit a spectrum of sociality within a single taxonomic family, ranging from strictly solitary to highly social species (Faulkes et al., 1997). Solitary species are typically polygamous whereas social species tend to be more monogamous. Social mole-rats live in family groups that exhibit a distinct reproductive division of labor (Jarvis, 1981; Bennett, 1988). Reproduction is restricted to a single female and one or two males, while the remainder of the colony comprises overlapping generations of subordinate animals that are reproductively suppressed. Mole-rats breed cooperatively, and the non-breeding individuals assist with the rearing of offspring and maintenance of the tunnel system (Jarvis, 1981; Bennett, 1988). Social mole-rat colonies exhibit linear dominance hierarchies where larger animals are dominant over smaller animals (Jacobs et al., 1991), but breeding animals are always dominant over non-breeding animals. In other rodents, both dominance and reproductive status have been shown to influence AHN (Tanapat et al., 1999; Kozorovitskiy and Gould, 2004). Therefore, the difference in social structures between species and the within species status differences in the mole-rat model provide abundant opportunities for empirical testing of predictions in a comparative setting.

Age and Longevity

Laboratory mice and rats have maximum lifespans of under 5 years (Gorbunova et al., 2008), whereas their free-living counterparts may have a much shorter life expectancy. Similar sized mole-rats, especially the social species, can attain ages three to six-fold that of laboratory animals. In captivity, the age of 16 years have been recorded for social *Fukomys* mole-rats (Dammann et al., 2011) and the age of 32 years for naked mole-rats (*Heterocephalus glaber*) (Buffenstein and Jarvis, 2002). An exponential decline in AHN is apparent in both long and short-lived species, but the slower maturation of longer lived species may offer a larger window for experimental manipulation of the baseline AHN.

MOLE-RAT NEUROGENESIS

Morphologically, the dentate gyrus of mole-rats is comparatively smaller than that of other rodents, with fewer granule cells (Amrein et al., 2014). Mole-rats in general have very low levels of neurogenesis in the hippocampus (Amrein et al., 2014; Penz et al., 2015; Oosthuizen and Amrein, 2016). Normalized proliferating cell numbers of mole-rats are comparable with that

of other rodents however the normalized young neurons are lower (Amrein et al., 2014).

Habitat Complexity

The lower survival rate of young neurons in mole-rats supports a habitat-dependent modulation of neurogenesis. The habitat complexity of mole-rat burrow systems is very low when compared to the highly complex three-dimensional environments of surface dwelling rodents. The sealed burrow systems of mole-rats lack external cues and therefore present a very homogenous and stable habitat (Burda et al., 1990).

Despite the overall low habitat complexity, the length and complexity of mole-rat burrows differ between species, it depends on a number of factors including sociality, habitat type, resource availability, and population density (Le Comber et al., 2002). The burrow systems of Damaraland mole-rats (*Fukomys damarensis*) can reach up to 2 km in length (Bennett and Faulkes, 2000), while burrow systems of solitary species such as the Cape mole-rat (*Georychus capensis*) are generally much shorter (Thomas et al., 2012). Within the context of the subterranean niche, interspecies differences in hippocampal neurogenesis that is consistent with the relative length and complexity of the burrows of the different species, is evident. The social and solitary species have similar numbers of granule cells despite size differences in the species [Cape: 150–200 g; Highveld (*Cryptomys hottentotus pretoriae*; intermediately social species): 80–120 g; Damaraland: 120–150 g; Bennett and Faulkes, 2000, pers. obs.], however both the Highveld and Damaraland mole-rats have more proliferating cells compared to Cape mole-rats (Ki67 staining) (Amrein et al., 2014; Oosthuizen and Amrein, 2016). The numbers of young neurons show large within species variation, thus young neuron numbers of the individual species show some overlap.

Social Status

Despite the low rate of neurogenesis, a status dependent amount of hippocampal neurogenesis is evident in the social Damaraland mole-rats. Seemingly in contrast with results from laboratory rodents, the breeding females, or queens, have lower numbers of both proliferating cells and young neurons compared to subordinate colony members (Oosthuizen and Amrein, 2016) (**Figure 2**). A similar occurrence is observed in the naked mole-rat, where breeding animals were found to have significantly less young neurons, as visualized by doublecortin (DCX) immunoreactive neurons, compared to the non-breeding animals (Peragine et al., 2014). Differential AHN in breeding and non-breeding mole-rats may potentially have an endocrinological basis. Both reproductive hormones and stress hormones have been shown to modulate neurogenesis in laboratory rodents (Cameron and Gould, 1994; Gould and Tanapat, 1999; Tanapat et al., 1999).

In highly social species such as the Damaraland mole-rat and the naked mole-rat, the breeding females have higher estrogen levels compared to non-breeding animals (Bennett and Jarvis, 1988; Faulkes et al., 1990; Bennett, 1994), thus one would also expect an upregulation of neurogenic cells, yet the opposite is true (Peragine et al., 2014; Oosthuizen and Amrein, 2016). In the case of mole-rats, estrogen appears to rather downregulate AHN. Similarly, cell proliferation is inhibited in the dentate gyrus of female meadow voles in the breeding season, when high estrogen levels are present, compared to females out of the breeding season, although more cells survive in the reproductively active females (Galea and McEwen, 1999; Ormerod and Galea, 2001). A potential mechanism for the disparity in the effect of estrogen on AHN may be related to the density of the estrogen receptor α in the dentate gyrus. In voles, estrogen increased the density of the estrogen receptor α (ERα) (Fowler et al., 2005), however this increase was region specific and no difference was observed in the dentate gyrus. In mole-rats, non-breeding Damaraland mole-rat females express lower levels of ERα compared to the breeders in brain regions important for reproduction (Voigt et al., 2014). The density of the ERα has not been investigated in the DG of mole-rats thus far, but could potentially also show differential expression between breeder and non-breeder mole-rats. In naked mole-rats, no significant relationships could

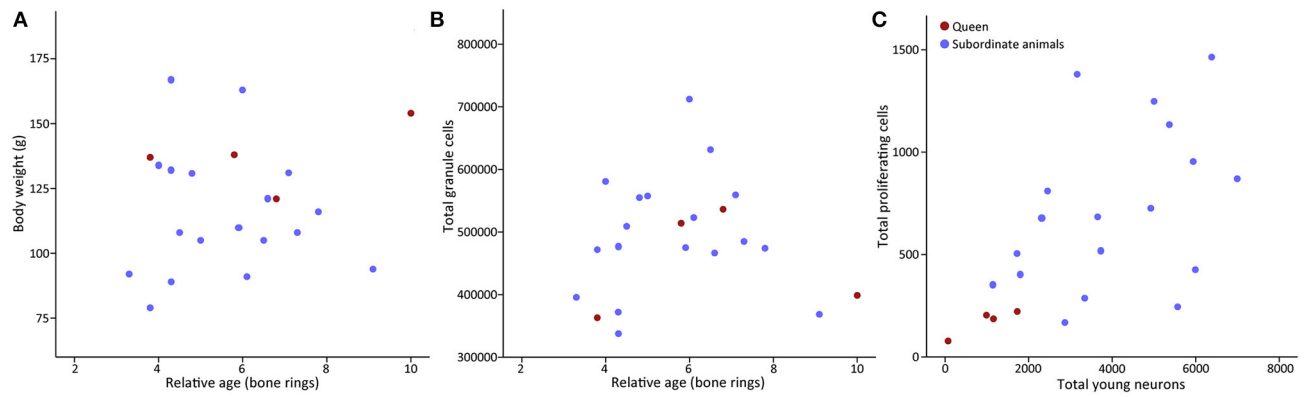

FIGURE 2 | Scatter plots of relative age x body weight, total granule cells × relative age, and proliferation × young neurons in Damaraland mole-rats. **(A)** The body weight of Damaraland mole-rats does not increase with relative age, **(B)** total granule cells remains stable with relative age, and **(C)** a scatter plot of proliferating cells (Ki67) and young neurons (PSA-NCAM) in dominant and subordinate Damaraland mole-rats (Modified from (Oosthuizen and Amrein, 2016), with permission from Elsevier).

be identified between circulating gonadal steroids and DCX (Peragine et al., 2014), however this do not exclude potential differences in proliferating cells or receptors for the hormones.

Stress hormones have not been exhaustively investigated in mole-rats in terms of social status in the colony. It appears that when the social structure is stable, there is no difference cortisol levels between breeding and non-breeding animals (Clarke and Faulkes, 1998; Clarke et al., 2001), but instability in the social structure is associated with increased cortisol levels in non-breeding animals compared to the breeding animals (Clarke and Faulkes, 1997). In congruence with this, a higher concentration of CRF receptor binding sites is present in non-breeding naked mole-rats (Beery et al., 2016). In addition, CRF receptor binding sites also differ between solitary and social mole-rat species (Coen et al., 2015), where differences in proliferating cells have been shown. Stress hormones are also expressed in response to running and exercise, where it is associated with an upregulation of AHN (Stranahan et al., 2006). Non-breeding Damaraland mole-rat females show higher levels of locomotor activity than the breeding females (Oosthuizen and Bennett, 2015), therefore increased activity could, at least in part, explain the higher AHN in non-breeding mole-rats.

Age and Longevity

In agreement with their increased life expectancies, mole-rats have long gestation times and subsequent postnatal development is slower than other rodents. Like other animals, mole-rats also show a steep decline in neurogenesis at a relatively young age (Penz et al., 2015). A slow postnatal development may increase the expected window for higher levels of neurogenesis seen in all young animals between birth and puberty (Penz et al., 2015). In mole-rats, puberty is reached around the age of 1 year, when neurogenesis should start to decline exponentially (Bennett and Faulkes, 2000; Penz et al., 2015), however this has not been tested empirically.

Cognitive Activity

As a result of their lightless environment, subterranean animals rely on other mechanisms such as tactile stimuli and memory to navigate their burrow systems (du Toit et al., 2012). Despite the relatively uniform habitat of the sealed tunnel systems, the difference in tunnel length and complexity appears to be sufficient stimulation to induce learning differences in the different species. Damaraland mole-rats with longer and more complex burrow systems, show superior learning abilities compared to the solitary Cape mole-rat (Costanzo et al., 2009; Oosthuizen et al., 2013), Oosthuizen, unpublished data). The enhanced learning abilities of Damaraland mole-rats are associated with more proliferating cells compared to Cape mole-rats (Amrein et al., 2014; Oosthuizen and Amrein, 2016). Although the basal level of neurogenesis differs with social status in highly social species, there is no corresponding difference in learning abilities.

CONCLUSIONS

Neurogenesis studies performed on conventional laboratory rodents by far outnumber those on wild species. Research on laboratory animals is necessary as laboratory models are very useful and convenient tools for the fundamental understanding of the molecular basis and the regulation of neurogenesis, however they have limitations. Laboratory animals live in a completely uniform habitat without natural predators and are bred to minimize variability. To comprehend the functional and adaptive significance of neurogenesis, the environmental, genetic and physiological variation of natural populations is essential. It is important to appreciate that the adaptive value of neurogenesis is species specific. In many instances, natural animal populations show very different and more varied physiological and neurological responses compared to their laboratory counterparts.

This perspective primarily illustrates the diversity in environmental conditions, social structures and longevity in rodent species. Animal models that display a different set of species-specific features may provide insight into the functional and adaptive significance of adult neurogenesis. Mole-rats differ from conventional laboratory animals in a number of important ways, specifically social structure and longevity. Mole-rats (and indeed other natural rodent populations) are not suggested as a replacement for conventional laboratory rodents in neurogenesis research, but rather to complement the existing body of information. Ultimately, understanding the functional and adaptive context of adult neurogenesis will require research on both laboratory animals and natural rodent populations.

AUTHOR CONTRIBUTIONS

The author confirms being the sole contributor of this work and approved it for publication.

REFERENCES

Aimone, J. B., Li, Y., Lee, S. W., Clemenson, G. D., Deng, W., and Gage, F. H. (2014). Regulation and function of adult neurogenesis: from genes to cognition. *Physiol. Rev.* 94, 991–1026. doi: 10.1152/physrev.00004.2014

Amrein, I. (2015). Adult hippocamal neurogenesis in natural populations of mammals. *Cold Spring Harb. Perspect. Biol.* 7:a021295. doi: 10.1101/cshperspect.a021295

Amrein, I., Becker, A. S., Engler, S., Huang, S. H., Muller, J., Slomianka, L., et al. (2014). Adult neurogenesis and its anatomical context in the hippocampus of three mole-rat species. *Front. Neuroanat.* 8:39. doi: 10.3389/fnana.2014.00039

Amrein, I., Dechmann, D. K. N., Winter, Y., and Lipp, H. P. (2007). Absent or low rate of adult neurogenesis in the hippocampus of bats (Chiroptera). *PLoS ONE* 2:e455. doi: 10.1371/journal.pone.0000455

Amrein, I., Slomianka, L., Poletaeva, I. I., Bologova, N. V., and Lipp, H. P. (2004). Marked species and age-dependent differences in cell proliferation and neurogenesis in the hippocampus of wild-living rodents. *Hippocampus* 14, 1000–1010. doi: 10.1002/hipo.20018

Beery, A. K., Bicks, L., Mooney, S. J., Goodwin, N. L., and Holmes, M. M. (2016). Sex, social status, and CRF receptor densities in naked mole-rats. *J. Comp. Neurol.* 524, 228–243. doi: 10.1002/cne.23834

Ben Abdallah, N. M., Slomianka, L., Vyssotski, A. L., and Lipp, H. P. (2010). Early age-related changes in adult hippocampal neurogenesis in C57 mice. *Neurobiol. Aging* 31, 151–161. doi: 10.1016/j.neurobiolaging.2008.03.002

Bennett, N. C. (1988). *The Trend Towards Sociality in Three Species of Southern African Mole-Rats Bathyergidae: Causes and Consequences*. Ph.D., University of Cape Town.

Bennett, N. C. (1994). Reproductive suppression in social *Cryptomys damarensis* colonies - a lifetime of socially-induced sterility in males and females (Rodentia: Bathyergidae). *J. Zool. Lond.* 234, 25–39. doi: 10.1111/j.1469-7998.1994.tb06054.x

Bennett, N. C., and Faulkes, C. G. (2000). *African Mole-Rats: Ecology and Eusociality*. Cambridge, UK: Cambridge University Press.

Bennett, N. C., and Jarvis, J. U. (1988). The social structure and reproductive biology of colonies of the mole-rat, *Cryptomys damarensis* (Rodentia, Bathyergidae). *J. Mammal.* 69, 293–302. doi: 10.2307/1381379

Brown, J., Cooper-Kuhn, C. M., Kempermann, G., Van Praag, H., Winkler, J., Gage, F. H., et al. (2003). Enriched environment and physical activity stimulate hippocampal but not olfactory bulb neurogenesis. *Eur. J. Neurosci.* 17, 2042–2046. doi: 10.1046/j.1460-9568.2003.02647.x

Buffenstein, R., and Jarvis, J. U. (2002). The naked mole-rat - a new record for the oldest living rodent. *Sci. Aging Knowl. Environ.* 21:7. doi: 10.1126/sageke.2002.21.pe7

Burda, H., Bruns, V., and Muller, J. (1990). *Evolution of Subterranean Mammals a the Organismal and Molecular Levels*. New York, NY: Wiley.

Cameron, H.A., and Gould, E. (1994). Adult neurogenesis is regulated by adrenal steroids in the dentate gyrus. *Neuroscience* 612, 203–209.

Cavegn, N., van Dijk, R. M., Menges, D., Brettschneider, H., Phalanndwa, M., Chimimba, C. T., et al. (2013). Habitat-specific shaping of proliferation and neuronal differentiation in adult hippocampal neurogenesis of wild rodents. *Front. Neurosci.* 7:59. doi: 10.3389/fnins.2013.00059

Clarke, F. M., and Faulkes, C. G. (1997). Dominance and queen succession in captive colonies of the eusocial naked mole-rat, *Heterocephalus glaber*. *Proc. R. Soc. Lond.* 264, 993–1000. doi: 10.1098/rspb.1997.0137

Clarke, F. M., and Faulkes, C. G. (1998). Hormonal and behavioural corelates of male dominance and reproductive status in captive colonies of the naked mole-rat, *Heterocephalus glaber*. *Proc. R. Soc. Lond. B.* 265, 1391–1399. doi: 10.1098/rspb.1998.0447

Clarke, F. M., Miethe, G. H., and Bennett, N. C. (2001). Reproductive suppression in female Damaraland mole-rats *Cryptomys damarensis*: dominant control or self-restraint? *Proc. R. Soc. Lond.* 268, 899–909. doi: 10.1098/rspb.2000.1426

Coen, C. W., Kalamatianos, T., Oosthuizen, M. K., Poorun, R., Faulkes, C. G., and Bennett, N. C. (2015). Sociality and the telencephalic distribution of corticotrophin-releasing factor, urocortin 3, and binding sites for CRF type 1 and type 2 receptors: a comparative study of eusocial naked mole-rats and solitary Cape mole-rats. *J. Comp. Neurol.* 523, 2344–2371. doi: 10.1002/cne.23796

Costanzo, M. S., Bennett, N. C., and Lutermann, H. (2009). Spatial learning and memory in African mole-rats: the role of sociality and sex. *Physiol. Behav.* 96, 128–134. doi: 10.1016/j.physbeh.2008.09.008

Dammann, P., Sumbera, R., Masmann, C., Scherag, A., and Burda, H. (2011). Extended longevity of reproductives appears to be common in Fukomys mole-rats (Rodentia, Bathyergidae). *PLoS ONE* 6:e18757. doi: 10.1371/journal.pone.0018757

Dobrossy, M. D., Drapeau, E., Aurousseau, C., Le Moal, M., Piazza, P. V., and Abrous, D. N. (2003). Differential effects of learning on neurogenesis: learning increases or decreases the number of newly born cells depending on their birth date. *Mol. Psychiatry* 8, 974–982. doi: 10.1038/sj.mp.4001419

du Toit, L., Bennett, N. C., Nickless, A., and Whiting, M. J. (2012). Influence of spatial environment on maze learning in an African mole-rat. *Anim. Cogn.* 15, 797–806. doi: 10.1007/s10071-012-0503-0

Duarte-Guterman, P., Yagi, S., Chow, C., and Galea, L. A. (2015). Hippocampal learning, memory, and neurogenesis: effects of sex and estrogens across the lifespan in adults. *Horm. Behav.* 74, 37–52. doi: 10.1016/j.yhbeh.2015.05.024

Faulkes, C. G., Abbott, D. H., and Jarvis, J. U. M. (1990). Social suppresion of ovarian cyclicity in captive and wild colonies of naked mole-rats, *Heterocephalus glaber*. *J. Reprod. Fert.* 88, 559–568. doi: 10.1530/jrf.0.0880559

Faulkes, C. G., Bennett, N. C., Bruford, M. W., O'Brien, H. P., Aguilar, G. H., and Jarvis, J. U. (1997). Ecological constraints drive social evolution in the African mole-rats. *Proc. Biol. Sci.* 264, 1619–1627.

Fowler, C. D., Johnson, F., and Wang, Z. (2005). Estrogen regulation of cell proliferation and distribution of estrogen receptor-alpha in the brains of adult female prairie and meadow voles. *J. Comp. Neurol.* 489, 166–179. doi: 10.1002/cne.20638

Fowler, C. D., Liu, Y., and Wang, Z. (2008). Estrogen and adult neurogenesis in the amygdala and hypothalamus. *Brain Res. Rev.* 57, 342–351. doi: 10.1016/j.brainresrev.2007.06.011

Gage, F. H. (2000). Mammalian neural stem cells. *Science* 287:1433. doi: 10.1126/science.287.5457.1433

Galea, L. A. M., and McEwen, B. S. (1999). Sex and seasonal differences in the rate of cell proliferation in the dentate gyrus of adult wild meadow voles. *Neuroscience* 89, 955–964. doi: 10.1016/S0306-4522(98)00345-5

Garthe, A., Behr, J., and Kempermann, G. (2009). Adult-generated hippocampal neurons allow the flexible use of spatially precise learning strategies. *PLoS ONE* 4:e5464. doi: 10.1371/journal.pone.0005464

Gorbunova, V., Bozzella, M. J., and Seluanov, A. (2008). Rodents for comparative aging studies: from mice to bevers. *Age* 30, 111–119. doi: 10.1007/s11357-008-9053-4

Gould, E., and Tanapat, P. (1999). Stress and hippocampal neurogenesis. *Biol. Pshychiatry* 46, 1472–1479. doi: 10.1016/S0006-3223(99)00247-4

Gould, E., Beylin, A., Tanapat, P., Reeves, A., and Shors, T. J. (1999a). Learning enhances adult neurogenesis in the hippocampal formation. *Nat. Neurosci.* 2, 260–265.

Gould, E., McEwen, B. S., Tanapat, P., Galea, L. A. M., and Fuchs, E. (1997). Neurogenesis in the dentate gyrus of the adult tree shrew is regulated by psychosocial stress and NMDA receptor activation. *J. Neurosci. Methods* 17, 2492–2498.

Gould, E., Tanapat, P., Hastings, N. B., and Shors, T. J. (1999b). Neurogenesis in adulthood: a possible role in learning. *Trends in Cogn. Sci.* 3, 186–192.

Gould, E., Tanapat, P., McEwen, B., Flügge, G., and Fuchs, E. (1998). Proliferation of granule cell precursors in the dentate gyrus of adult monkeys is diminished by stress. *Proc. Natl. Acad. Sci. U.S.A.* 95, 3168–3171. doi: 10.1073/pnas.95.6.3168

Groves, J. O., Leslie, I., Huang, G. J., McHugh, S. B., Taylor, A., Mott, R., et al. (2013). Ablating adult neurogenesis in the rat has no effect on spatial processing: evidence from a novel pharmacogenetic model. *PLoS Genet* 9:e1003718. doi: 10.1371/journal.pgen.1003718

Hedrich, H. J. (2012). *The Laboratory Mouse*. London, UK: Academic Press.

Jacobs, D. S., Bennett, N. C., Jarvis, J. U. M., and Crowe, T. M. (1991). The colony structure and dominance hierarchy of the Damaraland mole-rat, *Cryptomys damarensis* (Rodentia: Bathyergidae), from Namibia. *J. Zool. Lond.* 224, 553–576. doi: 10.1111/j.1469-7998.1991.tb03785.x

Jaholkowski, P., Kiryk, A., Jedynak, P., Ben Abdallah, N. M., Knapska, E., Kowalczyk, A., et al. (2009). New hippocampal neurons are not obligatory for memory formation; cyclin D2 knockout mice with no adult brain neurogenesis show learning. *Learn. Mem.* 16, 439–451. doi: 10.1101/lm.1459709

Jarvis, J. U. M. (1981). Eusociality in a mammal - cooperative breeding in the naked mole-rat *Heterocephalus glaber* colonies. *Science* 212, 571–573. doi: 10.1126/science.7209555

Jessberger, S., and Gage, F. H. (2014). Adult neurogenesis: bridging the gap between mice and humans. *Trends Cell Biol.* 24, 558–563. doi: 10.1016/j.tcb.2014.07.003

Kempermann, G. (2012). New neurons for 'survival of the fittest. *Nat. Rev. Neurosci.* 13, 727–736. doi: 10.1038/nrn3319

Kempermann, G., Brandon, E. P., and Gage, F. H. (1998). Environmental stimulation of 129/SvJ mice causes increased cell proliferation and neurogenesis in the adult dentate gyrus. *Curr. Biol.* 8, 939–942. doi: 10.1016/S0960-9822(07)00377-6

Kempermann, G., Kuhn, H. G., and Gage, F. H. (1997a). Genetic influence on neurogenesis in the dentate gyrus of adult mice. *Proc. Natl. Acad. Sci. U.S.A.* 94, 10409–10414.

Kempermann, G., Kuhn, H. G., and Gage, F. H. (1997b). More hippocampal neurons in adult mice living in an enriched environment. *Nature* 386, 493–495.

Kozorovitskiy, Y., and Gould, E. (2004). Dominance hierarchy influences adult neurogenesis in the dentate gyrus. *J. Neurosci.* 24, 6755–6759. doi: 10.1523/JNEUROSCI.0345-04.2004

Kuhn, H. G., Dickenson-Anson, H., and Gage, F. H. (1996). Neurogenesis in the dentate gyrus of the adult rat: age-related decrease of neuronal progenitor proliferation. *J. Neurosci.* 16, 2027–2033.

Le Comber, S. C., Spinks, A. C., Bennett, N. C., Jarvis, J. U. M., and Faulkes, C. G. (2002). Fractal dimension of African mole-rat burrows. *Canad. J. Zool.* 80, 436–441. doi: 10.1139/z02-026

Lemaire, V., Koehl, M., Le Moal, M., and Abrous, D. N. (2000). Prenatal stress produces learning deficits associated with an inhibition of neurogenesis in the hippocampus. *PNAS* 97, 11032–11037. doi: 10.1073/pnas.97.20.11032

Lieberwirth, C., and Wang, Z. (2012). The social environment and neurogenesis in the adult mammalian brain. *Front. Hum. Neurosci.* 6:118. doi: 10.3389/fnhum.2012.00118

Lund, M. (1975). Social mechanisms and social structure in rats and mice. *Ecol. Bull.* 19, 255–260.

Nillson, M., Perfilieva, E., Johansson, U., Orwar, O., and Eriksson, P. (1999). Enriched environment increases neurogenesis in the adult rat dentate gyrus and improves spatial memory. *J. Neurobiol.* 39, 569–578. doi: 10.1002/(SICI)1097-4695(19990615)39:4<569::AID-NEU10>3.0.CO;2-F

Oosthuizen, M. K., and Amrein, I. (2016). Trading new neurons for status: Adult hippocampal neurogenesis in eusocial Damaraland mole-rats. *Neuroscience* 324, 227–237. doi: 10.1016/j.neuroscience.2016.03.020

Oosthuizen, M. K., and Bennett, N. C. (2015). The effect of ambient temperature on locomotor activity patterns in reproductive and non-reproductive female Damaraland mole-rats. *J. Zool.* 297, 1–8. doi: 10.1111/jzo.12254

Oosthuizen, M. K., Scheibler, A. G., Bennett, N. C., and Amrein, I. (2013). Effects of laboratory housing on exploratory behaviour, novelty discrimination and spatial reference memory in a subterranean, solitary rodent, the Cape mole-rat (*Georychus capensis*). *PLoS ONE* 8:e75863. doi: 10.1371/journal.pone.0075863

Ormerod, B. K., and Galea, L. (2001). Reproductive status influences cell proliferation and cell survival in the dentate gyrus of adult female meadow voles: a possible regulatory role for estradiol. *Neuroscience* 102, 369–379. doi: 10.1016/S0306-4522(00)00474-7

Penz, O. K., Fuzik, J., Kurek, A. B., Romanov, R., Larson, J., Park, T. J., et al. (2015). Protracted brain development in a rodent model of extreme longevity. *Sci. Rep.* 5:11592. doi: 10.1038/srep11592

Peragine, D. E., Simpson, J. A., Mooney, S. J., Lovern, M. B., and Holmes, M. M. (2014). Social regulation of adult neurogenesis in a eusocial mammal. *Neuroscience* 268, 10–20. doi: 10.1016/j.neuroscience.2014.02.044

Schoenfeld, T. J., and Gould, E. (2012). Stress, stress hormones, and adult neurogenesis. *Exp. Neurol.* 233, 12–21. doi: 10.1016/j.expneurol.2011.01.008

Snyder, J. S., Hong, N. S., McDonald, R. J., and Wojtowicz, J. M. (2005). A role for adult neurogenesis in spatial long-term memory. *Neuroscience* 130, 843–852. doi: 10.1016/j.neuroscience.2004.10.009

Stranahan, A. M., Khalil, D., and Gould, E. (2006). Social isolation delays the positive effects of running on adult neurogenesis. *Nat. Neurosci.* 9, 526–533. doi: 10.1038/nn1668

Tanapat, P., Hastings, N. B., Reeves, A., and Gould, E. (1999). Estrogen stimulates a transient increase in the number of new neurons in the dentate gyrus of the adult female rat. *J. Neurosci.* 19, 5792–5801.

Thomas, H. G., Bateman, P. W., Scantlebury, M., Bennett, N. C., and Hayssen, V. (2012). Season but not sex influences burrow length and complexity in the non-sexually dimorphic solitary Cape mole-rat (Rodentia: Bathyergidae). *J. Zool.* 288, 214–221. doi: 10.1111/j.1469-7998.2012.00944.x

Thomas, R. M., Hotsenpiller, G., and Peterson, D. A. (2007). Acute Psychosocial stress reduces cell survival in adult hippocampal neurogenesis without altering proliferation. *J. Neurosci.* 27, 2734–2743. doi: 10.1523/JNEUROSCI.3849-06.2007

Toth, L. A., Kregel, K., Leon, L., and Musch, T. I. (2011). Environmental enrichment of laboratory rodents: the answer depends on the question. *Comp. Med.* 61, 314–321.

Voigt, C., Gahr, M., Leitner, S., Lutermann, H., and Bennett, N. C. (2014). Breeding status and social environment differentially affect the expression of sex steroid receptor and aromatase mRNA in the brain of female Damaraland mole-rats. *Front. Zool.* 11:38. doi: 10.1186/1742-9994-11-38

Westenbroek, C., Den Boer, J. A., Veenhuis, M., and Ter Horst, G. J. (2004). Chronic stress and social housing differentially affect neurogenesis in male and female rats. *Brain Res. Bull.* 64, 303–308. doi: 10.1016/j.brainresbull.2004.08.006

Winocur, G., Wojtowicz, J. M., Sekeres, M., Snyder, J. S., and Wang, S. (2006). Inhibition of neurogenesis interferes wit hhippicampus-dependent memory function. *Hippocampus* 16, 296–304. doi: 10.1002/hipo.20163

Wu, M. V., Shamy, J. L., Bedi, G., Choi, C.-W., Wall, M. M., Arango, V., et al. (2014). Impact of social status and antidepressant treatment on neurogenesis in the baboon hippocampus. *Neuropsychopharmacology* 39, 1861–1871. doi: 10.1038/npp.2014.33

Conflict of Interest Statement: The author declares that the research was conducted in the absence of any commercial or financial relationships that could be construed as a potential conflict of interest.

frontiers in Neuroscience

MINI REVIEW
published: 20 July 2018
doi: 10.3389/fnins.2018.00497

Humans and Dolphins: Decline and Fall of Adult Neurogenesis

*Roberta Parolisi[1], Bruno Cozzi[2] and Luca Bonfanti[1,3]**

[1] NICO – Neuroscience Institute Cavalieri Ottolenghi, Turin, Italy, [2] Department of Comparative Biomedicine and Food Science, University of Padua, Padua, Italy, [3] Department of Veterinary Sciences, University of Turin, Turin, Italy

Pre-clinical research is carried out on animal models, mostly laboratory rodents, with the ultimate aim of translating the acquired knowledge to humans. In the last decades, adult neurogenesis (AN) has been intensively studied since it is viewed as a tool for fostering brain plasticity, possibly repair. Yet, occurrence, location, and rate of AN vary among mammals: the capability for constitutive neuronal production is substantially reduced when comparing small-brained, short living (laboratory rodents) and large-brained, long-living species (humans, dolphins). Several difficulties concerning scarce availability of fresh tissues, technical limits and ethical concerns did contribute in delaying and diverting the achievement of the picture of neurogenic plasticity in large-brained mammals. Some reports appeared in the last few years, starting to shed more light on this issue. Despite technical limits, data from recent studies mostly converge to indicate that neurogenesis is vestigial, or possibly absent, in regions of the adult human brain where in rodents neuronal addition continues into adult life. Analyses carried out in dolphins, mammals devoid of olfaction, but descendant of ancestors provided with olfaction, has shown disappearance of neurogenesis in both neonatal and adult individuals. Heterogeneity in mammalian structural plasticity remains largely underestimated by scientists focusing their research in rodents. Comparative studies are the key to understand the function of AN and the possible translational significance of neuronal replacement in humans. Here, we summarize comparative studies on AN and discuss the evolutionary implications of variations on the recruitment of new neurons in different regions and different species.

Keywords: adult neurogenesis, brain plasticity and aging, comparative anatomy, doublecortin, immature neurons

OPEN ACCESS

Edited by:
Vincent Tropepe,
University of Toronto, Canada

Reviewed by:
Francis G. Szele,
University of Oxford, United Kingdom
Jose Manuel Garcia-Verdugo,
Universitat de València, Spain

***Correspondence:**
Luca Bonfanti
luca.bonfanti@unito.it

Specialty section:
This article was submitted to Neurogenesis, a section of the journal Frontiers in Neuroscience

Received: *09 May 2018*
Accepted: *02 July 2018*
Published: *20 July 2018*

Citation:
Parolisi R, Cozzi B and Bonfanti L (2018) Humans and Dolphins: Decline and Fall of Adult Neurogenesis. Front. Neurosci. 12:497. doi: 10.3389/fnins.2018.00497

INTRODUCTION

After long debate since its first demonstration (Altman and Das, 1965), adult neurogenesis (AN) became accepted in birds in the 1980s by the direct illustration of long-range neuronal migration and the demonstration that the new cells had physiological properties of functional neurons (Paton and Nottebohm, 1984). Ten years later, the use of genetic tools to label the newborn neurons was functional to demonstrate the long migration and integration of new neurons in the mouse brain (Lois and Alvarez-Buylla, 1994; Suhonen et al., 1996). Laboratory rodents are considered by the vast majority of scientists the best (maybe the "only") animal model for biomedical research and for translational science in humans. Comparative studies in other mammals are still considered as either oddities or scarcely useful duplicates. Mice and humans share striking biological similarities, but important differences and biases also emerge when complex biological

processes are concerned (Bolker, 2017). Brain structural plasticity and its adaptation to different environment and differences in animal behavior are a typical example (Lipp and Bonfanti, 2016; Faykoo-Martinez et al., 2017). If basic neuronal stem cell biology can be similar in all mammals, the behavior of their differentiated neuronal progeny can substantially vary in brains whose neuroanatomies and development/postnatal growth also differ (Workman et al., 2013). It is well known that AN is highly reduced as to its rate, anatomical extension, reparative capacity when comparing non-mammalian vertebrates with mammals (Grandel et al., 2006; Bonfanti, 2011; Kempermann, 2016; **Figure 1A**). Mammals are often considered homogeneous in their capability to undergo structural plasticity, nevertheless, the occurrence, location and rate of neurogenesis substantially differ when comparing laboratory rodents with large-brained, long-living species (Lipp and Bonfanti, 2016; Paredes et al., 2016; Parolisi et al., 2017). This fact is still underestimated by many scientists working in the field. This mini-review is intended to draw attention to evolutionary issues linked to mammalian AN, in the light of recent studies carried out on humans and dolphins.

ADULT NEUROGENESIS IN MICE AND HUMANS: THE NUMBERS

The two main neurogenic sites, the subventricular zone (SVZ) of the lateral ventricles and the subgranular zone (SGZ) in the hippocampal dentate gyrus (DG), are less active in adult humans than in adult rodents. Differences concerning the SVZ are quite striking: changes occurring in early postnatal human infants lead to the disappearance of the rostral migratory stream (RMS) around 18 months of age (Sanai et al., 2011). Then, only rare migrating neurons are observed in the SVZ and it remains unclear if these few cells can make the very long journey from the ventricle to their final destination in the olfactory bulb (OB; Sanai et al., 2011; Wang et al., 2011; Conover and Todd, 2017). The picture appears quite different in laboratory rodents, in which the SVZ is still active in adults and retains dividing stem cell populations throughout life. In mice, it provides continuous delivery of new neurons into the OB through chain migration in the RMS (estimated in ∼10,000 cells/day out of ∼180,000 newly generated cells in the whole SVZ region in a 3-month-old mice; Lois and Alvarez-Buylla, 1994; Ponti et al., 2013; Bordiuk et al., 2014). Nevertheless, stem cell activity/neurogenesis levels are quite reduced with age also in these rodents (Shook et al., 2012; Obernier et al., 2018).

Adult hippocampal neurogenesis has been suggested to be retained into adulthood in different mammalian species (Amrein, 2015), including humans (Kempermann, 2016). Yet, a substantial reduction in the rate of neurogenesis occurs from young to adult age also in the DG of all species, including mice (in C57BL/6 mice, the reduction in proliferation is 10-fold, from 0.76 – percentage of Ki-67+ cells/granule cells – at 2 months to 0.08 at 9 months of age; Ben Abdallah et al., 2010). What about humans? A highly cited study published in cell and carried out using a technique based on incorporation of radioactive ^{14}C left from nuclear explosions in the 1950s (Spalding et al., 2013) showed that the early decay of hippocampal neurogenesis in humans is less severe, claiming that its rate at 40 years of age is comparable with the C57BL/6 laboratory mouse at 9–12 months. In fact, the authors infer such "comparable" daily turnover of new granule cells (also reported in Bergmann et al., 2015) from a calculation based on a typo error in the Ben Abdallah et al.'s (2010) paper: the number expressing the negative exponential curve (changes in proliferating cells in the SGZ) is reported as $Y = 1051$, yet it was in reality $Y = 10051$. The mistake is easily identifiable by checking the raw data of the histograms reporting the number of Ki-67+ cells. The true relation (humans: 700 new cells out of 20 million granule cells = 0.0035%; mice at 9 months: 416 out of 0.5 million granule cells = 0.083%) is indicated in **Figure 2A**. Thus, men and mice appear to differ highly in hippocampal neurogenesis occurring at adult ages, the turnover rate in older humans being 10–20 times lower than in mice (see **Figure 2A** and Lipp and Bonfanti, 2016, for more detail). A similar rate has been found in the hippocampus of non-human primates, i.e., the adult macaque monkeys (Kornack and Rakic, 1999). Due to the technical limitations of using postmortem human brain samples and to a lack of robust, histological/immunocytochemical data, direct evaluation of human hippocampal neurogenesis remained open for several years. Then, three reports appeared in 2018. A detailed study carried out on postmortem and intraoperative samples of the human hippocampus showed that proliferating progenitors and young neurons in the DG sharply decline in the first year of life and only a few isolated young neurons can be detected by 7–13 years of age (Sorrells et al., 2018; **Figure 2D**). Very similar data emerge from another detailed report performed in the human hippocampus from early gestation to aging adults (Cipriani et al., 2018). These studies come to the conclusion that if AN continues in the adult DG, this process must be extremely rare. Finally, in a study claiming maintenance of neurogenesis in adult human hippocampus (Boldrini et al., 2018), actually various molecular markers were found associated to different stages of immature neurons, which do not show the typical aspect of recently generated neuroblasts. All these studies employed a large battery of antibodies on a great number of human specimens, indicating that most antigens are detectable in postmortem tissue (Arellano et al., 2018). The Sorrells et al.'s (2018) work performed the more complete histologic analysis (whole sections of SGZ neurogenic site examined through ages). All papers substantially show a similar landscape, though the interpretation of data highly differ in the Boldrini report. Indeed, even in the absence of constitutive niches, genesis of isolated neurons cannot be excluded. Further studies involving post-surgical resection work and single cell RNAseq from human neurogenic zones may help to define their developmental potential over time.

The majority of mammals does show adult hippocampal neurogenesis to some extent, with exceptions in dolphins, humans and some bats (Amrein et al., 2007; Patzke et al., 2015; Sorrells et al., 2018; **Figures 2B,C,E**). Neurogenesis seems to be under selective pressure. Under an evolutionary profile, humans have it during the youngest ages that likely had the greatest phylogenetic importance in the past. Open questions about adult human neurogenesis include: (i) are low levels of neurogenesis functionally relevant? (ii) are there

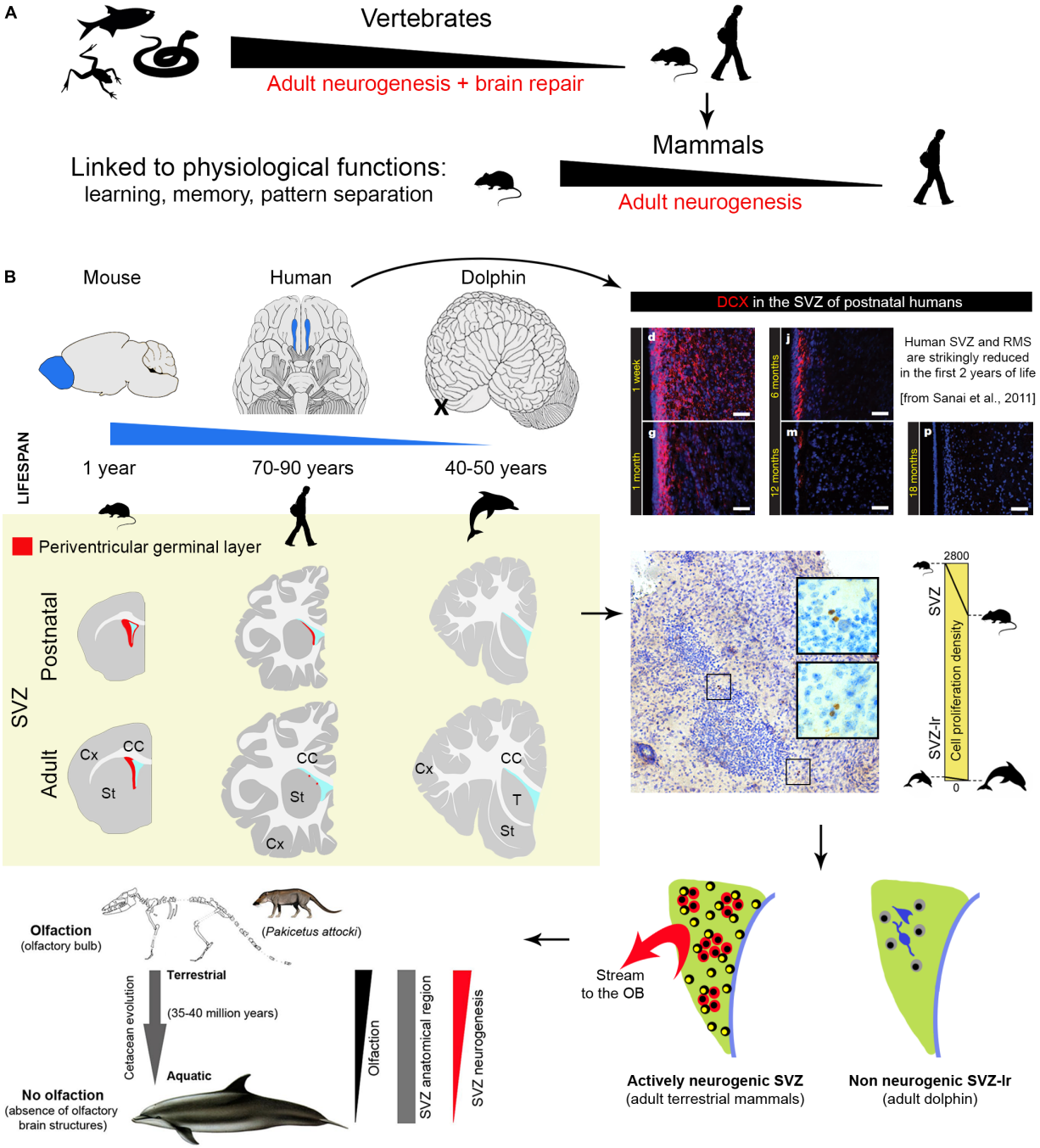

FIGURE 1 | Comparison of central nervous system plasticity and adult neurogenesis in the animal world. **(A)** Strong reduction of brain neurogenic and reparative capacity occurs in vertebrates from non-mammals to mammals. **(B)** Among mammals, striking reduction is detectable in SVZ neurogenesis (a process which in laboratory rodents provides new neurons for the olfactory bulb throughout life) of large brained, long living species with reduced (humans) and absent (dolphins) olfactory brain structures. Images adapted from Sanai et al. (2011) and Parolisi et al. (2017) (reproduced with permission of Nature Publishing Group and Springer). *Yellow panel*: schematic representation of the reduction of SVZ neurogenesis in different animal species and at different ages (continuous red line, SGZ neurogenic niche; red dots, occurrence of scattered newly born/immature neurons).

vestigial/quiescent remnants of stem cell niches and can these be reactivated in some way? Some authors, considering that the new neurons within the DG, even a low number, can be highly functional (at least in animal models), argue that "there has been evolution toward neurogenesis-based plasticity rather than away from it" (Kempermann, 2016). At present, no systematic, fully comparable studies are available on a wide range of mammalian species to support this view or evaluate the importance of

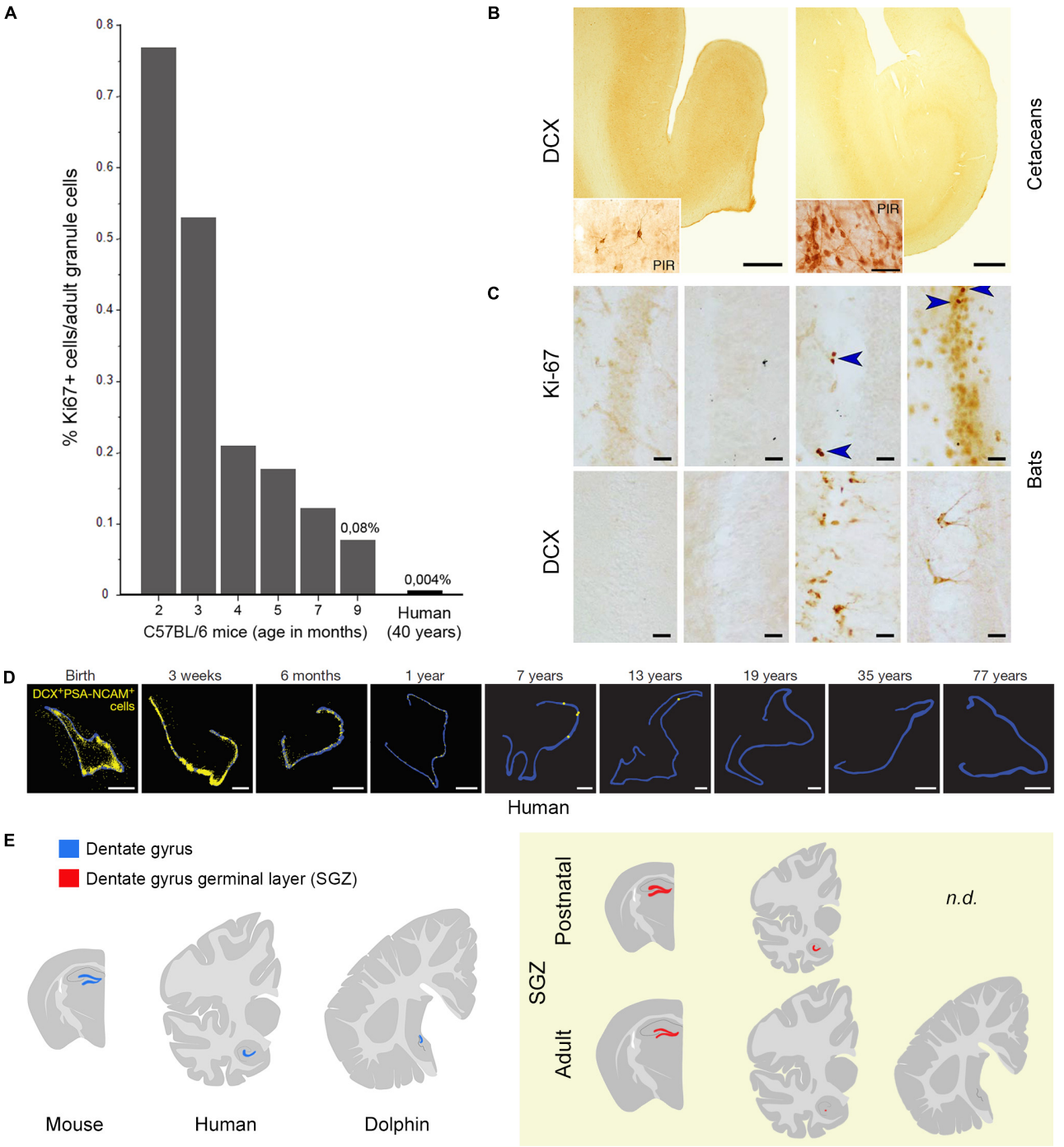

FIGURE 2 | Substantial reduction or absence of neurogenic activity in the hippocampus of mice **(A)**, humans **(A,D)**, dolphins **(B)**, and bats **(C)**. **(A)** Percentage of Ki67+ cells as related to the total granule cell number (roughly corresponding to daily turnover) in C57BL/6 mice at different age levels (as reported in Ben Abdallah et al., 2010) and estimated percentage in human hippocampi as indicated by Spalding et al. (2013) and Bergmann et al. (2015); reproduced from Lipp and Bonfanti (2016), with permission of S. Karger AG, Basel. **(B)** No doublecortin (DCX) is detectable in the hippocampi of cetaceans (harbor porpoise, *Phocoena phocoena*, left; minke whale, *Balaenoptera acutorostrata*, right; adapted from Patzke et al., 2015 with permission from Springer); PIR, piriform cortex used as a positive control. **(C)** Absent or very low occurrence of cell proliferation (Ki-67 antigen) and immature neurons (DCX) in the hippocampus of bats; from left to right: *Phyllostomus discolor*, *Hipposideros cyclops*, *Hipposideros caffer*, *Mops condylurus*. Adapted from Amrein et al. (2007). Arrowheads: Ki-67+ nuclei. **(D)** The number of DCX+/PSA-NCAM+ cells (yellow) declines in the human dentate gyrus (blue outline) from infancy into childhood (reproduced from Sorrells et al., 2018 with permission of Nature Publishing Group). **(E)** *Yellow panel*: schematic representation of the reduction of dentate gyrus neurogenesis in different animal species and at different ages (continuous red line, SGZ neurogenic niche; red dots, occurrence of scattered newly born/immature neurons).

conservation in AN. Really comparable studies would involve the count of dividing and DCX+ cells, in relation to the count of the different cell populations residing in the hippocampus of different species (primarily granule cells, whose number can undergo substantial individual variations: between 10 and 30 million in humans; Simic et al., 1997). An existent analysis, mostly based in rodent species (van Dijk et al., 2016) indicates that the rate of the neurogenesis varies widely, either due to differences in the rates of neuronal birth or to different rates in neurogenesis decline. A wider, systematic analysis involving different mammalian orders is lacking.

ABSENCE OF POSTNATAL NEUROGENESIS IN THE DOLPHIN BRAIN

Dolphins are large-brained, highly gyrencephalic, long-living mammals endowed with high cognitive abilities and sophisticated navigation systems (Marriott et al., 2013). The adaptation to aquatic life promoted the evolution of features (echolocation, composite language, capacity to elaborate intricate social skills) related to their ecological niche and sometimes similar in complexity to humans (Cozzi et al., 2017; van Kann et al., 2017). Among several aspects worthy of a comparative study on neurogenic activity in dolphins, we focused on a unique trait: the absence of olfaction/olfactory brain structures (Oelschläger, 2008; Berta et al., 2014; Cozzi et al., 2017). This is not simply due to dolphins not needing olfaction because of their aquatic adaptation. Fish have olfaction and olfactory systems similar to that of other vertebrates, supporting behaviors crucial for survival (Kermen et al., 2013). Instead, dolphins have developed echolocation for navigation, foraging, and tracking of prey (Marriott et al., 2013), thus, unlike terrestrial mammals (and fish), toothed whales have completely lost olfaction (Oelschläger, 2008; Cozzi et al., 2017). Since the SVZ of the lateral ventricles provides neuronal progeny destined for the OB and linked to olfactory discrimination (Lledo and Valley, 2016; Zhuo et al., 2016), we investigated the periventricular region of neonatal and adult dolphins in search for neurogenic activity. The typical germinal layer described in neonatal mammals (Tramontin et al., 2003; Peretto et al., 2005) was absent at birth in dolphins (Parolisi et al., 2015), replaced by a vestigial remnant (SVZ-like region; SVZ-lr) hosting small spots of non-proliferating cells beneath the ventricular wall (Parolisi et al., 2017; **Figure 1B**). In the neonatal SVZ-lr, Ki-67 antigen localization revealed very low numbers (negligible density) of dividing cells: 34-fold lower than in the germinal layer of the cerebellar cortex of the same animals, 62-fold lower than in the SVZ of neonatal rodents, 47-fold lower than in adult rodents (**Figure 1B**). A similar, very small number of SVZ-lr Ki-67 labeled cells was found in adults (Parolisi et al., 2017). The SVZ-lr area was similar to that in mice, whose brain is 3000-fold smaller if the weight or volume are considered. In dolphins, soon after birth, it appears compartmentalized into cell clusters (a feature reminiscent of AN sites), intermingled with neurons that express mature neuronal markers. Hence, in the dolphin SVZ-lr an early exhaustion of cell division is followed by a local, unknown rate of neuronal maturation. The absence of clear signs of active neurogenesis in aquatic mammals devoid of working olfaction/OB is apparently in contrast with the existence of an SVZ-lr throughout their lifespan. The explanation might be found in their evolutionary history, that started as terrestrial Cetartiodactyls that returned to the sea 35–40 million years ago (Thewissen et al., 2001). The terrestrial ancestors of dolphins were wolf-sized mammals endowed with olfactory structures (*Pakicetus*; Kishida et al., 2015), that underwent a gradual transition from land to sea, losing along the way the capacity to perceive odors (Thewissen et al., 2001). Thus, the vestigial, short-lived SVZ in humans, along with the not working SVZ-lr in dolphins, strongly support the view that AN is maintained in evolution only depending on strict relationships with its functional need(s).

WHY IS ADULT NEUROGENESIS HIGHLY REDUCED OR ABSENT IN SOME MAMMALS?

The most likely explanation for the general reduction of AN in humans with respect to rodents might be related to the reduced importance of specific brain functions linked to survival, somehow replaced by other (higher) cognitive functions. This potential explanation acquires relevance when olfaction/olfactory brain structures (SVZ neurogenesis) are concerned. Although olfaction in humans is considered more impactful than previously thought (in term of total amount of neurons; McGann, 2017), the relative size of the OB with respect to the whole brain volume (0.01% of the human brain compared to 2% of the mouse brain) and the importance of olfaction for survival are quite reduced when compared to rodents (see **Figure 1B**). For this reason, we recently expressly searched the periventricular region of dolphins for neurogenic processes. The persistence of a vestigial remnant (functionally inactive) of the SVZ neurogenic niche in dolphins strongly suggests that periventricular neurogenesis reduction/disappearance occurs in parallel with reduction/disappearance of olfactory brain structures across evolution (Parolisi et al., 2017). Previous observations failing to detect DCX+ cells in the hippocampus of cetaceans (Patzke et al., 2015) suggest that AN does not continue into adult life in toothed whales. Interestingly, another group of mammals showing absence, or very low levels, of hippocampal neurogenesis, the bats (especially Microchiroptera; Amrein et al., 2007; Amrein, 2015; Chawana et al., 2016), are also endowed with echolocation. Unlike dolphins, bats possess a well-developed SVZ neurogenic niche and RMS (olfaction is important in their life; Jones et al., 2013), thus confirming the mutual relationships between the occurrence/rate of AN, its function, and the ecological niches in which a particular species evolved (see Amrein, 2015). Anyway, the link between low neurogenesis – long lifespan – large brain is broken up by the microchiroptera and naked mole-rats, both long-lived species but with small brains, thus adding further levels of complexity.

How these data can be put together in the context of AN reduction? Several studies indicate that olfactory systems held a

paramount importance in early mammalian evolution working as a reference system for spatial navigation for the location of food sources and mates (Rowe et al., 2011; Jacobs, 2012). These olfactory systems were mostly linked to paleocortical–hippocampal structures, subsequently replaced/integrated by the expansion of the isocortex as a "multimodal interface" for behavioral navigation based on vision and audition (Aboitiz and Montiel, 2015). Indeed, with respect to brain mass, the isocortex has "positive allometry": larger mammalian brains become progressively more composed of cortex, ranging from under 20% in relative volume in small shrews and rodents to over 80% in humans (Hofman, 1989; Finlay and Darlington, 1995). From an evolutionary perspective, the major expansion of the isocortex possibly took place "when other senses (vision, audition) began to provide information to the hippocampus to generate multimodal, bidimensional orientation maps" (Aboitiz and Montiel, 2015) and/or to improve long-term memory (e.g., in primates; Reep et al., 2007). Cetaceans did not develop vision to the extent of primates, but essentially base their orientation and navigation on echolocation, a combination of sound emission and perception that requires no olfactory structures for the detection of faraway targets (Marriott et al., 2013).

In the complexity of mammalian plasticity, research focused on single animal species or directed only to highly standardized models, minimizes genetic and environmental variation and may result misleading in a translational perspective (Bolker, 2017). If AN is concerned, models based on laboratory rodents are too simplistic if we consider the different neuroanatomies and the species-specific adaptations of mammals (Lipp and Bonfanti, 2016; Faykoo-Martinez et al., 2017). For instance, in a recent report, no significant change in the number of newly born neurons was detectable in young sheep forced to exercise (Swanson et al., 2017), sharply in contrast with rodents (Vivar and van Praag, 2017). The baseline exercise for lambs only consists of brief episodes of exploratory play and feeding activities, in contrast with the long-sustained periods of exercise required by rodents for feeding and survival. This difference further highlights how AN modulation is linked to species-specific natural behaviors (function-based need), rather than to a stimulus *per se*. Indeed, laboratory mice are not even a model for their wild counterpart, since physical activity (or the lack of) does not alter neurogenesis in wild rodents (Amrein, 2015).

Interestingly, in humans, primates, dolphins or naked mole rat, newly born DCX+ neurons can persist in the neurogenic areas long after their proliferation in a sort of prolonged maturation that does not take place in short-living rodents (Kornack and Rakic, 1999; Knoth et al., 2010; Kohler et al., 2011; Brus et al., 2013; Penz et al., 2015; Parolisi et al., 2017). The maturation of neurons in long-living species might be delayed to compensate for the strong reduction in the number of new neurons. Interestingly, the recent studies in the adult human hippocampus essentially show the existence of various kinds/stages of immature neurons.

CONCLUSIONS AND FUTURE PERSPECTIVES

Three features of AN are crucial when considering its translational value: (i) its substantial decrease in humans and other long-living, large-brained mammals; (ii) its decrease with the age of the individuals (in both SVZ and hippocampus); and (iii) a scarce propensity/efficacy for lesion-induced repair in mammals. These constraints seem to strongly depend on evolutionary pathways (Weil et al., 2008). Evolution drives the occurrence, rate and type of plasticity among mammals, and interspecies differences must be taken into account when translating results from mice to humans. In parallel, mechanistic studies in mice may still guide future induction efforts or transplantation in humans. Current efforts are aimed at identifying and fostering the endogenous/exogenous sources of stem cells. However, future angles should also contemplate the search for other forms of plasticity potentially adopted by different species in alternative or in addition to the genesis of new neurons. In long-living species, it is more common to find DCX+ neurons which maintain markers of immaturity for a long time. This suggests that other forms of plasticity might compensate the loss of continuous neurogenesis (apparently not compatible with the acquisition of higher cognitive functions). An example consists of the so called "immature neurons": non-newly generated, DCX+ cells which are born prenatally but persist through time in an immature state in non-neurogenic regions (Gómez-Climent et al., 2008; functional hypothesis reviewed in Bonfanti and Nacher, 2012; König et al., 2016). We recently showed that immature neurons are by far more present in sheep than in rodents, thus supporting the existence of distinct, possibly alternative, forms of structural plasticity in some mammals (Piumatti et al., 2017; Palazzo et al., 2018).

AUTHOR CONTRIBUTIONS

LB wrote the article. BC and RP contributed to writing the article.

ACKNOWLEDGMENTS

We thank Arturo Alvarez-Buylla, Irmgard Amrein, and Lutz Slomianka for reading the manuscript and for their precious suggestions.

REFERENCES

Aboitiz, F., and Montiel, J. F. (2015). Olfaction, navigation, and the origin of isocortex. *Front. Neurosci.* 9:402. doi: 10.3389/fnins.2015.00402

Altman, J., and Das, G. D. (1965). Post-natal origin of microneurones in the rat brain. *Nature* 207, 953–956. doi: 10.1038/207953a0

Amrein, I. (2015). Adult hippocampal neurogenesis in natural populations of mammals. *Cold Spring Harb. Perspect. Biol.* 7:a021295. doi: 10.1101/cshperspect.a021295

Amrein, I., Dechmann, D. K., Winter, Y., and Lipp, H. P. (2007). Absent or low rate of adult neurogenesis in the hippocampus of bats (Chiroptera). *PLoS One* 2:e455. doi: 10.1371/journal.pone.0000455

Arellano, J. I., Harding, B., and Thomas, J. L. (2018). Adult human hippocampus: no new neurons in sight. *Cereb. Cortex* 28, 2479–2481. doi: 10.1093/cercor/bhy106

Ben Abdallah, N. M., Slomianka, L., Vyssotski, A. L., and Lipp, H. P. (2010). Early age-related changes in adult hippocampal neurogenesis in C57 mice. *Neurobiol. Aging* 31, 151–161. doi: 10.1016/j.neurobiolaging.2008.03.002

Bergmann, O., Spalding, K. L., and Frisen, J. (2015). Adult neurogenesis in humans. *Cold Spring Harb. Perspect. Biol.* 7:a018994. doi: 10.1101/cshperspect.a018994

Berta, A., Ekdale, E. G., and Cranford, T. W. (2014). Review of the cetacean nose: form, function, and evolution. *Anat. Rec.* 297, 2205–2215. doi: 10.1002/ar.23034

Boldrini, M., Fulmore, C. A., Tartt, A. N., Simeon, L. R., Pavlova, I., Poposka, V., et al. (2018). Human hippocampal neurogenesis persists throughout aging. *Cell Stem Cell* 22:589-599.e5. doi: 10.1016/j.stem.2018.03.015

Bolker, J. A. (2017). Animal models in translational research: Rosetta stone or stumbling block? *Bioessays* 39:1700089. doi: 10.1002/bies.201700089

Bonfanti, L. (2011). From hydra regeneration to human brain structural plasticity: a long trip through narrowing roads. *ScientificWorldJournal* 11, 1270–1299. doi: 10.1100/tsw.2011.113

Bonfanti, L., and Nacher, J. (2012). New scenarios for neuronal structural plasticity in non-neurogenic brain parenchyma: the case of cortical layer II immature neurons. *Prog. Neurobiol.* 98, 1–15. doi: 10.1016/j.pneurobio.2012.05.002

Bordiuk, O. L., Smith, K., Morin, P. J., and Semenov, M. V. (2014). Cell proliferation and neurogenesis in adult mouse brain. *PLoS One* 9:e111453. doi: 10.1371/journal.pone.0111453

Brus, M., Meurisse, M., Gheusi, G., Keller, M., Lledo, P. M., and Levy, F. (2013). Dynamics of olfactory and hippocampal neurogenesis in adult sheep. *J. Comp. Neurol.* 521, 169–188. doi: 10.1002/cne.23169

Chawana, R., Patzke, N., Alagaili, A. N., Bennett, N. C., Mohammed, O. B., Kaswera-Kyamakya, C., et al. (2016). The distribution of Ki-67 and doublecortin immunopositive cells in the brains of three Microchiropteran. species, Hipposideros fuliginosus, Triaenops persicus, and Asellia tridens. *Anat. Rec.* 299, 1548–1560. doi: 10.1002/ar.23460

Cipriani, S., Ferrer, A., Arinica, I., Kovacs, G., Verney, C., Nardelli, J., et al. (2018). Hippocampal radial glial subtypes and their neurogenic potential in human fetuses and healthy and Alzheimer disease adults. *Cereb. Cortex* 28, 2458–2478. doi: 10.1093/cercor/bhy096

Conover, J. C., and Todd, K. L. (2017). Development and aging of a brain neural stem cell niche. *Exp. Gerontol.* 94, 9–13. doi: 10.1016/j.exger.2016.11.007

Cozzi, B., Huggenberger, S., and Oelschläger, H. H. A. (eds). (2017). "Chapter 6: brain, spinal cord, and cranial nerves," in *The Anatomy of Dolphins: Insights into Body Structure and Function* (London: Academic Press), 191–285.

Faykoo-Martinez, M., Toor, I., and Holmes, M. M. (2017). Solving the neurogenesis puzzle: looking for pieces outside the traditional box. *Front. Neurosci.* 11:505. doi: 10.3389/fnins.2017.00505

Finlay, B. L., and Darlington, R. B. (1995). Linked regularities in the development and evolution of mammalian brains. *Science* 268, 1578–1584. doi: 10.1126/science.7777856

Gómez-Climent, M. A., Castillo-Gómez, E., Varea, E., Guirado, R., Blasco-Ibáñez, J. M., Crespo, C., et al. (2008). A population of prenatally generated cells in the rat paleocortex maintains an immature neuronal phenotype into adulthood. *Cereb. Cortex* 18, 2229–2240. doi: 10.1093/cercor/bhm255

Grandel, H., Kaslin, J., Ganz, J., Wenzel, I., and Brand, M. (2006). Neural stem cells and neurogenesis in the adult zebrafish brain: origin, proliferation dynamics, migration and cell fate. *Dev. Biol.* 295, 263–277. doi: 10.1016/j.ydbio.2006.03.040

Hofman, M. A. (1989). On the evolution and geometry of the brain in mammals. *Prog. Neurobiol.* 32, 137–158. doi: 10.1016/0301-0082(89)90013-0

Jacobs, L. F. (2012). From chemotaxis to the cognitive map: the function of olfaction. *Proc. Natl. Acad. Sci. U.S.A.* 109, 10693–10700. doi: 10.1073/pnas.1201880109

Jones, G., Teeling, E. C., and Rossiter, S. J. (2013). From the ultrasonic to the infrared: molecular evolution and the sensory biology of bats. *Front. Physiol.* 4:117. doi: 10.3389/fphys.2013.00117

Kempermann, G. (2016). Adult neurogenesis: an evolutionary perspective. *Cold Spring Harb. Perspect. Biol.* 8:a018986. doi: 10.1101/cshperspect.a018986

Kermen, F., Franco, L. M., Wyatt, C., and Yaksi, E. (2013). Neural circuits mediating olfactory-driven behavior in fish. *Front. Neural Circuits* 7:62. doi: 10.3389/fncir.2013.00062

Kishida, T., Thewissen, J. G. M., Hayakawa, T., Imai, H., and Agata, K. (2015). Aquatic adaptation and the evolution of smell and taste in whales. *Zoological Lett.* 1:9. doi: 10.1186/s40851-014-0002

Knoth, R., Singec, I., Ditter, M., Pantazis, G., Capetian, P., Meyer, R. P., et al. (2010). Murine features of neurogenesis in the human hippocampus across the lifespan from 0 to 100 years. *PLoS One* 5:e8809. doi: 10.1371/journal.pone.0008809

Kohler, S. J., Williams, N. I., Stanton, G. B., Camerond, J. L., and Greenough, W. T. (2011). Maturation time of new granule cells in the dentate gyrus of adult macaque monkeys exceeds six months. *Proc. Natl. Acad. Sci. U.S.A.* 108, 10326–10331. doi: 10.1073/pnas.1017099108

König, R., Benedetti, B., Rotheneichner, P., O'Sullivan, A., Kreutzer, C., Belles, M., et al. (2016). Distribution and fate of DCX/PSA-NCAM expressing cells in the adult mammalian cortex: a local reservoir for adult cortical neuroplasticity? *Front. Biol.* 11, 193–213. doi: 10.1007/s11515-016-1403-5

Kornack, D. R., and Rakic, P. (1999). Continuation of neurogenesis in the hippocampus of the adult macaque monkey. *Proc. Natl. Acad. Sci. U.S.A.* 96, 5768–5773. doi: 10.1073/pnas.96.10.5768

Lipp, H. P., and Bonfanti, L. (2016). Adult neurogenesis in mammals: variations and confusions. *Brain Behav. Evol.* 87, 205–221. doi: 10.1159/000446905

Lledo, P. M., and Valley, M. (2016). Adult olfactory bulb neurogenesis. *Cold Spring Harb. Perspect. Biol.* 8:a018945. doi: 10.1101/cshperspect.a018945

Lois, C., and Alvarez-Buylla, A. (1994). Long-distance neuronal migration in the adult mammalian brain. *Science* 264, 1145–1148. doi: 10.1126/science.8178174

Marriott, S., Cowan, E., Cohen, J., and Hallock, R. M. (2013). Somatosensation, echolocation, and underwater sniffing: adaptations allow mammals without traditional olfactory capabilities to forage for food underwater. *Zoolog. Sci.* 30, 69–75. doi: 10.2108/zsj.30.69

McGann, J. P. (2017). Poor human olfaction is a 19th-century myth. *Science* 356:eaam7263. doi: 10.1126/science.aam7263

Obernier, K., Cebrian-Silla, A., Thomson, M., Parraguez, J. I., Anderson, R., Guinto, C., et al. (2018). Adult neurogenesis is sustained by symmetric self-renewal and differentiation. *Cell Stem Cell* 22, 221–234.e8. doi: 10.1016/j.stem.2018.01.003

Oelschläger, H. H. A. (2008). The dolphin brain-a challenge for synthetic neurobiology. *Brain Res. Bull.* 75, 450–459. doi: 10.1016/j.brainresbull.2007.10.051

Palazzo, O., La Rosa, C., Piumatti, M., and Bonfanti, L. (2018). Do large brains of long-living mammals prefer non-newly generated, immature neurons? *Neural Regen. Res.* 13, 633–634. doi: 10.4103/1673-5374.230282

Paredes, M. F., Sorrells, S. F., Garcia-Verdugo, J. M., and Alvarez-Buylla, A. (2016). Brain size and limits to adult neurogenesis. *J. Comp. Neurol.* 524, 646–664. doi: 10.1002/cne.23896

Parolisi, R., Cozzi, B., and Bonfanti, L. (2017). Non-neurogenic SVZ-like niche in dolphins, mammals devoid of olfaction. *Brain Struct. Funct.* 222, 2625–2639. doi: 10.1007/s00429-016-1361-3

Parolisi, R., Peruffo, A., Messina, S., Panin, M., Montelli, S., Giurisato, M., et al. (2015). Forebrain neuroanatomy of the neonatal and juvenile dolphin (*T. truncatus* and *S. coeruloalba*). *Front. Neuroanat.* 9:140. doi: 10.3389/fnana.2015.00140

Paton, J. A., and Nottebohm, F. (1984). Neurons generated in adult brain are recruited into functional circuits. *Science* 225, 1046–1048. doi: 10.1126/science.6474166

Patzke, N., Spocter, M. A., Karlsson, K. Æ., Bertelsen, M. F., Haagensen, M., Chawana, R., et al. (2015). In contrast to many other mammals, cetaceans have relatively small hippocampi that appear to lack adult neurogenesis. *Brain Struct. Funct.* 220, 361–383. doi: 10.1007/s00429-013-0660-1

Penz, O. K., Fuzik, J., Kurek, A. B., Romanov, R., Larson, J., Park, T. J., et al. (2015). Protracted brain development in a rodent model of extreme longevity. *Sci. Rep.* 5:11592. doi: 10.1038/srep11592

Peretto, P., Giachino, C., Aimar, P., Fasolo, A., and Bonfanti, L. (2005). Chain formation and glial tube assembly in the shift from neonatal to adult subventricular zone of the rodent forebrain. *J. Comp. Neurol.* 487, 407–427. doi: 10.1002/cne.20576

Piumatti, M., Palazzo, O., La Rosa, C., Crociara, P., Parolisi, R., Luzzati, F., et al. (2017). Non-newly generated, "immature" neurons in the sheep brain are not restricted to cerebral cortex. *J. Neurosci.* 38, 826–842. doi: 10.1523/JNEUROSCI.1781-17.2017

Ponti, G., Obernier, K., Guinto, C., Jose, L., Bonfanti, L., and Alvarez-Buylla, A. (2013). Cell cycle and lineage progression of neural progenitors in the ventricular-subventricular zones of adult mice. *Proc. Natl. Acad. Sci. U.S.A.* 110, E1045–E1054. doi: 10.1073/pnas.1219563110

Reep, R. L., Finlay, B. L., and Darlington, R. B. (2007). The limbic system in mammalian brain evolution. *Brain Behav. Evol.* 70, 57–70. doi: 10.1159/000101491

Rowe, T. B., Macrini, T., and Luo, Z. X. (2011). Fossil evidence on origin of mammalian brain. *Science* 332, 955–957. doi: 10.1126/science.1203117

Sanai, N., Nguyen, T., Ihrie, R. A., Mirzadeh, Z., Tsai, H.-H., Wong, M., et al. (2011). Corridors of migrating neurons in the human brain and their decline during infancy. *Nature* 478, 382–386. doi: 10.1038/nature10487

Shook, B. A., Manz, D. H., Peters, J. J., Kang, S., and Conover, J. C. (2012). Spatiotemporal changes to the subventricular zone stem cell pool through aging. *J. Neurosci.* 32, 6947–6956. doi: 10.1523/JNEUROSCI.5987-11.2012

Simic, G., Kostovic, I., Winblad, B., and Bogdanovic, N. (1997). Volume and number of neurons of the human hippocampal formation in normal aging and Alzheimer's disease. *J. Comp. Neurol.* 379, 482–494. doi: 10.1002/(SICI)1096-9861(19970324)379:4<482::AID-CNE2>3.0.CO;2-Z

Sorrells, S. F., Paredes, M. F., Cebrian-Silla, A., Sandoval, K., Qi, D., Kelley, K. W., et al. (2018). Human hippocampal neurogenesis drops sharply in children to undetectable levels in adults. *Nature* 555, 377–381. doi: 10.1038/nature25975

Spalding, K. L., Bergmann, O., Alkass, K., Bernard, S., Salehpour, M., Huttner, H. B., et al. (2013). Dynamics of hippocampal neurogenesis in adult humans. *Cell* 153, 1219–1227. doi: 10.1016/j.cell.2013.05.002

Suhonen, J. O., Peterson, D. A., Ray, J., and Gage, F. H. (1996). Differentiation of adult hippocampus-derived progenitors into olfactory neurons in vivo. *Nature* 383, 624–627. doi: 10.1038/383624a0

Swanson, M. E. V., Murray, H. C., Oliver, M. H., Waldvogel, H. J., Firth, E. C., and Curtis, M. A. (2017). Imposed running exercise does not alter cell proliferation in the neurogenic niches of young lambs. *J. Anim. Sci.* 95, 4381–4390. doi: 10.2527/jas2017.1710

Thewissen, J. G., Williams, E. M., Roe, L. J., and Hussain, S. T. (2001). Skeletons of terrestrial cetaceans and the relationship of whales to artiodactyls. *Nature* 413, 277–281. doi: 10.1038/35095005

Tramontin, A. D., Garcìa-Verdugo, J. M., Lim, D. A., and Alvarez-Buylla, A. (2003). Postnatal development of radial glia and the ventricular zone (VZ): a continuum of the neural stem cell compartment. *Cereb. Cortex* 13, 580–587. doi: 10.1093/cercor/13.6.580

van Dijk, R. M., Huang, S. H., Slomianka, L., and Amrein, I. (2016). Taxonomic separation of hippocampal networks: principal cell populations and adult neurogenesis. *Front. Neuroanat.* 10:22. doi: 10.3389/fnana.2016.00022

van Kann, E., Cozzi, B., Hof, P. R., and Oelschläger, H. H. A. (2017). Qualitative and quantitative analysis of primary neocortical areas in selected mammals. *Brain Behav. Evol.* 90, 193–210. doi: 10.1159/000477431

Vivar, C., and van Praag, H. (2017). Running changes the brain: the long and the short of it. *Physiology (Bethesda)* 32, 410–424. doi: 10.1152/physiol.00017.2017

Wang, C., Liu, F., Liu, Y.-Y., Zhao, C.-H., You, Y., Wang, L., et al. (2011). Identification and characterization of neuroblasts in the subventricular zone and rostral migratory stream of the adult human brain. *Cell Res.* 21, 1534–1550. doi: 10.1038/cr.2011.83

Weil, Z. M., Norman, G. J., De Vries, A. C., and Nelson, R. J. (2008). The injured nervous system: a Darwinian perspective. *Prog. Neurobiol.* 86, 48–59. doi: 10.1016/j.pneurobio.2008.06.001

Workman, A. D., Charvet, C. J., Clancy, B., Darlington, R. B., and Finlay, B. L. (2013). Modeling transformations of neurodevelopmental sequences across mammalian species. *J. Neurosci.* 33, 7368–7383. doi: 10.1523/JNEUROSCI.5746-12.2013

Zhuo, J. M., Tseng, H. A., Desai, M., Bucklin, M. E., Mohammed, A. I., Robinson, N. T., et al. (2016). Young adult born neurons enhance hippocampal dependent performance via influences on bilateral networks. *Elife* 5:e22429. doi: 10.7554/eLife.22429

Conflict of Interest Statement: The authors declare that the research was conducted in the absence of any commercial or financial relationships that could be construed as a potential conflict of interest.

frontiers in Neuroscience

ORIGINAL RESEARCH
published: 01 March 2017
doi: 10.3389/fnins.2017.00097

Increased Testosterone Decreases Medial Cortical Volume and Neurogenesis in Territorial Side-Blotched Lizards (*Uta stansburiana*)

Lara D. LaDage[1], Timothy C. Roth II[2], Cynthia J. Downs[3], Barry Sinervo[4] and Vladimir V. Pravosudov[5]*

[1] Division of Mathematics and Natural Sciences, Penn State University Altoona, Altoona, PA, USA, [2] Department of Psychology, Franklin and Marshall College, Lancaster, PA, USA, [3] Biology Department, Hamilton College, Clinton, NY, USA, [4] Department of Ecology and Evolutionary Biology, University of California, Santa Cruz, CA, USA, [5] Department of Biology, University of Nevada, Reno, NV, USA

Variation in an animal's spatial environment can induce variation in the hippocampus, an area of the brain involved in spatial cognitive processing. Specifically, increased spatial area use is correlated with increased hippocampal attributes, such as volume and neurogenesis. In the side-blotched lizard (*Uta stansburiana*), males demonstrate alternative reproductive tactics and are either territorial—defending large, clearly defined spatial boundaries—or non-territorial—traversing home ranges that are smaller than the territorial males' territories. Our previous work demonstrated cortical volume (reptilian hippocampal homolog) correlates with these spatial niches. We found that territorial holders have larger medial cortices than non-territory holders, yet these differences in the neural architecture demonstrated some degree of plasticity as well. Although we have demonstrated a link among territoriality, spatial use, and brain plasticity, the mechanisms that underlie this relationship are unclear. Previous studies found that higher testosterone levels can induce increased use of the spatial area and can cause an upregulation in hippocampal attributes. Thus, testosterone may be the mechanistic link between spatial area use and the brain. What remains unclear, however, is if testosterone can affect the cortices independent of spatial experiences and whether testosterone differentially interacts with territorial status to produce the resultant cortical phenotype. In this study, we compared neurogenesis as measured by the total number of doublecortin-positive cells and cortical volume between territorial and non-territorial males supplemented with testosterone. We found no significant differences in the number of doublecortin-positive cells or cortical volume among control territorial, control non-territorial, and testosterone-supplemented non-territorial males, while testosterone-supplemented territorial males had smaller medial cortices containing fewer doublecortin-positive cells. These results demonstrate that testosterone can modulate medial cortical attributes outside of differential spatial processing experiences but that territorial males appear to be more sensitive to alterations in testosterone levels compared with non-territorial males.

Keywords: testosterone, neurogenesis, medial cortex, dorsal cortex, lizards, *Uta stansburiana*

OPEN ACCESS

Edited by:
Luca Bonfanti, University of Turin, Italy

Reviewed by:
Paolo Peretto, University of Turin, Italy
Gustavo M. Somoza, Instituto de Investigaciones Biotecnológicas-Instituto Tecnológico de Chascomús (IIB-INTECH), Argentina

****Correspondence:***
Lara D. LaDage
ldl18@psu.edu

Specialty section:
This article was submitted to Neurogenesis, a section of the journal Frontiers in Neuroscience

Received: *14 January 2017*
Accepted: *14 February 2017*
Published: *01 March 2017*

Citation:
LaDage LD, Roth II TC, Downs CJ, Sinervo B and Pravosudov VV (2017) Increased Testosterone Decreases Medial Cortical Volume and Neurogenesis in Territorial Side-Blotched Lizards (Uta stansburiana). Front. Neurosci. 11:97. doi: 10.3389/fnins.2017.00097

INTRODUCTION

Animals that defend clearly delineated territories are in part reliant upon spatial memory to remember territorial boundaries and determine the location of territorial neighbors (Falls, 1982; Godard, 1991; McGregor and Westby, 1992; Sherry, 1998; Bee and Gerhardt, 2001). However, territory size can vary among individuals suggesting that individuals likely have differential demands on spatial cognitive processing based on the size of the defended territory. In support of this, previous studies in a variety of taxa have demonstrated that individuals that hold territories, hold larger territories, or traverse larger home ranges have better spatial memory. Further, these individuals also have larger hippocampi, the area of the brain largely responsible for spatial memory processing, with more new hippocampal neurons, presumably to subserve the increased demands on spatial cognition (Gaulin and Fitzgerald, 1986, 1989; Jacobs et al., 1990; Galea and McEwen, 1999; Amrein et al., 2004; Roth et al., 2006; LaDage et al., 2009, 2013; Holding et al., 2012). Consequently, there is a positive relationship among territoriality, spatial area use, spatial cognition, and the underlying neural substrate supporting spatial cognition.

What remains unclear is the mechanism underlying the correlation among territoriality, spatial cognition, and the brain. During the breeding season, territorial behavior and territory size have been linked to testosterone, in that increased levels of testosterone correlate with increased territory size and improve spatial cognition in mammals, birds, and lizards (e.g., Wingfield, 1984; DeNardo and Sinervo, 1994; Moss et al., 1994; Sinervo et al., 2000; Veiga et al., 2001; Ketterson et al., 1996; Spritzer et al., 2011). Variation in hormone levels can also directly affect the hippocampus and these changes can be maintained long-term in mammals (e.g., Gould et al., 1990; Roof and Havens, 1992; Woolley and McEwen, 1992; Cooke et al., 1998; Galea et al., 1999). Specifically, in birds and mammals, testosterone levels correlate with increased brain substructure volume and increased neurogenesis rates (e.g., Roof and Havens, 1992; Absil et al., 2003; Galea et al., 2006). While testosterone has been linked to both territoriality and hippocampal attributes, it remains unclear if testosterone is the underlying mechanism that links the two and, if so, whether variation in testosterone can directly alter brain attributes, outside of spatial area use experiences.

While many of the aforementioned studies have leveraged naturally occurring hormonal changes across seasons, between the sexes, or across species to examine these relationships, there are genetic, population-level, and other life history variables that can introduce variance not attributable to differences in neuroendocrinology (e.g., Knapp, 2003; Moore, 1991; LaDage, 2016). One way to circumvent some of these issues is to utilize model species that demonstrate polymorphisms within a sex. Polymorphisms allow individuals to engage in different strategies to increase reproductive success and also correlate with differences in other dimensions, such as morphology, physiology, and other life history characteristics (e.g., Sinervo et al., 2000; Crews and Moore, 2005). Thus, the use of a polymorphic species allows for naturally occurring intrasexual differences yet controls for potentially confounding variables associated with intersexual, population-level, or interspecific differences not related to the neuroendocrinology axis. This approach has been relatively successful, particularly in reptiles, and much research has been directed toward understanding the hormonal influences on the organization and activation of physiological, morphological, and behavioral differences within polymorphic species (e.g., Moore, 1991).

In the current study, we used side-blotched lizards (*Uta stansburiana*), a polymorphic species in which male morphotypes differ in space use, hormonal profile, and brain attributes. In our target population, males are found in one of the three morphotypes and all morphs are genetically determined by a single locus (OBY locus) (orange morph: *oo*, *bo*, *yo*; blue morph: *bb*; yellow morph: *by*, *yy*) (Sinervo et al., 2001, 2006). Each morph has a different space use strategy: the orange morph occupies and defends large territories, the blue morph occupies and defends smaller territories while the yellow morph does not hold or defend a territory, and its home range is smaller than the territories of the other two morphs (Sinervo and Lively, 1996; Sinervo et al., 2000, 2006; Zamudio and Sinervo, 2000).

Territorial predisposition in side-blotched lizards is associated with differences in territory size, testosterone profiles, and cortical attributes. Previous studies in this and other polymorphic lizard species have found that territorial morphotypes have higher levels of testosterone than non-territorial males (e.g., DeNardo and Sinervo, 1994; Wikelski et al., 2005; Olsson et al., 2007) and this is one mechanism that can directly modulate spatial area use. For example, experimentally elevating testosterone levels in non-territorial males induces an increase in home range size similar to home range sizes seen in un-manipulated territorial males (DeNardo and Sinervo, 1994; Sinervo et al., 2000; Wikelski et al., 2005) suggesting that testosterone is sufficient to regulate spatial area use.

However, whether testosterone is the modulating mechanism underlying changes in spatial area use and the brain is still unknown. Our previous research indicates that the putative reptilian hippocampal homologs, the dorsal and medial cortices (Butler, 1976), are larger in territorial than non-territorial males (LaDage et al., 2009) yet these differences are not fixed and can vary based on environmental experiences (LaDage et al., 2013, 2016). Further, territorial predisposition can modulate the effects of environmental experiences on cortical plasticity in that only territorial males upregulate neurogenesis in the face of increased spatial area use, possibly due to territorial males' higher reliance on spatial processing (LaDage et al., 2013). Thus, known factors that influence neural plasticity can also differentially modulate that plasticity based on territorial status.

Since there is a relationship between testosterone and the brain, as well as between testosterone and territoriality, and if testosterone is the mechanistic mediator between territorial predisposition and the brain, experimentally elevating testosterone levels should increase cortical attributes, independent of spatial use experiences. We predicted that, in individuals hatched and raised with identical spatial area experiences, testosterone supplementation would increase cortical attributes in all males, regardless of territorial predisposition. Further, because territorial predisposition

has been found to modulate cortical attributes, we also predicted that territorial males would be more sensitive to changes in testosterone because territorial males are more dependent on spatial cognition within the context of territorial defense. Thus, while testosterone may upregulate cortical attributes in both territorial and non-territorial males, the effects should be more dramatic in territorial males.

MATERIALS AND METHODS

Subjects

In March 2010, adult male and non-gravid female side-blotched lizards were collected near Los Baños Grandes, California and transported to the University of Nevada, Reno. Morphotypes were determined by external morphological characteristics (e.g., Sinervo and Lively, 1996) in that homozygote males have solid throat colors: (*oo*) males have purely orange throats, blue males (*bb*) have purely blue throat coloration, and yellow males (*yy*) have pure yellow throats. Because male throat coloration easily identifies morphotype, males and females were assigned to breeding enclosures (20-L terraria) to facilitate the production of primarily homozygous morphotypic offspring (LaDage et al., 2013, 2016). Females were subjected to abdominal palpitations every other day and gravid females were transferred to individual ovipositing enclosures until laying [enclosure size: 22 × 14 × 13.5 cm with a moist layer of peat/sand (3:1)]. Ovipositing enclosures were checked for eggs every morning and, after oviposition, females were returned to their breeding enclosure.

Eggs were collected from ovipositing enclosures and individually incubated at 28 ± 1°C until the emergence of hatchlings (35–45 days, L. LaDage, personal observation). To prevent pseudoreplication, only one male offspring per mated pair was used in the current experiment. Male hatchlings were individually housed (enclosure size: 22 × 14 × 13.5 cm), fed live crickets dusted with calcium and vitamins each day, and supplied with water *ad libitum*. The temperature of the laboratory was maintained at 20°C and cages were supplemented with above-cage basking lights which provided a thermal gradient from 25 to 40°C. All lights were kept on a cycle mirroring ambient across the year (e.g., 10L:14D in December, 16L:8D in June). Individuals were raised until adulthood (>9 mo) before being subjected to the experimental treatment thus assessing the activational role of testosterone rather than the organizational (Moore, 1991). All procedures were approved by the Institutional Animal Care and Use Committee at the University of Nevada, Reno (2009-00434) in accordance with the guidelines of the American Veterinary Medical Association.

Experimental Protocol

Our previous studies indicate no neurobiological differences in cortical volume between orange and blue territorial males (LaDage et al., 2009, 2013) suggesting that brain attributes are likely regulated by how morphotypes use space rather than the size of the space *per se* (e.g., Clint, 2012). Thus, we collapsed morphotypes into territorial predisposition, with orange and blue males comprising the territorial group and yellow males comprising the non-territorial group. We randomly assigned territorial and non-territorial males to either a control or testosterone-supplemented treatment group ($n = 12$ for territorial, $n = 9$ for non-territorial at the conclusion of the study). A 3 mm length of Silastic medical grade tubing (Dow Corning 602–305) was filled with saline (control group) or 1 mm testosterone (Sigma T1500) (supplemented group). Implants were sealed at each end with silicone sealant and soaked in saline for 24 h before implantation (DeNardo and Licht, 1993; DeNardo and Sinervo, 1994). All subjects were subcutaneously anesthetized with 0.2% lidocaine, a small incision was made in the flank, and the implant was placed intracoelomically through the incision (DeNardo and Sinervo, 1994). These implants have been shown to maintain elevated levels of testosterone for at least 3 months in this species (DeNardo and Licht, 1993; DeNardo and Sinervo, 1994). After implantation, subjects were returned to their home enclosures for 2 months, which allowed for an adequate amount of time in which testosterone could possibly affect cortical attributes (e.g., Delgado-Gonzalez et al., 2011). Further, because implantation occurred in April, all males were well into breeding age and, in their natural habitat, would have exhibited increased levels of testosterone and territory establishment/defense (e.g., Ferguson and Fox, 1984; Wilson and Wingfield, 1994).

Testosterone Assays

To assess baseline and terminal testosterone levels, as well as the success of our implants in elevating testosterone, we collected blood in all subjects the week before implantation and at the time of sacrifice. Blood was collected via the retro-orbital sinus using two to three 20 ul heparinized microcapillary tubes and kept on ice for no more than 3 h. We centrifuged samples to isolate the plasma and froze plasma samples at −80°C until processed (<3 months). We quantified testosterone concentrations (pg/ml) using a commercially available ELISA kit (#ADI-900-065, Enzo, Farmingdale, NY 11735) (Robertson et al., 2011). Prior to use, we validated the kits for *Uta* by created a dilution curve of unknown samples (Buchanan and Goldsmith, 2004); we found parallelism between standards and *Uta* samples. All samples were quantified using kits from the same lot, and we used the protocol included with the kit. End absorbances were quantified on a 405 nm plate reader (Thermo Scientific Multiskan Ascent). Samples were tested in duplicate at the predetermined optimal dilution of 1:20. Because some samples had testosterone levels that were outside the standard curve, we reassayed these samples at more dilute concentrations until they fell within the ideal part of the standard curve; repeated assays were at either 1:40 or 1:500.

Tissue Processing

After 2 months in their respective treatment groups, all individuals were anesthetized with a lethal overdose of Nembutal (510 mg/kg of 50 mg/ml sodium pentobarbital), then transcardially perfused with 0.1 M phosphate buffered saline for 10 min followed by a 15–20 min perfusion of 10% methanol-free formalin (from paraformaldehyde). Brains were extracted and post-fixed for 24 h in 10% methanol-free formalin (from paraformaldehyde), cryoprotected in 15% sucrose for 24 h, 30% sucrose for another 24 h, and finally

flash-frozen on dry ice. Brains were stored at −80°C until sectioning. Brains were sectioned in the coronal plane every 40 μm (Leica CM 3050S, −20°C). Sections were divided into two series. One series was mounted and Nissl-stained with thionin to visualize cortical boundaries while the second series was subjected to immunohistochemistry to visualize the production of new neurons (e.g., LaDage et al., 2013, 2016).

Immunohistochemistry

To visualize new neurons, the second series of tissue sections were processed for the expression of doublecortin, an endogenous protein expressed by immature, migrating neurons, which co-labels with other markers specific to new neurons (Brown et al., 2003; Rao and Shetty, 2004; Couillard-Despres et al., 2005; Hairston et al., 2005; Balthazart et al., 2008; Luzzati et al., 2009; Delgado-Gonzalez et al., 2011). In lizards, doublecortin expression in new neurons lasts between 7 and 90 days, although 2 weeks to 30 days is more typical (Lopez-Garcia et al., 1990; Ramirez-Castillejo et al., 2002; Marchioro et al., 2005; Delgado-Gonzalez et al., 2011). After these neurons migrate and become incorporated into the existing neural architecture, expression of doublecortin ceases while expression of mature neuronal proteins begins (Mullen et al., 1992; Brown et al., 2003). Thus, in lizards, quantifying doublecortin protein expression encompasses the majority of the neurons in the immature stages of development.

To visualized doublecortin expression, sections were washed in tris (hydroxymethyl) aminomethane-buffered saline (TBS), incubated in 30% hydrogen peroxide plus TBS (1:50) at room temperature for 30 min, washed in TBS, incubated in blocking buffer (normal horse serum, 1:33.3; Triton X-100, 1:39.8; and TBS) at room temperature for 30 min, and then incubated in anti-doublecortin antibody plus blocking buffer (1:200; Santa Cruz Biotechnology, Santa Cruz, CA; SC-8066) overnight (approximately 18 h) at 4°C. The following day, sections were washed in TBS, incubated in biotinylated horse anti-goat antibody in blocking buffer (1:200; Vector Laboratories, Burlingame, CA; BA-9500) at room temperature for 2 h, washed in TBS, incubated in a Vectastain Elite ABC kit (Vector Laboratories, PK-6100) at room temperature for 1 h, washed in TBS, reacted with diaminobenzidine-nickel kit (DAB-Ni; Vector Laboratories, SK-4100) at room temperature for 1 min and again washed in TBS and mounted on slides. We also performed a negative control to account for nonspecific binding of the secondary antibody. To do so, we repeated this protocol, but replaced the anti-doublecortin antibody with TBS during overnight incubation. The elimination of the antibody suppressed staining, thus indicating that our protocol was specifically staining cells expressing doublecortin.

Brain Analysis

In the reptilian brain, the medial and dorsal cortices exhibit structural and functional homologies to the hippocampus of other vertebrates (e.g., Grisham and Powers, 1990; Reiner, 1991, 1993; Butler, 1994; Petrillo et al., 1994; Reiman Avigan and Schade Powers, 1995; Striedter, 1997; Rodríguez et al., 2002; López et al., 2003; Striedter, 2016) thus both areas were measured in their entirety. We used standard stereological methods (StereoInvestigator, Microbrightfield, Inc., Williston, VT; Leica M4000B microscope) to estimate the remainder of the telencephalon (total telencephalon minus the dorsal and medial cortical volumes), the dorsal cortex, and the medial cortex volumes in nissl- stained slides, as well as production of new neurons in the dorsal and medial cortices in doublecortin-stained slides. All methods have been previously optimized for this species (LaDage et al., 2009, 2013, 2016) and all coefficients of error were <0.10 (Gundersen et al., 1999).

For nissl-stained slides, the left and right hemispheres of the cortical regions and the remainder of the telencephalon were contoured on every section (**Figure 1**). Volumes were estimated with the Cavalieri procedure (Gundersen and Jensen, 1987) using a 200 μm grid for the cortical regions and a 300 μm grid for the remainder of the telencephalon. Because of the section thickness necessary for stereological estimations of doublecortin-positive cells, the high density of cells within the cell layers of the cortices rendered mature cell bodies indistinguishable (e.g., Ulinski, 1990). Consequently, performing unbiased stereological estimations of total number of neurons was not feasible.

New neuron counts were performed on the doublecortin-stained sections (**Figure 2**); the left and right hemispheres of the cortical regions were contoured and new neurons were counted exhaustively with the Optical Fractionator procedure (counting frame: 70 × 70 μm, grid: 70 μm, dissector height: 5 μm). All doublecortin-positive cells were counted including migrating fusiform cells typically aligned perpendicular to the ventricular zone as well as the more mature, spherical phenotype (e.g., Pérez-Cañellas and García-Verdugo, 1996; **Figure 3**). All slides were measured blind to treatment group and territorial identity. Due to histological artifacts, not all brain regions could be analyzed in all animals.

Statistical Methods

There were no differences between the left and right hemispheres for any of the measured variables (paired *t*-tests: all $p > 0.097$) thus data from the left and right hemispheres were summed and subsequent analyses were performed on the pooled data. Homogeneity of variances was assessed with Levene's test and, if the assumption was not met, data were either log or square root transformed to conform to the assumption ($p > 0.072$ for all variables after transformation). Using repeated-measures GLM, we tested for differences in weight and testosterone levels before and after implantation based on territorial predisposition and treatment. We assessed changes in the overall telencephalon volume using GLM with body mass as a covariate to ascertain the effects of territorial predisposition and treatment on overall brain size, outside of changes due to allometry. We also used GLM to assess the effects of territorial predisposition and treatment on the volumes of the dorsal and medial cortices, using remainder of the telencephalon volume as a covariate. Doing so assured that our results were specific to changes in the cortices of the telencephalon, rather than global changes in the brain. Finally, we also used GLM to assess the effects of territorial predisposition and treatment on the production of new neurons in the medial

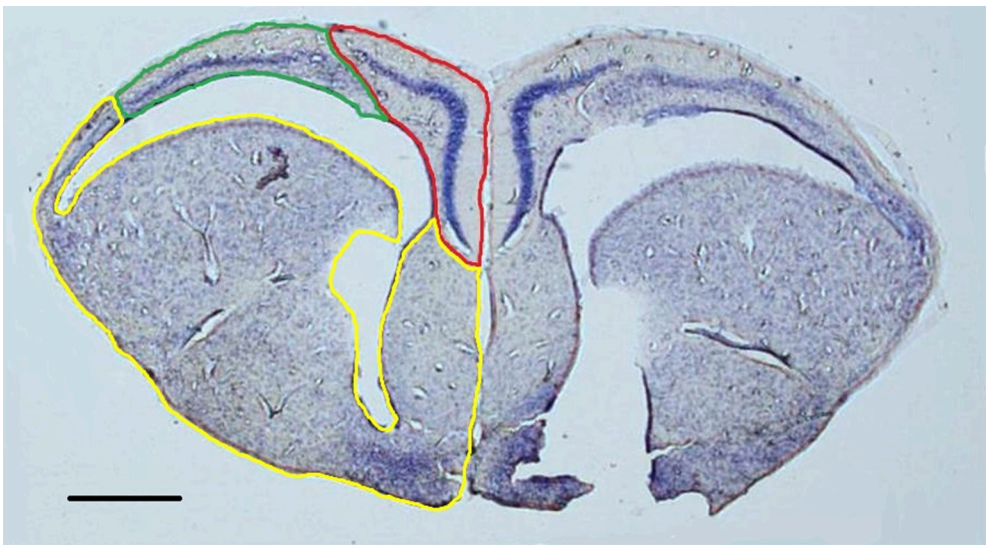

FIGURE 1 | Representative nissl-stained section (1.25x) with the medial cortex (red), dorsal cortex (green), and remainder of the telencephalon (yellow) outlined in the left hemisphere. Both hemispheres were contoured in order to construct volumetric estimations. Scale bar = 500 μm.

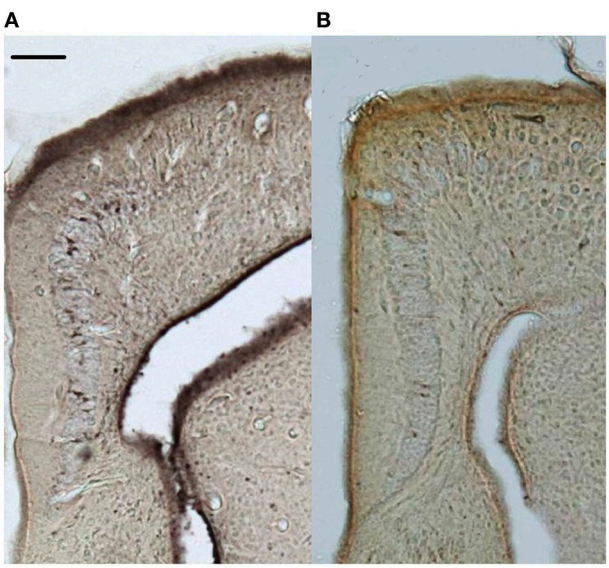

FIGURE 2 | Representative doublecortin-stained sections (5x) of the medial cortices from (A) control and **(B)** supplemented territorial male side-blotched lizards (*Uta stansburiana*). Scale bar = 100 μm.

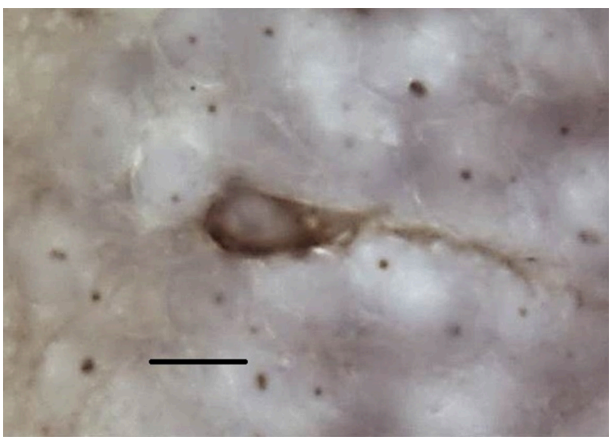

FIGURE 3 | Representative doublecortin-positive cell at 100x. Scale bar = 10 μm.

and dorsal cortices, with either dorsal or medial cortex volume as a covariate, essentially assessing new neuron density in these substructures (e.g., LaDage et al., 2013). We also performed analyses without covariates to ascertain any statistical differences when not controlling for the covariates. Testosterone levels did not correlate with changes in brain attributes so was not used as a covariate in the analyses (all $r^2 < 0.160$, $p > 0.081$). All analyses were conducted with SPSS for Windows, v. 21.0 (IBM Corp.) and we considered results to be statistically significant if $p < 0.05$.

RESULTS

There were no significant differences in weight before or after implantation between territorial and non-territorial males, control and treatment groups, nor a significant effect of the interaction [territorial predisposition: $F_{(1, 17)} = 0.292$, $p = 0.596$; treatment: $F_{(1, 17)} = 3.177$, $p = 0.093$; interaction: $F_{(1, 17)} = 0.871$, $p = 0.364$]. However, testosterone levels were significantly higher after implantation [$F_{(1, 17)} = 69.847$, $p < 0.001$] and higher in males who received testosterone implants [$F_{(1, 17)} = 157.321$, $p < 0.001$]; territorial predisposition and the interaction among time point, territorial predisposition, and treatment did not significantly affect testosterone levels [territorial predisposition: $F_{(1, 17)} = 0.106$, $p = 0.748$; interaction: $F_{(1, 17)} = 0.365$, $p = 0.554$] (**Figure 4**).

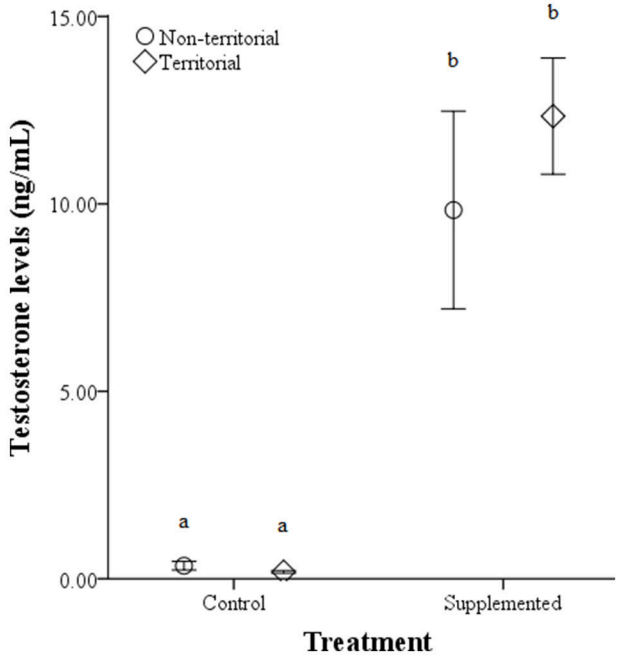

FIGURE 4 | Circulating testosterone levels (ng/mL) ± SEM in non-territorial (open circles) and territorial (diamonds) male side-blotched lizards (*Uta stansburiana*). Individuals were either subjected to testosterone implants (supplemented) or an empty vehicle (control) for 2 months. Implants were sufficient to raise testosterone levels similarly in non-territorial and territorial males. Different letters indicate statistically significant differences ($p \leq 0.05$).

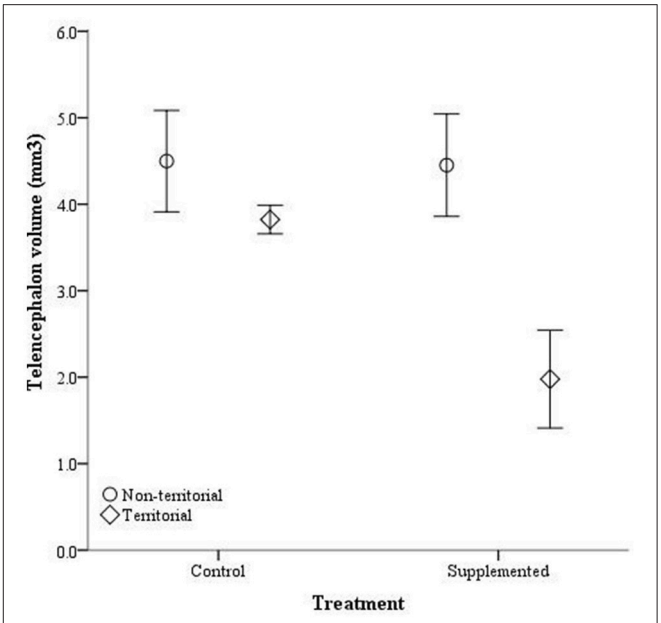

FIGURE 5 | Absolute telencephalon volume (mm^3) ± SEM in non-territorial (open circles) and territorial (diamonds) male side-blotched lizards (*Uta stansburiana*). Individuals were either subjected to testosterone implants (supplemented) or an empty vehicle (control) for 2 months. Supplemented territorial males had smaller telencephalons than any other group ($p = 0.013$).

After males were subjected to the experimental protocol, telencephalon volume, when controlled for variation in body weight, significantly differed based on the weight covariate [$F_{(1, 14)} = 6.60$, $p = 0.022$], territorial status [$F_{(1, 14)} = 16.061$, $p = 0.011$], and the interaction between territorial status and treatment [$F_{(1, 14)} = 4.728$, $p = 0.047$]; treatment was not significant [$F_{(1, 14)} = 2.905$, $p = 0.11$] (**Figure 5**). When excluding the body weight covariate in the analysis, we obtained comparable results [territorial status: $F_{(1, 15)} = 9.268$, $p = 0.008$; treatment: $F_{(1, 15)} = 3.347$, $p = 0.087$; interaction: $F_{(1, 15)} = 3.023$, $p = 0.013$]. When controlling for remainder of the telencephalon volume, we found that dorsal cortical volume was not significantly affected by the covariate [$F_{(1, 13)} = 0.573$, $p = 0.462$], territorial status [$F_{(1, 13)} = 0.015$, $p = 0.904$], treatment [$F_{(1, 13)} = 0.022$, $p = 0.886$], or the interaction [$F_{(1, 13)} = 134$, $p = 0.720$]; analyses without the covariate yielded similar results [territorial status: $F_{(1, 16)} = 0.484$, $p = 0.497$; treatment: $F_{(1, 16)} = 0.002$, $p = 0.963$; interaction: $F_{(1, 16)} = 0.627$, $p = 0.440$]. Medial cortical volume, when adjusted for volume of the remainder of the telencephalon, significantly differed based on the covariate [$F_{(1, 13)} = 7.418$, $p = 0.017$] but was not significantly affected by the other variables [territorial status: $F_{(1, 13)} = 0.285$, $p = 0.602$; treatment: $F_{(1, 13)} = 0.141$, $p = 0.741$; interaction: $F_{(1, 13)} = 4.235$, $p = 0.06$]. However, when volume of remainder of the telencephalon was not included as a covariate, there was a significant effect of territorial status [$F_{(1, 16)} = 5.505$, $p = 0.032$] and the interaction between territorial status and treatment [$F_{(1, 14)} = 7.635$, $p = 0.014$] on medial cortical volume; treatment alone was not significant [$F_{(1, 14)} = 0.587$, $p = 0.455$] (**Figure 6**).

The number of doublecortin-positive cells did not significantly differ in the dorsal cortex for any of the independent variables, either with dorsal cortical volume included as a covariate [dorsal cortex volume: $F_{(1, 14)} = 3.764$, $p = 0.074$; territorial status: $F_{(1, 14)} = 0.027$, $p = 0.872$; treatment: $F_{(1, 14)} = 1.203$, $p = 0.293$; interaction: $F_{(1, 14)} = 4.27$, $p = 0.059$] or without [territorial status: $F_{(1, 15)} = 0.063$, $p = 0.805$; treatment: $F_{(1, 15)} = 629$, $p = 0.440$; interaction: $F_{(1, 13)} = 3.726$, $p = 0.073$]. Similarly, the number of doublecortin-positive cells in the medial cortex, when medial cortical volume was included as a covariate, was not significantly affected by the covariate [$F_{(1,14)} = 0.067$, $p = 0.799$], territorial status [$F_{(1, 14)} = 3.780$, $p = 0.072$], treatment [$F_{(1, 14)} = 2.453$, $p = 0.140$], or the interaction between territorial status and treatment [$F_{(1, 14)} = 2.756$, $p = 0.119$]. However, when the covariate was not included, territorial status [$F_{(1, 16)} = 5.891$, $p = 0.027$] and the interaction between territorial status and treatment [$F_{(1, 16)} = 4.513$, $p = 0.05$] significantly affected the number of doublecortin-positive cells in the medial cortex while treatment alone was not a significant predictor [$F_{(1, 16)} = 2.586$, $p = 0.127$] (**Figure 7**).

DISCUSSION

The Effects of Testosterone on the Brain

We found that testosterone supplementation had a direct effect on brain attributes outside of differential environmental

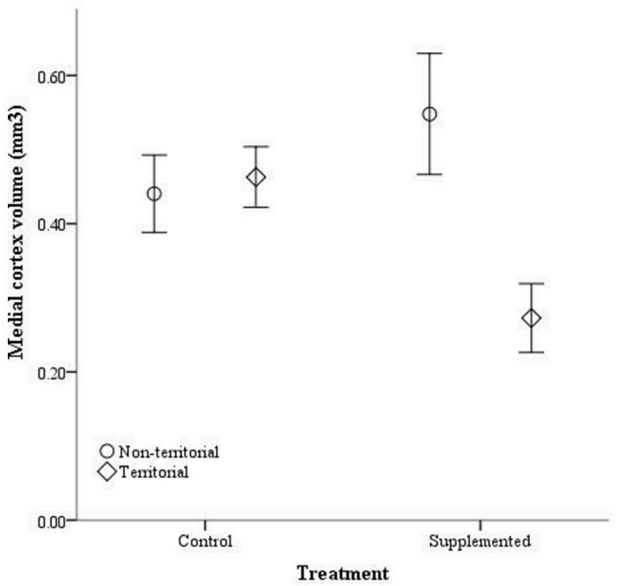

FIGURE 6 | Absolute medial cortex volume (mm^3) ± SEM in non-territorial (open circles) and territorial (diamonds) male side-blotched lizards (*Uta stansburiana*). Individuals were either subjected to testosterone implants (supplemented) or an empty vehicle (control) for 2 months. Supplemented territorial males had smaller medial cortices than any other group ($p = 0.014$).

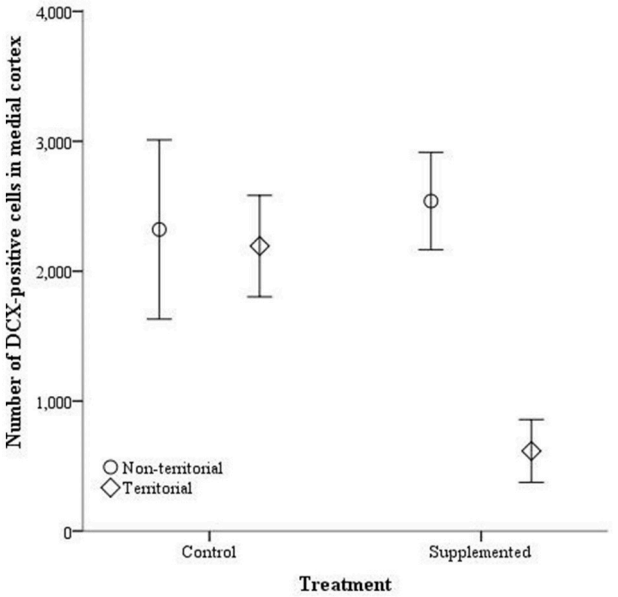

FIGURE 7 | The total number of doublecortin-positive cells in the medial cortex ± SEM in non-territorial (open circles) and territorial (diamonds) male side-blotched lizards (*Uta stansburiana*). Individuals were either subjected to testosterone implants (supplemented) or an empty vehicle (control) for 2 months. Supplemented territorial males had fewer doublecortin-positive cells in the medial cortex compared with the other groups ($p = 0.05$).

experiences. Two months after testosterone implantation, telencephalon volume, medial cortical volume, and the total number of doublecortin-positive cells in the medial cortex were downregulated in adult territorial males despite no concurrent change in spatial environmental experiences. Interestingly, controlling for the telencephalon volume in analyses of medial cortical volume and controlling for the medial cortical volume in the analyses of the total number of new neurons (which effectively analyses neuron density) rendered all analyses non-significant, suggesting that variation in absolute volume and the production of new neurons within the medial cortex is likely a product of proportional downregulation of neural attributes more globally across the entire telencephalon. There were no significant effects of elevated testosterone on any measurements of the dorsal cortex, regardless of covariate inclusion or exclusion in the analyses.

Although we determined that testosterone can directly modulate medial cortical attributes, it was not in the direction predicted. Many studies, primarily in rodent and bird models, have demonstrated that increased testosterone levels upregulate volume and neurogenesis in certain brain regions. For instance, seasonal changes in testosterone have been positively correlated with changes in brain attributes (e.g., Rasika et al., 1994; Galea et al., 2006) and reproductively active males demonstrate increased new neuron survival compared with reproductively inactive males (e.g., Ormerod and Galea, 2003), both of which suggest that testosterone may be one potential mechanism directly and positively regulating brain attributes. Experimental evidence tends to support the positive correlation between testosterone and brain plasticity; testosterone supplementation has been associated with increased volume and survival of new neurons in particular brain regions (Rasika et al., 1994; Alvarez-Buylla and Kirn, 1997; Galea et al., 1999, 2006, 2008, 2013; Absil et al., 2003; Spritzer and Galea, 2007; Galea, 2008; Balthazart and Ball, 2016). However, some studies have found that testosterone supplementation has no effect on neurogenesis (Pfau et al., 2010; Zhang et al., 2010; Carrier and Kabbaj, 2012) and, in some cases, testosterone suppresses neurogenesis (Brannvall et al., 2005; Estrada et al., 2006; Buwalda et al., 2010; Allen et al., 2014).

Although these results are seemingly contradictory, methodological factors may contribute to the discordance. For instance, Hamson et al. (2013) suggested that, in rodent models, testosterone's positive effects on hippocampal neurogenesis may occur between 16 and 30 days, whereas elevated testosterone exposure outside of that window may have detrimental effects, indicating that testosterone supplementation may have differential effects based on the duration of exposure (Buwalda et al., 2010; Spritzer et al., 2011). Further, the effects of testosterone supplementation can be dependent on dosage (e.g., Galea et al., 1999), route of administration (e.g., injection, implants), timing of supplementation vs. application of an exogenous neurogenesis marker (Spritzer and Galea, 2007; Allen et al., 2014), interact with environmental cues/seasonality (e.g., Moore, 1988; Bernard and Ball, 1997; O'Bryant and Wilczynski, 2010), and may differ based on species (e.g., Powers, 2016). Previous studies have used testosterone supplementation that was shorter in duration (<2 months) and no previous

study has used a reptilian species to examine the effects of testosterone on neurogenesis. Further, our study utilized doublecortin, an endogenous marker that generates a combined measure of proliferation and survival (Rao and Shetty, 2004), precluding separation of the two. Our study confirmed that testosterone supplementation caused a decrease in doublecortin expression in territorial males but testosterone may have downregulated neuronal proliferation while not affecting, or even positively affecting, neuron survival. Utilization of an exogenous label, such as BrdU, and sacrificing at various time points would allow for detangling the contribution of cellular proliferation vs. survival rates to overall neurogenesis rates. Alternatively, utilization of an endogenous marker expressed only during proliferation would elucidate the effects of testosterone exclusively on the proliferative stage of neurogenesis. Because our and previous studies differ on many of the aforementioned methodological components, generalizability of the effects of testosterone on the brain remains equivocal.

Interestingly, while testosterone supplementation within the laboratory setting was sufficient to elevate testosterone levels and induce neural plasticity, testosterone levels are at least four times higher in the field than what we found in the current study (average 48–203 ng/mL in the field [variation based on morphotype and season, Sinervo et al., 2000] vs. average 11.3 ng/mL in supplemented individuals in the current study). Further, previous literature suggests that our implants should have elevated and maintained testosterone at physiologically-relevant levels in this species (DeNardo and Licht, 1993; DeNardo and Sinervo, 1994). However, our study differed in that our supplementation treatment lasted 2 months; no previous studies in this species have examined supplemented hormone levels past 1 month thus the effects of longer-term supplementation are unknown. Additionally, in ectothermic taxonomic groups, individuals subjected to higher temperatures are thought to clear testosterone quicker (e.g., Pearson et al., 1976; Krohmer et al., 1987). We maintained ideal thermoregulatory conditions within the laboratory; temperatures were consistent from day to day and basking temperatures were higher than the average temperatures at the field site for April and May. Thus, it is possible that the higher average temperatures found in the laboratory were sufficient to clear the supplemented testosterone faster in our animals. Alternatively, but unlikely, all of our implants could have released large amount of testosterones very early while releasing less toward the end of the treatment. While we could have taken blood samples more frequently to assess testosterone levels throughout the 2 month experimental time frame, oversampling would have induced stress in our animals which is a strong down regulator of neurogenesis (e.g., Schoenfeld and Gould, 2012). Regardless of the consistency of testosterone release, the testosterone levels were significantly higher in implanted animals at the end of our 2 month treatment indicating that the implants were functional. Altering methodological protocol to artificially elevate testosterone levels to that seen in the field should be essential for future studies; doing so may yield different results that found in the current study.

Considering that we did not castrate our subjects, endogenous levels of testosterone should have also contributed to overall circulating levels of testosterone. However, environmental components, particularly in the laboratory, can affect homeostatic control of testosterone levels. For instance, previous studies have found that endogenous testosterone levels are typically lower in laboratory-reared species, including reptiles, and this may be due to environmental factors in the laboratory that differ from those in the field (e.g., Callard et al., 1976; Licht et al., 1985; Krohmer et al., 1987; Moore et al., 1991; Soto-Gamboa et al., 2005; Calisi and Bentley, 2009). Changes in day length have often been shown to be important in inducing changes in testosterone levels, reproductive physiology, and behavior, particularly in the laboratory (e.g., Wingfield and Kenagy, 1991). However, our changes in day length mimicked ambient and thus was likely not the modulator of these differences. Further, many reptiles do not demonstrate reproductive responses to changes in photoperiod (e.g., Ferrell, 1984; Moore et al., 1984). Temperature appears to be more important to changes in reproductive physiology (e.g., Pearson et al., 1976; Krohmer et al., 1987) and we maintained temperatures that should have been ideal for upregulating testosterone production. An alternative possibility is that our subjects were not allowed social interactions during the protocol yet social interactions are important modulators of androgen levels in this species (Wingfield et al., 1990). Males in our study were raised in isolation while males in the field typically engage in agonistic interactions with other males and come in contact with many females during the breeding season (e.g., Zamudio and Sinervo, 2000). Because of the lack of opportunity for territorial and reproductive behaviors in our study, we would expect testosterone levels to be much lower than those found in the field. While it is unclear what caused either a downregulation in testosterone after the 2 months treatment or did not allow supplementation to achieve levels seen in the field, even a modest elevation of testosterone within the laboratory setting was still sufficient to downregulate telencephalon volume, medial cortex volume, and neurogenesis in supplemented territorial males. It is not, however, unreasonable to expect that testosterone levels that more closely parallel levels in the field would have more dramatic effects on neural attributes.

While testosterone downregulated cortical attributes in the medial cortex of territorial males, it had no effect on any of the measured neural attributes in the dorsal cortex, whether the covariate was included or not, suggesting that the effects of testosterone may be region-specific. In support of this, previous studies have found that testosterone differentially modulates volume in different brain regions in birds and lizards (Balthazart et al., 2008; Small et al., 2015; Wilson, 2015; Balthazart and Ball, 2016) and only increases cell proliferation in the ventricular zone in canaries (Barker et al., 2014) and the amygdala in rodents (Fowler et al., 2003). While both the medial and dorsal cortices are involved with spatial cognition, they serve slightly different functions—the medial cortex concerns spatial learning and the dorsal cortex is involved in spatial mapping (Grisham and Powers, 1990; Petrillo et al., 1994; Reiman Avigan and Schade Powers, 1995; Rodríguez et al., 2002; López et al., 2003). This

suggests that the effects of testosterone could differ based on structural and functional differences between the medial and dorsal cortices. Further, the medial and dorsal cortices vary in the absolute number of new neurons as well as modulation of new neuron production rates. More new neurons are produced and incorporated into the medial cortex (Font et al., 2002) and spatial use experiences only upregulate new neuron production in the medial cortex (LaDage et al., 2013). Thus, while steroid hormones can cross the blood-brain barrier, certain regions of the brain, particularly in regions demonstrating more plasticity, may be more susceptible to testosterone and other hormonal influences.

The effects of testosterone on the brain has been shown to occur through an androgen-specific mechanism (e.g., Spritzer and Galea, 2007), possibly through androgen receptors (ARs) (e.g., Galea, 2008). Nuclear ARs are commonly found in areas associated with reproductive behavior (e.g., Simerly et al., 1990). Some other areas of the brain, including the cortices in lizards, are also AR-immunoreactive suggesting that testosterone could possibly have a direct effect on brain attributes in these regions as well (e.g., Simerly et al., 1990; Clancy et al., 1992; Young et al., 1994; Moga et al., 2000; Rosen et al., 2002; Sarkey et al., 2008). In a recent study, Hamson et al. (2013) demonstrated that the survival of new neurons in the mammalian dentate gyrus can be regulated by testosterone and that this occurs via ARs. However, new neurons in the dentate gyrus did not express ARs suggesting that testosterone indirectly modulates neurogenesis in this area, possible via other hippocampal regions that contain high densities of ARs and are known to have regulatory effects on neurogenesis (Hamson et al., 2013). Interestingly, Brannvall et al. (2005) also demonstrated that androgens act through ARs to modulate neurogenesis but, unlike the previous study, they found that neural stem cells within the dentate gyrus did express ARs, suggesting a possible direct effect of testosterone on proliferating cells in that area. Unfortunately, their methodology precluded identification of these cells as neurons or glia. Thus, while testosterone is correlated with neurogenesis, it is still equivocal if the effect of testosterone is direct and mediated through ARs on new neurons. Testosterone could also have indirect effects as it can be converted to estradiol and several other reduced androgens. Thus, the effect of testosterone could be quite broad and mediated through other signaling mechanisms that could affect neurogenesis and other neural attributes (e.g., Rasika et al., 1999; Harley et al., 2000; Smith et al., 2002; Hebbard et al., 2003; MacLusky et al., 2006; Hamson et al., 2013; Allen et al., 2014).

Territorial Predisposition Modulates the Relationship between Testosterone and the Brain

In some species, males that adopt alternative mating strategies also have variation in testosterone levels that can differently organize or activate the nervous system (e.g., Marler et al., 1999; Rhen and Crews, 2002; Aubin-Horth et al., 2005; Crews and Moore, 2005; Bass and Forlano, 2008; Schunter et al., 2014). While we found that testosterone implants elevated testosterone levels similarly between territorial and non-territorial males, testosterone-implanted non-territorial males demonstrated no detectable changes in cortical attributes when compared with control groups while supplemented territorial males downregulated cortical attributes. Thus, testosterone supplementation appears to differentially affect males contingent upon territorial predisposition, despite territorial and non-territorial males having similar beginning and end testosterone levels. In the field, territorial predisposition, testosterone, and spatial area use co-vary; territorial males have naturally elevated testosterone levels compared with non-territorial males (Sinervo et al., 2000) and testosterone is associated with increased activity and home range size (e.g., DeNardo and Sinervo, 1994; Sinervo et al., 2000). Also, previous studies in this species have determined that territorial predisposition modulates the differential effects of testosterone on other physiological measures. For instance, increasing testosterone increases endurance and sprint speed in non-territorial but not territorial males suggesting that territorial males are at their physiological limits for these variables (Mills et al., 2008). Also, our previous work demonstrated that increasing spatial area use increased rates of neurogenesis in territorial males but not in non-territorial males (LaDage et al., 2013). Thus, territorial predisposition correlates with differences in a variety of physiological measures including neural plasticity.

Other physiological factors, such as differences in homeostatic mechanisms, target tissue response, or synergy with other hormones may also contribute to the differential morphotypic modulation of neural attributes, yet it is still unclear how these factors interact with testosterone and morphotype to produce the neural phenotype. For example, Knapp (2003) proposed that non-territorial morphs may be insensitive to testosterone relative to territorial males due to fewer androgen receptors, which would support our results that non-territorial males did not differ from controls despite having elevated testosterone levels. This explanation, however, does not explain reduced neural attributes in territorial males. An alternative explanation, but not mutually exclusive, concerns testosterone and its possible morphotypic-specific interactions with other hormones. Testosterone and social behaviors demonstrate a reciprocal positive relationship with each other but an increase in both also correlates with increased glucocorticoid release, presumably to mobilize energy stores for reproductive behaviors (e.g., Emerson and Hess, 2001; Moore and Jessop, 2003; Wilczynski et al., 2005). However, chronically high levels of glucocorticoids can subsequently suppress testosterone and social behaviors, likely for energy recovery (e.g., Emerson and Hess, 2001). Previous studies have also demonstrated that the relationship between testosterone and glucocorticoids can also be modulated by territorial status. In tree lizards (*Urosaurus ornatus*), both territorial and non-territorial males increase glucocorticoids in response to a stressor. However, only non-territorial males demonstrated a concurrent decrease in testosterone, indicating different downstream homeostatic responses to elevated glucocorticoids (Knapp and Moore, 1995, 1996, 1997). In rodent models, high levels of glucocorticoids strongly downregulate hippocampal neurogenesis (reviewed in Schoenfeld and Gould, 2012; Saaltink and Vreugdenhil,

2014), thus there may be a link among increased testosterone, increased glucocorticoids, and decreased neurogenesis and this may be modulated by territorial predisposition. Territorial and non-territorial males may differ in sensitivity to elevated levels of glucocorticoids, possibly via differential expression of glucocorticoid receptors or differences in homeostatic stress reactivity (e.g., LaDage, 2015), which would in turn differentially modulate rates of neurogenesis. In the current study, if increased testosterone concurrently increased glucocorticoids and if territorial males were unable to downregulate glucocorticoids in the face of constantly elevated testosterone while non-territorial males could, it would not be surprising that territorial males demonstrated downregulated neural attributes while non-territorial males did not. However, we did not measure circulating glucocorticoid levels or glucocorticoid receptor expression therefore the relationship between testosterone, glucocorticoids, and the brain remains to be tested.

CONCLUSIONS

We found that supplementing testosterone, outside of variation in spatial use experiences, was sufficient to directly downregulate telencephalon volume, medial cortical volume and neurogenesis. Analyses controlling for the overall telencephalon or medial cortex volumes indicated that medial cortical volume and neurogenesis may correlate with more global downregulated changes in the brain as the densities of new neurons were not different between treatment and control while the total numbers were. Overall, these results are counter to previous studies in rodents demonstrating that testosterone upregulates neural attributes but this discrepancy could be a result of methodology differences. As of now, there is a paucity of literature on the effects of testosterone on the hippocampus, particularly in non-model species (e.g., Powers, 2016), thus precluding meaningful generalizations at this point. Interestingly, downregulation of cortical attributes was only seen in territorial males indicating that territorial predisposition can modulate the effects of testosterone on the brain. Although morphotypes may demonstrate similar levels of testosterone, they may differ in response to such (e.g., Moore, 1988; Baird and Hews, 2007) leading to morphotypic variation in neuroendocrine pathways, downstream physiological effects, and subsequent behaviors (e.g., Knapp, 2003). Presumably, morphotypic-specific responses to testosterone are based on naturally selected behaviors and life histories that confer differential fitness benefits for morphotypes (e.g., Crews and Moore, 2005).

Studies that examine the mechanistic basis of the effects of testosterone on the brain could elucidate if testosterone, estradiol, and reduced androgens act directly, through ARs on new neurons, or indirectly to control the production and survival of new neurons as well as other forms of brain plasticity. From a functional perspective, it is still unknown if testosterone is sufficient to induce differences in spatial memory ability between territorial and non-territorial males and, if so, whether neurogenesis is a necessary process used to encode those spatial memories. Similarly, differential spatial use or social experiences may also induce changes in brain plasticity differently than that found in studies that constrain those experiences. Ultimately, the current study underscores the importance of understanding how naturally-selected morphotypic differences in the neuroendocrine axis may alter neural plasticity in ways that could not be predicted from clinical studies in rodent models. Understanding the interplay among circulating hormones, spatial use, and polymorphic differences would aid our understanding of the control and functional significance of neurogenesis and other forms of brain plasticity.

AUTHOR CONTRIBUTIONS

LL, VP, and BS designed the experiments. LL, TR, and CD performed the experiments. LL performed the immunohistochemistry and stereology. LL, TR, and VP analyzed and interpreted the data. LL drafted the paper and all authors critically reviewed, revised, and approved the final version of the paper.

FUNDING

This research was supported by a National Science Foundation award to LL, VP, and BS (IOS-0918268). VP was also supported by the National Science Foundation award (IOS-1351295).

ACKNOWLEDGMENTS

We thank K. Kappes and F. Gonzalez for assistance in data collection. We would also like to thank Drs. Amrein and Bonfanti for this timely research topic on neurogenesis in non-model species.

REFERENCES

Absil, P., Pinxten, R., Balthazart, J., and Eens, M. (2003). Effect of age and testosterone on autumnal neurogenesis in male European starlings (*Sturnus vulgaris*). *Behav. Brain Res.* 143, 15–30. doi: 10.1016/S0166-4328(03)00006-8

Allen, K. M., Fung, S. J., Rothmond, D. A., Noble, P. L., and Weickert, C. S. (2014). Gonadectomy increases neurogenesis in the male adolescent rhesus macaque hippocampus. *Hippocampus* 24, 225–238. doi: 10.1002/hipo.22217

Alvarez-Buylla, A., and Kirn, J. R. (1997). Birth, migration, incorporation, and death of vocal control neurons in adult songbirds. *J. Neurobiol.* 33, 585–601.

Amrein, I., Slomianka, L., Poletaeva, I. I., Bologova, N. V., and Lipp, H.-P. (2004). Marked species and age-dependent differences in cell proliferation and neurogenesis in the hippocampus of wild-living rodents. *Hippocampus* 14, 1000–1010. doi: 10.1002/hipo.20018

Aubin-Horth, N., Landry, C. R., Letcher, B. H., and Hofmann, H. A. (2005). Alternative life histories shape brain gene expression profiles in males of the same population. *Proc. R. Soc. Lond. B Biol. Sci.* 272, 1655–1662. doi: 10.1098/rspb.2005.3125

Baird, T. A., and Hews, D. K. (2007). Hormone levels in territorial and non-territorial male collared lizards. *Physiol. Behav.* 92, 755–763. doi: 10.1016/j.physbeh.2007.05.069

Balthazart, J., and Ball, G. F. (2016). Endocrine and social regulation of adult neurogenesis in songbirds. *Front. Neuroendocrinol.* 41, 3–22. doi: 10.1016/j.yfrne.2016.03.003

Balthazart, J., Boseret, G., Konkle, A. T., Hurley, L. L., and Ball, G. F. (2008). Doublecortin as a marker of adult neuroplasticity in the canary song control nucleus HVC. *Eur. J. Neurosci.* 27, 801–817. doi: 10.1111/j.1460-9568.2008.06059.x

Barker, J. M., Ball, G. F., and Balthazart, J. (2014). Anatomically discrete sex differences and enhancement by testosterone of cell proliferation in the telencephalic ventricle zone of the adult canary brain. *J. Chem. Neuroanat.* 55, 1–8. doi: 10.1016/j.jchemneu.2013.10.005

Bass, A. H., and Forlano, P. M. (2008). "Neuroendocrine mechanisms of alternative reproductive tactics: the chemical language of reproductive and social plasticity," in *Alternative Reproductive Tactics: An Integrative Approach*, eds R. F. Oliveira, M. Taborsky, and H. J. Brockmann (Cambridge: Cambridge University Press), 109–131.

Bee, M. A., and Gerhardt, H. C. (2001). Neighbour-stranger discrimination by territorial male bullfrogs (*Rana catesbeiana*): II. Perceptual basis. *Anim. Behav.* 62, 1141–1150. doi: 10.1006/anbe.2001.1852

Bernard, D. J., and Ball, G. F. (1997). Photoperiodic condition modulates the effects of testosterone on song control nuclei volumes in male European starlings. *Gen. Comp. Endocrinol.* 105, 276–283. doi: 10.1006/gcen.1996.6829

Brannvall, K., Bogdanovic, N., Korhonen, L., and Lindholm, D. (2005). 19-Nortestosterone influences neural stem cell proliferation and neurogenesis in the rat brain. *Eur. J. Neurosci.* 21, 871–878. doi: 10.1111/j.1460-9568.2005.03942.x

Brown, J. P., Couillard-Despres, S., Cooper-Kuhn, C. M., Winkler, J., Aigner, L., and Kuhn, H. G. (2003). Transient expression of doublecortin during adult neurogenesis. *J. Comp. Neurol.* 467, 1–10. doi: 10.1002/cne.10874

Buchanan, K. L., and Goldsmith, A. R. (2004). Noninvasive endocrine data for behavioural studies: the importance of validation. *Anim. Behav.* 67, 183–185. doi: 10.1016/j.anbehav.2003.09.002

Butler, A. B. (1976). Telencephalon of the lizard *Gekko gecko*: some connections of the cortex and dorsal ventricular ridge. *Brain Behav. Evol.* 13, 396–417 doi: 10.1159/000123824

Butler, A. B. (1994). The evolution of the dorsal pallium in the telencephalon of amniotes: cladistic analysis and a new hypothesis. *Brain Res. Rev.* 19, 66–101. doi: 10.1016/0165-0173(94)90004-3

Buwalda, B., van der Borght, K., Koolhass, J. M., and McEwen, B. S. (2010). Testosterone decrease does not play a major role in the suppression of hippocampal cell proliferation following social defeat stress in rats. *Physiol. Behav.* 101, 719–725. doi: 10.1016/j.physbeh.2010.08.010

Calisi, R. M., and Bentley, G. E. (2009). Lab and field experiments: are they the same animals? *Hormones Behav.* 56, 1–10. doi: 10.1016/j.yhbeh.2009.02.010

Callard, I. P., Callard, G. V., Lance, V., and Eccles, S. (1976). Seasonal changes in testicular structure and function and the effects of gonadotropins in the freshwater turtle, *Chrysemys picta*. *Gen. Comp. Endocrinol.* 30, 535–536. doi: 10.1016/0016-6480(76)90086-1

Carrier, N., and Kabbaj, M. (2012). Extracellular signal-regulated kinase 2 signaling in the hippocampal dentate gyrus mediates the antidepressant effects of testosterone. *Biol. Psych.* 71, 642–651. doi: 10.1016/j.biopsych.2011.11.028

Clancy, A. N., Bonsall, R. W., and Michael, R. P. (1992). Immunohistochemical labeling of androgen receptors in the brain of rat and monkey. *Life Sci.* 50, 409–417. doi: 10.1016/0024-3205(92)90375-Y

Clint, E. K. (2012). Male superiority in spatial navigation: adaptation or side effect? *Q. Rev. Biol.* 87, 289–313. doi: 10.1086/668168

Cooke, B., Hegstrom, C. D., Villeneuve, L. S., and Breedlove, S. M. (1998). Sexual differentiation of the vertebrate brain: principles and mechanisms. *Front. Neuroendocrinol.* 19, 323–362. doi: 10.1006/frne.1998.0171

Couillard-Despres, D., Winner, B., Schaubeck, S., Aigner, R., Vroemen, M., Weidner, N., et al. (2005). Doublecortin expression levels in adult brain reflect neurogenesis. *Eur. J. Neurosci.* 21, 1–14. doi: 10.1111/j.1460-9568.2004.03813.x

Crews, D., and Moore, M. C. (2005). Historical contributions of research on reptiles to behavioral neuroendocrinology. *Hormones Behav.* 48, 384–394. doi: 10.1016/j.yhbeh.2005.04.003

Delgado-Gonzalez, F. J., Gonzalez-Granero, S., Trjillo-Trujillo, C. M., Garcia-Verdugo, J. M., and Damas-Hernandez, M. C. (2011). Study of adult neurogenesis in the *Gallotia galloti* lizard during different seasons. *Brain Res.* 1390, 50–58. doi: 10.1016/j.brainres.2011.03.027

DeNardo, D. F., and Licht, P. (1993). Effects of corticosterone on social behavior of male lizards. *Hormones Behav.* 27, 184–199. doi: 10.1006/hbeh.1993.1014

DeNardo, D. F., and Sinervo, B. (1994). Effects of steroid hormone interaction on activity and home-range size of male lizards. *Hormones Behav.* 28, 273–287. doi: 10.1006/hbeh.1994.1023

Emerson, S. B., and Hess, D. L. (2001). Glucocorticoids, androgens, testis mass, and the energetics of vocalization in breeding male frogs. *Hormones Behav.* 39, 59–69. doi: 10.1006/hbeh.2000.1635

Estrada, M., Varshney, A., and Ehrlich, B. E. (2006). Elevated testosterone induces apoptosis in neuronal cells. *J. Biol. Chem.* 281, 25492–25501. doi: 10.1074/jbc.M603193200

Falls, J. B. (1982). "Individual recognition by sounds in birds," in *Acoustic communication in Birds*, eds D. E. Kroodsma and E. H. Miller (New York, NY: Academic Press), 237–278.

Ferguson, G. W., and Fox, S. F. (1984). Annual variation of survival advantage of large juvenile side-blotched lizards, *Uta stansburiana*: its causes and evolutionary significance. *Evolution* 38, 342–349. doi: 10.2307/2408492

Ferrell, B. R. (1984). Photoperiodism in the lizard, *Anolis carolinensis*. *Comp. Physiol. Biochem.* 232, 19–27. doi: 10.1002/jez.1402320104

Font, E., Desfilis, E., Pérez-Cañellas, M. M., and Garcia-Verdugo, J. M. (2002). Neurogenesis and neuronal regeneration in the adult reptilian brain. *Brain Behav. Evol.* 58, 276–295. doi: 10.1159/000057570

Fowler, C. D., Freeman, M. E., and Wang, Z. (2003). Newly proliferated cells in the adult male amygdala are affected by gonadal steroid hormones. *J. Neurobiol.* 57, 257–269. doi: 10.1002/neu.10273

Galea, L. A. (2008). Gonadal hormone modulation of neurogenesis in the dentate gyrus of adult male and female rodents. *Brain Res. Rev.* 57, 332–341. doi: 10.1016/j.brainresrev.2007.05.008

Galea, L. A., and McEwen, B. S. (1999). Sex and seasonal changes in the rate of cell proliferation in the dentate gyrus of adult wild meadow voles. *Neuroscience* 89, 955–964. doi: 10.1002/hipo.20154

Galea, L. A. M., Perrot-Sinal, T. S., Kavaliers, M., and Ossenkopp, K.-P. (1999). Relations of hippocampal volume and dentate gyrus width to gonadal hormone levels in male and female meadow voles. *Brain Res.* 821, 383–391. doi: 10.1016/S0006-8993(99)01100-2

Galea, L. A., Spritzer, M. D., Barker, J. M., and Pawluski, J. L., (2006). Gonadal hormone modulation of hippocampal neurogenesis in the adult. *Hippocampus* 16, 225–232. doi: 10.1002/hipo.20154

Galea, L. A. M., Uban, K. A., Epp, J. R., Brummelte, S., Barha, C. K., Wilson, W. L., et al. (2008). Endocrine regulation of cognition and neuroplasticity: our pursuit to unveil the complex interaction between hormones, the brain, and behavior. *Can. J. Exp. Psychol.* 62, 247–260. doi: 10.1037/a0014501

Galea, L. A., Wainwright, S. R., Roes, M. M., Duarte-Guteman, P., Chow, C., and Hamson, D. K. (2013). Sex, hormones and neurogenesis in the hippocampus: hormonal modulation of neurogenesis and potential functional implications. *J. Neuroendocrinol.* 25, 1039–1061. doi: 10.1111/jne.12070

Gaulin, S. J. C., and Fitzgerald, R. W. (1986). Sex differences in spatial ability: an evolutionary hypothesis and test. *Am. Nat.* 127, 74–88. doi: 10.1086/284468

Gaulin, S. J. C., and Fitzgerald, R. W. (1989). Sexual selection for spatial-learning ability. *Anim. Behav.* 37, 322–331. doi: 10.1016/0003-3472(89)90121-8

Godard, R. (1991). Long-term memory of individual neighbours in a migratory songbird. *Nature* 350, 228–229. doi: 10.1038/350228a0

Gould, E., Woolley, C. S., and McEwen, B. S. (1990). Short-term glucocorticoid manipulations affect neuronal morphology and survival in the adult dentate gyrus. *Neuroscience* 37, 367–375. doi: 10.1016/0306-4522(90)90407-U

Grisham, W., and Powers, A. S. (1990). Effects of dorsal and medial cortex lesion on reversals in turtles. *Physiol. Behav.* 47, 43–49. doi: 10.1016/0031-9384(90)90040-B

Gundersen, H. J., Jensen, E. B., Kieu, K., and Nielsen, J. (1999). The efficiency of systematic sampling in stereology–reconsidered. *J. Microscopy* 193, 199–211. doi: 10.1046/j.1365-2818.1999.00457.x

Gundersen, H. J., and Jensen, E. B. (1987). The efficacy of systematic sampling in stereology and its predictions. *J. Microscopy* 147, 229–263. doi: 10.1111/j.1365-2818.1987.tb02837.x

Hairston, I. S., Little, M. T., Scanlon, M. D., Barakat, M. T., Palmer, T. D., Sapolsky, R. M., et al. (2005). Sleep restriction suppresses neurogenesis by hippocampus-dependent learning. *J. Neurophysiol.* 94, 4224–4233. doi: 10.1152/jn.00218.2005

Hamson, D. K., Wainwright, S. R., Taylor, J. R., Jones, B. A., Watson, N. V., and Galea, L. A. (2013). Androgens increase survival of adult-born neurons in the dentate gyrus by an androgen receptor-dependent mechanism in male rats. *Endocrinology* 154, 3294–3304. doi: 10.1210/en.2013-1129

Harley, C. W., Malsbury, C. W., Squires, A., and Brown, R. A. (2000). Testosterone decreases CA1 plasticity *in vivo* in gonadectomized male rates. *Hippocampus* 10, 693–697. doi: 10.1002/1098-1063(2000)10:6<693::AID-HIPO1007>3.0.CO;2-G

Hebbard, P. C., King, R. R., Malsbury, C. W., and Harley, C. W. (2003). Two organizational effects of pubertal testosterone in male rats: transient social memory and a shift away from long-term potentiation following a tetanus in hippocampal CA1. *Exp. Neurol.* 182, 470–475. doi: 10.1016/S0014-4886(03)00119-5

Holding, M. L., Frazier, J. A., Taylor, E. N., and Strand, C. R. (2012). Experimentally altered navigational demands induce changes in the cortical forebrain of free-ranging norther pacific rattlesnakes (*Crotalus o. oreganus). Brain Behav. Evol.* 79, 144–154. doi: 10.1159/000335034

Jacobs, L. F., Gaulin, S. J., Sherry, D. F., and Hoffman, G. E. (1990). Evolution of spatial cognition: sex-specific patterns of spatial behavior predict hippocampal size. *Proc. Natl. Acad. Sci. U.S.A.* 87, 6349–6352. doi: 10.1073/pnas.87.16.6349

Ketterson, E. D., Nolan, V., Cawthorn, M. J., Parker, P. G., and Ziegenfus, C. (1996). Phenotypic engineering: using hormones to explore the mechanistic and function bases of phenotypic variation in nature. *Ibis* 138, 70–86. doi: 10.1111/j.1474-919X.1996.tb04769.x

Knapp, R. (2003). Alternative reproductive tactics: the next generation of studies. *Int. Comp. Biol.* 43, 658–668. doi: 10.1093/icb/43.5.658

Knapp, R., and Moore, M. C. (1995). Hormonal responses to aggression vary in different types of agonistic encounters in male tree lizards, *Urosaurus ornatus. Hormones Behav.* 29, 85–105. doi: 10.1006/hbeh.1995.1007

Knapp, R., and Moore, M. C. (1996). Male morphs in tree lizards, *Urosaurus ornatus*, have different delayed hormonal responses to aggressive encounters. *Anim. Behav.* 52, 1045–1055. doi: 10.1006/anbe.1996.0251

Knapp, R., and Moore, M. C. (1997). Male morphs in tree lizards have different testosterone responses to elevated levels of corticosterone. *Gen. Comp. Endocrinol.* 107, 273–279. doi: 10.1006/gcen.1997.6923

Krohmer, R. W., Grassman, M., and Crews, D. (1987). Annual reproductive cycle in the male red-sided garter snake, *Thamnophis sirtalis parietalis*: Field and laboratory studies. *Gen. Comp. Endocrinol.* 68, 64–75. doi: 10.1016/0016-6480(87)90061-X

LaDage, L. D. (2015). Environmental change, the stress response, and neurogenesis. *Int. Comp. Biol.* 55, 372–383. doi: 10.1093/icb/icv040

LaDage, L. D. (2016). Factors that modulate neurogenesis: a top-down approach. *Brain Behav. Evol.* 87, 184–190. doi: 10.1159/000446906

LaDage, L. D., Maged, R. M., Forney, M. V., Roth, T. C., Sinervo, B., and Pravosudov, V. V. (2013). Interaction between territoriality, spatial environment, and hippocampal neurogenesis in male side-blotched lizards. *Behav. Neurosci.* 127, 555–565. doi: 10.1037/a0032852

LaDage, L. D., Riggs, B. J., Sinervo, B., and Pravosudov, V. V. (2009). Dorsal cortex volume in male side-blotched lizards, *Uta stansburiana*, is associated with different space use strategies. *Anim. Behav.* 78, 91–96. doi: 10.1016/j.anbehav.2009.03.020

LaDage, L. D., Roth, T. C., Sinervo, B., and Pravosudov, V. V. (2016). Environmental experiences influence cortical volume in territorial and non-territorial side-blotched lizard, *Uta stansburiana*. *Anim. Behav.* 115, 11–18. doi: 10.1016/j.anbehav.2016.01.029

Licht, P., Breitenbach, G. L., and Congdon, J. D. (1985). Sreasonal cycles in testicular activity, gonadotropin, and thyroxine in the painted turtle, *Chrysemys picta*, under natural conditions. *Gen. Comp. Endocrinol.* 59, 130–139.

Lopez-Garcia, C., Molowny, A., Garcia-Verdugo, J. M., Martinez-Guijarro, F. J., and Bernabeu, A. (1990). Late generated neurons in the medial cortex of adult lizards send axons that reach the Timm-reactive zones. *Dev. Brain Res.* 57, 249–254. doi: 10.1016/0165-3806(90)90050-9

López, J. C., Vargas, J. P., Gómez, Y., and Salas, C. (2003). Spatial and non-spatial learning in turtles: the role of medial cortex. *Behav. Brain Res.* 143, 109–120. doi: 10.1016/S0166-4328(03)00030-5

Luzzati, F., Bonfanti, L., Fasolo, A., and Peretto, P. (2009). DCX and PSA-NCAM expression identifies a population of neurosn preferentially distributed in associateive areas of different pallial derivatives and vertebrate species. *Cereb. Cortex* 19, 1028–1041. doi: 10.1093/cercor/bhn145

MacLusky, N. J., Hajszan, T., Prange-Kiel, J., and Leranth, C. (2006). Androgen modulation of hippocampal synaptic plasticity. *Neuroscience* 138, 957–965. doi: 10.1016/j.neuroscience.2005.12.054

Marchioro, M., Nunes, J. M., Rabelo Ramalho, A. M., Molowny, A., Perez-Martinez, E., Ponsoda, X., et al. (2005). Postnatal neurogenesis in the medial cortex of the tropical lizard *Tropidurus hispidus*. *Neuroscience* 134, 407–143. doi: 10.1016/j.neuroscience.2005.04.014

Marler, C. A., Boyd, S. K., and Wilczynski, W. (1999). Forebrain arginine vasotocin correlates of alternative male mating strategies in cricket frogs. *Hormones Behav.* 36, 53–61 doi: 10.1006/hbeh.1999.1524

McGregor, P. K., and Westby, G. W. M. (1992). Discrimination of individually characteristic electric organ discharge by a weakly electric fish. *Anim. Behav.* 43, 977–986. doi: 10.1016/S0003-3472(06)80011-4

Mills, S. C., Hazard, L., Lancaster, L., Mappes, T., Miles, D., Oksanen, T. A., et al. (2008). Gonadotropin hormone modulation of testosterone, immune function, performance, and behavioral trade-offs among male morphs of the lizard *Uta stansburiana*. *Am. Nat.* 171, 339–357. doi: 10.1086/527520

Moga, M. M., Geib, B. M., Zhou, D., and Prins, G. S. (2000). Androgen receptor-immunoreactivity in the forebrain of the Eastern Fence lizard (*Sceloporus undulatus*). *Brain Res.* 879, 174–182. doi: 10.1016/S0006-8993(00)02771-2

Moore, I. T., and Jessop, T. S. (2003). Stress, reproduction and adrenocortical modulation in amphibians and reptiles. *Hormones Behav.* 43, 39–47. doi: 10.1016/S0018-506X(02)00038-7

Moore, M. C. (1988). Testosterone control of territorial behavior: tonic-release implants fully restore seasonal and short-term aggressive responses in free-living castrated lizards. *Gen. Comp. Endocrinol.* 70, 450–459. doi: 10.1016/0016-6480(88)90121-9

Moore, M. C. (1991). Application of organization-activation theory to alternative male reproductive strategies: a review. *Hormones Behav.* 25, 154–179. doi: 10.1016/0018-506X(91)90048-M

Moore, M. C., Thompson, C. W., and Marler, C. A. (1991). Reciprocal changes in corticosterone and testosterone levels following acute and chronic handling stress in the tree lizard, *Urosaurus ornatus*. *Gen. Comp. Endocrinol*81, 217–226. doi: 10.1016/0016-6480(91)90006-R

Moore, M. C., Whittier, J. M., and Crews, D. (1984). Environmental control of seasonal reproduction in a parthenogenetic lizard *Cnemidophorus uniparens*. *Physiol. Zool.* 57, 544–549. doi: 10.1086/physzool.57.5.30163946

Moss, R., Parr, R., and Lambin, X. (1994). Effects of testosterone on breeding density, breeding success and survival of red grouse. *Proc. R. Soc. Lond. B Biol. Sci.* 258, 175–180. doi: 10.1098/rspb.1994.0159

Mullen, R. J., Buck, C. R., and Smith, A. M. (1992). NeuN, a neuronal specific nuclear protein in vertebrates. *Development* 116, 201–211.

O'Bryant, E. L., and Wilczynski, W. (2010). Changes in plasma testosterone levels and brain AVT cell number during the breeding season in the green treefrog. *Brain Behav. Evol.* 75, 271–281. doi: 10.1159/000316084

Olsson, M., Healey, M., and Astheimer, L. (2007). Afternoon T: testosterone level is higher in red than yellow male polychromatic lizards. *Physiol. Behav.* 91, 531–534. doi: 10.1016/j.physbeh.2007.04.025

Ormerod, B. K., and Galea, L. A. (2003). Reproductive status influences the survival of new cells in the dentate gyrus of adult male meadow voles. *Neurosci. Lett.* 346, 25–28. doi: 10.1016/S0304-3940(03)00546-9

Pearson, A. K., Tsui, H. W., and Licht, P. (1976). Effect of temperature on spermatogenesis, on the production and action of androgens and on the

ultrastructure of gonadotropic cells in the lizard *Anolis carolinensis*. *J. Exp. Zool. A* 195, 291–303.

Pérez-Cañellas, M., and García-Verdugo, J. M. (1996). Adult neurogenesisin the telencephalon of a lizard: a [3H]thymidine autoradiographic and bromodeoxyuridine immunocytochemical study. *Dev. Brain Res.* 93, 49–61.

Petrillo, M., Ritter, C. A., and Schade-Powers, A. (1994). A role for acetylcholine in spatial memory in turtles. *Physiol. Behav.* 56, 135–141. doi: 10.1016/0031-9384(94)90271-2

Pfau, D. R., Potter, S. Y., DeNardo, D. F., Taylor, E. N., and Strand, C. R. (2010). "Effects of testosterone and captivity on medial and dorsal cortex volumes and neurogenesis in adult male western fence lizards," in *Sceloporus Occidentalis. SICB Annual Meeting Abstracts* (Seattle, WA).

Powers, A. S. (2016). Plasticity and adult neurogenesis in amphibians and reptiles: more questions than answers. *Brain Behav. Evol.* 87, 175–183. doi: 10.1159/000447047

Ramirez-Castillejo, C., Nacher, J., Molowny, A., Ponsoda, X., and Lopez-Garcia, C. (2002). PSA-NCA immunocytochemistry in the cerebral cortex and other telencephalic areas of the lizard *Podarcis hispanica*: differential expression during medial cortex neuronal regeneration. *J. Comp. Neurol.* 453, 145–156. doi: 10.1002/cne.10390

Rao, M. S., and Shetty, A. K. (2004). Efficacy of doublecrotin as a marker to analyze the absolute number and dendritic growth of newly generated neurons in the adult dentate gyrus. *Eur. J. Neurosci.* 19, 234–246. doi: 10.1111/j.0953-816X.2003.03123.x

Rasika, S., Alvarez-Buylla, A., and Nottebohm, F. (1999). BDNF mediates the effects of testosterone on the survival of new neurons in an adult brain. *Neuron* 22, 53–62. doi: 10.1016/S0896-6273(00)80678-9

Rasika, S., Nottebohm, F., and Alvarez-Buylla, A. (1994). Testosterone increases the recruitment and/or survival of new high vocal center neurons in adult female canaries. *Proc. Natl. Acad. Sci. U.S.A.* 91, 7854–7858. doi: 10.1073/pnas.91.17.7854

Reiman Avigan, M., and Schade Powers, A. (1995). The effects of MK-801 injections and dorsal cortex lesions on maze learning in turtles (*Chrysemys picta*). *Psychobiology* 23, 63–68.

Reiner, A. (1991). A comparison of the neurotransmitter-specific and neuropeptide-specific neuronal cell types present in turtle cortex to those present in mammalian isocortex: Implications for the evolution of isocortex. *Brain Behav. Evol.* 38, 53–72. doi: 10.1159/000114379

Reiner, A. (1993). Neurotransmitter organization and connections of turtle cortex: Implications for the evolution of mammalian isocortex. *Comp. Biochem. Physiol. Comp. Physiol.* 104, 735–748. doi: 10.1016/0300-9629(93)90149-X

Rhen, T., and Crews, D. (2002). Variation in reproductive behavior within a sex: neural systems and endocrine activation. *J. Neuroendocrinol.* 14, 517–531. doi: 10.1046/j.1365-2826.2002.00820.x

Robertson, J. M., Hoversten, K., Gruendler, M., Poorten, T. J., Hews, D. K., and Rosenblum, E. B. (2011). Colonization of novel White Sands habitat is associated with changes in lizard anti-predator behavior. *Biol. J. Linn. Soc.* 103, 657–667. doi: 10.1111/j.1095-8312.2011.01644.x

Rodríguez, F., López, J. C., Vargas, J. P., Gomez, Y., Broglio, C., and Salas, C. (2002). Conservation of spatial memory function in the pallial forebrain of reptiles and ray-finned fishes. *J. Neurosci.* 22, 2894–2903.

Roof, R. L., and Havens, M. D. (1992). Testosterone improves maze performance and induces development of a male hippocampus in females. *Brain Res.* 572, 310–313. doi: 10.1016/0006-8993(92)90491-Q

Rosen, G., O'Bryant, E., Matthews, J., Zacharewski, T., and Wade, J. (2002). Distribution of androgen receptor mRNA expression and immunoreactivity in the brain of the green anole lizard. *J. Neuroendocrinol.* 14, 19–28. doi: 10.1046/j.0007-1331.2001.00735.x

Roth, E. D., Lutterschmidt, W. I., and Wilson, D. A. (2006). Relative medial and dorsal cortex volume in relation to sex differences in spatial ecology of a snake population. *Brain Behav. Evol.* 67, 103–110. doi: 10.1159/000089183

Saaltink, D. J., and Vreugdenhil, E. (2014). Stress, glucocorticoid receptors, and adult neurogenesis: a balance between excitation and inhibition? *Cell. Mol. Life Sci.* 71, 2499–2515. doi: 10.1007/s00018-014-1568-5

Sarkey, S., Azcoitia, I., Garcia-Segura, L. M., Garcia-Ovejero, D., and DonCarlos, L. L. (2008). Classical androgen receptors in non-classical sites in the brain. *Hormones Behav.* 53, 753–764. doi: 10.1016/j.yhbeh.2008.02.015

Schoenfeld, T., and Gould, E. (2012). Stress, stress hormones, and adult neurogenesis. *Exp. Neurol.* 233, 12–21. doi: 10.1016/j.expneurol.2011.01.008

Schunter, C., Vollmer, S. V., Macpherson, E., and Pascual, M. (2014). Transcriptome analyses and differential gene expression in a non-model fish species with alternative mating tactics. *BMC Genomics* 15:167. doi: 10.1186/1471-2164-15-167

Sherry, D. F. (1998). "The ecology and neurobiology of spatial memory," in *Cognitive Ecology*, ed R. Dukas (Chicago, IL: University of Chicago Press), 261–296.

Simerly, R. B., Change, C., Muramatsu, M., and Swanson, L. W. (1990). Distribution of androgen and estrogen receptor mRNA-containing cells in the rat brain: an in situ hybridization study. *J. Comp. Neurol.* 294, 76–95. doi: 10.1002/cne.902940107

Sinervo, B., Bleay, C., and Adamopoulou, C. (2001). Social causes of correlational selection and the resolution of a heritable throat color polymorphism in a lizard. *Evolution* 55, 2040–2052. doi: 10.1111/j.0014-3820.2001.tb01320.x

Sinervo, B., Calsbeek, R., Comendant, T., Both, C., Adamopoulou, C., and Clobert, J. (2006). Genetic and maternal determinants of effective dispersal: the effect of sire genotype and size at birth in side-blotched lizards. *Am. Nat.* 168, 88–99. doi: 10.1086/505765

Sinervo, B., and Lively, C. M. (1996). The rock-paper-scissors game and the evolution of alternative male strategies. *Nature* 380, 240–243. doi: 10.1038/380240a0

Sinervo, B., Miles, D. B., Frankino, A., Klukowski, M., and DeNardo, D. F. (2000). Testosterone, endurance, and Darwinian fitness: natural and sexual selection on the physiological bases of alternative male behaviors in side-blotched lizards. *Hormones Behav.* 38, 222–233. doi: 10.1006/hbeh.2000.1622

Small, T. W., Brenowitz, E. A., Wojtenek, W., and Moore, I. T. (2015). Testosterone mediates seasonal growth of the song control nuclei in a tropical bird. *Brain Behav. Evol.* 86, 110–121. doi: 10.1159/000437412

Smith, M. D., Jones, L. S., and Wilson, M. A. (2002). Sex differences in hippocampal slice excitability: role of testosterone. *Neuroscience* 109, 517–530. doi: 10.1016/S0306-4522(01)00490-0

Soto-Gamboa, M., Villalon, M., and Bozinovic, F. (2005). Social cues and hormone levels in male *Octodon degus* (Rodentia): a field test of the challenge hypothesis. *Hormones Behav.* 47, 311–318. doi: 10.1016/j.yhbeh.2004.11.010

Spritzer, M. D., Daviau, E. D., Coneeny, M. K., Engelman, S. M., Prince, W. T., and Rodriguez-Wisdom, K. N. (2011). Effects of testosterone on spatial learning and memory in adult male rats. *Hormones Behav.* 59, 484–496. doi: 10.1016/j.yhbeh.2011.01.009

Spritzer, M. D., and Galea, L. A. M. (2007). Testosterone and dihydrotestosterone, but not estradiol, enhance survival of new hippocampal neurons in adult male rats. *Dev. Neurobiol.* 67, 1321–1333. doi: 10.1002/dneu.20457

Striedter, G. F. (1997). The telencephalon of tetrapods in evolution. *Brain Behav. Evol.* 49, 205–213. doi: 10.1159/000112992

Striedter, G. F. (2016). Evolution of the hippocampus in reptiles and birds. *J. Comp. Neurol.* 524, 496–517. doi: 10.1002/cne.23803

Ulinski, P. S. (1990). "The cerebral cortex of reptiles," in *Cerebral Cortex*, *Vol. 8A: Comparative Structure and Evolution of Cerebral Cortex Part I,* eds E. G. Jones and A. Peters (New York, NY: Plenum), 139–215.

Veiga, J. P., Moreno, J., Cordero, P. J., and Minguez, E. (2001). Territory size and polygyny in the spotless starling: resource-holding potential or social inertia? *Can. J. Zool.* 79, 195–1956. doi: 10.1139/z01-161

Wikelski, M., Steiger, S. S., Gall, B., and Nelson, K. N. (2005). Sex, drugs and mating role: testosterone-induced phenotype-switching in Galapagos marine iguanas. *Behav. Ecol.* 16, 260–268. doi: 10.1093/beheco/arh160

Wilczynski, W., Lynch, K. S., and O'Bryant, E. L. (2005). Current research in amphibians: studies integrating endocrinology, behavior, and neurobiology. *Hormones Behav.* 48, 440–450. doi: 10.1016/j.yhbeh.2005.06.001

Wilson, B. S., and Wingfield, J. C. (1994). Seasonal and interpopulational variation in plasma levels of corticosterone in the side-blotched lizard (*Uta stansburiana*). *Physiol. Zool.* 67, 1025–1049. doi: 10.1086/physzool.67.4.30163877

Wilson, R. C. (2015). *Effects of Testosterone on the Spatial Ecology, Coloration, and Brain Regions in Western Fence Lizards, Sceloporus occidentalis*. Master's thesis, California Polytechnic State University-San Luis Obispo.

Wingfield, J. C. (1984). Androgens and mating systems: testosterone-induced polygyny in normally monogamous birds. *Auk* 101, 665–671. doi: 10.2307/4086893

Wingfield, J. C., Hegner, R. E., Dufty, A. M., and Ball, G. F. (1990). The Challenge hypothesis: theoretical implications for patterns of testosterone secretion, mating systems, and breeding strategies. *Am. Nat.* 136, 829–846. doi: 10.1086/285134

Wingfield, J. C., and Kenagy, G. J. (1991). "Natural regulation of reproductive cycles," in *Vertebrate Endocrinology: Fundamentals and Biomedical Implications*, Vol. 4, eds P. B. M. Schreibman and R. E. Jones (New York, NY: Academic Press), 181–241.

Woolley, C. S., and McEwen, B. S. (1992). Estradiol mediates fluctuation in hippocampal synapse density during the estrous cycle in the adult rat. *J. Neurosci.* 12, 2549–2554.

Young, L. J., Lopreato, G. F., Horan, K., and Crews, D. (1994). Cloning and in situ hybridization analysis of estrogen receptor, progesterone and androgen receptor expression in the brain of whiptail lizards (*Cnemidophorus uniparens* and *C. inoratus). J. Comp. Neurol.* 347, 288–300. doi: 10.1002/cne.903470210

Zamudio, K. R., and Sinervo, B. (2000). Polygyny, mate-guarding, and posthumous fertilization as alternative male mating strategies. *Proc. Natl. Acad. Sci. U.S.A.* 97, 14427–14432. doi: 10.1073/pnas.011544998

Zhang, Z., Yang, R., Zhou, R., Li, L., Sokabe, M., and Chen, L. (2010). Progesterone promotes the survival of newborn neurons in the dentate gyrus of adult male mice. *Hippocampus* 20, 402–412. doi: 10.1002/hipo.20642

Conflict of Interest Statement: The authors declare that the research was conducted in the absence of any commercial or financial relationships that could be construed as a potential conflict of interest.

The reviewer PP and handling Editor declared their shared affiliation, and the handling Editor states that the process nevertheless met the standards of a fair and objective review.

frontiers in Neuroscience

ORIGINAL RESEARCH
published: 07 June 2017
doi: 10.3389/fnins.2017.00323

Maturation, Behavioral Activation, and Connectivity of Adult-Born Medium Spiny Neurons in a Striatal Song Nucleus

Jennifer Kosubek-Langer, Lydia Schulze and Constance Scharff*

Animal Behavior, Freie Universität Berlin, Berlin, Germany

Neurogenesis continues in the adult songbird brain. Many telencephalic song control regions incorporate new neurons into their existing circuits in adulthood. One song nucleus that receives many new neurons is Area X. Because this striatal region is crucial for song learning and song maintenance the recruitment of new neurons into Area X could influence these processes. As an entry point into addressing this possibility, we investigated the maturation and connectivity within the song circuit and behavioral activation of newly generated Area X neurons. Using BrdU birth dating and virally mediated GFP expression we followed adult-generated neurons from their place of birth in the ventricle to their place of incorporation into Area X. We show that newborn neurons receive glutamatergic input from pallial/cortical song nuclei. Additionally, backfills revealed that the new neurons connect to pallidal-like projection neurons that innervate the thalamus. Using *in situ* hybridization, we found that new neurons express the mRNA for D1- and D2-type dopamine receptors. Employing DARPP-32 (dopamine and cAMP-regulated phosphoprotein of 32 kDa) and EGR-1 (early growth response protein 1) as markers for neural maturation and activation, we established that at 42 days after labeling approximately 80% of new neurons were mature medium spiny neurons (MSNs) and could be activated by singing behavior. Finally, we compared the MSN density in Area X of birds up to seven years of age and found a significant increase with age, indicating that new neurons are constantly added to the nucleus. In summary, we provide evidence that newborn MSNs in Area X constantly functionally integrate into the circuit and are thus likely to play a role in the maintenance and regulation of adult song.

Keywords: adult neurogenesis, songbird, basal ganglia, Area X, EGR-1, DARPP-32, dopamine

OPEN ACCESS

Edited by:
Irmgard Amrein,
University of Zurich, Switzerland

Reviewed by:
Tom V. Smulders,
Newcastle University, United Kingdom
Antonia Marin-Burgin,
IBioBA-CONICET-Max Planck Society Partner, Argentina

****Correspondence:***
Jennifer Kosubek-Langer
jennifer.kosubek@fu-berlin.de

Specialty section:
This article was submitted to Neurogenesis, a section of the journal Frontiers in Neuroscience

Received: *24 March 2017*
Accepted: *23 May 2017*
Published: *07 June 2017*

Citation:
Kosubek-Langer J, Schulze L and Scharff C (2017) Maturation, Behavioral Activation, and Connectivity of Adult-Born Medium Spiny Neurons in a Striatal Song Nucleus. Front. Neurosci. 11:323. doi: 10.3389/fnins.2017.00323

INTRODUCTION

Adult neurogenesis is an enigmatic trait. Only some neurons continue to be generated in adulthood whereas the majority are born during development and persist throughout the animal's life. Why these differences exist is still not known but much progress has been made elucidating the mechanism and function of adult neurogenesis during the past decades (Song et al., 2016). Neurons born in adulthood originate in regions adjacent to the ventricles that also give rise to neurons during development. From these neurogenic niches, neural precursors delaminate and then migrate through the dense parenchyma, incorporate into functional circuits and influence behavior (Paredes et al., 2016).

Considerable differences exist with respect to the extent of adult neurogenesis in different species. As a rule of thumb, adult-born new neurons are recruited to many brain regions in vertebrates like teleost fish, amphibians, and reptiles, whereas in birds the extent is still widespread but more restricted to the forebrain (Kaslin et al., 2008). In mammals, there are even fewer regions that continue to recruit new neurons in adulthood, principally the dentate gyrus (DG) of the hippocampal formation (Kempermann et al., 2015) and the olfactory bulb (Lim and Alvarez-Buylla, 2016). Interestingly, in rats, rabbits, monkeys and humans but not in mice, adult-generated neurons have also been observed in the striatum (Bedard et al., 2002; Dayer et al., 2005; Tonchev et al., 2005; Luzzati et al., 2006; Ernst et al., 2014). In these cases, the newly generated neurons belong primarily to the class of GABAergic interneurons, which constitute less than 5% of the striatal neurons (Tepper et al., 2010). The most abundant striatal cell type are medium spiny projection neurons (MSNs) (Gerfen and Wilson, 1996). In adult rodents, generation of MSNs has only been reported in response to experimentally induced stroke, ischemia, or lesions (Arvidsson et al., 2002; Tattersfield et al., 2004; Hou et al., 2008). In contrast, in songbirds adult MSNs keep immigrating in substantial numbers into the striatum under natural conditions (Alvarez-Buylla et al., 1990). Striatal newborn neurons originate from the progenitor containing subpallial region in the lateral ventricle that expresses the transcription factors ISL-1/2, NKX2.1, and DLX but not TBR1 (Scott and Lois, 2007). Of particular interest is the recruitment of MSNs into Area X (Nordeen and Nordeen, 1988; Rochefort et al., 2007; Scott and Lois, 2007) a region unique to songbirds relevant for song plasticity in juveniles and adults (Sohrabji et al., 1990; Scharff and Nottebohm, 1991; Jarvis et al., 1998; Hessler and Doupe, 1999; Woolley et al., 2014). In songbirds, new neurons destined for Area X migrate between 1,000 and 2,000 μm to their final destination.

The dynamics of neural recruitment are best understood in the DG and the olfactory bulb. In the former, new neurons are added, whereas in the latter, they replace older neurons that undergo apoptosis (Crespo et al., 1986; Imayoshi et al., 2008). In both cases, the time it takes for new neurons to incorporate into preexisting circuits is similar (Deshpande et al., 2013). In songbirds, the dynamics of neural recruitment have only been studied in the pallial/cortical song control region HVC (proper name, **Figure 1A**), where glutamatergic projection neurons undergo neurogenesis (Kirn et al., 1999; Scott and Lois, 2007; Tokarev et al., 2016).

To gain insight into the integration of GABAergic MSNs into existing circuits, we studied their differentiation, connectivity and activation by singing in Area X. To do so we traced new neurons by injections of green fluorescent protein (GFP)-expressing lentivirus into the lateral wall of the lateral ventricle and with systemic injections of the cell birth marker 5-bromo-2′-deoxyuridine (BrdU). We also injected retrograde tracer into one of the target regions of Area X, and used immuno- and *in situ*-histochemistry to characterize the new neurons. We report that adult born MSNs receive glutamatergic and dopaminergic input, connect to pallidal-like projection neurons and are activated during singing like older, resident MSNs.

Because new HVC neurons seem to replace older ones in canaries (Kirn and Nottebohm, 1993), whereas in zebra finches constant neuronal addition was observed (Walton et al., 2012) we also addressed the issue of replacement vs. addition. We quantified neuron numbers in adult zebra finches of varying age and found that the density of MSNs in Area X increased with age, supporting the idea of neuron addition rather than replacement. Overall, our results suggest that Area X receives a constant addition of functional new GABAergic MSNs.

MATERIALS AND METHODS

Animals

Adult male zebra finches (*Taeniopygia guttata*) were bred and housed at the Department of Animal Behavior at Freie Universität Berlin. The colony was kept under a 12:12 h light:dark-cycle and food and water were available *ad libitum*. All procedures were reviewed and approved by the veterinary department of the Freie Universität Berlin and by the ethics committee of the Regional Office for Health and Social Affairs Berlin (LAGeSo). The permit numbers are G0116/13 and G0296/15. In total, we used 53 adult male zebra finches. For the expression analysis of the early growth response protein 1 (EGR-1) and the dopamine- and cAMP-regulated neuronal phosphoprotein (DARPP-32) in newborn cells we used 29 birds (age 462 ± 158 days, mean ± standard deviation, SD). Dopamine (DA) receptor expression was studied in 5 birds (age 172 days ± 13 days, mean ± SD). Five birds received lentiviral injections (age 367 days ± 109 days, mean ± SD). Density measures in Area X were performed in 14 birds (age ranging from 372 to 2,526 days).

BrdU Injections

Birds for EGR-1 and DA receptor analysis received BrdU (50 μg/g) via intramuscular injections in the mornings for 5 consecutive days. Birds were assigned to three groups with different survival times after BrdU injection (21, 31, and 42 days). We choose the first survival time to be 21 days, because BrdU+ neurons in Area X were previously shown to express immediate early genes after singing at that time (Tokarev et al., 2016).

Song Monitoring

For subsequent EGR-1 analysis, birds were kept in sound attenuated chambers for three nights and were perfused in the morning of the 4th day 1.5 h after the lights went on. Vocalizations were continuously monitored via Sound Analysis Pro (Tchernichovski et al., 2000). During those 1.5 h birds had to sing at least 150 motifs to be included in the subsequent analysis of EGR-1 expression.

Birds that received lentiviral injections and retrograde tracer were isolated in sound attenuated chambers for one night before sacrifice. Birds were kept from singing by the experimenter sitting nearby for 1.5 h after lights went on in the morning and then killed. This was necessary because we used some of the brain sections in another experiment to be reported elsewhere.

Birds used for DA receptor analysis were decapitated without previous song monitoring and their brains were quickly dissected

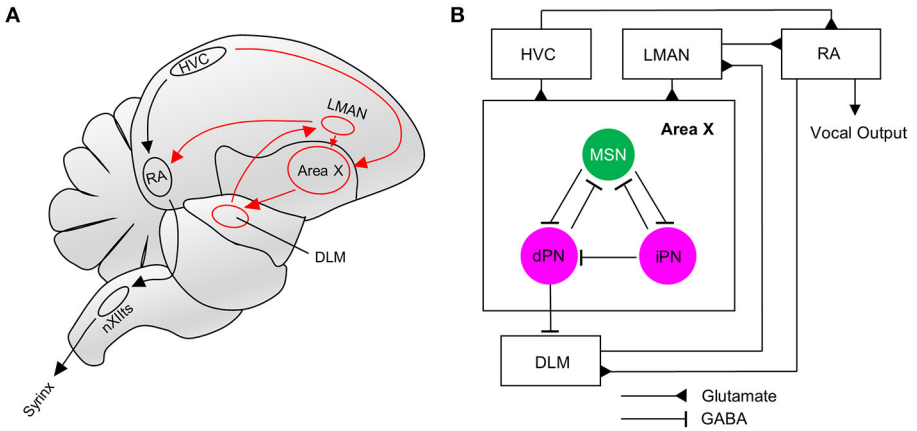

FIGURE 1 | The song system and connectivity within Area X. **(A)** The song motor pathway (shown in black) controls the vocal organ (syrinx) via HVC->RA->nXIIts. The anterior forebrain pathway (AFP, shown in red) forms a cortico-basal ganglia-thalamic-cortical loop, connecting HVC and RA via Area X->DLM->LMAN. **(B)** Neurons in Area X receive glutamatergic innervations from HVC and LMAN. MSNs in Area X inhibit direct and indirect pallidal-like neurons (dPN, iPN). Both types can project to MSNs, but only dPNs project to the thalamic nucleus DLM that connects to RA via LMAN (Farries et al., 2005; Goldberg et al., 2010). RA directly innervates the AFP via DLM. RA, Robust nucleus of the arcopallium; LMAN, Lateral magnocellular nucleus of the anterior nidopallium; XII, Nucleus; NXIIts, tracheosyringeal part; DLM, Dorsal lateral nucleus of the medial thalamus.

1.5 h after the lights went on. All birds were killed by isoflurane overdose.

Lentiviral Vector Injection and Backfill

To label progenitors in the lateral wall of the ventricle, the lentiviral expression vector pFUGW (Lois et al., 2002) containing a GFP reporter gene was stereotactically injected into the ventricular zone under isofluorane anesthesia. Birds were fixed in a stereotaxic head holder, with the beak in a 45° angle from the vertical axis. In each hemisphere, we injected four sites with approximately 200 µl of viral construct using the following coordinates relative to the bifurcation of the midsagittal sinus: anterior-posterior 3.8–4.1, medial-lateral −1.3/+1.3, dorsal-ventral −5.0, injection angle AP 10°. To label pallidal-like projection neurons, we injected approximately 600 µl tetramethylrhodamine coupled with biotin (BDA, 3,000 MW, Molecular Probes) into DLM 4–5 days before sacrifice at day 42. We used the following coordinates: anterior-posterior 1.2, medial-lateral −1.3/+1.3, dorsal-ventral −4.5. After surgeries birds were transferred to their home cages. To confirm that the virus infected proliferating cells, some birds were injected with BrdU (50 µg/g) on the day of surgery.

Immunohistochemistry and Image Analysis

For immunohistochemistry birds were overdosed with isoflurane and then perfused transcardially with phosphate-buffered saline (PBS) followed by 4% paraformaldehyde (PFA) in PBS. After dissection, brains were post-fixed for one night, washed for another night in PBS and cut sagitally or coronally into 50 µm sections using a vibrating microtome (VT1000S, Leica). For BrdU antigen retrieval, sections were incubated in 2 N HCl for 30 min at 37°C and neutralized with borate buffer. All other immunostainings were performed according to standard protocols. The following antibodies were used; primary: anti EGR-1 (rabbit, Santa Cruz sc-189), anti DARPP-32 (mouse, kindly provided by H.C. Hemmings, Jr., Weill Cornell Medical College, New York), anti DARPP-32 (rabbit, abcam ab40801), anti BrdU (rat, Bio-Rad MCA2060), anti VGLUT2 (mouse, abcam ab79157), anti GFP (rabbit, abcam ab290). Fluorescent Secondary: anti-rabbit-Alexa-Fluor-568 (life technologies, A10042), anti-mouse-Alexa-Flour-568 (Life technologies, A10037), anti-rat-Alexa-Fluor-488 (Life Technologies, A21208), anti-rabbit-Alexa-Fluor-488 (Life Technologies, A21206). Biotinylated dextran signal was amplified using Streptavidin-Alexa-Fluor-568 (Life Technologies, S11226). Sections were counterstained with 4′,6-Diamidin-2-phenylindol (DAPI, Serva). Z-Stacks were obtained with a SP8 confocal microscope (Leica) and processed using the Fiji software package (Schindelin et al., 2012). Colors of images were adjusted ("false-colored") to improve visibility, particularly for readers with red-green blindness. Axons were traced using the Simple Neurite Tracer plugin in Fiji (Schindelin et al., 2012), starting at the soma and using the smooth axonal morphology (in contrast to spiny dendrites) as a criterion. MSN density was analyzed in 40 µm sagittal sections containing Area X. For each bird, we analyzed two to four different sections of both hemispheres. Within those we counted the number of labeled neurons in at least eight stacks, each with the measures 100 × 100 × 8 µm and used the average of those to calculate density. We counted all nuclei (DAPI+) and all DARPP-32+ cells using the cell counter plugin in the Fiji software package (Schindelin et al., 2012).

In situ Hybridization

Hemispheres of birds used for *in situ* hybridization were separately frozen in Tissue-Tek O.T.C. Compound medium (Sakura) and stored at −80°C. Hemispheres were cut in 12 µm sagittal sections using a cryostat (Cryo-Star HM 560

Cryostat, MICROM). Sections were fixed with 4% PFA for 10 min and then acetylated with 0.25% acetic anhydride in triethanolamine for 10 min. Sections were rinsed in 2x in saline sodium citrate (SSC) buffer, dehydrated (75% EtOH, 95% EtOH, and 100% EtOH, each for 2 min) and air dried. Sections were prehybridized for 1 h at 60°C in a hybridization mix consisting of 50% deionized formamide, 5x SSC (pH 4.5), 2% blocking reagent (Roche, 11096176001) in 1x maleic acid buffer, 2% sodium dodecyl sulfate, yeast tRNA (Invitrogen, 0.25 mg/ml), and heparin (Polysciences, 0.1 mg/ml). Sections were hybridized overnight with 1% digoxigenin or fluorescin labeled RNA probe in hybridization mix at 60°C in a mineral oil bath. The next day, slides were rinsed twice with chloroform followed by 2x SSC and 1x SSC. A series of post-hybridization washes followed: 30 min in 1x SSC containing 50% formamide at hybridization temperature (60°C). Then, sections were washed once in 2x SSC and twice in 0.2x SSC 20 min each at hybridization temperature. After the post-hybridization washing steps, sections were washed twice in 1x MABT (pH 7.5), consisting of 100 mM maleic acid, 150 mM NaCl and 0.1% Tween-20. Afterwards, sections were incubated in 1x Roti-ImmunoBlock (Carl Roth) in 1x MABT for 30 min, then with either alkaline phosphatase (AP)-conjugated sheep anti-DIG antibody (Roche) or AP-conjugated sheep anti-fluorescein antibody (Roche), that were diluted 1:200 in 1x Roti-ImmunoBlock in 1x MABT. Slices were incubated overnight at 4°C in a humidity chamber. After antibody incubation, slides were washed with 1x MABT 4 times for 5 min and equilibrated in alkaline phosphatase buffer NTMT, consisting of 100 mM NaCl, 100 mM Tris hydrochloride pH 9.5, 50 mM $MgCl_2$ and 0.1% Tween-20 for 10 min. AP-labeled probes were detected colorimetrically via the nitro blue tetrazolium/5-Bromo-4-chloro-3-indolyl phosphate substrate system (NBT/BCIP; Roche). NBT (final concentration: 337.5 µg/ml) and BCIP (final concentration: 175 µg/ml) were diluted in NTMT and slices were covered with this solution. Slices were incubated for 6–8 h, then fresh NBT/BCIP solution was added and sections were incubated overnight. The reaction was stopped by 10 min of incubation in a stop solution consisting of 10 mM Tris hydrochloride pH 8.0 and 1 mM EDTA. Afterwards, slides were washed three times with 1x PBS for 5 min. Sections were further used for immunohistochemical BrdU detection (see Immunohistochemistry) and examined with a Zeiss Axiovert 200 fluorescent microscope.

Analysis and Statistics

Data were analyzed with the data analysis software R (R Development Core Team, 2013) and GraphPad Prism version 5.00 (GraphPad Software, San Diego California USA). Data for EGR-1, DARPP-32 and DA receptor expression passed the D'Agostino's K^2 test for normal distribution and were then evaluated with an analysis of variance (ANOVA) followed by a *post hoc* Tukey's Honestly Significant Difference test (HSD). To test the correlation between DARPP-32 density and age, we performed a linear regression analysis. Significance level was $p < 0.05$ for all tests.

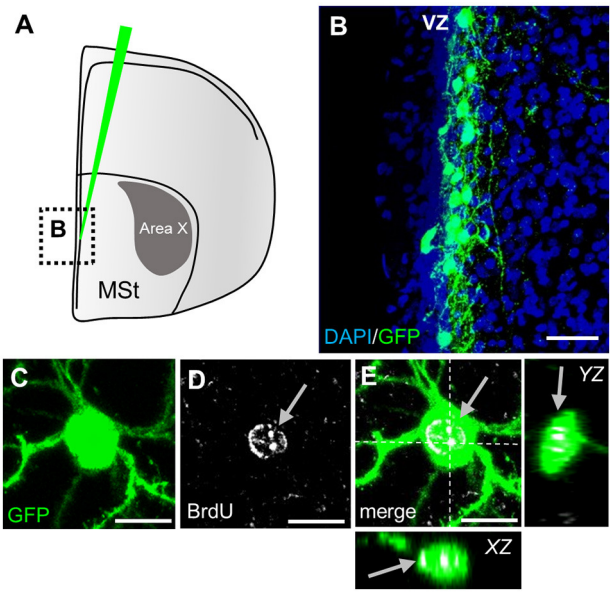

FIGURE 2 | Labeling of striatal progenitors. **(A)** Lentiviral vector injections were surgically targeted at the wall of the lateral ventricle adjacent to the medial striatum (MSt). The area outlined is depicted in B. **(B)** Many cells in the ventricular zone (VZ) were infected, as shown by virally mediated GFP expression in a coronal section. The ventricle is on the left side of the image. **(C–E)** GFP+ neuron in the striatum recently divided and incorporated BrdU (arrows). Dashed lines **(E)** indicate the planes used to generate orthogonal views of the Z-stack (*YZ, XZ*). Scale bars: 25 µm **(B)**, 10 µm **(C–E)**.

RESULTS

Newborn MSNs Receive Glutamatergic Input and Connect to Pallidal Output Neurons

To investigate whether and when newborn neurons in Area X are integrated into existing circuits, we used a lentivirally mediated approach to label progenitor cells in the striatal ventricular zone of adult male zebra finches (**Figures 2A,B**). By 31 days post injection (dpi), newly generated neurons in Area X exhibited the typical MSN morphology with relatively small nuclei (5–9 µm) and spiny dendrites. Co-labeling with BrdU confirmed that GFP+ cells in Area X recently divided and originated from the progenitor pool (**Figures 2C–E**).

Newly generated granule neurons in the adult murine DG first receive long-range cortical inputs at 3 weeks of age, whereas granule cells in the olfactory bulb connect already at 2 weeks of age to presynaptic cortical neurons (Deshpande et al., 2013). We wanted to know if and when newborn MSNs in Area X receive glutamatergic inputs from afferent cortical song nuclei. Using VGLUT2 (vesicular glutamate transporter 2) (**Figure 3A**) as a marker we found glutamatergic synapses at spines of newly generated MSNs at 31 dpi (**Figures 3B–E**). These glutamatergic innervations are likely to originate from the pallial song nuclei HVC and LMAN (**Figure 1**). We also noticed spines without VGLUT2 immunoreactivity (**Figures 3B,F–H**).

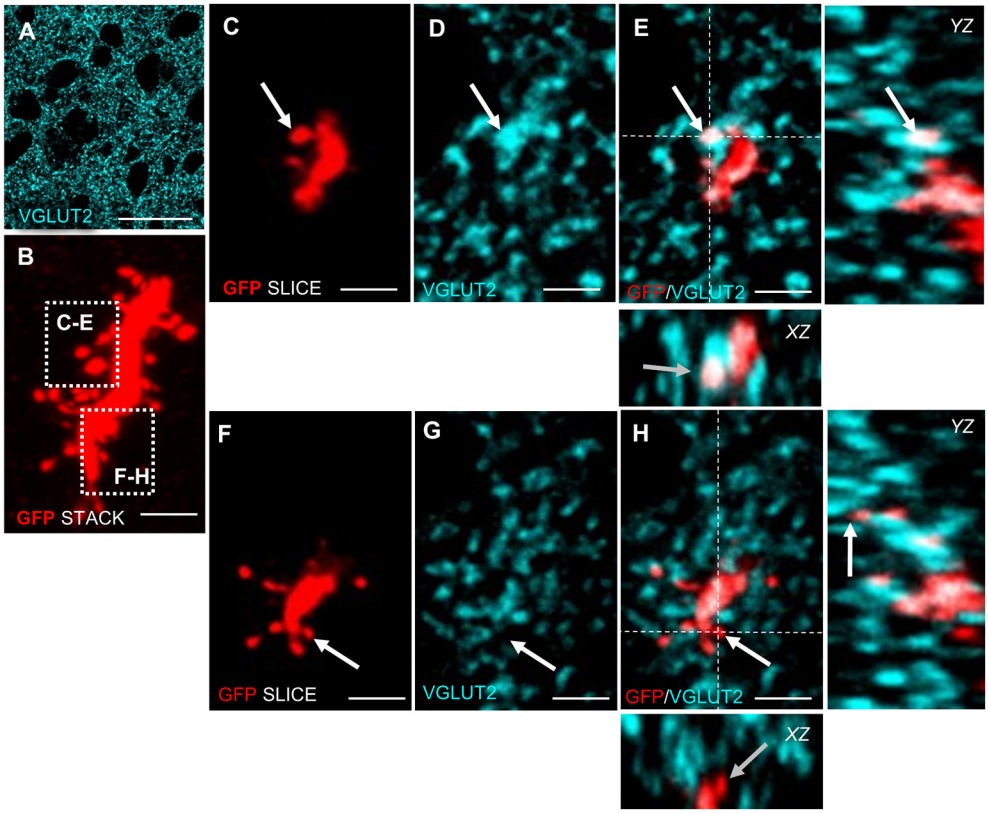

FIGURE 3 | Adult generated MSNs in Area X receive glutamatergic input. **(A)** VGLUT2 is expressed in a punctate pattern in the neuropil, corresponding to presynaptic glutamatergic terminals in Area X. **(B)** High-resolution scan of an adult generated MSN dendrite (GFP+, red). The Z-scan was collapsed. The focus planes of spines in dashed boxes are shown in **C–H**. **(C–E)** Arrow points to a dendritic spine of an adult generated MSN that colocalized with VGLUT2. **(F–H)** Arrow points to a spine of new MSN that did not colocalize with VGLUT2. Dashed lines **(E,H)** indicate the planes used to generate orthogonal views of the Z-stack (*YZ, XZ*). Scale bars: 2.5 μm **(B–H)**, 25 μm **(A)**.

After confirming glutamatergic input onto new MSNs, we tested if they contribute to signal transmission via pallidal-like output neurons. In the adult HVC, newborn projection neurons were found to be connected to their target nucleus at 3 weeks of age (Tokarev et al., 2016). We therefore predicted that newborn MSNs connected to their target cells in a similar way. Additional to GFP-labeling of progenitors in the VZ, we retrogradely labeled one class of pallidal-like neurons that project directly from Area X to the thalamic nucleus DLM (**Figures 1**, **4A,B**; Goldberg et al., 2013).This neuron type is considered to be homologous to primate internal pallidal neurons (Goldberg and Fee, 2010). Retrogradely labeled neurons had big somata and smooth, aspiny dendrites; consistent with this cell type (Reiner et al., 2004; **Figure 4C**). We found connections from newborn MSNs to pallidal-like neurons at 31 dpi and 42 dpi. We observed connections between axons and axonal boutons of new MSNs and dendrites of pallidal-like neurons; in that case, axons often wrapped around pallidal-like neuronal dendrites (**Figures 4G–J**). Additionally, their axons were often found in close apposition to the somata of pallidal-like neurons (**Figures 4D–F**). We specifically searched for backfilled pallidal-like neurons with new MSNs (GFP+) nearby. At 31 dpi, we observed that in a fraction of 0.73 of pallidal-like neurons, new MSN axons contacted their dendrites. In a fraction of 0.27 of pallidal-like neurons, both their somata and dendrites received contacts by new MSNs axons (in total 22 pallidal-like neurons, 2 animals). At 42 dpi, we found that in a fraction of 0.69 of pallidal-like neurons, new MSN axons contacted their dendrites. In a fraction of 0.31 of pallidal-like neurons, both their somata and dendrites received contacts by new MSNs axons (in total 26 pallidal-like neurons, 2 animals).

Newborn MSNs Receive Dopaminergic Innervation

Besides glutamatergic input from the song nuclei HVC and LMAN, MSNs in Area X also receive dopaminergic innervations from the ventral tegmental area (VTA) and the substantia nigra pars compacta (SNc), (Lewis et al., 1981; Bottjer, 1993; Gale et al., 2008). DA signaling via D1 receptors modulates social context dependent song variability; DA concentration in Area X is higher during female directed courtship song than when birds sing by themselves (Sasaki et al., 2006; Leblois et al., 2010). DA signaling can either be activating or inhibiting, depending on the receptor it is binding to Gerfen and Surmeier (2011). DA

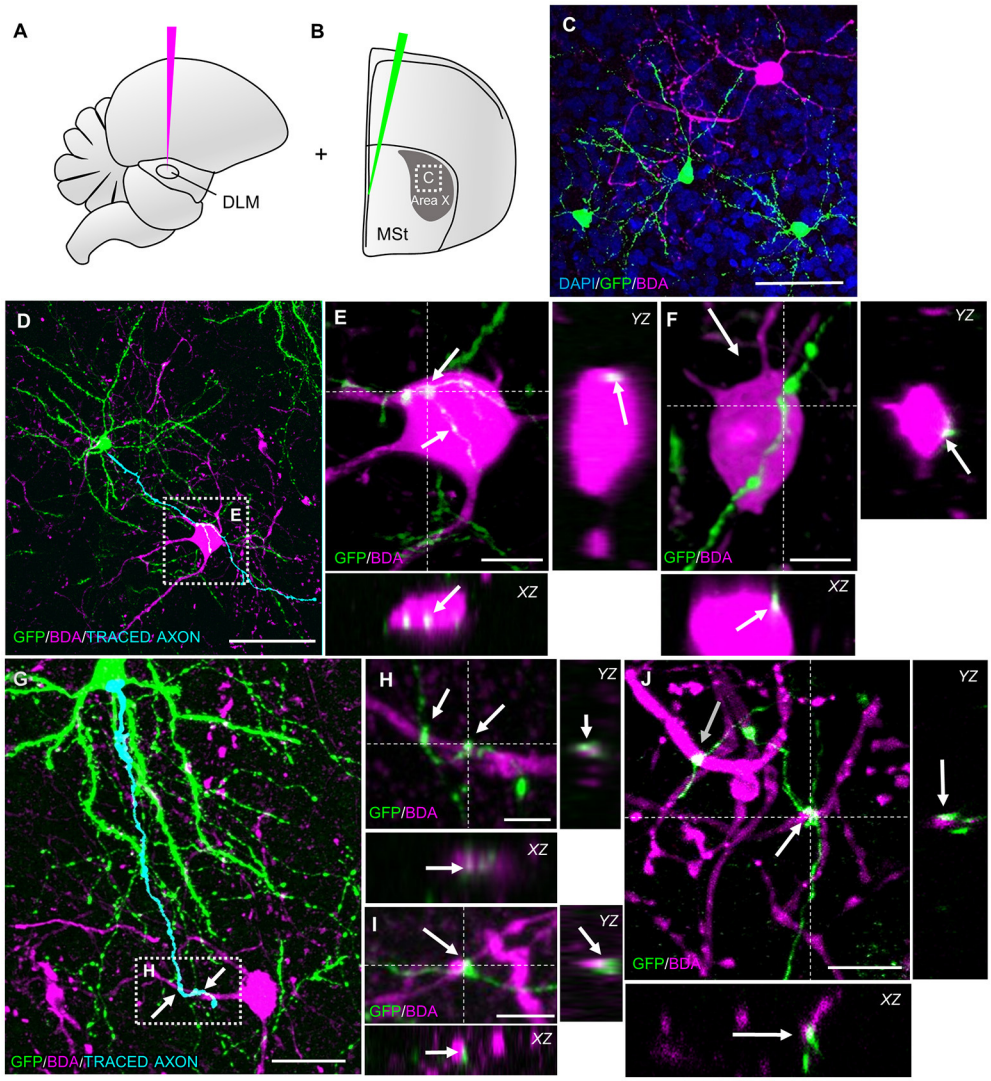

FIGURE 4 | New MSNs have axosomatic and axodendritic contacts to pallidal-like projection neurons in Area X. **(A)** Pallidal-like projection neurons in Area X were labeled via retrograde tracing. BDA was injected into thalamic nucleus DLM, the target of pallidal-like projection neurons in Area X. **(B)** Additionally, progenitors were labeled in the VZ via lentivirally mediated GFP expression. The area outlined is depicted in **C**. **(C)** Newborn MSNs (GFP+) and pallidal-like neurons were both present in sections of Area X. **(D)** The axon of a newborn MSN passed the soma of a pallidal-like projection neuron (BDA). The pallidal-like neuron in the dashed box is magnified in **E**,**F**. **(E,F)** Axosomatic contacts (arrows) of new MSN on pallidal-like neuron somata. **(G)** The axon a newborn MSN wrapped around dendrites of a pallidal-like neuron. The area in the dashed box is magnified in **H**. **(H–J)** Axodendritic contacts (arrows) of newborn MSN onto pallidal-like neurons. Dashed lines **(E,F,H–J)** indicate the planes used to generate orthogonal views of the Z-stack (*YZ, XZ*). Scale bars: 5 μm **(H,I)**, 10 μm **(E,F,J)**, 25 μm **(G)**, 50 μm **(C,D)**.

binding to D1-like receptors rises the resting potential and hence increases the chance of an action potential, whereas DA binding to D2-like receptors has the opposite effect. Neurons in the avian striatum express four types of dopamine receptors. Different from mice, up to 50% of MSNs in songbirds express both D1 and D2 receptor types (Kubikova et al., 2010). To test if newborn neurons differ from older, resident neurons in Area X in their expression of DA receptors, we combined *in situ* hybridization to detect DA receptor mRNA with BrdU labeling (**Figures 5A–G**). Because the majority of new neurons were mature at 42 days after BrdU labeling (**Figure 6L**), we decided to analyze DA receptor expression at that point. We found that a fraction of 0.89 ± 0.03 of new neurons expressed D1A, 0.94 ± 0.02 D1B, and 0.69 ± 0.03 D2 receptor mRNA (**Figure 5H**).

These results did not differ statistically from DA receptor mRNA expression values we found in non-BrdU labeled cells (0.9 ± 0.08 D1A, 0.95 ± 0.05 D1B, and 0.66 ± 0.08 D2). The averages of single-labeled D1A and D2 cells added up to more than 1, indicating that at least a fraction of 0.58 of BrdU+ cells co-expressed both receptor types. The averages of single-labeled D1B and D2 indicate that at least a fraction of 0.63 of BrdU+ cells co-expressed D1B and D2 receptors.

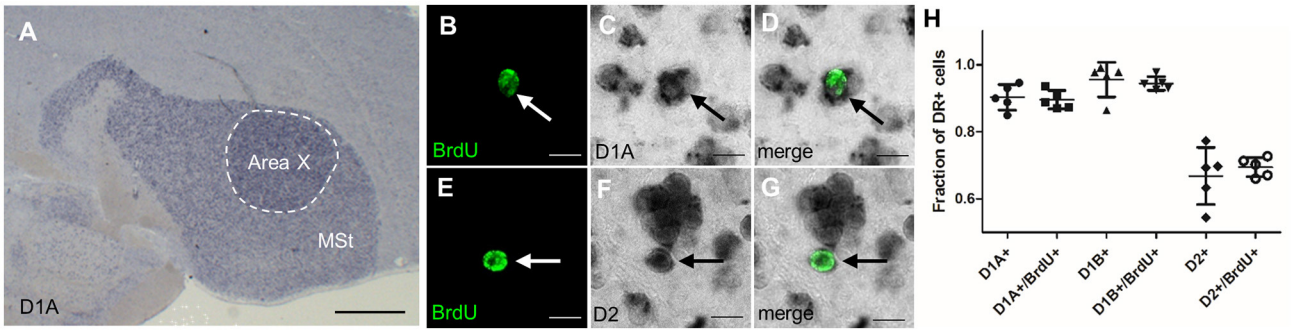

FIGURE 5 | Newborn MSNs do not differ from mature MSNs in their DA receptor expression. **(A)** Dopamine receptors were highly expressed in the MSt and Area X shown here for D1A in a non-fluorescent *in situ* hybridization (blue precipitate). **(B–D)** New MSNs (BrdU+, arrow, fluorescent green label) expressed dopamine receptor D1A (dark precipitate). **(E–G)** New MSNs (BrdU+, arrow) expressed DA receptor D2. **(H)** There was no significant difference in the expression of dopamine receptor types between older neurons (BrdU-) and 42-day-old neurons (BrdU+). One data point represents one animal. Shown are mean and SD. Scale bars: 10 μm **(B–F)**, 500 μm **(A)**.

Age Dependent Activation of Newborn MSNs during Singing Behavior

Having confirmed that newborn MSNs receive both glutamatergic and dopaminergic input and are connected to output neurons, we tested if they participate in signal transduction during singing. We used the immediate early gene EGR-1 as an indicator for neuronal activity (Knapska and Kaczmarek, 2004) in Area X and quantified its expression after singing in new neurons at different survival times (**Figure 6A**). Undirected singing resulted in elevated EGR-1 expression in Area X (**Figure 6B**), as expected (Jarvis et al., 1998; Mello and Ribeiro, 1998).

The fraction of singing-activated, newborn neurons in Area X (BrdU+/EGR-1+, **Figures 6C–F**) cells increased from 0.18 ± 0.17 at 21 dpi to 0.72 ±0.07 at 42 dpi ($F = 13.05$, $p = 0.00038$, **Figure 6K**). There was no significant difference in activation of new neurons between 21 and 31 dpi ($F = 13.05$, $p = 0.149$), but between 31 and 42 dpi ($F = 13.05$, $p = 0.019$, **Figure 6K**). Additionally, we evaluated the maturation course and quantified the expression of the MSN marker DARPP-32 in newborn neurons (BrdU+/DARPP-32+, **Figures 6G–J**). DARPP-32 expression significantly increased from 0.0075 ± 0.015 at 21 dpi to 0.44 ± 0.09 at 31 dpi ($F = 180.8$, $p = 6.3 \times 10^{-6}$) to 0.9 ±0.01 at 42 dpi ($F = 180.8$, $p = 8.3 \times 10^{-6}$, **Figure 6L**).

Age Dependent MSN Density in Area X

When studying adult neurogenesis, it is always of concern whether newly-generated neurons are added continuously to an existing circuit or if they replace older neurons. Both strategies can occur in the same organism: newly generated granule cells in the mouse DG are added to the existing cell pool, whereas in the olfactory bulb new granule cells replace old neurons (Crespo et al., 1986; Imayoshi et al., 2008).

In the canary song control nucleus HVC, newly generated projection neurons are replaced seasonally, while in the zebra finch HVC, new neurons are continuously added to the existing circuit (Walton et al., 2012). To investigate which strategy applies in Area X of zebra finches, we quantified the density of MSNs in zebra finches at different ages. MSN density in Area X increased significantly between 1 and 6 years of age (linear regression, $R^2 = 0.679$ $p = 0.0003$, **Figure 7G**). MSN packing density increased from 78 × 10^4 cells/mm^3 in Area X of a 1-year-old zebra finch (**Figures 7A–C**) to 163 × 10^4 cells/mm^3 in as 6-year-old zebra finch (**Figures 7D–F**). Assuming an Area X size of 1.532 mm^3 (Nixdorf-Bergweiler, 1996) the total number of MSNs in Area X more than doubled from 1.2 to 2.5 million within 5 years. The fraction of MSNs out of all DAPI+ cells also increased significantly with MSN density (linear regression, $R^2 = 0.34$ $p = 0.0286$, **Figure 7H**).

DISCUSSION

In the present study, we investigated key features of adult-generated MSN that integrate into the avian striatal song nucleus Area X. Area X receives long-range cortical glutamatergic innervations from premotor nuclei HVC and LMAN (Bottjer and Johnson, 1997). We tested whether newborn MSNs in Area X receive this input by searching for glutamatergic presynaptic terminals on GFP-labeled newborn neurons after their migration from the ventricular zone. We found those contacts as early as 31 dpi. This time frame of being contacted by long-range excitatory input is similar to that reported for newborn hippocampal granule cells in mice (Deshpande et al., 2013), even though the migration distance of new MSNs from the VZ to Area X is considerably longer. This suggests that glutamatergic innervation of adult-born neurons is more a question of absolute age than a question of time of arrival at their final destination. We did not find presynaptic terminals on all dendritic spines, perhaps because those were in the process of being contacted or eliminated (Ramiro-Cortes et al., 2014).

Besides glutamate, dopaminergic innervation from VTA and SNc is the second main input to Area X (Lewis et al., 1981; Bottjer, 1993; Gale et al., 2008). By combining BrdU birth

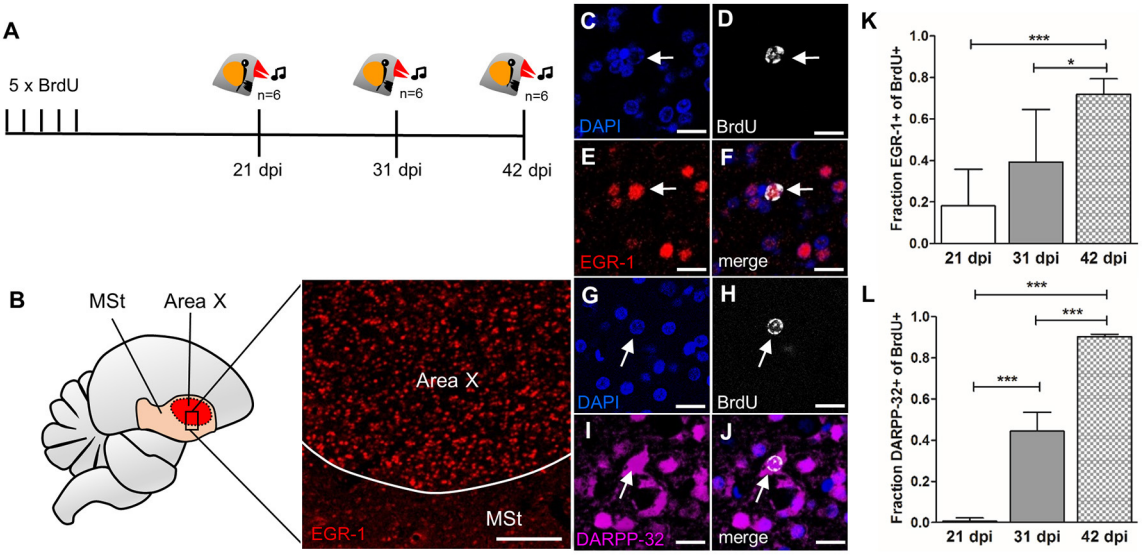

FIGURE 6 | Newborn MSNs are activated during singing in an age-dependent manner. **(A)** Experimental design: Adult male zebra finches ($n = 6$ per age group) received BrdU injections and were sacrificed at 21, 31, or 42 dpi after singing. **(B)** Region specific EGR-1 expression in Area X but not in the surrounding striatum after singing. **(C–F)** Newborn neuron (31 dpi, arrow) expressed EGR-1 after singing. **(G–J)** Newborn neuron (31 dpi arrow) expressed DARPP-32. **(K)** The fraction of new cells (BrdU+) that were activated after singing (EGR-1+) increased significantly between 21 and 42 dpi and between 31 and 42 dpi (shown are mean and SD). **(L)** The fraction of new cells (BrdU+) that express DARPP-32 increased significantly from 21 to 42 dpi (shown are mean and SD). $^{*}P \leq 0.05$; $^{***}P \leq 0.001$. Scale bars: 10 μm **(C–J)**, 100 μm **(B)**.

dating with *in situ* hybridization for DA receptors we established that 6-weeks old MSNs in Area X expressed mRNA for D1- and D2-type receptors in the same fractions as older, resident neurons. This suggests that newborn Area X neurons participate in dopaminergic signaling in the same way as older neurons do. It would be interesting to test if a time-dependent dopamine receptor expression in new neurons was crucial for specific stages of neurogenesis. For example, dopaminergic innervation via D3 receptors stimulates the very early process of progenitor proliferation in mammals and birds (Coronas et al., 2004; Lukacova et al., 2016) and in new murine granular cells, D1-type receptor expression is found earlier than D2-type receptor expression (Mu et al., 2011).

Having established the inputs onto new MSNs we were interested in their connection to pallidal-like projection neurons inside Area X. Direct pallidal-like neurons project to thalamic nucleus DLM and exhibit different firing patterns than indirect pallidal-like neurons (Goldberg and Fee, 2010; Woolley et al., 2014). We observed terminal boutons of newborn MSNs in close proximity to somata and dendrites of direct pallidal-like neurons. This suggests that newborn Area X neurons participate in signal transduction via the pallidal-like projection neurons. Future studies might address whether the innervation and connectivity to output neurons occurs even earlier than by 31 days after generation in the VZ, the time point we chose.

Given that newborn MSN have the morphological hallmarks to receive and transmit signals within Area X, we tested whether they are active during production of undirected song, which is known to induce EGR-1 protein expression (Jarvis et al., 1998; Mello and Ribeiro, 1998). We found that 20% of 21 day old MSN expressed EGR-1 after singing, but DARPP-32 was not detected in any MSN at that age. By 42 days of age, the majority of newborn MSNs expressed both proteins, raising the possibility that new MSNs may have to be physiologically active to trigger their further maturation. This is consistent with the fact that in mammals EGR-1 acts as a transcriptional activator of DARPP-32 (Keilani et al., 2012). One interpretation of our data is that singing-driven EGR-1 triggers maturation of newborn MSNs. This idea is supported indirectly; in mammals, the brain-derived neurotrophic factor (BDNF) enhances EGR-1 binding to the *Darpp-32* gene (Keilani et al., 2012). In canaries, BDNF levels are positively correlated with singing and enhance the survival of newly recruited HVC neurons (Rasika et al., 1999; Li et al., 2000). Similar mechanisms were shown in rodents; voluntary running exercise increases BDNF levels (Kobilo et al., 2011) and individual running activity positively correlates with rates of neurogenesis in the DG (Kodali et al., 2016). If overall individual singing activity influenced neuronal maturation via a BDNF/EGR-1/DARPP-32 pathway, it could explain the high variance in the fraction of activated new MSN during the early maturation phase (31 dpi) in contrast to the later maturation phase (42 dpi). New neurons that survived by then might have reached a stable state, whereas others that were not reliably EGR-1 activated by behavior were eliminated, similar to mechanisms found in the DG of mice (Veyrac et al., 2013).

Are new neurons in Area X added to existing circuits as a replacement of neurons that have died or are they added to the existing cell pool? In the songbird HVC both strategies exist: in canary HVC, seasonal fluctuations in projection neuron death and the recruitment of new neurons are correlated and

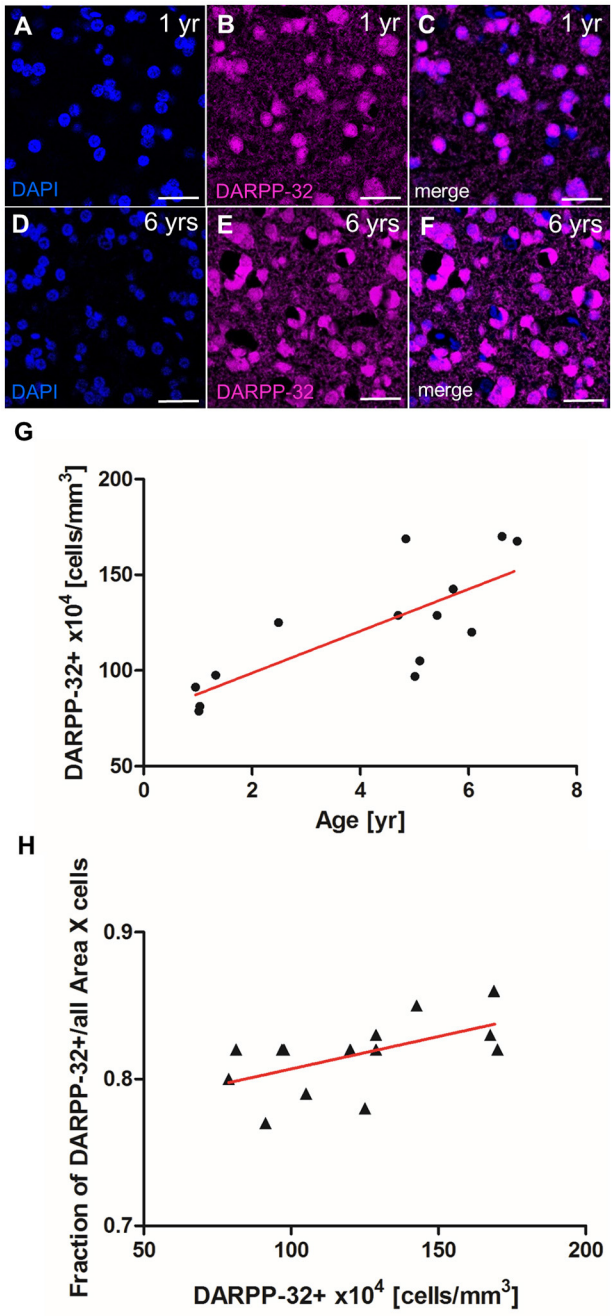

FIGURE 7 | MSN density in Area X increases with age. **(A–C)** MSNs (DARPP-32+) in Area X of a 1-year-old zebra finch male. **(D–F)** MSN (DARPP-32+) in Area X of a 6-year-old zebra finch male. **(G)** The density of MSNs (Darpp-32+) increased significantly with age. **(H)** The fraction of MSNs (DARPP-32+) of all DAPI+ nuclei increased with MSN density. In **(G,H)** one data point represents one animal (mean of both hemispheres). Scale bars: 20 μm **(A–F)**.

the peaks of neural recruitment coincide with the incorporation of new song elements. Together these data are consistent with a replacement strategy (Kirn et al., 1994). In the zebra finch HVC, new projection neurons are added constantly to HVC, resulting in an increasing density within the nucleus (Walton et al., 2012). Correlative evidence suggests that the age-dependent decline of new neuron addition in HVC is associated with increasing song stereotypy (Pytte et al., 2007). Together, these data are best explained by an addition strategy. In the present dataset, we show that the density of DARPP-32 positive MSNs in Area X increased significantly with age, implying that new MSNs were constantly added to the circuit. This does not exclude the possibility that some new neurons replaced apoptotic cells. In fact, experimentally induced apoptosis correlates with replacement by new neurons in zebra finch HVC (Scharff et al., 2000). Further, we found that the fraction of cells that were DARPP-32+ relative to all Area X cells also increased with age. Since the DARPP-32 neurons constitute the majority of cells that undergo adult neurogenesis, this finding emphasizes that increased cell density in Area X is a consequence of continued recruitment of newly born MSN during the course of aging.

Our findings suggest that, once matured, newborn MSNs fulfill the same function as older, resident MSNs, at least concerning the features we analyzed. MSNs function via feed forward inhibition, e.g. sparsely spiking MSNs inhibit tonically active pallidal-like projection neurons. Their high frequency bursts can evoke spiking of DLM neurons via inhibitory rebound (Person and Perkel, 2005, 2007; Kojima and Doupe, 2009). This process in modulated by dopaminergic signals from VTA/SNc. Dopaminergic neurons in VTA/SNc encode performance errors in singing zebra finches (Gadagkar et al., 2016).

We end on some speculations how constant addition of new neurons might affect the AFP and in turn the motor pathway. Constant MSN addition in face of an unchanged number of pallidal-like neurons would be expected to cause stronger inhibitory MSN action on pallidal-like neurons. In turn, DLM would experience fewer inhibitory rebound spikes, causing lower activation of LMAN neurons. Ultimately this would result in reduced excitation of motor nucleus RA by the AFP. If this hypothesis holds true, signaling through the AFP would diminish, as birds get older. In adult birds, the AFP mediates differences in song variability (Hessler and Doupe, 1999; Woolley et al., 2014). Song variability, including deterioration, can be induced experimentally by distorting auditory feedback via deafening or tracheosyringeal nerve cut (Williams and McKibben, 1992; Hough and Volman, 2002; Nordeen and Nordeen, 2010). The AFP seems to mediate this degradation process, since lesions of the AFP output nucleus LMAN prevent song deterioration after auditory feedback distortion (Brainard and Doupe, 2000). Interestingly, song deterioration after deafening is less severe in old birds compared to young birds, and song becomes more stereotyped with age, consistent with our hypothesis (Lombardino and Nottebohm, 2000; Brainard and Doupe, 2001; Pytte et al., 2007, 2012). This scenario does not exclude the possibility that new MSNs initially might undergo a narrow plastic phase, during which they can be tuned and possibly counteract song drift. In summary, we demonstrate that within a month after their generation newly generated MSNs in Area X of adult zebra finches are connected to other song nuclei and participate in neuronal firing during song production. The net increase of Area X neurons with age

might provide a mechanism to achieve the equilibrium between plasticity and stereotypy needed to sustain adult song behavior.

ETHICS STATEMENT

This study was carried out in accordance with the governmental law (TierSchG). The protocol was approved by the LAGeSo, Berlin.

AUTHOR CONTRIBUTIONS

JK and CS planned experiments, JK and LS conducted experiments, JK and CS wrote the manuscript.

FUNDING

JK was funded by the Elsa Neumann scholarship by the state of Berlin.

REFERENCES

Alvarez-Buylla, A., Theelen, M., and Nottebohm, F. (1990). Proliferation "hot spots" in adult avian ventricular zone reveal radial cell division. *Neuron* 5, 101–109.

Arvidsson, A., Collin, T., Kirik, D., Kokaia, Z., and Lindvall, O. (2002). Neuronal replacement from endogenous precursors in the adult brain after stroke. *Nat. Med.* 8, 963–970. doi: 10.1038/nm747

Bedard, A., Cossette, M., Levesque, M., and Parent, A. (2002). Proliferating cells can differentiate into neurons in the striatum of normal adult monkey. *Neurosci. Lett.* 328, 213–216. doi: 10.1016/S0304-3940(02)00530-X

Bottjer, S. W. (1993). The distribution of tyrosine hydroxylase immunoreactivity in the brains of male and female zebra finches. *J. Neurobiol.* 24, 51–69. doi: 10.1002/neu.480240105

Bottjer, S. W., and Johnson, F. (1997). Circuits, hormones, and learning: vocal behavior in songbirds. *J. Neurobiol.* 33, 602–618.

Brainard, M. S., and Doupe, A. J. (2000). Interruption of a basal ganglia-forebrain circuit prevents plasticity of learned vocalizations. *Nature* 404, 762–766. doi: 10.1038/35008083

Brainard, M. S., and Doupe, A. J. (2001). Postlearning consolidation of birdsong: stabilizing effects of age and anterior forebrain lesions. *J Neurosci* 21, 2501–2517.

Coronas, V., Bantubungi, K., Fombonne, J., Krantic, S., Schiffmann, S. N., and Roger, M. (2004). Dopamine D3 receptor stimulation promotes the proliferation of cells derived from the post-natal subventricular zone. *J. Neurochem.* 91, 1292–1301. doi: 10.1111/j.1471-4159.2004.02823.x

Crespo, D., Stanfield, B. B., and Cowan, W. M. (1986). Evidence that late-generated granule cells do not simply replace earlier formed neurons in the rat dentate gyrus. *Exp. Brain Res.* 62, 541–548.

Dayer, A. G., Cleaver, K. M., Abouantoun, T., and Cameron, H. A. (2005). New GABAergic interneurons in the adult neocortex and striatum are generated from different precursors. *J. Cell Biol.* 168, 415–427. doi: 10.1083/jcb.200407053

Deshpande, A., Bergami, M., Ghanem, A., Conzelmann, K. K., Lepier, A., Gotz, M., et al. (2013). Retrograde monosynaptic tracing reveals the temporal evolution of inputs onto new neurons in the adult dentate gyrus and olfactory bulb. *Proc. Natl. Acad. Sci. U.S.A.* 110, E1152–1161. doi: 10.1073/pnas.1218991110

Ernst, A., Alkass, K., Bernard, S., Salehpour, M., Perl, S., Tisdale, J., et al. (2014). Neurogenesis in the striatum of the adult human brain. *Cell* 156, 1072–1083. doi: 10.1016/j.cell.2014.01.044

Farries, M. A., Ding, L., and Perkel, D. J. (2005). Evidence for "direct" and "indirect" pathways through the song system basal ganglia. *J. Comp. Neurol.* 484, 93–104. doi: 10.1002/cne.20464

Gadagkar, V., Puzerey, P. A., Chen, R., Baird-Daniel, E., Farhang, A. R., and Goldberg, J. H. (2016). Dopamine neurons encode performance error in singing birds. *Science* 354, 1278–1282. doi: 10.1126/science.aah6837

Gale, S. D., Person, A. L., and Perkel, D. J. (2008). A novel basal ganglia pathway forms a loop linking a vocal learning circuit with its dopaminergic input. *J. Comp. Neurol.* 508, 824–839. doi: 10.1002/cne.21700

Gerfen, C. R., and Surmeier, D. J. (2011). Modulation of striatal projection systems by dopamine. *Annu. Rev. Neurosci.* 34, 441–466. doi: 10.1146/annurev-neuro-061010-113641

Gerfen, C. R., and Wilson, C. J. (1996). "Chapter II: The basal ganglia," in *Handbook of Chemical Neuroanatomy*, eds A. B. L. W. Swanson and T. Hökfelt (Amsterdam: Elsevier), 371–468.

Goldberg, J. H., Adler, A., Bergman, H., and Fee, M. S. (2010). Singing-related neural activity distinguishes two putative pallidal cell types in the songbird basal ganglia: comparison to the primate internal and external pallidal segments. *J. Neurosci.* 30, 7088–7098. doi: 10.1523/JNEUROSCI.0168-10.2010

Goldberg, J. H., Farries, M. A., and Fee, M. S. (2013). Basal ganglia output to the thalamus: still a paradox. *Trends Neurosci.* 36, 695–705. doi: 10.1016/j.tins.2013.09.001

Goldberg, J. H., and Fee, M. S. (2010). Singing-related neural activity distinguishes four classes of putative striatal neurons in the songbird basal ganglia. *J. Neurophysiol.* 103, 2002–2014. doi: 10.1152/jn.01038.2009

Hessler, N. A., and Doupe, A. J. (1999). Singing-related neural activity in a dorsal forebrain-basal ganglia circuit of adult zebra finches. *J. Neurosci.* 19, 10461–10481.

Hou, S. W., Wang, Y. Q., Xu, M., Shen, D. H., Wang, J. J., Huang, F., et al. (2008). Functional integration of newly generated neurons into striatum after cerebral ischemia in the adult rat brain. *Stroke* 39, 2837–2844. doi: 10.1161/STROKEAHA.107.510982

Hough, G. E. II, and Volman, S. F. (2002). Short-term and long-term effects of vocal distortion on song maintenance in zebra finches. *J. Neurosci.* 22, 1177–1186.

Imayoshi, I., Sakamoto, M., Ohtsuka, T., Takao, K., Miyakawa, T., Yamaguchi, M., et al. (2008). Roles of continuous neurogenesis in the structural and functional integrity of the adult forebrain. *Nat. Neurosci.* 11, 1153–1161. doi: 10.1038/nn.2185

Jarvis, E. D., Scharff, C., Grossman, M. R., Ramos, J. A., and Nottebohm, F. (1998). For whom the bird sings: context-dependent gene expression. *Neuron* 21, 775–788.

Kaslin, J., Ganz, J., and Brand, M. (2008). Proliferation, neurogenesis and regeneration in the non-mammalian vertebrate brain. *Philos. Trans. R Soc. Lond. B Biol. Sci.* 363, 101–122. doi: 10.1098/rstb.2006.2015

Keilani, S., Chandwani, S., Dolios, G., Bogush, A., Beck, H., Hatzopoulos, A. K., et al. (2012). Egr-1 induces DARPP-32 expression in striatal medium spiny neurons via a conserved intragenic element. *J. Neurosci.* 32, 6808–6818. doi: 10.1523/JNEUROSCI.5448-11.2012

Kempermann, G., Song, H., and Gage, F. H. (2015). Neurogenesis in the Adult Hippocampus. *Cold Spring Harb. Perspect. Biol.* 7:a018812. doi: 10.1101/cshperspect.a018812

Kirn, J., O'Loughlin, B., Kasparian, S., and Nottebohm, F. (1994). Cell death and neuronal recruitment in the high vocal center of adult male canaries are temporally related to changes in song. *Proc. Natl. Acad. Sci. U.S.A.* 91, 7844–7848.

Kirn, J. R., Fishman, Y., Sasportas, K., Alvarez-Buylla, A., and Nottebohm, F. (1999). Fate of new neurons in adult canary high vocal center during the first 30 days after their formation. *J. Comp. Neurol.* 411, 487–494.

Kirn, J. R., and Nottebohm, F. (1993). Direct evidence for loss and replacement of projection neurons in adult canary brain. *J. Neurosci.* 13, 1654–1663.

Knapska, E., and Kaczmarek, L. (2004). A gene for neuronal plasticity in the mammalian brain: Zif268/Egr-1/NGFI-A/Krox-24/TIS8/ZENK? *Prog. Neurobiol.* 74, 183–211. doi: 10.1016/j.pneurobio.2004.05.007

Kobilo, T., Liu, Q. R., Gandhi, K., Mughal, M., Shaham, Y., and van Praag, H. (2011). Running is the neurogenic and neurotrophic stimulus in environmental enrichment. *Learn. Mem.* 18, 605–609. doi: 10.1101/lm.2283011

Kodali, M., Megahed, T., Mishra, V., Shuai, B., Hattiangady, B., and Shetty, A. K. (2016). Voluntary running exercise-mediated enhanced neurogenesis does not obliterate retrograde spatial memory. *J. Neurosci.* 36, 8112–8122. doi: 10.1523/JNEUROSCI.0766-16.2016

Kojima, S., and Doupe, A. J. (2009). Activity propagation in an avian basal ganglia-thalamocortical circuit essential for vocal learning. *J. Neurosci.* 29, 4782–4793. doi: 10.1523/JNEUROSCI.4903-08.2009

Kubikova, L., Wada, K., and Jarvis, E. D. (2010). Dopamine receptors in a songbird brain. *J. Comp. Neurol.* 518, 741–769. doi: 10.1002/cne.22255

Leblois, A., Wendel, B. J., and Perkel, D. J. (2010). Striatal dopamine modulates basal ganglia output and regulates social context-dependent behavioral variability through D1 receptors. *J. Neurosci.* 30, 5730–5743. doi: 10.1523/JNEUROSCI.5974-09.2010

Lewis, J. W., Ryan, S. M., Arnold, A. P., and Butcher, L. L. (1981). Evidence for a catecholaminergic projection to area X in the zebra finch. *J. Comp. Neurol.* 196, 347–354. doi: 10.1002/cne.901960212

Li, X. C., Jarvis, E. D., Alvarez-Borda, B., Lim, D. A., and Nottebohm, F. (2000). A relationship between behavior, neurotrophin expression, and new neuron survival. *Proc. Natl. Acad. Sci. U.S.A.* 97, 8584–8589. doi: 10.1073/pnas.140222497

Lim, D. A., and Alvarez-Buylla, A. (2016). The adult ventricular-subventricular zone (V-SVZ) and olfactory bulb (OB) neurogenesis. *Cold Spring Harb. Perspect. Biol.* 8:pii: a018820. doi: 10.1101/cshperspect.a018820

Lois, C., Hong, E. J., Pease, S., Brown, E. J., and Baltimore, D. (2002). Germline transmission and tissue-specific expression of transgenes delivered by lentiviral vectors. *Science* 295, 868–872. doi: 10.1126/science.1067081

Lombardino, A. J., and Nottebohm, F. (2000). Age at deafening affects the stability of learned song in adult male zebra finches. *J. Neurosci.* 20, 5054–5064.

Lukacova, K., Pavukova, E., Kostal, L., Bilcik, B., and Kubikova, L. (2016). Dopamine D3 receptors modulate the rate of neuronal recovery, cell recruitment in Area X, and song tempo after neurotoxic damage in songbirds. *Neuroscience* 331, 158–168. doi: 10.1016/j.neuroscience.2016.06.032

Luzzati, F., De Marchis, S., Fasolo, A., and Peretto, P. (2006). Neurogenesis in the caudate nucleus of the adult rabbit. *J. Neurosci.* 26, 609–621. doi: 10.1523/JNEUROSCI.4371-05.2006

Mello, C. V., and Ribeiro, S. (1998). ZENK protein regulation by song in the brain of songbirds. *J. Comp. Neurol.* 393, 426–438.

Mu, Y., Zhao, C., and Gage, F. H. (2011). Dopaminergic modulation of cortical inputs during maturation of adult-born dentate granule cells. *J. Neurosci.* 31, 4113–4123. doi: 10.1523/JNEUROSCI.4913-10.2011

Nixdorf-Bergweiler, B. E. (1996). Divergent and parallel development in volume sizes of telencephalic song nuclei in male and female zebra finches. *J. Comp. Neurol.* 375, 445–456. doi: 10.1002/(SICI)1096-9861(19961118)375:3<445::AID-CNE7>3.0.CO;2-2

Nordeen, K. W., and Nordeen, E. J. (1988). Projection neurons within a vocal motor pathway are born during song learning in zebra finches. *Nature* 334, 149–151. doi: 10.1038/334149a0

Nordeen, K. W., and Nordeen, E. J. (2010). Deafening-induced vocal deterioration in adult songbirds is reversed by disrupting a basal ganglia-forebrain circuit. *J. Neurosci.* 30, 7392–7400. doi: 10.1523/JNEUROSCI.6181-09.2010

Paredes, M. F., Sorrells, S. F., Garcia-Verdugo, J. M., and Alvarez-Buylla, A. (2016). Brain size and limits to adult neurogenesis. *J. Comp. Neurol.* 524, 646–664. doi: 10.1002/cne.23896

Person, A. L., and Perkel, D. J. (2005). Unitary IPSPs drive precise thalamic spiking in a circuit required for learning. *Neuron* 46, 129–140. doi: 10.1016/j.neuron.2004.12.057

Person, A. L., and Perkel, D. J. (2007). Pallidal neuron activity increases during sensory relay through thalamus in a songbird circuit essential for learning. *J. Neurosci.* 27, 8687–8698. doi: 10.1523/JNEUROSCI.2045-07.2007

Pytte, C. L., George, S., Korman, S., David, E., Bogdan, D., and Kirn, J. R. (2012). Adult neurogenesis is associated with the maintenance of a stereotyped, learned motor behavior. *J. Neurosci.* 32, 7052–7057. doi: 10.1523/JNEUROSCI.5385-11.2012

Pytte, C. L., Gerson, M., Miller, J., and Kirn, J. R. (2007). Increasing stereotypy in adult zebra finch song correlates with a declining rate of adult neurogenesis. *Dev. Neurobiol.* 67, 1699–1720. doi: 10.1002/dneu0.20520

Ramiro-Cortes, Y., Hobbiss, A. F., and Israely, I. (2014). Synaptic competition in structural plasticity and cognitive function. *Philos. Trans. R Soc. Lond. B. Biol. Sci.* 369:20130157. doi: 10.1098/rstb.2013.0157

Rasika, S., Alvarez-Buylla, A., and Nottebohm, F. (1999). BDNF mediates the effects of testosterone on the survival of new neurons in an adult brain. *Neuron* 22, 53–62.

R Development Core Team (2013). *R: A Language and Environment for Statistical Computing*. Vienna: R Foundation for Statistical Computing.

Reiner, A., Laverghetta, A. V., Meade, C. A., Cuthbertson, S. L., and Bottjer, S. W. (2004). An immunohistochemical and pathway tracing study of the striatopallidal organization of area X in the male zebra finch. *J. Comp. Neurol.* 469, 239–261. doi: 10.1002/cne.11012

Rochefort, C., He, X., Scotto-Lomassese, S., and Scharff, C. (2007). Recruitment of FoxP2-expressing neurons to area X varies during song development. *Dev. Neurobiol.* 67, 809–817. doi: 10.1002/dneu.20393

Sasaki, A., Sotnikova, T. D., Gainetdinov, R. R., and Jarvis, E. D. (2006). Social context-dependent singing-regulated dopamine. *J. Neurosci.* 26, 9010–9014. doi: 10.1523/JNEUROSCI.1335-06.2006

Scharff, C., Kirn, J. R., Grossman, M., Macklis, J. D., and Nottebohm, F. (2000). Targeted neuronal death affects neuronal replacement and vocal behavior in adult songbirds. *Neuron* 25, 481–492. doi: 10.1016/S0896-6273(00)80910-1

Scharff, C., and Nottebohm, F. (1991). A comparative-study of the behavioral deficits following lesions of various parts of the zebra finch song system - implications for vocal learning. *J. Neurosci.* 11, 2896–2913.

Schindelin, J., Arganda-Carreras, I., Frise, E., Kaynig, V., Longair, M., Pietzsch, T., et al. (2012). Fiji: an open-source platform for biological-image analysis. *Nat. Methods* 9, 676–682. doi: 10.1038/nmeth.2019

Scott, B. B., and Lois, C. (2007). Developmental origin and identity of song system neurons born during vocal learning in songbirds. *J. Comp. Neurol.* 502, 202–214. doi: 10.1002/cne.21296.

Sohrabji, F., Nordeen, E. J., and Nordeen, K. W. (1990). Selective impairment of song learning following lesions of a forebrain nucleus in the juvenile zebra finch. *Behav. Neural Biol.* 53, 51–63.

Song, J., Olsen, R. H. J., Sun, J., Ming, G. L., and Song, H. (2016). Neuronal circuitry mechanisms regulating adult mammalian neurogenesis. *Cold Spring Harb. Perspect. Biol.* 8. doi: 10.1101/cshperspect.a018937

Tattersfield, A. S., Croon, R. J., Liu, Y. W., Kells, A. P., Faull, R. L., and Connor, B. (2004). Neurogenesis in the striatum of the quinolinic acid lesion model of Huntington's disease. *Neuroscience* 127, 319–332. doi: 10.1016/j.neuroscience.2004.04.061

Tchernichovski, O., Nottebohm, F., Ho, C. E., Pesaran, B., and Mitra, P. P. (2000). A procedure for an automated measurement of song similarity. *Anim. Behav.* 59, 1167–1176. doi: 10.1006/anbe.1999.1416

Tepper, J. M., Tecuapetla, F., Koos, T., and Ibanez-Sandoval, O. (2010). Heterogeneity and diversity of striatal GABAergic interneurons. *Front. Neuroanat.* 4:150. doi: 10.3389/fnana.2010.00150

Tokarev, K., Boender, A. J., Claßen, G. A. E., and Scharff, C. (2016). Young, active and well-connected: adult-born neurons in the zebra finch are activated during singing. *Brain Struct. Funct.* 221, 1833–1843. doi: 10.1007/s00429-015-1006-y

Tonchev, A. B., Yamashima, T., Sawamoto, K., and Okano, H. (2005). Enhanced proliferation of progenitor cells in the subventricular zone and limited neuronal production in the striatum and neocortex of adult macaque monkeys after global cerebral ischemia. *J. Neurosci. Res.* 81, 776–788. doi: 10.1002/jnr.20604

Veyrac, A., Gros, A., Bruel-Jungerman, E., Rochefort, C., Kleine Borgmann, F. B., Jessberger, S., et al. (2013). Zif268/egr1 gene controls the selection, maturation and functional integration of adult hippocampal newborn neurons by learning. *Proc. Natl. Acad. Sci. U.S.A.* 110, 7062–7067. doi: 10.1073/pnas.1220558110

Walton, C., Pariser, E., and Nottebohm, F. (2012). The zebra finch paradox: song is little changed, but number of neurons doubles. *J. Neurosci.* 32, 761–774. doi: 10.1523/JNEUROSCI.3434-11.2012

Williams, H., and McKibben, J. R. (1992). Changes in stereotyped central motor patterns controlling vocalization are induced by peripheral nerve injury. *Behav. Neural. Biol.* 57, 67–78.

Woolley, S. C., Rajan, R., Joshua, M., and Doupe, A. J. (2014). Emergence of context-dependent variability across a basal ganglia network. *Neuron* 82, 208–223. doi: 10.1016/j.neuron.2014.01.039

Conflict of Interest Statement: The authors declare that the research was conducted in the absence of any commercial or financial relationships that could be construed as a potential conflict of interest.

frontiers in Neuroscience

ORIGINAL RESEARCH
published: 23 August 2016
doi: 10.3389/fnins.2016.00387

Neuroblast Distribution after Cortical Impact Is Influenced by White Matter Injury in the Immature Gyrencephalic Brain

*Sabrina R. Taylor[1], Colin M. Smith[2], Kristen L. Keeley[2], Declan McGuone[3], Carter P. Dodge[4], Ann-Christine Duhaime[2,5] and Beth A. Costine[2,5]**

[1] Department of Physical Medicine and Rehabilitation, Spaulding Rehabilitation Hospital, Charlestown, MA, USA, [2] Brain Trauma Lab, Department of Neurosurgery, Massachusetts General Hospital, Boston, MA, USA, [3] The Office of Chief Medical Examiner, New York, NY, USA, [4] Department of Anesthesiology, Dartmouth Medical School, Children's Hospital at Dartmouth, Lebanon, PA, USA, [5] Department of Neurosurgery, Harvard Medical School, Boston, MA, USA

Cortical contusions are a common type of traumatic brain injury (TBI) in children. Current knowledge of neuroblast response to cortical injury arises primarily from studies utilizing aspiration or cryoinjury in rodents. In infants and children, cortical impact affects both gray and white matter and any neurogenic response may be complicated by the large expanse of white matter between the subventricular zone (SVZ) and the cortex, and the large number of neuroblasts in transit along the major white matter tracts to populate brain regions. Previously, we described an age-dependent increase of neuroblasts in the SVZ in response to cortical impact in the immature gyrencephalic brain. Here, we investigate if neuroblasts target the injury, if white matter injury influences repair efforts, and if postnatal population of brain regions are disrupted. Piglets received a cortical impact to the rostral gyrus cortex or sham surgery at postnatal day (PND) 7, BrdU 2 days prior to (PND 5 and 6) or after injury (PND 7 and 8), and brains were collected at PND 14. Injury did not alter the number of neuroblasts in the white matter between the SVZ and the rostral gyrus. In the gray matter of the injury site, neuroblast density was increased in cavitated lesions, and the number of $BrdU^+$ neuroblasts was increased, but comprised less than 1% of all neuroblasts. In the white matter of the injury site, neuroblasts with differentiating morphology were densely arranged along the cavity edge. In a ventral migratory stream, neuroblast density was greater in subjects with a cavitated lesion, indicating that TBI may alter postnatal development of regions supplied by that stream. Cortical impact in the immature gyrencephalic brain produced complicated and variable lesions, increased neuroblast density in cavitated gray matter, resulted in potentially differentiating neuroblasts in the white matter, and may alter the postnatal population of brain regions utilizing a population of neuroblasts that were born prior to PND 5. This platform may be useful to continue to study potential complications of white matter injury and alterations of postnatal population of brain regions, which may contribute to the chronic effects of TBI in children.

Keywords: neurogenesis, neuroplasticity, gyrencephalic, pediatric brain injury, traumatic brain injury, calretinin, interstitial neurons

OPEN ACCESS

Edited by:
Luca Bonfanti, University of Turin, Italy

Reviewed by:
Francis G. Szele, University of Oxford, UK
Enrica Boda, University of Turin, Italy

***Correspondence:**
Beth A. Costine
bcostine@mgh.harvard.edu

Specialty section:
This article was submitted to Neurogenesis, a section of the journal Frontiers in Neuroscience

Received: *25 May 2016*
Accepted: *08 August 2016*
Published: *23 August 2016*

Citation:
Taylor SR, Smith CM, Keeley KL, McGuone D, Dodge CP, Duhaime A-C and Costine BA (2016) Neuroblast Distribution after Cortical Impact Is Influenced by White Matter Injury in the Immature Gyrencephalic Brain. Front. Neurosci. 10:387. doi: 10.3389/fnins.2016.00387

INTRODUCTION

Traumatic brain injury (TBI) is the leading cause of death and disability in children, and yet, all promising neuroprotective treatments developed in rodent models have failed in preclinical trials to date (Margulies and Hicks, 2009). One treatment strategy may be the stimulation of innate neuro-regenerative mechanisms to support or replace damaged neurons (Longhi et al., 2004). The effect of TBI on neurogenesis is commonly studied in the hippocampus where TBI has been shown to stimulate neurogenesis in the hippocampal niche in both immature and adult rodent models (Dash et al., 2001; Rola et al., 2006) less studied is the migration of neuroblasts from the subventricular zone (SVZ) to a cortical injury where neuroblasts have been observed to differentiate around the lesion cavity in gray matter in rodent models of TBI (Covey et al., 2010; Saha et al., 2013). In rodent models of stroke, inhibition of neurogenesis has been demonstrated to exacerbate damage (Jin et al., 2010; Marlier et al., 2015). Migration of neuroblasts to the injury and the capacity of neuroblasts to aid in injury repair may be species-specific emphasizing the importance of studying neurogenesis and response to injury in the gyrencephalic brain (Cattaneo and Bonfanti, 2014; Peretto and Bonfanti, 2015). It has yet to be determined if neurogenesis and the targeting of neuroblasts to the injury site is a helpful strategy promoting recovery in the gyrencephalic brain where TBI results in significant white matter injury (Wilde et al., 2006; Wu et al., 2010).

In our large animal model, cortical impact affects both cortical gray matter and cerebral white matter as it deforms 50% of the distance from the cortical gyral crest to the lateral ventricles and thus models blunt impact head injury in children who have deformable skulls and display preferential white matter injury (Duhaime et al., 2000; Missios et al., 2009). We have previously demonstrated an increase in lesion size with increasing age despite injury input parameters scaled for brain growth, and have demonstrated a developmental decrease in the area of the SVZ with increasing age (Costine et al., 2015). In response to scaled cortical impact, the area of neuroblasts in the SVZ increases, but is age-dependent with an increase in piglets developmentally similar to infants (PND 7) and toddlers (PND 30), and no response in piglets developmentally similar to human pre-adolescents (4 months; Costine et al., 2015). The uninjured PND 14 piglet brain has 2 million neuroblasts with a migratory morphology throughout the major white matter tracts (Costine et al., 2015). Neuroblasts are observed to migrate out of the SVZ into the periventricular white matter with the number decreasing with increased age (Sanai et al., 2011; Taylor et al., 2013; Costine et al., 2015).

Blunt impact head trauma during immaturity may not only cause foci of injury, but may also disrupt the normal developmental program of postnatal population of specific brain regions (De Marchis et al., 2004; Sanai et al., 2011; Costine et al., 2015). In normal early postnatal development in gyrencephalic species, large populations of neuroblasts are found in a migratory morphology in the major white matter tracts (Sanai et al., 2011; Costine et al., 2015). The SVZ generates neuroblasts that migrate to distant brain regions via distinct pathways, migratory streams to the olfactory bulbs (where population continues past infancy), prefrontal cortex, and possibly the nucleus accumbens (De Marchis et al., 2004; Sanai et al., 2011). An attempt to repair a traumatic injury in the immature brain may interrupt the postnatal population of specific brain regions resulting in misdirection of migrating neuroblasts from regions undergoing postnatal population or delay progression through damaged white matter. Stalled migration of neuroblasts may potentially result in ectopic foci of neurons, which may act as a substrate for aberrant electrical activity and post-traumatic epilepsy (Taylor et al., 2013; Petit et al., 2014; Irimia and Van Horn, 2015). In addition, mechanical disruption of the structural integrity of gyral white matter tracts following TBI may further impede migration of neuroblasts to the cortical gray matter. In the immature gyrencephalic brain, which utilizes extensive white matter tracts for neuroblast migration during postnatal brain development, disruption of migration patterns might exacerbate complications from TBI (Scharfman and Hen, 2007; Scharfman and McCloskey, 2009; Costine et al., 2015).

Here, we continue our investigation of neuroblasts after cortical impact or sham surgery. We describe for the first time the active postnatal population of the claustrum, which plays a role in the integration of sensory information. The objectives of these experiments were to determine if a cortical impact in the immature gyrencephalic brain results in (1) neuroblasts that target the injury site, (2) disruption of normal postnatal population of the claustrum, and lastly, (3) to determine if neuroblasts in these areas were born before or after cortical impact. Specifically, we administered bromodeoxyuridine (BrdU) just prior to or after TBI or sham surgery in PND 7 piglets and analyzed the brain 7 days after injury. Neuroblasts with or without BrdU were quantified in the white matter tracts leading from the SVZ to the injury, within the injured rostral gyrus, and in a ventral migratory stream that leads to the claustrum, which is normally undergoing active population by neuroblasts at PND 14.

MATERIALS AND METHODS

Surgery, BrdU Administration, and Brain Collection

Twenty-nine male, Yorkshire piglets (Earle Parsons and Sons, Inc., Hadley, MA) were housed and fed as previously described after arrival at PND 5 (Costine et al., 2015). Milk replacer was removed overnight prior to surgery and piglets were given a liquid electrolyte solution (BlueLite; TechMix, Inc., Stewart, MN). A total of two piglets died before the end of the experiment: one anesthetic death in a 7 day old piglet likely due to a relative overdose of isoflurane and one piglet was euthanized before the end of the experiment due to illness that developed prior to the start to the experiment (scours, weakness, and weight loss). Four of the sham piglets developed a hematoma at the site of dural incision (discussion below). After careful consideration, these piglets were excluded as the pathology indicated a tissue response to injury that may have interfered with their ability to serve as true shams. A total of 23 piglets were used for

analysis. All protocols and procedures were in accordance with the guidelines of the American Veterinary Association and the National Institutes of Health, and were approved by the Animal Care and Use Committee at Massachusetts General Hospital.

Piglets were randomly assigned to a 2 × 2 factorial array experiment with time of BrdU and injury as the main effects resulting in four groups: (1) sham surgery, BrdU before surgery, $n = 5$, (2) sham surgery, BrdU after surgery, $n = 4$, (3) injury, BrdU before surgery, $n = 7$, and (4) injury, BrdU after surgery, $n = 7$. Piglets received a total of 4 injections (**Table 1**); BrdU (50 mg/kg; IP) or vehicle (saline) was administered as previously described while piglets were lightly anesthetized with isoflurane once per day (Costine et al., 2015). The different time points in administration of BrdU was to compare the number of $BrdU^+$ neurons before relative to after injury, in order to identify whether injury itself stimulated the formation of new neurons from the SVZ within the first days after trauma.

Surgery and anesthesia protocols were employed as previously described (Missios et al., 2009; Costine et al., 2015). Briefly, on PND 7, anesthesia was induced and maintained with isoflurane mixed with room air and piglets were mechanically ventilated. Piglets received buprenorphine (0.005 mg/kg, IM), and heart rate, blood pressure, end tidal CO_2, oxygen saturation, and body temperature were monitored and maintained within a narrow range (Missios et al., 2009). As previously described, a craniectomy to create a 2 cm burr hole in the skull was performed over the right coronal suture exposing the rostral gyrus, the somatosensory cortex with somatotopy to the snout (Missios et al., 2009). This site was chosen to create a pathologically significant, but clinically silent lesion that we have previously characterized (Duhaime et al., 2000, 2003; Missios et al., 2009). The dura was incised to expose the cortical surface and a spring-loaded indentation device was secured to the skull with screws. The device contained an indentor tip scaled to displace 1% of brain volume in 4 ms (Duhaime et al., 2000; Missios et al., 2009). After injury, the dura was re-approximated and the skin was closed. Sham piglets underwent the surgery at PND 7 without deployment of the indentor. After seven sham surgeries had been performed, it was observed that four sham piglets developed cortical hematomas. It was postulated the incised dura bled onto the cortical surface, and the dura was scored but left intact in the remaining six sham animals. No additional hematomas were observed. Animals were recovered from general anesthesia and weighed daily before euthanasia on day 7 post-injury as an indicator of general health. Average daily gain was not different between sham and injured piglets (0.14 ± 0.2 vs. 0.13 ± 0.2 kg/day; $P = 0.6$).

Seven days after injury (PND 14), piglets were deeply anesthetized and euthanized via exsanguination by transcardial perfusion with 0.9% saline followed by 10% buffered formalin as previously described (Missios et al., 2009; Costine et al., 2015). The brain was removed, post-fixed overnight at 4°C, and coronally sliced into 5 mm blocks starting at the anterior edge of the rostral gyrus. The three adjacent 5 mm coronal blocks containing the injury site and SVZ were post-fixed in 10% buffered formalin overnight at 4°C then cryoprotected in 30% sucrose in phosphate buffered saline (PBS) over 2–3 days at 4°C. Blocks were embedded in optimum cutting temperature compound (OCT, Tissue-Tek®), frozen, and stored at −80°C. Frozen sections were made (50 μm) and every other section was mounted on poly-L-lysine-coated microscope slides (Superfrost® Plus, Fisherbrand®, Fisher Scientific, Pittsburgh, PA), dried, and stored at −80°C.

Histologic Analysis

In order to ascertain the presence and severity of injury, two 10 μm sections from each piglet (one from each hemisphere) were obtained just caudal to the impact site. The sections were stained with Luxol-fast-blue/hematoxylin-eosin (LH&E) and were analyzed by a neuropathologist (DM) blinded to injury and hemisphere for contusional injury, hemorrhage, necrosis, and acute and chronic inflammation.

Immunofluorescence was used to assess the effect of trauma on cell types indicative of neurogenesis (DCX^+, $BrdU^+$, and $DCX^+/BrdU^+$ cells) or markers of early neuronal differentiation (calretinin) or mature neurons (NeuN) as previously described (Costine et al., 2015; Sarnat, 2015). Between all steps, sections were washed three times in 0.1 M tris-buffered saline (TBS; 1 M Tris-HCl, 1.5 M NaCl; pH 7.5). Mounted tissue was rehydrated in TBS followed by permeabilization in 1% Triton X-100 (ICN Biomedicals, Aurora, OH) in TBS (TBST) for 20 min. Sections were placed in 10 mM citric acid buffer (pH 6.0) in a pressure cooker (DAKO, Carpinteria, CA) reaching 120°C for 10 min and 90°C for 20 min for concurrent antigen retrieval and DNA denaturation (Tang et al., 2007). The tissue was allowed to equilibrate to room temperature for 30 min before blocking with 5% donkey serum/TBST (TBSTD, ab7475, Abcam, Cambridge, MA) for 30 min. Sections were incubated in various combinations of the following primary antibodies: goat anti-human DCX (sc-8066, Santa Cruz Biotechnology, Santa Cruz, CA; 1:100), mouse anti-BrdU (ab8152, Abcam; 1:75), rabbit anti-calretinin (ab702, Abcam; 1:100), mouse anti-CD68 (M0876, Dako; 1:100), anti-mouse NeuN (MAB377; Millipore;1:100) and were diluted in TBSTD overnight at 4°C.

TABLE 1 | Timeline and treatment of piglets.

Day	Day-2	Day-1	Day 0 Injury or sham	Day 1 post-injury	Day 2 post-injury	Day 3 post-injury	Day 4 post-injury	Day 5 post-injury	Day 6 post-injury	Day 7 post-injury
Age	PND 5	PND 6	PND 7	PND 8	PND 9	PND 10	PND 11	PND 12	PND 13	PND 14
BrdU before	BrdU	BrdU	Vehicle	Vehicle						
BrdU after	Vehicle	Vehicle	BrdU	BrdU						Brain collection

We previously determined that this DCX antibody does not co-localize with markers of astrocytes nor microglia (Taylor et al., 2013). After washing the primary antibody, sections were incubated in Alexa Fluor 488 donkey anti-goat (for DCX) and Alexa Fluor 568 donkey anti-mouse (for BrdU) or Alexa Fluor 568 donkey anti-rabbit (for calretinin;1:200, Invitrogen, Carlsbad, CA) or Alexa Fluor 488 donkey-anti-mouse for CD68 or NeuN for 2 h at room temperature protected from light. Sections were then coated with Vectashield Mounting Medium with 4′,6-diamidino-2-phenylindole (DAPI) to detect all nuclei (Vector Laboratories, Inc., Burlingame, CA) or were incubated for 15 min in 0.5 μM TO-PRO®-3 Iodide in PBS (TOPRO; Thermofisher Scientific, Cambridge, MA) and cover slipped. Negative control sections excluded primary antibodies. In the absence of primary antibody, some blood vessel structures were observed. In the center of the lesion cavity, auto-fluorescence of red blood cells and perhaps other cellular debris was observed and was not imaged. Black holes in images are artifact from freezing that was primarily observed in gray matter.

Stereological Quantification of Cell Types in the White Matter Tract Leading from the SVZ to the Rostral Gyrus

The total numbers of DCX^+ ("neuroblasts"), $BrdU^+$("$BrdU^+$ cells"), and $DCX^+/BrdU^+$ cells ("$BrdU^+$ neuroblasts") in the white matter from the SVZ to the site of injury (**Figure 1A**) were quantified with the optical fractionator method (Francis et al., 2006). A Nikon TE-2000 microscope with a motorized XYZ stage was used for quantification. Quantification was completed on 13–18 sections per animal (6–9 sections per hemisphere), which were positioned every 1200 μm after a random start within the first 12 sections. Sections were coded and identifiers removed on the slide for analysis. Briefly, the Stereo Investigator software was used to draw a contour around the white matter from the abventricular SVZ to the impact site on the cortex including the centrum semiovale (the white matter under the gray matter in the cerebrum; **Figure 1A**) using a 2x objective. Once the region of interest had been outlined, quantification of cells was carried out using a 20x objective. The sampling scheme was as follows: sampling grid: 859 × 1255 μm (with random orientation); counting frame: 200 × 200 μm; dissector height: 30 μm; and guard zones: 5 μm. Every DCX^+, $BrdU^+$, and $DCX^+/BrdU^+$ cell was tagged with a specific marker and tracked in the Stereo Investigator section manager to avoid over-counting. When the specific tags for DCX^+ and $BrdU^+$ cells were proximally located, co-localization was confirmed at 40x before tagging the cell with a third tag for $DCX^+/BrdU^+$ cells. The area of the region of interest was determined using Stereo Investigator, and the total numbers (N) of DCX^+, $BrdU^+$, and $DCX^+/BrdU^+$ cells were then calculated with the optical fractionator formula: $N = \frac{1}{ssf} \times \frac{1}{asf} \times \frac{1}{hsf} \times \sum Q^-$. For this experiment the section sampling fraction (ssf) was $\frac{1}{24}$, the area sampling fraction (asf) was $\frac{1}{27}$, and the height sampling fraction (hsf) was $\sim\frac{30}{36}$. As before, $\sum Q^-$ was the total count of particles sampled for the entire white matter area.

DCX^+ cells were characterized as neuroblasts if they had an elongated morphology with uni—or bi-polar processes to indicate migration ("neuroblasts"). Cells were considered $BrdU^+$ if they had nuclei, visualized with DAPI, which were positive for BrdU ("$BrdU^+$ cells," not co-localized with DCX). Neuroblasts were quantified as newborn cells if the nucleus was positive for BrdU with a surrounding cytoplasm positive for DCX ("$BrdU^+$ neuroblasts," **Figures 1E–H**).

Quantification of Cells in Region of the Injury, a Ventral Migratory Stream, and Claustrum

To further investigate the region of the injury and other brain regions where injury may affect neuroblast density, microphotographs were analyzed as a more time efficient method than stereology. The other advantage was that microphotographs could be quantified by multiple workers blinded to the treatment (without having access to view the tissue section on the microscope), and easily audited by multiple workers. Images were obtained using a 20x objective with the microscope and camera (described above) of four fields in 2 sections from each piglet for the following regions: rostral gyrus gray matter, rostral gyrus white matter, a ventral migratory stream in the external capsule, and the claustrum. Sections were selected from the contralateral hemisphere of sham piglets or the ipsilateral hemisphere of injured piglets. To ensure neuroblasts were quantified in injured sections, we required evidence of injury in the section analyzed that were binned into 2 categories: (1) large cavitation through the gray matter extending into the gyral white matter and sometimes deeper into the subcortical white matter: "$cavity^+$ lesion," (2) disruption in the gray matter of the gyral crest surface at the impact site only: "$cavity^-$ lesion." One injured piglet was excluded as an area of injury was not visible on immunofluorescence in multiple sections evaluated (though an injury was observed for that piglet on tissue stained with LH&E). To select the area for imaging in the rostral gyrus, the entire gyrus was evaluated for areas of high neuroblast density, and 1–2 photos were obtained for gray or white matter. Thereafter, images were obtained for gray matter in the dorsal portion of the gyrus dorsal to the termination of the gyral white matter and mid-gyrus to the right and left of gyral white matter. White matter images were obtained at evenly spaced distances along the gyral white matter spanning the tract. Cortical layer II pyramidal neurons were DCX^+ in all piglets and this layer was often disrupted in injured piglets and was, therefore, not included in imaging for cell quantification (**Figures 2B,C**). In images removed of subject and treatment identifiers, the numbers of DCX ("neuroblasts"), BrdU ("$BrdU^+$ cells"), and DCX/BrdU cells ("$BrdU^+$ neuroblasts") were quantified using the "Cell Counter" plugin of ImageJ (National Institutes of Health, Bethesda, MD). The eight fields per region per piglet per cell type ($BrdU^+$, $BrdU^+$ neuroblasts, neuroblasts) were averaged and the maximum count was identified.

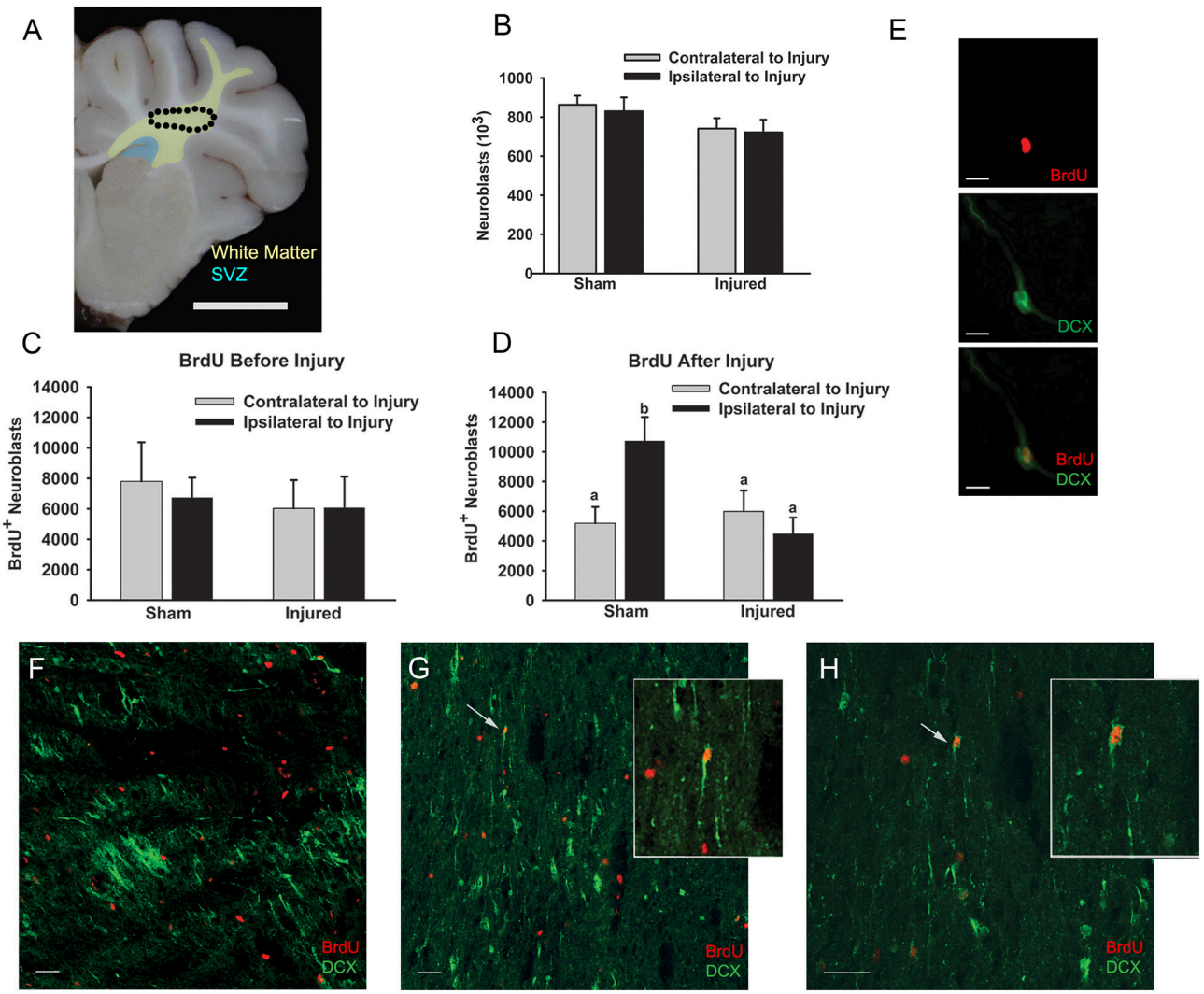

FIGURE 1 | Cortical impact did not alter the number of neuroblasts or BrdU$^+$ neuroblasts in the white matter tracts leading to the injury. Piglets received cortical impact or sham surgeries on PND 7 with BrdU administered prior to injury or after injury, and the brains were collected at PND 14. **(A)** Schematic illustrating the SVZ (blue) and the white matter where neuroblasts were quantified (yellow) including the corpus callosum, centrum semiovale (circle), and the white matter of the rostral gyrus. The number of neuroblasts **(B)** and the number of BrdU$^+$ neuroblasts when BrdU was given before **(C)** or after **(D)** injury was not greater in injured vs. sham piglets as determined with two-way ANOVA followed by Fisher's LSD *post-hoc* analyses. **(D)** However, the number of BrdU$^+$ neuroblasts in the ipsilateral hemisphere of sham piglets was greater than the contralateral hemisphere and both hemispheres of injured piglets (^{a,b}Means ± SEM with different letters differ, $P < 0.05$). **(E)** High power photomicrograph demonstrating DCX (green) and BrdU (red) co-labeling in a neuroblast with a migratory morphology. **(F)** Neuroblasts and BrdU$^+$ cells in the corpus collosum of sham piglets. **(G,H)** Neuroblasts and BrdU$^+$ cells in the white matter of the rostral gyrus of sham piglets with arrows indicating BrdU$^+$ neuroblasts. Inset: Increased magnification of BrdU$^+$ neuroblasts. Scale bars: **(A)** = 1 cm; **(F–H)** = 20 μm; **(E)** = 10 μm.

Preliminary Analysis of Neuroblast Morphology in Regions of Injured White Matter

To further characterize the morphology of neuroblasts according to the region within the injured white matter, photomicrographs of the white matter were analyzed in a subset of piglets with cavity$^+$ lesions ($n = 2$). Using the "Simple Neurite Tracer" plugin in ImageJ, neuroblasts, as detected with DCX, were analyzed in single plane or z stack photomicrographs in the injured white matter either adjacent to the cavity ($n = 244$ neuroblasts in three photomicrographs; **Figure 4**) or in the injured white matter at a distance from the cavity ($n = 143$ neuroblasts in three photomicrographs). The total number of branches was recorded per neuroblast. The mean number of branches per neuroblasts in each injury location and the percentage of unipolar (no branches), bipolar (1 branch off the neuroblast), and multipolar neuroblasts (2 or more branches off the neuroblast) per injury location were determined. For example, the neuroblast in **Figure 1E** is considered "unipolar" with only the main neuroblast. The neuroblast in **Figure 4E**

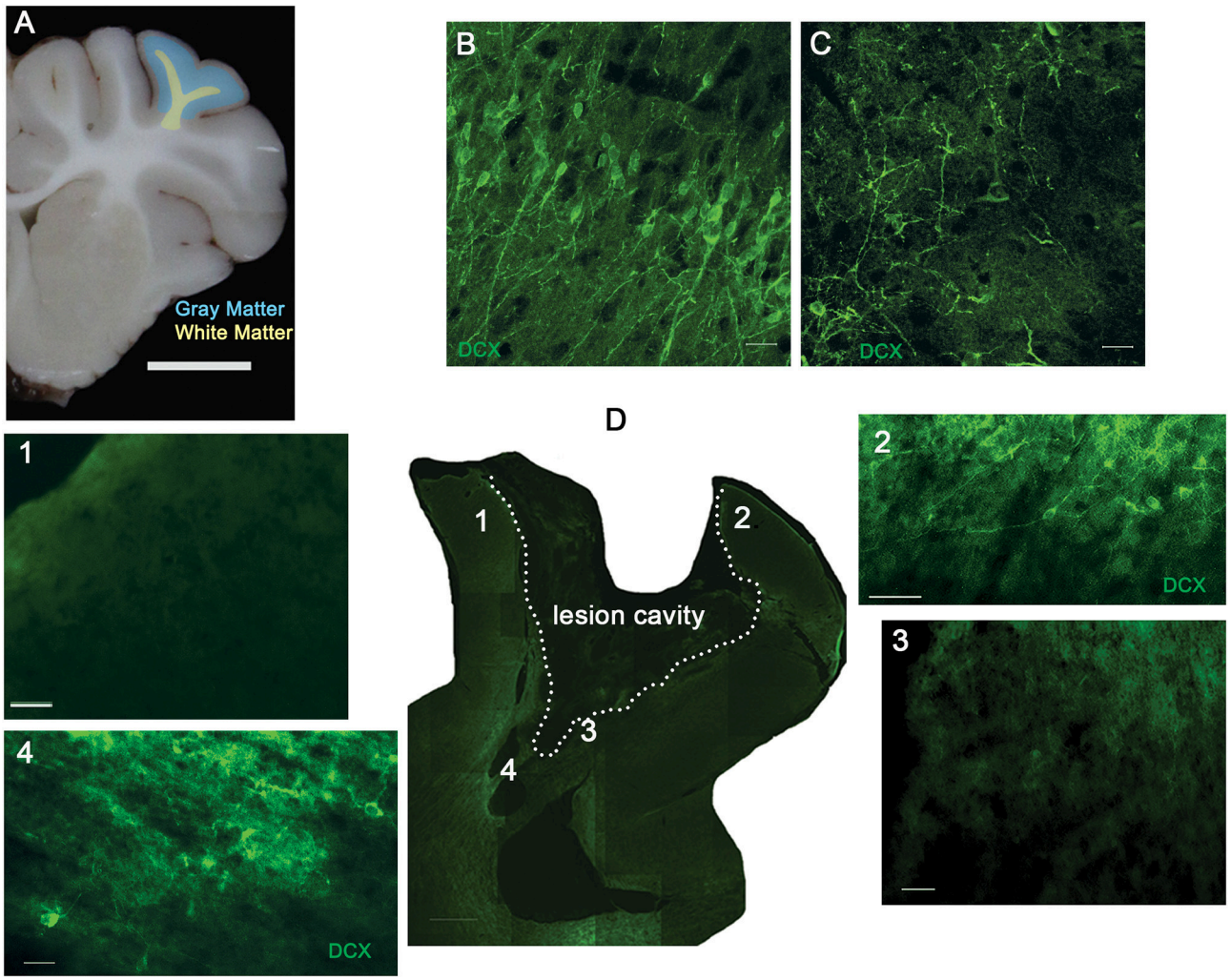

FIGURE 2 | The density of neuroblasts throughout the lesion is variable. Piglets received cortical impact or sham surgery on PND 7, and the brain was collected at PND 14. **(A)** Schematic illustrating the location of the cortical impact and resulting lesion in the rostral gyrus gray matter (blue) and rostral gyrus white matter (yellow). The second layer of the rostral gyrus contained pyramidal neurons positive for DCX (green) in sham piglets **(B)** that was disrupted in injured piglets **(C)**. **(D)** Low power view of the injured rostral gyrus with a lesion cavity outlined (broken line, "cavity$^+$") with higher power images demonstrating a lack of neuroblasts in the gray matter **(1)**, disruption of the second layer **(2)**, lack of neuroblasts in the white matter adjacent to the lesion cavity **(3)**, and increased neuroblast density in the white matter at the base of the gyrus **(4)**. Scale bars: **(A)** = 1 cm; **(D)** = 200 μm; **(D1–D4)** = 50 μm; **(B,C)** = 20 μm.

was considered "multipolar" with three branches + the main neuroblast.

Statistical Analysis

For the stereological investigation of white matter tracts, the main effects of the timing of BrdU administration, injury, and their interaction on cell numbers (neuroblasts, BrdU$^+$ cells, and BrdU$^+$ neuroblasts) were analyzed with two-way analysis of variance (ANOVA) followed by Fisher's Least Significant Difference (Fisher's LSD) *post-hoc* analyses. For quantification of cells at the injury site, no differences in the time of BrdU administration on BrdU$^+$ neuroblasts were detected via a Student's *t*-Test, therefore, these groups were combined. The differences in the density of BrdU$^+$ cells, neuroblasts, and BrdU$^+$ neuroblasts in the rostral gyrus white matter, rostral gyrus gray matter, external capsule, and claustrum were compared in injured vs. sham piglets using unpaired Student's *t*-Tests. The difference in the number of neuroblast branches per neuroblast in the injured white matter at the cavity edge vs. at a distance from the cavity edge in the injured white matter were tested with an unpaired Student's *t*-Test. The main effect of injury on the maximum density of neuroblasts in piglets binned for lesion type ("cavity$^+$ lesion" or "cavity$^-$ lesion") were determined via a one-way ANOVA followed by Tukey-Kramer Multiple Comparisons Test. All values were expressed as means ± SEM. $P < 0.05$ were considered significant. $P \leq 0.08$ were considered as a tendency to be significant. Statistical analyses were performed using SPSS Statistics software version 20 (IBM, Armonk, NY) or Prism® version 6.03 (GraphPad, San Diego, CA).

RESULTS

Effect of Cortical Impact on Neuroblast Quantity in the Cerebral White Matter Leading to the Injured Rostral Gyrus

In this immature gyrencephalic species, neuroblasts appear to travel along the extensive white matter tracts from the SVZ to the cortical gyri. To determine if a greater number of neuroblasts were in the white matter between the SVZ and the injured rostral gyrus compared to sham injured animals, neuroblasts were quantified within the corpus callosum adjacent to the SVZ, centrum semiovale, and white matter of the rostral gyrus ipsilateral and contralateral to injury (**Figures 1A, E–H**) in injured and sham piglets. BrdU was administered daily for 2 days prior to injury (PND 5 and 6) or after injury (PND 7 and 8) to determine the timing of the birth of the neuroblasts in the white matter 7 days after injury (PND 14; **Table 1**). The numbers of $BrdU^+$ cells were not different if BrdU was given before or after sham surgery ($4.6 \times 10^6 \pm 1.0 \times 10^6$ vs. $3.51 \times 10^6 \pm 0.49 \times 10^6$) or injury ($3.8 \times 10^6 \pm 1.4 \times 10^6$ vs. $3.3 \times 10^6 \pm 8.5 \times 10^6$) indicating that there was no effect of piglet age at the time of BrdU injection (5–6 PND vs. 8–9 PND) on proliferation and that an additional proliferative effect on cell genesis due to the injury was not observed in the white matter tracts leading to the injury. Neither the number of neuroblasts nor the number of $BrdU^+$ neuroblasts when BrdU was given before injury differed among injured vs. sham piglets (**Figures 1B,C**). Unexpectedly, the number of $BrdU^+$ neuroblasts in the ipsilateral hemisphere of sham piglets was greater than the contralateral and both hemispheres of injured piglets when BrdU was administered after injury (main effect of hemisphere, $P = 0.32$, main effect of injury, $P = 0.051$, interaction, $P = 0.027$, Fisher's LSD, $P < 0.05$; **Figure 1D**).

Cortical Impact Produces Different Patterns of Tissue Damage in the Piglet

The rostral gyrus of all injured piglets demonstrated microscopic evidence of apoptosis, hemorrhage, necrosis, acute or chronic inflammation, reactive astrocytes, microgliosis, macrophages, and axonal swellings (data not shown). The response to impact resulted in variable injury patterns, therefore, data was analyzed among all lesion types and also binned into two categories: (1) large cavitation through the gray matter extending through the cortical ribbon into the gyral white matter and sometimes extending into the centrum semiovale: "$cavity^+$ lesion," (2) disruption to the impact site of the cortical gray matter only: "$cavity^-$ lesion." These categories reflect the extent of tissue disruption and magnitude of the visible lesion. We did not observe lesions extending to the SVZ in this age of piglets.

Neuroblast Density Is Increased at the Injury, but the Density Is Highly Variable

Because there was no effect of injury on the total number of neuroblasts or $BrdU^+$ neuroblasts in the white matter leading from the SVZ to the injury, we sought to determine if neuroblasts were concentrated at the site of injury in the rostral gyrus. Both the gray matter and white matter of the rostral gyrus was analyzed with the white matter being a subset of the entire white matter tract analyzed above (**Figure 2A**). Not surprisingly, neurons in layer II of the rostral gyrus were DCX^+ and displayed a differentiated, mature neuronal morphology (**Figure 2B**). This layer was disrupted by the injury and was not included in the analysis (**Figures 2C,D2**). Neuroblast density was variable in the gray matter and white matter of the injured rostral gyrus. In $cavity^+$ lesions (**Figure 2D**), the gray matter of the dorsal rostral gyrus was devoid of neuroblasts (DCX was below the level of detection) in gray matter that remained intact (**Figures 2D1,D3**) while pockets of dense neuroblasts were found at ventral portions of the gyrus in the white matter adjacent to lesion cavities (**Figures 2D4**, **4B–J**).

The mean neuroblast density was approximately two-fold greater in the gray matter of the rostral gyrus among all lesion types in injured vs. sham piglets, but was not significant ($P = 0.09$; **Figures 3A,B**). Due to within-subject variability of neuroblast distribution within each subject, the maximum density per field per piglet was also identified. Maximum neuroblast density was greater ($P < 0.05$) in the gray matter and tended to be greater ($P = 0.08$) in the white matter of the rostral gyrus of injured piglets vs. sham piglets (**Figure 3C**). When binned into lesion category, the increase in maximum neuroblast density was due to an increase in $cavity^+$ lesions only (ANOVA $P = 0.0029$; Tukey-Cramer: $cavity^+$ lesion vs. sham $P < 0.01$, Tukey-Cramer: $cavity^+$ lesion vs. $cavity^-$ lesion $P < 0.05$; **Figure 3D**). As expected, injury increased the number of $BrdU^+$ cells in the rostral gyrus gray matter and white matter ($P < 0.05$; **Figure 3E**), of which only 10% were neuroblasts (**Figure 3F**). The number of neuroblasts that were $BrdU^+$ did not differ when BrdU was administered before or after injury and these groups were therefore combined for analyses. The number of $BrdU^+$ neuroblasts was greater in injured gray matter ($P < 0.05$), but not gyral white matter (**Figure 3F**). Only 1% of neuroblasts at the injury were $BrdU^+$ (**Figures 3B,F**).

Apparent Differentiation of Neuroblasts in the Injured White Matter in Some $Cavity^+$ Lesions

Dense meshworks of neuroblasts displaying a differentiating morphology were observed in some ventral portions along the edge of the lesion cavity in the white matter (**Figures 4A–F**). In a preliminary analysis of injured white matter, neuroblasts adjacent to the cavity edge had a greater number of neurites than neuroblasts at a distance away from the cavity edge (2.05 ± 0.1 vs. 1.10 ± 0.03, $P < 0.001$; 1 main branch only = unipolar neuroblasts, 2 = bipolar neuroblasts consisting of the main branch + 1 neurite, 3 + = multipolar neuroblasts; $N = 387$ neuroblasts; **Figures 4S–U**). In injured white matter at a distance from the cavity, 91% of neuroblasts were unipolar, 7.6% were bipolar, and only 1.4% were multipolar (**Figure 4S**). The majority of neuroblasts in injured white matter at a distance from the cavity appeared to be in a simple migratory phenotype (**Figure 4T**). The maximum number of

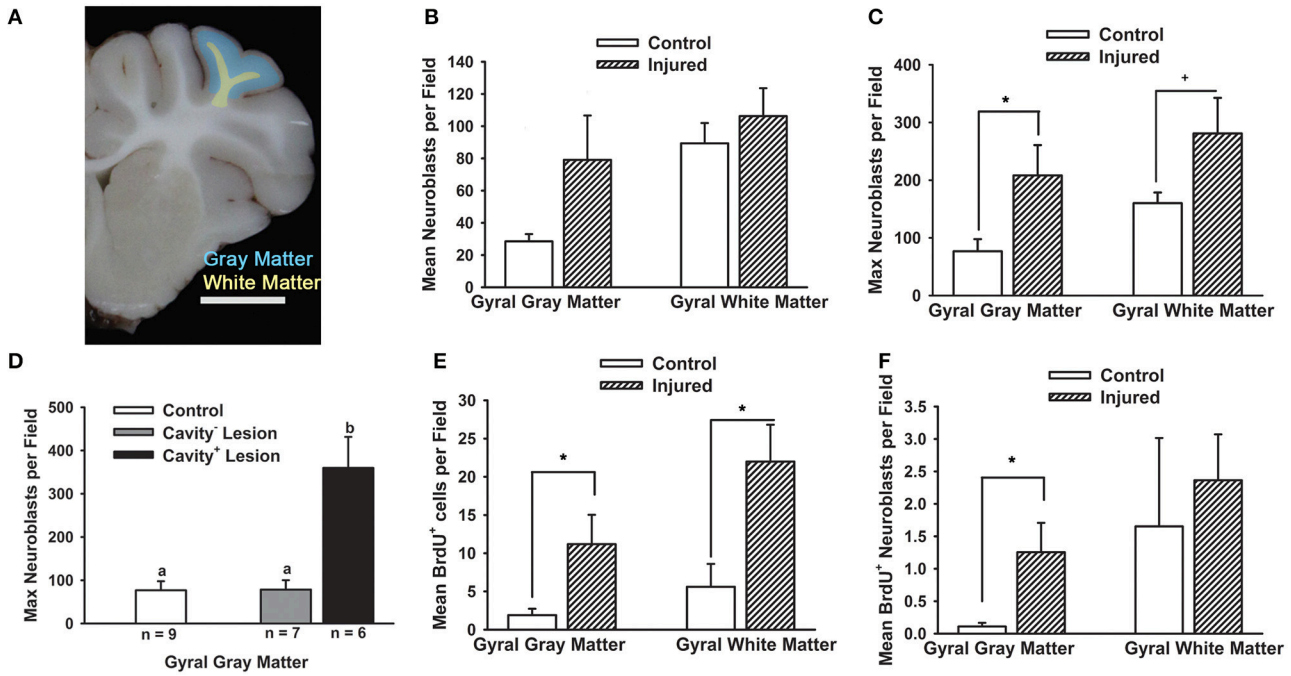

FIGURE 3 | Cortical impact increases the density of neuroblasts in the gray matter and white matter dependent on lesion type. Piglets received cortical impact or sham surgery on PND 7 and the brain was collected at PND 14. The mean density of neuroblasts (average of eight fields per region per piglet) and max density of neuroblasts (field with the greatest density) in each region was compared in injured vs. sham piglets via Student's *t*-Tests. **(A)** Schematic illustrating the location of the cortical impact and resulting lesion in the rostral gyrus gray matter (blue) and rostral gyrus white matter (yellow). **(B)** The mean neuroblast density was not greater ($P = 0.09$) in injured vs. sham piglets. **(C)** The maximum neuroblast density was greater ($^*P < 0.05$) in the gray matter and tended to be greater ($^+P = 0.08$) in the white matter of the rostral gyrus. **(D)** Piglets were binned into categories of lesion type based on pattern and extent, and neuroblast density was compared among groups via a one way ANOVA followed by Tukey-Kramer Multiple Comparisons Test. Injured piglets with a cavity$^+$ lesion had a greater maximum density of neuroblasts than piglets with "cavity$^-$" lesions (^{a,b}Means ± SEM with different letters differ, $P < 0.05$). **(E)** The mean number of BrdU$^+$ cells per field was greater in the gray and white matter of injured vs. sham piglets ($^*P < 0.05$). **(F)** The mean number of BrdU$^+$ neuroblasts per field was greater in injured rostral gyrus gray matter ($^*P < 0.05$), though the number is extremely low.

neurites observed to branch off of multipolar neuroblasts in this region was 2 neurites. In contrast, in the region adjacent to the cavity in the white matter, 52.5% were unipolar, 23% were bipolar, and 24.5% were multipolar (**Figure 4S**). Of multipolar neuroblasts adjacent to the cavity, 30% had 5 or more branches having up to 10 neurites. Often, neurites from multipolar neuroblasts were observed to be in close proximity to other neurites from other multipolar neuroblasts (**Figure 4U**). The white matter adjacent the white cavity had a mixture of neuroblasts in a migratory and a differentiating morphology.

To further investigate these neurons that appear to be sprouting neurites, we probed calretinin, a marker of GABAergic neurons expressed early in differentiation. As expected, calretinin$^+$ neuroblasts were observed throughout the gray matter, but were also observed at the cavity edge intermixed with DCX$^+$ neuroblasts (**Figures 4G–J**). We rarely observed co-labeling of calretinin and DCX in the same neuron (**Figures 4K–N**). Also in the injured white matter, but not on the cavity edge were small, round macrophages that were CD68$^+$ (**Figures 4O–R**).

Cortical Impact Does Not Disrupt Postnatal Population of the Claustrum

As TBI during childhood is superimposed upon ongoing development, we investigated the effect of TBI on an actively postnatally-populating region in the piglet. In coronal sections of sham or injured piglets, large chains of neuroblasts of a migratory morphology appeared to be exiting the ventral SVZ into the external capsule and then a portion were observed to enter the claustrum (**Figures 5A,D**). Within the claustrum, neuroblast morphology varied according to region. In the dorsal claustrum, neuroblasts were observed in long, narrow chains (**Figure 5D1**). In the central claustrum, individual neuroblasts were present in either a differentiating or a migratory morphology and chains were absent (**Figure 5D2**). In the ventral claustrum, a mix of large chains of neuroblasts and individual migratory or neuroblasts with a differentiating morphology was observed (**Figure 5D3**). The density of neuroblasts in the external capsule and in the claustrum was not different in response to injury (**Figure 5B**), but the maximum density of neuroblasts was greater in the external capsule in cavity$^+$ lesions than sham or cavity$^-$ lesions ($P < 0.05$; **Figure 5C**). The density of neuroblasts in the claustrum was

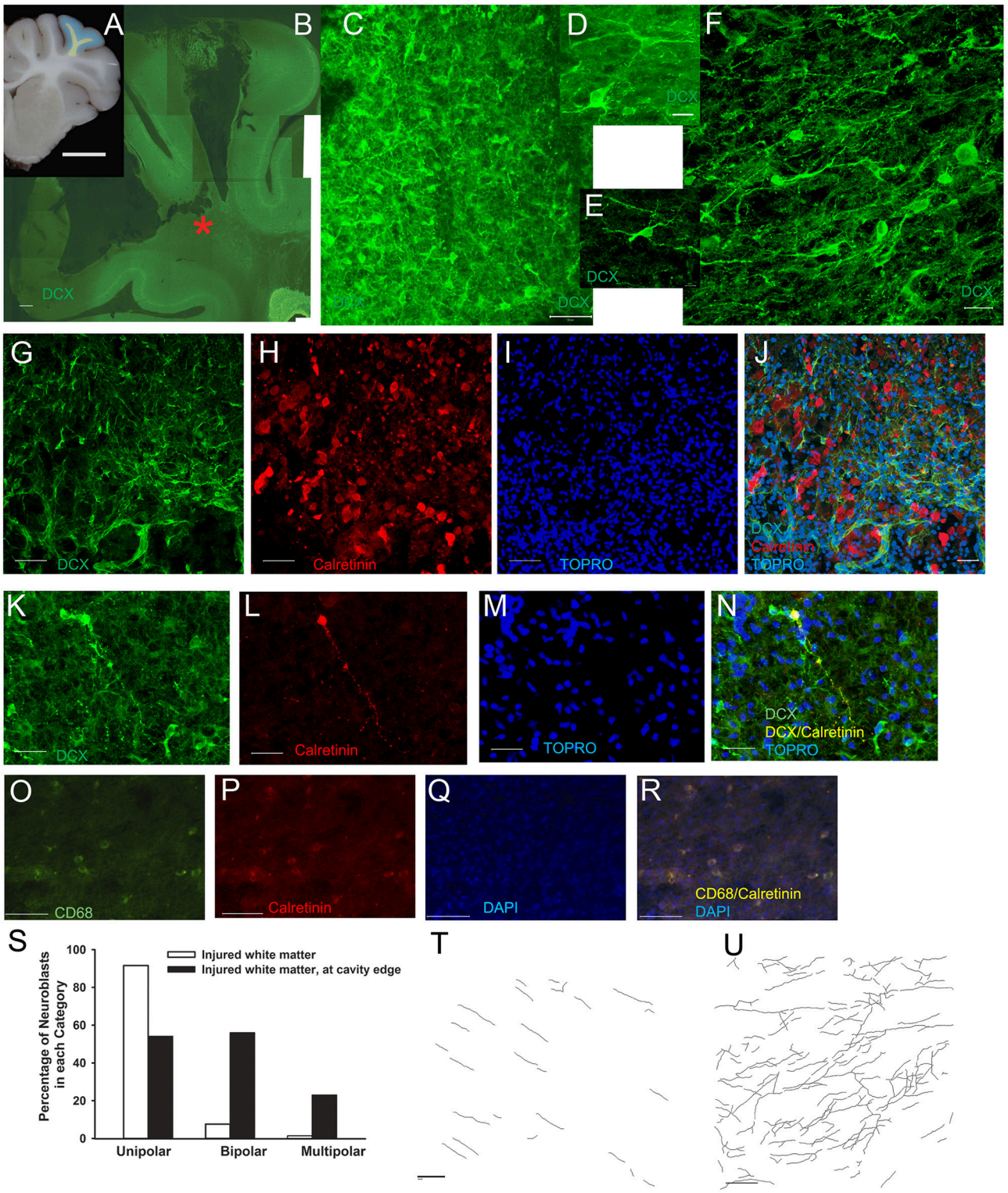

FIGURE 4 | Neuroblasts in injured white matter appear to be differentiating. In cavity$^+$ lesions, neuroblasts along the edge of the cavity were observed have a differentiating morphology. The white matter of the rostral gyrus was examined (yellow; **A**), and neuroblasts were densely arranged at the edge of the cavity at the ventral portion of the gyral white matter (red star; **B**). **(C–F)** Higher power images of the dense meshwork of neuroblasts in the injured rostral gyrus white matter indicated by the red star in **(B)**. **(D,E)** Neuroblasts (green) with a multipolar, differentiating morphology with 4–5 neurites at the cavity edge intermixed with calretinin$^+$ neurons (red). **(K–N)** A few neuroblasts (green) in the injured white matter were found to co-localize with calretinin (red; yellow when co-localized). **(O–R)** In the injured

(Continued)

FIGURE 4 | Continued
white matter (not on the cavity edge), small groups of small, round macrophages were faintly positive for CD68 (green) and faintly positive for calretinin (red; yellow when co-localized). **(S)** At the cavity edge, neuroblasts had a greater number of neurites ($P < 0.001$) with a larger percentage of bipolar and multipolar neuroblasts than in the injured white matter not adjacent to the cavity edge. **(T,U)** Maximum projection of neurite tracing in injured white matter distant from the cavity edge **(T)** and at the cavity edge **(U)** in injured piglets with a cavity$^+$ lesion. Scale bars: **(A)** = 1 cm; **(B)** = 500 μm; **(K–R)** = 100 μm; **(C,G–J,T,U)** = 50 μm; **(F)** = 20 μm; **(D**,**E)** = 10 μm.

two-fold denser than in injured rostral gyrus highlighting the apparent prioritization of the immature brain to continue with development.

DISCUSSION

This is the first study to determine the effect of cortical impact on the distribution of neuroblasts in the white matter path to the injury, at the injury, and at an actively postnatally-populating region in any species. Various models of injury and stroke in adult and immature rodents have shown that neuroblasts migrate from the SVZ to striatum or cortex where they replace, at least temporarily, injured neurons (Gordon et al., 2007; Li et al., 2008; Jin et al., 2010; Saha et al., 2013). However, the cortex of rodents, which lacks gyri and gyral white matter that may complicate repair efforts after TBI, may not accurately model the mechanisms of injury and repair in children; additionally, models thus far of TBI do not use an impact event to cause the injury but aspiration or freezing (Sundholm-Peters et al., 2005; Covey et al., 2010; Saha et al., 2013). We have previously described ectopic neurons in the damaged white matter of a child after TBI in a region excised for extra-temporal epilepsy and hypothesized that neuroblasts traveling to the injured gyrencephalic brain may result in epileptic foci (Taylor et al., 2013). An additional incidental finding was a clinically silent infarct in the subcortical white matter in a 1 month old infant who died of sepsis where an increased density of neuroblasts was observed around the infarct (Taylor et al., 2013). We hypothesize that neurogenesis stimulated by TBI and other causes of focal brain damage in the gyrencephalic brain may contribute to post-traumatic sequelae in addition to injury repair, in contrast to the predominant hypothesis in the TBI literature that neuroblasts target the injury to aid in successful repair without detriment.

In our model where both the gray matter and white matter of the rostral gyrus are damaged from cortical impact, we found a greater density of neuroblasts in gyral gray matter compared to sham piglets, but only in lesions that were cavitated. Within cavity$^+$ lesions, neuroblasts were most dense at the ventral portion of the gyri and were noticeably absent in dorsal portions of the gyri appearing to abandon attempts at salvage. It is difficult to compare the neuroblast distribution in gray matter in our model to the response to a cortical lesion from to aspiration or cryoinjury in the lissencephalic brain as these papers only describe the ventral or ventral and lateral portion of the lesion, which demonstrates increased neuroblast density in the gray matter in immature (Covey et al., 2010) and adult mice (Saha et al., 2013), but does not describe the dorsal portions of the lesion. One paper in adult mice reported an absence of neuroblasts in the gray matter adjacent to a lesion when the aspiration lesion did not have gray matter present between the lesion cavity and corpus collosum (Sundholm-Peters et al., 2005). In rodent studies, the low variability of lesion size after injury to the cortex is due to either biological uniformity specific to this species, due to the exclusion of variable lesions, or that these models of TBI do not use a cortical impact (Covey et al., 2010; Saha et al., 2013). Certainly, an impact model of TBI creates a complicated and cluttered tissue response. Increased neuroblast density at the lesion may be achieved by, (1) re-direction and concentration of neuroblasts to the ventral portion of the gyrus, which has more potential for salvage and repair then the damaged dorsal portions of the gyrus, (2) apoptosis and/or necrosis of neuroblasts in the dorsal portion, (3) decreased binding of antibodies the dorsal injured gyri, or (4) closer proximity to the SVZ (Covey et al., 2010; Saha et al., 2013; Costine et al., 2015). In this experiment, we have not determined if the neuroblasts are specifically targeting the cavity or, conversely, if neuroblasts migrating along gyral white matter tracts are collecting in the white matter creating a bottleneck of neuroblasts. It is possible that a longer piglet survival time might reveal a greater number of neuroblasts in the dorsal regions of the injured gyri. We hypothesized that damaged gyral white matter tracts may impede neuroblasts from reaching damaged gyral gray matter. Indeed, there were a lower number of BrdU$^+$ neuroblasts in the white matter leading from the SVZ to the rostral gyrus ipsilateral to injury in injured vs. sham piglets (**Figure 1D**). It is conceivable that the burr hole and dural manipulation stimulates the release of cytokines that may attract neuroblasts in surgical sham subjects, but the number of neuroblasts responding to the cytokines may be impeded by white matter damage in injured subjects (Tang et al., 2014). In large brained species, the distance of the diffusion of the cytokines from the injury relative to the size of the brain may limit the distance where neuroblasts may be actively recruited.

An additional finding at the injury site was the apparent differentiation of neuroblasts in damaged white matter. Within cavity$^+$ lesions, neuroblasts were densely arranged adjacent to a portion of the lesion cavity edge in the ventral portion of the gyri. This is similar to work in rodents revealing differentiating neuroblasts in the gray matter lesion (Covey et al., 2010; Saha et al., 2013), but shifted to the white matter in this gyrencephalic species. In the dense network of neuroblasts in the white matter, a large proportion of neuroblasts were observed to have several neurites. To further investigate these neuroblasts, we probed for calretinin, an early marker of differentiation; calretinin is a calcium-binding protein expressed in GABAergic neurons including a subset of interstitial neurons (Suárez-Solá et al., 2009; Wu and Sun, 2015). Calretinin$^+$ cells with neuronal

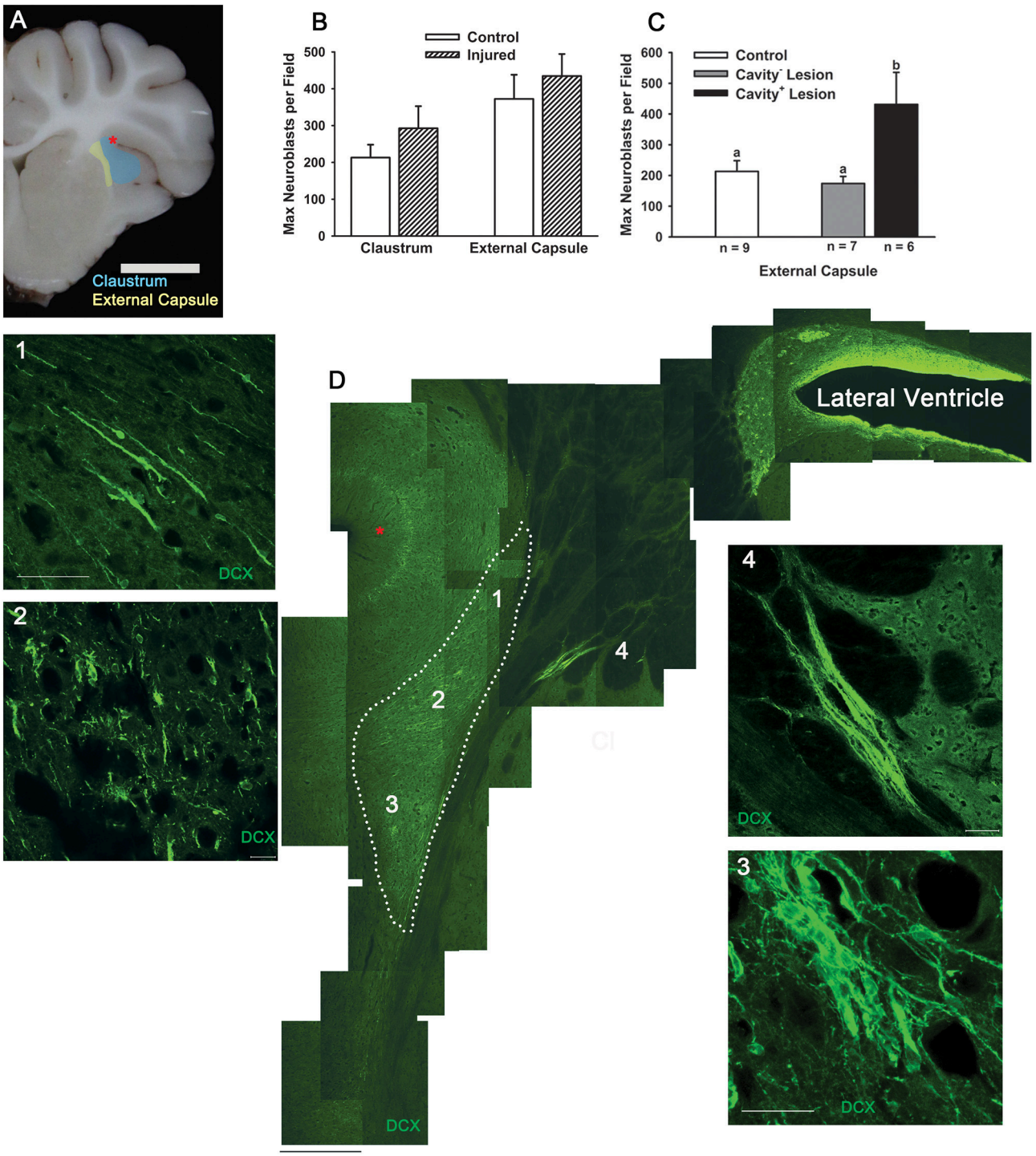

FIGURE 5 | Cortical impact does not reduce the number of neuroblasts in the claustrum. We observed large chains of neuroblasts traveling from the SVZ through the external capsule and entering the claustrum in sham piglets. We compared the density of neuroblasts in the external capsule and claustrum in piglets injured or receiving sham surgery at PND 7 and brains collected at PND 14. **(A)** Neuroblasts were quantified in the white matter (yellow) ventral to the SVZ and in the white matter adjacent to the claustrum (Cl, blue). **(B)** The maximum density of neuroblasts in the external capsule and claustrum in injured piglets were not different from sham piglets. In injured piglets, the density of neuroblasts in the claustrum was nearly three-fold greater than in the injured gray matter of the rostral gyrus indicating that postnatal population of this region is still prioritized after TBI in the gyrencephalic brain. **(C)** When piglets were binned according to lesion type, the neuroblast density was greater in the external capsule in piglets with "cavity^{+} lesions" than shams or "cavity^{-} lesions" (^{a,b}Means ± SEM with different letters differ, $P < 0.05$). **(D)** Low power view of the SVZ, ventral white matter, external capsule, and claustrum (Cl, indicated with broken line) with neuroblasts detected with DCX

(Continued)

FIGURE 5 | Continued
(green) with the red star corresponding to the sulci marked with a red star in **(A)**. **(D1)** In the dorsal claustrum, long and thick chains of neuroblasts are observed in a migratory morphology. **(D2,D3)** In the ventral claustrum, neuroblasts are extremely dense with individual neuroblasts and various sizes of clusters. **(D4)** A large cluster of neuroblasts approximately 1000 μm in length appears to migrate through the external capsule. Scale bars: **(A)** = 1 cm; **(D)** = 200 μm; **(D4)** = 100 μm; **(D1–D3)** = 20 μm.

morphology were located throughout the white matter of injured and sham piglets. In injured piglets, some calretinin$^+$/DCX$^+$ neurons and NeuN$^+$/calretinin$^-$ neurons were in the white matter. This population may be resident interstitial cells or newly differentiated neurons in the white matter in response to injury. In the gyrencephalic brain, interstitial neurons mediate brain development and persist into adulthood in the gyral white matter; this population is absent in rodents (Suárez-Solá et al., 2009). Future studies will aim to quantify neurons in the white matter at different time points after injury as well as further characterize the injury environment and these potentially differentiating neuroblasts. While the migration of neuroblasts in the corpus callosum has been examined after TBI, neuroblasts with a differentiating morphology in the white matter have not yet been described after TBI in any species (Sundholm-Peters et al., 2005; Covey et al., 2010; Saha et al., 2013). The only phenomena similar to what we describe here is in humans where neuroblasts localized to a white matter infarct in an infant (Taylor et al., 2013) and around chronic white matter lesions in adult multiple sclerosis patients (Chang et al., 2008). Focal differentiation of neuroblasts around white matter lesions post-TBI in the human brain may be an attempt at a "quick fix" with long-lasting effects.

The role of potentially differentiating neuroblasts in the white matter after cortical impact is not known. One possibility is a recapitulation of development as calretinin$^+$ interstitial neurons are crucial to development (Suárez-Solá et al., 2009; Wu and Sun, 2015). Vertical plasticity has been described in human children with hydranencephaly where the children developed functions ascribed to the neocortex in the near-complete absence of a neocortex (Shewmon et al., 1999). These children were born with scarce neocortex and lacked neocortical functions as infants and toddlers, but developed neocortical functions during childhood. The neurologists treating these children proposed that the functions ascribed to the cortex developed subcortically (Shewmon et al., 1999). This population of differentiating neuroblasts may be transient and temporarily supply growth factors to the injured white matter and then regress. Alternatively, ectopic neurons that persist may develop into direct epileptic foci or indirectly through influencing surrounding circuits (Petit et al., 2014). Though neurons generated from the SVZ in healthy subjects are GABAergic, the possibility of neurons from the SVZ serving as epileptic foci is supported by work in stroke models where SVZ-derived differentiated neurons in the cortex generated excitatory post-synaptic currents (Lai et al., 2008). Furthermore, GABA is depolarizing in the immature brain and GABAergic neurons revert back being excitatory after injury, which may be a recapitulation of development (van den Pol et al., 1996; Wu and Sun, 2015). Repair mechanisms may have both beneficial and deleterious long-term effects.

Of the neuroblasts at the injury site, less than 1% were born (BrdU$^+$) in the 2 days before or the 2 days after injury. This low percentage is similar to our previous work estimating the total number of neuroblasts in the entire white matter in sham or injured piglets (Costine et al., 2015). There was no effect of injury on the number of BrdU$^+$ neuroblasts in the white matter in the current experiment (the white matter tract leading from the SVZ to the injury) or our past experiment (all white matter). However, we did find an increased number of BrdU$^+$ neuroblasts at the lesion site in the gray matter though they comprised a very small portion of total neuroblasts. We can conclude that the majority of neuroblasts that arrived at the lesion were born prior to PND 4, and likely were born prior to birth. An increase in neuroblast density at the lesion was largely achieved without stimulation of cell division to create new neuroblasts, which is similar to work in immature rodents where only 10% of neuroblasts were BrdU$^+$ when BrdU was administered for 4 days post-injury (Covey et al., 2010). The low percentage of neuroblasts labeled with BrdU reported here and reported in immature rodents (Covey et al., 2010) is in contrast to adult rodents (Sundholm-Peters et al., 2005). In uninjured adult mice, the number of BrdU$^+$ neuroblasts in the corpus callosum were doubled in response to injury to the cortex (Sundholm-Peters et al., 2005). In the early postnatal brain where an abundance of neuroblasts are migrating throughout the white matter, a further increase in the production of neuroblasts to support lesion repair may not be possible.

In gyrencephalic species where the white matter is abundant, the number of neuroblasts in the white matter does not predict the number of neuroblasts collected at the lesion site. In our unbiased quantification of neuroblasts in the white matter from the SVZ leading to the injured rostral gyrus including the corpus callosum, centrum semiovale, and gyral white matter, there was no effect of cortical impact on the number of neuroblasts though we found an increase in the density of neuroblasts at the lesion site. In the uninjured PND 14 piglet, we have previously demonstrated large chains of neuroblasts moving rostrally in the rostral migratory stream, and demonstrate a ventrolateral migratory stream in our current work (Costine et al., 2015). In addition to these major pathways, all white matter of the neocortex contained individual or small chains of neuroblasts with a migratory morphology (Costine et al., 2015). The persistence of doublecortin protein in differentiated neurons in cortical layer II, which was damaged after cortical impact, is similar to other higher mammals, has been demonstrated to persist into adulthood, and is hypothesized to impart increased complexity through continued plasticity of GABAergic

interneurons in higher mammals, but does not persist through adulthood in rodent species (Cai et al., 2009; Radonjic et al., 2014). In contrast, neuroblasts produced in the SVZ in healthy postnatal rodents fail to enter the neocortex after the regression of radial glia possibly due to the absence of white matter tracts entering the neocortex (Brazel, 2003). Any postnatal population of the neocortex in the Yorkshire/Landrace piglet may impart plasticity, but does not increase the total number of neurons as neocortical neuron number does not increase from birth to adulthood in piglets, similar to humans (Jelsing, 2006). The immature gyrencephalic brain appears to use white matter tracts in the neocortex as highways for postnatal neocortex development, and to continue the analogy—the population of cars on a highway (white matter) to a city cannot be used to estimate the population of the city (lesion site).

We sought to determine if the developing gyrencephalic brain prioritized development over injury repair or vice versa. The postnatal population of the olfactory bulb via the rostral migratory stream is the most studied among species including rodents, piglets, and humans (Sundholm-Peters et al., 2005; Sanai et al., 2011; Costine et al., 2015). Neuroblasts also migrate from the SVZ into the ventral migratory stream (Sanai et al., 2011) and have been found to populate the Islands of Calleja in rodents (De Marchis et al., 2004). Here, we observed a large population of neuroblasts moving from the SVZ into a ventral migratory stream and into the claustrum. Postnatal development of the claustrum has been described in the rat, rabbit, and cat, and the specific role of migrating neuroblasts populating the claustrum up to PND 4 was hypothesized to occur to explain the late differentiation of interneurons (Adinolfi and Levine, 1986; Wójcik et al., 2002; Kowianski et al., 2008). Here, we demonstrate this predicted postnatal population of interneurons in the claustrum of piglets at PND 14, which is later than observed in rodents, perhaps allows greater plasticity to this brain region that is important in cross-modal sensory integration. After TBI, the density of neuroblasts in the claustrum was not diminished. This is similar to adult rodents where migration to the olfactory bulb was not diminished even with an increased number of neuroblasts migrating dorsally to the cortical lesion (Sundholm-Peters et al., 2005). Most of the neuroblasts in the claustrum and gray matter of the rostral gyrus were born prior to PND 5 as $BrdU^+$ neuroblasts were rare in both regions when BrdU was administered as early as PND 5. Though the density of neuroblasts in the claustrum was not altered from TBI, the density of neuroblasts in the external capsule was greater in subjects with $cavity^+$ lesions. In the immature piglet brain, it appears that cortical impact may induce neuroblasts to concentrate in lesions with a cavity without compromising development of brain regions, and may potentially result in greater postnatal population of other brain regions.

In conclusion, cortical impact to the rostral gyrus of the immature piglet brain increased the density of neuroblasts in the gray matter and unexpectedly caused focal densities of neuroblasts in the injured white matter. Consistent with other models of injury in immature animals, injury did not stimulate de novo neurons. However, unlike TBI models in rodents, both the lesion pattern and neuroblast distribution in the lesion cortex were heterogeneous. Neuroblast density was increased in the gray matter, but this increase was in cavitated lesions only. In the white matter, neuroblasts aligned along the edge of the cavity and had a differentiating morphology. This meshwork of potentially differentiating neuroblasts may become interstitial neurons, may develop into new cortex via vertical plasticity, may be support the re-building of white matter recapitulating development, may support repair temporarily and regress, or may ultimately develop into epileptic foci responsible for some of the long-term effects of TBI. Immature gyrencephalic animals can serve as a platform to study TBI in infants and children where white matter, which is preferentially vulnerable after TBI, may complicate the repair response. Future work will focus on the interplay of neuroblasts and interstitial neurons in white matter repair, the potential for this remodeled white matter to create post-traumatic epileptic foci, to determine if postnatal population of brain regions is affected, and to examine the potential effect of age on these processes during immaturity. If it is determined that neuroblast differentiation impedes white matter recovery in the gyrencephalic brain, then modulation and even repression of the targeting of neuroblasts to white matter injury may improve recovery in infants and children after TBI.

AUTHOR CONTRIBUTIONS

BC, ST, and AD designed the experiments. ST, KK, and CD performed the animal experiments. ST, BC, CS, and KK performed the immunohistochemistry and quantification. BC, AD, ST, and DM analyzed and interpreted the data. BC and ST drafted the paper. All authors critically reviewed, revised, and approved the final version of the paper.

ACKNOWLEDGMENTS

This work was supported by the Nicholas T. Zervas Chair of Harvard Medical School, the Joel Alan Viktor Research Fund and John G. Price Memorial Fund at Massachusetts General Hospital to AD, NICHD grant K01HD083759 to BC, and the MGH Neuroscience Center Imaging Core supported by NINDS grant 5P30NS045776. This work was conducted with support from Harvard Catalyst, The Harvard Clinical and Translational Science Center (National Center for Research Resources and the National Center for Advancing Translational Sciences, National Institutes of Health Award UL1 TR001102) and financial contributions from Harvard University and its affiliated academic healthcare centers. The content is solely the responsibility of the authors and does not necessarily represent the official views of Harvard Catalyst, Harvard University and its affiliated academic healthcare centers, or the National Institutes of Health. The authors express their gratitude to Rebecca Zhu, Christopher Seufert, Marissa Fiorello, and Monica Shifman for their assistance with animal handling, immunohistochemistry, and quantification. We thank George Price for his assistance with immunohistochemistry and assistance with the preparation of the results section of the manuscript.

REFERENCES

Adinolfi, A. M., and Levine, M. S. (1986). An autoradiographic study of the postnatal development of pericruciate cortical projections to the neostriatum and the claustrum of the cat. *Brain Res.* 389, 99–108. doi: 10.1016/0165-3806(86)90177-X

Brazel, C. (2003). Roles of the mammalian subventricular zone in brain development. *Prog. Neurobiol.* 69, 49–69. doi: 10.1016/S0301-0082(03)00002-9

Cai, Y., Xiong, K., Chu, Y., Luo, D.-W., Luo, X.-G., Yuan, X.-Y., et al. (2009). Doublecortin expression in adult cat and primate cerebral cortex relates to immature neurons that develop into GABAergic subgroups. *Exp. Neurol.* 216, 342–356. doi: 10.1016/j.expneurol.2008.12.008

Cattaneo, E., and Bonfanti, L. (2014). Therapeutic potential of neural stem cells: greater in people's perception than in their brains? *Front. Neurosci.* 8:79. doi: 10.3389/fnins.2014.00079

Chang, A., Smith, M. C., Yin, X., Fox, R. J., Staugaitis, S. M., and Trapp, B. D. (2008). Neurogenesis in the chronic lesions of multiple sclerosis. *Brain* 131(Pt 9), 2366–2375. doi: 10.1093/brain/awn157

Costine, B. A., Missios, S., Taylor, S. R., McGuone, D., Smith, C. M., Dodge, C. P., et al. (2015). The subventricular zone in the immature piglet brain: anatomy and exodus of neuroblasts into white matter after traumatic brain injury. *Dev. Neurosci.* 37, 115–130. doi: 10.1159/000369091

Covey, M. V., Jiang, Y., Alli, V. V., Yang, Z., and Levison, S. W. (2010). Defining the critical period for neocortical neurogenesis after pediatric brain injury. *Dev. Neurosci.* 32, 488–498. doi: 10.1159/000321607

Dash, P. K., Mach, S. A., and Moore, A. N. (2001). Enhanced neurogenesis in the rodent hippocampus following traumatic brain injury. *J. Neurosci. Res.* 63, 313–319. doi: 10.1002/1097-4547(20010215)63:4<313::AID-JNR1025>3.0.CO;2-4

De Marchis, S., Fasolo, A., and Puche, A. C. (2004). Subventricular zone-derived neuronal progenitors migrate into the subcortical forebrain of postnatal mice. *J. Comp. Neurol.* 476, 290–300. doi: 10.1002/cne.20217

Duhaime, A. C., Hunter, J. V., Grate, L. L., Kim, A., Golden, J., Demidenko, E., et al. (2003). Magnetic resonance imaging studies of age-dependent responses to scaled focal brain injury in the piglet. *J. Neurosurg.* 99, 542–548. doi: 10.3171/jns.2003.99.3.0542

Duhaime, A. C., Margulies, S. S., Durham, S. R., O'Rourke, M. M., Golden, J. A., Marwaha, S., et al. (2000). Maturation-dependent response of the piglet brain to scaled cortical impact. *J. Neurosurg.* 93, 455–462. doi: 10.3171/jns.2000.93.3.0455

Francis, H. W., Rivas, A., Lehar, M., Saito, Y., Mouton, P. R., and Ryugo, D. K. (2006). Efficient quantification of afferent cochlear ultrastructure using design-based stereology. *J. Neurosci. Methods* 150, 150–158. doi: 10.1016/j.jneumeth.2005.06.020

Gordon, R. J., Tattersfield, A. S., Vazey, E. M., Kells, A. P., McGregor, A. L., Hughes, S. M., et al. (2007). Temporal profile of subventricular zone progenitor cell migration following quinolinic acid-induced striatal cell loss. *Neuroscience* 146, 1704–1718. doi: 10.1016/j.neuroscience.2007.03.011

Irimia, A., and Van Horn, J. D. (2015). Epileptogenic focus localization in treatment-resistant post-traumatic epilepsy. *J. Clin. Neurosci.* 22, 627–631. doi: 10.1016/j.jocn.2014.09.019

Jelsing, J. (2006). The postnatal development of neocortical neurons and glial cells in the Gottingen minipig and the domestic pig brain. *J. Exp. Biol.* 209, 1454–1462. doi: 10.1242/jeb.02141

Jin, K., Wang, X., Xie, L., Mao, X. O., and Greenberg, D. A. (2010). Transgenic ablation of doublecortin-expressing cells suppresses adult neurogenesis and worsens stroke outcome in mice. *Proc. Natl. Acad. Sci. U.S.A.* 107, 7993–7998. doi: 10.1073/pnas.1000154107

Kowianski, P., Morys, J. M., Dziewiatkowski, J., Wójcik, S., Sidor-Kaczmarek, J., and Morys, J. (2008). NPY-, SOM- and VIP-containing interneurons in postnatal development of the rat claustrum. *Brain Res. Bull.* 76, 565–571. doi: 10.1016/j.brainresbull.2008.04.004

Lai, B., Mao, X. O., Xie, L., Jin, K., and Greenberg, D. A. (2008). Electrophysiological neurodifferentiation of subventricular zone-derived precursor cells following stroke. *Neurosci. Lett.* 442, 305–308. doi: 10.1016/j.neulet.2008.07.032

Li, W. L., Yu, S. P., Ogle, M. E., Ding, X. S., and Wei, L. (2008). Enhanced neurogenesis and cell migration following focal ischemia and peripheral stimulation in mice. *Dev. Neurobiol.* 68, 1474–1486. doi: 10.1002/dneu.20674

Longhi, L., Watson, D. J., Saatman, K. E., Thompson, H. J., Zhang, C., Fujimoto, S., et al. (2004). *Ex vivo* gene therapy using targeted engraftment of NGF-expressing human NT2N neurons attenuates cognitive deficits following traumatic brain injury in mice. *J. Neurotrauma* 21, 1723–1736. doi: 10.1089/neu.2004.21.1723

Margulies, S., and Hicks, R. (2009). Combination therapies for traumatic brain injury: prospective considerations. *J. Neurotrauma* 26, 925–939. doi: 10.1089/neu.2008.0794

Marlier, Q., Verteneuil, S., Vandenbosch, R., and Malgrange, B. (2015). Mechanisms and functional significance of stroke-induced neurogenesis. *Front. Neurosci.* 9:458. doi: 10.3389/fnins.2015.00458

Missios, S., Harris, B. T., Dodge, C. P., Simoni, M. K., Costine, B. A., Lee, Y. L., et al. (2009). Scaled cortical impact in immature swine: effect of age and gender on lesion volume. *J. Neurotrauma* 26, 1943–1951. doi: 10.1089/neu.2009.0956

Peretto, P., and Bonfanti, L. (2015). Adult neurogenesis 20 years later: physiological function vs. brain repair. *Front. Neurosci.* 9:71. doi: 10.3389/fnins.2015.00071

Petit, L. F., Jalabert, M., Buhler, E., Malvache, A., Peret, A., Chauvin, Y., et al. (2014). Normotopic cortex is the major contributor to epilepsy in experimental double cortex. *Ann. Neurol.* 76, 428–442. doi: 10.1002/ana.24237

Radonjic, N. V., Ayoub, A. E., Memi, F., Yu, X., Maroof, A., Jakovcevski, I., et al. (2014). Diversity of cortical interneurons in primates: the role of the dorsal proliferative niche. *Cell Rep.* 9, 2139–2151. doi: 10.1016/j.celrep.2014.11.026

Rola, R., Mizumatsu, S., Otsuka, S., Morhardt, D. R., Noble-Haeusslein, L. J., Fishman, K., et al. (2006). Alterations in hippocampal neurogenesis following traumatic brain injury in mice. *Exp. Neurol.* 202, 189–199. doi: 10.1016/j.expneurol.2006.05.034

Saha, B., Peron, S., Murray, K., Jaber, M., and Gaillard, A. (2013). Cortical lesion stimulates adult subventricular zone neural progenitor cell proliferation and migration to the site of injury. *Stem Cell Res.* 11, 965–977. doi: 10.1016/j.scr.2013.06.006

Sanai, N., Nguyen, T., Ihrie, R. A., Mirzadeh, Z., Tsai, H. H., Wong, M., et al. (2011). Corridors of migrating neurons in the human brain and their decline during infancy. *Nature* 478, 382–386. doi: 10.1038/nature10487

Sarnat, H. B. (2015). Immunocytochemical markers of neuronal maturation in human diagnostic neuropathology. *Cell Tissue Res.* 359, 279–294. doi: 10.1007/s00441-014-1988-4

Scharfman, H. E., and Hen, R. (2007). Is more neurogenesis always better? *Science* 315, 336–338. doi: 10.1126/science.1138711

Scharfman, H. E., and McCloskey, D. P. (2009). Postnatal neurogenesis as a therapeutic target in temporal lobe epilepsy. *Epilepsy Res.* 85, 150–161. doi: 10.1016/j.eplepsyres.2009.03.006

Shewmon, D. A., Holmes, G. L., and Byrne, P. A. (1999). Consciousness in congenitally decorticate children: developmental vegetative state as self-fulfilling prophecy. *Dev. Med. Child Neurol.* 41, 364–374. doi: 10.1017/S0012162299000821

Suárez-Solá, M. L., González-Delgado, F. J., Pueyo-Morlans, M., Medina-Bolívar, O. C., Hernández-Acosta, N. C., González-Gómez, M., et al. (2009). Neurons in the white matter of the adult human neocortex. *Front. Neuroanat.* 3:7. doi: 10.3389/neuro.05.007.2009

Sundholm-Peters, N. L., Yang, H. K. C., Goings, G. E., Walker, A. S., and Szele, F. G. (2005). Subventricular zone neuroblasts emigrate toward cortical lesions. *J. Neuropathol. Exp. Neurol.* 64, 1089–1100. doi: 10.1097/01.jnen.0000190066.13312.8f

Tang, S. K., Knobloch, R. A., Maucksch, C., and Connor, B. (2014). Redirection of doublecortin-positive cell migration by over-expression of the chemokines MCP-1, MIP-1alpha and GRO-alpha in the adult rat brain. *Neuroscience* 260, 240–248. doi: 10.1016/j.neuroscience.2013.1012.1022

Tang, X., Falls, D. L., Li, X., Lane, T., and Luskin, M. B. (2007). Antigen-retrieval procedure for bromodeoxyuridine immunolabeling with concurrent labeling of nuclear DNA and antigens damaged by HCl pretreatment. *J. Neurosci.* 27, 5837–5844. doi: 10.1523/JNEUROSCI.5048-06.2007

Taylor, S. R., Smith, C., Harris, B. T., Costine, B., and Duhaime, A. C. (2013). Maturation-dependent response of neurogenesis after traumatic brain injury in children. *J. Neurosurg. Pediatr.* 12, 545–554. doi: 10.3171/2013.8.peds13154

van den Pol, A. N., Obrietan, K., and Chen, G. (1996). Excitatory actions of GABA after neuronal trauma. *J. Neurosci.* 16, 4283–4292.

Wilde, E. A., Bigler, E. D., Haider, J. M., Chu, Z., Levin, H. S., Li, X., et al. (2006). Vulnerability of the anterior commissure in moderate to severe pediatric traumatic brain injury. *J. Child Neurol.* 21, 769–776. doi: 10.1177/08830738060210090201

Wójcik, S., Dziewiatkowski, J., Kowianski, P., Ludkiewicz, B., Jagalska-Majewska, H., and Morys, J. (2002). Qualitative and quantitative study of the postnatal development of the rabbit claustrum. *Int. J. Dev. Neurosci.* 20, 113–123. doi: 10.1016/S0306-4522(02)00084-2

Wu, C., and Sun, D. (2015). GABA receptors in brain development, function, and injury. *Metab. Brain Dis.* 30, 367–379. doi: 10.1007/s11011-014-9560-1

Wu, T. C., Wilde, E. A., Bigler, E. D., Li, X., Merkley, T. L., Yallampalli, R., et al. (2010). Longitudinal changes in the corpus callosum following pediatric traumatic brain injury injury. *Dev. Neurosci.* 32, 361–373. doi: 10.1159/000317058

Conflict of Interest Statement: The authors declare that the research was conducted in the absence of any commercial or financial relationships that could be construed as a potential conflict of interest.

The reviewer EB and handling Editor declared that even though they share the institution they work at different departments, and the handling Editor states that the process met the standards of a fair and objective review.

frontiers in Neuroscience

ORIGINAL RESEARCH
published: 15 November 2016
doi: 10.3389/fnins.2016.00523

Oct4 Methylation-Mediated Silencing As an Epigenetic Barrier Preventing Müller Glia Dedifferentiation in a Murine Model of Retinal Injury

*Luis I. Reyes-Aguirre and Monica Lamas **

Departamento de Farmacobiología, Centro de Investigación y de Estudios Avanzados-Sede Sur, México, Mexico

Müller glia (MG) is the most abundant glial type in the vertebrate retina. Among its many functions, it is capable of responding to injury by dedifferentiating, proliferating, and differentiating into every cell types lost to damage. This regenerative ability is notoriously absent in mammals. We have previously reported that cultured mammalian MG undergoes a partial dedifferentiation, but fails to fully acquire a progenitor phenotype and differentiate into neurons. This might be explained by a mnemonic mechanism comprised by epigenetic traits, such as DNA methylation. To achieve a better understanding of this epigenetic memory, we studied the expression of pluripotency-associated genes, such as *Oct4*, *Nanog,* and *Lin28*, which have been reported as necessary for regeneration in fish, at early times after NMDA-induced retinal injury in a mouse experimental model. We found that although Oct4 is expressed rapidly after damage (4 hpi), it is silenced at 24 hpi. This correlates with a significant decrease in the DNA methyltransferase *Dnmt3b* expression, which returns to basal levels at 24 hpi. By MS-PCR, we observed a decrease in *Oct4* methylation levels at 4 and 12 hpi, before returning to a fully methylated state at 24 hpi. To demonstrate that these changes are restricted to MG, we separated these cells using a GLAST antibody coupled with magnetic beads. Finally, intravitreous administration of the DNA-methyltransferase inhibitor SGI-1027 induced *Oct4* expression at 24 hpi in MG. Our results suggest that mammalian MG injury-induced dedifferentiation could be restricted by DNA methylation, which rapidly silences *Oct4* expression, preventing multipotency acquisition.

Keywords: Müller glia, DNA methylation, retinal progenitors

Key Points

A silencing event upon the pluripotency marker Oct4 expression occurs in mice Müller glia after retinal damage.

This event correlates with decreased DNA methyltransferase expression and Oct4 methylation profile.

OPEN ACCESS

Edited by:
Luca Bonfanti,
University of Turin, Italy

Reviewed by:
Krishna Vadodaria,
Salk Institute for Biological Studies, USA
Ola Hermanson,
Karolinska Institutet, Sweden

****Correspondence:***
Monica Lamas
mlamas@cinvestav.mx

Specialty section:
This article was submitted to Neurogenesis, a section of the journal Frontiers in Neuroscience

Received: *25 July 2016*
Accepted: *28 October 2016*
Published: *15 November 2016*

Citation:
Reyes-Aguirre LI and Lamas M (2016) Oct4 Methylation-Mediated Silencing As an Epigenetic Barrier Preventing Müller Glia Dedifferentiation in a Murine Model of Retinal Injury. Front. Neurosci. 10:523. doi: 10.3389/fnins.2016.00523

INTRODUCTION

Müller glia (MG) is responsible for the maintenance of retinal homeostasis and neural nourishment (Pfeiffer-Guglielmi et al., 2005), protection against oxidative stress (Schütte and Werner, 1998), maintenance of the blood-retinal barrier (BRB; Bringmann et al., 2006), growth factor release (Eichler et al., 2001), and even light guidance to the photoreceptor layer (Agte et al., 2011).

MG is remarkably capable of regenerating damaged neurons, albeit in a very restricted number of vertebrates, particularly teleost fish, by dedifferentiating and acquiring a progenitor phenotype. This is revealed by a drastic change in MG's gene expression program, as they down-regulate and eventually lose the expression of its specific markers cellular retinaldehyde-binding protein (CRALBP) and glutamine synthase (GS), while up-regulating progenitor-associated markers such as *ascl1a*, *chx10,* and *six3*, and genes usually expressed by pluripotent cells, like *oct4*, *lin28*, *sox2*, *klf4,* and c-*myc* (Raymond et al., 2006; Bernardos et al., 2007; Fischer and Bongini, 2010; Ramachandran et al., 2010). These pluripotency-associated markers are usually present in embryonic stem cells (ESCs) and are often regarded as fundamental for the generation of iPSCs (Takahashi and Yamanaka, 2006; Hochedlinger and Plath, 2009). Notably, *Oct4* has been described as both necessary and sufficient for direct induction of multipotency in adult neural stem cells (NSCs; Kim et al., 2009). The dedifferentiation stage allows MG to proliferate and then differentiate into neurons and completely restore visual function.

In mammals, MG responds to damage by becoming reactive and hypertrophic, in a process known as reactive gliosis which involves the up-regulation of glial fibrillary acidic protein (GFAP) and GS, as well as uncontrolled proliferation (Fawcett and Asher, 1999). Far from restoring visual function, this ultimately contributes to neurodegeneration and loss of visual function. While naturally occurring dedifferentiation-mediated regeneration is missing in these organisms, several research groups have demonstrated that, under specific conditions, mammalian MG has the basic machinery needed to initiate such a process, acquiring a progenitor phenotype, and even differentiating to other cellular types, although with varying grades of success (Ooto et al., 2004; Karl et al., 2008; Abrahan et al., 2009; Stutz et al., 2014).

We have previously reported that low, sub-toxic concentrations of glutamate are enough to trigger the expression of some progenitor-associated markers (*Lin28* and *Chx10*, and nestin) in most Müller cells in culture, at very short times after treatment (1 and 4 h). However, only 2% of the allegedly dedifferentiated cells expressed early neuronal markers after applying proven differentiation protocols, and none of them fully acquired a neuronal phenotype. Also, cells in culture failed to down-regulate the MG-specific markers CRALBP and GS (Reyes-Aguirre et al., 2013). We reasoned that this partial dedifferentiation could be explained by a mnemonic mechanism restricting treated cells to a glial phenotype. Such a mechanism can be seamlessly associated with epigenetics, since the transcriptional machinery responsible for changes in gene expression is controlled by epigenetic traits.

DNA methylation is the most stable among epigenetic mechanisms, and is considered the main device of epigenetic memory. It involves the covalent bonding of methyl groups to the C-5 position of the cytosine ring within a DNA sequence, mediated by DNA methyltransferases (DNMTs; Jin et al., 2011). This modification correlates negatively with gene transcription and it is consistently observed in high levels throughout the genome of somatic cells. Three major DNA methyltransferases have been identified in mammals: DNMT1, classically considered a maintenance methyltransferase (Rhee et al., 2012) and DNMT3a and DNMT3b, which can initiate methylation of previously unmethylated DNA (Chen et al., 2003). This modification is reversed by DNA demethylation, which, in the absence of an specific demethylase, potentially involves several different proteins, including TET, GADD45, and deaminases (Rai et al., 2008, 2010).

In this study, we identified changes in the expression of pluripotency-associated genes, previously reported in zebrafish, in a mammalian retinal injury model, at early time points after damage. We suggest a possible correlation between changes in these genes and in those related to DNA methylation and demethylation, whose blockage should enhance MG dedifferentiation.

MATERIALS AND METHODS

Animal Subjects

Adult (6–10 weeks) C57BL/6J mice were used for all lesion experiments and subsequent analysis. Animals were housed under standard conditions with access to water and food *ad libitum*. All procedures were performed under protocols approved by the internal animal care committee (CICUAL–CINVESTAV), and following the guidelines of the Association for Research in Vision and Ophthalmology (ARVO) Statement for the Use of Animals in Ophthalmic and Vision Research.

NMDA Intravitreal Injection and Eye Extraction

Mice were anesthetised with pentobarbital (0.1 mg per 10 g body weight) by an i.p. injection. Tetracaine topical anesthetic was applied to the eyes before the intravitreal injection, as well as a tropicamide/phenylephrine ophthalmic solution. The animals were then placed on a head mount, and a 30G needle was carefully inserted at the upper temporal ora serrata in the left eye, delivering 250 mM N-methyl-D-aspartate (NMDA) (Sigma) into the vitreous humor. The right eye remained intact as a control. After the injection, mice were returned to their home cages for recovery, with food and water *ad libitum*. Eyes were enucleated at 4, 12, 18, and 24 h post injury (hpi), and prepared for further analysis.

Immunohistochemistry

After enucleation, eyes were fixed with a 4% paraformaldehyde (PFA) solution for 1 h at 4°C. Following fixation, the anterior region was removed and the posterior part cryopreserved in

a 30% sucrose solution overnight at 4°C. Then, eyes were embedded in OCT compound (Tissue-Tek, Sakura Finetek, USA) and frozen for cryo-sectioning with a microtome (Leica), obtaining 10 μm retinal sections placed on coated slides (Biocare Medical, USA), which were air-dried for 1 h at room temperature (RT) and then hydrated for 30 min with phosphate buffered saline (PBS). The slides were placed in a wet chamber and blocked with a 0.3% Triton X-100 solution containing 1% bovine serum albumin (BSA) and 5% goat serum for 1 h at RT. Primary antibodies against nestin (1:200; Millipore, Billerica, MA, USA, MAB353), and glutamine synthase (GS) (1:100; Abcam, AB16802), were diluted in PBS and allowed to bind to the slides overnight at 4°C. After several rounds of washing, the slides were incubated with the secondary antibodies Alexa 488 anti-mouse (1:500; Molecular Probes, Eugene, OR, USA) and/or Alexa 568 anti-rabbit (1:500; Molecular Probes, Eugene, OR, USA), diluted in PBS with 4′,6-diamidino-2-phenylindole (DAPI; 1:15000; Sigma) for 1 h and 30 min at RT. The slides were then mounted with DABCO, and viewed on an epifluorescence microscope Zeiss Axiovert 40 CFL, coupled with a digital camera Carl Zeiss Axiocam MRm, with AxioVision Rel.4.8 software.

Terminal Deoxynucleotidyl Transferase dUTP Nick-End Labeling (TUNEL) Assay

Cell death was analyzed in slides from eyes enucleated 24 hpi, using the *in situ* Cell Death Detection Kit, Fluorescein (Roche Diagnostics, GmbH, Mannheim, Germany), according to manufacturer's instructions. As a positive control, some slides were incubated with 200 U/ml DNase I (Sigma) for 10 min at RT.

RNA Extraction, RT-PCR, and qPCR

Total RNA was isolated from enucleated eyes using Trizol (Invitrogen, CA, USA), from which complementary DNA was synthesized using Oligo dT and Superscript-II reverse transcriptase (Invitrogen). Specific cDNAs were amplified by PCR over 30–40 cycles, using *Taq* polymerase (Fermentas) and gene-specific primers (**Table 1**), under the following conditions: denaturation at 95°C for 30 s, annealing at 50–60°C (this temperature was changed according to the primers' Tm) for 15 s, and extension at 72°C for 30 s. The PCR products were resolved on 1.5% agarose gels containing 25 ng/ml ethidium bromide, and visualized in an UV EpiChem^3 Darkroom transilluminator. Images were captured using the LabWorks 4.5 software (BioImaging Systems, UVP, Upland, CA, USA). Embryonic (E10) cDNA was used as a positive control, while non-template samples were negative controls.

Quantitative PCR reactions were performed using KAPA SYBR FAST (Kappa BioSystems, Wilmington, MA, USA) master mix on the PikoReal Real-time PCR System (Thermo Scientific), for 35 cycles as following: denaturation at 94°C for 10 s, annealing at 50–60°C for 30 s, and extension at 72°C for 30 s. Reactions for each primer were performed in triplicate. The $\Delta\Delta$CT method was used to determine mRNA levels in control and injured retinas. All data were normalized to GAPDH mRNA expression levels.

TABLE 1 | Primers used for RT-PCR and qPCR analysis.

Gene		Sequence
Oct4	Forward	TCTTTCCACCAGGCCCCCGGCTC
	Reverse	TGCGGGCGGACATGGGGGAGATCC
Nanog	Forward	GACTGAGATATGGCTTGCTC
	Reverse	CTTTCTGAGGGATAGGGTCT
Klf4	Forward	GGCGAGTCTGACATGGCTG
	Reverse	GCTGGACGCAGTGTCTTCTC
Pax6	Forward	CGGAGGGAGTAAGCCAAGA
	Reverse	AAGGGCACTCCCGTTTATACT
Lin28	Forward	AGGCGGTGGAGTTCACCTTTAAGA
	Reverse	AGCTTGCATTCCTTGGCATGATGG
Sox2	Forward	TAGAGCTAGACTCCGGGCGATGA
	Reverse	TTGCCTTAAACAAGACCACGAAA
C-myc	Forward	TGACCTAACTCGAGGAGGAGCTGGAATC
	Reverse	AAGTTTGAGGCAGTTAAAATTATGGCTG
DNMT1	Forward	CCTAGTTCCGTGGCTACGAGGAGAA
	Reverse	TCTCTCTCCTCTGCAGCCGACTCA
DNMT3a	Forward	GCCGAATTGTGTCTTGGTGGATGACA
	Reverse	CCTGGTGGAATGCACTGCAGAAGGA
DNMT3b	Forward	TGGGTACAGTGGTTTGGTGA
	Reverse	GCCCTTGTTGTTGGTGACTT
Gadd45a	Forward	CCTGCACTGTGTGCTGGTGA
	Reverse	CCACTGATCCATGTAGCGACTTTC
Gadd45b	Forward	CCTGGCCATAGACGAAGAAG
	Reverse	AGCCTCTGCATGCCTGATAC
Tet1	Forward	GAGCCTGTTCCTCGATGTGG
	Reverse	CAAACCCACCTGAGGCTGTT
Tet2	Forward	GCCATTCTCAGGAGTCACTGC
	Reverse	ACTTCTCGATTGTCTTCTCTATTGAGG
Tet3	Forward	GGTCACAGCCTGCATGGACT
	Reverse	AGCGATTGTCTTCCTTGGTCAG
GAPDH	Forward	ACTGGCATGGCCTTCCGTGTTCCTA
	Reverse	TCAGTGTAGCCCAAGATGCCCTTC

Bisulphite Conversion and Methylation-Specific PCR (MSPCR)

After eye enucleation and retinal extraction, genomic DNA was extracted with the EpiTect Fast DNA Bisulfite Kit (Qiagen, Hilden, Germany), and then treated for bisulphite conversion and purified according to manufacturer's instructions. MSPCR was performed using the EpiTect MSP kit (Qiagen, Hilden, Germany) master mix and previously reported specific primers

for the methylated and unmethylated forms of *Oct4* (Wang et al., 2013; **Table 2**). DNA was amplified for 40 cycles, which comprised a denaturation step at 94°C for 15 s, annealing at 50°C for 30 s, and extension at 72°C for 30 s. The resulting products were resolved on 1.5% agarose gels containing 25 ng/ml ethidium bromide, and visualized in an UV EpiChem^3 Darkroom transilluminator. Images were captured using the LabWorks 4.5 software (BioImaging Systems, UVP, Upland, CA, USA). Samples treated with CpG methyltransferase M.SssI (New England BioLabs, Ipswich, MA, USA) were used as positive methylation controls.

High Resolution Melting (HRM) Analysis

DNA was amplified for HRM analysis on the PikoReal Real-time PCR System (Thermo Scientific), using a Luminaris Color HRM (Thermo Scientific) master mix, in a volume of 20 µl, containing 20 ng of DNA. Thermal cycling conditions were as follows: denaturation at 95°C for 10 s, annealing at 50°C for 30 s, and extension at 72°C for 30 s, for 40 cycles. Samples were then melted from 40 to 99°C, with a melting rate of 0.2°C/s. All HRM data were collected and analyzed by the dedicated PikoReal software (Thermo Scientific, version 2.2). Normalization of HRM curves was performed by the same software, as well as calculation of closest standard call (value attributed to each sample with respect to a methylation standard). All analysis were performed in triplicate. Genomic DNA from intact retinas, treated with CpG methyltransferase M.SssI (New England BioLabs, Ipswich, MA, USA) was used as methylation standard.

Magnetic-Activated Cell Sorting (MACS)

As previously reported (Eberle et al., 2014), isolated retinas were dissociated in DMEM containing 0.5% trypsin (Sigma) for 20 min at 37°C. The enzymatic reaction was inhibited by transferring the tissue to DMEM containing 10% fetal calf serum. Additional mechanical dissociation was performed by triturating cells with a 1 ml plastic tip and then a fire-polished glass Pasteur pipette. Cells were resuspended in MACS buffer and incubated with a rabbit anti-mouse primary antibody against GLAST (1:200; Novus Biologicals, Littleton, CO, USA, NB100-1869) for 5 min at 4°C, washed in MACS buffer, and then centrifuged. The cell pellet was resuspended in MACS buffer and incubated with 0.1 ml of goat anti-rabbit IgG magnetic beads (Miltenyi Biotec, Bergisch Gladbach, Germany) for 15 min at 4°C. Magnetic separation was performed according to manufacturer's instructions on a QuadroMACS separator, using LS columns (Miltenyi Biotec, Bergisch Gladbach, Germany). Briefly, the cells were placed on a column fixed to the separator and flow through (GLAST-negative cells) was collected. Then, GLAST-positive fraction was eluted by loading 5 ml MACS buffer and immediately applying pressure with the supplied plunger. Cells from both fractions were then prepared for further analysis.

TABLE 2 | Primers for MSPCR for Oct4.

Gene		Sequence
Oct4 M	Forward	GGTTTTAGAAATAATTGGTATACG
	Reverse	CTATTAACACTACACCCTCTCGAC
Oct4 U	Forward	TGGTTTTAGAAATAATTGGTATATGA
	Reverse	CCTATTAACACTACACCCTCTCAAC

M, methylated allele; U, unmethylated allele.

SGI-1027 Intravitreal Injection

DNA methyltransferase inhibitor SGI-1027 (Sigma) was dissolved in 0.05% DMSO, and injected intravitreally following the same procedure as NMDA injection (10 µM in 2 µl), 24 h before retinal injury.

Statistical Analysis

All experiments were performed by triplicate and all data are expressed as mean ± SEM. Statistical significance of the differences was assessed by a one-way analysis of variance (ANOVA), followed by a Tukey test for *post-hoc* comparisons, or by Student's *t*-test.

RESULTS

Expression of Pluripotency-Associated Markers after Retinal Injury

We demonstrated the excitotoxic effect of the NMDA injection by a TUNEL assay, comparing injured retinas (at 24 hpi) with positive controls. NMDA produced massive cellular death throughout all retinal layers (**Figure 1A**), as well as a general disruption of the laminar structure of the retina. MG response to damage was assessed by immunofluorescence against GS and nestin, a filamentous protein usually found in progenitor cells. Intact retinas (**Figure 1B**) lack nestin-immunopositive cells. After 24 hpi, co-labeling of nestin and GS is observable across the inner nuclear layer (INL), reflecting MG early dedifferentiation (**Figure 1C**).

To characterize the early molecular events during MG response to NMDA-induced injury in rodent retina *in vivo*, we analyzed the changes in expression of pluripotency-associated genes of retinas extracted at 4, 12, 18, and 24 hpi (**Figure 2A**) from a group of mice ($n = 12$, 3 per group). We found that *Oct4* and *Nanog*, both regarded as essential for pluripotency acquisition and maintenance, rapidly increase their expression after 4 and 12 hpi. However, this change is transient, and both genes become undetectable at 24 hpi. *Klf4* and *Pax6* also appear to have a transient expression, since both are substantially reduced after 18 hpi. In contrast, *Lin28* and *Sox2* maintain their expression throughout all time points. To validate these data, we performed qPCR analysis and determined the relative expression level of each gene. A one way ANOVA revealed that *Oct4* and *Nanog* reach an expression peak at 4 hpi ($p < 0.001$, when compared to controls) and then reduce their levels at 18 and 24 hpi (**Figure 2B**). In a similar fashion, *Klf4* exhibits a significant increase at 4, 12, and 18 hpi ($p < 0.01$) and then a reduction at 24 hpi. *Pax6* actually undergoes a slight decrease at 4 hpi ($p < 0.05$), before increasing its

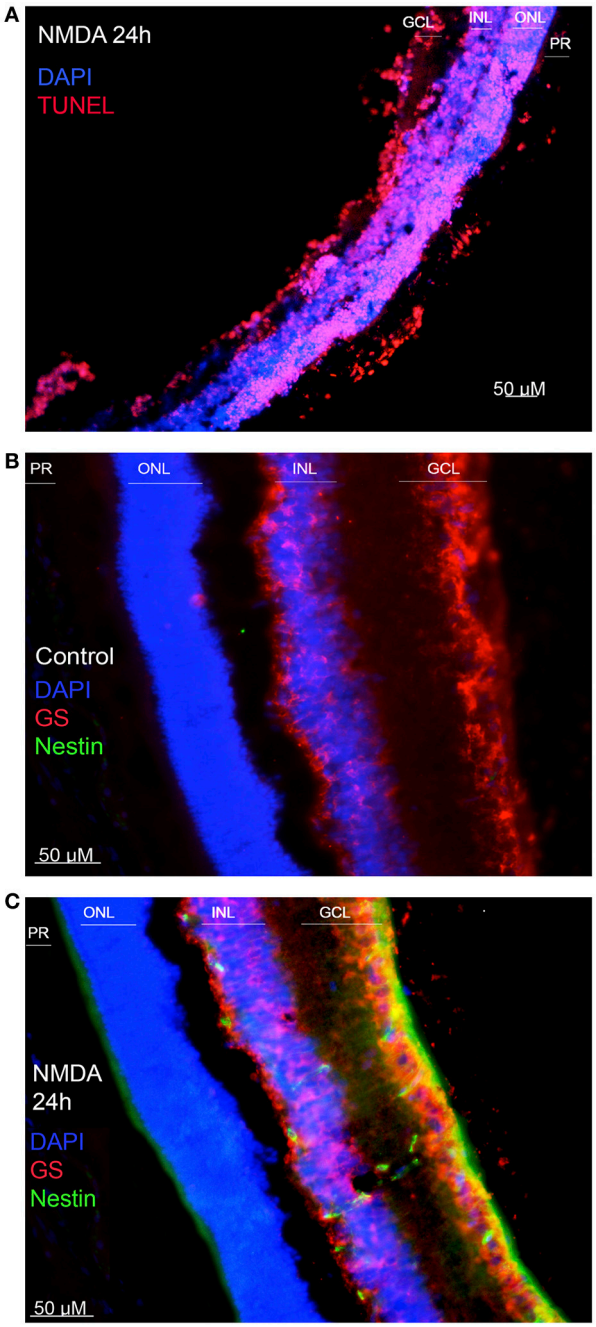

FIGURE 1 | ***Effect of NMDA injury.*** **(A)** TUNEL test performed on a damaged retina, 24 h after injury. Cell nuclei are shown in blue, and apoptotic cells in red. **(B)** Immunofluorescence against nestin and glutamine synthase (GS) on an intact retina. MG, positive to GS, is shown in red. No nestin-positive cells are detected. **(C)** Immunofluorescence against the same markers on a damaged retina, extracted 24 h after injury. Co-labeling of GS (red) and nestin (green) indicates that MG are expressing the progenitor-associated marker as a response to damage. (ONL, outer nuclear layer; INL, inner nuclear layer; GCL, ganglion cell layer; PR, photoreceptor layer). Calibration bar: 50 µm.

expression levels at 12 and 18 hpi (**Figure 2C**). In order to achieve a better visualization of the changes in mRNA levels for each gene, we compiled the data and performed a logarithmic transformation (**Figure 2D**). The resulting graph shows the expression dynamics of the evaluated pluripotency-associated genes.

Expression of Markers Associated to DNA Methylation and Demethylation

The transient expression of pluripotency-associated genes suggests the presence of a silencing mechanism acting on MG at 24 hpi. Since DNA methylation is considered the main device of epigenetic memory (Vierbuchen and Wernig, 2012), we chose to analyse the expression of genes encoding DNA methyltransferases and Gadd proteins, by RT-PCR (**Figures 3A,B**). As expected, we did not observe any change in the expression levels of the maintenance methyltransferase *Dnmt1*, but the expression of *Dnmt3a* and *3b*, which are involved in *de novo* methylation of DNA, is diminished at 4 and 12 hpi. Gadd proteins, associated with DNA demethylation, also exhibited changes in their expression profiles. Particularly, we found a significant increase of *Gadd45b* at 4 and 12 hpi. These mRNA is then drastically reduced at 18 and 24 hpi. Quantification of gene expression changes by qPCR demonstrated that *Dnmt3b* exhibits a biphasic, time-dependent decrease, which becomes statistically significant (by an ANOVA test) at 12 hpi ($p < 0.01$), before reverting to its basal levels. *Gadd45b* also shows a significant increase at 4 hpi ($p < 0.001$), and then returns to normal levels (**Figure 3B**). We also analyzed the expression of the genes that encode active DNA demethylation-associated Tet proteins (**Figure 3C**), and observed that, unexpectedly, the expression of *Tet1* is decreased at 12 hpi ($p < 0.05$); *Tet2* is decreased at 4 and 12 hpi ($p < 0.01$ and 0.05, respectively), and *Tet3* at 4, 12, and 24 hpi ($p < 0.001$, 0.001, and $p < 0.01$, respectively). We then performed a logarithmic transformation of data in order to achieve a better visualization, and compared the changes in the expression of *Dnmt3b* and *Gadd45b* with those of *Oct4* and *Nanog* (**Figure 3D**). Noteworthy, the expression peak of pluripotency genes correlates with a major decrease in *Dnmt3b* levels (at 4 and 12 hpi), and with a significant increase in *Gadd45b*.

Oct4 Methylation Profile in Injured Retina

Given the apparent correlation between *Oct4*, *Dnmt3b,* and *Gadd45b*, we reasoned that *Oct4* DNA methylation profile might exhibit changes at different times post injury. To demonstrate this, we extracted genomic DNA from another group of mice ($n = 12$, 3 per group) and performed a methylation-specific PCR analysis, using previously tested primers, which recognize the methylated form of *Oct4* (Wang et al., 2013). We observed a decrease in methylated *Oct4* at 4 and 12 hpi, with an apparent return to basal levels at 24 hpi (**Figure 4A**). Assuming the limitations of MS-PCR, we also performed an HRM analysis, using several dilutions of DNA treated with CpG methyltransferase M.SssI as a methylation standard. By using an ANOVA test, we observed that NMDA injury induced a significant decrease in *Oct4* methylation after 4 and 12 hpi (down to 20% when compared to the fully methylated standard; $p < 0.001$; **Figure 4B**). Afterwards, DNA methylation tends to increase, up to 60% when compared

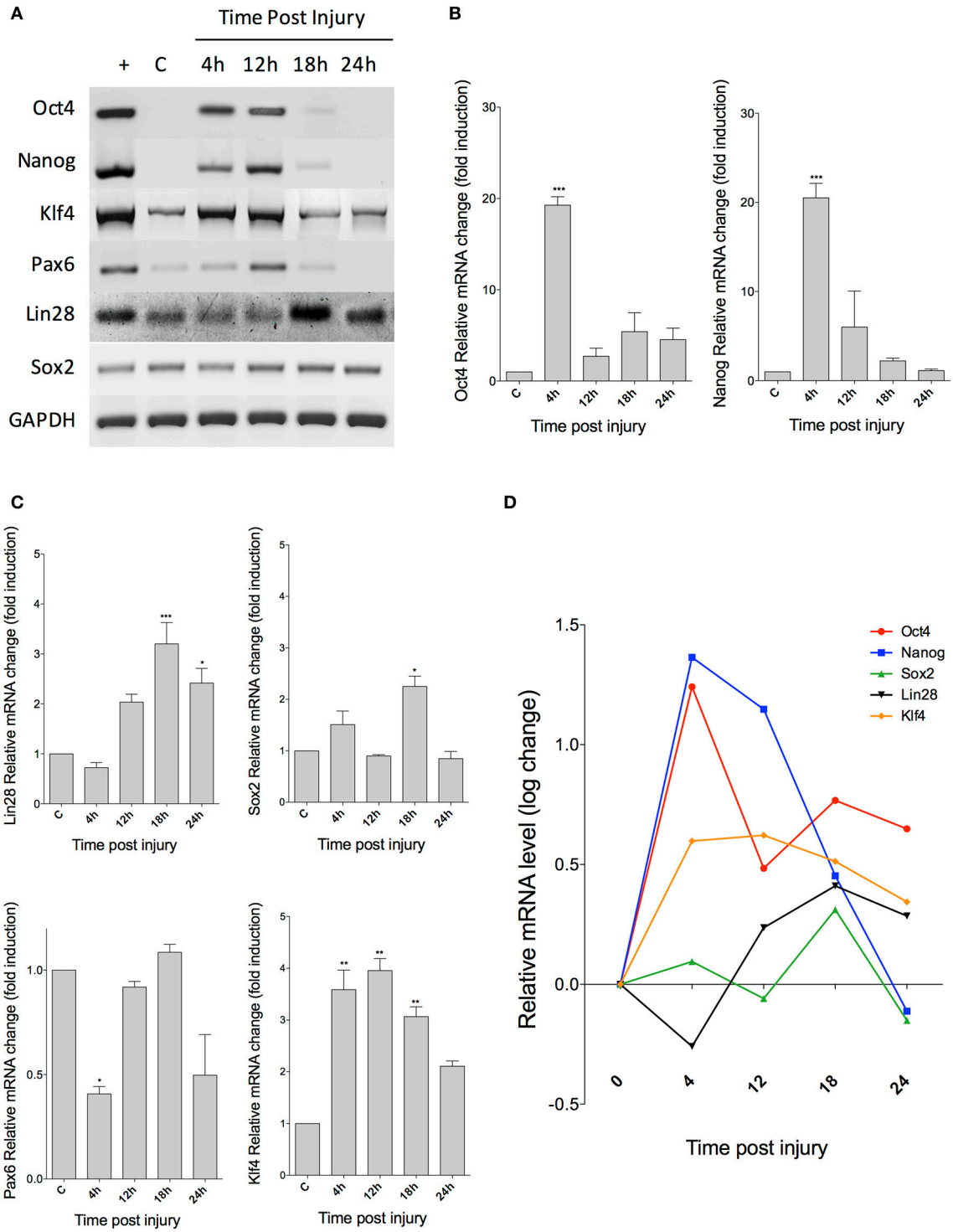

FIGURE 2 | ***Expression of pluripotency-associated markers in injured retina*****. (A)** RT-PCR analysis reveals the changes in expression of several markers at the indicated times after injury. C, control; +, embryonic cDNA as positive control. **(B)** Real-time PCR quantification of Oct4 and Nanog expression levels **(C)** qPCR analysis for Lin28, Sox2, Pax6, and Klf4. **(D)** Change dynamics for all markers after a logarithmic transformation of data to allow a better visualization of the expression pattern for each gene. (ANOVA: ***$p < 0.001$; **$p < 0.01$; *$p < 0.05$).

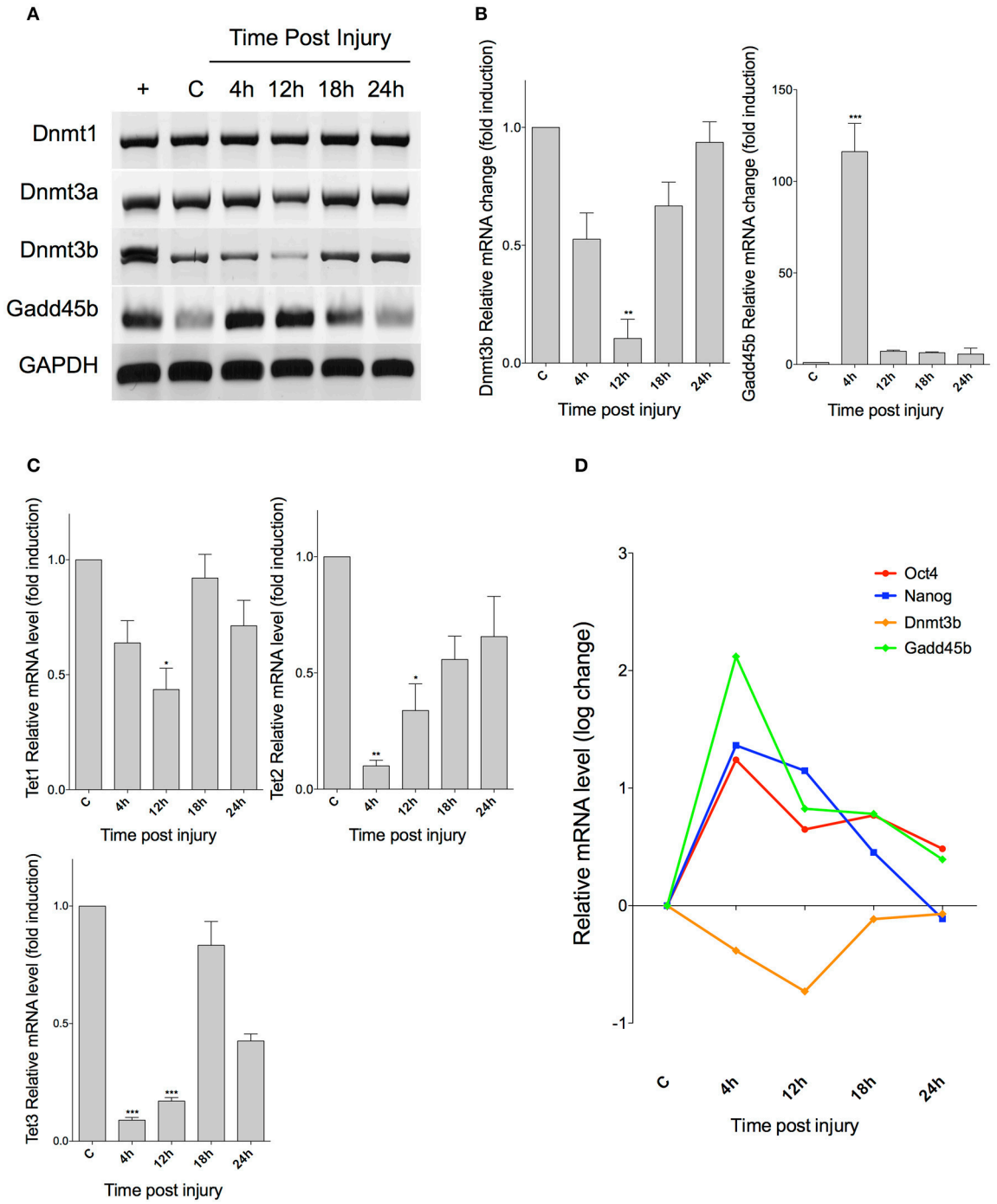

FIGURE 3 | ***Expression of markers associated to DNA methylation and demethylation after retinal injury in vivo.*** **(A)** RT-PCR analysis for genes encoding for DNA methyltransferases (Dnmt1, Dnmt3a, and Dnmt3b), and a Gadd45 protein, associated with repair-based DNA demethylation. C, control; +, embryonic cDNA used as positive control. **(B)** qPCR analysis of Dnmt3b and Gadd45b. **(C)** qPCR for DNA demethylation-associated Tet proteins. **(D)** Comparison between expression changes in pluripotency-associated genes and methylation and demethylation-associated markers (ANOVA; ***$p < 0.001$; **$p < 0.01$; *$p < 0.05$).

with the standard ($p < 0.001$) at 18 hpi, and around 88% at 24 hpi ($p < 0.01$). These results indicate a tendency of Oct4 to return to its fully methylated state as damage proceeds.

Damage Response in Mice is Restricted to MG

To evaluate whether the expression changes we observed are happening exclusively in MG, and not in other cell types in

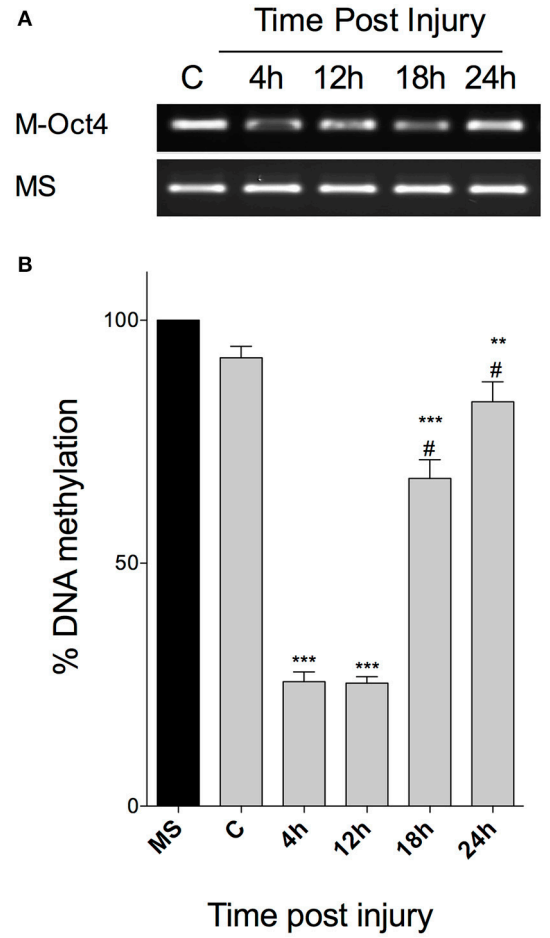

FIGURE 4 | *Oct4 methylation profile after retinal injury in vivo.* (A) MS-PCR of Oct4, with primers specific to its methylated form, resolved in an agarose gel. M-Oct4, Methylated form of Oct4; fully methylated DNA was used as an internal control. **(B)** Representation of the percentage of Oct4 methylation at different times after injury, calculated after HRM analysis, and compared to a methylation standard. (ANOVA; ***$p < 0.001$; **$p < 0.01$, when compared to the fully methylated standard (MS); #$p < 0.001$, when compared with 4 and 12 hpi).

the retina, we separated Müller cells by magnetic associated cell sorting (MACS) after extracting retinas from 12 mice (3 per condition). This procedure depends on a reliable surface marker, and we chose the glutamate transporter GLAST, mainly expressed in radial glia in the central nervous system and specific to MG in the retina (Namekata et al., 2009). First, we confirmed that Slc1a3 (which encodes GLAST) maintains its expression levels *in vivo* after retinal injury (**Figure 5A**), making GLAST a suitable marker for MACS in our injury model. As a validation to our cell sorting results, we found that the GLAST-positive fraction shares the expression of both *Slc1a3* (GLAST) and *Glul* (GS) with cultured MG. In contrast, the GLAST-negative fraction expresses the photoreceptor marker *Nrl*, also found in a whole, intact retina sample (**Figure 5B**). We extracted total RNA from both GLAST-positive and negative fractions of injured retina for qPCR analysis, and found that changes in *Oct4* expression are restricted to the positive fraction, i.e., MG, closely resembling the pattern previously found in whole retina (**Figure 5C**). We obtained similar results after quantifying *Nanog* (**Figure 5D**), *Lin28* (**Figure 5E**), and *Dnmt3b* (**Figure 5F**). These genes are expressed exclusively in MG after retinal injury, and show no significant changes in GLAST-negative cells, after statistical analysis by a Student's *t*-test.

DNA Methylation Blockage Maintains Oct4 Expression at 24 hpi

To demonstrate a causal relationship between DNA methylation and *Oct4* silencing, we intravitreally administered SGI-1027, a DNA-methyltransferase inhibitor which has been shown to block and degrade DNMT1, DNMT3a, and DNMT3b (Yoo et al., 2013; Gros et al., 2015), to a group of mice ($n = 10$, 5 per condition). We evaluated the expression of *Oct4* in GLAST-positive and negative fractions of retinas injured in the presence and absence of SGI-1027. The retinas were extracted 24 h after NMDA injection, since the aforementioned pluripotency-associated marker was silenced at this time in previous experiments. Our results show that SGI-1027 allows the sustained expression of *Oct4* after retinal injury, only in the GLAST-positive fraction of retinas (**Figure 6A**). This increase was revealed to be statistically significant (Student's *t*-test) by qPCR analysis ($p < 0.001$, when compared to control; $p < 0.001$ when compared to damaged retinas at 24 hpi without SGI-1027 treatment; **Figure 6B**). These results suggest that DNA methylation could be involved in *Oct4* silencing at 24 hpi *in vivo*, and restrict this response to MG.

DISCUSSION

In this study, with the purpose of unveiling the critical mechanisms that impair damage- induced Müller glia dedifferentiation in mammals, we used an experimental murine model to study the kinetics and regulatory mechanisms of the expression of pluripotency-associated genes at early times after injury. We contrasted our results to thoroughly characterized data obtained in fish, and we identified, in mice, a silencing event upon *Oct4* expression that is not evident in the regenerating fish retina. We demonstrate that this event, that is restricted to Müller glia, correlates with a significant decrease in DNA methyltransferase expression and *Oct4* methylation profile. Furthermore, we suggest that intravitreous administration of a DNA-methyltransferase inhibitor refrains this silencing event *in vivo* and induces a sustained expression of *Oct4* after injury.

Seminal work has described the changes in gene expression at early time points after retinal injury in zebrafish MG, revealing a reprogramming process that drives these cells from a glial to a progenitor-like phenotype, and involves a significant increase in mRNA levels of pluripotency-associated genes (Ramachandran et al., 2010). While this particular study focused on the role of *ascl1a* and *lin28*, it also described changes in *oct4* throughout the regeneration process. This pluripotency gene is expressed in zebrafish quiescent MG and increases its levels after retinal injury; its expression is then sustained for several days, and tends to revert to basal levels a week after damage onset. The presence

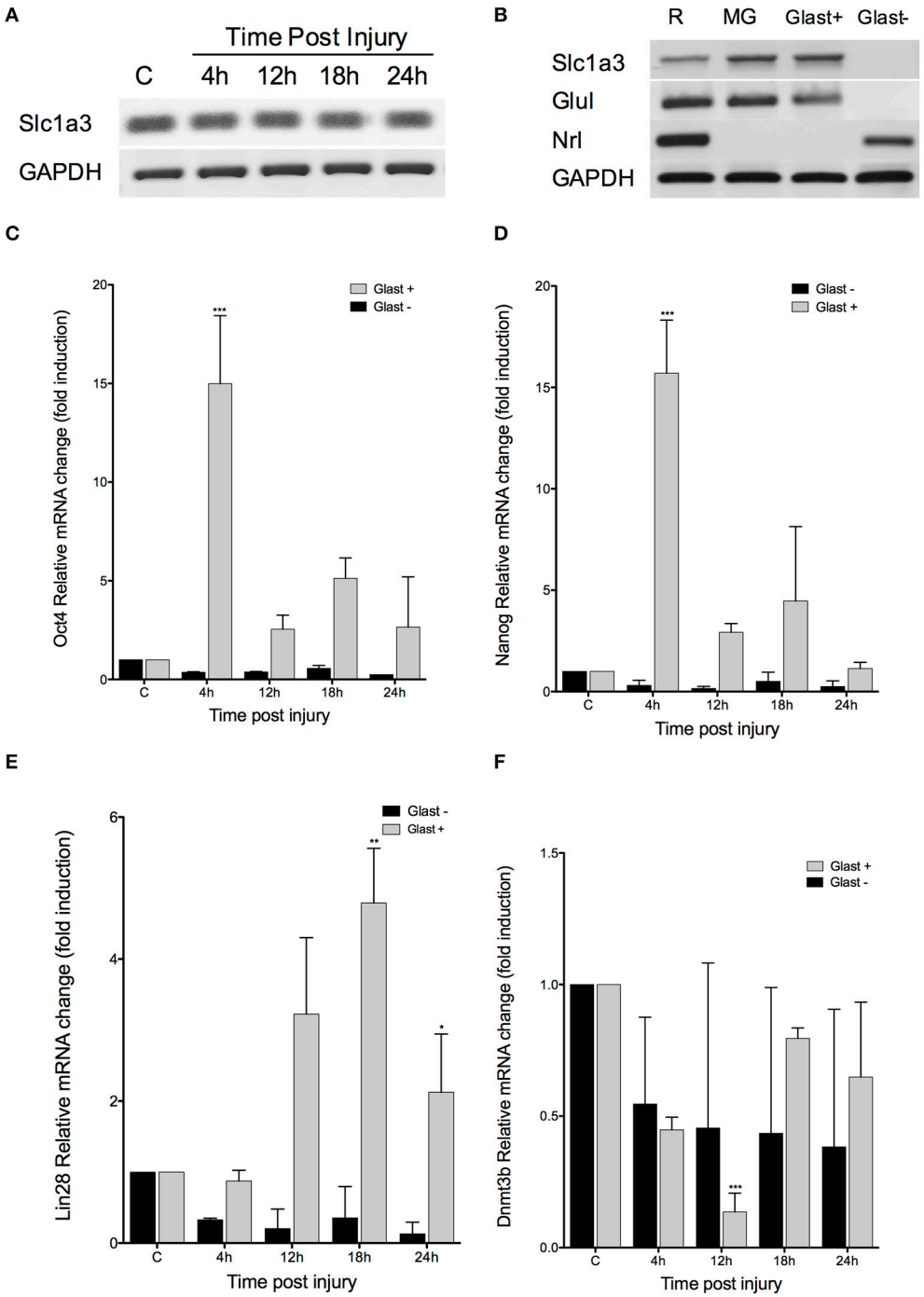

FIGURE 5 | *Damage response is restricted to MG.* **(A)** RT-PCR analysis for Slc1a3, the gene encoding GLAST, at the indicated times after injury. **(B)** RT-PCR for MG and a photoreceptor-specific marker (Nrl) in GLAST-positive and negative fractions, after MACS in intact retinas. **(C–F)** qPCR quantification of Oct4, Nanog, Lin28, and Dnmt3b expression levels at the indicated time after injury in MACS GLAST-positive and negative fraction; C, intact retina as control (Student's *t*-test; $^{***}p < 0.001$; $^{**}p < 0.01$; $^{*}p < 0.05$).

of a pluripotency-associated transcription factor in basal MG has been considered a reflection of its amenability to revert to a less-differentiated state and initiate retinal regeneration. Our results regarding *Oct4* expression in injured mammalian retina greatly differ from the aforementioned observations in fish, and, to our knowledge, comprise the first characterisation of changes in the expression of *Oct4* at different time points after retinal injury in mice. We have proved that excitotoxic injury rapidly induces

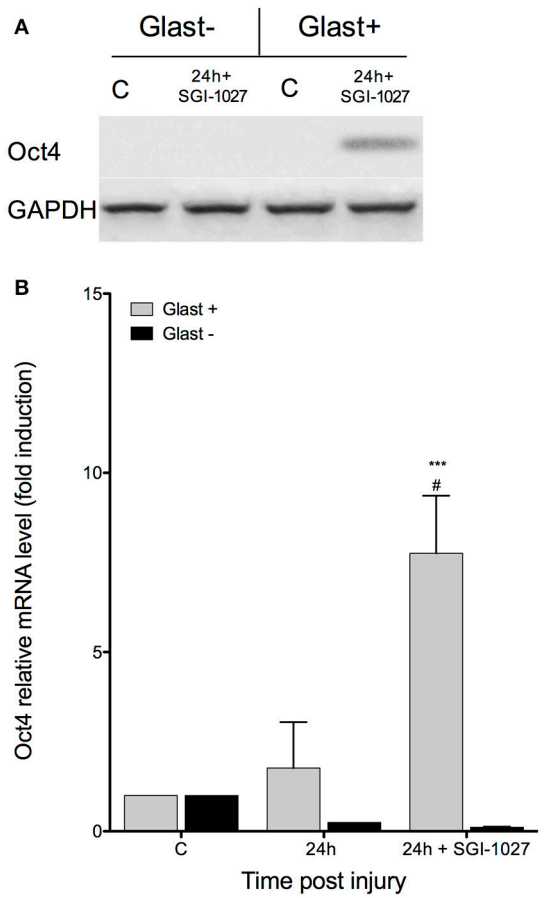

FIGURE 6 | ***SGI-1027 sustains Oct4 expression at 24 hpi.*** **(A)** RT-PCR analysis for Oct4 in MACS GLAST-positive and negative fractions of retinas treated with SGI-1027; C, intact retina as control. **(B)** qPCR quantification of Oct4 expression at 24 hpi in untreated retinas and those treated with SGI-1027. (Student's *t*-test; $^{***}p < 0.001$, when compared to controls; $^{\#}p < 0.001$, when compared with Oct4 expression in untreated retina at 24 hpi).

the expression of this pluripotency-associated gene, as early as 4 hpi.

This result is relevant as *Oct4* expression in the early stages of regeneration suggests similarities among tissue regeneration and pluripotency induction, and impels the question of how further down the road of pluripotency lies the dedifferentiated MG. While no direct observations of *Oct4* effect on retinal regeneration have been reported, there is evidence of impaired fin regrowth by its knockdown at several points during regeneration in zebrafish (Christen et al., 2010). The levels of this gene are not up-regulated in regenerating tissue at levels comparable to those of iPSCs, so it might be insufficient to confer real pluripotency. However, its expression may fulfill a stoichiometric requirement that might enable cells to dedifferentiate to a multipotent state (Eminli et al., 2008; Christen et al., 2010). This possibility deserves further investigation.

Our observations contribute to establishing the dynamics of *Oct4* in the damaged mammalian retina and its striking differences from zebrafish. The demonstration that *Oct4* expression peaks shortly after retinal injury and is rapidly silenced raises the question of whether such silencing constitutes one, of many, mechanisms preventing the successful dedifferentiation of MG, and potentially cell regeneration, in mammals. From the assumption that the core idea of dedifferentiation (that is, the deletion of a genetic program and subsequent acquisition of a different one) involves a certain kind of reprogramming, we could speculate that the rapid repression of *Oct4* may reflect the fast onset of a mnemonic mechanism, potentially involved in the maintenance of glial identity.

Having observed a sudden silencing of *Oct4* after 12 hpi, we reasoned that this pluripotency-associated gene might be rapidly methylated. There is a well-documented correlation between DNA methylation and gene repression. The relative stability and heritability of DNA methylation establishes it as the main mechanism of epigenetic memory, understood as the remaining characteristics of original chromatin after reprogramming (Vierbuchen and Wernig, 2012). We measured the expression levels of enzymes responsible for the addition of methyl groups to DNA (DNMTs) and proteins associated with demethylation. Our results indicate that maintenance *Dnmt1* (Bostick et al., 2007) kept its expression levels at all times after injury, whereas we observed a significant decrease in *Dnmt3b*, that coincided with the expression peak of *Oct4*. This enzyme is traditionally considered a *de novo* methyltransferase, responsible of initiating methylation of previously unmethylated DNA (Chen et al., 2003). Orthologs to this enzyme have been identified in zebrafish, and are expressed at critical points during development of the lens and retina, particularly in the ciliary marginal zone (CMZ), where they are thought to maintain the proliferative properties of this area (Seritrakul and Gross, 2014; Takayama et al., 2014). While extensive characterization of DNMTs expression in mammalian retina is lacking, there is a report of low levels of these enzymes in MG, when compared with other cell types in the neural retina, which might account for its progenitor-like properties (Nasonkin et al., 2011).

It has been observed that *Dnmt3b* orthologs are expressed in blastema cells during fin regeneration in zebrafish, following an interesting expression pattern, i.e., they are absent before and immediately after amputation, and then their expression is induced 3 days after damage, suggesting a crucial involvement in the recovery of 5-methyl-cytosine (5 mC) levels (Takayama et al., 2014). Our results resemble these observations. The significant reduction, and further return to basal levels, in *Dnmt3b* expression that we observe may reflect the involvement of this enzyme in the recovery of methylation levels, in our case, of *Oct4* and other pluripotency-associated genes. To our knowledge, there are no previous reports regarding DNMTs in injured mammalian retina.

Accompanying *Dnmt3b* dynamics, we observed a significant increase in *Gadd45b* expression levels. This gene encodes the protein GADD45b, associated with DNA demethylation, a process that has been deemed necessary for a proper dedifferentiation. GADD45 proteins participate in repair-based DNA demethylation by recruiting the base-excision or the nucleotide-excision repair machinery (BER and NER, respectively; Jung et al., 2007; Schäfer, 2013). Interestingly,

it has been reported that *Gadd45* gene expression can be induced by cellular stress (Hollander and Fornace, 2002), ultimately initiating GADD45-mediated DNA demethylation which, notably, seems to be restricted to single genes (Schmitz et al., 2009; Gavin et al., 2012; Schäfer et al., 2013), without affecting global DNA demethylation (Engel et al., 2009).

These previous results lead us to speculate about a potential correlation between *Gadd45b* expression peak and *Oct4* induction. Our findings may suggest an effect of this demethylation system on *Oct4*, which might be rapidly reversed by *Dnmt3b* return to basal levels and recovery of methylation. However, more tests are needed to fully demonstrate this notion. It is known that *Oct4* expression can be induced by *Gadd45* transfection; also, *Oct4* demethylation is inhibited by *Gadd45a* knockdown in *Xenopus* (Barreto et al., 2007), so this suggested correlation might be plausible. While data on DNA demethylation after retinal injury are still scarce, it has been reported that *Gadd45b* is induced during the transition from MG to MG-derived progenitors in injured zebrafish (Powell et al., 2013), and during MG partial dedifferentiation after glutamate stimuli in cultured mammalian MG (Reyes-Aguirre et al., 2013).

Interestingly, we also observed a significant decrease in *Tet1*, *Tet2,* and *Tet3*. These genes encode the homonymous proteins, which have been shown to promote demethylation by oxidizing 5 mC recruiting excision mechanisms (He et al., 2011), or preventing the proper maintenance of methylation patterns throughout cellular divisions, since they are not recognized by DNMT1 (Valinluck and Sowers, 2007). Direct evidence of Tet role in retina regeneration is still lacking. Reports in zebrafish found discrete, often non-significant changes in Tet relative mRNA levels during transition from MG to MG-derived progenitors, as well as a slight decrease 15 h post injury.

Another striking difference between our data and previously reported results in zebrafish regards the methylation state of pluripotency-associated genes. Powell et al. (2013) reported that promoters of pluripotency and regeneration-associated genes, including *Oct4*, are hypomethylated in quiescent MG. This may contribute to the progenitor-like properties of these cells (Powell et al., 2013). Surprisingly, these authors reported the same hypomethylation of the *Oct4* promoter in basal mouse MG. Our HRM results seem to contradict these findings, since we did not observe *Oct4* expression in intact retinas, nor in quiescent, MACS-separated Müller cells. The pluripotency-associated gene was only induced after retinal injury, and its methylation status in control conditions was similar to a fully methylated standard. A possible explanation for this difference might lay on the evaluated regions. Instead of focusing in *Oct4* promoter, we used specific primers for the first exon, driven by previous reports regarding the close relationship between transcriptional silencing and methylation of this region (Brenet et al., 2011).

We evaluated the effect of a novel inhibitor of DNA methyltransferases, SGI-1027, on *Oct4* expression. Notably, we found that previously tested concentrations of the inhibitor (Simó-Riudalbas et al., 2011) partially revert *Oct4* silencing at 24 hpi. SGI-1027 is a quinolone derivative, which displays inhibitory activity toward DNMT1, DNMT3A, and DNMT3B (Datta et al., 2009). It has been previously reported that regulation of DNA methylation accompanies the reprogramming of MG to progenitor cells in zebrafish, and that global inhibition of methylation by 5-dAza may activate genes associated to reprogramming, but also to proliferation, migration, and differentiation (Powell et al., 2013). These evidences comprise the only precedent of DNA methylation inhibition in injured retina, and its contribution to MG reprogramming.

Studies regarding the effect of *Oct4* expression maintenance on later stages of retina regeneration, are still needed. However, we would like to speculate that preventing the silencing of this pluripotency-associated gene at specific times after injury might improve the transition from MG to retinal progenitors, driving the process of MG-mediated retina regeneration in mammals one step further.

AUTHOR CONTRIBUTIONS

LR and ML conceived the experiments, LR carried out the experiments, LR and ML analyzed data. Both authors were involved in writing the article and had final approval of the submitted and published versions.

ACKNOWLEDGMENTS

The authors wish to express their gratitude to A. Huerta (Cinvestav) and to all the members of Dr. Lamas' laboratory. This work was supported by grants from Conacyt (219847) to ML. LR was a doctoral fellowship recipient from Conacyt. Additional support from the Mexican Society for Stem Cell Research (SOMICET) has also been granted (Project 27109).

REFERENCES

Abrahan, C. E., Insua, M. F., Politi, L. E., German, O. L., and Rotstein, N. P. (2009). Oxidative stress promotes proliferation and dedifferentiation of retina glial cells *in vitro*. *J. Neurosci. Res.* 87, 964–977. doi: 10.1002/jnr.21903

Agte, S., Junek, S., Matthias, S., Ulbricht, E., Erdmann, I., Wurm, A., et al. (2011). Müller glial cell-provided cellular light guidance through the vital guinea-pig retina. *Biophys. J.* 101, 2611–2619. doi: 10.1016/j.bpj.2011.09.062

Barreto, G., Schäfer, A., Marhold, J., Stach, D., Swaminathan, S., Handa, V., et al. (2007). Gadd45a promotes epigenetic gene activation by repair-mediated DNA demethylation. *Nature* 445, 671–675. doi: 10.1038/nature05515

Bernardos, R. L., Barthel, L. K., Meyers, J. R., and Raymond, P. A. (2007). Late-stage neuronal progenitors in the retina are radial Müller glia that function as retinal stem cells. *J. Neurosci.* 27, 7028–7040. doi: 10.1523/JNEUROSCI.1624-07.2007

Bostick, M., Kim, J. K., Estève, P.-O., Clark, A., Pradhan, S., and Jacobsen, S. E. (2007). UHRF1 plays a role in maintaining DNA methylation in mammalian cells. *Science* 317, 1760–1764. doi: 10.1126/science.1147939

Brenet, F., Moh, M., Funk, P., Feierstein, E., Viale, A. J., Socci, N. D., et al. (2011). DNA methylation of the first exon is tightly linked to transcriptional silencing. *PLoS ONE* 6:e14524. doi: 10.1371/journal.pone.0014524

Bringmann, A., Pannicke, T., Grosche, J., Francke, M., Wiedemann, P., Skatchkov, S. N., et al. (2006). Müller cells in the healthy and diseased retina. *Prog. Retin. Eye Res.* 25, 397–424. doi: 10.1016/j.preteyeres.2006.05.003

Chen, T., Ueda, Y., Dodge, J. E., Wang, Z., and Li, E. (2003). Establishment and maintenance of genomic methylation patterns in mouse embryonic stem cells by Dnmt3a and Dnmt3b. *Mol. Cell. Biol.* 23, 5594–5605. doi: 10.1128/MCB.23.16.5594-5605.2003

Christen, B., Robles, V., Raya, M., Paramonov, I., and Izpisúa Belmonte, J. C. (2010). Regeneration and reprogramming compared. *BMC Biol.* 8:5. doi: 10.1186/1741-7007-8-5

Datta, J., Ghoshal, K., Denny, W. A., Gamage, S. A., Brooke, D. G., Phiasivongsa, P., et al. (2009). A new class of quinoline-based DNA hypomethylating agents reactivates tumor suppressor genes by blocking DNA methyltransferase 1 activity and inducing its degradation. *Cancer Res.* 69, 4277–4285. doi: 10.1158/0008-5472.CAN-08-3669

Eberle, D., Santos-Ferreira, T., Grahl, S., and Ader, M. (2014). Subretinal transplantation of MACS purified photoreceptor precursor cells into the adult mouse retina. *J. Vis. Exp.* e50932. doi: 10.3791/50932

Eichler, H., Meckies, J., Schmut, N., Kern, S., Klüter, H., and Zieger, W. (2001). Aspects of donation and processing of stem cell transplants from umbilical cord blood. *Z. Geburtshilfe Neonatol.* 205, 218–223. doi: 10.1055/s-2001-19053

Eminli, S., Utikal, J., Arnold, K., Jaenisch, R., and Hochedlinger, K. (2008). Reprogramming of neural progenitor cells into induced pluripotent stem cells in the absence of exogenous Sox2 expression. *Stem Cells* 26, 2467–2474. doi: 10.1634/stemcells.2008-0317

Engel, N., Tront, J. S., Erinle, T., Nguyen, N., Latham, K. E., Sapienza, C., et al. (2009). Conserved DNA methylation in Gadd45a(-/-) mice. *Epigenetics* 4, 98–99. doi: 10.4161/epi.4.2.7858

Fawcett, J. W., and Asher, R. A. (1999). The glial scar and central nervous system repair. *Brain Res. Bull.* 49, 377–391. doi: 10.1016/S0361-9230(99)00072-6

Fischer, A. J., and Bongini, R. (2010). Turning Müller glia into neural progenitors in the retina. *Mol. Neurobiol.* 42, 199–209. doi: 10.1007/s12035-010-8152-2

Gavin, D. P., Sharma, R. P., Chase, K. A., Matrisciano, F., Dong, E., and Guidotti, A. (2012). Growth arrest and DNA-damage-inducible, beta (GADD45b)-mediated DNA demethylation in major psychosis. *Neuropsychopharmacology* 37, 531–542. doi: 10.1038/npp.2011.221

Gros, C., Fleury, L., Nahoum, V., Faux, C., Valente, S., Labella, D., et al. (2015). New insights on the mechanism of quinoline-based DNA methyltransferase inhibitors. *J. Biol. Chem.* 290, 6293–6302. doi: 10.1074/jbc.M114.594671

He, Y. F., Li, B. Z., Li, Z., Liu, P., Wang, Y., Tang, Q., et al. (2011). Tet-mediated formation of 5-carboxylcytosine and its excision by TDG in mammalian DNA. *Science* 333, 1303–1307. doi: 10.1126/science.1210944

Hochedlinger, K., and Plath, K. (2009). Epigenetic reprogramming and induced pluripotency. *Development* 136, 509–523. doi: 10.1242/dev.020867

Hollander, M. C., and Fornace, A. J. (2002). Genomic instability, centrosome amplification, cell cycle checkpoints and Gadd45a. *Oncogene* 21, 6228–6233. doi: 10.1038/sj.onc.1205774

Jin, B., Li, Y., and Robertson, K. D. (2011). DNA methylation: superior or subordinate in the epigenetic hierarchy? *Genes Cancer* 2, 607–617. doi: 10.1177/1947601910393957

Jung, H. J., Kim, E. H., Mun, J. Y., Park, S., Smith, M. L., Han, S. S., et al. (2007). Base excision DNA repair defect in Gadd45a-deficient cells. *Oncogene* 26, 7517–7525. doi: 10.1038/sj.onc.1210557

Karl, M. O., Hayes, S., Nelson, B. R., Tan, K., Buckingham, B., and Reh, T. A. (2008). Stimulation of neural regeneration in the mouse retina. *Proc. Natl. Acad. Sci. U.S.A.* 105, 19508–19513. doi: 10.1073/pnas.0807453105

Kim, J. B., Greber, B., Araúzo-Bravo, M. J., Meyer, J., Park, K. I., Zaehres, H., et al. (2009). Direct reprogramming of human neural stem cells by OCT4. *Nature* 461, 649–643. doi: 10.1038/nature08436

Namekata, K., Harada, C., Guo, X., Kikushima, K., Kimura, A., Fuse, N., et al. (2009). Interleukin-1 attenuates normal tension glaucoma-like retinal degeneration in EAAC1-deficient mice. *Neurosci. Lett.* 465, 160–164. doi: 10.1016/j.neulet.2009.09.029

Nasonkin, I. O., Lazo, K., Hambright, D., Brooks, M., Fariss, R., and Swaroop, A. (2011). Distinct nuclear localization patterns of DNA methyltransferases in developing and mature mammalian retina. *J. Comp. Neurol.* 519, 1914–1930. doi: 10.1002/cne.22613

Ooto, S., Akagi, T., Kageyama, R., Akita, J., Mandai, M., Honda, Y., et al. (2004). Potential for neural regeneration after neurotoxic injury in the adult mammalian retina. *Proc. Natl. Acad. Sci. U.S.A.* 101, 13654–13659. doi: 10.1073/pnas.0402129101

Pfeiffer-Guglielmi, B., Francke, M., Reichenbach, A., Fleckenstein, B., Jung, G., and Hamprecht, B. (2005). Glycogen phosphorylase isozyme pattern in mammalian retinal Müller (glial) cells and in astrocytes of retina and optic nerve. *Glia* 49, 84–95. doi: 10.1002/glia.20102

Powell, C., Grant, A. R., Cornblath, E., and Goldman, D. (2013). Analysis of DNA methylation reveals a partial reprogramming of the Müller glia genome during retina regeneration. *Proc. Natl. Acad. Sci. U.S.A.* 110, 19814–19819. doi: 10.1073/pnas.1312009110

Rai, K., Huggins, I. J., James, S. R., Karpf, A. R., Jones, D. A., and Cairns, B. R. (2008). DNA demethylation in zebrafish involves the coupling of a deaminase, a glycosylase, and gadd45. *Cell* 135, 1201–1212. doi: 10.1016/j.cell.2008.11.042

Rai, K., Jafri, I. F., Chidester, S., James, S. R., Karpf, A. R., Cairns, B. R., et al. (2010). Dnmt3 and G9a cooperate for tissue-specific development in zebrafish. *J. Biol. Chem.* 285, 4110–4121. doi: 10.1074/jbc.M109.073676

Ramachandran, R., Fausett, B. V., and Goldman, D. (2010). Ascl1a regulates Müller glia dedifferentiation and retinal regeneration through a Lin-28-dependent, let-7 microRNA signalling pathway. *Nat. Cell Biol.* 12, 1101–1107. doi: 10.1038/ncb2115

Raymond, P. A., Barthel, L. K., Bernardos, R. L., and Perkowski, J. J. (2006). Molecular characterization of retinal stem cells and their niches in adult zebrafish. *BMC Dev. Biol.* 6:36. doi: 10.1186/1471-213X-6-36

Reyes-Aguirre, L. I., Ferraro, S., Quintero, H., Sánchez-Serrano, S. L., Gómez-Montalvo, A., and Lamas, M. (2013). Glutamate-induced epigenetic and morphological changes allow rat Müller cell dedifferentiation but not further acquisition of a photoreceptor phenotype. *Neuroscience* 254, 347–360. doi: 10.1016/j.neuroscience.2013.09.048

Rhee, K. D., Yu, J., Zhao, C. Y., Fan, G., and Yang, X. J. (2012). Dnmt1-dependent DNA methylation is essential for photoreceptor terminal differentiation and retinal neuron survival. *Cell Death Dis.* 3:e427. doi: 10.1038/cddis.2012.165

Schäfer, A. (2013). Gadd45 proteins: key players of repair-mediated DNA demethylation. *Adv. Exp. Med. Biol.* 793, 35–50. doi: 10.1007/978-1-4614-8289-5_3

Schäfer, A., Karaulanov, E., Stapf, U., Döderlein, G., and Niehrs, C. (2013). Ing1 functions in DNA demethylation by directing Gadd45a to H3K4me3. *Genes Dev.* 27, 261–273. doi: 10.1101/gad.186916.112

Schmitz, K. M., Schmitt, N., Hoffmann-Rohrer, U., Schäfer, A., Grummt, I., and Mayer, C. (2009). TAF12 recruits Gadd45a and the nucleotide excision repair complex to the promoter of rRNA genes leading to active DNA demethylation. *Mol. Cell* 33, 344–353. doi: 10.1016/j.molcel.2009.01.015

Schütte, M., and Werner, P. (1998). Redistribution of glutathione in the ischemic rat retina. *Neurosci. Lett.* 246, 53–56. doi: 10.1016/S0304-3940(98)00229-8

Seritrakul, P., and Gross, J. M. (2014). Expression of the *de novo* DNA methyltransferases (dnmt3 - dnmt8) during zebrafish lens development. *Dev. Dyn.* 243, 350–356. doi: 10.1002/dvdy.24077

Simó-Riudalbas, L., Melo, S. A., and Esteller, M. (2011). DNMT3B gene amplification predicts resistance to DNA demethylating drugs. *Genes Chromosomes Cancer* 50, 527–534. doi: 10.1002/gcc.20877

Stutz, B., Conceição, F. S., da, Santos, L. E., Cadilhe, D. V., Fleming, R. L., Acquarone, M., et al. (2014). Murine dopaminergic Müller cells restore motor function in a model of Parkinson's disease. *J. Neurochem.* 128, 829–840. doi: 10.1111/jnc.12475

Takahashi, K., and Yamanaka, S. (2006). Induction of pluripotent stem cells from mouse embryonic and adult fibroblast cultures by defined factors. *Cell* 126, 663–676. doi: 10.1016/j.cell.2006.07.024

Takayama, K., Shimoda, N., Takanaga, S., Hozumi, S., and Kikuchi, Y. (2014). Expression patterns of dnmt3aa, dnmt3ab, and dnmt4 during development and fin regeneration in zebrafish. *Gene Expr. Patterns* 14, 105–110. doi: 10.1016/j.gep.2014.01.005

Valinluck, V., and Sowers, L. C. (2007). Endogenous cytosine damage products alter the site selectivity of human DNA maintenance methyltransferase DNMT1. *Cancer Res.* 67, 946–950. doi: 10.1158/0008-5472.CAN-06-3123

Vierbuchen, T., and Wernig, M. (2012). Molecular roadblocks for cellular reprogramming. *Mol. Cell* 47, 827–838. doi: 10.1016/j.molcel.2012.09.008

Wang, J., Fu, Y. H., Wang, W. S., Wang, D. M., and Zhou, Z. Y. (2013). Oct4 methylation in induced differentiation of bone mesenchymal stem cells. *Zhongguo Yi Xue Ke Xue Yuan Xue Bao* 35, 275–280. doi: 10.3881/j.issn.1000-503X.2013.03.007

Yoo, J., Choi, S., and Medina-Franco, J. L. (2013). Molecular modeling studies of the novel inhibitors of DNA methyltransferases SGI-1027 and CBC12: implications for the mechanism of inhibition of DNMTs. *PLoS ONE* 8:e62152. doi: 10.1371/journal.pone.0062152

Conflict of Interest Statement: The authors declare that the research was conducted in the absence of any commercial or financial relationships that could be construed as a potential conflict of interest.

frontiers in Neuroscience

ORIGINAL RESEARCH
published: 01 June 2018
doi: 10.3389/fnins.2018.00364

Sexually Dimorphic Patterns of Cell Proliferation in the Brain Are Linked to Seasonal Life-History Transitions in Red-Sided Garter Snakes

Deborah I. Lutterschmidt, Ashley R. Lucas, Ritta A. Karam, Vicky T. Nguyen and Meghann R. Rasmussen*

Department of Biology, Portland State University, Portland, OR, United States

Seasonal rhythms in physiology and behavior are widespread across diverse taxonomic groups and may be mediated by seasonal changes in neurogenesis, including cell proliferation, migration, and differentiation. We examined if cell proliferation in the brain is associated with the seasonal life-history transition from spring breeding to migration and summer foraging in a free-ranging population of red-sided garter snakes (*Thamnophis sirtalis*) in Manitoba, Canada. We used the thymidine analog 5-bromo-2′-deoxyuridine (BrdU) to label newly proliferated cells within the brain of adult snakes collected from the den during the mating season or from a road located along their migratory route. To assess rates of cell migration, we further categorized BrdU-labeled cells according to their location within the ventricular zone or parenchymal region of the nucleus sphericus (homolog of the amygdala), preoptic area/hypothalamus, septal nucleus, and cortex (homolog of the hippocampus). We found that cell proliferation and cell migration varied significantly with sex, the migratory status of snakes, and reproductive behavior in males. In most regions of interest, patterns of cell proliferation were sexually dimorphic, with males having significantly more BrdU-labeled cells than females prior to migration. However, during the initial stages of migration, females exhibited a significant increase in cell proliferation within the nucleus sphericus, hypothalamus, and septal nucleus, but not in any subregion of the cortex. In contrast, migrating males exhibited a significant increase in cell proliferation within the medial cortex but no other brain region. Because it is unlikely that the medial cortex plays a sexually dimorphic role in spatial memory during spring migration, we speculate that cell proliferation within the male medial cortex is associated with regulation of the hypothalamus-pituitary-adrenal axis. Finally, the only brain region where cell migration into the parenchymal region varied significantly with sex or migratory status was the hypothalamus. These results suggest that the migration of newly proliferated cells and/or the continued division of undifferentiated cells are activated earlier or to a greater extent in the hypothalamus. Our data suggest that sexually dimorphic changes in cell proliferation and cell migration in the adult brain may mediate sex differences in the timing of seasonal life-history transitions.

Keywords: life-history stage, reproduction, courtship behavior, migration, dispersal, foraging, neurogenesis, reptile

OPEN ACCESS

Edited by:
Irmgard Amrein, ETH Zürich, Switzerland

Reviewed by:
Lara LaDage, Penn State Altoona, United States
Michael Brand, Technische Universität Dresden, Germany

****Correspondence:***
Deborah I. Lutterschmidt
d.lutterschmidt@pdx.edu

Specialty section:
This article was submitted to Neurogenesis, a section of the journal Frontiers in Neuroscience

Received: *21 October 2017*
Accepted: *09 May 2018*
Published: *01 June 2018*

Citation:
Lutterschmidt DI, Lucas AR, Karam RA, Nguyen VT and Rasmussen MR (2018) Sexually Dimorphic Patterns of Cell Proliferation in the Brain Are Linked to Seasonal Life-History Transitions in Red-Sided Garter Snakes. Front. Neurosci. 12:364. doi: 10.3389/fnins.2018.00364

INTRODUCTION

Seasonal changes in physiology and behavior are often associated with specific life-history stages, during which an organism is well suited to engage in particular functions within the appropriate environmental context. Examples of such life-history stages include reproduction, migration, parenting, foraging, and even territoriality vs. affiliative behavior. Critically, interactions between environmental conditions and resource availability can relegate life-history stages to a specific time of year and/or geographic locale. Transitions between life-history stages are therefore often characterized by dramatic behavioral changes that result from a shift in motivation to pursue one resource over another. While the mechanisms regulating life-history transitions are poorly understood, the concomitant changes in motivation suggest that a combination of mechanisms involving neuromodulation and neuroplasticity is likely.

One form of neuroplasticity that could contribute to seasonal changes in both appetitive and consummatory behaviors is neurogenesis. Post-natal neurogenesis is defined as the birth and maturation of new neurons that add to or replace neurons in the existing circuitry of the adult brain (e.g., Lindsey and Tropepe, 2006). Neurogenesis involves 5 different phases: cell proliferation within the ventricular zone (i.e., usually but not always within the ependymal layer of a ventricle), cell migration into the parenchyma, cell differentiation and maturation, cell integration into the existing synaptic network, and cell survival. It is hypothesized that seasonal changes in neurogenesis may regulate seasonal cycles in physiology and behavior (see review in Ebling, 2015). For example, both seasonal and circadian variation in cell proliferation, migration, and/or death has been described in many vertebrate and some invertebrate taxa (e.g., Goergen et al., 2002; Hansen and Schmidt, 2004; Vidal Pizarro et al., 2004; Dawley et al., 2006; Lindsey and Tropepe, 2006; Schmidt, 2007; Barnea and Pravosudov, 2011; Delgado-Gonzalez et al., 2011; Font et al., 2012; Smarr et al., 2014; Brenowitz, 2015; Sherry and MacDougall-Shackleton, 2015; Balthazart and Ball, 2016; Migaud et al., 2016; Akle et al., 2017; Yang et al., 2017). Moreover, there is now substantial evidence that the integration of new neurons into existing synaptic circuits in the adult brain contributes to both synaptic plasticity (e.g., long-term potentiation) and environmentally-induced plasticity (e.g., effects of enrichment and exercise) (Sahay et al., 2011; Singer et al., 2011; Alonso et al., 2012; Iscru et al., 2013; Patten et al., 2013; Darcy et al., 2014; Bergami et al., 2015; Temprana et al., 2015; Sakalem et al., 2017). Two questions that emerge prominently from these findings are: What function does such plasticity play in an animal's physiological and behavioral ecology, and how is neurogenesis regulated seasonally?

One of the most extensively studied functions associated with neurogenesis is its role in regulating learning and memory, including hippocampus-dependent spatial learning and memory (reviewed in Amrein and Lipp, 2009; Barnea and Pravosudov, 2011; Lieberwirth et al., 2016). Although early studies sometimes reported contradictory results regarding the association between neurogenesis and spatial learning (e.g., Nilsson et al., 1999; Meshi et al., 2006), it is now evident that the effects of neurogenesis depend on multiple processes, including the differential survival of relatively mature neurons, the death of relatively immature cells, and the timing of differentiation and integration of the surviving cells into existing synaptic circuits (Dupret et al., 2007; Farioli-Vecchioli et al., 2008). In an ecological context, neurogenesis-associated changes in spatial learning and memory have significant functional consequences for both survival and reproductive fitness. For example, in food-storing birds such as black capped chickadees (*Poecile atricapillus*), seasonal changes in neurogenesis and neuronal recruitment in the hippocampus are temporally linked to food-caching and retrieval behavior during the autumn and winter months (Hoshooley and Sherry, 2007; Hoshooley et al., 2007; Sherry and Hoshooley, 2010; Sherry and MacDougall-Shackleton, 2015). Increased neurogenesis appears to be critical to the process of spatial learning during food caching, as treatment of birds with the cell proliferation inhibitor methylazoxymethanol significantly decreased their performance on a spatial learning task (Hall et al., 2014). Spatial learning and memory is also critical to the process of migrating from one geographic locale to another, especially in animals that are faithful to a particular breeding territory, hibernacula, or foraging site. Several studies suggest that seasonal changes in hippocampal neurogenesis are associated with migratory behavior in birds (LaDage et al., 2011; Barkan et al., 2014; also see review in Barnea and Pravosudov, 2011). Whether a similar association between neurogenesis and seasonal migration exists in other vertebrate groups has not been directly examined. However, several key studies indicate that variation in hippocampal neurogenesis and/or volume is indeed positively correlated with the spatial memory demands of defending territorial boundaries, establishing social hierarchies, and determining home range size in ectotherms (Roth et al., 2006; LaDage et al., 2009, 2013; Holding et al., 2012, also see review in Powers, 2016).

Because spatial learning and memory is regulated by the hippocampus, a majority of studies on the function of neurogenesis have necessarily focused on cell proliferation, migration, differentiation, and integration within this region of the brain. This is especially true in mammals, where the regions of proliferative activity are limited to the subventricular zone of the lateral ventricles and the subgranular zone of the dentate gyrus within the hippocampus. In non-mammalian animals, however, the sites of neurogenesis are more widespread throughout the brain, and the rate of cell proliferation within these brain regions is much greater than that in mammals (Lindsey and Tropepe, 2006; Kaslin et al., 2008). Thus, we have relatively little information about the potential role of neurogenesis in other neurogenic brain regions, including the hypothalamus and amygdala, which are important in modulating reproductive and social behaviors. An additional area of complexity in understanding the role of neurogenesis is the existence of sex differences in both basal rates of cell proliferation, migration, and differentiation in the adult brain as well as neurogenic responses to environmental and social stimuli (Spritzer et al., 2017; see reviews in Duarte-Guterman et al., 2015; Frick et al., 2015; Holmes, 2016; Mahmoud et al., 2016; Powers, 2016; Heberden, 2017). Such results indicate that sex steroid hormones, which also vary seasonally in most vertebrates, play a critical role in

modulating the processes that characterize neurogenesis both within the hippocampus and in extra-hippocampal regions. To better understand the function of neurogenesis, it will be helpful to explore sex differences in neurogenic processes while simultaneously mapping these differences onto known sex differences in seasonal physiology and behavior. For example, it is well known that in many seasonally breeding animals, males often become reproductively active and migrate to the breeding grounds prior to females (Ball and Ketterson, 2008). The mechanisms that mediate these differences in reproductive timing, however, are unknown.

In the current study, we examined if changes in cell proliferation and cell migration during the spring are associated with the seasonal life-history transition from spring breeding to migration and summer foraging in a free-ranging population of red-sided garter snakes (*Thamnophis sirtalis parietalis*) in south central Manitoba, Canada. Although many vertebrates exhibit seasonal rhythms in physiology and behavior, one of the most spectacular examples is the spring emergence of more than 30,000 garter snakes from a single hibernaculum following 8 months of winter dormancy. In late April through May, males emerge from underground dens in large numbers and immediately begin searching for mates. Similar to many vertebrates with lek-like mating aggregations (Ball and Ketterson, 2008), male snakes emerge in much larger numbers than females early in the mating season. Approximately 1–2 weeks after males first begin to emerge from the hibernaculum, females begin emerging in increasing numbers. Upon emergence, a female garter snake can be courted by up to 100 males in a single mating ball (Joy and Crews, 1985). Neither male nor female snakes eat during winter dormancy or the mating season; rather, as breeding activity wanes, snakes disperse from the den site and migrate up to 18 km to summer foraging areas, where food is abundant and competition is less fierce (Gregory and Stewart, 1975). Most female garter snakes disperse from the den within 24 h of emergence [DIL, unpublished data; also see (Shine et al., 2006)]. In contrast, many male snakes stay within the vicinity of the den for up to several weeks, searching for and courting newly emerging females (Shine et al., 2001). The factors mediating the sexually dimorphic timing of this life-history transition are unknown, but seasonal changes in neurogenesis may play a central role during migration. Importantly, red-sided garter snakes are typically faithful to their hibernaculum and return to the same den site during the fall to prepare for another cycle of winter dormancy. Thus, enhanced spatial memory during spring migration may be critical for navigating the fall return to the hibernaculum. We previously reported that patterns of cell proliferation and cell migration in the brain vary seasonally in adult male red-sided garter snakes (Maine et al., 2014b). In this study, we asked if patterns of post-embryonic cell proliferation and cell migration vary with sex or migration status during the spring mating season.

METHODS

These experiments were performed in the field with free-ranging red-sided garter snakes in the Interlake region of Manitoba, Canada. All animals were collected from 14 to 18 May 2012. Experimental protocols were approved by the Portland State University Animal Care and Use Committee and were performed under the authority of Wildlife Scientific Permit WB12691 issued by the Manitoba Department of Sustainable Development.

Experimental Design

Experiment 1. Variation in Cell Proliferation Related to Sex and Migratory Status

We asked if there are sex differences in cell proliferation and/or cell migration within the brain, and if these differences are related to changes in migratory behavior of snakes during the spring mating season. Similar to Cease et al. (2007) and Dayger and Lutterschmidt (2017), we compared non-migratory snakes collected from the den site to migratory snakes collected at the beginning of their seasonal migration to the summer feeding grounds. We used a road located approximately 1 km from the den along the migration route to aid in intercepting migrating snakes.

During the spring, female snakes collected from the road typically have visible copulatory plug residue, indicating that they mated prior to migrating from the breeding grounds. We therefore compared migrating female snakes ($n = 10$) to mated females collected from the den ($n = 11$). Females were collected from actively mating pairs and held in outdoor arenas until copulation was completed; successful mating was confirmed by the presence of a mating plug in the cloaca.

Similarly, we wanted to compare courting males collected from the den ($n = 10$) to migrating males that were still exhibiting courtship behavior. During the spring, migrating males collected at the road exhibit two different behavioral phenotypes: some males continue to actively court females while others do not, presumably because they are further along in the seasonal transition to summer feeding activity (e.g., Lutterschmidt and Maine, 2014; Lucas et al., 2017). While it is not feasible to control for variation in male sexual experience in this study (i.e., it is not possible to determine whether an individual male mated previously or how many matings a male achieved prior to migration), all snakes were sexually mature and of similar body size, which suggests they were also of similar age. We used a well-established ethogram of male courtship behavior (Lutterschmidt et al., 2004; modified from Crews, 1984; Moore et al., 2000) to categorize the reproductive status of each male as courting or non-courting. Of the 22 migrating males collected from the road in this study, 10 male snakes exhibited courtship scores ≥ 2, behaviors that are only expressed in a reproductive context (Crews, 1984). These males were classified as "courting" and included in Experiment 1, while the remaining 12 snakes were classified as "non-courting" and reserved for Experiment 2. Thus, we examined changes in cell proliferation related to migratory status without introducing the confounding variable of differences in reproductive status.

Experiment 2. Variation in Cell Proliferation Related to Reproductive Status

We next asked if variation in cell proliferation and/or cell migration within the adult brain is associated with the

seasonal life-history transition from reproductive to non-reproductive status. To address this question, we needed to distinguish changes related to migration from those related to changes in reproductive behavior. We therefore focused on the differences between reproductive and post-reproductive snakes while keeping migratory status constant. We compared cell proliferation between the 10 courting males and 12 non-courting males collected from the road during the initial stages of spring migration. To determine changes related to reproductive status in females, we collected an additional 10 females from the den immediately upon spring emergence and prior to mating. We then compared cell proliferation between these unmated females and the 11 mated females collected from the den during Experiment 1. We confirmed unmated status by verifying the absence of a mating plug in the cloaca.

Animal Housing and Tissue Collection

Immediately upon capture, blood samples (200 μl) were collected within 3 min using tuberculin syringes and heparinized needles. Animals were weighed and their snout-vent length (SVL) measured before they were scale clipped on the ventrum with a unique number. All animals were adult snakes with a mean SVL of 47.2 cm (±0.67 SEM) for males and 54.6 cm (±0.96 SEM) for females; these sizes are generally indicative of adult status in *T. sirtalis parietalis* (Crews et al., 1985; Conant and Collins, 1998). Snakes then received two pulse injections of 100 mg kg^{-1} body mass 5-bromo-2′-deoxyuridine (BrdU) as in Almli and Wilczynski (2007) and Maine et al. (2014b); injections were administered sequentially into two different regions of the peritoneal cavity. BrdU is a thymidine analog that is incorporated into the DNA of mitotic cells. Our previous studies indicate that injection with BrdU does not alter reproductive behavior or brain neuropeptides in male red-sided garter snakes (Maine et al., 2014b; DIL, unpublished data). Snakes were housed in semi-natural outdoor arenas (1 × 1 × 1 m) containing a hide box and water bowl. Snakes were not offered food because they do not eat during the spring mating season. Previous studies in red-sided garter snakes have demonstrated that these housing conditions do not induce significant stress responses (Moore and Mason, 2001; Cease et al., 2007; Lutterschmidt and Maine, 2014).

Four days after their initial capture, a second blood sample was collected before snakes were euthanized with a lethal overdose of 1% sodium Brevital. Male courtship behavior was assessed prior to final tissue collection. We chose this sampling regime because it allowed us to more accurately assess the behavioral phenotypes of migrating males without the influence of capture and handling immediately preceding courtship trials (Cease et al., 2007; Lutterschmidt and Maine, 2014), it maximized our chances of observing changes in cell proliferation related to the post-mating estradiol surge in females (Whittier et al., 1987a), and it optimized the labeling of newly proliferated cells by BrdU treatment (Maine et al., 2014b).

Brains were immersion-fixed in 4% paraformaldehyde in 0.1 M phosphate buffer (pH 7.2) for 16–18 h at 4°C. Tissues were then transferred to 0.1 M phosphate buffer and stored at 4°C until sectioning. Brains were cryoprotected in 30% sucrose in 0.1 M phosphate buffer and cut on a cryostat (Leica 3050S) into four alternate series of 25-μm coronal sections. Tissues were thaw-mounted onto subbed slides (Fisherbrand Superfrost Plus) and stored at −20°C. One series of tissue was used to examine differences in cell proliferation and cell migration via BrdU immunohistochemistry. Two additional tissue series were used to examine differences in arginine vasotocin and neuropeptide Y immunoreactivity among snakes, as well as the relationship between these neuropeptides and plasma steroid hormones. These data are the subject of independent analyses presented in Lucas et al. (2017).

Immunohistochemistry

We examined potential differences in cell proliferation among snakes using BrdU immunohistochemistry methods identical to those described by Maine et al. (2014b). Briefly, antigen retrieval was performed by incubating slides in 2 N HCl in 0.1 M phosphate-buffered saline (PBS; pH 7.4) at 37°C for 30 min to denature the DNA. BrdU immunoreactivity was examined using a rat anti-BrdU antiserum (OBT0030, Accurate Chemical, Westbury, NY, USA) at a dilution of 1:5,000 in PBS containing 0.3% Triton X and 10% normal goat serum. Sections were incubated with primary antibody for 48 h at 4°C in a humid chamber. Primary antibody signal was amplified by incubation with biotinylated goat anti-rat IgG secondary antibody (BA-9400, Vector Labs Inc., Burlingame, CA, USA) diluted 1:400 followed by avidin conjugated to horseradish peroxidase (Elite ABC peroxidase kit, Vector Labs, Inc.). Primary antibody binding was visualized using 0.25 mg/ml diaminobenzidine in 0.2% hydrogen peroxide in 0.05 M Tris buffer (pH 7.2). Tissues were counterstained for 1 min in hematoxylin, dehydrated in a graded ethanol series, cleared with Citrisolv (Fisher Scientific, Pittsburgh, PA, USA) and coverslipped.

Histology and Cell Quantification

Stained tissue was examined using an Olympus BX40 microscope with a QIClick digital camera and QImaging software (QImaging, Surrey, Bristish Columbia, Canada). Locations of BrdU-immunoreactive (ir) cells were mapped onto standard anatomical brain sections adapted from Krohmer et al. (2010) and Martínez-Marcos et al. (2001, 2005). Newly proliferated, BrdU-ir cells were regionally distributed in the adult red-sided garter snake brain as shown in **Figure 1**. BrdU-ir cells occurred mainly in the ventricular zone (i.e., the ependymal cell layer of the ventricle) and the immediately adjacent tissue, especially in forebrain regions. An additional atlas and detailed description of the locations of BrdU-ir cells throughout the brain of red-sided garter snakes can be found in Maine et al. (2014b). Similar to our previous study, we quantified BrdU-ir cell number in the nucleus sphericus (NS), anterior dorsal ventricular ridge, anterior, lateral, and medial septal nucleus (SN), preoptic area, hypothalamus, and medial, dorsal, and lateral regions of the cortex. Because distinct boundaries could not be consistently established between the BrdU-ir cell populations in the NS and anterior dorsal ventricular ridge, labeled cells located in the anterior dorsal ventricular ridge were grouped into and analyzed with the NS. Similarly, distinct boundaries could not be identified between labeled nuclei in the preoptic area and

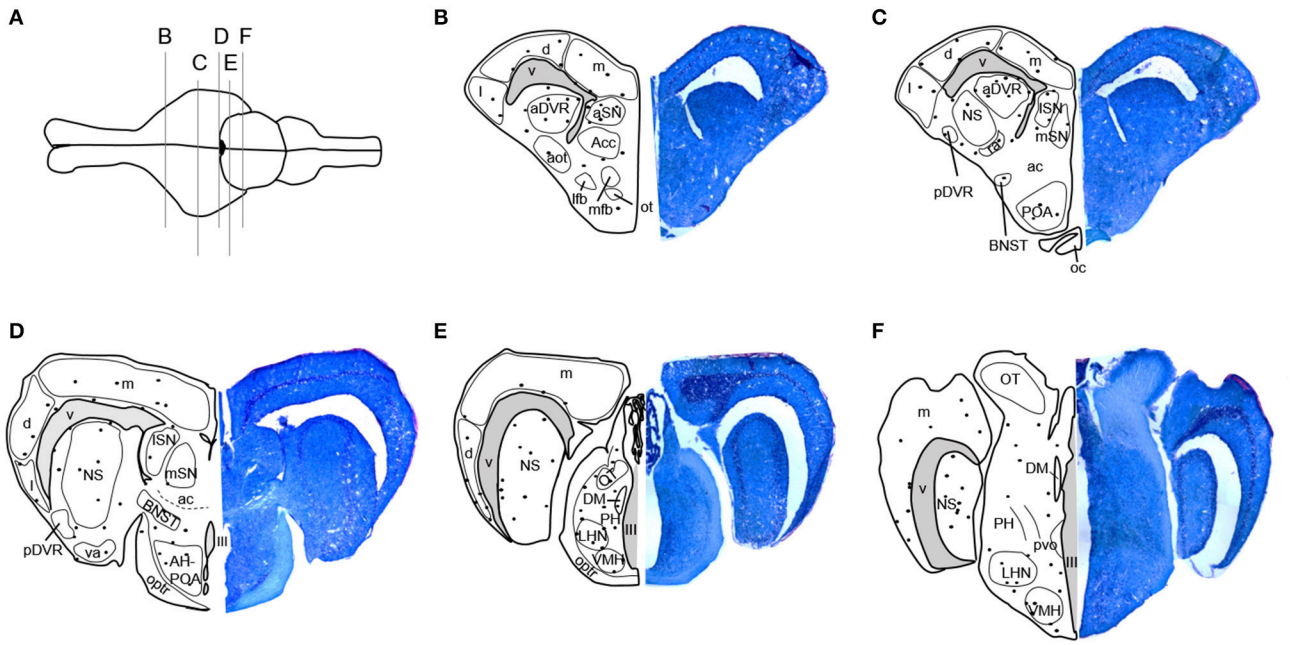

FIGURE 1 | Distribution of BrdU-immunoreactive cells in the brain of adult red-sided garter snakes (*Thamnophis sirtalis parietalis*). **(A)** Schematic showing the dorsal view of the snake brain; the rostral portion of the brain is oriented to the left. The labeled vertical lines indicate the level of sections through BrdU-immunoreactive cell populations from the **(B–F)** rostral through caudal telencephalon. We quantified BrdU-labeled nuclei in the combined nucleus sphericus and anterior dorsal ventricular ridge, combined anterior preoptic area and hypothalamus, septal nucleus, and medial, dorsal, and lateral cortex. Solid black circles indicate locations of immunoreactive nuclei. Tissue sections to the right of each schematic are counterstained with toluidine blue. See Maine et al. (2014b) for a detailed atlas of BrdU-ir cells throughout the brain of red-sided garter snakes, including hindbrain structures. aot, Accessory olfactory tract; Acc, Accumbens; ac, Anterior commissure; aDVR, Anterior dorsal ventricular ridge; AH, Anterior hypothalamus; aSN, Anterior septal nucleus; BNST, Bed nucleus of the stria terminalis; d, Dorsal cortex; DM, Dorsomedial thalamic nucleus; l, Lateral cortex; lfb, Lateral forebrain bundle; LHN, Lateral hypothalamic nucleus; lSN, Lateral septal nucleus; m, Medial cortex; mfb, Medial forebrain bundle; mSN, Medial septal nucleus; NS, Nucleus sphericus; III, Oculomotor nerve; ot, Olfactory tubercle; oc, Optic chiasm; OT, Optic tectum; optr, Optic tract; pvo, Paraventricular organ; PH, Periventricular hypothalamic nucleus; pDVR, Posterior dorsal ventricular ridge; POA, Preoptic area; ra, Rostral amygdaloid nucleus; va, Ventral amygdaloid nucleus; V, Ventricle; VMH, Ventromedial hypothalamic nucleus.

hypothalamus, and thus labeled cells within these regions were combined for analysis.

Animals were coded so that the observer was blind to the identity of individuals. Within each brain region, the total number of BrdU-ir nuclei was quantified manually in every tissue section throughout the region of interest following the methods of Maine et al. (2014b). When BrdU-ir nuclei were located within a bilateral brain region (i.e., all regions of interest except the hypothalamus), cells were quantified in one hemisphere only, as there are no significant differences in BrdU-ir cell number between hemispheres in red-sided garter snakes (Maine et al., 2014b). Labeled nuclei were further categorized by their location relative to the ventricle following the methods of Almli and Wilczynski (2009) and Maine et al. (2014b). As in these studies, we selected 50 μm as a relative boundary for categorizing cells as newly proliferating vs. migrating into the surrounding brain tissue. A BrdU-ir cell was considered to be located within the ventricular zone if it was within 50 μm of a ventricle (**Figure 2**). If the BrdU-labeled cell was located more than 50 μm from the ependymal layer of the ventricle it was categorized as being located within the parenchymal region (Almli and Wilczynski, 2009; Maine et al., 2014b). Cell category was also confirmed by nucleus shape, as cells located close to the ventricle have nuclei that are circular in shape, while cells migrating away from the ventricle have nuclei that are elongated and oval in shape (**Figure 2**; Almli and Wilczynski, 2007, 2009; Delgado-Gonzalez et al., 2011). For each region of interest, we therefore report the number of BrdU-ir cells in the ventricular zone vs. the parenchymal region.

We followed the calculations and criteria described by Laberge et al. (2008) and used in Maine et al. (2014b) to account for missing and/or damaged sections. Within each region of interest, the number of BrdU-ir cells for an individual was calculated as the total number of labeled cells divided by the total number of usable brain sections multiplied by the average number of brain sections for a given region across all animals. We calculated the total number of labeled cells in males and females separately, because body size (and therefore brain size) is sexually dimorphic. These counting methods allowed us to retain more animals in the statistical analyses, in contrast to eliminating an animal if two or more consecutive sections were missing or damaged (e.g., Lutterschmidt and Wilczynski, 2012). The mean number of missing or damaged sections across all animals and regions was 1.19 ± 0.04 SEM (5.46% ± 0.19 SEM). Any animal missing greater than 33% of its sections within a region of interest was excluded from analyses.

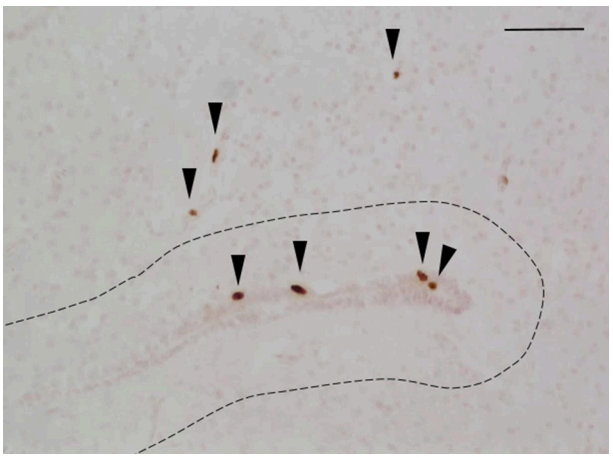

FIGURE 2 | Example photomicrograph showing BrdU-labeled cells in the brain of red-sided garter snakes (*Thamnophis sirtalis parietalis*). Arrows indicate BrdU-immunoreactive nuclei; scale bar = 50 μm. The dashed line delineates a distance of 50 μm from the ependymal layer of the lateral ventricle, which was used to further categorize labeled cells as being located within the ventricular zone (within 50 μm of the ventricle) or parenchymal region (more than 50 μm from the ependymal layer of the ventricle). Arrow heads point toward the ventral region of the tissue section.

Final sample sizes for each region of interest are listed in **Tables 1**, **2**.

Statistical Analyses

Data were transformed where necessary to meet the assumptions of parametric analysis. All data exhibited equal variance among groups. When data transformation could not correct for non-normality, we used a non-parametric Mann-Whitney *U*-test or a Scheirer-Ray-Hare extension of the Kruskal-Wallis ANOVA. We used SigmaPlot 12.0 (Systat Software) for all statistical analyses.

In Experiment 1, we first used *t*-tests within each sex to confirm that body size did not differ between den- and road-collected snakes. Using the same individual snakes included in this study, Lucas et al. (2017) showed that the volume of both the medial cortex and NS are positively related to the SVL of snakes. Thus, SVL can be used as a proxy for brain region volume in red-sided garter snakes. Because body size is sexually dimorphic in this population, with females being larger than males, we corrected our cell counts for potential sex differences in brain volume by dividing the total number of ir cells for each individual by its SVL. We then compared these SVL-corrected data using a general linear model two-way ANOVA with sex and migratory status as between-subjects factors for each brain region of interest. Significant main effects from these analyses were further examined using Tukey's multiple comparisons tests.

In Experiment 2, we used *t*-tests to confirm that body size of snakes did not differ between reproductive states. We then used a *t*-test within each region of interest to compare BrdU-ir cell number between reproductive conditions: courting and non-courting males collected from the road and mated and unmated females collected from the den. Data were not corrected for SVL because these analyses compared cell proliferation and cell migration within each sex, and there was very little variation in SVL among either male (mean ± SEM: 47.2 ± 0.67 cm) or female (54.6 ± 0.96 cm) snakes. These comparisons allowed us to assess potential differences in cell proliferation and cell migration related to changes in reproductive behavior while holding migratory status constant.

RESULTS

Body size (snout-vent-length) did not vary significantly between migrating snakes collected from the road and non-migrating snakes collected from the den for either males ($t = 1.336$, $df = 18$, $P = 0.198$) or females ($t = 0.844$, $df = 19$, $P = 0.409$). Similarly, there were no significant differences in SVL between courting and non-courting males ($t = 0.058$, $df = 20$, $P = 0.954$) or unmated and mated females ($t = 1.423$, $df = 19$, $P = 0.171$).

Experiment 1. Variation in Cell Proliferation Related to Sex and Migratory Status

Table 1 summarizes the effects of sex and migratory status on newly proliferated and migrating cells within each brain region of interest; results from multiple comparisons tests, where appropriate, are shown in **Figures 3–6**. The number of BrdU-labeled cells observed in the ventricular zone varied significantly with the main effects of sex in the NS (**Figure 3A**) and the medial and dorsal cortex (**Figures 6A,B**). Males had more labeled cells than females in each region, even after accounting for sex differences in snout-vent length. Within the NS and SN (**Figures 3A**, **5A**), migrating snakes collected from the road had significantly more BrdU-ir cells in the ventricular zone than non-migrating snakes collected from the den. However, we observed a significant interaction between sex and migratory status within the NS as well as the hypothalamus (**Figures 3A**, **4A**), indicating that the sex differences observed in the number of BrdU-labeled cells within the ventricular zone of these regions depended on the snakes' migratory status.

In all regions of interest except the hypothalamus, the number of migrating BrdU-labeled cells observed in the parenchymal region did not vary significantly with sex or the migratory status of snakes (**Table 1**). All interactions between factors in these regions were also statistically non-significant. Within the hypothalamus, the number of BrdU-ir cells in the parenchymal region varied significantly with sex, and there was a statistically significant interaction between sex and the migratory status of snakes (**Figure 4B**).

Experiment 2. Variation in Cell Proliferation Related to Reproductive Status

We asked if changes in BrdU-ir cell number in the brain are related to the transition from courting to non-courting in males or from unmated to mated status in females. **Table 2**

TABLE 1 | Differences in SVL-corrected BrdU-positive cell number related to sex and migratory status in adult red-sided garter snakes within the nucleus sphericus (NS), hypothalamus (HYP), septal nucleus (SN), medial cortex (MC), dorsal cortex (DC), and lateral cortex (LC).

Location of BrdU-ir cells	Brain region	Final sample sizes	Sex	Migratory status	Interaction
Ventricular zone	NS	20 (10), 21 (11)	$F_{(1, 37)} = 7.550$, $\mathbf{P = 0.009}$	$F_{(1, 37)} = 6.461$, $\mathbf{P = 0.015}$	$F_{(1, 37)} = 13.622$, $\mathbf{P < 0.001}$
	HYP	19 (10), 20 (11)	$F_{(1, 35)} = 0.226$, $P = 0.637$	$F_{(1, 35)} = 3.419$, $P = 0.073$	$F_{(1, 35)} = 10.013$, $\mathbf{P = 0.003}$
	SN	20 (10), 21 (11)	$H_{(1, 37)} = 1.262$, $P = 0.261$	$H_{(1, 37)} = 4.624$, $\mathbf{P = 0.031}$	$H_{(1, 37)} = 2.679$, $P = 0.102$
	MC	20 (10), 20 (11)	$F_{(1, 36)} = 10.947$, $\mathbf{P = 0.002}$	$F_{(1, 36)} = 3.480$, $P = 0.070$	$F_{(1, 36)} = 1.853$, $P = 0.182$
	DC	20 (10), 20 (11)	$F_{(1, 36)} = 14.472$, $\mathbf{P < 0.001}$	$F_{(1, 36)} = 1.814$, $P = 0.187$	$F_{(1, 36)} = 0.007$, $P = 0.931$
	LC	20 (10), 19 (11)	$H_{(1, 35)} = 1.519$, $P = 0.218$	$H_{(1, 35)} = 3.421$, $P = 0.072$	$H_{(1, 35)} = 1.278$, $P = 0.258$
Parenchyma	NS	20 (10), 21 (11)	$F_{(1, 37)} = 0.001$, $P = 0.976$	$F_{(1, 37)} = 0.446$, $P = 0.509$	$F_{(1, 37)} = 2.940$, $P = 0.095$
	HYP	19 (10), 20 (11)	$F_{(1, 35)} = 7.059$, $\mathbf{P = 0.012}$	$F_{(1, 35)} = 3.514$, $P = 0.069$	$F_{(1, 35)} = 34.405$, $\mathbf{P < 0.001}$
	SN	20 (10), 21 (11)	$F_{(1, 37)} = 2.204$, $P = 0.146$	$F_{(1, 37)} = 1.596$, $P = 0.214$	$F_{(1, 37)} = 3.452$, $P = 0.071$
	MC	20 (10), 20 (11)	$F_{(1, 36)} = 0.526$, $P = 0.473$	$F_{(1, 36)} = 0.585$, $P = 0.449$	$F_{(1, 36)} = 0.371$, $P = 0.546$
	DC	20 (10), 20 (11)	$H_{(1, 36)} = 0.501$, $P = 0.479$	$H_{(1, 36)} = 0.585$, $P = 0.444$	$H_{(1, 36)} = 0.050$, $P = 0.823$
	LC	20 (10), 19 (11)	$F_{(1, 35)} = 3.418$, $P = 0.073$	$F_{(1, 35)} = 0.097$, $P = 0.757$	$F_{(1, 35)} = 2.683$, $P = 0.110$

Labeled cells were categorized as newly proliferated if they were found within the ventricular zone of each region of interest and migrating if they were found within the parenchymal region more than 50 μm from the ventricular zone. Sample sizes are given as total number of males (non-migrating males collected from the den), total number of females (non-migrating females collected from the den). All statistics are the main effects of factors from a general linear model multifactor ANOVA (F statistics) or a non-parametric Scheirer-Ray-Hare extension of a Kruskal-Wallis ANOVA (H statistics) within each region of interest. Statistically significant P-values are highlighted in bold font.

TABLE 2 | Variation in BrdU-labeled cell number related to reproductive status in adult red-sided garter snakes within the nucleus sphericus (NS), hypothalamus (HYP), septal nucleus (SN), medial cortex (MC), dorsal cortex (DC), and lateral cortex (LC).

Comparison	Brain region	Final sample sizes	Proliferating cells in the ventricular zone	Migrating cells in the parenchymal region
Courting vs. non-courting males	NS	10, 12	$t = -2.082$, $\mathbf{P = 0.050}$	$t = -0.668$, $P = 0.512$
	HYP	9, 10	$t = -0.963$, $P = 0.349$	$t = -2.349$, $\mathbf{P = 0.031}$
	SN	10, 11	$t = -1.172$, $P = 0.256$	$U = 51.50$, $P = 0.828$
	MC	10, 11	$t = 3.201$, $\mathbf{P = 0.005}$	$t = 1.881$, $P = 0.075$
	DC	10, 11	$U = 27.00$, $\mathbf{P = 0.040}$	$U = 23.00$, $\mathbf{P = 0.016}$
	LC	10, 11	$U = 40.00$, $P = 0.280$	$U = 46.00$, $P = 0.476$
Unmated vs. mated females	NS	10, 11	$t = 0.334$, $P = 0.742$	$U = 32.50$, $P = 0.121$
	HYP	10, 11	$t = 0.082$, $P = 0.936$	$t = 0.674$, $P = 0.508$
	SN	8, 11	$U = 28.50$, $P = 0.152$	$t = 0.916$, $P = 0.372$
	MC	10, 9	$U = 37.00$, $P = 0.495$	$t = -0.449$, $P = 0.659$
	DC	10, 11	$U = 47.00$, $P = 0.507$	$t = 1.467$, $P = 0.159$
	LC	10, 11	$U = 40.00$, $P = 0.094$	$t = 1.164$, $P = 0.259$

Labeled cells were categorized as newly proliferated if they were found within the ventricular zone of each region of interest and migrating if they were found within the parenchymal region more than 50 μm from the ventricular zone. Final sample sizes are given as courting, non-courting males collected from the road and unmated, mated females collected from the den. All statistics are from a t-test (t statistics) or non-parametric rank sum test (U statistics) within each region of interest. Statistically significant P-values are highlighted in bold font.

and **Figures 7**, **8** show the effects of reproductive status on the number of newly proliferated and migrating cells within each brain region of interest. In summary, non-courting males had significantly more BrdU-ir cells in the ventricular zone of the NS (**Figure 7A**) and the parenchymal region of the hypothalamus (**Figure 7E**) compared to courting males. In contrast, BrdU-labeled cell number was significantly lower in non-courting males within the ventricular zone of the medial (**Figure 8A**) and dorsal (**Figure 8B**) cortex as well as the parenchymal region of the dorsal cortex (**Figure 8E**). In female snakes, BrdU-labeled cell number within the ventricular zone and parenchymal region did not vary significantly with reproductive status in any brain region of interest (**Table 2**; data not shown).

DISCUSSION

We found that cell proliferation and cell migration in the adult brain of red-sided garter snakes varied significantly with sex, the migratory status of snakes, and reproductive behavior in males. Furthermore, the patterns of these differences varied among the regions of interest. Four general patterns emerge from these data: (1) Prior to migration from the den site, male snakes

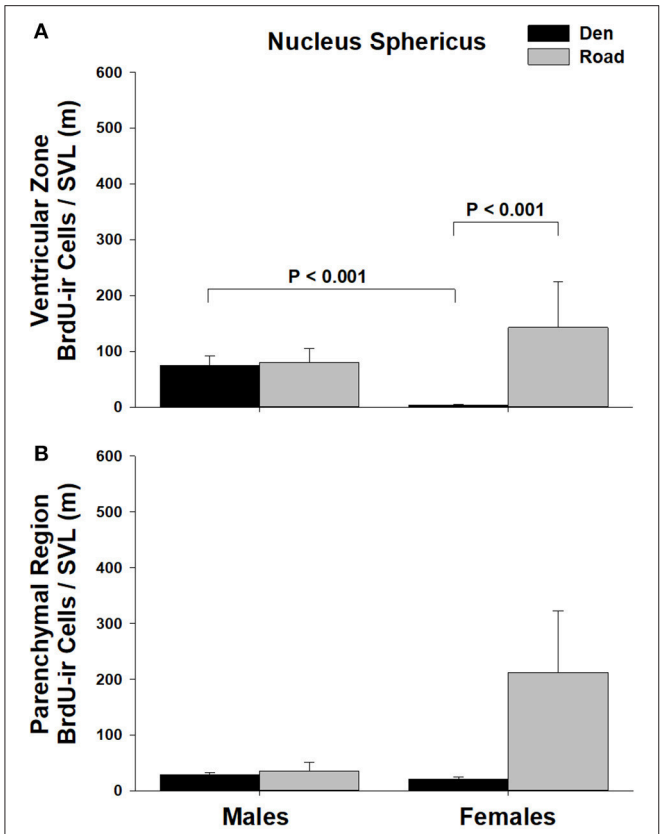

FIGURE 3 | Effects of sex and migratory status on the number of BrdU-immunoreactive (ir) cells in the **(A)** ventricular zone or **(B)** parenchymal region of the nucleus sphericus (NS) in red-sided garter snakes (*Thamnophis sirtalis parietalis*). We captured snakes from the den prior to migration from the breeding grounds; migratory snakes were intercepted on a road located 1 km from the den along the migratory route. Similar to Lucas et al. (2017), we corrected BrdU-ir cell number for sex differences in body size by dividing the number of labeled cells within each individual by its snout-vent length (SVL). Each bar is the mean number of labeled cells +1 SEM. Statistics are from multiple comparisons tests.

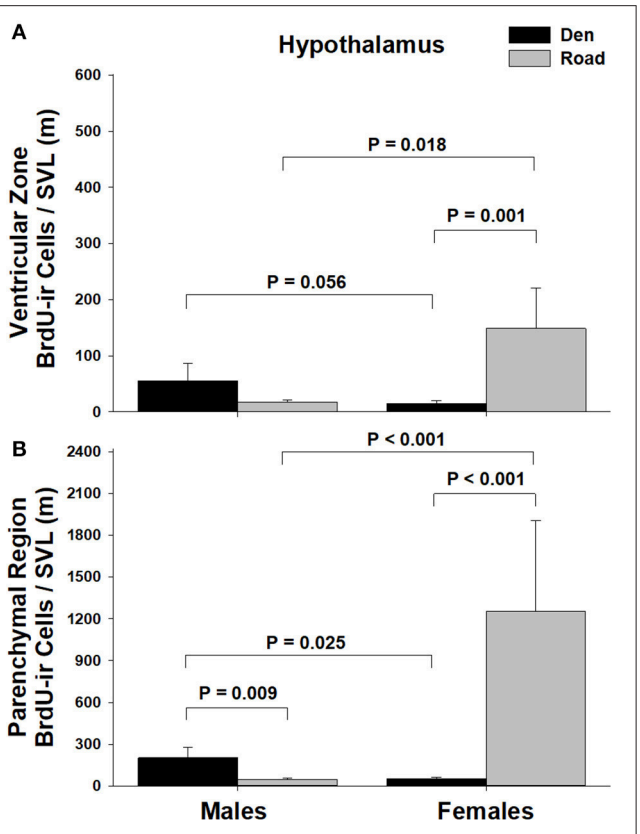

FIGURE 4 | Effects of sex and migratory status on the number of BrdU-immunoreactive (ir) cells in the **(A)** ventricular zone or **(B)** parenchymal region of the hypothalamus in red-sided garter snakes (*Thamnophis sirtalis parietalis*). We captured snakes from the den prior to migration from the breeding grounds; migratory snakes were intercepted on a road located 1 km from the den along the migratory route. Similar to Lucas et al. (2017), we corrected BrdU-ir cell number for sex differences in body size by dividing the number of labeled cells within each individual by its snout-vent length (SVL). Each bar is the mean number of labeled cells + 1 SEM. Statistics are from multiple comparisons tests.

exhibited higher levels of cell proliferation in the ventricular zone of all brain regions compared to females (but this difference was not statistically significant in the medial and lateral cortex); (2) Compared to females collected from the den, migrating female snakes exhibited a statistically significant increase in cell proliferation within the ventricular zone of all brain regions except the cortex (all subregions), whereas migrating males exhibited a significant increase in cell proliferation within the medial cortex but no other brain region; (3) The only brain region where cell migration into the parenchymal region varied significantly with sex or migratory status was the hypothalamus; and (4) In females, changes in cell proliferation and cell migration during dispersal from the breeding grounds were unrelated to changes in reproductive status, whereas in males changes in cell proliferation and cell migration were observed in response to both dispersal as well as changing reproductive behavior.

An important feature of this study is the inclusion of both hippocampal and extra-hippocampal regions of interest, which will be necessary for expanding our understanding of the function and regulation of neurogenesis beyond spatial learning and memory. As in Maine et al. (2014b), we quantified cell proliferation and cell migration within the NS, hypothalamus, SN, and cortex. Similar to other vertebrates, the NS, hypothalamus, and SN are involved in regulating reproductive behavior in red-sided garter snakes: the NS and hypothalamus contain sex steroid-concentrating neurons (Halpern et al., 1982); the NS and POA/hypothalamus exhibit seasonal changes in aromatase activity (Krohmer et al., 2010); and lesions to the NS, SN, and POA/hypothalamus prior to winter dormancy alter the courtship behavior of male snakes (Krohmer and Crews, 1987a,b). Results from the latter studies suggest that the NS and SN inhibit sexual behavior, while the POA/hypothalamus facilitates reproductive behavior. In addition to its role in reproduction, the NS of reptiles is a homolog of the mammalian amygdala (Ubeda-Bañon et al., 2011) and receives input directly from vomeronasal projections (Wang and Halpern, 1988; Lanuza and Halpern, 1997, 1998).

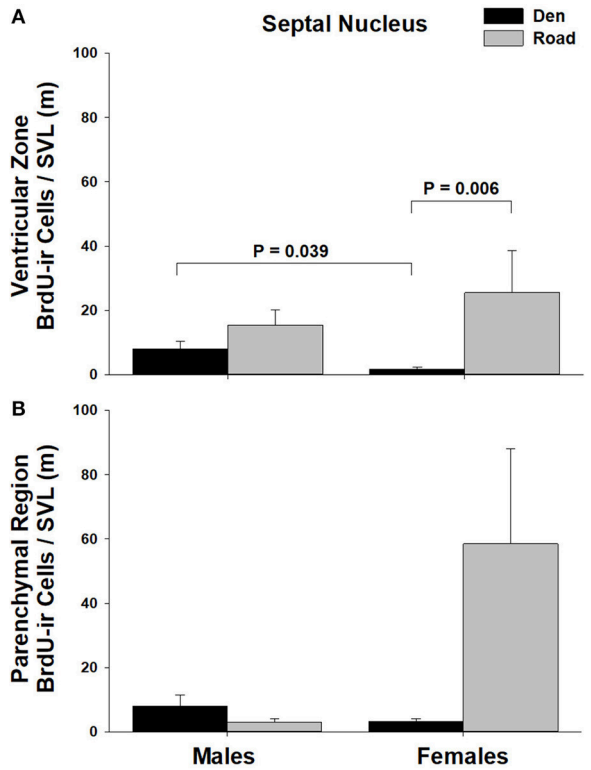

FIGURE 5 | Effects of sex and migratory status on the number of BrdU-immunoreactive (ir) cells in the **(A)** ventricular zone or **(B)** parenchymal region of the septal nucleus (SN) in red-sided garter snakes (*Thamnophis sirtalis parietalis*). We captured snakes from the den prior to migration from the breeding grounds; migratory snakes were intercepted on a road located 1 km from the den along the migratory route. Similar to Lucas et al. (2017), we corrected BrdU-ir cell number for sex differences in body size by dividing the number of labeled cells within each individual by its snout-vent length (SVL). Each bar is the mean number of labeled cells +1 SEM. Statistics are from multiple comparisons tests.

Together, the vomeronasal-NS system mediates reproductive responses of male garter snakes to the female sexual attractiveness pheromone (Mason et al., 1989) and responses of both sexes to food chemical cues. Finally, the medial cortex is a structural and functional homolog of the mammalian hippocampus; the dorsal cortex plays a similar role but to a lesser extent (Butler and Hodos, 2005). We quantified the number of BrdU-labeled cells within each cortical subregion separately to better understand if changes in cell proliferation are associated with the spatial memory required for migration. Our data suggest that sexually dimorphic changes in cell proliferation and cell migration in the adult brain contribute to sex differences in the seasonal life-history transition from reproduction to migration and foraging behavior in red-sided garter snakes.

Sexually Dimorphic Cell Proliferation in the Brain of Breeding Snakes

Even after correcting for sex differences in body length, male snakes collected from the den site had significantly more newly proliferated cells within the ventricular zone of the NS, hypothalamus, SN, and dorsal cortex compared to females. This trend was also present in the medial and lateral portions of the cortex, but these differences were not statistically significant. The observed sex differences were specific to premigratory snakes: after snakes dispersed from the den, migration-related changes in cell proliferation altered the patterns of sex differences. For example, migrating females had significantly more BrdU-labeled cells in the hypothalamus than migrating males (discussed in the next section). We suggest that sex differences in cell proliferation prior to migration are associated with temporal differences in spring emergence and dispersal from the hibernaculum between sexes.

As in most studies of male red-sided garter snakes, it is not possible to determine how much time elapsed between the emergence of each individual male and its collection. In contrast, premigratory females are collected immediately upon or very soon after spring emergence, because they typically disperse from the den within 24 h. Thus, it is extremely likely that the duration of terrestrial activity (and therefore acclimation to environmental cues such as temperature) prior to collection differed between sexes. This difference may be associated with the higher levels of cell proliferation observed within the ventricular zone of males. There is precedence for this hypothesis in previous studies of baseline glucose concentrations and oxygen consumption in red-sided garter snakes (Crews et al., 1987; Maine et al., 2014a). For example, male snakes collected from the den had significantly higher baseline glucose concentrations than females. The authors hypothesized that the sex difference was related to differences in the timing of emergence and the duration of spring activity prior to collection. In male red-sided garter snakes, Maine et al. (2014b) reported that neither cell proliferation nor cell migration into the parenchyma changed over time during the spring mating season. However, changes in cell proliferation during and immediately following spring emergence have not been investigated in either sex. Such studies are necessary to determine if males also exhibit low rates of cell proliferation immediately upon spring emergence, and whether rates of cell proliferation increase during the first several days post-emergence. For example, it is likely that acclimation to spring-like environmental cues and/or increased motor activity resulting directly from spring emergence itself are associated with increases in both metabolic and mitotic processes. Such results would suggest that the observed differences in cell proliferation are a result of, rather than the cause of, sex differences in the timing of spring emergence.

The processes that characterize neurogenesis are subject to hormonal regulation, and therefore the influence of sex steroid hormones (or other sexually dimorphic endocrine factors, including glucocorticoid "stress" hormones) on cell proliferation and migration may contribute to the sex differences reported here (see reviews in Balthazart and Ball, 2016; Dunlap, 2016; Mahmoud et al., 2016; Powers, 2016). For example, treatment of territorial, but not non-territorial male side-blotched lizards (*Uta stansburiana*) with testosterone decreased the volume of the medial cortex and reduced the number of doublecortin-positive cells, an indicator of immature, migrating neurons (LaDage et al., 2017). Pellegrini et al. (2007) showed that radial glial cells in the zebrafish forebrain express aromatase, the enzyme

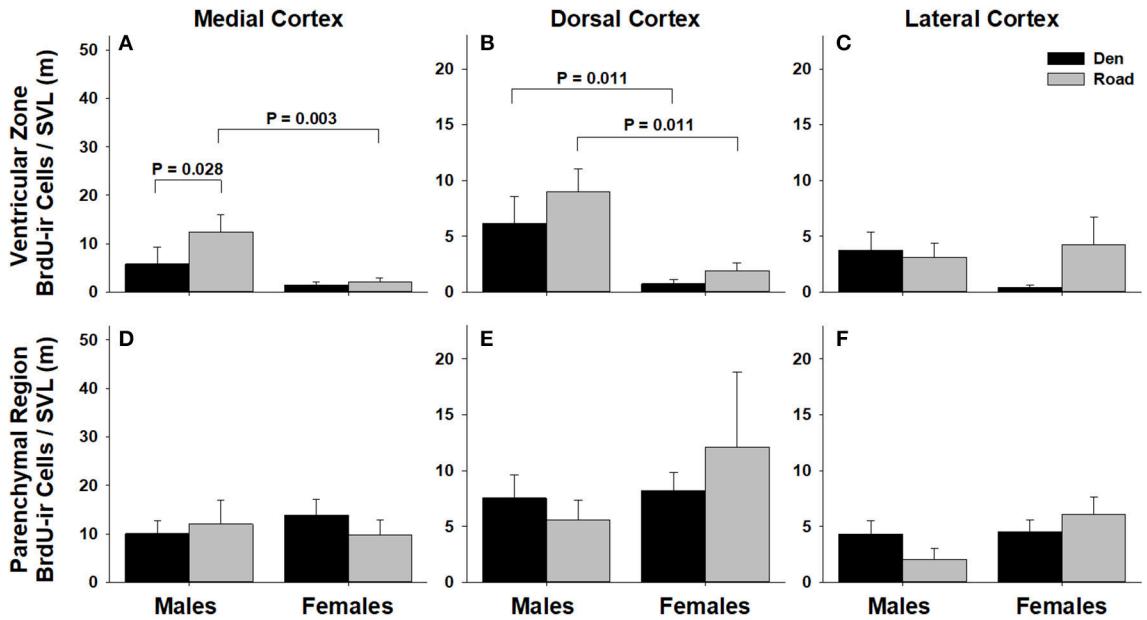

FIGURE 6 | Effects of sex and migratory status on the number of BrdU-immunoreactive (ir) cells in the ventricular zone or parenchymal region of the medial cortex **(A,D)**, dorsal cortex **(B,E)**, and lateral cortex **(C,F)** in red-sided garter snakes (*Thamnophis sirtalis parietalis*). We captured snakes from the den prior to migration from the breeding grounds; migratory snakes were intercepted on a road located 1 km from the den along the migratory route. Similar to Lucas et al. (2017), we corrected BrdU-ir cell number for sex differences in body size by dividing the number of labeled cells within each individual by its snout-vent length (SVL). Each bar is the mean number of labeled cells +1 SEM. Statistics are from multiple comparisons tests.

that synthesizes estrogens from androgens. The mitotic rate of these progenitor cells as well as the migration of their newly-formed daughter cells are, surprisingly, inhibited by treatments that elevate brain estrogen levels (Diotel et al., 2013). Whether aromatase expression in radial glial cells is unique to teleosts or a conserved feature of vertebrates is not yet clear (Coumailleau et al., 2015). Nevertheless, these and other studies demonstrate that sex steroids contribute to both sex and seasonal variation in neurogenesis.

Because red-sided garter snakes exhibit a temporally dissociated reproductive pattern (reviewed in Lutterschmidt, 2012), the observed sex differences in cell proliferation and migration may not be mediated by sex steroids. For example, plasma androgens are low and declining during breeding in male snakes (e.g., Crews et al., 1984; Krohmer et al., 1987; Whittier et al., 1987b; Moore et al., 2001; Lutterschmidt and Mason, 2009), and estradiol concentrations of unmated females are low or undetectable during the mating season (Whittier et al., 1987a; Dayger et al., 2013; Dayger and Lutterschmidt, 2016, 2017). Although females exhibit an estradiol surge post-mating (Whittier et al., 1987a), we did not observe differences in cell proliferation or cell migration between unmated and mated females. It is possible that either the sex differences observed here are independent of gonadal sex steroid hormones, or that the sex differences in seasonal neurogenesis are established during winter dormancy, when plasma sex steroid hormones are elevated in both males and females in response to low temperature dormancy (Lutterschmidt and Mason, 2009). Neither of these hypotheses exclude the possibility that brain-derived neurosteroids mediate sex differences in cell proliferation during winter dormancy and/or spring mating. The timecourse of neurogenic changes during winter dormancy has not yet been characterized in any ectothermic vertebrate (but see Cerri et al., 2009), and such data will be necessary for evaluating these hypotheses.

Sex Differences in Cell Proliferation Related to Snake Migration

After dispersing from the den during the spring mating season, migrating females collected from the road showed a statistically significant increase in cell proliferation within the ventricular zone of the NS, hypothalamus, and SN. In contrast, cell proliferation within these same brain regions did not vary significantly with migratory status in males. These observations support and expand upon the hypothesis described in the previous section: females exhibit low levels of cell proliferation compared to males immediately post-emergence, and cell proliferation increases once females have been terrestrially active for a period of time comparable to that of males. Alternatively, it is possible that sexually dimorphic changes in cell proliferation during migration are associated with concomitant changes in other behaviors, such as reproductive or foraging behaviors. For example, most migrating male snakes continue to court females even as they migrate away from the breeding grounds (Lutterschmidt and Maine, 2014; Lucas et al., 2017), and cell proliferation within the NS of males varied significantly with reproductive status but not migratory status. Similarly, increased cell proliferation within the NS, hypothalamus, and/or SN of

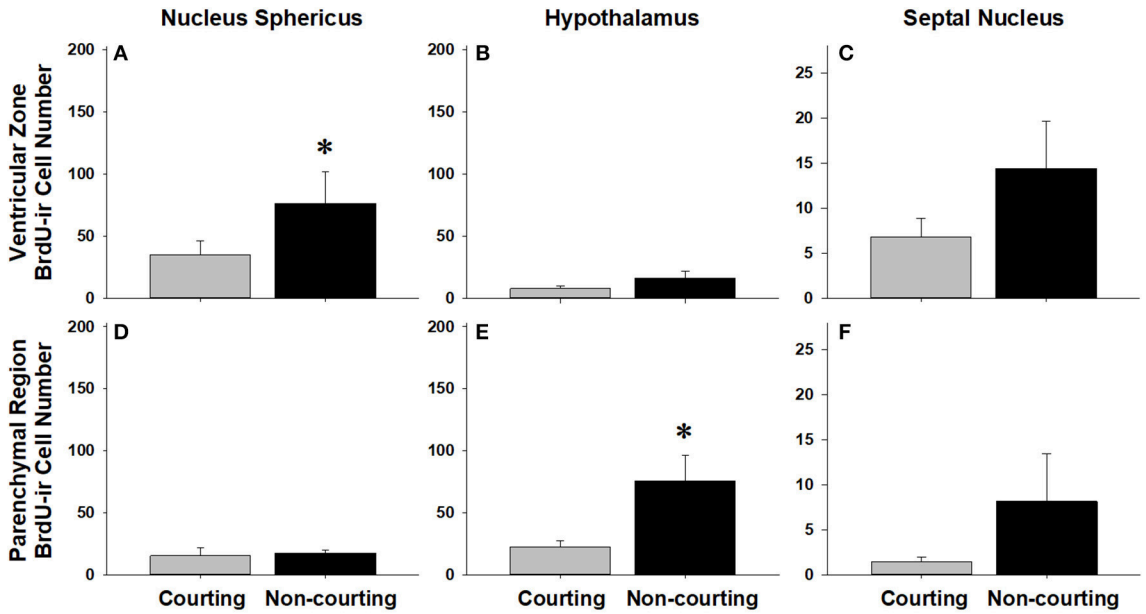

FIGURE 7 | Influence of male reproductive status on the number of BrdU-immunoreactive (ir) cells in the ventricular zone or parenchymal region of the nucleus sphericus **(A,D)**, hypothalamus **(B,E)**, and septal nucleus **(C,F)** in red-sided garter snakes (*Thamnophis sirtalis parietalis*). Both courting and non-courting males were collected from the road after they had dispersed from the den to control for possible differences in migratory status. Each bar is the mean number of labeled cells +1 SEM. Asterisks indicate significant differences in BrdU cell number between courting and non-courting males.

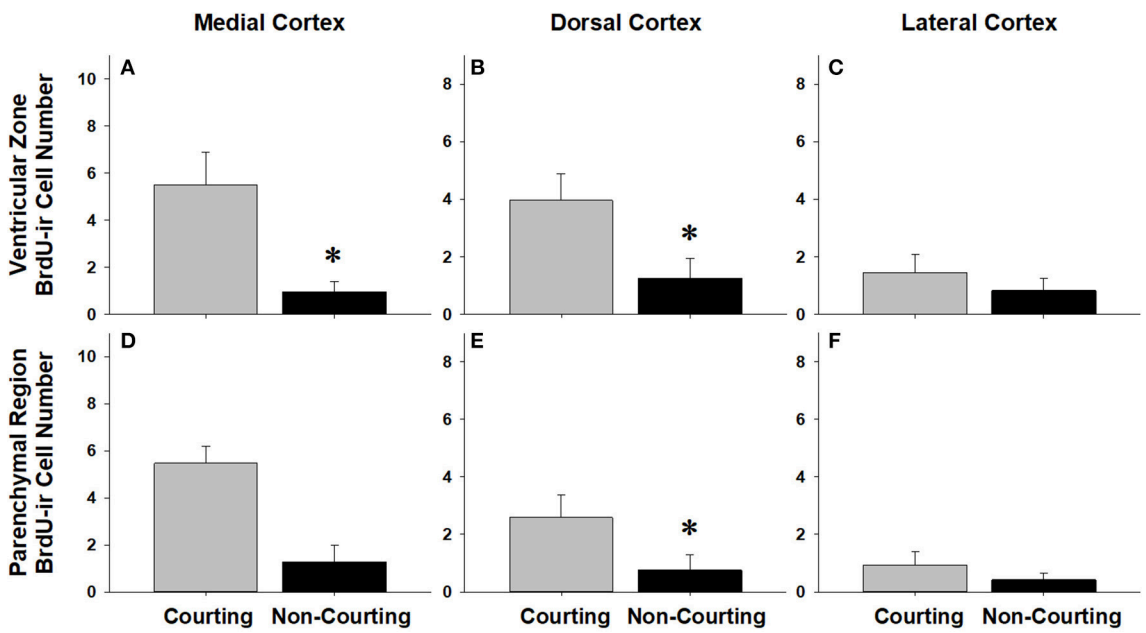

FIGURE 8 | Influence of male reproductive status on the number of BrdU-immunoreactive (ir) cells in the ventricular zone or parenchymal region of the medial cortex **(A,D)**, dorsal cortex **(B,E)**, and lateral cortex **(C,F)** in red-sided garter snakes (*Thamnophis sirtalis parietalis*). Both courting and non-courting males were collected from the road after they had dispersed from the den to control for possible differences in migratory status. Each bar is the mean number of labeled cells +1 SEM. Asterisks indicate significant differences in BrdU cell number between courting and non-courting males.

females after dispersal from the den may be related to the activation of foraging behavior. Preliminary data suggest that a significant proportion of females pursue feeding opportunities and eat soon after emerging from winter dormancy (DIL, unpublished data). This is in stark contrast to males, which will refuse food in lieu of courtship opportunities for up to

several weeks post-emergence (Crews et al., 1987; O'Donnell et al., 2004; Lutterschmidt and Maine, 2014), even as they begin migrating to the feeding grounds (Lucas et al., 2017; DIL, unpublished data). Evaluating which of these hypotheses best explains the sex differences in cell proliferation after dispersal will require a detailed timecourse focused on the later stages of migration in both sexes. It is also possible that sex differences in navigational strategies are associated with different patterns of spatial memory development and spatial learning (e.g., Roth and Krochmal, 2015), which could in turn contribute to the observed sex differences in cell proliferation and cell migration. The navigational mechanisms utilized by red-sided garter snakes during migration to and from the hibernaculum are not yet known.

Surprisingly, there were no migration-related changes in cell proliferation within any subregion of the cortex in females, whereas the only migration-related change in cell proliferation observed in males occurred within the medial cortex. The reptilian medial cortex is a structural and functional homolog of the avian and mammalian hippocampus (Butler and Hodos, 2005), and variation in cortical neurogenesis and/or volume is positively correlated with territory and home range size in reptiles (Roth et al., 2006; LaDage et al., 2009; Powers, 2016). While it is possible that the increase in cell proliferation within the medial cortex of migrating males is related to changing spatial learning and memory demands, it is unlikely that such a change would be sexually dimorphic, as females also migrate similar distances to summer feeding areas. We speculate that the significant increase in cell proliferation within the medial cortex of migrating males is involved in regulating changes in the sensitivity of the hypothalamic-pituitary-adrenal (HPA) axis during the spring. It is well established that male red-sided garter snakes exhibit decreased sensitivity to capture stress during the mating season (e.g., Moore et al., 2000, 2001; Lutterschmidt and Mason, 2005; Cease et al., 2007). Further, breeding males are less sensitive to adrenocorticotrophic hormone (ACTH) challenge compared to both females and fall-collected males (Dayger and Lutterschmidt, 2016). One possible explanation for decreased activity of the HPA axis is a change in its negative feedback regulation by the hippocampus. For example, neuropeptide Y (NPY)-positive cells within the hippocampus have a neuromodulatory influence on the sensitivity of the HPA axis in rats (Thorsell et al., 2000; Heilig and Thorsell, 2002; Morales-Medina et al., 2010; Schneider et al., 2013). Intriguingly, we observed sexually dimorphic changes in NPY-positive cell number in the cortex of the same animals used in this study: non-courting males had significantly more NPY-labeled cells in the cortex compared to courting males, whereas females showed no change in NPY-labeled cell number in relation to either changing migratory or reproductive status (Lucas et al., 2017). It is possible that increased cell proliferation within the medial cortex of migrating males contributes to the seasonal changes in cortical NPY cell number reported in Lucas et al. (2017), and that changing NPY cell number in turn mediates seasonal changes in HPA axis sensitivity and/or activity. Studies using double-labeling techniques to determine the fate of newly proliferated, BrdU-labeled cortical cells are necessary to determine this possibility. It would also be interesting to test if blocking cell proliferation pharmacologically during spring migration alters the sensitivity of the HPA axis.

Regional Variation in Cell Migration Into the Parenchyma

In the adult brain, new cells are born from dividing radial glial cells located within the ependymal layer of the ventricles. These newly-born cells are undifferentiated and can develop into either neurons or glial cells as they migrate to their final destination in the parenchyma. Lopez-Garcia et al. (1990) reported that a minimum of 7 days is required for newly proliferated cells to differentiate into neurons in Iberian wall lizards (*Podarcis hispanica*). We observed BrdU-labeled cells within the parenchymal region 4 days after treatment with BrdU. Because our 4-day timecourse is likely not long enough for new cells to migrate into the parenchyma and/or fully differentiate into mature neurons or glia, it is possible that the presence of BrdU-positive cells within the parenchyma of all brain regions in this study results from the continued division of newly proliferated cells (i.e., transient amplification) (Delgado-Gonzalez et al., 2011). Regardless of the cause, our results indicate significant variation among brain regions in cell migration and/or continued cell division within the parenchyma during the spring mating season.

The only brain region where the number of BrdU-labeled cells within the parenchymal region varied significantly with sex or migratory status was the hypothalamus. Similar to differences in cell proliferation, males had significantly more BrdU-labeled cells in the parenchymal region compared to females prior to migration, but migrating females showed a significant increase in BrdU-labeled cell number within the parenchyma, resulting in a reversal of the sex difference. Our results suggest that cell proliferation and/or cell migration are activated earlier or to a greater extent in the hypothalamus compared to other brain regions. Because the processes of neurogenesis are influenced by environmental temperature (Powers, 2016), it is possible that the differences reported here are established during low-temperature winter dormancy. For example, in the tropical lizard *Tropidurus hispidus*, acclimation to low temperatures decreases cell migration but not cell proliferation (Marchioro et al., 2012). Similar results were reported in Iberian wall lizards (*P. hispanica*) (Ramirez et al., 1997). In red-sided garter snakes, several different neuroendocrine factors and hypothalamic circuits are known to be highly responsive to low temperature winter dormancy (Krohmer and Lutterschmidt, 2011; Lutterschmidt, 2012), and therefore temperature-induced changes in cell proliferation or cell migration within the hypothalamus could explain the differences in BrdU-labeled cell number within the parenchymal region reported here.

Changes in Cell Proliferation Related to Reproductive Status

In females, changes in cell proliferation during dispersal from the breeding grounds were unrelated to changes in reproductive status, as there were no significant differences in cell proliferation or migration between mated and unmated females in any

brain region. In males, changes in cell proliferation and cell migration were observed in response to both dispersal and changing reproductive behavior. We propose that the pattern of these changes in males reflects the timecourse of neurogenesis from spring emergence and the activation of courtship behavior to migration and the cessation of reproductive behavior. For example, non-courting males exhibited more cell proliferation in the NS and more cell migration into the parenchyma of the hypothalamus than courting males. These changes mirror those observed in migrating females, suggesting that males do exhibit a similar increase in cell proliferation and cell migration during dispersal from the den, but only after courtship behavior has waned. This hypothesis may also explain why cell migration within the hypothalamus initially decreases in courting males collected from the road (**Figure 4B**), but subsequently increases as males transition to non-courting status (**Figure 7E**). Similarly, migrating males that still express courtship behavior exhibit a significant increase in cell proliferation within the medial cortex, but as migrating males transition to non-courting reproductive status, there is a subsequent and significant decrease in cell proliferation within the medial and dorsal cortex and a decrease in cell migration within the dorsal cortex (and probably the medial cortex: $P = 0.075$). Collectively, these results suggest that there is a timecourse of changes in cell proliferation and migration in males during the spring mating season, from courting females at the breeding grounds, to simultaneously migrating but continuing to court females if the opportunity arises, and finally to migrating to summer foraging areas as reproductive behavior wanes and feeding behavior is activated.

CONCLUSIONS

In summary, we found that cell proliferation and cell migration in the adult brain of red-sided garter snakes varied significantly with sex, the migratory status of snakes, and reproductive behavior in males. Our data suggest that changes in cell proliferation and cell migration within the adult brain are involved in the seasonal life-history transition from reproduction to migration and foraging behavior in red-sided garter snakes. Moreover, differences in the observed patterns of cell proliferation and cell migration between males and females may contribute to known sex differences in the timing of this life-history transition during the spring mating season. To better understand how the processes of neurogenesis contribute to seasonal changes in physiology and behavior, future research directions should include elucidating the timecourse of neurogenic changes during multiple life-history stages, especially winter dormancy, emergence, and migration. Subsequent studies could then determine if the newly proliferated cells differentiate into primarily neurons or glial cells, as well as the neurochemical phenotype of the surviving, mature cells. Finally, knowing if and how physiology and behavior change when rates of cell proliferation and cell migration are altered pharmacologically will be critical for understanding the functional significance of post-embryonic neurogenesis to seasonal rhythms and, ultimately, reproductive fitness.

AUTHOR CONTRIBUTIONS

DL and AL designed and conducted the experiments. AL performed the immunohistochemistry assay. AL, RK, VN, and MR quantified the immunoreactive cell data. DL and AL analyzed and interpreted the data. DL wrote the paper.

FUNDING

Partial funding for this work was provided by a Forbes-Lea Student Research Grant from the Portland State University Biology Department to AL and a Portland State University Faculty Enhancement Grant and National Science Foundation grant IOS-1355203 to DL. The PSU Upward Bound Program, a federally-funded TRiO program, provided stipend support to VN as a participant in the Summer Research Internship Program for high school students. This article's publication was funded by the Portland State University Open Access Article Processing Charge Fund, administered by the Portland State University Library.

ACKNOWLEDGMENTS

We thank the Manitoba Department of Conservation and Dave Roberts for logistical support in Manitoba, Canada. Catherine Dayger, Christopher Friesen, and Robert Mason provided assistance in the field.

REFERENCES

Akle, V., Stankiewicz, A. J., Kharchenko, V., Yu, L., Kharchenko, P. V., and Zhdanova, I. V. (2017). Circadian kinetics of cell cycle progression in adult neurogenic niches of a diurnal vertebrate. *J. Neurosci.* 37, 1900–1909. doi: 10.1523/JNEUROSCI.3222-16.2017

Almli, L. M., and Wilczynski, W. (2007). Regional distribution and migration of proliferating cell populations in the adult brain of *Hyla cinerea* (Anura, Amphibia). *Brain Res.* 1159, 112–118. doi: 10.1016/j.brainres.2007.05.020

Almli, L. M., and Wilczynski, W. (2009). Sex-specific modulation of cell proliferation by socially relevant stimuli in the adult green treefrog brain (*Hyla cinerea*). *Brain Behav. Evol.* 74, 143–154. doi: 10.1159/000235963

Alonso, M., Lepousez, G., Wagner, S., Bardy, C., Gabellec, M.-M., Torquet, N., et al. (2012). Activation of adult-born neurons facilitates learning and memory. *Nat. Neurosci.* 15, 897–904. doi: 10.1038/nn.3108

Amrein, I., and Lipp, H. P. (2009). Adult hippocampal neurogenesis of mammals: evolution and life history. *Biol. Lett.* 5, 141–144. doi: 10.1098/rsbl.2008.0511

Ball, G. F., and Ketterson, E. D. (2008). Sex differences in the response to environmental cues regulating seasonal reproduction in birds. *Philos. Trans. R. Soc. Lond. B. Biol. Sci.* 363, 231–246. doi: 10.1098/rstb.2007.2137

Balthazart, J., and Ball, G. F. (2016). Endocrine and social regulation of adult neurogenesis in songbirds. *Front. Neuroendocrinol.* 41, 3–22. doi: 10.1016/j.yfrne.2016.03.003

Barkan, S., Yom-Tov, Y., and Barnea, A. (2014). A possible relation between new neuronal recruitment and migratory behavior in *Acrocephalus warblers*. *Dev. Neurobiol.* 74, 1194–1209. doi: 10.1002/dneu.22198

Barnea, A., and Pravosudov, V. (2011). Birds as a model to study adult neurogenesis: bridging evolutionary, comparative and neuroethological approaches. *Eur. J. Neurosci.* 34, 884–907. doi: 10.1111/j.1460-9568.2011.07851.x

Bergami, M., Masserdotti, G., Temprana, S. G., Motori, E., Eriksson, T. M., Göbel, J., et al. (2015). A critical period for experience-dependent remodeling of adult-born neuron connectivity. *Neuron* 85, 710–717. doi: 10.1016/j.neuron.2015.01.001

Brenowitz, E. A. (2015). Transsynaptic trophic effects of steroid hormones in an avian model of adult brain plasticity. *Front. Neuroendocrinol.* 37, 119–128. doi: 10.1016/j.yfrne.2014.09.003

Butler, A., and Hodos, W. (2005). *Comparative Vertebrate Neuroanatomy: Evolution and Adaptation*. New York, NY: Wiley-Liss.

Cease, A. J., Lutterschmidt, D. I., and Mason, R. T. (2007). Corticosterone and the transition from courtship behavior to dispersal in male red-sided garter snakes (*Thamnophis sirtalis parietalis*). *Gen. Comp. Endocrinol.* 150, 124–131. doi: 10.1016/j.ygcen.2006.07.022

Cerri, S., Bottiroli, G., Bottone, M. G., Barni, S., and Bernocchi, G. (2009). Cell proliferation and death in the brain of active and hibernating frogs. *J. Anat.* 215, 124–131. doi: 10.1111/j.1469-7580.2009.01101.x

Conant, R., and Collins, J. T. (1998). *Peterson Field Guide to Reptiles and Amphibians: Eastern and Central North America*. New York, NY: Houghton Mifflin.

Coumailleau, P., Pellegrini, E., Adrio, F., Diotel, N., Cano-Nicolau, J., Nasri, A., et al. (2015). Aromatase, estrogen receptors and brain development in fish and amphibians. *Biochim. Biophys. Acta* 1849, 152–162. doi: 10.1016/j.bbagrm.2014.07.002

Crews, D. (1984). Gamete production, sex hormone secretion, and mating behavior uncoupled. *Horm. Behav.* 18, 22–28. doi: 10.1016/0018-506X(84)90047-3

Crews, D., Camazine, B., Diamond, M., Mason, R., Tokarz, R. R., and Garstka, W. R. (1984). Hormonal independence of courtship behavior in the male garter snake. *Horm. Behav.* 18, 29–41. doi: 10.1016/0018-506X(84)90048-5

Crews, D., Diamond, M. A., Whittier, J., and Mason, R. (1985). Small male body size in garter snake depends on testes. *Am. J. Physiol.* 249, R62–R66. doi: 10.1152/ajpregu.1985.249.1.R62

Crews, D., Grassman, M., Garstka, W. R., Halpert, A., and Camazine, B. (1987). Sex and seasonal differences in metabolism in the red-sided garter snake, *Thamnophis sirtalis parietalis*. *Can. J. Zool.* 65, 2362–2368. doi: 10.1139/z87-357

Darcy, M. J., Trouche, S., Jin, S. X., and Feig, L. A. (2014). Ras-GRF2 mediates long-term potentiation, survival, and response to an enriched environment of newborn neurons in the hippocampus. *Hippocampus* 24, 1317–1329. doi: 10.1002/hipo.22313

Dawley, E. M., Nelsen, M., Lopata, A., Schwartz, J., and Bierly, A. (2006). Cell birth and survival following seasonal periods of cell proliferation in the chemosensory epithelia of red-backed salamanders, *Plethodon cinereus*. *Brain Behav. Evol.* 68, 26–36. doi: 10.1159/000092311

Dayger, C. A., Cease, A. J., and Lutterschmidt, D. I. (2013). Responses to capture stress and exogenous corticosterone vary with body condition in female red-sided garter snakes (*Thamnophis sirtalis parietalis*). *Horm. Behav.* 64, 748–754. doi: 10.1016/j.yhbeh.2013.09.003

Dayger, C. A., and Lutterschmidt, D. I. (2016). Seasonal and sex differences in responsiveness to adrenocorticotropic hormone contribute to stress response plasticity in red-sided garter snakes (*Thamnophis sirtalis parietalis*). *J. Exp. Biol.* 219, 1022–1030. doi: 10.1242/jeb.130450

Dayger, C. A., and Lutterschmidt, D. I. (2017). Patterns of stress responses shift during seasonal life-history transitions: an analysis comparing baseline, maximal and integrated corticosterone in female red-sided garter snakes (*Thamnophis sirtalis parietalis*). *Gen. Comp. Endocrinol.* 246, 29–36. doi: 10.1016/j.ygcen.2017.03.008

Delgado-Gonzalez, F. J., Gonzalez-Granero, S., Trujillo-Trujillo, C. M., García-Verdugo, J. M., and Damas-Hernandez, M. C. (2011). Study of adult neurogenesis in the *Gallotia galloti* lizard during different seasons. *Brain Res.* 1390, 50–58. doi: 10.1016/j.brainres.2011.03.027

Diotel, N., Vaillant, C., Gabbero, C., Mironov, S., Fostier, A., Gueguen, M. M., et al. (2013). Effects of estradiol in adult neurogenesis and brain repair in zebrafish. *Horm. Behav.* 63, 193–207. doi: 10.1016/j.yhbeh.2012.04.003

Duarte-Guterman, P., Yagi, S., Chow, C., and Galea, L. A. (2015). Hippocampal learning, memory, and neurogenesis: effects of sex and estrogens across the lifespan in adults. *Horm. Behav.* 74, 37–52. doi: 10.1016/j.yhbeh.2015.05.024

Dunlap, K. D. (2016). Fish neurogenesis in context: assessing environmental influences on brain plasticity within a highly labile physiology and morphology. *Brain Behav. Evol.* 87, 156–166. doi: 10.1159/000446907

Dupret, D., Fabre, A., Döbrössy, M. D., Panatier, A., Rodríguez, J. J., Lamarque, S., et al. (2007). Spatial learning depends on both the addition and removal of new hippocampal neurons. *PLoS Biol.* 5:e214. doi: 10.1371/journal.pbio.0050214

Ebling, F. J. (2015). Hypothalamic control of seasonal changes in food intake and body weight. *Front. Neuroendocrinol.* 37, 97–107. doi: 10.1016/j.yfrne.2014.10.003

Farioli-Vecchioli, S., Saraulli, D., Costanzi, M., Pacioni, S., Cinà, I., Aceti, M., et al. (2008). The timing of differentiation of adult hippocampal neurons is crucial for spatial memory. *PLoS Biol.* 6:e246. doi: 10.1371/journal.pbio.0060246

Font, E., Barbosa, D., Sampedro, C., and Carazo, P. (2012). Social behavior, chemical communication, and adult neurogenesis: studies of scent mark function in Podarcis wall lizards. *Gen. Comp. Endocrinol.* 177, 9–17. doi: 10.1016/j.ygcen.2012.02.015

Frick, K. M., Kim, J., Tuscher, J. J., and Fortress, A. M. (2015). Sex steroid hormones matter for learning and memory: estrogenic regulation of hippocampal function in male and female rodents. *Learn. Mem.* 22, 472–493. doi: 10.1101/lm.037267.114

Goergen, E. M., Bagay, L. A., Rehm, K., Benton, J. L., and Beltz, B. S. (2002). Circadian control of neurogenesis. *J. Neurobiol.* 53, 90–95. doi: 10.1002/neu.10095

Gregory, P. T., and Stewart, K. W. (1975). Long-distance dispersal and feeding strategy of red-sided garter snake (*Thamnophis sirtalis parietalis*) in Interlake of Manitoba. *Can. J. Zool.* 53, 238–245. doi: 10.1139/z75-030

Hall, Z. J., Delaney, S., and Sherry, D. F. (2014). Inhibition of cell proliferation in black-capped chickadees suggests a role for neurogenesis in spatial learning. *Dev. Neurobiol.* 74, 1002–1010. doi: 10.1002/dneu.22180

Halpern, M., Morrell, J. I., and Pfaff, D. W. (1982). Cellular [3H]estradiol and [3H]testosterone localization in the brains of garter snakes: an autoradiographic study. *Gen. Comp. Endocrinol.* 46, 211–224. doi: 10.1016/0016-6480(82)90203-9

Hansen, A., and Schmidt, M. (2004). Influence of season and environment on adult neurogenesis in the central olfactory pathway of the shore crab, *Carcinus maenas*. *Brain Res.* 1025, 85–97. doi: 10.1016/j.brainres.2004.08.001

Heberden, C. (2017). Sex steroids and neurogenesis. *Biochem. Pharmacol.* 141, 56–62. doi: 10.1016/j.bcp.2017.05.019

Heilig, M., and Thorsell, A. (2002). Brain neuropeptide Y (NPY) in stress and alcohol dependence. *Rev. Neurosci.* 13, 85–94. doi: 10.1515/REVNEURO.2002.13.1.85

Holding, M. L., Frazier, J. A., Taylor, E. N., and Strand, C. R. (2012). Experimentally altered navigational demands induce changes in the cortical forebrain of free-ranging northern pacific rattlesnakes (*Crotalus o. oreganus*). *Brain Behav. Evol.* 79, 144–154. doi: 10.1159/000335034

Holmes, M. M. (2016). Social regulation of adult neurogenesis: a comparative approach. *Front. Neuroendocrinol.* 41, 59–70. doi: 10.1016/j.yfrne.2016.02.001

Hoshooley, J. S., Phillmore, L. S., Sherry, D. F., and MacDougall-Shackleton, S. A. (2007). Annual cycle of the black-capped chickadee: seasonality of food-storing and the hippocampus. *Brain Behav. Evol.* 69, 161–168. doi: 10.1159/000096984

Hoshooley, J. S., and Sherry, D. F. (2007). Greater hippocampal neuronal recruitment in food-storing than in non-food-storing birds. *Dev. Neurobiol.* 67, 406–414. doi: 10.1002/dneu.20316

Iscru, E., Ahmed, T., Coremans, V., Bozzi, Y., Caleo, M., Conway, E. M., et al. (2013). Loss of survivin in neural precursor cells results in impaired long-term potentiation in the dentate gyrus and CA1-region. *Neuroscience* 231, 413–419. doi: 10.1016/j.neuroscience.2012.10.049

Joy, J. E., and Crews, D. (1985). Social dynamics of group courtship behavior in male red-sided garter snakes (*Thamnophis sirtalis parietalis*). *J. Comp. Psychol.* 99, 145–149. doi: 10.1037/0735-7036.99.2.145

Kaslin, J., Ganz, J., and Brand, M. (2008). Proliferation, neurogenesis and regeneration in the non-mammalian vertebrate brain. *Philos. Trans. R. Soc. Lond. B. Biol. Sci.* 363, 101–122. doi: 10.1098/rstb.2006.2015

Krohmer, R. W., Boyle, M. H., Lutterschmidt, D. I., and Mason, R. T. (2010). Seasonal aromatase activity in the brain of the male red-sided garter snake. *Horm. Behav.* 58, 485–492. doi: 10.1016/j.yhbeh.2010.04.011

Krohmer, R. W., and Crews, D. (1987a). Facilitation of courtship behavior in the male red-sided garter snake (*Thamnophis sirtalis parietalis*) following lesions of the septum or nucleus sphericus. *Physiol. Behav.* 40, 759–765. doi: 10.1016/0031-9384(87)90280-0

Krohmer, R. W., and Crews, D. (1987b). Temperature activation of courtship behavior in the male red-sided garter snake (*Thamnophis sirtalis parietalis*): role of the anterior hypothalamus-preoptic area. *Behav. Neurosci.* 101, 228–236. doi: 10.1037/0735-7044.101.2.228

Krohmer, R. W., Grassman, M., and Crews, D. (1987). Annual reproductive-cycle in the male red-sided garter snake, *Thamnophis sirtalis parietalis* - Field and laboratory studies. *Gen. Comp. Endocrinol.* 68, 64–75. doi: 10.1016/0016-6480(87)90061-X

Krohmer, R. W., and Lutterschmidt, D. I. (2011). "Environmental and neuroendocrine control of reproduction in snakes," in *Reproductive Biology and Phylogeny, Vol. 9, Reproductive Biology and Phylogeny of Snakes (R.D. Aldridge and D.M. Sever, Volume Editors)*, ed B. G. M. Jamieson (Boca Raton, FL: CRC Press), 289–346.

Laberge, F., Feldhoff, R. C., Feldhoff, P. W., and Houck, L. D. (2008). Courtship pheromone-induced c-Fos-like immunolabeling in the female salamander brain. *Neuroscience* 151, 329–339. doi: 10.1016/j.neuroscience.2007.11.006

LaDage, L. D., Maged, R. M., Forney, M. V., Roth, T. C., Sinervo, B., and Pravosudov, V. V. (2013). Interaction between territoriality, spatial environment, and hippocampal neurogenesis in male side-blotched lizards. *Behav. Neurosci.* 127, 555–565. doi: 10.1037/a0032852

LaDage, L. D., Riggs, B. J., Sinervo, B., and Pravosudov, V. V. (2009). Dorsal cortex volume in male side-blotched lizards (*Uta stansburiana*) is associated with different space use strategies. *Anim. Behav.* 78, 91–96. doi: 10.1016/j.anbehav.2009.03.020

LaDage, L. D., Roth, T. C., Downs, C. J., Sinervo, B., and Pravosudov, V. V. (2017). Increased testosterone decreases medial cortical volume and neurogenesis in territorial side-blotched lizards (*Uta stansburiana*). *Front. Neurosci.* 11:97. doi: 10.3389/fnins.2017.00097

LaDage, L. D., Roth, T. C. II., and Pravosudov, V. V. (2011). Hippocampal neurogenesis is associated with migratory behaviour in adult but not juvenile sparrows (*Zonotrichia leucophrys* ssp.). *Proc. Biol. Sci.* 278, 138–143. doi: 10.1098/rspb.2010.0861

Lanuza, E., and Halpern, M. (1997). Afferent and efferent connections of the nucleus sphericus in the snake *Thamnophis sirtalis*: convergence of olfactory and vomeronasal information in the lateral cortex and the amygdala. *J. Comp. Neurol.* 385, 627–640. doi: 10.1002/(SICI)1096-9861(19970908)385:4<627::AID-CNE8>3.0.CO;2-5

Lanuza, E., and Halpern, M. (1998). Efferents and centrifugal afferents of the main and accessory olfactory bulbs in the snake *Thamnophis sirtalis*. *Brain Behav. Evol.* 51, 1–22. doi: 10.1159/000006525

Lieberwirth, C., Pan, Y., Liu, Y., Zhang, Z., and Wang, Z. (2016). Hippocampal adult neurogenesis: its regulation and potential role in spatial learning and memory. *Brain Res.* 1644, 127–140. doi: 10.1016/j.brainres.2016.05.015

Lindsey, B. W., and Tropepe, V. (2006). A comparative framework for understanding the biological principles of adult neurogenesis. *Prog. Neurobiol.* 80, 281–307. doi: 10.1016/j.pneurobio.2006.11.007

Lopez-Garcia, C., Molowny, A., Garcia-Verdugo, J. M., Martinez-Guijarro, F. J., and Bernabeu, A. (1990). Late generated neurons in the medial cortex of adult lizards send axons that reach the Timm-reactive zones. *Brain Res. Dev. Brain Res.* 57, 249–254. doi: 10.1016/0165-3806(90)90050-9

Lucas, A. R., Richards, D. Y., Ramirez, L. M., and Lutterschmidt, D. I. (2017). Arginine vasotocin and neuropeptide Y vary with seasonal life-history transitions in garter snakes. *Integr. Comp. Biol.* 57, 1166–1183. doi: 10.1093/icb/icx107

Lutterschmidt, D. I. (2012). Chronobiology of reproduction in garter snakes: neuroendocrine mechanisms and geographic variation. *Gen. Comp. Endocrinol.* 176, 448–455. doi: 10.1016/j.ygcen.2011.12.015

Lutterschmidt, D. I., Lemaster, M. P., and Mason, R. T. (2004). Effects of melatonin on the behavioral and hormonal responses of red-sided garter snakes (*Thamnophis sirtalis parietalis*) to exogenous corticosterone. *Horm. Behav.* 46, 692–702. doi: 10.1016/j.yhbeh.2004.06.013

Lutterschmidt, D. I., and Maine, A. R. (2014). Sex or candy? Neuroendocrine regulation of the seasonal transition from courtship to feeding behavior in male red-sided garter snakes (*Thamnophis sirtalis parietalis*). *Horm. Behav.* 66, 120–134. doi: 10.1016/j.yhbeh.2014.01.011

Lutterschmidt, D. I., and Mason, R. T. (2005). A serotonin receptor antagonist, but not melatonin, modulates hormonal responses to capture stress in two populations of garter snakes (*Thamnophis sirtalis parietalis* and *Thamnophis sirtalis concinnus*). *Gen. Comp. Endocrinol.* 141, 259–270. doi: 10.1016/j.ygcen.2005.01.012

Lutterschmidt, D. I., and Mason, R. T. (2009). Endocrine mechanisms mediating temperature-induced reproductive behavior in red-sided garter snakes (*Thamnophis sirtalis parietalis*). *J. Exp. Biol.* 212, 3108–3118. doi: 10.1242/jeb.033100

Lutterschmidt, D. I., and Wilczynski, W. (2012). Sexually dimorphic effects of melatonin on brain arginine vasotocin immunoreactivity in green treefrogs (*Hyla cinerea*). *Brain Behav. Evol.* 80, 222–232. doi: 10.1159/000341238

Mahmoud, R., Wainwright, S. R., and Galea, L. A. (2016). Sex hormones and adult hippocampal neurogenesis: regulation, implications, and potential mechanisms. *Front. Neuroendocrinol.* 41, 129–152. doi: 10.1016/j.yfrne.2016.03.002

Maine, A. R., Dayger, C. A., Richards, D. Y., Ramirez, L. M., and Lutterschmidt, D. I. (2014a). "Migration to summer feeding grounds is associated with changes in plasma glucocorticoids and glucose in red-sided garter snakes (*Thamnophis sirtalis*)," *Presented at The Society for Integrative Comparative Biology Annual Meeting 2014* (Austin, TX).

Maine, A. R., Powers, S. D., and Lutterschmidt, D. I. (2014b). Seasonal variation in cell proliferation and cell migration in the brain of adult red-sided garter snakes (*Thamnophis sirtalis parietalis*). *Brain Behav. Evol.* 84, 181–196. doi: 10.1159/000364778

Marchioro, M., Pimentel Hde, C., Santos, M. L., Lima, M. M., Dos Santos, J. R., Martí, X. P., et al. (2012). Low temperature-acclimation impairs cellular migration in the adult cerebral cortex of the tropical lizard, *Tropidurus hispidus* (Spix, 1825) (Squamata: Tropiduridae). *Arch. Ital. Biol.* 150, 22–30. doi: 10.4449/aib.v149i5.1381

Martínez-Marcos, A., Ubeda-Bañón, I., and Halpern, M. (2001). Neural substrates for tongue-flicking behavior in snakes. *J. Comp. Neurol.* 432, 75–87. doi: 10.1002/cne.1089

Martinez-Marcos, A., Ubeda-Bañon, I., Lanuza, E., and Halpern, M. (2005). Efferent connections of the "olfactostriatum": a specialized vomeronasal structure within the basal ganglia of snakes. *J. Chem. Neuroanat.* 29, 217–226. doi: 10.1016/j.jchemneu.2005.02.001

Mason, R. T., Fales, H. M., Jones, T. H., Pannell, L. K., Chinn, J. W., and Crews, D. (1989). Sex pheromones in snakes. *Science* 245, 290–293. doi: 10.1126/science.2749261

Meshi, D., Drew, M. R., Saxe, M., Ansorge, M. S., David, D., Santarelli, L., et al. (2006). Hippocampal neurogenesis is not required for behavioral effects of environmental enrichment. *Nat. Neurosci.* 9, 729–731. doi: 10.1038/nn1696

Migaud, M., Butruille, L., Duittoz, A., Pillon, D., and Batailler, M. (2016). Adult neurogenesis and reproductive functions in mammals. *Theriogenology* 86, 313–323. doi: 10.1016/j.theriogenology.2016.04.044

Moore, I. T., Greene, M. J., and Mason, R. T. (2001). Environmental and seasonal adaptations of the adrenocortical and gonadal responses to capture stress in two populations of the male garter snake, *Thamnophis sirtalis*. *J. Exp. Zool.* 289, 99–108. doi: 10.1002/1097-010X(20010201)289:2<99::AID-JEZ3>3.0.CO;2-Z

Moore, I. T., Lemaster, M. P., and Mason, R. T. (2000). Behavioural and hormonal responses to capture stress in the male red-sided garter snake, *Thamnophis sirtalis parietalis*. *Anim. Behav.* 59, 529–534. doi: 10.1006/anbe.1999.1344

Moore, I. T., and Mason, R. T. (2001). Behavioral and hormonal responses to corticosterone in the male red-sided garter snake, *Thamnophis sirtalis parietalis*. *Physiol. Behav.* 72, 669–674. doi: 10.1016/S0031-9384(01)00413-9

Morales-Medina, J. C., Dumont, Y., and Quirion, R. (2010). A possible role of neuropeptide Y in depression and stress. *Brain Res.* 1314, 194–205. doi: 10.1016/j.brainres.2009.09.077

Nilsson, M., Perfilieva, E., Johansson, U., Orwar, O., and Eriksson, P. S. (1999). Enriched environment increases neurogenesis in the adult rat dentate gyrus and improves spatial memory. *J. Neurobiol.* 39, 569–578. doi: 10.1002/(SICI)1097-4695(19990615)39:4<569::AID-NEU10>3.0.CO;2-F

O'Donnell, R. P., Shine, R., and Mason, R. T. (2004). Seasonal anorexia in the male red-sided garter snake, *Thamnophis sirtalis parietalis*. *Behav. Ecol. Sociobiol.* 56, 413–419. doi: 10.1007/s00265-004-0801-x

Patten, A. R., Sickmann, H., Hryciw, B. N., Kucharsky, T., Parton, R., Kernick, A., et al. (2013). Long-term exercise is needed to enhance synaptic plasticity in the hippocampus. *Learn. Mem.* 20, 642–647. doi: 10.1101/lm.030635.113

Pellegrini, E., Mouriec, K., Anglade, I., Menuet, A., Le Page, Y., Gueguen, M. M., et al. (2007). Identification of aromatase-positive radial glial cells as progenitor cells in the ventricular layer of the forebrain in zebrafish. *J. Comp. Neurol.* 501, 150–167. doi: 10.1002/cne.21222

Powers, A. S. (2016). Plasticity and adult neurogenesis in amphibians and reptiles: more questions than answers. *Brain Behav. Evol.* 87, 175–183. doi: 10.1159/000447047

Ramirez, C., Nacher, J., Molowny, A., Sanchez-Sanchez, F., Irurzun, A., and Lopez-Garcia, C. (1997). Photoperiod-temperature and neuroblast proliferation-migration in the adult lizard cortex. *Neuroreport* 8, 2337–2342. doi: 10.1097/00001756-199707070-00047

Roth, E. D., Lutterschmidt, W. I., and Wilson, D. A. (2006). Relative medial and dorsal cortex volume in relation to sex differences in spatial ecology of a snake population. *Brain Behav. Evol.* 67, 103–110. doi: 10.1159/000089183

Roth, T. C., and Krochmal, A. R. (2015). The role of age-specific learning and experience for turtles navigating a changing landscape. *Curr. Biol.* 25, 333–337. doi: 10.1016/j.cub.2014.11.048

Sahay, A., Scobie, K. N., Hill, A. S., O'carroll, C. M., Kheirbek, M. A., Burghardt, N. S., et al. (2011). Increasing adult hippocampal neurogenesis is sufficient to improve pattern separation. *Nature* 472, 466–470. doi: 10.1038/nature 09817

Sakalem, M. E., Seidenbecher, T., Zhang, M., Saffari, R., Kravchenko, M., Wordemann, S., et al. (2017). Environmental enrichment and physical exercise revert behavioral and electrophysiological impairments caused by reduced adult neurogenesis. *Hippocampus* 27, 36–51. doi: 10.1002/hipo.22669

Schmidt, M. (2007). The olfactory pathway of decapod crustaceans–an invertebrate model for life-long neurogenesis. *Chem. Senses* 32, 365–384. doi: 10.1093/chemse/bjm008

Schneider, J. E., Wise, J. D., Benton, N. A., Brozek, J. M., and Keen-Rhinehart, E. (2013). When do we eat? Ingestive behavior, survival, and reproductive success. *Horm. Behav.* 64, 702–728. doi: 10.1016/j.yhbeh.2013.07.005

Sherry, D. F., and Hoshooley, J. S. (2010). Seasonal hippocampal plasticity in food-storing birds. *Philos. Trans. R. Soc. Lond. B. Biol. Sci.* 365, 933–943. doi: 10.1098/rstb.2009.0220

Sherry, D. F., and MacDougall-Shackleton, S. A. (2015). Seasonal change in the avian hippocampus. *Front. Neuroendocrinol.* 37, 158–167. doi: 10.1016/j.yfrne.2014.11.008

Shine, R., Elphick, M. J., Harlow, P. S., Moore, I. T., Lemaster, M. P., and Mason, R. T. (2001). Movements, mating, and dispersal of red-sided gartersnakes (*Thamnophis sirtalis parietalis*) from a communal den in Manitoba. *Copeia* 2001, 82–91. doi: 10.1643/0045-8511(2001)001[0082:MMADOR]2.0.CO;2

Shine, R., Langkilde, T., Wall, M., and Mason, R. T. (2006). Temporal dynamics of emergence and dispersal of garter snakes from a communal den in Manitoba. *Wildlife Res.* 33, 103–111. doi: 10.1071/WR05030

Singer, B. H., Gamelli, A. E., Fuller, C. L., Temme, S. J., Parent, J. M., and Murphy, G. G. (2011). Compensatory network changes in the dentate gyrus restore long-term potentiation following ablation of neurogenesis in young-adult mice. *Proc. Natl. Acad. Sci. U.S.A.* 108, 5437–5442. doi: 10.1073/pnas.1015425108

Smarr, B. L., Jennings, K. J., Driscoll, J. R., and Kriegsfeld, L. J. (2014). A time to remember: the role of circadian clocks in learning and memory. *Behav. Neurosci.* 128, 283–303. doi: 10.1037/a0035963

Spritzer, M. D., Panning, A. W., Engelman, S. M., Prince, W. T., Casler, A. E., Georgakas, J. E., et al. (2017). Seasonal and sex differences in cell proliferation, neurogenesis, and cell death within the dentate gyrus of adult wild-caught meadow voles. *Neuroscience* 360, 155–165. doi: 10.1016/j.neuroscience.2017.07.046

Temprana, S. G., Mongiat, L. A., Yang, S. M., Trinchero, M. F., Alvarez, D. D., Kropff, E., et al. (2015). Delayed coupling to feedback inhibition during a critical period for the integration of adult-born granule cells. *Neuron* 85, 116–130. doi: 10.1016/j.neuron.2014.11.023

Thorsell, A., Michalkiewicz, M., Dumont, Y., Quirion, R., Caberlotto, L., Rimondini, R., et al. (2000). Behavioral insensitivity to restraint stress, absent fear suppression of behavior and impaired spatial learning in transgenic rats with hippocampal neuropeptide Y overexpression. *Proc. Natl. Acad. Sci. U.S.A.* 97, 12852–12857. doi: 10.1073/pnas.220232997

Ubeda-Bañon, I., Pro-Sistiaga, P., Mohedano-Moriano, A., Saiz-Sanchez, D., De La Rosa-Prieto, C., Gutierrez-Castellanos, N., et al. (2011). Cladistic analysis of olfactory and vomeronasal systems. *Front. Neuroanat.* 5:3. doi: 10.3389/fnana.2011.00003

Vidal Pizarro, I., Swain, G. P., and Selzer, M. E. (2004). Cell proliferation in the lamprey central nervous system. *J. Comp. Neurol.* 469, 298–310. doi: 10.1002/cne.11013

Wang, R. T., and Halpern, M. (1988). Neurogenesis in the vomeronasal epithelium of adult garter snakes: 3. use of H3-thymidine autoradiography to trace the genesis and migration of bipolar neurons. *Am. J. Anat.* 183, 178–185. doi: 10.1002/aja.1001830208

Whittier, J. M., Mason, R. T., and Crews, D. (1987a). Plasma steroid-hormone levels of female red-sided garter snakes, *Thamnophis sirtalis parietalis* - Relationship to mating and gestation. *Gen. Comp. Endocrinol.* 67, 33–43. doi: 10.1016/0016-6480(87)90202-4

Whittier, J. M., Mason, R. T., Crews, D., and Licht, P. (1987b). Role of light and temperature in the regulation of reproduction in the red-sided garter snake, *Thamnophis sirtalis parietalis*. *Can. J. Zool.* 65, 2090–2096. doi: 10.1139/z87-320

Yang, C., Wang, L., Xing, X., Gao, Y., and Guo, L. (2017). Seasonal variation in telencephalon cell proliferation in adult female tsinling dwarf skinks (*Scincella tsinlingensis*). *Brain Res.* 1662, 7–15. doi: 10.1016/j.brainres.2017.02.015

Conflict of Interest Statement: The authors declare that the research was conducted in the absence of any commercial or financial relationships that could be construed as a potential conflict of interest.

frontiers in Neuroscience

PERSPECTIVE
published: 08 September 2017
doi: 10.3389/fnins.2017.00505

Solving the Neurogenesis Puzzle: Looking for Pieces Outside the Traditional Box

Mariela Faykoo-Martinez[1], *Ilapreet Toor*[2] *and Melissa M. Holmes*[1, 2, 3]*

[1] Department of Cell and Systems Biology, University of Toronto, Toronto, ON, Canada, [2] Department of Ecology and Evolutionary Biology, University of Toronto, Toronto, ON, Canada, [3] Department of Psychology, University of Toronto Mississauga, Mississauga, ON, Canada

The vast majority of what is considered fact about adult neurogenesis comes from research on laboratory mice and rats: where it happens, how it works, what it does. However, this relative exclusive focus on two rodent species has resulted in a bias on how we think about adult neurogenesis. While it might not *prevent* us from making conclusions about the evolutionary significance of the process or even prevent us from generalizing to diverse mammals, it certainly does not help us achieve these outcomes. Here, we argue that there is every reason to expect striking species differences in adult neurogenesis: where it happens, how it works, what it does. Species-specific adaptations in brain and behavior are paramount to survival and reproduction in diverse ecological niches and it is naive to think adult neurogenesis escaped these evolutionary pressures. A neuroethological approach to the study of adult neurogenesis is essential for a comprehensive understanding of the phenomenon. Furthermore, most of us are guilty of making strong assertions about our data in order to have impact yet this ultimately creates bias in how work is performed, interpreted, and applied. By taking a step back and actually placing our results in a much larger, non-biomedical context, we can help to reduce dogmatic thinking and create a framework for discovery.

Keywords: comparative, neuroethology, neurogenesis, reproduction, social behavior

OPEN ACCESS

Edited by:
Irmgard Amrein,
University of Zurich, Switzerland

Reviewed by:
Walter Wilczynski,
Georgia State University, United States
Margaret Ann Mohr,
David Geffen School of Medicine at UCLA, United States

***Correspondence:**
Melissa M. Holmes
melissa.holmes@utoronto.ca

Specialty section:
This article was submitted to Neurogenesis, a section of the journal Frontiers in Neuroscience

Received: *08 July 2017*
Accepted: *25 August 2017*
Published: *08 September 2017*

Citation:
Faykoo-Martinez M, Toor I and Holmes MM (2017) Solving the Neurogenesis Puzzle: Looking for Pieces Outside the Traditional Box. Front. Neurosci. 11:505. doi: 10.3389/fnins.2017.00505

With his prescient metaphor of the laboratory rat (*Ratticus norvegicus*) as the Pied Piper leading experimentalists away from the path to discovery, Frank Beach shed light on the increasing species bias in fundamental biomedical research (Beach, 1950). Now, nearly 70 years later, history appears to rhyme as scientists are led not by one but two species, with the second being the standard laboratory mouse, *Mus musculus*. While it might not be the case for all disciplines (see Adkins-Regan, 1990; Shettleworth, 2009 for further discussion of Beach, 1950), we believe the study of adult neurogenesis is an example of a field now saturated with research using these two traditional mammalian laboratory models. This species bias appears to result from active choice as scientists have failed to embrace studying adult neurogenesis in non-traditional models (i.e., not mice or rats) twice since the conception of the field. First, Altman's original publication on adult neurogenesis in the rat (Altman, 1962) was trailed by similar findings in the guinea pig (*Cavia porcellus*; Altman and Das, 1967). The second instance occurred two decades later when the study of adult neurogenesis was reinvigorated with the relatively simultaneous findings of Bayer et al. in rats (Bayer et al., 1982) and Goldman and Nottebohm in canaries (*Serinus carinia*; Goldman and Nottebohm, 1983). As publication history shows, scientists largely, albeit not exclusively, chose the route of the rat/mouse:

a Web of Science search performed August 8, 2017 returns 14,344 hits using the search term "adult neurogenesis" for the period 1990–2017 (+ "mouse" = 6,251; + "rat" = 6,563; + "bird" = 175; + "canary" = 110; + "guinea pig" = 83). However, if we are to truly understand adult neurogenesis, including the puzzle of how and why it varies across species, we need to consider approaches that might require "out of the box" thinking, so to speak.

Here, we acknowledge the significance of mouse and rat research for establishing the current depth of knowledge about adult neurogenesis, but we argue for a contrasting approach: it is by studying a wide variety of species across vertebrate groups that we will gain a broader understanding of neurogenesis, including species differences in neurogenic brain regions, and the proximate and ultimate mechanisms underlying this diversity. We believe the rat/mouse-bias has led many scientists off the path to pioneering discoveries, and toward parametric manipulations and/or redundant findings with comparatively less advancement of knowledge. For example, it is widely agreed that the dentate gyrus of the hippocampus (DG) and the subventricular zone of the forebrain (SVZ) are canonical mammalian neurogenic regions (Messier et al., 1958; Altman, 1963; Altman and Das, 1965a,b; Kaplan and Hinds, 1977; Kaplan and Bell, 1984; rev. in Braun and Jessberger, 2013). These two regions contain adult neural stem cells (NSC) and are spontaneously and robustly neurogenic, with adult generated neurons integrating into functional neural circuits. By contrast, the neurogenic ability of other brain regions is a topic of active scientific debate. These "non-neurogenic" regions are thought to either not contain adult NSC or, if they do, significant perturbations are often required to trigger neurogenesis and/or permit cell survival (e.g., stroke can trigger neurogenesis in the adult mouse striatum by reprogramming astrocytes to produce neuroblasts; Magnusson et al., 2014). To be sure, we have gained tremendous depth of insight into mechanisms influencing hippocampal and subventricular neurogenesis but there is much to be gained by actively integrating a "breadth" approach. It is our perspective that, in lieu of using invasive perturbations in mice and rats to explore neurogenesis outside of traditional niches, we should capitalize on naturally-occurring phenomena in other animals to inform this debate.

The need for the study of diverse species is exemplified by the debate over adult neurogenesis in the cerebellum. In teleosts, cerebellar neurogenesis persisting into adulthood is well-accepted (rev. in Zupanc, 2006). Cells are born and migrate from and within the cerebellum, with roughly half possessing a neuronal phenotype and integrating into existing networks of cerebellar neurons. By contrast, the cerebellum has long been considered the most static region within the adult mammalian brain (Altman, 1969), with researchers rejecting the prospect of constitutive cerebellar neurogenesis despite some evidence of cell proliferation (albeit glial phenotypes) in the cerebellum of mice and rats (Grimaldi and Rossi, 2006; Su et al., 2014) and manipulation-induced generation of neurons in the cerebellum of cats and mice (Tighilet et al., 2007; Kumar et al., 2014). Yet, evidence supports the presence of constitutively active neuronal and glial progenitors in the cerebellar cortex of peripubertal and adult rabbits (*Orictolagus cuniculus*), perhaps owing to the longevity of rabbits as compared to other mammalian species studied (Ponti et al., 2006, 2008). If we were to consider results from rats and mice as conclusive, we might underestimate the existence of cerebellar neurogenesis in mammals. Instead, to address the continued skepticism surrounding cerebellar adult neurogenesis, we can test the longevity hypothesis by studying the phenomena in other long-lived mammalian species [e.g., Eastern gray squirrel (24 years; *Sciurus carolinensis*), naked mole-rat (28 years; *Heterocephalus glaber*; Gorbunova et al., 2008), little brown bat (34 years; *Myotis lucifugus*; Austad, 2009)].

Thus, in a turn from the current approach that focuses on the use of essentially only two laboratory models to represent all mammals, we need to move toward a paradigm that celebrates and capitalizes on the remarkable variability between species. Evolution has sculpted animals to be well-suited to their physical and social environments and each species faces unique pressures and challenges depending on their ecological niche. Yet, the current approach in much biomedical research is to over-generalize findings across species in an effort to translate to humans. Rather, we need to pursue and promote the idea of evolutionary experimentation, which focuses on the natural mechanisms that evolution has provided to solve biological problems (Buffenstein et al., 2014). Indeed, by returning to the roots of the field we see that evolutionary experimentation was instrumental in generating widespread acceptance of adult neurogenesis (rev. in Balthazart and Ball, 2016). Nottebohm's original finding of adult neurogenesis in the female canary (Goldman and Nottebohm, 1983) came at a time when the dogma was that no new neurons were born in adulthood, certainly not in mammals. However, by capitalizing on the remarkable production and perception of song in canaries, which varies by season, Nottebohm and colleagues demonstrated naturally-occurring adult neurogenesis that was linked to species-specific reproductive behavior. Importantly, these adult generated neurons are found in regions of the song circuit, *not* exclusively regions homologous with the dentate gyrus and subventricular zone. Given the significance of these comparative data to the field's origins, we should collectively reflect on the various factors that have contributed to the rat/mouse species bias present today.

Not surprisingly, given their direct relevance to reproductive fitness, species-specific adaptations in sociosexual behavior provide a rich opportunity to explore atypical neurogenic patterns. **Table 1** outlines a diverse list of other species in which adult neurogenesis linked to sociosexual adaptations has been identified, or at least suggested, in "non-neurogenic niches." While the available data might not always conclusively demonstrate constitutive neurogenesis in "non-neurogenic" regions, they should open the door for more research rather than simply be dismissed as impossible or irrelevant. Changes in the social and reproductive environment can have profound influences on an organism's survival and fitness and a small but growing literature reveals how these transitions appear to influence neurogenesis in "non-neurogenic" brain regions. As in the songbird brain, season influences adult neurogenesis in sheep (*Ovies aries)*. Specifically, increased cell proliferation

TABLE 1 | Evidence for adult neurogenesis in non-neurogenic niches in non-traditional animals likely attributed to sociosexual adaptations.

Species	Region	Notes
African cichlid fish (*Astatotilapia burtoni*)	Central posterior thalamic nucleus; nucleus of the lateral recess; preoptic area; periventricular nucleus of the posterior tuberculum; ventral nucleus of the ventral telencephalon	Increased cell proliferation in socially-dominant males (Muraska et al., 2012)
Golden hamster	Posterior medial amygdala	Testosterone increases cell proliferation, but not cell survival (Antzoulatos et al., 2008)
Green treefrog (*Hyla cinerea)*	Pre-optic area (male only), infundibular hypothalamus	Acoustic stimuli (mating chorus) increased cell proliferation (Almli and Wilczynski, 2012)
Iberian wall lizard (*Podarcis hispanica)*	Main and accessory olfactory bulbs, lateral cortex, nucleus sphericus	Males demonstrated increased cell proliferation and enhanced responsiveness to social chemical stimuli (Sampedro et al., 2008)
Meadow vole	Posterior cortical and posterior medial nuclei of amygdala	Estradiol treatment increases cell proliferation as compared to prairie voles (Fowler et al., 2005)
Prairie vole	Amygdala, hypothalamus	Male-exposure increases cell proliferation as compared to isolation (Fowler et al., 2002)
Red-sided garter snake (*Thanophis sirtalis parietalis)*	Septal nucleus, nucleus sphericus, pre-optic area, hypothalamus	Increased cell proliferation during the fall (Maine et al., 2014)
Ring dove	Pre-optic area	GnRH neuron regeneration in response to electrolytic damage (Cheng et al., 2011)
Soay sheep	Thalamus, hypothalamus (including median eminence, tanycyte projection zone)	Short photoperiod increases cell proliferation (Migaud et al., 2011; Hazlerigg et al., 2013)
Zebra finch (*Taeniopygia guttata)*	High vocal center, neostriatum caudale, Area X	Large group pairing increases new cell survival (Lipkind et al., 2002)
Zebrafish (*Danio rerio)*	Ventral telencephalon, diencephalic periventricular pre-optic area, dorsal hypothalamic nuclei	Estradiol treatments decreases cell proliferation (Makantasi and Dermon, 2014)

This is not an exhaustive list; rather, it demonstrates the diversity of species and regions in which evidence for adult-generated neurons exists.

occurs when animals are housed in short photoperiod (Migaud et al., 2011) and a higher number of doublecortin-expressing cells, thought to be immature neurons, are also seen in short day conditions (Batailler et al., 2016). These newly born cells are located in hypothalamic nuclei (e.g., arcuate nucleus) that are critically involved in neuroendocrine control of reproduction and sheep are seasonal breeders (Migaud et al., 2011). Similarly, an increased number of newly born cells is seen in the hypothalamus of Golden hamsters (*Mesocricetus auratus*), also seasonal breeders, housed in short photoperiods and at least some of these cells will survive and express neuronal markers (Huang et al., 1998). The effects of photoperiod on adult neurogenesis in Golden hamsters are also seen in the cingulate cortex and retrosplenial cortex in addition to the canonical neurogenic niche, the DG (Huang et al., 1998). Social environment manipulations alter adult neurogenesis in prairie voles (*Microtus ochrogaster*), which are highly affiliative and form strong, stable opposite-sex pair bonds. Being paired with a male increases adult-born neurons in the amygdala and hypothalamus of females compared to single-housed females; same-sex paired females are intermediate on these measures, suggesting both social and reproductive cues are influencing neurogenic processes (Fowler et al., 2002). Indeed, social isolation reduces cell survival, proliferation, and neuronal differentiation in the amygdala of female prairie voles, proliferation in the medial pre-optic area and survival in the ventromedial hypothalamus (Lieberwirth et al., 2012). Female prairie voles seem more sensitive than males to these social and reproductive manipulations as exposure to opposite-sex soiled bedding increases cell proliferation in the amygdala of females but not males; effects in the hypothalamus were not reported (Liu et al., 2014). The effects of sociosexual cues on adult-generated neurons in the amygdala and hypothalamus of female prairie voles are likely due to their species-specific affiliative adaptations. They exhibit increased cell proliferation and survival in the hypothalamus and amygdala compared to female meadow voles (*Microtus pennsylvanicus*), which do not form pair-bonds; no species differences were detected in the DG (Pan et al., 2016). Furthermore, adult proliferating and surviving cells in the amygdala and hypothalamus are correlated with social affiliation and recognition behaviors while no significant relationships between DG neurogenesis and these behaviors were detected (Pan et al., 2016).

Puberty is arguably the most profound transition in both reproductive and social functioning that an organism will experience. In rats, pubertal animals show sex-specific patterns of cell birth that correspond to adult sex differences in brain region morphology: males have greater cell addition in the sexually dimorphic nucleus of the pre-optic area and the medial amygdala, whereas females have more newly born cells in the anteroventral periventricular nucleus (AVPV; Ahmed et al., 2008). Indeed, these newly generated cells might have tremendous significance for the onset of adult-typical neuroendocrine function and reproductive behaviors.

For example, increased cell proliferation in the AVPV of pubertal females might be associated with the female-specific spike in luteinizing hormone that begins at puberty due to the kisspeptin neuron population in the AVPV (Mohr et al., 2016). Perhaps not surprising given that puberty is a virtually ubiquitous developmental process in mammals, pubertally-born cells are also seen in the medial pre-optic area, arcuate nucleus, and medial amygdala (i.e., hypothalamic and amygdalar regions) of male Golden hamsters (Mohr and Sisk, 2013). Importantly, a subset of these cells go on to express mature neuronal markers and activate during an interaction with a potential female mate (Mohr and Sisk, 2013). Adult ring doves (*Streptopelia risoria*) of both sexes can produce new GnRH neurons in the pre-optic area of the hypothalamus in response to electrolytic damage (Cheng et al., 2011). Given that these neurons are essential for successful reproduction (e.g., Mantei et al., 2008), the ability to regenerate the neural population is extremely adaptive. Collectively, pubertal and/or adult sculpting of hypothalamic neural circuits via neurogenesis may prove to be critically important for successful social and reproductive function and thus warrants much future investigation.

Our own work utilizes naked mole-rats to investigate how reproductive and social transitions might influence adult neurogenesis in both canonical and non-canonical neurogenic regions. Naked mole-rats are eusocial and live in a rigid social hierarchy dominated by a single reproductive female who breeds with one to three males while all others in the colony are sexually suppressed and socially subordinate (Jarvis, 1981). Subordinates are further differentiated into subcastes: soldiers, responsible for colony defense, and workers, responsible for colony maintenance and pup care. Through removal from the suppressive environmental cues imposed by breeders, subordinates undergo a one-way transition to sexual maturation and can compete for dominance, providing the opportunity to study how the social environment influences adult neural plasticity and, in turn, how adult neurogenesis contributes to behavioral differences. To date, our work suggests that the DG, piriform cortex, and basolateral amygdala (BLA) have increased neurogenesis, based on doublecortin staining, in subordinate animals relative to dominants (Peragine et al., 2014). Interestingly, female animals removed from their colony and paired with a female show evidence of increased neurogenesis in the basolateral amygdala (BLA) relative to animals paired with males (Peragine et al., 2016). This might reflect the role of the BLA in mediating stress and threat in other mammals (Levinson et al., 1980; Fanselow and LeDoux, 1999; Jacobs et al., 2006) coupled with the unique female-dominant aspect of naked mole-rat social organization. Next, we aim to capitalize on the socially-mediated pubertal transition of naked mole-rats to gain more insight into the significance of hypothalamic neurogenesis seen in other species. Our preliminary explorations indicate a population of BrdU-labeled cells in the arcuate nucleus of the hypothalamus (**Figure 1**). We hypothesize that this population of proliferating cells is related to the role of the arcuate nucleus in regulating reproduction through downstream effects on gonadotropin releasing and inhibitory hormones, similar to the pubertally born putative kisspeptin AVPV neurons in rats discussed above (Mohr et al., 2016). Indeed, we have recently demonstrated that naked mole-rats have a unique population of neurons expressing the gonadotropin-inhibitory hormone ligand, RFRP-3, in the arcuate nucleus and that subordinates have significantly greater RFRP immunofluorescence in this region (Peragine et al., 2017). Determining whether the adult-generated cells in the arcuate nucleus mature and influence neuroendocrine signaling is a critical next step.

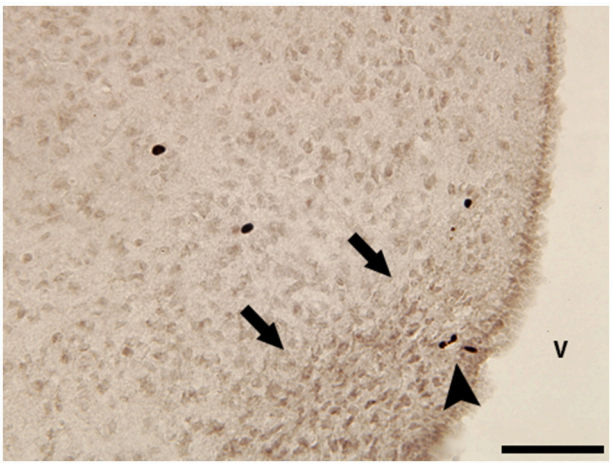

FIGURE 1 | Photomicrograph of BrdU-immunoreactive (ir) cells in the hypothalamus of a subordinate female naked mole-rat collected 2 h after a single BrdU injection. Black arrowhead points to small group of BrdU-ir cells within the boundaries of the arcuate nucleus (black arrows). V, 3rd ventricle. Scale bar = 50 μm.

In sum, we by no means intend to minimize the importance of the SVZ or DG work in mice and rats. There have been tremendous advances in the mechanistic understanding of adult neurogenesis by focusing on these regions in these species. Nor are we the first to consider how the concerns raised by Beach (1950) apply to a particular research area (e.g., Adkins-Regan, 1990; Shettleworth, 2009). Indeed, similar to the views presented by Adkins-Regan (1990) and Shettleworth (2009), we acknowledge the fascinating and not insubstantial comparative neurogenesis work done to date. However, we argue that a strong species bias exists in the neurogenesis literature and that this bias serves to promote dogmatic thinking, ultimately impeding on creativity and advancement of knowledge. If one thinks of a research question as a puzzle, we can appreciate that we need to put together many pieces to reveal the complete image. In the case of adult neurogenesis, one can think of that puzzle very specifically (e.g., "adult neurogenesis as a process in mice and/or rats") or as a broad, general phenomenon. The types of pieces needed to solve the puzzle will differ, to be sure, but the problem is thinking you are working on one puzzle when you are actually working on another. If it is our goal to solve the puzzle of "adult neurogenesis," including both proximate and ultimate questions, we must pursue this goal with rigor: accepting or rejecting a

hypothesis (i.e., neurogenesis in a "non-neurogenic" niche) based on substantial comparative evidence. History does not need to continue to rhyme as it has in the time since Beach's manifesto (Beach, 1950) to experimental psychologists. We must go back to the roots of the field and assume the role of Altman who, despite the prolific Ramón y Cajal deeming the adult brain static, pursued the idea of adult neurogenesis in the face of emphatic assertions backed by experimental evidence (Ramón y Cajal, 1928; Altman, 1962). By pursuing evolutionary experimentation with an open yet critical mind, the future will not be that of the lab rat leading the scientist, but the scientist leading the vast diversity of species along the path to discovery.

AUTHOR CONTRIBUTIONS

MFM, IT, and MMH all discussed the perspective to be presented and planned the manuscript. MFM and MMH wrote the manuscript. MFM, IT, and MMH revised the manuscript.

FUNDING

This work was funded by NSERC Discovery Grant 402633 and an Ontario Early Researcher Award to MMH. IT is the recipient of an Ontario Graduate Scholarship and MFM is the recipient of a NSERC USRA.

REFERENCES

Adkins-Regan, E. (1990). Is the snark still a boojum? The comparative approach to reproductive behavior. *Neurosci. Biobehav. Rev.* 14, 243–252. doi: 10.1016/S0149-7634(05)80224-6

Ahmed, E. I., Zehr, J. L., Schulz, K. M., Lorenz, B. H., DonCarlos, L. L., and Sisk, C. L. (2008). Pubertal hormones modulate the addition of new cells to sexually dimorphic brain regions. *Nat. Neurosci.* 11, 995–997. doi: 10.1038/nn.2178

Almli, L. M., and Wilczynski, W. (2012). Socially modulated cell proliferation is independent of gonadal steroid hormones in the brain of the adult green treefrog (*Hyla cinerea*). *Brain. Behav. Evol.* 79, 170–180. doi: 10.1159/000335037

Altman, J. (1962). Are new neurons formed in the brains of adult mammals? *Science* 135, 1127–1128. doi: 10.1126/science.135.3509.1127

Altman, J. (1963). Autoradiographic investigation of cell proliferation in the brains of rats and cats. *Anat. Rec.* 145, 573–591. doi: 10.1002/ar.1091450409

Altman, J. (1969). Autoradiographic and histological studies of postnatal neurogenesis. III. Dating the time of production and onset of differentiation of cerebellar microneurons in rats. *J. Comp. Neurol.* 136, 269–293. doi: 10.1002/cne.901360303

Altman, J., and Das, G. D. (1965a). Autoradiographic and histological evidence of postnatal hippocampal neurogenesis in rats. *J. Comp. Neurol.* 124, 319–336. doi: 10.1002/cne.901240303

Altman, J., and Das, G. D. (1965b). Post-natal origin of microneurones in the rat brain. *Nature* 207, 953–956. doi: 10.1038/207953a0

Altman, J., and Das, G. D. (1967). Postnatal neurogenesis in the guinea-pig. *Nature* 214, 1098–1101. doi: 10.1038/2141098a0

Antzoulatos, E., Magorien, J. E., and Wood, R. I. (2008). Cell proliferation and survival in the mating circuit of adult male hamsters: effects of testosterone and sexual behavior. *Horm. Behav.* 54, 735–740. doi: 10.1016/j.yhbeh.2008.08.001

Austad, S. N. (2009). Comparative biology of gaining. *J. Gerontol. A. Biol. Sci. Med. Sci.* 64, 199–201. doi: 10.1093/gerona/gln060

Balthazart, J., and Ball, G. F. (2016). Endocrine and social regulation of adult neurogenesis in songbirds. *Front. Neuroendocrinol.* 41, 3–22. doi: 10.1016/j.yfrne.2016.03.003

Batailler, M., Derouet, L., Butruille, L., and Migaud, M. (2016). Sensitivity to the photoperiod and potential migratory features of neuroblasts in the adult sheep hypothalamus. *Brain Struct. Funct.* 221, 3301–3314. doi: 10.1007/s00429-015-1101-0

Bayer, S. A., Yackel, J. W., and Puri, P. S. (1982). Neurons in the rat dentate gyrus granule layer substantially increase during juvenile and adult life. *Science* 216, 890–892. doi: 10.1126/science.7079742

Beach, F. A. (1950). The snark was a boojum. *Am. Psychol.* 5, 115–124. doi: 10.1037/h0056510

Braun, S. M. G., and Jessberger, S. (2013). Adult neurogenesis in the mammalian brain. *Front. Biol.* 8, 295–304. doi: 10.1007/s11515-013-1263-1

Buffenstein, R., Nelson, O. L., and Corbit, K. C. (2014). Questioning the preclinical paradigm: natural, extreme biology as an alternative discovery platform. *Aging* 6, 913–920. doi: 10.18632/aging.100704

Cheng, M.-F., Alexander, K., Zhou, S., Bonder, E., and Chuang, L.-S. (2011). Newborn GnRH neurons in the adult forebrain of the ring dove. *Horm. Behav.* 60, 94–104. doi: 10.1016/j.yhbeh.2011.03.008

Fanselow, M. S., and LeDoux, J. E. (1999). Why we think plasticity underlying Pavlovian fear conditioning occurs in the basolateral amygdala. *Neuron* 23, 229–232. doi: 10.1016/S0896-6273(00)80775-8

Fowler, C. D., Johnson, F., and Wang, Z. (2005). Estrogen regulation of cell proliferation and distribution of estrogen receptor-α in the brains of adult female prairie and meadow voles. *J. Comp. Neurol.* 489, 166–179. doi: 10.1002/cne.20638

Fowler, C. D., Liu, Y., Ouimet, C., and Wang, Z. (2002). The effects of social environment on adult neurogenesis in the female prairie vole. *J. Neurobiol.* 51, 115–128. doi: 10.1002/neu.10042

Goldman, S. A., and Nottebohm, F. (1983). Neuronal production, migration, and differentiation in a vocal control nucleus of the adult female canary brain. *Proc. Natl. Acad. Sci. U.S.A.* 80, 2390–2394. doi: 10.1073/pnas.80.8.2390

Gorbunova, V., Bozzella, M. J., and Seluanov, A. (2008). Rodents for comparative aging studies: from mice to beavers. *Age* 30:111. doi: 10.1007/s11357-008-9053-4

Grimaldi, P., and Rossi, F. (2006). Lack of neurogenesis in the adult rat cerebellum after Purkinje cell degeneration and growth factor infusion. *Eur. J. Neurosci.* 23, 2657–2668. doi: 10.1111/j.1460-9568.2006.04803.x

Hazlerigg, D. G., Wyse, C. A., Dardente, H., Hanon, E. A., and Lincoln, G. A. (2013). Photoperiodic variation on CD45-Positive cells and cell proliferation in the mediobasal hypothalamus of the soay sheep. *Chronobiol. Int.* 30, 548–558. doi: 10.3109/07420528.2012.754450

Huang, L., DeVries, G. J., and Bittman, E. L. (1998). Photoperiod regulates neuronal bromodeoxyuridine labeling in the brain of a seasonally breeding mammal. *J. Neurobiol.* 36, 410–420. doi: 10.1002/(SICI)1097-4695(19980905)36:3<410::AID-NEU8>3.0.CO;2-Z

Jacobs, C., Van Den Broeck,W., and Simoens, P. (2006). Increased volume and neuronal number of the basolateral nuclear group of the amygdaloid body in aggressive dogs. *Behav. Brain Res.* 170, 119–125. doi: 10.1016/j.bbr.2006.02.011

Jarvis, J. U. M. (1981). Eusociality in a mammal: cooperative breeding in naked mole-rat colonies. *Science* 212, 571–573. doi: 10.1126/science.7209555

Kaplan, M. S., and Bell, D. H. (1984). Mitotic neuroblasts in the 9-day-old and 11-month-old rodent hippocampus. *J. Neurosci.* 4, 1429–1441.

Kaplan, M. S., and Hinds, J. W.,(1977). Neurogenesis in the adult rat: electron microscopic analysis of light radioautographs. *Science* 197, 1092–1094. doi: 10.1126/science.887941

Kumar, M., Csaba, Z., Peineau, S., Srivastava, R., Rasika, S., Mani, S., et al. (2014). Endogenous cerebellar neurogenesis in adult mice with progressive ataxia. *Ann. Clin. Trans. Neurol.* 1, 968–981. doi: 10.1002/acn3.137

Levinson, D., Reeves, D., and Buchanan, D. (1980). Reductions in aggression and dominance status in guinea pigs following bilateral lesions in the basolateral amygdala or lateral septum. *Physiol. Behav.* 25, 963–971 doi: 10.1016/0031-9384(80)90318-2

Lieberwirth, C., Liu, Y., Jia, X., and Wang, Z. (2012). Social isolation impairs adult neurogenesis in the limbic system and alters behaviors in female prairie voles. *Horm. Behav.* 62, 357–366. doi: 10.1016/j.yhbeh.2012.03.005

Lipkind, D., Nottebohm, F., Rado, R., and Barnea, A. (2002). Social change affects the survival of new neurons in the forebrain of adult songbirds. *Behav. Brain. Res.* 133, 31–43. doi: 10.1016/S0166-4328(01)00416-8

Liu, Y., Lieberwirth, C., Jia, X., Curtis, J. T., Meredith, M., and Wang, Z. X. (2014). Chemosensory cues affect amygdaloid neurogenesis and alters behaviors in the socially monogamous prairie vole. *Eur. J. Neurosci.* 39, 1632–1641. doi: 10.1111/ejn.12531

Magnusson, J. P., Göritz, C., Tatarishvili, J., Dias, D. O., Smith, E. M. K., Lindvall, O., et al. (2014). A latent neurogenic program in astrocytes regulated by Notch signaling in the mouse. *Science* 346, 237–241. doi: 10.1126/science.346.6206.237

Maine, A. R., Powers, S. D., and Lutterschmidt, D. I. (2014). Seasonal variation in cell proliferation and cell migration in the brain of adult red-sided garter snakes (*Thamnophis sirtalis* parietalis). *Brain. Behav. Evol.* 84, 181–196. doi: 10.1159/000364778

Makantasi, P., and Dermon, C. R. (2014). Estradiol treatment decreases cell proliferation in the neurogenic zones of adult female zebrafish (*Danio rerio*) brain. *Neuroscience* 26, 306–320. doi: 10.1016/j.neuroscience.2014.06.071

Mantei, K. E., Ramakrishnan, S., Sharp, P. J., and Buntin, J. D. (2008). Courtship interactions stimulate rapid changes in GnRH synthesis in male ring doves. *Horm. Behav.* 54, 669–675. doi: 10.1016/j.yhbeh.2008.07.005

Messier, B., Leblond, C. P., and Smart, I. (1958). Presence of DNA synthesis and mitosis in the brain of young adult mice. *Exp. Cell. Res.* 14, 224–226. doi: 10.1016/0014-4827(58)90235-0

Migaud, M., Batailler, M., Pillon, D., Franceschini, I., and Malpaux, I. (2011). Seasonal changes in cell proliferation in the adult sheep brains and pars tuberalis. *J. Biol. Rhythms* 26, 486–496. doi: 10.1177/0748730411420062

Mohr, M. A., and Sisk, C. L. (2013). Pubertally born neurons and glia are functionally integrated into limbic and hypothalamic circuits of the male Syrian hamster. *Proc. Natl. Acad. Sci. U.S.A.* 110, 4792–4797. doi: 10.1073/pnas.1219443110

Mohr, M. A., Garcia, F. L., DonCarlos, L. L., and Sisk, C. L. (2016). Neurons and glial cells are added to the female rat anteroventral periventricular nucleus during puberty. *Endocrinology* 157, 2393–2402. doi: 10.1210/en.2015-2012

Muraska, K. P., Carpenter, R. E., and Fernald, R. D. (2012). Characterization of cell proliferation throughout the brain of the African cichlid fish *Astatotilapia burtoni* and its regulation by social status. *J. Comp. Neurol.* 520, 3471–3491. doi: 10.1002/cne.23100

Pan, Y., Liu, Y., Lieberwirth, C., Zhang, Z., and Wang, Z. (2016). Species differences in behavior and cell proliferation/survival in the adult brains of female meadow and prairie voles. *Neuroscience* 315, 259–270. doi: 10.1016/j.neuroscience.2015.12.026

Peragine, D. E., Pokarowski, M., Mendoze-Viveros, L., Swift-Gallant, A., Cheng, H.-Y. M., Bentley, G. E., et al. (2017). RFamide-related peptide-3 (RFRP-3) suppresses sexual maturation in a eusocial mammal. *Proc. Natl. Acad. Sci. U.S.A.* 114, 1207–1212. doi: 10.1073/pnas.1616913114

Peragine, D. E., Simpson, J. A., Mooney, S. J., Lovern, M. B., and Holmes, M. M. (2014). Social regulation of adult neurogenesis in a eusocial mammal. *Neuroscience* 268, 10–20. doi: 10.1016/j.neuroscience.2014.02.044

Peragine, D. E., Yousuf, Y., Fu, Y., Swift-Gallant, A., Ginzberg, K., and Holmes, M. M. (2016). Contrasting effects of opposite- versus same-sex housing on hormones, behavior and neurogenesis in a eusocial mammal. *Horm. Behav.* 81, 28–37. doi: 10.1016/j.yhbeh.2016.03.005

Ponti, G., Peretto, P., and Bonfanti, L. (2006). A subpial, transitory germinal zone forms chains of neuronal precursors in the rabbit cerebellum. *Dev. Biol.* 294, 168–180. doi: 10.1016/j.ydbio.2006.02.037

Ponti, G., Peretto, P., and Bonfanti, L. (2008). Genesis of neuronal and glial progenitors in the cerebellar cortex of peripubertal and adult rabbits. *PLoS ONE* 3:e2366. doi: 10.1371/journal.pone.0002366

Ramón y Cajal, S. (1928). *Degeneration and Regeneration of the Nervous System*. New York, NY: Hafner.

Sampedro, C., Font, E., and Desfilis, E. (2008). Size variation and cell proliferation in chemosensory brain areas of a lizard (*Podarcis hispanica*): effects of sex and season. *Eur. J. Neurosci.* 28, 87–98. doi: 10.1111/j.1460-9568.2008.06287.x

Shettleworth, S. J. (2009). The evolution of comparative cognition: is the snark still a boojum? *Behav. Process.* 80, 210–217. doi: 10.1016/j.beproc.2008.09.001

Su, X., Guan, W., Yu, Y. C., and Fu, Y. (2014). Cerebellar stem cells do not produce neurons and astrocytes in adult mouse. *Biochem. Biophys. Res. Commun.* 450, 378–383. doi: 10.1016/j.bbrc.2014.05.131

Tighilet, B., Brezun, J. M., Sylvie, G. D., Gaubert, C., and Lacour, M. (2007). New neurons in the vestibular nuclei complex after unilateral vestibular neurectomy in the adult cat. *Eur. J. Neurosci.* 25, 47–58. doi: 10.1111/j.1460-9568.2006.05267.x

Zupanc, G. K. H. (2006). Neurogenesis and neuronal regeneration in the adult fish brain. *J. Comp. Physiol. A.* 192, 649–670. doi: 10.1007/s00359-006-0104-y

Conflict of Interest Statement: The authors declare that the research was conducted in the absence of any commercial or financial relationships that could be construed as a potential conflict of interest.

Advantages of publishing in Frontiers

OPEN ACCESS
Articles are free to read for greatest visibility and readership

FAST PUBLICATION
Around 90 days from submission to decision

HIGH QUALITY PEER-REVIEW
Rigorous, collaborative, and constructive peer-review

TRANSPARENT PEER-REVIEW
Editors and reviewers acknowledged by name on published articles

Frontiers
Avenue du Tribunal-Fédéral 34
1005 Lausanne | Switzerland

Visit us: www.frontiersin.org
Contact us: info@frontiersin.org | +41 21 510 17 00

REPRODUCIBILITY OF RESEARCH
Support open data and methods to enhance research reproducibility

DIGITAL PUBLISHING
Articles designed for optimal readership across devices

FOLLOW US
@frontiersin

IMPACT METRICS
Advanced article metrics track visibility across digital media

EXTENSIVE PROMOTION
Marketing and promotion of impactful research

LOOP RESEARCH NETWORK
Our network increases your article's readership